UNIVERSITY OF CAPE TOWN

THE EFFECTS OF PRENATAL AND EARLY-POSTNATAL ETHANOL EXPOSURE ON RAT BRAIN NEUROCHEMISTRY AND BEHAVIOUR

Patricia Cathryn Swart

Supervisor: Professor Vivienne A. Russell

Co-supervisor: Dr. Jacqueline J. Dimatelis

Submitted to the University of Cape Town
In fulfillment of the requirements for the degree

Doctor of Philosophy
Neuroscience (Physiology)

Department of Human Biology

Faculty of Health Sciences

UNIVERSITY OF CAPE TOWN

October 2017

ABSTRACT

Foetal alcohol spectrum disorder (FASD), the umbrella term used to describe the wide range of cognitive and behavioural deficits observed after exposure to alcohol *in utero*, is a major public health issue specifically in South Africa. South Africa is thought to have the highest prevalence of FASD in the world. FASD presents as a variety of learning and memory deficits as well as psychological disorders such as anxiety and depression but the underlying mechanisms are largely unknown and poorly understood. FASD, learning and memory processes and psychological disorders have been associated with changes in neural plasticity. Therefore, the research reported in this thesis describes ethanol-induced changes in neuroplasticity-related proteins, with specific reference to the extracellular signal-regulated kinase1/2 (ERK1/2) and glycogen synthase kinase-3-beta (GSK3β) signalling cascades, using two different animal models of FASD. Further, to elucidate additional mechanisms underlying the deficits observed in FASD, proteomic profiles were determined in order to illustrate large-scale ethanol-induced changes in proteins involved in energy metabolism, neurotransmitter signalling, redox regulation, protein metabolism and cytoskeletal structure in the rat brain. In addition, this research describes vinpocetine, a phosphodiesterase (PDE) type 1 inhibitor, as a possible treatment for disturbances caused by early exposure to ethanol and investigates the effects of additional early-life stress in animal models of FASD.

The first study, using a third-trimester equivalent animal model of FASD (4 g/kg/day i.p., 12 % v/v, P4 - P9), investigated early-postnatal ethanol-induced changes in adolescent rats. The results demonstrate that significant ethanol-induced changes can occur in rats that do not display overt behavioural deficits. Specifically, early-postnatal ethanol exposure decreased ERK1/2 activation in the prefrontal cortex (PFC) and increased ERK1/2 activation in the dorsal hippocampus (DH). Proteomic analysis revealed additional region-specific changes, for example, early-postnatal ethanol exposure increased the capacity for energy production in the PFC whereas in the DH, energy-related proteins were decreased compared to non-exposed controls. The PFC of rats exposed to early-postnatal ethanol was further characterized by an increased capacity for oxidative phosphorylation coupled with decreased antioxidant capacity. In addition, there was evidence that could lead to altered redox protein signaling in the DH of ethanol rats. Vinpocetine treatment of rats exposed to ethanol during early development

reduced ethanol-induced changes in ERK1/2 activity in the PFC and DH. Additional proteomic analysis of the ventral hippocampus (VH) demonstrated that vinpocetine also reduced postnatal-ethanol-induced changes in proteins related to energy metabolism, signaling, protein synthesis and cytoskeletal structure. Therefore, vinpocetine treatment of rats exposed to early-postnatal ethanol in conjunction with proteomic analysis has the potential to identify novel treatment targets to reduce the effects of ethanol on the developing brain.

The second animal study combined prenatal-ethanol exposure (0.066 % saccharin-sweetened, 10 % ethanol) with the maternal separation model of early-life stress (3 hours/day P2 – P14) in order to account for possible effects of early-life adversity in addition to *in utero* alcohol exposure. Adult rats exposed to prenatal-ethanol showed reduced weight gain, hyperactivity and a negative affective state which are characteristic of FASD. However, the combination of prenatal-ethanol exposure and early-life stress did not enhance behavioural changes. Rather, early-life stress subsequent to prenatal-ethanol exposure proved beneficial as shown by similar weight gain and activity levels to that of control rats. Similarly, early-life stress reduced prenatal-ethanol-induced increase in P-ERK1/2 signalling in both the PFC and DH. On the contrary, the combination of prenatal-ethanol exposure and early-life stress seemed to have an additive effect on protein changes in the PFC of adult rats as shown by a greater number of proteins related to energy, redox regulation, signaling and cytoskeletal structure being altered by the combination of these developmental insults. In addition, the DH appeared to be more susceptible to prenatal-ethanol exposure since a greater number of proteins were significantly changed by prenatal-ethanol exposure. However, the combination of prenatal-ethanol and maternal separation stress reduced the number of significantly altered proteins in the DH. These results further highlight the wide range and region-specific effects of prenatal-ethanol exposure on the brain and importantly demonstrate an interaction between prenatal-ethanol exposure and early-life stress. Therefore, it is important to account for the possible effects of early-life adversity when modeling FASD.

Results from these 2 studies highlight the long-term effects of ethanol exposure during early development on the rat brain and behaviour. In addition, these studies describe the importance of age at behavioural testing and tissue analysis and demonstrate the complexity of modeling FASD. Importantly, results demonstrate the need to account for the possible effects of early-life adversity when modeling FASD. Further, the results presented in this thesis highlight the

benefits of performing neurochemical analyses on rats that have not been subjected to prior stressors other than the model being investigated and further, to separately analyze functionally distinct brain regions. Both studies demonstrate long-term ethanol-induced changes in P-ERK1/2 signalling and proteins related to energy metabolism and redox regulation in the PFC and DH. These results provide a platform for future research with the potential to identify novel treatment targets. Together, the results presented in this thesis contribute valuable insight to the field of FASD and the animal models used to study this multifaceted disorder.

DECLARATION

I, **Patricia Cathryn Swart**, hereby declare that the work on which this dissertation/thesis is based is my original work (except where acknowledgements indicate otherwise) and that neither the whole work nor any part of it has been, is being, or is to be submitted for another degree in this or any other university. I empower the university to reproduce for the purpose of research either the whole or any portion of the contents in any manner whatsoever.

"This thesis has been submitted to the Turnitin module (or equivalent similarity and originality checking software) and I confirm that my supervisor has seen my report and any concerns revealed by such have been resolved with my supervisor."

Name: Patricia Cathryn Swart Student Number: SWRPAT003

Signature: Signed by candidate Date: 14 October 2017

ACKNOWLEDGEMENTS

To my supervisors, Professor Vivienne Russell and Dr. Jacqueline Dimatelis, I am so honored to have been your student and under your supervision. I have been fortunate enough to have had the greatest mentors and have learnt so much from your invaluable expertise. Thank you both so much for your guidance, support and patience over the years. Thank you for encouraging me and believing in me every step of the way. Prof, thank you for your constant support, willingness to help, comments, suggestions, and attention to detail. I have learnt so much from your many years of expertise and the guidance that brings. I truly value your dedication to your students. Moreover thank you for instilling confidence in me. I am so grateful to have had you as my supervisor. JD, thank you for being a constant source of support and encouraging me to pursue this PhD. Thank you for your hands-on approach and having the time and patience to train me, specifically, behavioural testing and the invaluable Western blotting technique. I am immensely grateful to have had you as a supervisor and even more so to call you a friend. I really admire your courage to change career paths and take the path less travelled in order to achieve your dreams. You are going to be an incredible medical doctor. Thank you!

There are many additional people to thank who contributed, in some way or another, to the completion of this PhD. I am immensely grateful for all their help and will attempt to express my gratitude in words.

To Nuraan Ismail and Abdul Kareem Samuels (AK), thank you so much for working beside me and ensuring the welfare of the animals used in this study. You made every effort to ensure that the animals remained healthy and happy. More importantly you helped me feel confident while working with rats. You have always been readily available to help in any capacity and I am always excited to see your smiling faces on campus.

Thank you to Christopher Currin for his assistance in conducting selected behavioural tests (MWM and cone test), which later formed part of his BSc (Med) Honours degree. Thank you to Dr Zac McDonald at the Centre for Proteomic and Genomic Research (CPGR) and Dr Maré Vlok (Central Analytics Facility, Tygerberg Medical Campus, University of Stellenbosch) for performing iTRAQ labeling and LC-MS on our tissue samples. The accuracy and reliability of the results have proved invaluable. I would highly recommend both their services. To Dr Maré

Vlok, thanks too for taking the time to explain aspects of iTRAQ labeling and LC-MS, your patience was highly appreciated.

To the Department of Human Biology, both its staff and its students in the Anatomy Building, thank you so much for making my time on UCT Medical Campus memorable. Your smiles and friendly greetings have always been warm and welcoming and have made for an incredible work environment. Help was always around the corner. Special mention to Charles Pelston, Bruce Dando, and Charles Harris who ensured things ran smoothly with regards to the maintenance of our liquid nitrogen storage facility, animal facility and behavioural rooms and in the case of load shedding went out of their way to ensure that the power to the equipment was never disrupted so that experimental procedures could continue. Special thanks to Charles Harris for constructing the behavioural apparatus and *in vitro* superfusion setup. Thanks to Nazeem Damon for looking after Lab 5.02 and Abbigale Van Der Westhuizen and the reception staff for all that they do. Thanks to Sharon Prince's Lab for the use of their plate reader and to the Katz Lab for use of the Beta counter. To Professor Asfree Gwanyanya, thank you for sharing your Western blot equipment and reagents in times of need and more importantly thank you for all your support, enthusiasm and words of encouragement. I would also like to thank Dr Kishor Bugarith, Dr Geney Gunston, Dr Gabi De Bie and Dr Paul Steyn for their continued support and interest. To Dr Vino Naidoo, Dr Joseph Raimondo and De Fleur Howells, thank you for your interest in my work and words of wisdom over the years.

I would also like to thank Adri Winckler and the Health Sciences Postgraduate Office team for their administrative support and advice.

When I started my postgraduate career in Lab 5.02 I was fortunate enough to be surrounded by senior postgraduate students: Hayley Tomes, Jacqueline Womersley, Toni-Lee Sterley and Jurgens Van Zyl, who taught me their ways, showed me the tricks of the trade and continue to be super supportive and encouraging. Thanks to Toni and Jurgens for all their advice and willingness to help me with western blots and tissue collection. To Jax, thanks for your continued faith in me, encouragement and introducing me to the wonderful world of yoga. To Hayley, you are a super star in more ways than one and I am so honoured to have you in my life. Your passion for science and learning is contagious. You have always been so supportive and you have always believed in me. I cannot describe the sense of balance and calmness your

presence has. I am so grateful for your positive vibes and the positive impact you have made on my life in general.

To my fellow postgrad friends who have travelled this journey with me: Katie Atmore, Matthew Amoni, Christopher Currin, Bianca Leigh Edwards, Emma Doubell, Anja de Lange (+Hayley Tomes = "Team Tapeworm") and Sylvia van Belle, thank you for all the memories, all the laughter and for always being there in my times of need (with coffee in hand) and being able to relate to the ups and downs of lab life.

To my friends and family, thank you for your continued love and support. Thank you for understanding my need to prioritize work. To my family, thank you for your support and always being in my corner. Thank you for understanding that I needed to be in Cape Town and that I needed to sacrifice family time for work. Thank you for your interest and curiosity in my work throughout this journey. Thank you for your patience and encouragement and for always believing in me. Thank you to my parents for affording me the opportunity to attend the University of Cape Town. Words cannot describe my love and gratitude. Thank you!

Without the financial assistance from the National Research Foundation, The University of Cape Town, Duncan Baxter and Harry Crossley Scholarships I would not have been able to complete this degree. Thank you to the friendly and helpful staff of the Postgraduate Funding Office.

"Any opinion, finding and conclusion or recommendation expressed in this material is that of the author(s) and the NRF does not accept any liability in this regard."

"The financial assistance of the National Research Foundation (NRF) towards this research is hereby acknowledged. Opinions expressed and conclusions arrived at, are those of the author and are not necessarily to be attributed to the NRF."

Contents

LIST OF RESEARCH OUTPUTS

PUBLICATIONS

Swart, P.C., Currin, C.B., Russell, V.A and Dimatelis, J.J. 2017. Early-ethanol exposure and vinpocetine treatment alter learning- and memory-related proteins in the rat hippocampus and prefrontal cortex. Journal of Neuroscience Research 95:1204–1215.

CONFERENCE OUTPUTS

IBRO-ISN Neuroscience School on Behavioural Bioassays in Neuroscience: Brain and Behaviour from Invertebrates to Small Mammals, Nairobi, Kenya, December 2014.

IBRO Writing Papers Workshop: Durban, KwaZulu-Natal, South Africa, 23 - 25 March 2015.

Society of Neuroscientists of Africa (SONA) Conference: Poster Presentation - Title: The effect of early alcohol exposure on the brain and behaviour in a third trimester equivalent animal model of FAS/FASD. Durban, KwaZulu-Natal, South Africa, March 2015.

South African Neuroscience Society (SANS) Symposium at the Biological Psychiatry Congress: Poster Presentation - Title: The effect of early-ethanol exposure on the brain and behaviour in a third trimester equivalent animal model of foetal alcohol spectrum disorders. Somerset West, Western Cape, South Africa, September 2015.

Society for Neuroscience (SfN) Meeting: Poster Presentation - Title: The effect of early-ethanol exposure on the brain and behaviour in a third trimester equivalent animal model of foetal alcohol spectrum disorders. Chicago, Illinois, October 2015.

10th Canadian IBRO School of Neuroscience: Montreal, 18 May - 02 June 2016.

Canadian Association of Neuroscience Meeting: Poster Presentation - Title: The long term effects of early-ethanol exposure on the developing rat brain: A proteomic study. Toronto, Canada, 29 May - 01 June 2016.

SANS Symposium: PowerPoint Presentation - Title: Early-ethanol exposure differentially alters energy-related proteins in the developing rat brain. University of Cape Town, South Africa, 11 December 2016.

SANS Symposium at the Biological Psychiatry Congress: Poster Presentation - Title: Vinpocetine treatment reverses early-ethanol exposure-induced protein changes in the rat brain. Somerset West, Western Cape, South Africa, 17 September 2017.

SfN Meeting: Poster Presentation - Title: Maternal separation reduced prenatal-ethanol-induced changes in hyperactivity and extracellular signal-regulated kinase activity. Washington DC, November 2017

IBRO Cape Town School Advanced Neuroscience Techniques: University of Cape Town, South Africa, 2 - 18 December 2017.

LIST OF ABBREVIATIONS

ADHD:	Attention-deficit/hyperactivity disorder
BAC:	Blood alcohol concentration
BDNF:	Brain-derived neurotrophic factor
CREB:	cAMP response element binding protein
DA:	Dopamine
DH:	Dorsal hippocampus
DMSO:	Dimethylsulfoxide
DOB:	Date of birth
ELISA:	Enzyme-linked immunosorbent assay
EPM:	Elevated plus maze
ERK1/2:	Extracellular signal-regulated kinase 1/2
EtOH:	Ethanol
FAS:	Foetal alcohol syndrome
FASD:	Foetal alcohol spectrum disorder
FST:	Forced swim test
GABA:	γ-aminobutyric acid
GD (*):	Gestational day (*)
GSK3β:	Glycogen synthase kinase three-beta
IQR:	Inter-quartile range
I.p:	Intraperitoneal injection
iTRAQ:	Isobaric tagging for relative and absolute quantitation
MKP-1:	Mitogen-activated protein kinase phosphatase-1
MS:	Maternal separation
nMS:	Non-maternally separated
NOT:	Novel object test
OFT:	Open field test
P (*):	Postnatal day (*)

P-ERK1/2:	Phosphorylated-extracellular signal-regulated kinase 1/2
P-CREB:	Phosphorylated-cAMP response element binding protein
P-GSK3β:	Phosphorylated-glycogen synthase kinase beta
PDE:	Phosphodiesterase
PFC:	Prefrontal cortex
SD:	Sprague-Dawley
SEM:	Standard error of the mean
SW:	Shapiro-Wilk test
VH:	Ventral hippocampus
MWM:	Morris Water Maze

LIST OF FIGURES AND TABLES

Chapter 1

Chapter 2

Chapter 4

Chapter 5

Chapter 6

CHAPTER 1: INTRODUCTION

FOETAL ALCOHOL SPECTRUM DISORDERS

The socioeconomic conditions and cultural drinking patterns (May et al., 2013a), lack of general awareness and many misconceptions regarding the safety of alcohol consumption during pregnancy have contributed to South Africa, specifically the Western Cape Province, having one of the highest rates of foetal alcohol syndrome (FAS) in the world (Olivier et al., 2016). FAS represents the most extreme outcome of exposure to alcohol *in utero* (Hoyme et al., 2016). The umbrella term used for the wide range of mild to severe neurobehavioural deficits observed after *in utero* alcohol exposure is foetal alcohol spectrum disorder (FASD) (Hoyme et al., 2016). Studies estimate that FASD occurs in 2.9 to 29 % of first grade learners across Gauteng, the Western Cape and the Northern Cape Province of South Africa (Olivier et al., 2016). Further, in a study done by May *et al*. (2013a), 25 % of the maternal sample population continued drinking heavily throughout pregnancy contributing to FASD occurring in 18.3 % to 25.9 % of the sample population in the Western Cape Province alone (May et al., 2016), the highest recorded prevalence rate in the world (Hoyme et al., 2016).

On the extreme end of the spectrum, the most severely affected individuals present with a specific pattern of facial features necessary for diagnosis of FAS. These features include short palpebral fissures, a smooth philtrum and a thin upper lip (Hoyme et al., 2016). In addition, the diagnosis of FAS requires the presence of growth deficiencies (pre- or postnatal), abnormal brain morphology and global intellectual impairments (executive function, learning and memory) or deficits in self-regulation (mood, negative affect, attention deficit and impulse control) (Hoyme et al., 2016). The remaining continuum of cognitive and neurobehavioural deficits may not present with the classic FAS facial features (Suttie and Foroud, 2013) but can be further categorized into partial FAS (pFAS), alcohol-related birth defects (ARBD), alcohol-related neurodevelopmental disorder (ARND) and neurobehavioural-disorder associated with prenatal alcohol exposure (ND-PAE) (Hoyme et al., 2016; Kable et al., 2016). All of the above fall under the umbrella term FASD.

Neurocognitive deficits associated with FASD include intellectual impairments (IQ); deficits in executive functioning (planning, organization and strategizing); learning and memory difficulties; and spatial impairments (drawing, direction, alignment) (Kable et al., 2016). For

instance, children with FASD, aged 6 - 12 years, had difficulty with organization, accuracy and memory as shown by drawing a complex diagram from memory after a 3 - 30 minute delay (Pei et al., 2011). And thirty-nine children, aged 3 - 5.5 years, had difficulty separating cards according to one parameter then again using a different parameter, and demonstrated increased impulsivity (delayed gratification task) compared to 50 age-matched non-exposed controls (Fuglestad et al., 2015). This study showed that impairments in executive function are identifiable before the age of 6 years. Moreover, at the age of 7, females with FASD appeared to have greater morphological differences and performed worse on non-verbal IQ tests compared to males with FASD, suggesting sexual dimorphism within in the continuum of FASD (May et al., 2017).

Further, deficits in adaptive functioning, such as communication, social interaction, daily living and fine and gross motor impairments are common in FASD (Kelly et al., 2000; O'Connor and Paley, 2009; Kable et al., 2016). For example, Grade 1 pupils diagnosed with FAS from a Western Cape South African cohort showed decreased cognitive motor function as shown by decreased hand-eye coordination (threading beads, drawing geometric shapes) (Adnams et al., 2001). In addition, children with FASD, aged 5 - 18 years, showed an increase in initial movement error when asked to reach out to randomly-selected objects during a virtual simulation compared to the control group (Williams et al., 2014). Further, within the FASD group, younger children (aged 5 - 6 years) performed markedly worse than older children (aged 15 - 18 years) on the same task (Williams et al., 2014) suggesting that motor deficits may become less severe with age.

FASD also encompass difficulties with self-regulation such as negative affect, attention deficit, hyperactivity and impulse control (Kable et al., 2016). In adolescence aggressive and addictive behaviour may also be observed (O'Connor and Paley, 2009). Additional symptoms include jitteriness, irritability and disruptions of sleep patterns (Mattson and Riley, 1998 & Paley, 2009 in Medina, 2011). Further, individuals exposed to alcohol *in utero* are more likely to have psychological disorders, such as anxiety and depression (O'Connor and Paley, 2009; Kable et al., 2016). Meta-analysis, in which the mean age was 10.9 years, showed that attention-deficit/hyperactivity disorder (ADHD), depression and anxiety disorders occurred in 50 %, 14 % and 7.8 % of the FASD population respectively versus control population (Weyrauch et al., 2017). The link between *in utero* alcohol exposure and psychological defects such as depression and anxiety disorders are not clearly understood.

The characteristics of the disorder persist into adulthood and individuals with FASD are at risk for adverse long-term life outcomes. For instance, the characteristic facial features of FAS diminish with age, however a thin upper lip, decreased height and microcephaly may be apparent in adulthood (Spohr et al., 2007). Further, adults with FASD (mean age 30 years) also showed deficits in executive function and social cognition (difficulty understanding social cues) (Rangmar et al., 2015b). In addition, out of 415 individuals diagnosed with FASD (age range 6 - 51, median age 14), 61 % had trouble at school, 60 % had an encounter with the law and 50 % had been detained in prison or a psychiatric facility (Streissguth et al., 2004). Adults born with FASD also have higher rates of unemployment and are more likely to abuse alcohol and other drugs (Rangmar et al., 2015a). Therefore, foetal alcohol exposure leads to persistent, debilitating cognitive and behavioural deficits resulting in a large scale public health issue.

The severity and diversity of the observed growth deficiencies and cognitive and psychological deficits depend on the timing, quantity and pattern of alcohol consumed during pregnancy (May et al., 2013b). In addition, the postnatal-environment may further influence the spectrum of disorders observed (Olson et al., 1998). Firstly, the timing of alcohol exposure is important because ethanol can alter the anatomical features developing at the time of exposure. Different processes and brain areas have different windows of vulnerability (Kleiber et al., 2013). Drinking during the 1st trimester versus abstaining from alcohol is 12 times more likely to result in cognitive and behavioural deficits (May et al., 2013b). Further, drinking during the 1st and 2nd trimester is 61 times more likely, and drinking during all three trimesters is 65 times more likely to result in cognitive and behavioural deficits than abstaining from alcohol (May et al., 2013b). Further, different behavioural deficits are associated with drinking in the respective trimesters. More anxiety and depression disorders have been observed after *in utero* alcohol exposure during the 1st trimester, and aggressive behaviour and language impairments have been associated with alcohol exposure during late pregnancy (O'Leary et al., 2010a). Further defining the time of exposure, by dividing the semesters in half showed that craniofacial, features such as the thin upper lip and short palpebral fissures, were strongly correlated with *in utero* alcohol exposure during the second half of the first trimester (Feldmann et al., 2011).

Secondly, the amount of alcohol consumed is an important factor. Approximately 2 hours after the maternal ingestion of alcohol, the foetal blood alcohol level (BAC) was approximately equivalent to that of the maternal intoxication level (Burd et al., 2012). Foetal exposure to

alcohol is prolonged because of its low rate of metabolism and intake of recycled amniotic fluid which then contains alcohol (Burd et al., 2012). Therefore, the foetus depends on the mother's metabolic capability to remove alcohol from the developing foetal system. The maternal ability to metabolize alcohol differs within the population due to genetic variation in alcohol metabolizing genes such as alcohol dehydrogenase (Jones, 2011; Lewis et al., 2012). Further, women who felt the effects of alcohol (i.e. who felt drunk) during pregnancy, which depends on the capacity to metabolize alcohol, had children with greater craniofacial differences compared to women who did not feel the effects (Muggli et al., 2017). Hence, women who consumed similar amounts of alcohol during pregnancy have children with different behavioural deficits of varying intensities. Further, the pattern of alcohol consumption contributes to the resulting BAC. Binge-drinking rather than the overall amount of alcohol consumed is associated with more severe cognitive deficits because binge-drinking patterns result in higher BACs than moderate-drinking patterns (Livy et al., 2003; Sokol et al., 2003; May and Gossage, 2011). In other words, drinking 5 units of alcohol on a single occasion is more deleterious to the fetus than drinking 1 unit of alcohol per day (moderate-drinking - low quantity of alcohol over an extended period of time). Binge-drinking 1 - 2 times per week during the 1st trimester was associated with more alcohol-related deficits compared to the group that abstained from drinking. In addition low to moderate-drinking was not associated with defects (O'Leary et al., 2010b). However, moderate-drinking has been associated with deficits in social skills, social conduct and mood while binge-like exposure was correlated with decreased cognitive function (Flak et al., 2014). Seven-year olds exposed to binge-like consumption of alcohol during gestation were more likely to have IQ's in the mentally disabled range and exhibit delinquent behaviour compared to the moderately-exposed group (Bailey et al., 2004). In addition, binge-drinking rather than moderate-drinking during the second trimester was associated with ADHD-like symptoms in 4 year old girls and in both genders at 7 years of age compared to controls (Sayal et al., 2009). However, the amount of alcohol that is safe to drink during pregnancy is undefined and even low levels of alcohol exposure may result in behavioural deficits and craniofacial abnormalities (Muggli et al., 2017). Further, if study participants are untruthful the measurements of maternal alcohol consumption may be inaccurate and unreliable (Caprara et al., 2006). Therefore, mothers who consumed a large amount of alcohol during pregnancy may be incorrectly classified as low to moderate-drinkers instead of heavy-drinkers and vice versa. This may also contribute to the variation reported in the literature (O'Leary et al., 2010a).

The brain continues to develop into early-adulthood and therefore it is vulnerable to the effects of a positive or negative postnatal-environment. A study showed that light-drinking during the 1st trimester was associated with higher scores on a Child Behaviour Checklist (positive outcomes) during a 14-year follow-up which the authors attributed to greater maternal self-control which suggests better parenting (Robinson et al., 2010). Further, early-environmental enrichment or being adopted by non-alcohol-abusing parents and raised in stable environments has been shown to increase the likelihood of positive long-term outcomes (Olson et al., 1998). However, more often than not, children born with FASD face adverse childhood experiences when living with alcohol-abusing parent/s such as, food insecurity, child neglect (such as decreased parental care and diminished health and safety), abuse (domestic violence, emotional and physical) and disrupted parent-child relationships (Anda et al., 2002; Choi et al., 2015). Therefore, early-life adversity may add further insult to the developing alcohol-exposed brain. Early-life stress alone results in persistent physiological and neurohormonal changes inducing a vulnerability to stressful events. For example, early-life stress can result in persistent changes in the ability of the HPA-axis to respond to stress (Faravelli, 2012). This may cause the brain to become sensitized to stressful events and increase the susceptibility to developing psychological disorders (McLaughlin et al., 2010). This vulnerability to stressful events can trigger, aggravate and increase the recurrence of psychological disorders (Mullen et al., 1996; Heim and Nemeroff, 2001; Carr et al., 2013; Grasso et al., 2013). For instance, early-life emotional or sexual abuse was shown to be predictive of major depressive disorder in adulthood (Saleh et al., 2017). However, the interaction between alcohol exposure *in utero* and exposure to childhood adversities and its effects on the developing brain has not been fully investigated.

Clinical studies have used neuroimaging techniques to provide insight into the structural and functional changes in the brain of individuals exposed to alcohol *in utero*. Studies have consistently reported decreased whole-brain volume (Treit et al., 2014; Donald et al., 2015a), as well as reduced cortical grey volume and thickness (Nardelli et al., 2011; Robertson et al., 2016). The volume of deep grey matter structures has also been shown to be significantly reduced in FASD (children aged 6 - 17) (Nardelli et al., 2011). For example, the hippocampus and basal ganglia were decreased in children with FASD (aged 6 - 9, 10 - 13 and 14 - 17) (Nardelli et al., 2011). Further, white matter integrity was significantly impaired in 2 - 4 week old infants exposed to alcohol *in utero* compared to non-exposed controls (Donald et al.,

2015b). These results highlight the differential structural changes in the brain after prenatal-alcohol exposure.

After birth, the brain continues to develop and neural networks undergo pruning and myelination to enhance efficiency and specialization. Studies have shown that this maturation process is significantly impaired after prenatal-alcohol exposure. For example, in 11 children with FASD, cortical thickness decreased less over a 2 to 4 year period compared to the control group, indicating decreased refinement of neural networks (Treit et al., 2014). Another study observed an association between a smaller change in cortical volume over time with lower IQ and increased craniofacial abnormalities (Lebel et al., 2012). An additional indication of neuronal maturation is gyrification. Children aged 9 -16 with FASD were shown to have less cortical gyrification (i.e. smoother cortical surface) compared to controls (Hendrickson et al., 2017). In addition, this study demonstrated an association between decreased gyrification and lower IQ levels in FASD (Hendrickson et al., 2017). Functional MRI showed that children with FASD, aged 10 - 17 years, versus age-matched controls had a greater path length (the distance between two functional nodes) which indicates inefficient neural connections and decreased plasticity (Wozniak et al., 2013). These results suggest a decreased capacity for neural plasticity in response to the postnatal-environment and hence neuronal maturation is significantly impaired after prenatal alcohol exposure. This would then lead to an overall decrease in neuronal efficiency which is in agreement with functional imaging studies. For example, within in the South African Cape Coloured cohort, children aged 8 - 12 years, diagnosed with FAS or partial FAS (pFAS) were able to process numbers just as well as the control group however, alcohol-exposed children activated more brain areas in order to perform the same number processing task (Meintjes et al., 2010). This result suggests a deficit in the functional integration of neuronal networks in FASD. Similarly, in an event-related potential Go/No-go task, children diagnosed with FASD, aged 11 - 13 years, demonstrated slower and less efficient processing and required greater neural activation to inhibit the response to the No-go stimulus (Burden et al., 2009). These neuroimaging studies showed that children exposed to alcohol *in utero* activated more neuronal networks than the control groups. This demonstrates that children with FASD may require greater neural activation (numerous brain regions) to perform the same cognitive task as healthy individuals. The above results suggest structural changes and impaired neuronal network maturation (decreased capacity for neural plasticity) can occur after *in utero* alcohol exposure which may result in decreased global neuronal efficiency.

The literature suggests that a decreased capacity for neural plasticity may occur after *in utero* alcohol exposure which would impair neuronal maturation and network refinement in response to stimuli from the postnatal-environment (example: learning and memory). However, prenatal-alcohol induced changes at the molecular level within the brain have yet to be fully elucidated. Therefore, there is a need to investigate the long-term molecular mechanisms involved in FASD in order to provide insight into specific deficits in the neuronal networks.

ANIMAL MODELS OF FASD

As described, the wide range of cognitive and behavioural deficits observed after *in utero* exposure to alcohol depends on a number of different factors (May et al., 2013b). Further, retrospective data regarding the quantity and timing of maternal alcohol consumption may often be inaccurate or unreliable. In addition, genetic, metabolic, nutritional and environmental factors further contribute to the continuum of FASD (Olson et al., 1998; Jones, 2011; Lewis et al., 2012). Therefore, studying FASD is particularly difficult in heterogeneous human populations. Hence, animal models are important tools which enable researchers to control and manipulate a variety of different variables.

When choosing an animal model of FASD it is important to note that the time-scale of embryonic development differs between humans and rodents, although the sequence of developmental events is roughly the same. The gestational period in rodent takes approximately 21 days which are equivalent to the first and second trimester of human pregnancy. The third trimester equivalent developmental stage occurs from postnatal day (P) 0 - P10 (Dobbing and Sands, 1979) (**Figure 1.1**). Therefore, when targeting structures or processes developing during the first and second trimester, such as cell proliferation, migration and differentiation ethanol must be administered from gestational day (GD) 0 - GD10 and/or GD11 - GD21 respectively (Kleiber et al., 2013). When targeting the third trimester equivalent developmental stage, a period of increased brain growth, synaptogenesis and myelination, ethanol needs to be administered directly to the pups from P0 - P10 (Dobbing and Sands, 1979). In this study, with regards to ethanol exposure in rodents, ethanol administered anywhere between GD0 and the date of birth (DOB) (± GD21) will be termed *prenatal-ethanol exposure* and alcohol administered during the third trimester equivalent stage from P0 - P10 will be termed *early-postnatal ethanol exposure* (**Figure 1.1**).

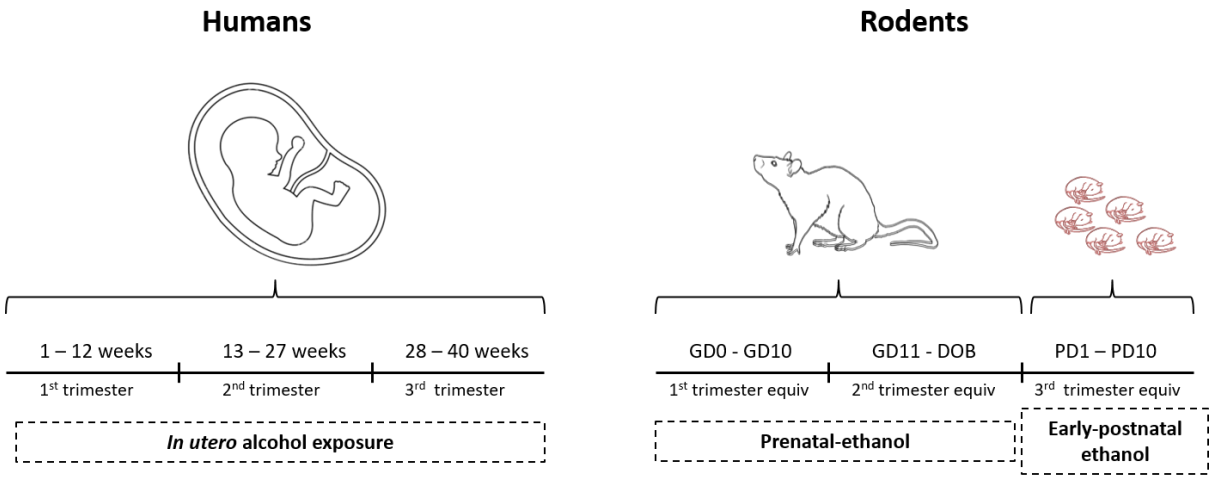

Figure 1.1: Time-scale of embryonic development in humans versus rodents.

In this study, prenatal-ethanol exposure will be used to describe ethanol administered between GD0 and the date of birth (DOB). Early-postnatal ethanol exposure will refer to ethanol administered between PD1 - PD10

In prenatal-ethanol exposure paradigms (GD0 - DOB), ethanol can be administered to the dam via gastric intubation /oral gavage (Thomas et al., 2010), ethanol-calorie derived liquid-diets (Patten *et al*., 2013), vaporization chambers (Oshiro et al., 2014), or dams can be trained to voluntary drink a saccharin-sweetened ethanol solution (Brady et al., 2012; Marquardt et al., 2014). Ethanol has also been administered via intraperitoneal (i.p.) injections to the dam during the first trimester equivalent developmental stage (Godin et al., 2010). Early-postnatal ethanol exposure paradigms involve administering ethanol directly to the pups via i.p injections (Filgueiras et al., 2010), gastric intubation (Hamilton et al., 2010; Tiwari and Chopra, 2011) and vaporization chambers (Puglia and Valenzuela, 2010; Granato et al., 2012). Ethanol can also be administered across all three trimester equivalents (throughout gestation and during the first 10 postnatal days). For example, dams received ethanol via gastric intubation from GD1 - GD22 and the pups received ethanol via gastric intubations from P4 - P10, thereby influencing all stages of development (Gil-Mohapel et al., 2011; Brocardo et al., 2012). In addition to the timing and route of ethanol exposure, researchers can manipulate the quantity and pattern of ethanol exposure which will influence the resultant BAC (Patten et al., 2014). Ethanol can be administered in a chronic, acute or binge-like manner. Chronic-ethanol exposure paradigms produce lower BACs than binge-like exposure paradigms (see **Table 1.1**). The BAC after ethanol exposure should be measured or based on previous literature in order to compare different animal models of FASD as well as to relate the quantity of ethanol to the cognitive

and behavioural deficits observed. Therefore, factors to consider when modeling FASD include the period of brain development (i.e. timing of exposure), route of administration, pattern and quantity of exposure, and the resulting BAC (**Table 1.1**).

Rodents exposed to ethanol during early-development develop morphological changes such as craniofacial abnormalities, decreased whole-brain volume (O'Leary-Moore et al., 2011) as well as diminished weight gain (Monk et al., 2012; An and Zhang, 2013; Brys et al., 2014) compared to non-exposed controls. More specifically, C57BL/6J foetuses showed median facial and forebrain defects on GD17 after the administration of 2 injections of ethanol (2.9 g/kg i.p.) on G7 (Godin et al., 2010). Similarly, the same protocol resulted in hypoplasia, short palpebral fissures, a short philtrum and a long upper lip in mice foetuses on GD17 (Lipinski et al., 2012). Wistar rats exposed to prenatal-ethanol (35 % ethanol liquid-diet) gained less weight compared to control rats from P7 - P40 (Brys et al., 2014) and SD rat pups exposed to early-postnatal ethanol (5 g/kg/day via oral intubation) from P4 - P9 gained less body weight than control rats during this time (Monk et al., 2012). Therefore, rodents exposed to ethanol during early-development phenotypically represent FASD.

Further, rodents exposed to ethanol develop abnormal behavioural traits characteristic of FASD. Prenatal- and early-postnatal ethanol-induced behavioural changes can be observed using a variety of different behavioural tests. For instance, ethanol-induced cognitive deficits can be analyzed using hippocampal-dependent tasks such as the Morris Water Maze (MWM) and the novel object recognition task (NOT) (Bevins and Besheer, 2006; Voorhees et al., 2013). For example, juvenile male Wistar rats exposed to prenatal-ethanol throughout gestation (4 g/kg/day , 20 % v/v, via oral gavage) took longer to find the hidden platform in the MWM compared to control rats (An and Zhang, 2013) indicating impaired spatial learning and memory. Decreased performance in the MWM was also observed in adolescent (P25 - P30) Long-Evans rats exposed to early-postnatal ethanol (5 g/kg i.p) on alternative days from P4 - P10 (peak BAC 239 ± 31 mg/dl) (Filgueiras *et al*., 2010). Learning deficits in the MWM were even observed in adolescent C57BL/6J mice after a single exposure to 0.03 ml/g ethanol (25 %) on GD8 (Incerti and Vink, 2010). Cognitive deficits after ethanol exposure during early-development have also been shown to occur in adult rodents. For example, adult SD rats (P65 - P66) exposed to 6 g/kg/day of 28.5 % ethanol from GD5 - GD20 demonstrated decreased working memory in the MWM (Thomas et al., 2010). Rats underwent a training trial in which they had 1 minute to find the hidden platform (training trial) then after 10 seconds on the

platform, rats were immediately placed in a different starting position and had to find the hidden platform using the visual cues (test trial). Rats exposed to prenatal-ethanol took longer to locate the hidden platform during the test trial which suggests a decreased capacity for working memory (Thomas et al., 2010). Further, adult C57BL/6 mice exposed to ethanol on P7 (2 x 2.5 g/kg) spent less time exploring the moved-object during an object placement task (Sadrian et al., 2012). This task involved a 5-minute habituation trial with 2 identical objects after which one of the objects was moved to a new location. Mice exposed to prenatal-ethanol did not explore the object at its second location which suggests impairments in spatial memory (Sadrian et al., 2012).

In order to evaluate ethanol-induced changes in affect state behavioural tests, such as the elevated plus maze (EPM) (Walf and Frye, 2007) and forced swim test (FST) (Slattery and Cryan, 2012), utilize the innate behavioural response to food, open spaces and aversive situations which can then be interpreted as anxiety- and / or depression-like behaviour. For example, adult SD rats exposed to ethanol throughout gestation (15 % ethanol derived liquid-diet) spent more time in the closed arms of the EPM compared to non-exposed control rats (Cullen et al., 2013) which is indicative of heightened anxiety-like behaviour. Adult SD rats exposed to ethanol across all 3 developmental periods (GD1 - GD21, 4.3 g/kg, 36 % ethanol, BAC = 155-195 mg/dL; P4 - P10, 4 g/kg, 12% ethanol, BAC = 228 ± 9 mg/dL) spent more time in the closed arms of the EPM and more time immobile in the FST indicating anxiety-like and depression-like behaviour respectively (Brocardo et al., 2012). In addition, to anxiety- and depression-like behaviour, and in parallel with human literature, rodents exposed to ethanol during early-development have been shown to exhibit hyperactivity which may be interpreted as ADHD-like behaviour (Schneider et al., 2011). For instance, Swiss-mice exposed to early-postnatal ethanol (5 g/kg/day i.p) from P2 - P8 showed increased locomotor activity at P30 when tested in the open field (Nunes *et al*., 2011) and adolescent SD rats exposed to early-postnatal ethanol from P4 - P9 were more active in the open field as suggested by the increased distance travelled compared to controls (Monk et al., 2012). In addition, SD rats exposed to prenatal-ethanol (4 - 6 g/kg/day 25 % ethanol, gastric intubation) travelled a greater distance than control rats in the open field indicating hyperactive behaviour (Kim *et al*., 2013). Further, male SD rats exposed to prenatal-ethanol (GD8 - GD20, 2 x 3 g/kg/day 20% ethanol via gastric intubation) showed ADHD-like behaviour in choice reaction time tasks, as shown by a greater variation in reaction time (Hausknecht and Acheson, 2005). Therefore, animal models of FASD

may also be used as a model for ADHD to explore the molecular mechanism behind the similar behavioural phenotype (Rojas-Mayorquín et al., 2016).

In some instances, there have been no observable quantitative cognitive or behavioural deficits after ethanol exposure. For example, SD rats exposed to prenatal-ethanol (6 g/kg/day) did not exhibit deficits in spatial memory using the standard MWM protocol on P45 compared to non-exposed controls (Thomas et al., 2010) and adult SD rats exposed to a 15 % ethanol-calorie derived liquid-diet throughout gestation were able to find the hidden platform in the MWM just as efficiently as control rats (Cullen et al., 2014). These results, in addition to the cognitive and anxiety-, depression- and ADHD-like behaviors described above, highlight the continuum of deficits observed after developmental-ethanol exposure in rodents which agrees with human clinical data. However, the molecular mechanisms underlying the observed behavioural abnormalities after ethanol exposure during development are less clear.

Table 1.1: Examples of ethanol exposure paradigms and behavioural phenotypes

Timing of exposure	Route of exposure	Pattern of exposure	Peak BAC	Age and Behaviour	Species	Reference
Prenatal-ethanol exposure ± GD0 - ± GD10 *(1st trimester equivalent)* ± GD11 - ± GD21 *(2nd trimester equivalent)*						
GD5 - GD20	Intubation	Binge-like	345 mg/dL	P65 - P66; Decreased performance in the MWM	SD rats	(Thomas et al., 2010)
GD6 - GD15	Intubation	Binge-like 3 - 6 g/kg 25 % v/v	Not described	P21 - P28; Hyperactivity in OFT	ICR mice and SD rats	(Kim et al., 2013)
GD7	I.p. injection	2 x 2.9 g/kg	400 - 466 mg/dL			(Godin et al., 2010)
GD8	I.p. injection	Acute 0.03 ml/g (25% ethanol)	Based on previous literature	P40 - P50; Learning deficits in MWM	C57BL/6J mice	(Incerti and Vink, 2010)
GD1 - GD21	Liquid diet	Chronic	135.40 ± 7.54 mg/dL			(Patten *et al*., 2013)
GD 1 - GD21	Intubation	Chronic	Based on previous literature	P36 - P44; Increase latency to reach hidden platform in MWM	Wistar rats	(An et al., 2013)
GD1 - GD21	Voluntary drinking	Chronic 0.066% saccharin-sweetened, 10 % ethanol	88.3 ± 11.5 mg/dL	P90 - P150; Decreased performance in hippocampal dependent tasks	C57BL/6J mice	(Brady et al., 2012)
GD1 - GD21	Voluntary drinking	Chronic 0.066% saccharin-sweetened, 10 % ethanol	80 - 90 mg/dL	Decreased executive function	C57BL/6J mice	(Marquardt et al., 2014)
GD9 - GD20	Inhalation	Chronic 5000 - 21 000 ppm/day	± 192 mg/dL	Impaired trace fear conditioning; Thigmotaxis in MWM	Long-Evans rats	(Oshiro et al., 2014)
Early-postnatal ethanol exposure ± P0 - P10 *(3rd trimester equivalent)*						
P2 - P8	I.p. injections	Binge-like 5 g/kg 25 % ethanol on alternate days	Based on previous literature	Increased locomotor activity in OFT	Swiss mice	(Nunes et al., 2011)
P7	I.p. injections	Binge-like 3 g/kg, 20 % ethanol	Based on previous literature	P70; Decreased performance in MWM	ICR mice	(Lee et al., 2015)

Timing of exposure	Route of exposure	Pattern of exposure	Peak BAC	Age and Behaviour	Species	Reference
P4 - P10	Intraperitoneal Injection	Binge-like 5 g/kg/ on alternate days	239 ± 31 mg/dL	P25 - P31 Decreased performance in MWM	Long-Evans rats	(Filgueiras et al., 2010)
P2 - P9	Inhalation	2 - 4.5 g/dL ethanol vapor				(Puglia and Valenzuela, 2010)
P2 - P6	Inhalation	2.5 ml (95% ethanol)/min	150 - 300 mg/dL			(Granato et al., 2012)
P4 - P9	Intubation	Binge-like 5.25 g/kg/day	333.5 ± 15.0 mg/dL			(Hamilton et al., 2010)
All three trimester equivalents GD0 - ± GD21 and P0 - P10						
GD1 - GD21 P4 - P10	Intubation	GD0 - GD21: 4.3 g/kg/day, 36 % ethanol; P4 - P10: 4 g/kg/day, 12 % ethanol	179.05 ± 41.01 mg/dL; 228 ± 9 mg/dL			(Gil-Mohapel et al., 2011; Brocardo et al., 2012)

[BAC = Blood alcohol concentration; GD = gestational day; P = postnatal day; MWM = Morris Water Maze; EPM = Elevated Plus Maze; OFT = Open Field test; FST = Forced Swim Test].

ETHANOL EXPOSURE AND THE DEVELOPING RAT BRAIN

Animal models have demonstrated the phenotypic and behavioural characteristics of FASD. Therefore, animal models of FASD have been used to investigate the structural, functional and molecular changes in the brain after ethanol exposure since the ethanol-induced changes underlying the observed cognitive and behavioural abnormalities observed in FASD still need to be fully elucidated.

The short-term effects of ethanol exposure have been studied in animal cell cultures, embryos, foetuses or pups sacrificed shortly after ethanol exposure. These short-term investigations, in parallel to the human condition, have demonstrated morphological changes such as decreased cell number, dendritic arborization and brain volume (Liesi, 1997; Kim et al., 2010). For example, decreased neurite outgrowth has been observed in cultured cerebellar neurons exposed to ethanol (Liesi, 1997). Further, cultured radial glial cells and cerebral cortical neurons obtained from embryos of Wistar rats exposed to a 5 % ethanol-derived liquid-diet

showed decreased cell proliferation and decreased number of neurons and astrocytes (Rubert et al., 2006). In addition, embryos obtained from SD rats on GD14 after exposure to prenatal-ethanol (2 - 4 g/kg/day) reduced proliferation of neuronal progenitor cells (Kim et al., 2010).

The observed decrease in brain volume after prenatal-ethanol exposure may be attributed to ethanol-induced excitatory or apoptotic neurodegeneration (Ikonomidou *et al*., 2000). Early studies of alcoholism showed that ethanol inhibits NMDA receptors and suggested compensatory mechanisms increase the number of NMDA receptors at the membrane in order to mitigate the insensitivity to glutamatergic neurotransmission (Tsai and Coyle, 1998). However, after the cessation of ethanol consumption, during the withdrawal period, the brain is vulnerable to excitotoxicity due to its hyper-excitable state (Tsai and Coyle, 1998). A similar process may occur during *in utero* ethanol exposure which may lead to excitation-induced neurodegeneration. For example, acute exposure to early-postnatal ethanol on P6 (6 g/kg) induced the co-expression of markers for glutamatergic activity (NMDA receptors) and cell death (caspase-3) in the hippocampus, striatum, and the prefrontal, somatosensory and motor cortices of Long-Evans rat pups 24 hours after exposure (Clements et al., 2012). Similarly, early-postnatal ethanol exposure (2 x 2.5 g/kg) on P7 induced neuronal cell death in the hippocampus of C57BL/6J mice on P8 (Sadrian et al., 2012). These studies suggest that ethanol exposure during the brain growth spurt induces wide-spread neuronal cell death via glutamatergic excitatory neurodegeneration. Apoptotic neurodegeneration, in which neuronal cells undergo programmed cell death due to insufficient stimulation and increased inhibition, can also occur after ethanol exposure due to ethanol's ability to block NMDA receptors and mimic GABAergic transmission. (Olney et al., 2002; Möykkynen and Korpi, 2012). These non-specific mechanisms of cell death may eliminate vital components of neuronal networks and impair further neuronal maturation and synapse formation which may result in inefficient neurotransmission (Kleiber et al., 2013). Specifically, the observed short-term effects of ethanol on glutamate receptors may induce persistent long-term changes in glutamatergic function and hence neural plasticity. For instance, brain slices from SD rat pups showed impaired LTP in the CA1 region of the hippocampus on P9 after the last dose of ethanol (2 - 4.5 g/dL, P2 - P9) (Puglia and Valenzuela, 2010). Deficits in LTP at this early stage of development may alter the maturation process and contribute to long-term deficits in neural plasticity after ethanol exposure during development. For example, ethanol exposure has been shown to impair neural plasticity in the primary visual cortex in animal models of ocular

dominance plasticity (Krahe et al., 2010; Lantz et al., 2012). The mechanism by which ocular dominance plasticity occurs is similar to learning and memory plasticity in the hippocampus. Both ocular dominance plasticity and learning and memory depend on NMDA receptor mediation and downstream intracellular signalling pathways (Lantz et al., 2012). For instance, adult C57BL6/J mice exposed to prenatal-ethanol (10 % ethanol, saccharin-sweetened solution, 4 hours/day) showed deficits in NMDA receptor-dependant LTP in the dentate gyrus in addition to altered NMDA subunit (decreased GluN2B, increased GluN1 and GluN3A) composition compared to non-exposed controls (Brady et al., 2013). This is supported by increased glutamate release and NMDA receptor stability after pre-treatment with novel peptides (Vink et al., 2005) thereby preventing prenatal-ethanol (0.03 ml/kg on GD8) induced spatial learning deficits in mice. Altered NMDA receptor-subunit composition and/or physiology may contribute to an imbalance between LTP and LTD which may affect learning and memory behaviour. For example, male and female adolescent Wistar rats exposed to prenatal-ethanol (4 g/kg/day, 20 % ethanol, gastric intubation) showed decreased performance in the MWM (An and Zhang, 2013). However, prenatal-ethanol exposure impaired LTP and enhanced LTD in the hippocampus of male rats whereas female rats exposed to prenatal-ethanol had enhanced LTP and decreased LTD even though female rats also performed poorly in the MWM (An and Zhang, 2013). Further, this result demonstrates ethanol may affect neural plasticity and LTP in the hippocampus in a sexually dimorphic manner (An and Zhang, 2015). Further, decreased firing rate of cortical pyramidal neurons was observed in Wistar rats (P30 - P60) exposed to early-postnatal ethanol from P2 - P6 via vaporization chambers (95 % ethanol, 2 ml/minute) (Granato et al., 2012) which may contribute to impaired LTP. Therefore, deficits in LTP in the hippocampus and cortical regions may contribute to the cognitive deficits obverse after ethanol exposure during early development.

Ethanol exposure during development has also been shown to impact the development of other neurotransmitter systems such as GABAergic and dopaminergic neurotransmission (Sari et al., 2010a). For instance, decreased levels of γ-aminobutyric acid (GABA) and dopamine (DA) were observed in mice foetuses on GD13 after exposure to prenatal-ethanol (25 % ethanol-calorie derived liquid-diet) from GD7 - GD13 with no significant changes in the levels of glutamate (Sari et al., 2010a) which may contribute to anxiety- and ADHD-like behaviour respectively. For example, offspring from SD rats exposed to prenatal-ethanol (6 g/kg/day, gastric intubation) from GD7 - GD20 showed decreased GABAergic function and decreased

anxiety-like behaviour in adulthood as shown by increased time in the centre zone of the open field compared to control rats (Zhou et al., 2010). Treatment with midazolam, which positively modulates GABAergic function, reduced anxiety-like behaviour to that of controls (Zhou et al., 2010). Therefore, anxiety-like behaviour after ethanol exposure may be associated with increased hyper-excitability of neuronal networks due to impairments in GABAergic neurotransmission. The observed behavioural abnormalities such as ADHD-like behaviour, increased susceptibility to substance abuse (drug addiction) and motor learning deficits observed after *in utero* alcohol exposure (Rangmar et al., 2015a; Weyrauch et al., 2017) suggests underlying alterations in dopaminergic function in the brain (Adinoff, 2004; Tripp and Wickens, 2009). For example, altered dopaminergic neurotransmission has been observed using the spontaneously hypertensive rat (SHR) model for ADHD, in which rats were shown to be hyperactive in the open field (Sagvolden, 2000; Warton et al., 2009; Womersley et al., 2011) and had increased DA release in the substantia nigra compare to WKY controls (Warton et al., 2009). In addition, dysfunction of the dopaminergic system is thought to be related to deficits in the vesicular stores of DA in the SHR model of ADHD (Russell et al., 1998; Warton et al., 2009). The deficits in dopaminergic neurotransmission observed in the SHR model of ADHD may also be apparent in animal models of FASD and may contribute to the ADHD-like behaviour observed after ethanol exposure during early development although the underlying, possibly overlapping, neurocircuitry is not yet fully understood. However, components of dopaminergic neurotransmission have been shown to be altered by ethanol exposure during development. For instance, rodents (mice and rats) exposed to prenatal-ethanol (0.5 - 6 g/kg/day) had increased levels of the DA transporter in the PFC and striatum as well as increased hyperactivity (Kim et al., 2013). Further, Schneider *et al*. (2005) showed that moderate prenatal-ethanol exposure in rhesus monkeys differentially alters dopaminergic function in the striatum according to timing of alcohol exposure during gestation. More specifically, prenatal-ethanol exposure during early-gestation results in reduced dopaminergic functioning whereas ethanol exposure from middle- to late-gestation results in heightened dopaminergic functioning (Schneider et al., 2005). In addition, after exposure to prenatal-ethanol, neuroimaging showed decreased DA receptor 1 (D1) binding in male Rhesus monkeys compared to controls (Converse et al., 2014). The authors attributed this to a compensatory mechanism in response to an ethanol-induced decrease in DA release, synthesis, DA metabolism and/or number of dopaminergic neurons. However, the mechanism underlying ethanol exposure-induced changes in dopaminergic neurotransmission are unclear.

The literature suggests ethanol exposure during early-development alters the function of neurotransmitter systems and receptors which would impair LTP or LTD and therefore neural plasticity and behaviour (Krahe et al., 2010; Lantz et al., 2012). However, plasticity further depends on additional structural and functional changes resulting from gene transcription and protein synthesis in order provide the molecular machinery needed to strengthen the synaptic connection. Hence, growth factors and intracellular signalling cascades downstream of membrane receptors are of significant interest. For instance, altered ethanol-induced NMDA receptor subunit composition (Brady et al., 2013) and impaired calcium-signalling (Granato et al., 2012) may alter downstream signalling molecules. In particular, extracellular signal-regulated kinase (ERK1/2) and glycogen synthase kinase-3 beta (GSK3β) are converging points for many signalling cascades that are involved in neurogenesis, differentiation, migration and survival (Moors et al., 2007). For example, the mitogen-activated protein kinase (MAPK) signalling cascade consists of a series of serine/threonine kinases, including Ras, Raf and MEK, that result in the phosphorylation of ERK1/2 (**Figure 1.2**). Activity of the MAPK pathway is mediated by several upstream activators and growth factors such as nerve growth factor, neurotrophins 3 - 6 and brain derived neurotrophic factor (BDNF) which bind to the family of tyrosine receptor kinases (Chao, 2003). Specifically, BDNF acts via tyrosine receptor kinase-beta (Trkβ) (Chao, 2003). Phosphorylated ERK1/2 leads to the phosphorylation and activation of the transcription factor, cAMP response element binding protein (CREB) resulting in gene expression and long-term effects of neurotrophic factors. In addition, the phosphatidylinositol 3-kinase (PI3K) / Akt (also known as protein kinase B) pathway results in the phosphorylation and *inactivation* of GSK3β (Li and Jope, 2010). BDNF is also a significant regulator of this pathway (Mai et al., 2002). The binding of BDNF to Trkβ activates PI3K, of which Akt is the primary target. Akt inhibits GSK3β activity via phosphorylation at serine 9 (Li and Jope, 2010). Numerous other extracellular stimuli mediate the activity of the PI3K/Akt signalling cascade (**Figure 1.2**). CREB is also a substrate of GSK3β, resulting in gene expression, synaptic plasticity and neurogenesis (Kaidanovich-Beilin and Woodgett, 2011; Bradley et al., 2012; Beurel et al., 2015). In summary, these neurotrophic signalling pathways play a role in synaptic plasticity by ultimately providing the machinery for LTP. For example, increased number of receptors, increased number of vesicles, increased synaptic size, trafficking of receptors and neurotransmitters (Kandel et al., 2014). Therefore, they are important in mechanisms of learning and memory (Lee and Son, 2009; Schmitt et al., 2009;

Peng et al., 2010; Chen et al., 2013; Goggin et al., 2014). In addition, these neurotrophic signalling pathways are also thought to play a role in depression and anxiety-related psychological disorders (Martinowich et al., 2007; Polter et al., 2010) and are therefore of particular interest with regards to the mechanisms underlying the behavioural deficits observed in FASD. Further, significant components and regulators (e.g. BDNF and MKP-1) of the P-ERK1/2- and GSK3β-signalling cascades are vulnerable to ethanol exposure. For example, in animal models of alcoholism, decreased levels P-ERK1/2 were observed in the hippocampus of Mongolian gerbils after chronic ethanol intake in adulthood (0.5 - 2 g/kg/day, for 3 weeks) (Kim et al., 2012). This was accompanied by decreased cell proliferation and depression-like behaviour in the FST (Kim et al., 2012). However, acute exposure to ethanol in adulthood (3 g/kg, 10 - 30 minutes before sacrifice) increased phosphorylation of ERK1/2 in the PFC of adult C57BL/6J mice (Agoglia et al., 2015). Further, in animal models of FASD, impaired ERK1/2 activation was observed in hippocampal slices taken from C57BL/6J mice (2 - 5 months) exposed to prenatal-ethanol (saccharin-sweetened 5% ethanol solution) (Samudio-Ruiz et al., 2009) and decreased phosphorylation of ERK1/2 was observed in mice sacrificed shortly after a high dose of ethanol on P7 (Subbanna et al., 2013). In addition, mitogen activated protein kinase-phosphatase 1 (MKP1), also known as dual specificity phosphatase-1 (DUSP1), dephosphorylates P-ERK1/2 and therefore is a negative regulator of the MAPK signalling pathway (Akbarian and Davis, 2010). Therefore, changes in P-ERK1/2 signalling due to ethanol exposure may be mediated by possible ethanol exposure-induced changes in MKP-1.

In adolescent rats, total levels of GSK3β were decreased and phosphorylation (ser9) of GSK3β was increased after prenatal-ethanol in the frontal cortex and hippocampus respectively (Goggin et al., 2014) thereby highlighting region-specific ethanol-induced changes in GSK3β in the brain. Although, the long-term *in vivo* ethanol-induced molecular changes in ERK1/2 and GSK3β signalling are relatively unexplored in the literature and no concluding picture can be constructed, the deficits in neuroplasticity observed after prenatal- and/or early-postnatal ethanol exposure may be due to the dysregulation of these kinases. This may be due ethanol-induced changes is upstream signalling molecules such as BDNF. For instance, 24 hours after the last dose of ethanol exposure (5.25 g/kg/day, P4 - P9) levels of BDNF were increased in the hippocampus but unchanged in the frontal cortex (Boschen et al., 2015). BDNF in the dentate gyrus has also been unchanged by exposure to ethanol during all three trimester equivalents in adult SD rats (Boehme et al., 2011). Further, early-postnatal ethanol exposure from P10 - P15 via ethanol vaporization chambers increased hippocampal levels of BDNF

mRNA on P16 and P20 but decreased BDNF mRNA levels in adulthood on P60 (Miki et al., 2008). These variable, age-dependent ethanol-induced changes in BDNF may affect the downstream regulation of ERK1/2- and GSK3β-signalling and contribute to ethanol-induced deficits in neural plasticity since irregular regulation of either the ERK1/2 or GSK3β will have downstream consequences on the transcription factor CREB. CREB has been shown to be altered by ethanol exposure. For instance, ferrets exposed to early-postnatal alcohol exposure (3.5 g/kg, 25 % ethanol) every other day from P10 to P30 had decreased levels of P-CREB and therefore a decreased capacity for neural plasticity in the visual cortex compare to non-exposed controls (Krahe et al., 2009).

In summary, short-term ethanol-induced cell death and structural changes may persist into adolescence and adulthood although the persistent impairments and functionality of the formed neuronal networks remain unclear. In parallel to human studies, animal studies suggest persistent ethanol exposure-induced changes in the capacity for neural plasticity. The mechanisms of neural plasticity have many regulatory components that may be susceptible to the teratogenic effect of ethanol exposure. For example, different neurotransmitter systems, specifically glutamatergic and dopaminergic neurotransmission, and the downstream ERK1/2- and GSK3β-intracellular signalling pathways contribute to the strength and efficiency of signal transduction. However, the *long-term* prenatal- and early-postnatal ethanol-induced changes (observed weeks to months after ethanol exposure (Gil-Mohapel et al., 2011; Kleiber et al., 2013)) in these regulatory components of neural plasticity are yet to be fully elucidated. In addition, ethanol-induced changes in the cellular environment will further affect the capacity for neural plasticity via energy production and redox balance.

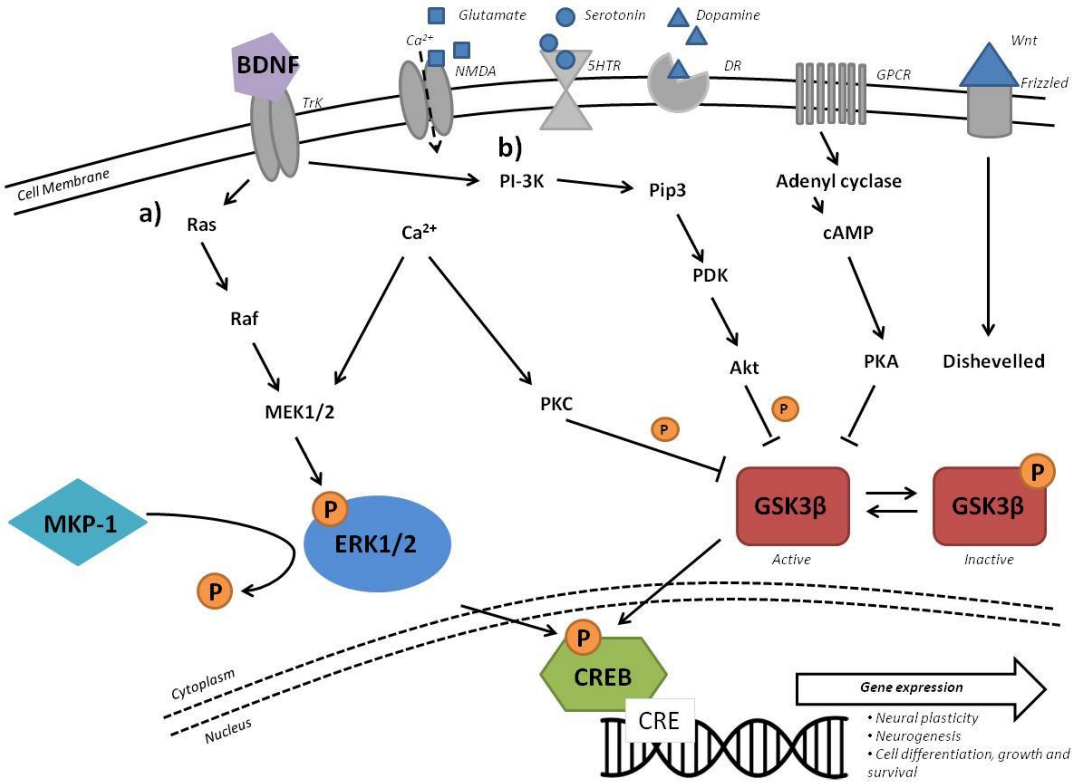

Figure 1.2: Neurotrophic signalling cascades

a) The mitogen-activate protein kinase (MAPK) signalling cascade. A cascade of therine/serine kinases result in the phosphorylation of ERK1/2. BDNF activates the MAPK via the tyrosine receptor kinase-beta (Trkβ). MKP-1 acts as a negative regulator of the MAPK pathway through the de-phosphorylation of ERK. ***b***) PI3K/Akt signalling pathway. GSK3β is *inactivated by phosphorylation* via numerous upstream molecules such as Akt, PKA and PKC. BDNF also mediates the activity of GSK3β via Trkβ. Wnt signalling also inhibits GSK3β. Both ERK1/2 and GSK3β result in the activation of the transcription factor CREB resulting in gene transcription and the machinery required for neural plasticity. [ERK1/2 = extracellular-signal regulated kinase; MKP-1 = mitogen activated protein kinase -1; PIP3 = Phosphatidylinositol-3,4,5-triphosphate; PI3K = phosphatidylinositol 3-kinase; GSK3β = glycogen synthase kinase-3 beta; BDNF = brain derived neurotrophic factor]

PHOSPHODIESTERASE INHIBITION

There is currently no treatment for FASD. However, phosphodiesterase (PDE) inhibitors have been used to target neural plasticity deficits (Krahe et al., 2009, 2010; Lantz et al., 2012) and therefore have the potential to elucidate possible treatment mechanism. Phosphodiesterases are enzymes that catalyze the hydrolysis of phosphate bonds in cAMP and cGMP. PDEs convert cAMP and cGMP to AMP and GMP respectively. PDEs are subdivided into families depending on their preferred substrate. For example, PDE4 acts on cAMP and PDE5 acts on cGMP whereas PDE1 act on both cAMP and cGMP pathways. Consequently, inhibiting the action of PDEs results in an increase of cAMP and cGMP which results in an increase in gene

transcription and hence gene expression via the phosphorylation of transcription factors such as CREB and serum response factor (SRF) respectively (Paul et al., 2010; Lantz et al., 2012).

The PDE inhibitor vinpocetine, is a type 1 PDE (PDE1) inhibitor and hence inhibits the hydrolysis of both cAMP to AMP and cGMP to GMP (**Figure 1.3**). Vinpocetine, has been shown to aid LTP, enhance dendritic spine complexity and restore ocular dominance plasticity in mice and ferrets (Lantz et al., 2012). This previous study showed that inhibition of conversion of both cAMP to AMP and cGMP to GMP are needed to restore ocular dominance plasticity (Lantz et al., 2012). Specifically, PDE4 inhibition by rolipram, which increases cAMP does not restore ocular dominance plasticity on its own (Krahe et al., 2010). However when rolipram is combined with a PDE5 inhibitor, vardenafil, neural plasticity is restored and results are similar to animals treated with a PDE1 inhibitor such as vinpocetine (Lantz et al., 2012). Therefore, the synergistic effect of increased cAMP and cGMP due to the inhibition of PDE1, by an inhibitor such as vinpocetine, is necessary to restore ocular dominance plasticity in the visual cortex after early-postnatal ethanol exposure (Lantz et al., 2012).

Vinpocetine has also been shown to increase performance on cognitive tests and restore learning and memory behaviour of animals exposed to ethanol during the early-developmental period (Filgueiras et al., 2010; Nunes et al., 2011; Lantz et al., 2012). For instance, vinpocetine treatment (20 mg/kg) of juvenile Long-Evans rats exposed to early-postnatal ethanol (5 g/kg/day, P4 - P9) performed better in the MWM compared to the untreated-ethanol-exposed controls (Filgueiras et al., 2010). Further, vinpocetine treatment of Swiss mice exposed to early-postnatal ethanol (5 g/kg, P2 - P8) reduced ethanol-induced hyperactivity behaviour (locomotor activity) and increased levels of cAMP in the frontal cortex and hippocampus (Nunes et al., 2011). In addition, vinpocetine has been shown to increase blood flow and metabolic activity, as well as protect against NMDA-induced excitotoxicity, ischemic insults and reactive oxygen species (Nivison-Smith *et al*., 2017) (**Figure 1.3**). Vinpocetine has also been shown to act as an anti-inflammatory agent via a mechanism independent of PDE inhibition (Jeon et al., 2010). In addition, it is not known how vinpocetine affects neural plasticity-related proteins such as components of the ERK1/2- and GSK3β-signalling cascades. Further, the additional benefits of vinpocetine-treatment such as increased blood flow and metabolic activity, as well as protection against reactive oxygen species (Nivison-Smith *et al*., 2017) suggest broader changes in proteins related to metabolic activity, redox regulation and

vasculature. Therefore, further investigation is required to provide insight into the neuroprotective mechanisms of vinpocetine and its potential use as a treatment for the deficits observed after ethanol exposure during early-development.

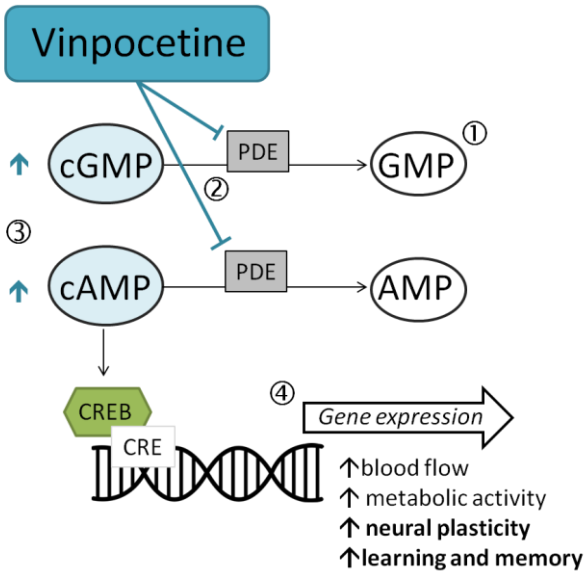

Figure 1.3: Phosphodiesterase inhibition and neural plasticity

1) Phosphodiesterases (PDEs) convert cAMP and cGMP to AMP and GMP respectively. **2**) Vinpocetine is a type 1 PDE inhibitor that prevents the conversion of both cAMP to AMP and cGMP to GMP. **3**) This results in increased levels of cAMP and cGMP. **4**) Increased levels of cAMP and cGMP promote transcription via CREB and SRF respectively. Neuroprotective benefits of vinpocetine treatment include increased blood flow, metabolic activity, and neural plasticity and therefore enhanced learning and memory.

EXPOSURE TO ALCOHOL *IN UTERO* AND EARLY-LIFE ADVERSITY

MATERNAL SEPARATION MODEL OF EARLY-LIFE STRESS

Experiencing early-life stress, such as physical or emotional abuse or neglect, is associated with the development of psychological disorders in adulthood (Mullen et al., 1996; Heim and Nemeroff, 2001; Carr et al., 2013; Grasso et al., 2013) due to persistent stress-induced functional and structural changes in neural circuitry (Faravelli, 2012). The non-linear effects of early-life stress, as a result of the nature, timing and duration of exposure as well as the genetic interaction, contribute to the wide variety and severity of observed psychological disorders (Mullen et al., 1996; Heim and Nemeroff, 2001; McLaughlin et al., 2010; Carr et al., 2013; Grasso et al., 2013). The maternal separation model is a valid animal model of early-life stress (Daniels et al., 2004; Ladd et al., 2004) and has been used by researchers to investigate

the effects of exposure to stress during early-development on the brain and behaviour. The maternal separation model involves separating the rat pups from the dam daily or sporadically during the first few weeks of life. For example, variations of the maternal separation model include separating the pups from the dam for 3 hours on a daily basis for the first 3 weeks of life (P2 - P21) (Aisa *et al*., 2007), or for 3 hours/day from P2 - P14 (Daniels *et al*., 2004; Ladd *et al*., 2004; El Khoury *et al*., 2006; Makena *et al*., 2012) (Dimatelis et al., 2013, 2016) as well as one 24 hour separation session during the first week of life (on P3 or P9) (Fabricius et al., 2008; Oomen et al., 2010) (**Table 1.2**).

The early-postnatal period (P2 - P14 in rats and P1 - P12 in mice), characterized by low levels of glucocorticoids and cortiscosterone, is termed the stress hypo-responsive period (Chen and Baram, 2016). During this time the HPA-axis does not efficiently regulate the stress response thereby creating an imbalance of stress mediators which can have long lasting structural and functional consequences in the brain which may contribute to the development of behavioural abnormalities later in life (Plotsky et al., 2005; Lippmann et al., 2007; Nishi et al., 2014). For instance, maternal separation stress during the stress hypo-responsive period leads to behavioural abnormalities, such as anxiety- and depression-like behaviour, in adolescent and adult rodents. Depression-like behaviour can be characterized by increased immobility in the FST (Slattery and Cryan, 2012) and decreased sucrose consumption in the sucrose-preference test (anhedonia) (Bessa, 2009). Anxiety-like behaviour can be indicated by an increased preference for dark or closed spaces over the innate response to explore novel environment. For instance, anxiety-like behaviour can be characterized by increased time spent in the closed arms of the EPM (Walf and Frye, 2007). In addition, the OFT, which is mostly used to measure locomotor activity, can also provide an indication of anxiety-like behaviour when the rats demonstrate a preference for the outer zone in which their vibrissae can stay in contact with the outer walls of the arena (thigmotaxis). For instance, maternally separated (3 hours/day, P2 - P14) juvenile SD rats spent more time immobile in the FST and more time in the closed arms of the EPM versus non-disturbed controls indicating depression- and anxiety-like behaviour respectively (Lee et al., 2007). Further, SD rats exposed to maternal separation stress (3 hours/day, P2 - P14) spent more time in the outer zone of the OFT on P28 compared to the non-separated controls (Makena et al., 2012). Adult Long-Evans rats separated for 3 hours/day (P2 - P14) have also been shown to have reduced locomotor activity in comparison to control rats in adulthood in the OFT (Lippmann et al., 2007). In addition, maternally separated rats have also been shown to exhibit longer and more ultrasonic vocalizations at 22 kHz (Dimatelis

et al., 2012, 2015). Rats emit ultrasonic vocalizations at different frequencies depending on their affective state. Vocalizations at 50 kHz (32 - 96 kHz, 30 - 50 ms duration) are reflective of a positive affective state whereas vocalizations at 22 kHz (range 18 - 32 kHz, 300 - 4000 ms duration) are produced in anticipation of aversive stimuli and therefore indicate the communication of a negative affective state (Portfors, 2007). In addition, adult Wistar rats exposed to a single 24-hour session of maternal separation on P3 showed impaired performance during the MWM (Oomen et al., 2010). This suggests that maternal separation stress can induce cognitive deficits in addition to the above behavioural deficits.

In some instances maternal separation stress did not generate depression- or anxiety-like behaviour (Shalev and Kafkafi, 2002; Marais et al., 2008; Dimatelis et al., 2015). For example, Long-Evans rats maternally separated from P3 - P14 for 3 hours/day did not show a decreased preference for sucrose or a difference in locomotor activity compared to controls. However, additional chronic-mild stress in later in life was shown to induce depression- or anxiety-like behaviour (Marais et al., 2008). Further, maternally separated rats (3 hours/day, P2 - P14) exposed to stressors in adulthood have elevated corticosterone levels compared to non-separated rats (Lippmann et al., 2007). These results demonstrate the differential response to stress in adulthood between separated and non-separated rats which may trigger the onset of depression- and anxiety-like behaviour. However, rats exposed to a single 24 hour session of maternal separation stress on P3 had higher levels of corticosterone in addition to enhanced contextual fear conditioning in adulthood compared to controls (Oomen et al., 2010). Therefore, suggesting that early-life stress may enable rats to better cope with stress later in life by optimally programming the brain to adapt to a stressful situation.
In addition to the above mentioned differential behavioural consequences of early-life stress, maternal separation has been shown to affect rodents in a sexually dimorphic manner. For instance, female SD rats maternally separated for 3 hours/day from P2 - P14 spent less time immobile in the FST and made shorter vocalizations of 22 kHz than non-separated controls (Dimatelis et al., 2015). Therefore, these rats did not display the conventional depressive-phenotype, indicating that this cohort of female rats were resistant to maternal separation stress.

The literature shows that rodents exposed to maternal separation stress develop anxiety- and depression-like behaviour and therefore can be used to investigate the multifaceted molecular

mechanisms underlying early-life adversity and the long-term behavioural consequences. These mechanisms are not yet fully elucidated however, similar to ethanol exposure during early development, neural plasticity and the ERK1/2- and GSK3β-signalling cascades have been implicated in the pathophysiology of early-life stress-induced psychological behavioural abnormalities (*described next*).

Table 1.2: Summary of observed behavioural-phenotypes after exposure to variations of the maternal separation paradigm.

Behaviour	Age	Behavioural Test	Maternal Separation	Species	Reference
Learning and memory	P60 - P75	MWM; NOT	3 hours/day from P2 - P21	Wistar	(Aisa *et al*., 2007)
	P90	MWM	24 hours on P3	Wistar	(Oomen et al., 2010)
Depression-like	P35	FST	1 hour/day from P2 - P14	SD	(Huang *et al*., 2006)
	P61 - P62	FST	3 hours/day from P1 - P14	SD	(Lee et al., 2007)
	P65	FST	3 hours/day from P2 - P14	FLS	(El Khoury et al., 2006)
	P65 - P67	UV; FST	3 hours/day from P2 - P14	SD	(Dimatelis et al., 2012)
	P60 - P75	FST; sucrose preference test	3 hours/day from P2 - P21	Wistar	(Aisa *et al*., 2007)
Anxiety-like	P28	OFT	3 hours/day from P2 - P14	SD	(Makena *et al*., 2012)
	P61 - P62	EPM	3 hours/day from P1 - P14	SD	(Lee et al., 2007)
Locomotor activity	P50 - P60	OFT	3 hours/day P2 - P14	Long-Evans	(Lippmann et al., 2007)

[MWM = Morris Water Maze; NOT = novel object test; FST = Forced swim test; UV = Ultrasonic vocalizations; OFT = open field test; EPM = elevated plus maze; SD = Sprague-Dawley; FLS = Flinders Sensitive Line]

MATERNAL SEPARATION AND THE ERK1/2- AND GSK3B-SIGNALLING CASCADES

There is evidence to suggest that neural plasticity deficits contribute to the development of anxiety- and depression-like behaviour after exposure to maternal separation stress. For instance, after a single 24 hour session of maternal separation stress on P3, adult Wistar rats showed decreased hippocampal neurogenesis and dendritic morphology (Oomen et al., 2010) and decreased LTP was observed in the Shaffer collaterals/CA1 synapses of aged-Wistar rats (±70 weeks) that were maternally separated for 3 hours/day from P2 - P14 compared to age-matched controls (Sousa et al., 2014). The HPA-axis hypo-responsive responsive period (P2 - P14 in rats) coincides with the brain growth spurt (Dobbing and Sands, 1979) as shown by a

rapid increase in synaptogenesis, dendritic complexity, spine formation and myelination. The ERK1/2- and GSK3β-intracellular signalling cascades are involved in neurogenesis, differentiation, migration and survival (Moors et al., 2007) and therefore have a significant role during this period of rapid brain maturation. However, components of these signalling cascades are susceptible to the effects of stress during this period due to crosstalk between glucocorticoid- and neurotrophin-signalling (Daskalakis et al., 2015). For example, 6 hours/day of maternal separation stress decreased levels of BDNF and P-ERK1/2 on P7 and decreased spine density on P21 in the hippocampus of SD rats (Ohta et al., 2017). This may be because corticosterone has been shown to increase MKP-1 which dephosphorylates P-ERK1/2 (Daskalakis et al., 2015) thereby reducing the activity of P-ERK1/2 and disrupting spine maturation. Further, there is evidence to suggest that there are significant long-term changes within the ERK1/2- and GSK3β-signalling pathways after exposure to maternal separation stress (Lippmann et al., 2007; Makena et al., 2012; Mozzaquatro et al., 2014; Dimatelis et al., 2015) which may contribute to the observed deficits in neural plasticity and development of anxiety- and depression-like behaviour. For instance, upstream of ERK1/2 and GSK3β, adult Long-Evans rats exposed to maternal separation stress for 3 hours/day from P2 - P14 had lower levels of BDNF in the hippocampus and striatum and were hypoactive in the open field compared to control rats (Lippmann et al., 2007). However, downstream of ERK1/2- and GSK3β-signalling levels of total CREB remained unchanged in maternally separated rats compared to controls (Lippmann et al., 2007). In addition, adult SD maternally separated rats (P2 - P14, 3 hours/day) showed impaired exercise-induced ERK1/2 activation and spent less time in the open arms of the EPM compared to non-separated rats demonstrating anxiety-like behaviour (Makena et al., 2012). Mice exposed to 3 hours/day of maternal separation stress from P2 - P21 showed decreased phosphorylation of GSK3β in the hippocampus and spent more time immobile in FST demonstrating depression-like behaviour compared to controls (Bian et al., 2015). Antidepressant treatment provides additional evidence for the involvement in ERK1/2- and GSK3β- signalling in the pathology of anxiety- and depression-like behaviour. For example, Swiss-mice treated with antidepressants spent less time immobile in the FST and had greater levels of P-ERK1/2 in the PFC and hippocampus compared to the non-treated controls (Mozzaquatro et al., 2014). This evidence suggests a dysregulation of these kinases may be involved in anxiety- and depression-like behaviours.

The maternal separation model of early-life stress induces persistent structural and functional changes in the brain which increases the vulnerability to depression- and anxiety-like behaviour in rodents. Similar behavioural-phenotypes and changes in the ERK-and GSK3β-signalling pathways were observed in both animal models of FASD and early-life stress. This indicates impairments in overlapping neuronal circuits. However, the interaction between exposure to ethanol *in utero* and postnatal-environmental adversities has not been investigated because early-life stress has not been included in animal models of FASD. By coupling prenatal-ethanol exposure with maternal separation stress we intended to provide a more representative and robust model of FASD in which the possible effect of childhood adversities are accounted for.

In summary, *in utero* alcohol exposure predominantly results in learning and memory deficits but anxiety and depression disorders are also commonly observed. Exposure to early-life stress increases vulnerability to the development of psychological disorders and to a lesser extent, the development of cognitive deficits. Both learning and memory processes and psychological disorders involve changes in neural plasticity, with specific reference to the ERK1/2 and GSK3β intracellular-signalling cascades (**Figure 1.4**). With reference to **Figure 1.4**, (i) as mentioned, components of these intracellular signalling cascades have been altered by prenatal- or early-postnatal ethanol exposure in animal models of FASD and in animals displaying deficits in learning and memory. However, there is a significant lack of the long-term, *in vivo* effects of ethanol exposure during development on these signalling pathways. (ii) Similarly, dysregulation of ERK1/2, GSK3β and components of these signalling cascades has been shown in animal models of early-life stress and in animals exhibiting anxiety- and depression-like behaviour. However, how these changes in neural plasticity-related proteins contribute to the development of behavioural abnormalities is not fully understood. Children exposed to alcohol *in utero* may face further adverse life events in childhood. However, this component of FASD is usually controlled for in human population studies and early-life adversity has not been factored into animal models of FASD. (iii) Therefore, there is a significant lack of literature on the possible interaction between prenatal-ethanol and early-life stress on the brain and behaviour. (iv) Since both prenatal-ethanol exposure and early-life stress have elicited changes in neural plasticity-related proteins, such as ERK1/2 and GSK3β and components of these signalling cascades, there may be an interaction between ethanol exposure and early-life stress on these signalling pathways. Therefore, investigating the effects of additional maternal

separation stress after prenatal-ethanol exposure on the brain may provide a better representation of the molecular mechanisms underlying the cognitive and behavioural deficits observed after exposure to alcohol *in utero* because the contribution of an adverse postnatal-environment is accounted for.

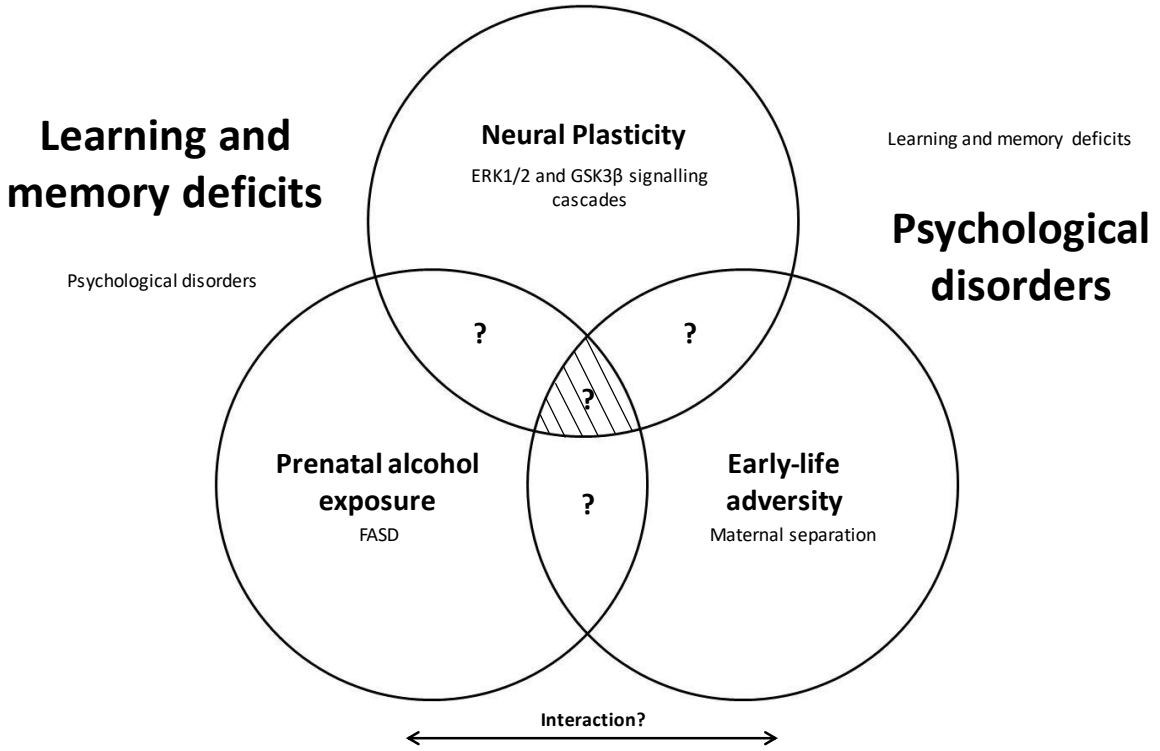

Figure 1.4: Prenatal-ethanol exposure and further early-life adversity

(**i**) The ERK1/2- and GSK3β-signalling cascades and prenatal-ethanol exposure are associated with learning and memory deficits.(**ii**) Psychological disorders and alterations in ERK1/2- and GSK3β-signalling cascades occur Safter exposure to early-life stress (maternal separation). (**iii**) Interaction between prenatal-ethanol exposure and early-life stress on behaviour. (**iv**) Interaction between prenatal-ethanol exposure and early-life stress on the ERK1/2- and GSK3β-signalling cascades.

Therefore, this study was done in order to investigate the long-term, *in vivo* effects of ethanol exposure during development on protein levels and intracellular-signalling pathways, specifically the ERK1/2 and GSK3β signaling cascades, to provide insight into how changes in these neural plasticity-related proteins contribute to the development of behavioural abnormalities observed in FASD. In addition, this work accounted for early-life stress in an animal model of FASD to investigate any interaction between ethanol exposure and early-life stress on neurochemistry and behaviour.

HYPOTHESES AND OBJECTIVES

The experiments described in Chapters 2 - 6 address the above gaps in the literature by utilizing two different animal models of FASD, a treatment in the form of a PDE type 1 inhibitor, additional early-life stress and determining the proteomic profile of specific brain regions following ethanol exposure. The following hypotheses were investigated by performing the associated objectives.

In Experiments 1 and 2 (described in Chapters 2 - 4), using an early-postnatal ethanol exposure animal model of FASD, the following were addressed:

1. The effects of early-postnatal ethanol exposure on behaviour and neurochemistry and the effectiveness of treatment with vinpocetine, a PDE type 1 inhibitor, in reducing ethanol-induced changes.
2. Changes in dopaminergic neurotransmission/glutamate receptor function following early-postnatal ethanol exposure.

In **Experiments 3 and 4** (described in Chapters 5 and 6), using prenatal-ethanol exposure followed by maternal separation stress, the following were addressed:

3. Prenatal-ethanol and/or maternal separation stress-induced changes in behaviour.
4. Prenatal-ethanol and/or maternal separation stress-induced changes in neurochemistry

Experiment 1

Hypothesis 1.1: Adolescent SD rats exposed to early-postnatal ethanol will show alterations in cognitive behaviour and changes in neural plasticity-related proteins in the prefrontal cortex (PFC) and dorsal hippocampus (DH).

> *Aim 1.1*: To elucidate the effects of early-postnatal ethanol exposure on learning and memory, and neuroplasticity-related proteins.
>
> > *Objective 1.1.1*: Adolescent male SD rats exposed to early-postnatal ethanol will be tested in the open field and MWM.

Objective 1.1.2: Changes in BDNF, MKP-1, P-ERK1/2, ERK1/2, P-GSK3B, GSK3B and synaptophysin will be measured in the PFC and DH using enzyme-linked immunosorbent assays (ELISA) and Western blot.

Hypothesis 1.2: Treatment of rats exposed to early-postnatal ethanol with the PDE1 inhibitor, vinpocetine, will restore behavioural changes and neural plasticity-related proteins.

Aim 1.2: To investigate the mechanism of action of vinpocetine and its effects on behaviour and neuroplasticity-related proteins.

Objective 1.2.1: Adolescent male SD rats exposed to early-postnatal ethanol will be treated with vinpocetine and tested in the open field and MWM.

Objective 1.2.2: Changes in BDNF, MKP-1, P-ERK1/2, ERK1/2, P-GSK3B, GSK3B and synaptophysin will be measured in the PFC and DH using ELISA and Western blot.

Hypothesis 1.3: Early-postnatal ethanol exposure and treatment with the PDE1 inhibitor, vinpocetine, will alter proteins in the ventral hippocampus (VH).

Aim 1.3: To investigate wide-spread early-postnatal ethanol-induced protein changes following vinpocetine treatment.

Objective 1.3: Perform proteomic analysis on VH tissue of adolescent male rats exposed to early-postnatal ethanol and treated with vinpocetine.

Hypothesis 1.4: Early-postnatal ethanol exposure will alter proteins in the PFC and DH of adolescent rats.

Aim 1.4: To investigate long-term early-postnatal ethanol-induced protein changes in the PFC and DH of rats which have not undergone handling or behavioural tests.

Objective 1.4.1: Perform proteomic analysis of PFC and DH tissue from adolescent control rats and rats exposed to early-postnatal ethanol.

Objective 1.4.2: Perform Western blot analyses of proteins in the PFC and DH highlighted by proteomic analysis to confirm proteomic data.

Experiment 2

Hypothesis 2.1: Adolescent male and female rats exposed to early-postnatal ethanol will have altered glutamatergic- and/or dopaminergic-neurotransmission in the striatum compared to non-exposed controls.

Aim 2.1: To investigate glutamate receptor function after early-postnatal ethanol exposure.

Objective 2.1: Measure the glutamate-stimulated release of radioactively labeled [^{3}H]-DA, from whole-striatal tissue collected from adolescent rats exposed to early-postnatal ethanol.

Experiment 3:

Hypothesis 3.1: Adult rats exposed to prenatal-ethanol will show learning and memory deficits and anxiety- and depression-like behaviour, as well as changes in neuroplasticity-related proteins compared to controls.

Aim 3.1: To elucidate the effects of prenatal-ethanol exposure on behaviour and the neural plasticity-related proteins, ERK1/2- and GSK3β, in the adult rat brain.

Objective 3.1.1: Assess the behaviour of male rats exposed to prenatal-ethanol using the NOT, ultrasonic vocalizations, EPM, OFT and FST.

Objective 3.1.2: Quantify neural plasticity-related proteins: BDNF, MKP-1, P-ERK1/2, ERK1/2, P-GSK3β, GSK3β and synaptophysin using Western Blot analysis in the PFC and DH of adult rats.

Hypothesis 3.2: Additional maternal separation stress will enhance prenatal-ethanol-induced behavioural deficits and changes in neuroplasticity-related proteins.

Aim 3.2: To account for possible early-life adversity experienced in addition to *in utero* alcohol exposure.

Objective 3.2.1: Assess the behaviour of male rats exposed to prenatal-ethanol and/or maternal separation stress using the NOT, ultrasonic vocalizations, EPM, OFT and FST.

Objective 3.2.2: Quantify neural plasticity-related proteins: BDNF, MKP-1, P-ERK1/2, ERK1/2, P-GSK3β, GSK3β and synaptophysin using Western Blot analysis in the PFC and DH of adult rats.

Experiment 4

Hypothesis 4.1: Prenatal-ethanol exposure and/or maternal separation stress will alter the proteome of the adult rat PFC and DH compared to non-exposed controls.

Aim 4.1: To provide a better representation of the molecular mechanisms underlying the behavioural deficits observed in FASD by accounting for possible additional early-life stress experienced in addition to *in utero* alcohol exposure.

Objective 4.1: Perform proteomic analysis of PFC and DH tissue of adult male rats exposed to prenatal-ethanol and/or maternal separation stress that did not undergo behavioural testing.

CHAPTER 2: THE EFFECTS OF EARLY-POSTNATAL ETHANOL EXPOSURE AND VINPOCETINE TREATMENT ON THE DEVELOPING RAT BRAIN.

Parts of this chapter have previously been published:
Swart PC, Currin CB, Russell VA and Dimatelis JJ (2017) Early-ethanol exposure and vinpocetine treatment alter learning- and memory-related proteins in the rat hippocampus and prefrontal cortex. Journal of Neuroscience Research. 95:1204–1215.

INTRODUCTION

The learning and memory deficits associated with exposure to alcohol *in utero* are especially prevalent during childhood and adolescence (Kodituwakku, 2007; Willoughby et al., 2008). In addition, FASD presents with motor deficits and behavioural pattern similar to those observed in ADHD (Mick et al., 2002; Kable et al., 2016). Neuronal cell loss during ethanol exposure was thought to be the cause of the persistent deficits (Ikonomidou *et al*., 2000). On average, the volume of brain areas, such as the hippocampus, was smaller (Nardelli et al., 2011) and a decrease in cortical thickness (Zhou et al., 2011) was observed in patients with FASD. However, the long-term functionality of the remaining cells still remains unclear. Evidence from animal models suggests that neuronal plasticity deficits and impaired neurotransmission underlie the learning and memory deficits observed after exposure to ethanol during the early stages of development (Krahe et al., 2010; Lantz et al., 2012).

In the present study, ethanol was administered during the third-trimester equivalent developmental stage (P0 - P10). Rats exposed to ethanol during the postnatal period have been shown to exhibit deficits in learning and memory (Filgueiras *et al*., 2010), and hyperactive behaviour (Nunes et al., 2011; Brocardo et al., 2012; Brys et al., 2014). Therefore, we aimed to measure learning and memory performance using the MWM, in which rats were trained (learning) to find a hidden platform given spatial cues and then had to remember the location of the platform during a test trial (memory) (Vorhees and Williams, 2006). In addition, we aimed to measure hyperactivity and anxiety-like behaviour in the OFT, as indicated by the distance travelled and time spent in the inner zone respectively. These behavioural tests have previously been used in our laboratory to assess learning and memory, hyperactivity, anxiety-like behaviour (Makena et al., 2012; McFie et al., 2012).

Growth factors and intracellular signalling cascades such as BDNF and its signalling pathways, comprising, amongst others, MKP-1, ERK1/2 and GSK3β have been implicated in developmental and learning and memory processes (Lee and Son, 2009; Schmitt et al., 2009; Peng et al., 2010; Chen et al., 2013; Goggin et al., 2014). Specifically, the kinases ERK1/2 and GSK3β are converging points for many signalling cascades that are involved in neurogenesis, differentiation, migration and survival of neuronal cells (Moors et al., 2007). Significant components of theses signalling cascades are vulnerable to ethanol exposure. Dysregulation of these kinases and their downstream substrates may underlie the observed deficits in neural plasticity and consequently neurotransmission and learning and memory. Deficits in neural-plasticity may be evidenced by long-term structural changes. For instance, West *et al*. (1981) and West and Hamre, (1985) demonstrated massive sprouting of the mossy fibre terminals after early-postnatal ethanol exposure (7 – 7.5 g/kg/day, P1 – P10). These structural changes persisted into adulthood resulting in a long-term footprint of early-postnatal ethanol exposure, possibly due to deficits in synaptic plasticity. Synaptophysin, a synaptic vesicle-related protein can then be used to indirectly measure synaptic density and identify deficits in neural plasticity as a consequence of early-postnatal ethanol exposure (Elibol-Can et al., 2014). However, a large portion of research investigating ethanol-induced changes in neural plasticity-related proteins has been conducted on cultured cells, embryos or on animals which were sacrificed shortly after ethanol administration (Sakai et al., 2005; Subbanna et al., 2013). Therefore, the long-term ethanol-induced changes in neural plasticity-related proteins still remain unclear. In this chapter we aimed to evaluate the long-term effects of ethanol exposure during the early-postnatal period on the above mentioned neural plasticity-related proteins in the PFC and DH of adolescent rats since these are key brain regions involved in cognitive function and learning and memory processes (Fanselow and Dong, 2010).

We further investigated whether early-postnatal ethanol-induced changes in learning and memory and neural plasticity-related proteins, could be reversed by treatment with vinpocetine, a type 1 PDE inhibitor (Lantz et al., 2012). Vinpocetine has been shown to facilitate long-term potentiation, enhance dendritic spine complexity, increase neuronal plasticity (Lantz et al., 2012), improve spatial learning in the MWM (Filgueiras *et al*., 2010) and reduce hyperactivity in animal models of FASD (Nunes et al., 2011). We hypothesized that adolescent rats exposed

to early-postnatal ethanol would take longer to find the hidden platform in the MWM and would have reduced levels of neural plasticity-related proteins in the PFC and DH. Further, treatment of rats exposed to early-postnatal ethanol with vinpocetine would restore neural plasticity-related proteins and therefore these rats would find the hidden platform in a similar time to that of controls.

Behavioural abnormalities such as ADHD-like behaviour and deficits in motor learning observed after *in utero* alcohol exposure (Rangmar et al., 2015a; Weyrauch et al., 2017) suggest underlying alterations in dopaminergic function in the brain (Adinoff, 2004; Tripp and Wickens, 2009). Therefore, this chapter also investigated the long-term early-postnatal ethanol-induced changes in dopaminergic neurotransmission as well as glutamate regulation of DA in the striatum of rats exposed to ethanol during the early-postnatal period. The striatum is highly innervated by dopaminergic neurons and therefore, early-postnatal ethanol-induced changes in dopaminergic neurotransmission should be evident in striatal tissue.

This chapter presents novel insight into the long-term effects of early-postnatal ethanol exposure and vinpocetine on neural plasticity-related proteins, specifically components of the ERK1/2- and GSK3β-signalling pathways, in the rat brain. In addition, this study provides insight into the effect of early-postnatal ethanol on dopaminergic neurotransmission and striatal glutamate receptor function in the adolescent rat brain.

METHODS

ANIMALS

Adult SD male and female rats were obtained from the University of Cape Town Faculty of Health Sciences Animal Unit and were housed in the nearby Satellite Animal Facility. Adult male and female rats were paired and housed together for breeding. Animals were housed in a 12 hour:12 hour light/dark cycle (lights on at 06:00) with *ad libitum* access to standard rat chow and water. The temperature was maintained at 23 ± 1 °C and the light intensity at ± 150 lux (range: 120-250). A single red tube was present in all cages as a source of environmental enrichment. Around the expected date of birth, the females were monitored twice daily to check for the presence of pups. When the dam gave birth (designated as P0) the adult male was immediately removed. On P2, the litter was sexed and culled to a maximum of 10 pups per litter (with a minimum of 2 female pups) to ensure equal suckling and nutrition from the dam. Ethical approval was obtained from the University of Cape Town Animal Ethics Committee [Project number: 014/002]. All experimental procedures aimed to minimize the pain and suffering of the animals used and adhered to the guidelines set out in the South African National Standard: The Care and Use of Animals for Scientific Purpose (2008).

EARLY-POSTNATAL ETHANOL EXPOSURE

Whole-litters were randomly assigned to either an early-postnatal ethanol exposed group (n = 8 litters) or a saline-control group (n = 9 litters). From P4 - P9, which is equivalent to the neurodevelopmental stage of the third trimester of human gestation (Dobbing and Sands, 1979), ethanol-exposed pups were administered ethanol (4 g/kg/day i.p, 12 % v/v) and saline-control pups were administered volume controlled saline (0.9 % NaCl i.p). The dose of ethanol chosen was based on previous studies in which the blood alcohol levels were measured and found to be 228 - 255 mg/dl (Goodlett and Peterson, 1995; Nunes et al., 2011; Brocardo et al., 2012; Patten et al., 2013a). These blood alcohol concentrations are considered to be high levels of intoxication (Marquardt and Brigman, 2016). All rats were weighed daily from P4 - P9 to monitor the effect of early-postnatal ethanol exposure on body weight. On P21, rat pups were weaned from the dam. Pups from the same litter were separated by sex and housed in groups of 2 - 3 rats per cage. Randomly selected male pups underwent drug treatment and behavioural

testing. The remaining rats were not treated and did not undergo behavioural testing. These rats were used in *in vitro* superfusion experiments (p.47) and proteomic analysis (*Chapter 4*, p.89).

DRUG TREATMENT

From P25 to P31 randomly selected male ethanol-exposed rats were administered vinpocetine (20 mg/kg/day i.p.), a PDE type 1 inhibitor (Sigma, St Louis, MO) or vehicle (dimethylsulfoxide [DMSO]; Calbiochem EMB Chemicals, San Diego, CA) (**Figure 2.1**). Similarly, randomly selected male saline-control rats were administered volume controlled DMSO i.p. This resulted in 3 experimental groups comprising of only male rats for behavioural testing and immunoassays: **control** (saline+DMSO, n = 17), **EtOH-** (EtOH+DMSO, n = 11) and **vinp-** (EtOH+vinpocetine, n = 11) rats. To minimize litter effects, a maximum of 2 pups from the same litter were assigned to the same experimental group, with the exception of three litters from which 3 pups were used. Injections were performed during the light phase (between 09:00 and 10:00) and the behaviour/sacrifice commenced 4 hours later (between 13:00 and 14:00). This was done in order to allow for vinpocetine to maximize cAMP levels (Filgueiras *et al*., 2010; Nunes *et al*., 2011).

BEHAVIOUR

Behavioural tests were conducted from P25 to P30 (**Figure 2.1**) during the light phase (between 13:00 and 16:00) using **control** (n = 11), **EtOH-** (n = 11) and **vinp-** (n = 17) rats. Rats were weighed daily throughout behavioural testing. All rats were habituated to the behavioural testing area one hour before the start of each test to decrease the stress due to the exposure to a novel environment as this would have an effect on the behavioural outcome. The behavioural equipment was cleaned with 70 % ethanol between rats to prevent the detection of another rats scent on the apparatus. Behaviour was recorded on a Sony Handicam video camera (DCR-SX838; Tokyo, Japan) mounted 1 m above the behavioural apparatus. This allowed for later behavioural analysis with Ethovision version 7.0 (Noldus Information Technology, Amsterdam, The Netherlands).

(Note: In this chapter the MWM and exposure to a novel object (cone) test were performed by Christopher B. Currin, a BSc (Med) Honours student in 2014)

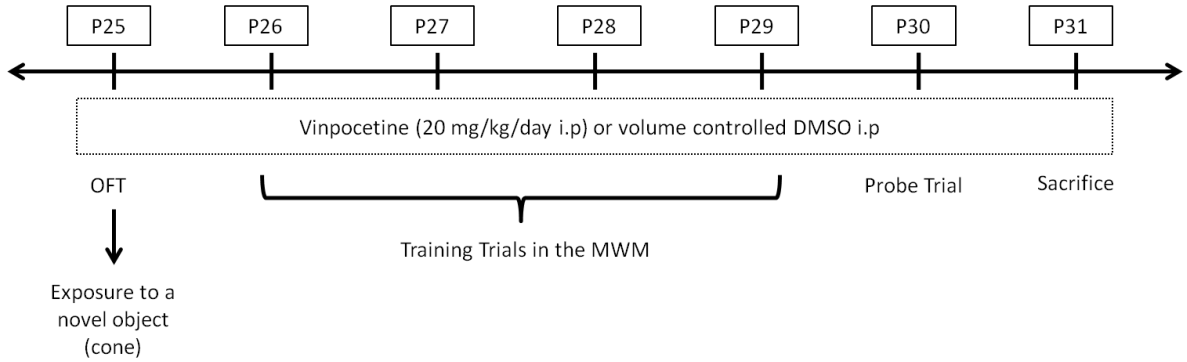

Figure 2.1: Treatment and behavioural timeline.

From P25 to P31, randomly selected male ethanol-exposed rats were treated with vinpocetine (20 mg/kg/day i.p) or vehicle (DMSO) 4 hours before behavioural testing or sacrifice. Male saline-control rats were administered DMSO in the same manner. Treated rats underwent behavioural analysis from P25 to P30. The open field test (OFT) took place on P25, followed by exposure to a novel object. From P26 to P29, rats underwent training in the Morris water maze (MWM), which concluded with the probe trial on P30. All rats were sacrificed on P31. [Experimental groups: control n = 11, (saline+DMSO); EtOH n = 11, (EtOH+DMSO); vinp n = 17, (EtOH+vinpocetine)]

OPEN FIELD TEST

The open field arena consists of a black box (100 cm x 100 cm x 50 cm; **Figure 2.2**) set up in a temperature controlled room (23 ± 1°C; 50 ± 20 Lux). On P25, rats were habituated in the same room with the open field arena one hour before the start of the test. Rats were individually placed in the bottom right hand corner of the open field arena facing the wall (represented by **X** in **Figure 2.2**) and left to explore the environment for 10 minutes (McFie et al., 2012). The inner zone was outlined by white tape. The time spent in the inner zone of the open field and the total distance travelled during the first 5 minutes were measured.

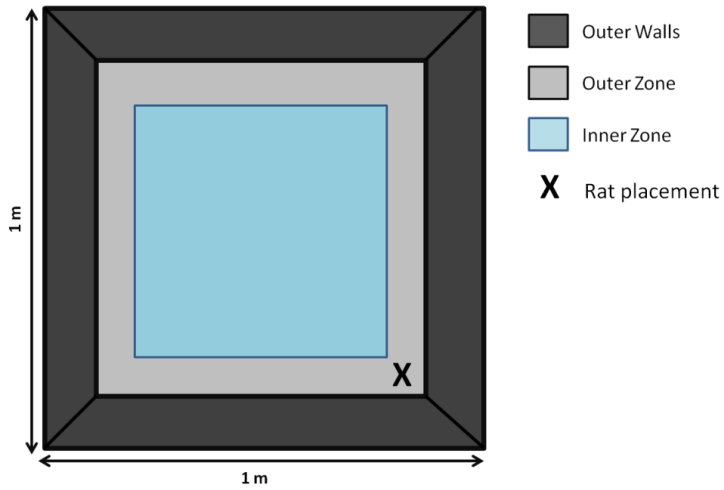

Figure 2.2: The open field test

The open field arena consists of a black box (1 m x 1 m x 50 cm). The arena was divided into an outer and inner zone, demarcated with white tape. On P25 rats were individually placed in the open field in the bottom right hand corner (**X**) and left to explore the environment for 10 minutes.

EXPOSURE TO A NOVEL OBJECT

Immediately after the OFT on P25, a novel object, a small-plastic, orange traffic cone (21.5 cm in diameter and 28 cm in height) was placed in the open field arena. The cone was placed so that it was approachable from the inner and outer zones of the open field (**Figure 2.3**). This position was kept constant for each rat. An area of 5 cm around the cone was designated the cone zone. Rats were placed back into the arena in the same manner as describe in the OFT and left to explore the environment and the cone for 5 minutes. The latency to approach the novel object and the amount of time spent in the cone zone was measured in addition to the OFT parameters described above.

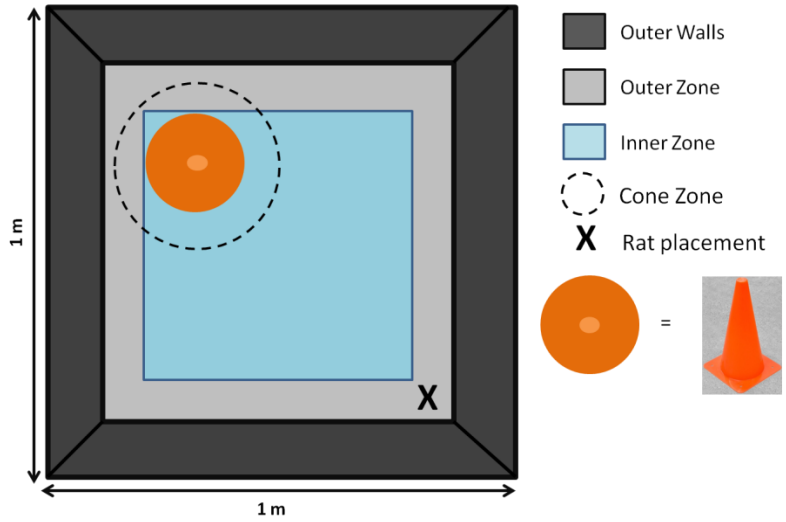

Figure 2.3: Exposure to a novel object.

After the OFT on P25, a small orange traffic cone was placed in the top left hand corner of the open field arena. The cone was approachable from both the inner and outer zones of the open field. An area around the cone was designated as the cone zone. Rats were placed back in the open field arena (**X**) and left to explore the environment and the cone for 5 minutes.

MORRIS WATER MAZE

From P26 - P30 spatial learning and memory were evaluated using the MWM. The MWM tank was 165 cm in diameter and the water (19 - 21°C) was filled up to a height of 33 cm (Vorhees and Williams, 2006; Filgueiras *et al*., 2010). The pool was divided into 4 quadrants (N, E, S and W) with external cues placed high up on the walls so that the rat could see the cues from the water level. The hidden platform (15 cm in diameter) was submerged 2 cm below the surface of the water and placed 21.5 cm from the side of the maze in the middle of the north-quadrant (**Figure 2.4**). The platform remained in the north quadrant throughout all 4 days of training (P26 - P29). Black powdered paint (non-toxic, water based) was used to colour the water to decrease the visibility of the platform and to enable Ethovision 7.0 to track the white rats against a dark background. Each rat performed four trials per day from P26 - P29. Rats were placed in the pool facing the wall of the MWM at randomly assigned starting positions. The rat had 2 minutes to reach the platform. If the rat was unable to find the platform within 2 minutes it was gently guided towards the platform. Rats had to remain on the platform for 15

seconds before being removed from the water in order to learn the position of the platform according to the localization of visual cues (Filgueiras *et al*., 2010).

For the probe trial on P30, the platform was removed from the MWM tank. Rats were individually placed in the south-quadrant and their behaviour was recorded for 1 minute. Rats were gently towel dried before being placed back in their home cages and placed under infrared lighting to completely dry before being returned to the satellite animal facility. Ethovision 7.0 was used to measure the latency to reach the platform during training and the time spent in each quadrant during the probe trial to identify impairments in spatial learning and memory.

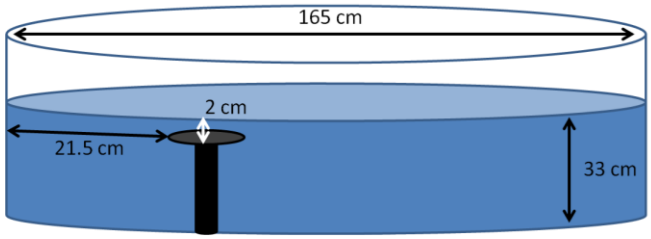

Figure 2.4: Morris water maze.

The MWM tank was 165 cm in diameter and the water was filled to a height of 33 cm. The platform was located 21.5 cm away from the side of the tank in the middle of the north-quadrant and submerged 2 cm below the surface of the water. Training in the MWM occurred daily from P26 - P29 and the probe trial took place on P30.

SACRIFICE

All rats were sacrificed without anesthesia using a rat guillotine on P31 during the light phase (between 13:00 and 15:00). Rats were habituated in a closed room next to the decapitation area one hour before sacrifice took place to decrease stress due to exposure to a novel environment. Immediately after decapitation the whole head of male **control** (saline+DMSO), **EtOH-** (EtOH+DMSO) and **vinp-** (EtOH+vinpocetine) rats as well as the whole-head of randomly selected male untreated, naïve-rats (experimental rats that did not undergo behavioural testing) rats (**saline-control; ethanol-exposed**) was submerged in liquid nitrogen for 5 seconds. This allowed for the immediate cooling of the brain in order to measure phosphorylated proteins (Makena et al., 2012). After removal of the olfactory bulb, PFC anterior to a coronal incision through the genu of the corpus callosum was rapidly removed and stored in liquid nitrogen. The remaining cortex was removed to expose the underlying hippocampus. The left and right hippocampi were gently separated from the

cortex. The dorsal one-third (DH) and ventral one-third (VH) of both left and right hippocampi were rapidly removed (Swart et al., 2017). The PFC, DH and VH were stored in liquid nitrogen until needed. The PFC and DH of control, EtOH- and Vinp-rats were used in ELISA (p. 42) and Western blot analysis (p. 45). The VH was used for proteomic analysis (*Chapter 3*, p. 68). The PFC and DH of saline-control and ethanol-exposed rats were used for proteomic analysis in *Chapter 4* (p. 89).

The remaining male *and female*, untreated, naïve-rats (**saline-control** and **ethanol-exposed)** were used in *in vitro* superfusion experiments. Immediately after decapitation whole brains were rapidly removed and placed in ice cold Krebs buffer (118 mM NaCl; 4.7 mM KCl; 1 mM NaH_2PO_4; 1.2 mM $MgCl_2$; 1.3 mM $CaCl_2$; 2.5 mM $NaHCO_3$; 11 mM $C_6H_{12}O_6$ and 0.04 mM EDTA) and used immediately in an *in vitro* superfusion analysis (p. 47)

IMMUNOASSAYS

SAMPLE PREPARATION

The PFC and DH from male **control**, **EtOH-** and **vinp**-rats were used in both ELISA and Western blot experiments. Therefore, the samples were prepared in such a way that the samples were compatible with both experimental techniques. DH and PFC tissue samples were weighed and added to 19x their weight of lysis buffer (137 mM NaCl; 20 mM Tris-HCl (ph 8.0); 1% NP-40; 10 % glycerol; 0.5 mM sodium vanadate; 1 mM phenylmethanesulfonyl fluoride solution (PMSF, Fluka); 10 µg/ml aprotinin; 1 µg/ml leupeptin) and protein inhibitor cocktail (Halt™ Protease & Phosphatase Inhibitor Cocktail, ThermoScientific). Samples were then sonnicated for 10 seconds. After sonication, samples were mixed on a vortex mixer and left to stand on ice for 20 minutes. Samples were then centrifuged at 17 200 *g* for 2 x 30 minutes at 4°C. Supernatants were collected and stored in liquid nitrogen until needed.

ELISA

BDNF E $_{max}$® ImmunoAssay System (Promega, 2 x 96 Wells, #G7610) was used to determine total free BDNF in the PFC and DH of male **control**, **EtOH-** and **Vinp**-rats. The protocol used was based on the Technical Bulletin for the products G7610 and G7611 provided by Promega (available at www.promega.com).

Ten micro-litres of anti-BDNF monoclonal antibody (mAB) was added to 9.99 ml of carbonate coating buffer (pH 9.7: 0.025 M Na_2CO_3 and 0.025 M $NaHCO_3$) to create the reagent required to coat a 96-well plate (CELLSTAR, Greiner Bio-One). One hundred microlitres of this reagent was then added to each well using a multichannel pipette (Labnet Excel^{TM} Electronic Pipette, Labnet International, Inc). The plate was then covered with parafilm and left to incubate overnight at 4°C.

Following overnight incubation, the contents of the wells were discarded and the plate was then manually washed once with TBS-T wash buffer (pH 7.6: 20 mm g Tris-HCl, 150 mM g NaCl and 0.05% Tween20) using a multichannel pipette. Two hundred micro-litres of Block and sample 1x buffer (42.4 ml of deionized water and 10.6 ml Block and sample 5x buffer stock solution) was then added to each well. The plate was then left to incubate at room temperature. This step blocks non-specific binding by covering the surface that was not covered by the anti-BDNF mAB.

Samples were diluted 19x in lysis buffer for compatibility with the Western Blot procedure and therefore samples were not diluted any further for the ELISA because samples need to fall within the range of the standard curve in order to determine accurate concentrations of BDNF present in the samples. Therefore, 100 µl of each experimental sample was added in duplicate to the plate in wells A1 - H10 (**Figure 2.5**). A 1:2 serial dilution using block and sample 1x buffer and diluted BDNF standard (500 pg/ml) was performed in duplicate in order to generate a linear standard curve from 7.8 - 500 pg/ml in wells A11 - H12 (**Figure 2.5**).

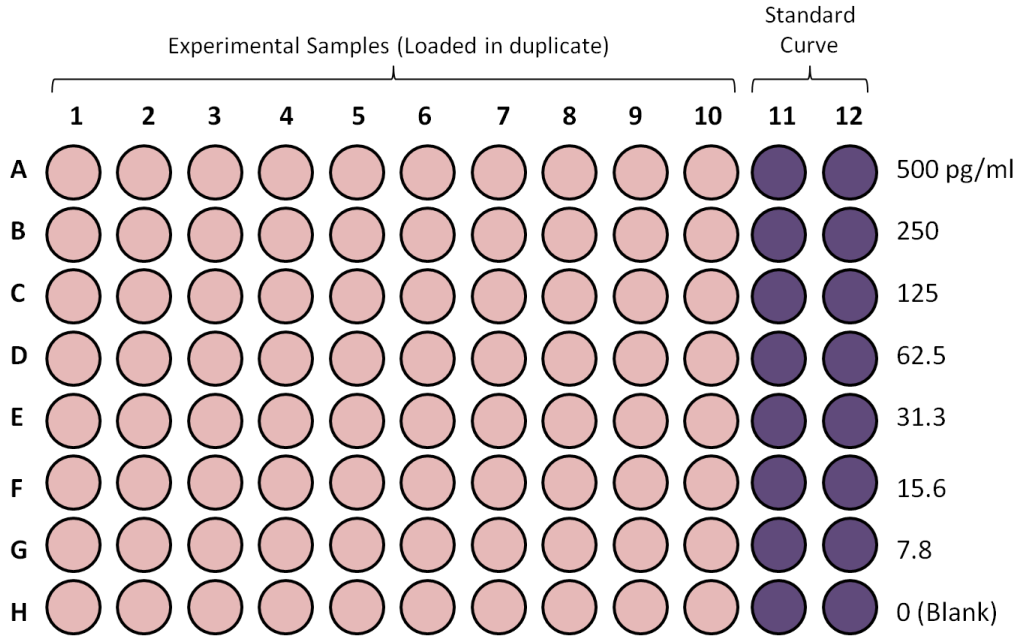

Figure 2.5: Schematic diagram of a 96-well plate showing the experimental samples and standard curve used to calculate BDNF concentration (pg/ml) in the PFC and DH.

After the addition of experimental samples and the BDNF standards, the plate was sealed with parafilm and left to incubate for 2 hours on a shaker (400 ± 100 rpm) (Vortemp 56, Labnet International, Inc) at room temperature.

Following incubation the plate was manually washed 5 times with TBS-T wash buffer. One hundred micro-litres of diluted anti-Human BDNF pAb (20 µl anti-Human BDNF pAb and 9.98 ml block and sample 1x buffer, 1:500 dilution) was then added to each well using the multichannel pipette. The plate was left to incubate for 2 hours at room temperature with shaking (400 ± 100 rpm).

After incubation the plate was washed 5 times with TBS-T wash buffer. One hundred microlitres of diluted anti-IgY HRP conjugate (50 µl anti-IgY HRP conjugate and 9.95 ml block and sample 1x buffer) was then added to each well and the plate was left to incubate at room temperature with shaking (400 ± 100 rpm) for 1 hour. This was followed by 5 manual washes with TBS-T wash buffer.

TMB One Solution (3,3' 5,5' tetramethylbenzidine) was then added to each well using a multichannel pipette. This substrate generates a blue colour when oxidized by peroxidase. The plate was placed on the shaker (400 ± 100 rpm) for 10 minutes while the blue colour developed.

The reaction was stopped by adding 100 µl of 1 M hydrochloric acid at which the colour changed from blue to yellow.

The absorbance values were recorded at 450 nm. For each 96-well plate a standard curve was constructed using the BDNF standards in wells A11 - H12 against the corresponding absorbance values (**Figure 2.6**). The BDNF concentration (pg/ml) of experimental samples was determined by the equation of the straight line generated by the standard curve and the respective absorbance value. The concentration of BDNF in the PFC was determined using the standard curve in **Figure 2.6a** and BDNF concentration in the DH was determined by using the standard curve in **Figure 2.6b**.

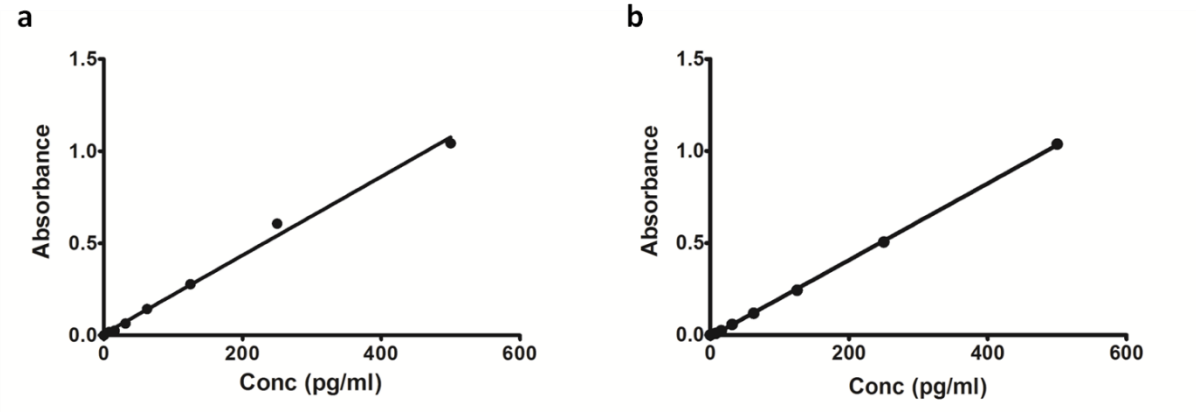

Figure 2.6: The standard curves used to calculate the concentration of BDNF in the PFC and DH

BDNF concentration (pg/ml) of experimental samples was determined by comparing the absorbance value of the experimental samples to that of the standards and reading the concentration off the respective standard curve in the (**a**) PFC and (**b**) DH.

WESTERN BLOT

Protein concentration of PFC and DH samples obtained from **control**, **EtOH**- and **Vinp**-rats was determined using the Pierce^{TM} BCA Protein Assay Kit (#23225, Thermo Scientific, Rockford, U.S.A.). Loading samples contained bromophenol blue sodium (Sigma-Aldrich), dithiothreitol (Promega, Madison, USA), lysis buffer and the respective lysate. Loading samples were boiled for 4 minutes at 97 °C, stored at -20 °C and re-boiled (4 minutes at 95 °C) then centrifuged briefly on the desk mini-centrifuge (Tomos, Laboratory Products) before use.

The optimal amount of protein (20 µg) determined during characterization was electrophoresed on 12% SDS-polyacrylamide gels for 1.5 hours (150 V) and then transferred (100 V) for 1 hour onto a Hybond nitrocellulose membrane (GE Healthcare, U.K.). The membranes were blocked overnight with 5 % bovine serum albumin (BSA) or 5 % milk and then immunolabelled with primary antibodies **(Table 2.1,** Phospho-p44/42 MAPK (Thr202/Tyr204) Rabbit mAb #4370, Cell Signalling, RRID AB_ 10234795 (P-ERK1/2): PFC 1 : 4 000 and DH 1 : 7 000; Phospho-GSK-3Beta (Ser 9)(5B3) Rabbit mAb, Cell Signalling, RRID AB_ 2115201 (P-GSK3β): PFC 1 : 4 000 and DH 1 : 2 000 ; MKP-1 (V-15): sc-119, Santa Cruz Biotechnology, Inc, RRID AB_ 2246131 (MKP-1): PFC 1 : 1 500 and DH 1 : 1 500 and Mouse monoclonal anti-synaptophysin, Abcam SY38 ab8049, RRID AB_ 444181 (Synaptophysin): PFC 1 : 60 000 and DH 1 : 60 000) against proteins of interest. Membranes were then incubated with the appropriate secondary HRP-conjugated antibodies (Goat anti-rabbit IgG (H+L)-HRP Conjugate, #170-6515, BioRad (GAR): P-ERK1/2, PFC 1 : 12 000, DH 1 : 14 000; P-GSK3β, PFC 1 : 10 000, DH 1 : 10 000; MKP-1, PFC 1 : 15 000, DH 1 : 15 000 and goat anti-mouse IgG (H+L)-HRP conjugate, #170-6515, Biorad (GAM): synaptophysin, PFC 1 : 10 000, DH 1 : 10 000). Membranes were stripped with 0.2 M NaOH for 5 minutes and immunolabelled for the respective reference protein (**Table 2.1**: (p44/42 MAPK (ERK1/2) antibody, Cell Signalling, RRID AB_ 823494 (T-ERK): PFC 1 : 2 000 and DH 1 : 2 000; GSK-3β (27C10) rabbit mAb, Cell Signalling, RRID AB_ 490890 (GSK3β): PFC 1 : 8 000 and DH 1 : 8 000; Monoclonal anti-alpha-tubulin antibody produced in mouse, T5168, Sigma-Aldrich, RRID AB_ 477579 (α-tubulin): DH 1 : 3 000 and anti-p38 MAP Kinase antibody produced in rabbit, M0800, Sigma Aldrich, RRID AB_260458 (P38): PFC 1 : 5 000). Secondary antibodies for the reference proteins were GAR: T-ERK: PFC 1 : 10 000, DH 1 : 10 000; GSK3β: PFC 1 : 14 000; DH 1 : 14 000; P38: PFC 1 : 5000 and GAM: α-Tubulin: DH 1 : 10 000). Membranes were then incubated with Clarity ^{TM} Western ECL Substrate (#170-5060, BioRad) and exposed to X-ray film (Medical X-Ray Film Blue, AGFA) to quantify the protein present. The density of each band was determined using UN-SCAN-IT Software Version 7.0 (Silk Scientific Inc, Utah, USA). The density of each band was expressed as a percentage of the mean density of all the bands representing the protein of interest on the X-ray film (pixel density percentage). The pixel density percentage of each band was then normalized to the pixel density percentage of its respective reference protein (*Pixel %*).

Table 2.1: Antibodies used for detection by Western blot.

Antibody	Abbreviation	Identifiers	MW	Concentration	
				PFC	DH
MKP-1 (V-15): sc-1199	MKP-1	Santa Cruz Biotechnology; Cat# sc-1199; RRID: AB_2246131; rabbit; polyclonal	40 kDa	1 : 1500	1 : 1500
Phospho-p44/42 MAPK (Erk1/2) (Thr202/Tyr204) (D13.14.4E) XP® Rabbit mAb	P-ERK1/2	Cell Signalling; Cat# 4370; RRID: AB_10234795; rabbit; monoclonal.	44 / 42 kDa	1 : 7000	1 : 4000
p44/42 MAPK (ERK1/2) Antibody	ERK1/2	Cell Signalling; Cat# 9102; RRID: AB_823494; rabbit, polyclonal.	44 / 42 kDa	1 : 2000	1 : 2000
Phospho-GSK-3β (Ser 9)(5B3) Rabbit mAb	P-GSK3β	Cell Signalling; Cat# 9323; RRID: AB_2115201; rabbit; monoclonal.	46 kDa	1 : 4000	1 : 2000
GSK-3β (27C10) Rabbit mAb	GSK3β	Cell Signalling; Cat# 9315; RRID: AB_490890; rabbit; monoclonal.	46 kDa	1 : 8000	1 : 8000
Mouse monoclonal [4E206] to Synaptophysin	Synaptophysin	Abcam; Cat# ab18008; RRID: AB_444181; mouse; monoclonal.	38 kDa	1 : 60000	1 : 60000
Monoclonal Anti-α-Tubulin antibody	α-Tubulin	Sigma-Aldrich; Cat# T5168; RRID: AB_477579; mouse; monoclonal.	50 kDa	-	1 : 3000
Anti-p38 MAK Kinase	P38	Sigma-Aldrich; Cat# M 0800; RRIDS: AB_260458; rabbit, monoclonal	38 kDa	1 : 5000	-

IN VITRO SUPERFUSION

The striatum of **saline-control** (n = 12 male, 11 female) and **ethanol-exposed** (n = 11 male, 12 female) rats was removed from both hemispheres after decapitation on P31 and immediately used in an *in vitro* superfusion experiment to measure the effect of early-postnatal ethanol exposure on glutamate receptor and dopaminergic function. This was done by radioactively

labeling DA stores and measuring stimulation-evoked release from dopaminergic terminals during 5-minute fractions using a method previously standardized in our laboratory (Russell, 2003; Tarr et al., 2004).

EXPERIMENTAL SET-UP

Fresh distilled water (dH_2O) was placed in large beakers in which the inlet and outlet tubes of the pump (Watson Marlow 295 S peristaltic pump, 30.5 rpm) were securely placed and the pump switched on and left to run for a few hours before the start of the experiment (**Figure 2.7**). This was done in order to remove any fluids that may have been present from previous experiments, to remove any dust that may have collected and to remove any blockages within the tubes. The water bath was also switched on early in order to allow the water to reach the desired temperature of 37 °C**.**

CHAMBER PREPARATION

Superfusion chambers were rinsed with dH_2O and then Krebs buffer before every *in vitro* superfusion experiment took place. All needles were pushed to the 0.5 ml mark and Krebs buffer added to each chamber. It was important to note that all needles were dripping in order to identify any blockages. A small cotton wool filter was pushed down on top of the needles and more Krebs buffer was added to the chambers. Again, all needles were checked for blockages by observing the drops of Krebs buffer collecting in the vials. All air bubbles were removed from the chambers. Needles were then plugged with pins and the chambers filled with Krebs buffer. The outlet tubes of the pump were later pushed down to the 0.8 ml mark after tissue slices were added to each chamber. Therefore, tissue slices were continually perfused in a volume of 0.3 ml.

CALCULATION OF FLOW RATE

The flow rate was frequently checked in order to identify any blockages within the tubes and to ensure an equal flow rate between chambers. The equipment was set up in the same way as described above however, only dH_2O was used. Empty collection vials were labeled (3 per chamber, i.e. 1.1; 1.2 and 1.3) and their weight (grams) was recorded. Collection vials were then placed in the superfusion rack and 3, 5-minute fractions of dH_2O were collected per chamber. Collection vials were then weighed again. The flow rate was calculated by subtracting the weight of the empty vial from the respective weight of the vial after the collection of dH_2O

during the 5-minute fraction. This value was then divided by 5 minutes to give a flow rate of ml/minute. The flow rate of each chamber was then represented as an average of 3 collection vials. A flow rate of 0.25 ± 0.02 ml per minute was accepted. If the flow rate of a chamber fell outside of this range the respective inlet and outlet tube was flushed with dH_2O prior to the start of an *in vitro* superfusion experiment and the chamber monitored during the experiment.

PREPARATION OF TISSUE SLICES

Four rats (2 male and 2 female) were used in each *in vitro* superfusion experiment. Rats were decapitated and whole brains were rapidly removed and immediately placed in an ice-cold solution of Krebs buffer aerated with carbogen for 15 minutes in order to maintain the pH at approximately 7.4.

The striatum was bilaterally dissected and chopped into 0.3 x 0.3 mm slices using the McWllwain Tissue Chopper and suspended in Krebs buffer containing 0.1 % ascorbic acid (incubation buffer). A 1 ml Gilson Pipette was used to break up tissue clumps. Slices were incubated in the incubation buffer for 15 minutes at 37 °C. After the 15 minute pre-incubation, 2.67 µl of radioactively labeled DA ([^{3}H]-DA, 9.25 MBq/ml, 21.2 Ci/mmol, Amersham biosciences UK limited) was added to the tissue slices. A further 15 minute incubation at 37 °C allows for the labeled [^{3}H]-DA to be taken up by the dopaminergic terminals and equilibrate with the endogenous DA. The added ascorbic acid reduces the metabolism of DA. Slices were then cooled on ice and the radioactive buffer was replaced with fresh incubation buffer. This was done in order to remove excess [^{3}H]-DA that was not taken up by the terminals. Slices were then suspended in 1 ml incubation buffer and transferred to the superfusion chambers.

GLUTAMATE- AND POTASSIUM-STIMULATED RELEASE OF [^{3}H]-DOPAMINE

Striatal slices from each brain were equally divided over 4 chambers and continually perfused with Krebs buffer (37 °C), at a flow rate of 0.25 ml per minute (Watson Marlow 295 S peristaltic pump, 30.5 rpm). The continual perfusion removed released neurotransmitter and prevented the re-uptake of [^{3}H]-DA. Slices were washed for 1.5 hours with Krebs buffer to remove any excess [^{3}H]-DA. Chambers were then manually moved to a row of discard vials and the motor was switched on. After which the collection of 5-minute fractions of eluate commenced. The motor was set to automatically move the chambers over to the next row of collection vials every 5 minutes (**Figure 2.8**).

The first 2x, 5-minute fractions established a baseline of [^{3}H]-DA release. During the 1st minute of the 3rd 5-minute fraction, [^{3}H]-DA release was evoked by exposing the tissue slices to 1 mM glutamate for 1 minute. After which a baseline release of [^{3}H]-DA was re-established during the collection of the next 3x, 5-minute fractions of eluate. During the 7th 5-minute fraction, [^{3}H]-DA release was evoked by exposing the tissue to a 25 mM potassium containing Krebs buffer solution for the 1st minute. Two subsequent 5-minute fractions of eluate were collected following potassium stimulation. During the 10th collection of eluate the inlet tubes were removed from the Krebs buffer and left to run dry. Once all the solution had been pumped through the chambers the pellet, containing the tissue slices and cotton wool filter was removed and left overnight in 0.1 M NaOH. This was done to lyse the tissue slices therefore releasing the remaining [^{3}H]-DA from the striatal tissue.

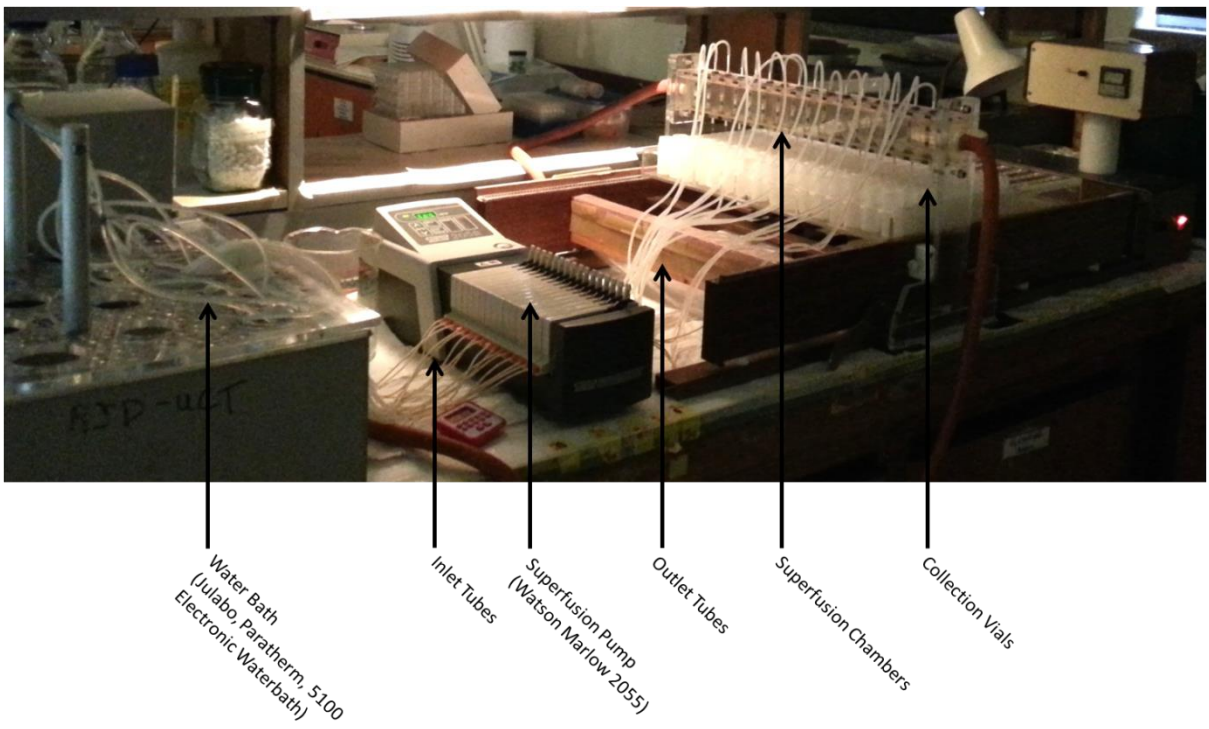

Figure 2.7: *In vitro* superfusion experimental set up.

The water bath and superfusion pump ensured that the tissue was continuously perfused with Krebs buffer (37 °C) at a flow rate of 2.5 ml/min. The outlet tubes were attached to the top of the superfusion chambers which emptied into a series of collections vials.

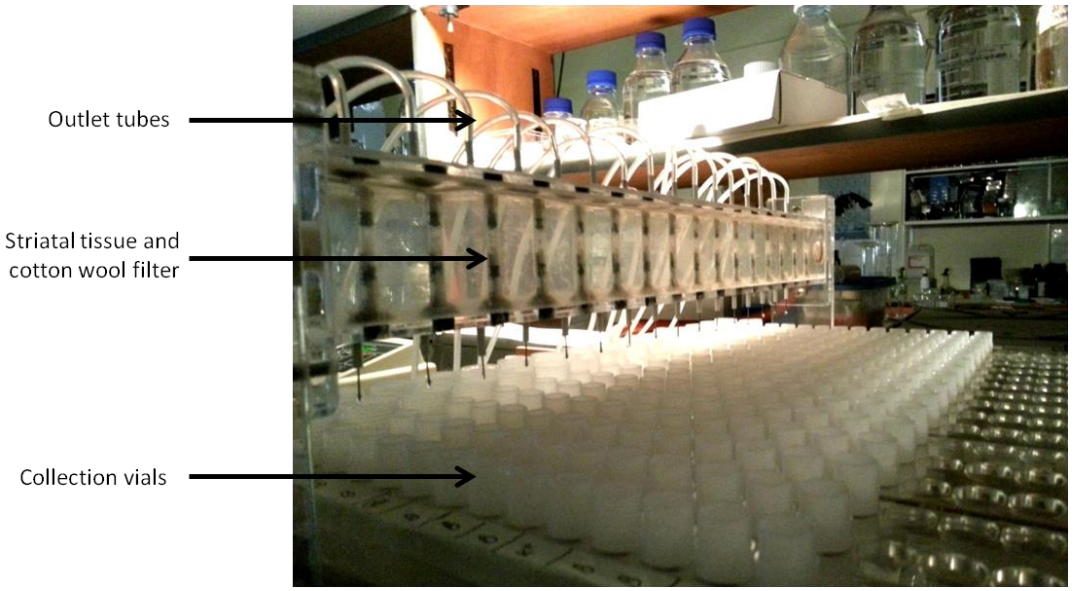

Figure 2.8: *In vitro* superfusion chambers.

Striatal tissue slices were placed on top of the cotton wool filter within the superfusion chambers. The outlet tubes were attached to the top of the superfusion chambers and allowed for the continuous perfusion of tissue slices with Krebs buffer. Superfusion chambers emptied into rows of collection vials.

CALCULATION OF FRACTIONAL RELEASE

Radioactivity in the 9 eluate fractions and the radioactivity at the end of the experiment (pellet vial) were measured using a Packard 1900 CA TRI-CARB liquid scintillation analyzer. This was done by adding 3.4 ml of scintillation fluid (Zinsser Analytic) to each vial following the overnight incubation of the pellet in 0.1 M NaOH. Vials were shaken vigorously to mix the contents in order for the energy emitted by the beta particles in the radioactive isotope [^{3}H] to transfer to the scintillation fluid in order for the radioactivity to be measured by the liquid scintillation analyzer.

The amount of radioactivity in each fraction of eluate was expressed as a percentage of the total radioactivity in that respective chamber in order to correct for the varying amount of tissue present in each superfusion chamber. Therefore the data were represented as a fractional release. To determine the amount of radioactivity released by glutamate or potassium the percentage of radioactivity in the preceding baseline eluate fraction was subtracted from the percentage evoked by the stimulation respectively. These calculations resulted in 2 stimulation peaks and were used as a representative of neurotransmitter release (**Figure 2.9**).

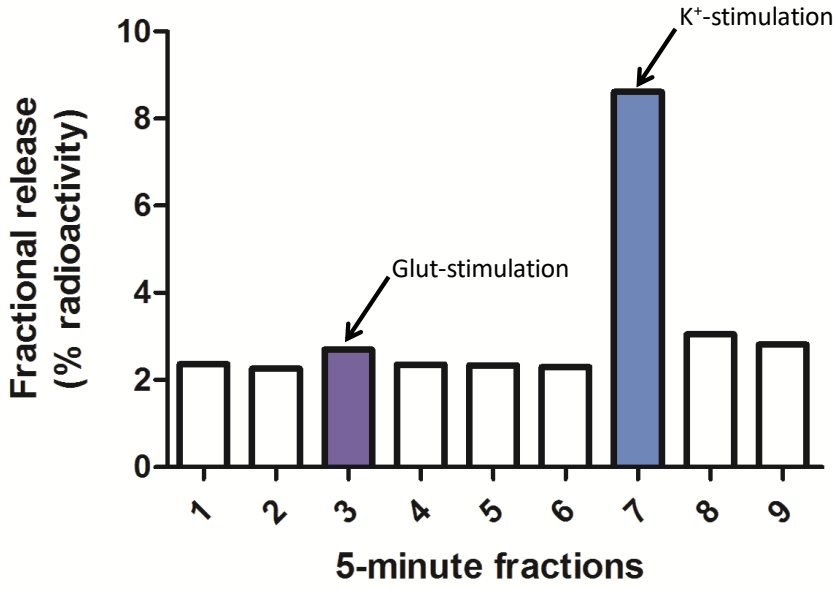

Figure 2.9: Calculation of fractional release.

The preceding baseline eluate, fraction-2 and fraction-6 for glutamate- (glut) and potassium- (K^+) stimulation respectively, was subtracted from the percentage evoked by the respective stimulation.

STATISTICS

Data collected from behavioural analysis, ELISA, Western blot and *in vitro* superfusion experiments were tested for normality using the Shapiro-Wilk test (SW). Depending on the spread of the data, normally distributed data (body weight; distance travelled in the OFT; latency to reach the platform in the MWM; time spent in the platform quadrant during the probe trial of the MWM; BDNF concentration; Western blot quantification of MKP-1, P-ERK1/2, ERK, GSK3β, P-GSK3β:GSK3β ratios, and synaptophysin in the PFC and DH; and Western blot quantification of P-ERK1/2 to ERK1/2 ratios and P-GSK3β in the DH) were analyzed by using parametric tests, which included one-way analysis of variance (ANOVA), repeated-measures ANOVA and Student t-tests followed by Duncan's post-hoc test when appropriate. If the data were not normally distributed (inner zone duration of the OFT, latency to reach the cone zone, cone zone duration, distance travelled during novel object exposure; Western blot quantification of PERK1/2 to ERK1/2 ratios, and P-GSK3β in the PFC; glutamate- and potassium-stimulated released of [^{3}H]-DA), nonparametric tests such as Friedman and the Kruskal-Wallis tests, followed by Bonferroni correction, were used when applicable. In addition, exploratory pairwise correlations were investigated to determine a possible relationship between behaviour and neurochemical measures (**Appendix A2**).

Parametric data were represented by the mean ± standard error of the mean (SEM) whereas non-parametric data were represented by the median and inter-quartile range (IQR). All data were analyzed in Statistica version 12 (StatSoft, Tulsa,OK). (**Appendix A2**, p. 270)

WEIGHT ANALYSIS

Pups were weighed daily during early-postnatal ethanol exposure from P4 - P9. Repeated-measures ANOVA showed no significant difference in weight gain between saline-control and ethanol-exposed rat pups (**Figure 2.10a**). Furthermore, Friedman ANOVA showed no significant difference in weight gain between control, EtOH- and vinp-rats from P25 - P30 during behavioural testing (**Figure 2.10b**). There was also no significant difference in body weight between experimental groups on P31, the day of sacrifice (Kruskal-Wallis, **Figure 2.10c**).

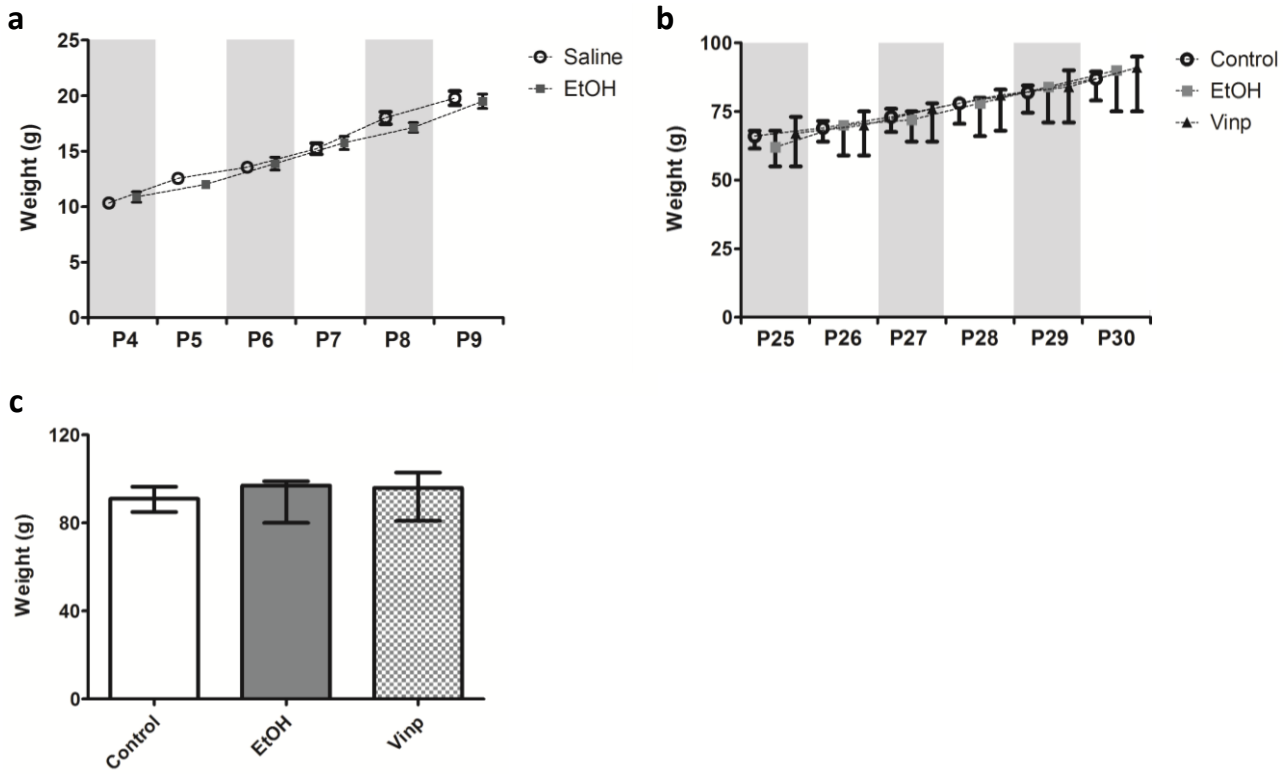

Figure 2.10: Body weight analysis.

(***a***) Weight gain during early-postnatal ethanol exposure. There was no significant difference between saline-control (n = 9 litters) and ethanol-exposed (n = 8 litters) rat pups in the amount of weight gained (repeated-measures ANOVA). The data are represented as the mean ± SEM of the average body weight per litter. (***b***) During behavioural testing from P25 - P30 there was no significant difference in weight gain between experimental groups (Friedman ANOVA). (***c***) On the day of sacrifice there was no difference in body weight (Kruskal-Wallis). The data were not normally distributed (SW, $p < 0.05$). The data represent the median and IQR.

BEHAVIOUR

OPEN FIELD TEST

The activity levels and anxiety-like behavior of **control** (n = 17), **EtOH-** (n = 11) and **vinp-** (n = 11) rats were measured on P25 in the OFT. There was no significant difference between treatment groups in the total distance moved (one-way ANOVA, **Figure 2.11a**) or in the distance moved per minute for the first 5 minutes of the OFT (repeated-measures ANOVA, **Figure 2.11b**). However, the distance travelled per minute decreased over time ($F_{(4, 337)} = 12.60$, $p < 0.0001$). There was no significant difference in the time spent in the inner zone of the open field arena between experimental groups (Kruskal-Wallis, **Figure 2.12**).

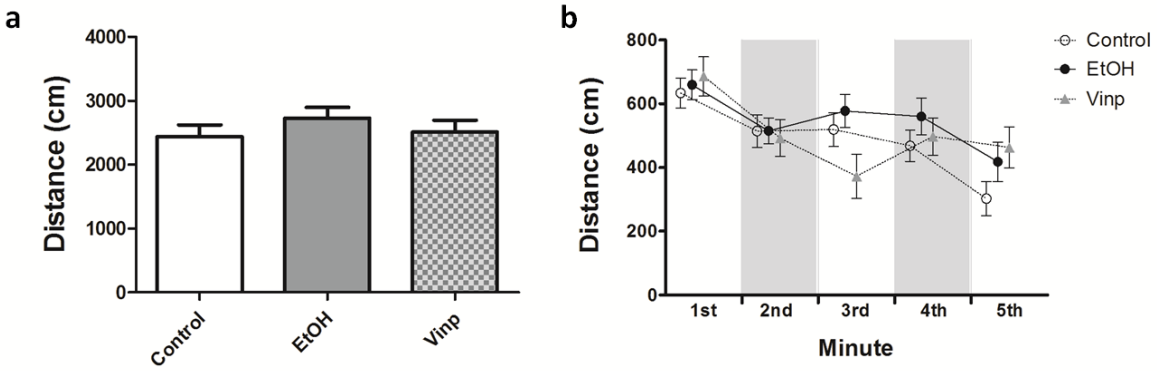

Figure 2.11: Total distance travelled and the distance traveled per minute for the first 5 minutes of the OFT.

(***a***) Distance travelled in the OFT. There was no significant difference between experimental groups (one-way ANOVA). (***b***) Repeated-measures ANOVA showed no significant difference in the distance travelled per minute for the first 5 minutes of the OFT. However, the distance travelled per minute decreased over time (Duncan's post-hoc test, $p < 0.05$). The data are normally distributed (SW, $p > 0.05$). The graphs represent the mean ± SEM. [control, n = 17; EtOH, n=11; vinp, n = 11].

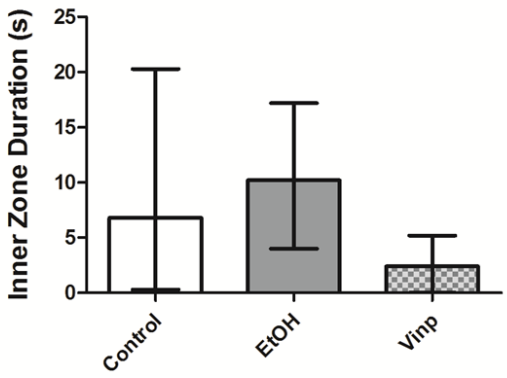

Figure 2.12: Time spent in the inner zone of the open field.

There was no significant difference between experimental groups in the amount of time spent in the inner zone of the OFT. The data were not normally distributed (SW, $p < 0.05$). The data represent the median and IQR. [control, n = 17; EtOH, n = 11; vinp, n = 11]

EXPOSURE TO A NOVEL OBJECT

Immediately after the OFT, an orange-plastic cone was placed in the open field arena. Rats were placed back in the arena and activity and exploratory-like behaviour were measured. There was no significant difference between control, EtOH- and vinp-rats in the distance travelled during the novel object (cone) test (Kruskal-Wallis). No significant difference was observed among experimental groups in the time spent in the cone zone. Further, there were no significant differences between experimental groups in latency to approach the cone zone or the frequency to enter the cone zone (Kruskal-Wallis) (**Table 2.2**).

Table 2.2: Behavioural results for the novel object (cone) test

		Distance (cm)	Cone zone duration (s)	Latency to reach the cone zone (s)	Frequency
Control	*(n = 17)*	841.25 ± 1374.77	18.00 ± 23.00	39.4 0 ± 139.80	3.00 ± 9.00
EtOH	*(n = 11)*	605.08 ± 1277.68	0.00 ± 35.80	0.00 ± 98.40	0.00 ± 8.00
Vinp	*(n = 11)*	420.28 ± 424.28	0.00 ± 0.00	0.00 ± 0.00	0.00 ± 0.00

The data are not normally distributed (SW, $p < 0.05$). The data represent the median and IQR.

MORRIS WATER MAZE

Spatial learning and memory was measured in the MWM from P26 - P30. Repeated-measures ANOVA showed no significant difference among experimental groups in the average latency to reach the platform during training in the MWM from P26 to P29 (**Figure 2.13a**). The average latency to reach the hidden platform decreased across all experimental groups from P26-28 (Duncan's post-hoc test, $p < 0.05$). During the probe trial on P30, no difference between groups in the time spent in the platform quadrant was revealed by one-way ANOVA (**Figure 2.13b**).

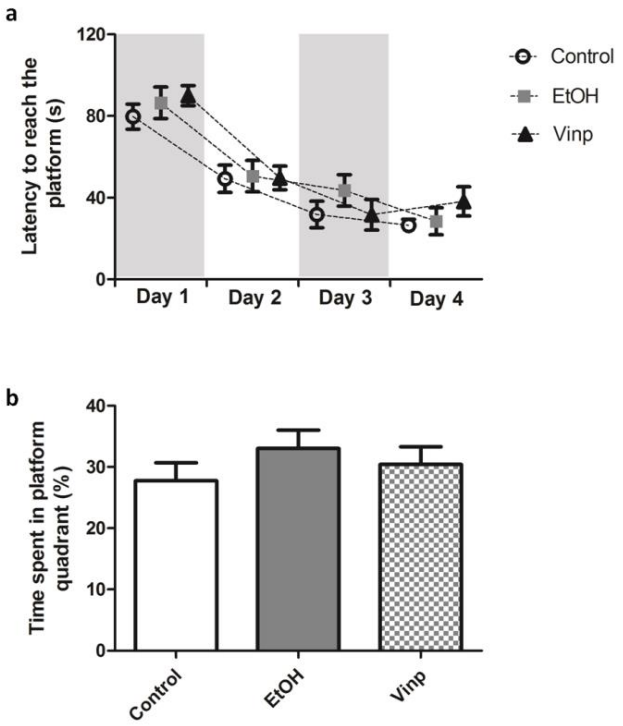

Figure 2.13: Latency to reach the platform and the percentage of time spent in the platform quadrant in the MWM

(***a***) The average latency to reach the platform during training from P26 to P29 was not significantly different between experimental groups (repeated-measures ANOVA). The latency to reach the platform decreased over training days 1-3 (Duncan's post-hoc test, $p < 0.05$). (***b***) The percentage of time spent in the platform quadrant during the probe trial. There were no significant differences between experimental groups (one-way ANOVA). The data are normally distributed (SW, $p > 0.05$). The graphs represent the mean ± SEM.

ELISA

Total free BDNF (pg/mg) was quantified in the PFC of **control** (n = 14), **EtOH-** (n = 11), and **Vinp-** (n = 11) rats and the DH of **control** (n = 15), **EtOH-** (n = 11), and **Vinp-** (n = 9) rats. One-way ANOVA revealed that there was a significant difference among experimental groups in the PFC. Vinp-rats had significantly less BDNF than control rats ($F_{(2,31)} = 5.02$, $p < 0.05$, **Figure 2.14a)**. There was no difference among treatment groups in BDNF concentration (pg/mg) in the DH (one-way ANOVA, **Figure 2.14b**).

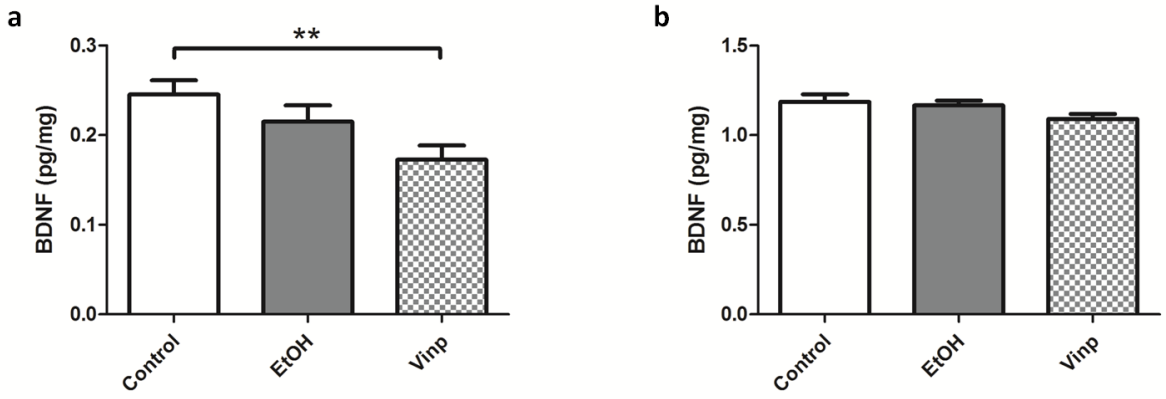

Figure 2.14: Total free brain-derived neurotrophic factor (BDNF) in the prefrontal cortex and dorsal hippocampus.

(***a***) BDNF concentration (pg/mg) in the PFC. Vinp-rats had significantly less BDNF than control rats (Duncan's-post-hoc test, $^{**}p < 0.01$). (***b***) BDNF concentration in the DH. There was no significant difference between experimental groups (one-way ANOVA). The data are normally distributed (SW, $p > 0.05$). The graphs represent the mean ± SEM.

WESTERN BLOT

MKP-1 was significantly increased in the PFC of Vinp rats (one-way ANOVA, $F_{(2,29)} = 56.4$, $p < 0.05$, **Figure 2.15a**). One-way ANOVA showed no difference among groups in MKP-1 levels in the DH (**Figure 2.15b**). In the PFC, there was no significant difference among experimental groups for levels of P-ERK1/2 (one-way ANOVA, **Figure 2.16b**). EtOH- and Vinp-rats had significantly more ERK1/2 than control rats (one-way ANOVA, $F_{(2,33)} = 5.5$, $p < 0.01$, **Figure 2.16c**), and EtOH-rats had significantly lower P-ERK1/2 to ERK1/2 ratios than control rats (Kruskal-Wallis, $H_{(2, N = 36)} = 8.1$, $p < 0.05$; **Figure 2.16d**). In the DH, there was no difference among experimental groups for the levels of P-ERK1/2 and ERK1/2 (one-way

ANOVA), whereas EtOH-rats had significantly more P-ERK1/2 relative to total ERK 1/2 than control rats (one-way ANOVA, $F_{(2, 29)} = 3.9$, $p < 0.05$; **Figure 2.16h**). In the PFC, Vinp-rats had significantly higher levels of P-GSK3β (Kruskal-Wallis, $H_{(2, N = 36)} = 7.5$, $p < 0.05$; **Figure 2.17b**) as well has higher levels of GSK3β (one way ANOVA, $F_{(2, 33)} = 4.2$, $p < 0.05$; **Figure 2.17c**) than control rats. There was no significant difference among treatment groups in P-GSK3β: total GSK3β ratios in the PFC (one-way ANOVA; **Figure 2.17d**). In the DH, P-GSK3β levels were elevated in EtOH- and Vinp-rats (one-way ANOVA, $F_{(2,33)} = 9.7$, $p < 0.05$; **Figure 2.17f**). There was no difference among groups in total GSK3β, whereas Vinp-rats had higher P GSK3β:GSK3β ratios than control and EtOH-rats in the DH (one-way ANOVA, $F_{(2,33)} = 6.2$, $p < 0.01$; **Figure 2.17h**). One-way ANOVA showed no significant difference among control, EtOH-, and Vinp-rats in synaptophysin levels in the PFC (**Figure 2.18b**). For the DH, one-way ANOVA showed that Vinp-rats had significantly more synaptophysin than control and EtOH-rats (one-way ANOVA, $F_{(2,33)} = 9.5$, $p < 0.01$; **Figure 2.18d**).

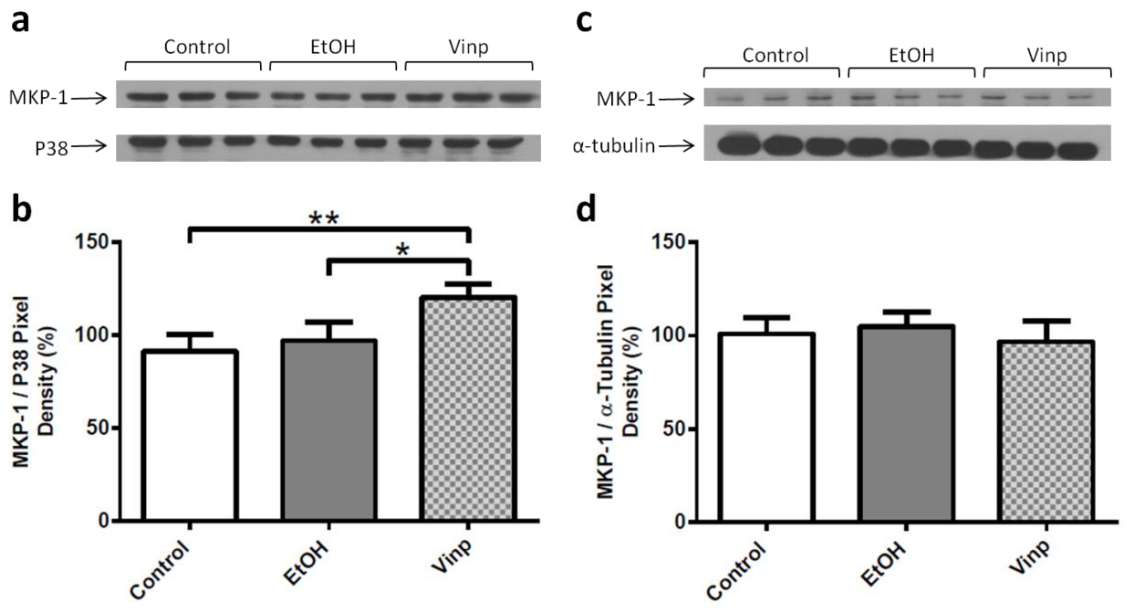

Figure 2.15: Western blot analysis of MKP-1 in the prefrontal cortex and dorsal hippocampus.

(***a***) Western blot of MKP-1 and the corresponding reference protein P38 in the PFC. (***b***) Vinp-rats had significantly more MKP-1 in the PFC compared to control and EtOH-rats (Duncan's post-hoc test, ***p* < 0.05, ****p* < 0.01). (***c***) Western blot of MKP-1 and the corresponding reference protein α-tubulin in the DH. (***d***) One-way ANOVA showed no significant differences among experimental groups. The data were normally distributed (SW, $p > 0.05$). The graphs represent mean ± SEM. [**control**, saline + DMSO (n = 11); **EtOH**, ethanol + DMSO (n = 10); **vinp**, ethanol + vinpocetine (n = 11)].

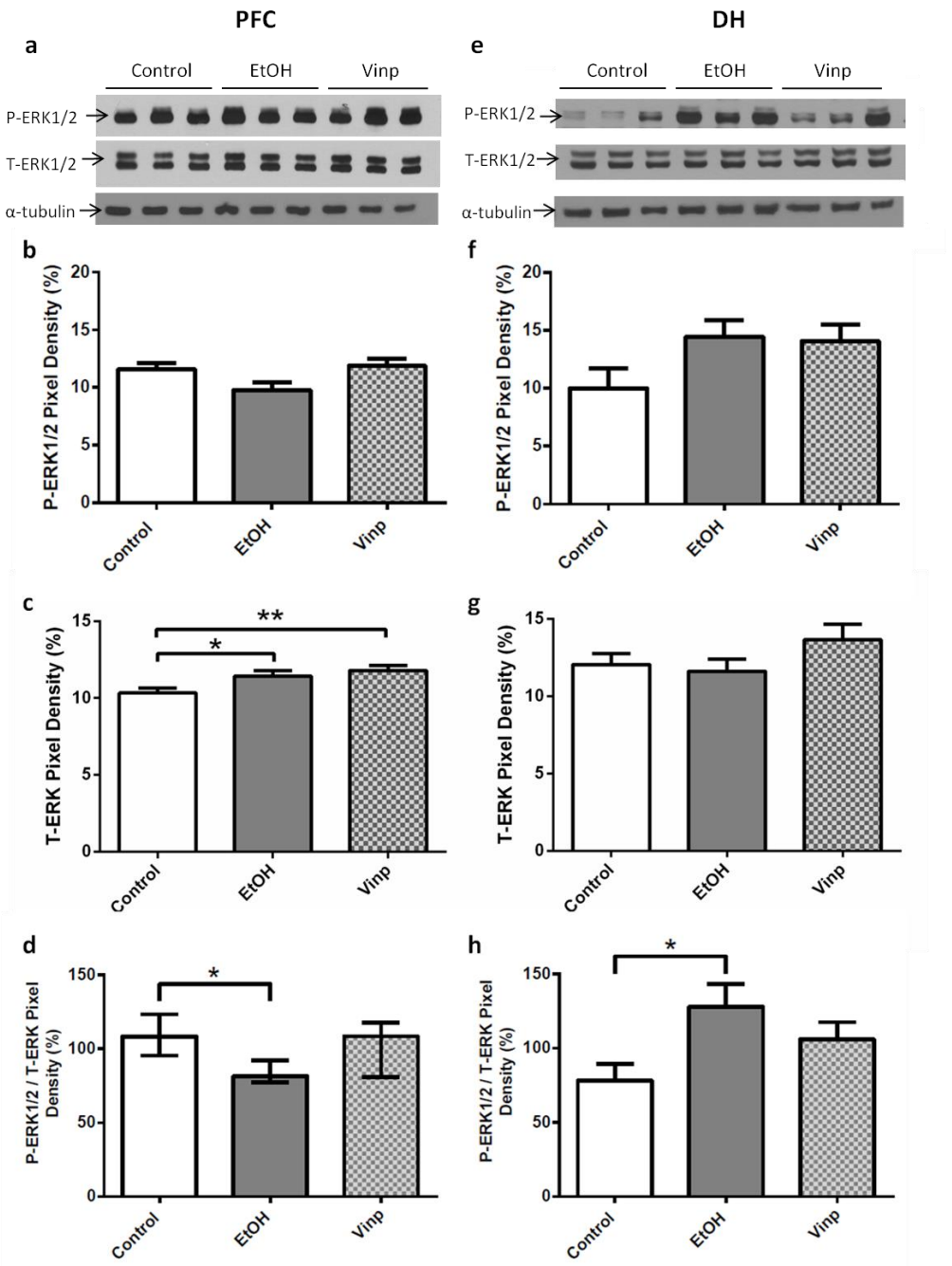

Figure 2.16: Western blot analysis of P-ERK1/2 and ERK1/2 in the prefrontal cortex and dorsal hippocampus.

(***a***) Western blot of P-ERK1/2, T-ERK and the corresponding reference protein, α-tubulin, in the PFC of **control** (n = 14), **EtOH-** (n = 11), and **Vinp-** (n = 11) rats. (***b***) Graph of P-ERK1/2 PFC. One-way ANOVA showed no significant difference among experimental groups. (***c***) Control rats had significantly less T-ERK than both EtOH- and Vinp- rats (Duncan's post-hoc test, * $p < 0.05$, ** $p < 0.01$) in the PFC. (***d***). EtOH-rats had significantly lower levels of P-ERK1/2 to T-ERK than control rats (Kruskal-Wallis, * $p < 0.05$) in the PFC. The data were not normally distributed (SW, $p < 0.05$). This graph represents the median and IQR. (***e***) Western blot of P-ERK1/2, T-ERK and the corresponding reference protein, α-tubulin, in the DH. (***f***) Graph of P-ERK1/2 in the DH. There were no significant differences among experimental groups (one-way ANOVA). (***g***) Graph of T-ERK in the DH. One-way ANOVA showed no significant differences among experimental groups. (***h***) EtOH-rats had significantly more P-ERK1/2 relative to T-ERK than control rats (Duncan's post-hoc test, * $p < 0.05$). The data were normally distributed except for those in **d** (SW, $p > 0.05$). The graphs represent the mean ± SEM. [**control**, saline + DMSO; **EtOH**, ethanol + DMSO; **vinp**, ethanol + vinpocetine].

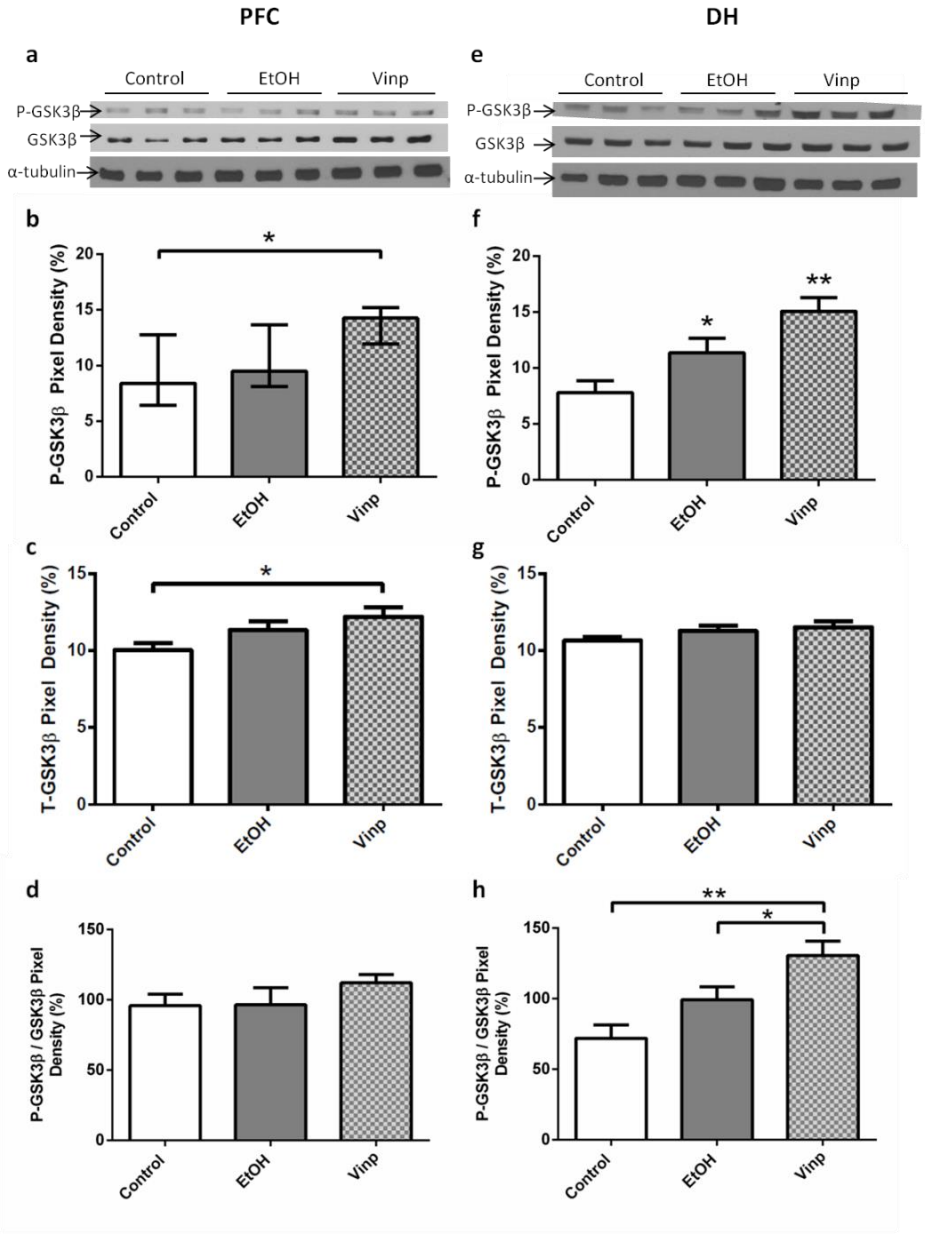

Figure 2.17: Western blot analysis of P-GSK3β and GSK3β in the prefrontal cortex and dorsal hippocampus.

(***a***) Western blot of P-GSK3β, GSK3β and the corresponding reference protein, α-tubulin, in the PFC of control, EtOH-, and Vinp-rats. (***b***) Vinp-rats had significantly more P-GSK3β than control rats in the PFC (Kruskal-Wallis, * $p < 0.05$). These data were not normally distributed (SW, $p < 0.05$). This graph represents the median and IQR. (***c***) Vinp-rats had significantly more GSK3β than control rats in the PFC (Duncan's post-hoc test, * $p < 0.05$). (***d***) One-way ANOVA showed no significant differences among experimental groups for the levels of P-GSK3β relative to GSK3β in the PFC. (***e***) Western blot of P-GSK3β, GSK3β and the corresponding reference protein, α-tubulin, in the DH of control, EtOH-, and vinp-rats. (***f***) Control rats had significantly less P-GSK3β than both EtOH- and vinp-rats (Duncan's post-hoc test, * $p < 0.05$, ** $p < 0.01$). (***g***) Graph of GSK3β in the DH. There were no significant differences among experimental groups (one-way ANOVA). (***h***) Vinp-rats had significantly more P-GSK3β relative to GSK3β than control and EtOH-rats (Duncan's post-hoc test, * $p < 0.05$, ** $p < 0.01$). The data were normally distributed except for those in **b** (SW, $p > 0.05$). Graphs represent the mean ± SEM. [**control**, saline + DMSO (n = 11); **EtOH**, ethanol + DMSO (n = 10); **vinp**, ethanol + vinpocetine (n = 11)].

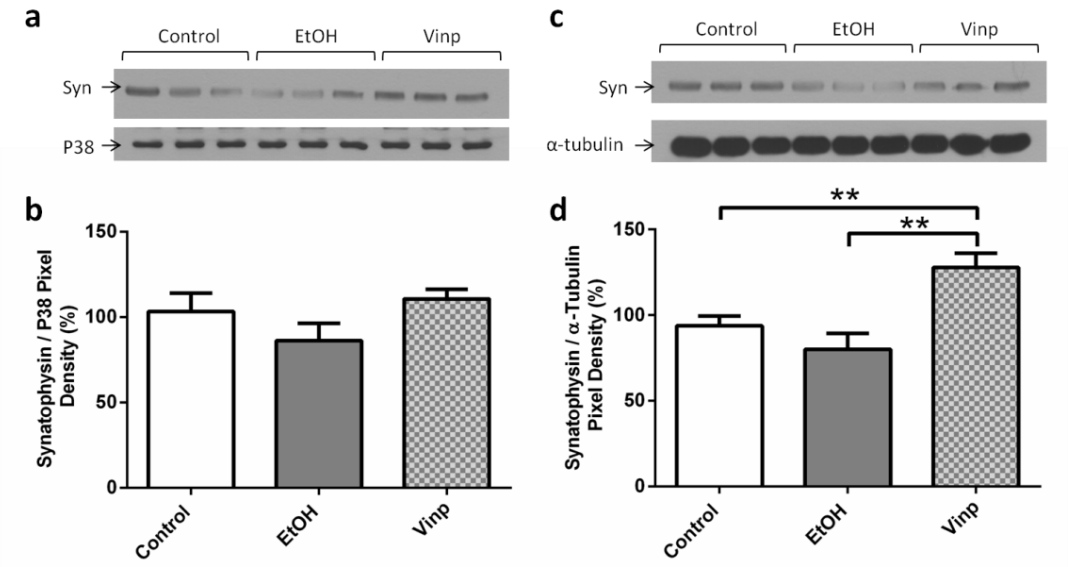

Figure 2.18: Western blot analysis of synaptophysin in the prefrontal cortex and dorsal hippocampus.

(***a***) Western blot of synaptophysin and the corresponding reference protein P38 in the PFC of control (n = 13), EtOH- (n = 11), and vinp- (n = 10) rats. (***b***) Graph of synaptophysin/ P38 in the PFC, expressed as a percentage. One-way ANOVA showed no significant differences among experimental groups. (***c***) Western blot of synaptophysin and the corresponding reference protein α-tubulin in the DH of control (n = 14), EtOH- (n = 11), and vinp- (n = 11) rats. (***d***) Graph of synaptophysin/α-tubulin in the DH. Vinp-rats had significantly more synaptophysin in the DH compared with control and EtOH-rats (Duncan's post-hoc test, ** $p < 0.01$). The data were normally distributed (SW, $p > 0.05$). The graphs represent mean ± SEM. [**control**, saline + DMSO; **EtOH**, ethanol + DMSO; **vinp**, ethanol + vinpocetine].

IN VITRO SUPERFUSION

The *in vitro* superfusion technique was used to measure the release of [^{3}H]-DA from striatal tissue of **control** (male n = 12, female n = 11) and **ethanol-exposed** (male n = 11, female n = 12) rats in response to stimulation with glutamate or potassium. Kruskal-Wallis analysis revealed no significant difference between experimental groups in the amount of [^{3}H]-DA released in response to glutamate-stimulation (Kruskal-Wallis, $H_{(3, N = 46)} = 6.92$, $p = 0.074$, **Figure 2.19a**). Further, investigation indicated a sex difference in the amount of [^{3}H]-DA released in response to glutamate-stimulation. Male rats released significantly more [^{3}H]-DA released in response to glutamate-stimulation compared to female rats (Kruskal-Wallis, $H_{(3, N = 46)} = 6.50$, $*p < 0.05$, **Figure 2.19a**).There was no significant difference between experimental groups in the amount of [^{3}H]-DA released in response to potassium stimulation (Kruskal-Wallis, **Figure 2.19b**).

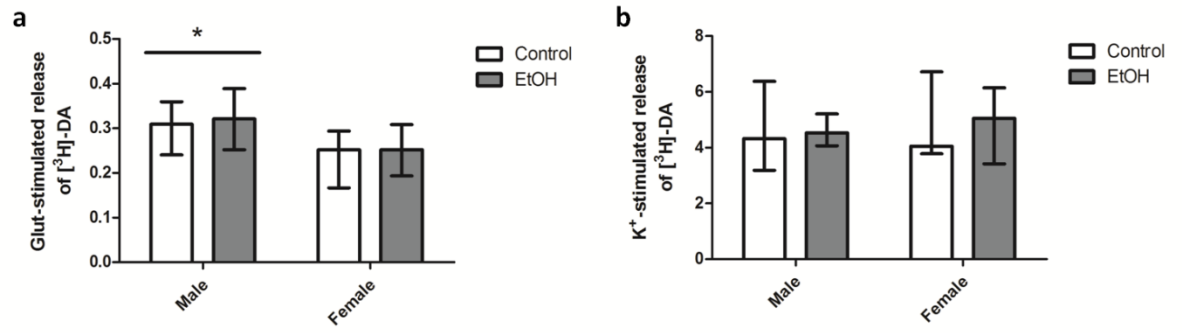

Figure 2.19: Glutamate- and potassium-stimulated release of [^{3}H]-dopamine from striatal tissue.

(**a**) Glutamate- (Glut) stimulated release of [^{3}H]-DA from striatal tissue of control (male n = 12, female n = 11) and EtOH- (male n = 11, female n = 12) rats. There was no significant difference between control and EtOH-rats (Kruskal-Wallis, $p > 0.05$). Male rats released significantly more [^{3}H]-DA in response to glut-stimulation than female rats (Kruskal-Wallis, * $p < 0.05$). (**b**) Potassium- (K^+) stimulated released of [^{3}H]-DA from striatal tissue of control (male n = 12, female n = 11) and EtOH- (male n = 11, female n = 12) rats. There was no significant difference between experimental groups (Kruskal-Wallis). The data are not normally distributed (SW, $p < 0.05$) and the graphs represent the median and IQR.

DISCUSSION

A key finding in this chapter was a significant early-postnatal ethanol-induced change in the function of the P-ERK1/2 signalling pathway in both the PFC and DH of rats that did not display overt behavioural deficits. Vinpocetine treatment of rats exposed to early-postnatal ethanol resulted in elevated MKP-1 and reduced BDNF levels in the PFC. It also reduced the effect of early-postnatal ethanol on the P-ERK1/2 signalling pathway in the PFC and DH and increased signalling via the P-GSK3β pathway in the DH. In agreement with this finding, synaptophysin, a synaptic vesicle-related protein, was increased in the DH of rats exposed to ethanol and treated with vinpocetine, consistent with suggestions that vinpocetine increases neural plasticity and dendritic spine complexity (Lantz *et al*. 2012).

EtOH-rats did not display any impairment of spatial learning and memory in the MWM. All experimental groups learned to find the hidden platform in the MWM as the latency to reach the platform decreased throughout the 4 days of training and there were no differences in the time spent in the platform quadrant during the probe trial. Early-postnatal ethanol's effect on learning and memory was not being masked by confounding factors since no difference in weight gain or activity level was observed. Body weight during early-postnatal ethanol exposure (P4 - P9) and during behavioural testing (P25 - P30) was not significantly different between experimental groups. Further, no difference in activity levels or anxiety-like behavior was observed in the OFT. No change in these parameters indicates that ethanol, administered at the dose and timing used in this study, did not have any adverse behavioural effects as reported in previous studies (in which ethanol was administered prenatally) where ethanol-exposed rats were shown to gain less weight than controls (Brocardo et al., 2012) and to exhibit hyperactivity (Kim et al., 2013) when ethanol was administered prenatally. In this study rats were housed with a single red tube as a source of environmental enrichment. Environmental enrichment has been shown to increase adult neurogenesis (Mustroph et al., 2012) and this may have rescued ethanol-induced deficits in the hippocampus and prevented spatial memory deficits (Hannigan *et al*., 1993; Nilsson *et al*., 1999; Hamilton *et al*., 2014) since previous studies have shown that binge-like exposure to ethanol during the third trimester equivalent induces spatial learning and memory deficits in the MWM (Goodlett and Peterson, 1995; Filgueiras *et al*., 2010; Banuelos *et al*., 2012).

Even though no overt learning and memory deficits were observed in the MWM, our results showed that activation of ERK1/2 (as shown by the P-ERK1/2 to ERK1/2 ratio) was significantly decreased in the PFC of EtOH-rats compared to controls. This was a novel finding and in contrast to the DH where P-ERK1/2 levels were elevated. Previous studies showed decreased levels of P-ERK1/2 in the hippocampus (Subbanna et al., 2013; DuPont et al., 2014), however, the timing and severity of ethanol exposure and pre-treatment of the animals differed from the present study. Subbanna *et al*. (2013) showed that ethanol (2 x 2.5 g/kg sc) administered on P7 caused neurodegeneration and inhibited phosphorylation of ERK1/2 for 4 to 24 hours after exposure. These authors did not determine the long-term effects of ethanol exposure. DuPont *et al* (2014) found diminished phosphorylation of ERK1/2 after trace fear conditioning in rats that had received ethanol at a dose of 5g/kg/day from P4 to P9. Our results indicate that timing is important and that the long-term effects of ethanol may be regionally specific, having opposite effects on the activity of the P-ERK1/2 pathway in PFC and DH.

Increased ERK1/2 and MKP-1 levels in the PFC may have accounted for the absence of an increase in P-ERK1/2 levels relative to total ERK1/2 in vinp-rats, since MKP-1 inhibits the phosphorylation of ERK1/2 (Davis et al., 2000; Owens and Keyse, 2007). This in turn may have resulted in the decrease in BDNF levels observed in the PFC of these rats.

Vinpocetine reduced the increase in hippocampal P-ERK1/2 observed in EtOH-rats. It also increased P-GSK3β, reducing the inhibitory activity of GSK3, thereby activating the mammalian target of rapamycin (mTOR) pathway and increasing gene transcription (Marsden, 2013). Vinpocetine is a type 1 PDE that increases levels of cAMP and cGMP levels, thereby increasing the activity of cAMP- and cGMP-dependent protein kinases. cAMP-dependent protein kinase phosphorylates many proteins including dopamine- and cAMP-regulated neuronal phosphoprotein (DARPP-32) which inhibits protein phosphatase-1, possibly accounting for the increased P-GSK3β levels observed and stimulation of the mTOR pathway. cAMP-dependent protein kinase also phosphorylates CREB which stimulates CREB-dependent transcription (Medina et al., 2006; Filgueiras et al., 2010; Nunes et al., 2011; Marsden, 2013). There are many pathways affected by increased cAMP and cGMP levels but activation of mTOR and P-CREB activation could possibly account for the increased levels of synaptophysin in the DH of vinpocetine-treated early-postnatal ethanol exposed rats. However, in line with the aim of this study there was no experimental group consisting of saline-control

rats treated with vinpocetine. Therefore, the protein alterations observed in early-postnatal ethanol exposed rats treated with vinpocetine must be interpreted with caution.

In the present study there was no evidence for early-postnatal ethanol-induced changes in glutamatergic and dopaminergic functioning in the striatum of rats exposed to early-postnatal ethanol as measured in a series of *in vitro* superfusion experiments. Differences in [^{3}H]-DA release between saline-control and early-postnatal ethanol exposed rats would have indicated the presence of impaired glutamate regulation of dopamine neurons in the striatum or a dysfunction of the dopamine neurons themselves. The striatum has functionally different areas that have been shown to release significantly different amounts of [^{3}H]-DA during *in vitro* superfusion procedures (Russell, 2003; Tarr et al., 2004). Therefore in this chapter, early-postnatal ethanol-induced effects on [^{3}H]-DA release in the striatum could have been masked because the whole striatum was used. Further, the timing of ethanol exposure may have influenced the results since Schneider *et al*. (2005) demonstrated opposing results in striatal dopamine functionality when ethanol was administered during the early- versus the late-gestational period. Ethanol administered during early-gestation resulted in blunted dopaminergic function whereas ethanol administration during late gestation resulted in heightened dopaminergic function (Schneider et al., 2005). However, we did observe a sex difference in the release of [^{3}H]-DA in response to glutamate stimulation. Adolescent female rats released significantly less [^{3}H]-DA than their male counter parts. Sex differences in dopaminergic neurotransmission may contribute to the observed sex-dependent susceptibility to ADHD. For example, males are 2-4 times more likely to develop ADHD (Andersen and Teicher, 2000).

The present study highlights the differential effects of early-postnatal ethanol exposure on the brain, the importance of timing (age of ethanol administration) and the amount of alcohol administered since this would have influenced the outcome (Livy et al., 2003; Mantha, 2013). The source of environmental enrichment (red tubes) in the housing conditions may have further influenced the results and possibly minimized ethanol-induced changes in behaviour and neural proteins. Future studies may wish to include more than one hippocampal-dependent task. Furthermore, the age at which the animals were sacrificed will also influence the results. The current study contributes to the understanding of the effects of early-postnatal ethanol exposure

on adolescent behaviour and neural proteins, providing insight into long-term early-postnatal ethanol-induced protein alterations in the rat brain.

Vinpocetine treatment of rats exposed to early-postnatal ethanol has the potential to identify novel treatment targets however more work is needed to fully elucidate the effects of early-postnatal ethanol exposure on the developing brain and resulting cognitive deficits as this chapter clearly demonstrates that not all animals exposed to early-postnatal ethanol develop overt behavioural impairments however ethanol does affect proteins closely involved in learning and memory.

CHAPTER 3: QUANTITATIVE ITRAQ AND LC-MS OF THE RAT BRAIN AFTER EARLY-POSTNATAL ETHANOL EXPOSURE AND VINPOCETINE TREATMENT

INTRODUCTION

The mechanisms underlying the cognitive and behavioural deficits observed after ethanol exposure during early-development are largely unknown. Wide-spread ethanol-induced neuronal cell death has been observed after ethanol exposure (Ikonomidou et al., 2000; Clements et al., 2012; Sadrian et al., 2012; Creeley et al., 2013) and this may contribute to the cognitive and behavioural deficits. However, little is known about functionality of the remaining neuronal networks. Resendiz *et al*. (2014) reviewed literature that suggested that ethanol affects epigenetic mechanisms during development thereby disrupting gene expression necessary for normal neuronal progression. Further, ethanol has also been shown to induce permanent changes in epigenetic mechanisms (Bekdash et al., 2013; Chater-diehl et al., 2016), thus obstructing or facilitating DNA transcription and changing protein expression. Persistent ethanol-induced epigenetic changes may ultimately reflect in the neuronal- and glial-proteome thereby altering neuronal processes.

In *Chapter 2* we investigated ethanol-induced changes in neuroplasticity-related proteins in the rat brain, such as the growth factor BDNF and proteins involved in ERK1/2- and GSK3β-signalling, using western blot analysis. However, ethanol's effect extends beyond these signalling pathways. Ethanol-induced epigenetic changes may alter the expression of many other proteins that are involved in energy metabolism, neurotransmitter signalling, redox regulation, protein metabolism and cytoskeletal structure. Western blotting is not suitable for investigating large-scale protein alterations. However, iTRAQ and LC-MS enables large-scale analysis of ethanol-induced protein changes in the brain via simultaneous identification and quantification of proteins (Aggarwal, *et al*., 2006). This high-throughput proteomic profiling technique may provide insight into the functionality of the neuronal networks after early-postnatal ethanol exposure.

In *Chapter 2*, we further hypothesized that vinpocetine would restore ethanol-induced changes in behaviour and neuroplasticity-related proteins since vinpocetine has been shown to increase blood flow and metabolic activity, as well as protect against NMDA-induced excitotoxicity,

ischemic insults and reactive oxygen species (Nivison-Smith *et al*., 2017). Vinpocetine has also been shown to increase performance on cognitive tests and restore learning and memory behaviour of animals exposed to ethanol during the early-developmental period (Filgueiras et al., 2010; Nunes et al., 2011; Lantz et al., 2012). This neuroprotective drug inhibits PDE1 activity thereby increasing levels of cAMP and cGMP. In *Chapter 2*, BDNF, MKP-1, ERK1/2, P-GSK3β, GSK3β, P-GSK3β/GSK3β and synaptophysin were altered in the PFC and/or DH of ethanol-exposed rats treated with vinpocetine. This is in agreement with inhibition of PDE1 and increased cAMP and cGMP activity. However, vinpocetine has also been shown to act as an anti-inflammatory agent via a mechanism independent of phosphodiesterase inhibition (Jean *et al*., 2010). Therefore, proteomic profiling was expected to provide further insight into the neuro-protective mechanisms of vinpocetine treatment after early-postnatal ethanol exposure.

This study used a large scale explorative approach by utilizing quantitative iTRAQ labeling and LC-MS to investigate the expression of proteins involved in energy metabolism, neurotransmitter signalling, redox regulation, protein metabolism and cytoskeletal structure in the ventral hippocampus (VH) of rats exposed to ethanol during the early-postnatal period. Further, vinpocetine was tested to determine whether it could reverse ethanol-induced protein alterations, hence providing insight into the mechanisms of this neuro-protective drug.

METHODS

ANIMALS

As describe in *Chapter 2* (p.36)

EARLY-POSTNATAL ETHANOL EXPOSURE

As described in *Chapter 2* (p. 36)

DRUG TREATMENT

As described in *Chapter 2* (p. 37). The resulting experimental groups are shown in **Figure 3.1**.

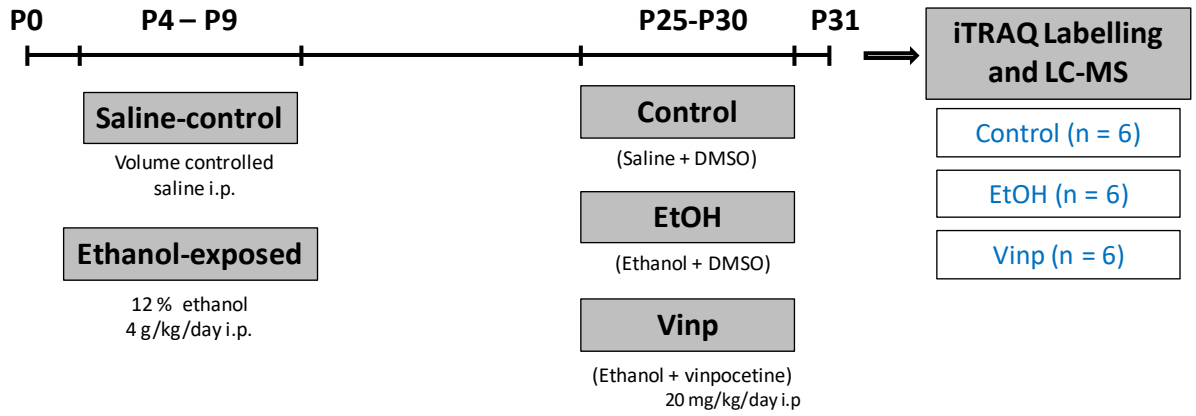

Figure 3.1: Experimental groups.

From P4 to P9 whole-litters were administered 12% ethanol (4 g/kg/day i.p.) or volume controlled saline. From P25 to P31, randomly selected ethanol-exposed rats were administered vinpocetine (20 mg/kg/day i.p.) prior to undergoing behavioural testing. The remaining ethanol-exposed and saline-control rats received volume controlled vehicle (DMSO). All rats were sacrificed on P31. For each experimental group, the ventral hippocampus from 6 male rats were pooled together for iTRAQ labeling and LC-MS.

BEHAVIOUR

The rats used in this chapter underwent behavioural testing in the open field, exposure to a novel object and in the MWM as described in *Chapter 2* from P25 - P30 (p. 37).

SACRIFICE

Animals were sacrificed as described in *Chapter 2* on P31 (p. 41). The VH was removed and stored in liquid nitrogen until later use.

PROTEOMICS

Six samples from each group were weighed (g) and pooled together accordingly (VH: control n = 6, EtOH n = 6, vinp n = 6). Samples were sonicated with triethylammonium bicarbonate (TEAB, Sigma) and Na_2CO_3 buffer (1M TEAB and 20 mM Na_2CO_3), lysozyme (100 pmol/µl) and protease inhibitor cocktail (Halt™ Protease & Phosphatase Inhibitor Cocktail, ThermoScientific). Following sonication, samples were incubated on ice for 1 hour and then centrifuged for 30 minutes at 17 200 g at 4 °C. The supernatant was removed and centrifuged a second time as before. The supernatant was then removed and kept on ice. Samples were thoroughly vortexed and split into technical triplicates (control; EtOH) or duplicates (vinp) and labeled 1 - 8. Samples were then transported on ice and handed over to the Centre for Proteomic and Genomic Research (CPGR) who carried out the methods described below.

PROTEIN DIGEST

Samples volume was adjusted using 50 mM TEAB to match protein concentration across samples. Aliquots containing 100 µg of protein were spiked with 1.5 µg β-casein (Sigma) and reduced by the addition of tris-(2-carboxyethyl)-phosphine (TCEP, Sigma) to a final concentration of 10 mM and incubated at 60 °C for 60 minutes. Methyl methane thiosulfonate (MMTS, Sigma) was subsequently added to a final concentration of 10 mM and incubated for 15 minutes at room temperature to achieve cysteine alkylation. Two vials of 20 µg modified trypsin (Promega) were each re-suspended in 20 µl MilliPore water and added to each sample in a 1:20 ratio of trypsin to protein. Samples were incubated at 37 °C for 18 hours to allow digestion to take place.

ISOBARIC TAGGING FOR RELATIVE AND ABSOLUTE QUANTITATION (ITRAQ)

Labeling of the samples with iTRAQ 8-plex (Applied Biosystems, 4390811) was performed according to the manufacturer's recommendations. Labeling occurred for 2 hours after which

2 µl aliquots of each sample were pooled together and successful labeling was confirmed. Analytical grade water (MilliPore) was added to each sample and incubated at room temperature to hydrolyse the excess labels. The 8 samples were combined, dried down (Speed Vac) and analyzed by LC-MS.

LIQUID-CHROMATOGRAPHY AND MASS SPECTROMETRY

LC−MS analysis was conducted with a Q-Exactive quadrupole-Orbitrap mass spectrometer (Thermo Fisher Scientific, USA) coupled with a Dionex Ultimate 3000 nano-HPLC system. The extracted peptide was dissolved in sample loading buffer (analytical grade water, 2.5 % acetonitrile (ACN), 0.1 % formic acid (FA)) and loaded on a C18 trap column (300 µm × 5mm ×5 µm). Chromatographic separation was performed with a C18 column (75 µm × 250 mm × 2µm). The solvent system employed was solvent A (water and 0.1% FA) and solvent B (80 % ACN and 0.1 % FA). The linear gradient for peptide separation was generated at 250 nL/minute with a gradient change from 6-18 % solvent B for 94 minutes then from 18-25% solvent B for 15 minutes.

The mass spectrometer was operated in positive ion mode with a capillary temperature of 320 °C. The applied electrospray voltage was 1.95 kV. Data were collected in the full scan mode and data-dependent MS/MS modes. In full scan mode, the maximum ion injection time was 100 ms, ions were collected in the mass range of 320-1750 m/z and acquired at a resolution of 70,000 at m/z 200.Data acquisition details are listed in **Table 3.1**.

Table 3.1: Data acquisition details

Full scan	
Resolution	70.000 (@ m/z 200)
AGC target value	3e6
Scan range	320 - 1750 m/z
Maximal injection time (ms)	100
Data-dependent MS/MS	
Inclusion	On
Resolution	17.500 (@ m/z 200)
AGC target	1e5
Maximal injection time (ms)	120
Loop count	15
Isolation window width (Da)	1
First fixed mass	100
NCE (%)	30
Data-dependent Series	
Underfill ratio (%)	1
Charge exclusion	Charge states 1.6 - 8.>8
Peptide match	Preferred
Exclusion isotopes	On
Dynamic Extinction	60

[*m/z* = mass-to-charge-ratio]

DATA ANALYSIS

The obtained MS spectra were processed with the MASCOT (Matrix Science, London, U.K.; version 2.5) search algorithm and searched against the Rattus sequence database (Source: UniprotKB-www.uniprot.org, filtered by "Organism – 'Rattus'", 10/06/2015) Search parameters are listed in **Table 3.2**. All identified peptides had an ion score above the Mascot peptide identity threshold (a high confidence score of 99% and a low false discovery rate (FDR) of 1 %). A target protein was considered identified if at least two such unique peptide matches were apparent for the protein. Protein probabilities were assigned by the Protein Proph*et al*gorithm (Nesvizhskii et al., 2003). Scaffold Q+ (version 4.4.5, Proteome Software Inc., Portland, OR) was used to quantify peptide and protein identifications.

Table 3.2: Details of search parameters

Type of search	MS / MS ion search
Quantitation	iTRAQ8plex (Applies Biosystems iTRAQ(TM) 8-plex
Enzyme	Trypsin
Fixed modifications	Methylio (C); iTRAQ8plex (N-term); iTRAQ8plex (K)
Variable modifications	Deamidated (NQ); Oxidation (M); iTRAQ8plex (Y)
Mass values	Monoisotopic
Protein mass	Unrestricted
Peptide mass tolerance	± 20 ppm
Fragment mass tolerance	± 20 mmu
Max missed cleavages	2
Instrument type	ESI-TRAP
Number of queries	97,844

[ppm = parts per million; mmu = milli mass units]

Acquired intensities in the experiment were globally normalized across all acquisition runs. Individual quantitative samples were normalized within each acquisition run. Intensities for each peptide identification were normalized within the assigned protein. The reference channels were normalized to produce a 1:1 fold change. All normalization calculations were performed using medians to multiplicatively normalize data.

Two data sets were obtained: the first compared EtOH to control (**EtOH:control**) and the second compared vinp to EtOH (**vinp:EtOH**). Data were represented as a fold change relative to the reference group. The tables list all proteins, organized into functional categories, that differed by more the 10 % (> 1.1-fold change relative to the reference group) and a fold change greater than 1.2 was used to identify differentially expressed proteins (Seshi, 2006; Unwin et al., 2006; Duthie et al., 2007; Ting et al., 2009; Williamson et al., 2016).

PROTEINS ALTERED BY EARLY-POSTNATAL ETHANOL EXPOSURE IN THE VENTRAL HIPPOCAMPUS

iTRAQ and LC-MS recognized 1 203 proteins. Of these, 32 proteins differed by 10 % (fold change greater than 1.1) in the VH of EtOH-rats versus control rats. Twenty-six of the identified proteins were downregulated (**Figure 3.2**). **Table 3.4** lists the 32 differentially expressed proteins organized into functional categories.

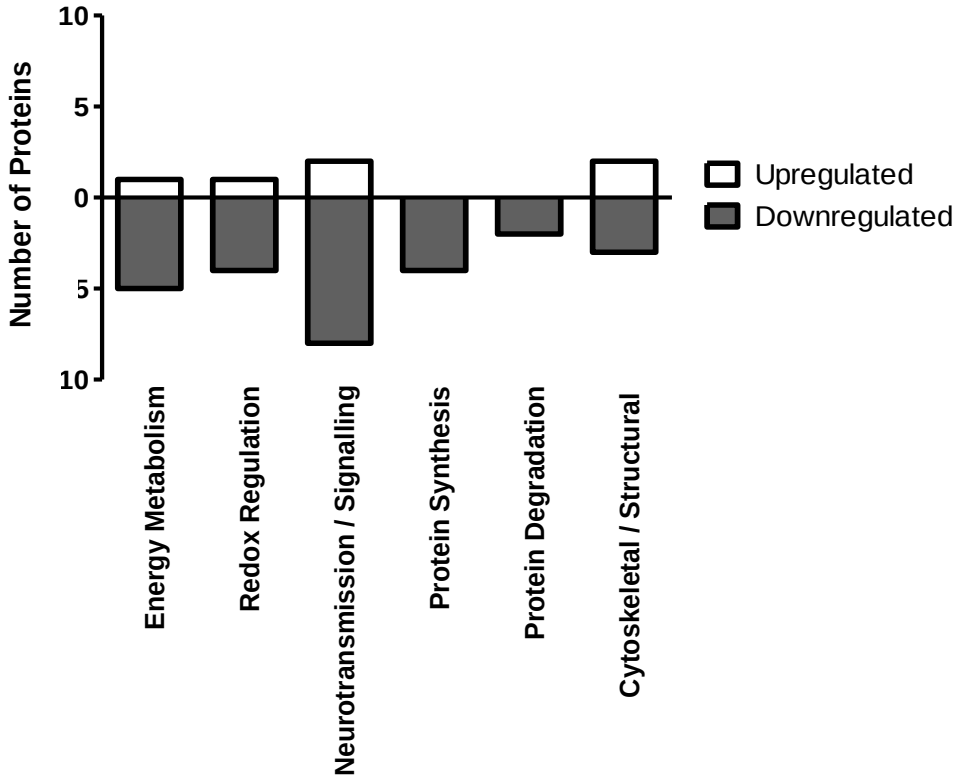

Figure 3.2: Number of upregulated and downregulated proteins (> 1.1-fold △) per functional category in the VH of EtOH-rats vs. control rats.

Ethanol exposure during the third trimester equivalent developmental stage decreased the expression of proteins related to metabolism in the VH of adolescent rats. For example, *non-specific lipid-transfer protein; mitochondrial NADH dehydrogenase [ubiquinone] 1 alpha subcomplex subunit 9*; and *mitochondrial carrier 2 protein* were downregulated in EtOH-rats versus control rats. Further, early-postnatal ethanol exposure decreased redox regulation-related proteins such as *6-phosphoglucolactonase; mitochondrial aldehyde dehydrogenase X,*

S-formylglutathione hydrolase and *glutathione S-transferase* (*protein RGD1561381)* in the VH.

Proteins related to neurotransmission were also downregulated by early-postnatal ethanol exposure in EtOH-rats compared to control rats. More specifically, *Ras-related protein Rab-3B; GTPase activating protein (SH3 domain) binding protein2; ADP-ribosylation factor GTPase-activating protein 1* and *G-protein-coupled receptor 21 (predicted), isoform CRA_a* were downregulated in EtOH-rats versus controls. *Eukaryotic translation initiation factor 3 subunit E, nucleobindin* and *CArG-binding factor A* are proteins related to the synthesis of proteins and these we downregulated in EtOH-rats versus control rats. In addition, the structure-related protein, *myelin proteolipid protein*, was also decreased in the VH of EtOH-rats compared to controls.

Ethanol exposure during the third trimester equivalent developmental stage also increased levels of several proteins in the VH compared to control rats. For example, *phosphorylase kinase-beta*, *cysteine sulfinic acid decarboxylase*, *actin beta-like 2 protein* and *thymosin beta-4* were all increased in EtOH-rats compared to controls.

Table 3.4: Proteins that differed by more than 10 % (> 1.1-fold △) in EtOH-rats relative to control rats in the VH.

Category	Protein		Accession no.	Cov (%)	Pep	EtOH : Control	Fold △	
Metabolism	**Phosphorylase kinase, beta**		**Q5RKH5**	**1.73**	**2**	**1.205**	**1.205**	↑
	Non-specific lipid-transfer protein	#	**F1LQ55**	**3.23**	**2**	**0.804**	**1.243**	↓
	Very-long-chain enoyl-CoA reductase		Q64232	10.4	3	0.874	1.145	↓
	D-beta-hydroxybutyrate dehydrogenase, mitochondrial		P29147	15.5	4	0.896	1.116	↓
	NADH dehydrogenase [ubiquinone] 1 alpha subcomplex subunit 9, mitochondrial		Q5BK63	14.1	4	0,880	1.136	↓
	Mitochondrial carrier 2		B0BN52	12.9	3	0.859	1.165	↓
Redox Regulation	Cysteine sulfinic acid decarboxylase	#	Q64611	7.10	2	1.130	1.130	↑
*(*Protein synthesis)*	**6-phosphogluconolactonase**		**G3V8D5**	**12.7**	**2**	**0.822**	**1.216**	↓
	Aldehyde dehydrogenase X, mitochondrial		G3V7I5	7.90	2	0.895	1.117	↓
	S-formylglutathione hydrolase		B0BNE5	12.8	2	0.898	1.113	↓
	Microsomal glutathione S-transferase		D3ZZQ8	34.2	3	0.851	1.175	↓
Neurotransmission / Signalling	Sodium- and chloride-dependent GABA transporter 1		P23978	4.67	2	1.136	1.136	↑
	Protein phosphatase methylesterase 1		Q4FZT2	5.70	2	1.108	1.108	↑
	Ras-related protein Rab-3B	#	Q63941	36.5	3	0.884	1.131	↓
	GTPase activating protein (SH3 domain) binding protein 2	#	Q6AY21	5.57	2	0.854	1.171	↓
	ADP-ribosylation factor GTPase-activating protein 1	#	Q62848	4.10	2	0.845	1.183	↓
	G protein-coupled receptor 21 (Predicted), isoform CRA_a	#	D3ZX42	2.91	2	0.842	1.188	↓
	Protein Sbf1 - SET binding factor		D3ZNN0	1.50	2	0.825	1.212	↓
	Ectonucleotide pyrophosphatase/phosphodiesterase family member 6		B0BND0	9.55	3	0.839	1.192	↓
	Vesicle-associated membrane protein 1 (Fragment)		F1M9V2	34.8	2	0.835	1.197	↓
*(*Energy Metabolism)*	Neurolysin, mitochondrial		P42676	2.84	2	0.877	1.141	↓
Protein Synthesis	**Eukaryotic translation initiation factor 3 subunit E**	#	**Q641X8**	**11.2**	**3**	**0.791**	**1.265**	↓
	Nucleobindin-1	#	Q63083	5.66	2	0.809	1.237	↓
	CArG-binding factor A	#	Q9QX80	20.7	4	0.900	1.111	↓
	Protein Vbp1 - Prefoldin subunit 3		M0R919	25.4	2	0.886	1.128	↓
Protein Degradation	Calpain small subunit 1		M0RD20	12.8	2	0.893	1.120	↓

Category	Protein		Accession no.	Cov (%)	Pep	EtOH : Control	Fold △	
	Aspartyl aminopeptidase		Q4V8H5	11.4	3	0.865	1.156	↓
Cytoskeletal / Structural	Protein Actbl2 - Actin, beta-like 2		D3ZRN3	33.2	2	1.224	1.224	↑
	Thymosin beta-4		P62329	29.5	2	1.103	1.103	↑
	Myelin proteolipid protein	**#**	**P60203**	**18.8**	**5**	**0.787**	**1.271**	↓
	Protein Mtmr1 - myotubularin related protein 1		D3ZKK5	6.33	3	0.894	1.118	↓
	Protein Surf4 - Surfeit 4, isoform CRA_a		D4A1D8	12.6	2	0.876	1.142	↓

[The number of exclusive unique peptides (Pep) represents the number of unique peptide sequences associated with that protein. The coverage percentage (Cov %) indicates the number of identified amino acids associated with that protein represented as a percentage of the total number of amino acids in that protein.(***** proteins play a role in more than one functional category; **#** protein expression reversed by vinpocetine treatment; red indicates a fold change great than 1.2 (20 %))]

Of the 1 203 proteins identified by iTRAQ and LC-MS, 22 proteins differed by 10 % (fold change greater than 1.1) in the VH of Vinp-rats versus EtOH-rats. Eighteen out of the 22 differentially expressed proteins were upregulated (**Figure 3.3**). **Table 3.5** lists the 22 differentially expressed proteins organized into functional categories.

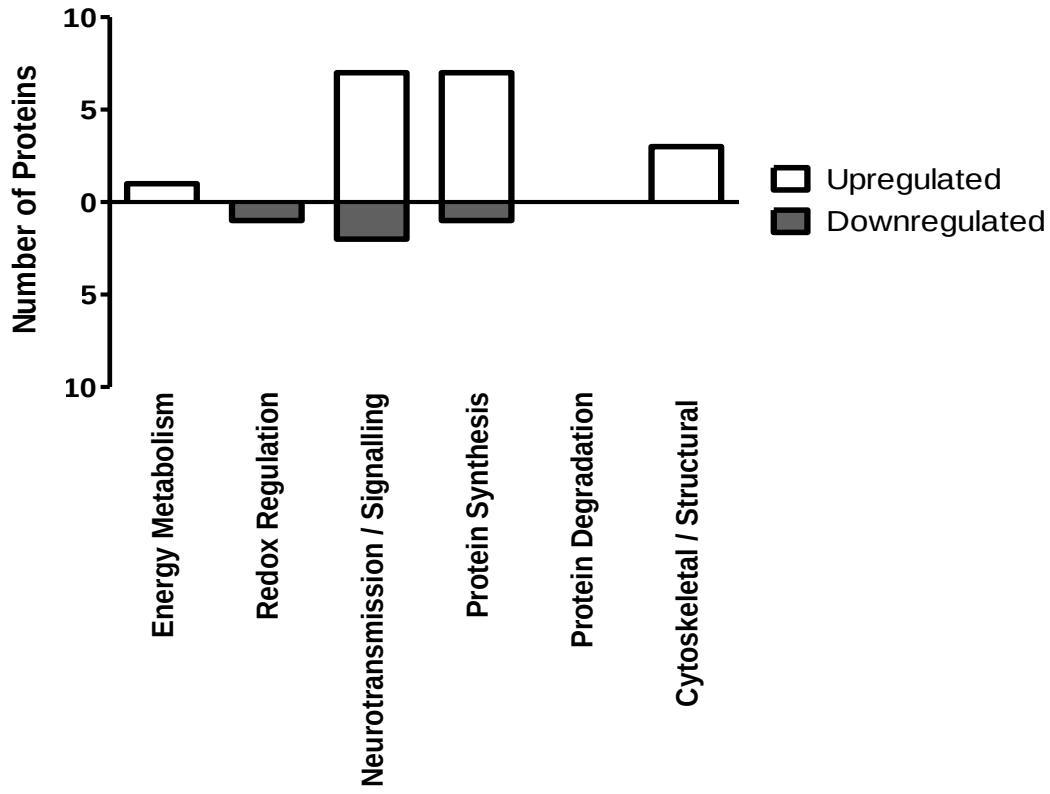

Figure 3.3: Number of upregulated and downregulated proteins (> 1.1-fold △) per functional category in the VH of vinp-rats vs. EtOH-rats.

Vinpocetine treatment of early-postnatal ethanol exposed rats had opposite effects on protein expression than early-postnatal ethanol exposure alone. Vinp-rats had higher levels of non-specific lipid-transfer protein than EtOH-rats. Further, *Ras-related protein Rab-3B; GTPase activating protein (SH3 domain) binding protein2; ADP-ribosylation factor GTPase-activating protein 1* and *G-protein-coupled receptor 21 (predicted), isoform CRA_a* were increased in vinp-rats compared to EtOH-rats. The protein synthesis-related proteins *eukaryotic translation initiation factor 3 subunit E, nucleobindin* and *CArG-binding factor A* were increased in vinp-rats relative to EtOH-rats. Myelin proteolipid protein was also now increased in vinp-rats

compared to EtOH-rats. In addition, vinp-rats showed greater levels of the *sodium -driven chloride bicarbonate exchanger* and *adenosine kinase* compared to EtOH-rats.

Table 3.5: Proteins that differed by more than 10 % (> 1.1-fold △) in Vinp-rats relative to EtOH-rats in the VH.

Category	Protein		Accession no.	Cov (%)	Pep	Vinp : EtOH	Fold △	
Metabolism	**Non-specific lipid-transfer protein**	#	**F1LQ55**	**3.23**	**2**	**1.377**	**1.377**	↑
Redox Regulation	Cysteine sulfinic acid decarboxylase	#	Q64611	7.10	2	0.884	1.132	↓
Neurotransmission / Signalling	**Sodium-driven chloride bicarbonate exchanger**		**D3ZGB5**	**3.91**	**2**	**1.300**	**1.300**	↑
	Ras-related protein Rab-3B	#	**Q63941**	**36.5**	**3**	**1.313**	**1.313**	↑
	ADP-ribosylation factor GTPase-activating protein 1	#	**Q62848**	**4.10**	**2**	**1.313**	**1.313**	↑
	Adenosine kinase		Q64640	9.14	2	1.177	1.177	↑
	G protein-coupled receptor 21 (Predicted), isoform CRA_a	#	D3ZX42	2.91	2	1.127	1.127	↑
	Guanine nucleotide-binding protein G(o) subunit alpha		P59215	55.6	16	1.117	1.117	↑
	GTPase activating protein (SH3 domain) binding protein 2	#	Q6AY21	5.57	2	1.114	1.114	↑
*(*Lipid Metabolism)*	SEC14-like 2 (S, cerevisiae)		Q5EBD0	11.9	3	0.875	1.143	↓
	Phosphatidylinositol 4-kinase alpha (PI4KA)		F1LRW9	1.27	2	0.881	1.135	↓
Protein Synthesis	**CArG-binding factor A**	#	**Q9QX80**	**20.7**	**4**	**1.258**	**1.258**	↑
	Nucleobindin-1	#	Q63083	5.66	2	1.146	1.146	↑
	Eukaryotic translation initiation factor 3 subunit E	#	Q641X8	11.2	3	1.136	1.136	↑
	Dolichyl-diphosphooligosaccharide--protein glycosyltransferase subunit 1		P07153	8.93	4	1.111	1.111	↑
	40S ribosomal protein S7		P62083	47.4	6	1.111	1.111	↑
	CHMP family, member 7 (Predicted), isoform CRA_a		D4A7H9	6.67	2	1.106	1.106	↑
	40S ribosomal protein S12		D3ZHB3	24.4	3	1.102	1.102	↑
	U5 small nuclear ribonucleoprotein 200 kDa helicase		F1LNJ2	1.40	2	0.899	1.112	↓
Cytoskeletal / Structural	**Protein Dsp - desmoplakin**		**F1LMV6**	**0.69**	**2**	**1.256**	**1.256**	↑
	Microtubule-associated protein RP/EB family member 1		Q66HR2	38.1	6	1.123	1.123	↑
	Myelin proteolipid protein	#	P60203	18.8	5	1.105	1.105	↑

[The number of exclusive unique peptides (Pep) represents the number of unique peptide sequences associated with that protein. The coverage percentage (Cov %) indicates the number of identified amino acids associated with that protein represented as a percentage of the total number of amino acids in that protein. (***** proteins play a role in more than one functional category; **#** protein expression reversed by vinpocetine treatment; red indicates a fold change great than 1.2 (20 %))]

DISCUSSION

In the present study we investigated early-postnatal ethanol-induced protein changes and the effect of vinpocetine treatment in the VH of adolescent rats exposed to ethanol during the third trimester equivalent neurodevelopmental stage. Exposure to ethanol during the early-postnatal period minimized the expression of proteins related to energy metabolism, redox regulation, signalling, protein metabolism and cytoskeletal structure in the VH compared to control rats. Importantly, vinpocetine treatment reversed several ethanol-induced changes in protein expression.

Exposure to early-postnatal ethanol downregulated metabolism-related proteins such as mitochondrial non-specific lipid-transfer protein, NADH dehydrogenase [ubiquinone] 1 alpha (subcomplex subunit 9) (NDUFA9), and mitochondrial carrier 2 in the VH. Non-specific lipid-transfer protein regulates peroxisomal fatty acid β-oxidation (Wouters et al., 1998) and NADH dehydrogenase [ubiquinone] 1 alpha (subcomplex subunit 9) is an accessory subunit of the mitochondrial respiratory chain involved in energy production (Hüttemann et al., 2012). The molecular mechanisms underlying the effects of ethanol exposure during the third trimester equivalent developmental stage of rodent models are largely unexplored in the literature. However, previous studies in which ethanol was administered prenatally, showed a decreased number and volume of mitochondria as well as a reduction in respiratory chain activity and decreased ATP synthase in the cerebrum of mice foetuses exposed to ethanol from GD6 to GD15 (Xu et al., 2005). In addition, decreased ATP production was observed in cultured cerebellar neurons obtained from P1 Long-Evans rat pups exposed to gestational alcohol (Chu et al., 2007). Further, proteomic analysis of brain tissue exposed to ethanol during development has not fully been investigated. However, a study by Sari *et al*. (2010) used a label-free proteomics technique and identified mitochondrial-related proteins in foetal mice brains exposed to prenatal-ethanol (pregnant dams were fed a 25% ethanol-derived liquid diet) from GD7 - GD13. In agreement with our results, Sari *et al*. (2010) found decreased levels of NADH dehydrogenase [ubiquinone] alpha subunit 9 and similarly decreased levels of mitochondrial carrier 1. These previous studies demonstrated the sensitivity of mitochondria to ethanol and the short-term effects of ethanol exposure during early development on the capacity for energy production in the rat brain. Results presented in the present study suggest that early-postnatal ethanol exposure induces persistent effects that may reduce the capacity for energy production in the long-term.

In the VH, 6-phosphogluconolactonase, was decreased in EtOH-rats compared to controls (> 1.2-fold change). Six-phosphogluconolactonase is involved in the pentose phosphate pathway and NADPH generation (Kruger and Von Schaewen, 2003). NADPH is used to generate glutathione (GSH) to combat reactive oxygen species (Magistretti and Allaman, 2015). Therefore, decreased activity of the pentose phosphate pathway may indicate an increased susceptibility to oxidative stress in the VH of EtOH-rats due to decreased capacity to generate GSH. Further, S-formylglutathione hydrolase and glutathione S-transferase were decreased by more than 10% in the VH of rats exposed to early-postnatal ethanol compared to controls. S-formylglutathione hydrolase increases levels of GSH whereas glutathione S-transferase decreases levels of GSH (Dringen, 2000; Haslam et al., 2002; Laborde, 2010). However, glutathione S-transferase decreases levels of GSH via S-glutathionylation, a cysteine posttranslational modification involving the addition of GSH to target proteins through disulfide bonds. S-glutathionylation provides protection against further oxidative stress-induced damage (Townsend et al., 2009). Hence, our results may suggest decreased capacity to protect against oxidative stress due to low GSH production and a low capacity to further use GSH in S-glutathionylation via glutathione S-transferase. GSH has previously been shown to be susceptible to effects of ethanol when ethanol has been administered prenatally. Decreased levels of GSH were observed in whole embryo cultures obtained from SD dams after gestational alcohol exposure (Jilek et al., 2015). In addition, decreased levels of GSH and increased lipid peroxidation were also observed in the brain of adult SD rats exposed to prenatal-ethanol (Patten et al., 2013b). These results in conjunction with results from the current study indicate the potential for oxidative stress and a shift from the normal cellular redox-state in the brain after early-ethanol exposure. The possible shift from the normal intracellular redox state may be as an indirect result of ethanol-induced dysregulation of mitochondrial function as suggest by Brocardo *et al*. (2011). A normal cellular redox environment is important for cellular processes and a disruption may lead to increased reactive oxygen species and therefore oxidative damage to DNA and proteins (Oktyabrsky and Smirnova, 2007). In addition, the redox environment may affect redox-sensitive protein kinase activity (Corcoran & Cotter *et al* 2013) and therefore altered redox state may lead to irregular cell signalling processes. Specifically, S-glutathionylation occurs in response to conditions of oxidative stress and results in the conjugation of GSH to target proteins which can alter their structure, function and cellular location (Xiong et al., 2011). Therefore, S-glutathionylation of

kinases, phosphatases and transcription factors can change cell signalling processes and may serve as a regulator of signal transduction pathways. Of particular interest, upstream regulators of P-ERK signaling are susceptible to S-glutathionylation. For instances, PKA is inactivated and the activity of Ras is increased after S-glutathionylation (Xiong et al., 2011). Inactivation of PKA which is activated by cAMP, will limit transcription and the potential for neural plasticity, whereas increased Ras activity may promote cellular proliferation (Xiong et al., 2011).

Early-postnatal ethanol exposure decreased levels of myelin proteolipid protein in the VH. Myelin proteolipid protein associates with myelin basic protein and plays a role in maintaining the myelin sheath. Myelination of axons is essential for rapid conduction of electrical signals necessary for optimal functioning. Importantly, myelin provides metabolic support and decreases the energy-cost of signal transduction (Bercury and Macklin, 2015). Previous studies have shown decreased myelin proteolipid protein mRNA expression in the hippocampus of adult SD rats exposed to chronic-ethanol (Lee et al., 2010) which may indicate the susceptibility of myelin proteolipid protein to ethanol-induced changes. In addition, rats exposed to the combination of prenatal- and early-postnatal ethanol showed delayed myelination and reduced myelin thickness of the optic nerve on P5, P10, and P15 (Phillips et al., 1991) and adult mice exposed to early-postnatal alcohol had decreased myelin basic protein in the corpus callosum (Newville et al., 2017). Interestingly, oligodendrocytes in spinal cord cultures obtained from ERK1/2 double-knock-out mice had lower levels of proteolipid protein and myelin basic protein (Ishii et al., 2012). The authors suggested that activation of ERK1/2 signalling in oligodendrocytes results in the expression of a specific cohort of genes involved in myelination. However, in *Chapter 2* we quantified ERK1/2 in the DH of the rats used in this current study and found increased levels of P-ERK1/2 to ERK1/2 in rats expose to early-postnatal ethanol. Therefore, our results do not correlate with those found by Ishii *et al*. (2012). Future studies may determine whether decreased myelin related-proteins, myelin sheath deficiencies and possibly altered conductive properties of axons occur in rats exposed to early-postnatal ethanol that display learning and memory and/or other overt behavioural deficits.

As shown, several proteins were downregulated in EtOH-rats. However, EtOH-rats also showed increased levels of phosphorylase kinase β (> 1.2-fold), cysteine sulfinic acid carboxylase, actin beta-like 2 and thymosin beta-4 (> 1.1-fold) compared to control rats. Phosphorylase kinase β activates glycogen phosphorylase necessary for glycogen metabolism (Shenolikar et al., 1979). Cysteine sulfinic acid carboxylase plays a role in taurine production which has a wide range of beneficial functions in the central nervous system (Ripps and Shen, 2012) Actin beta-like 2 protein in involved in cytoskeletal structure and integrity, including the shape of dendritic spines (Lei et al., 2016). Thymosin beta-like 2 promotes cell migration, differentiation and survival (Crockford et al., 2010). Interestingly, thymosin-beta 4 has been shown to be elevated in the hippocampus of C57BL/6 mice exposed to early-postnatal ethanol (4 g/kg/day) from P4 - P9 in conjunction with increased levels of P-ERK1/2 compared to controls (Zhang et al., 2016). This result is in agreement with the present study and we have previously observed increased levels of P-ERK1/2 to ERK1/2 in the DH of these rats (*Chapter 2*). Increased levels of the above mentioned proteins may indicate possible compensatory mechanisms in the rat brain after early- postnatal ethanol exposure.

In this study, vinpocetine treatment of rats to exposed early-postnatal ethanol reversed several ethanol-induced protein changes. Myelin proteolipid protein was restored in Vinp-rats as well as non-specific lipid-transfer protein. In addition, the membrane associated signalling proteins ras-related protein Rab-3B, ADP-ribosylation factor GTPase-activating protein 1 (>1.2-fold), GTPase activating protein (SH3 domain) binding protein 2 and G-protein coupled receptor 21 (>1.1-fold) were upregulated in Vinp-rats versus EtOH-rats pointing to restored cellular signalling. Protein synthesizing proteins such as CArG-binding factor A, nucleobindin-1, an eukaryotic translation initiation factor 3 subunit E, were also increased in Vinp-rats compared to EtOH-only rats. Our results are in agreement with previous studies in which vinpocetine is suggested to increase levels of cAMP and cGMP via PDE inhibition thereby activating intracellular-signalling cascades and subsequently transcription factors such as CREB and the serum response factor (SRF) (Medina, 2011) and hence increasing protein synthesis. Vinpocetine has been shown to restore plasticity in the visual cortex and behavioural deficits observed after exposure to ethanol during early development (Filgueiras et al., 2010; Nunes et al., 2011; Lantz et al., 2012).

In addition to restoring several ethanol-induced changes, vinp-rats had greater levels of the sodium driven chloride bicarbonate exchanger 1 and adenosine kinase. The sodium driven chloride bicarbonate exchanger mediates GABA signalling and maintains pH (Sinning et al., 2011). In response to increased levels of adenosine, adenosine kinase phosphorylates adenosine to form AMP (Park and Gupta, 2013). Vinpocetine increase levels of cAMP, through PDE inhibition, thereby decreasing levels of AMP therefore increased adenosine kinase may represent a compensatory mechanism to restore levels of AMP. However, more evidence is needed.

This study was limited by the number of identified proteins (> 1.1-fold) in the VH of EtOH-rats versus control (32 proteins) and the VH of Vinp-rats versus EtOH-rats (22 proteins). For instance, the current proteomic profiles of the VH did not detect the proteins quantified in *Chapter 2*. In addition, this study did not include an experimental group of saline-control rats treated with vinpocetine so the results should be interpreted with caution. Further, the proteomic analysis was performed on VH tissue obtained from rats that did not display overt behavioural deficits in the OFT and MWM (*Chapter 2*). However, in *Chapter 2* we observed significant early-postnatal ethanol-induced changes in P-ERK1/2 to ERK1/2 levels in the PFC and DH which were reduced by treatment with vinpocetine. Similarly, in this study we observed significant early-postnatal ethanol-induced protein changes in the VH of these rats.

This study demonstrated that exposure to ethanol during the third trimester neurodevelopmental stage can result in ethanol-induced changes in protein levels in the VH across different functional categories. In conjunction with previous studies, our results provide insight into ethanol-induced changes in proteins related to energy metabolism, redox-regulation and myelin in the brain. As demonstrated in *Chapter 2*, these rats did not display overt behavioural deficits even though significant ethanol-induced changes were observed in the brain. Therefore, further research is needed to identify if these early-postnatal ethanol-induced changes in the brain correlate with behavioural deficits observed after ethanol exposure during the early stages of development.

Importantly, vinpocetine-treatment reversed early-postnatal ethanol-induced changes in protein levels. Therefore, vinpocetine-treatment after early-postnatal ethanol exposure in conjunction with proteomic analysis has the potential to identify possible treatment targets.

However, further investigation is necessary because the rats used in the study did not display overt behavioural deficits.

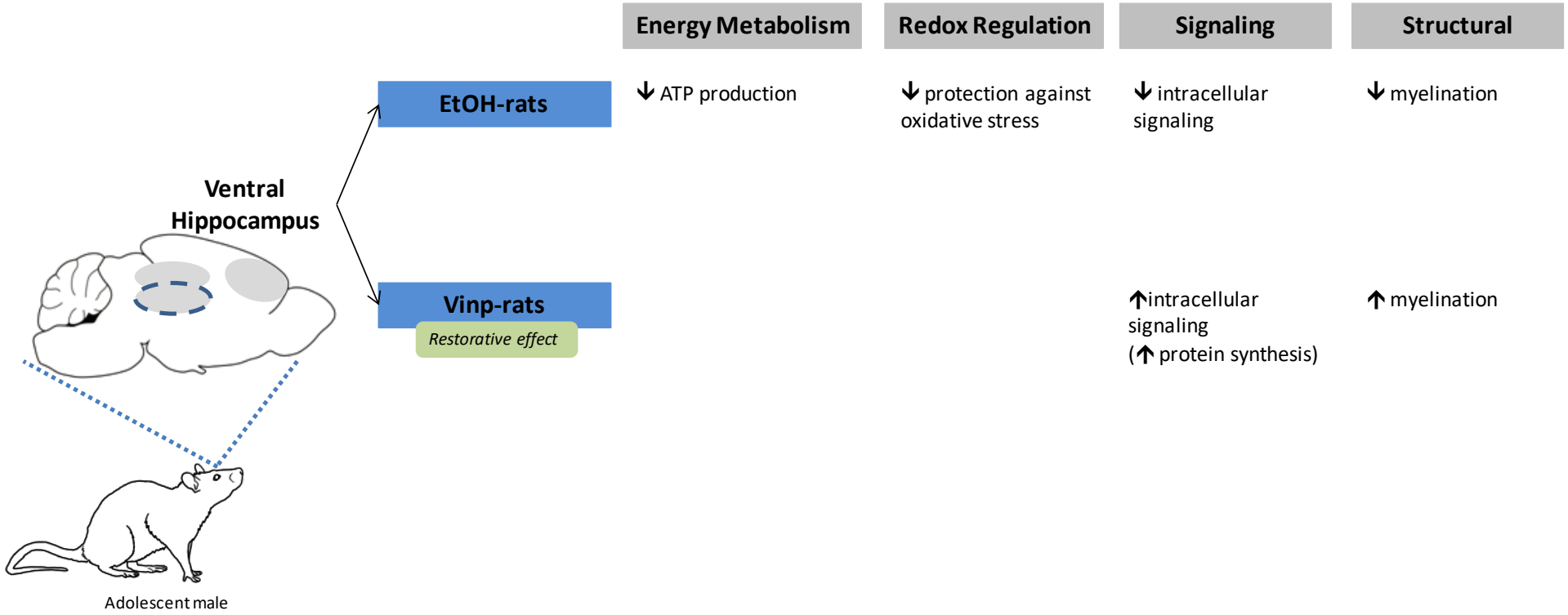

Figure 3.4: Summary of proteomic results in the *ventral hippocampus* after early-postnatal ethanol exposure and treatment with vinpocetine.

CHAPTER 4: PROTEOMIC ANALYSIS OF EARLY-POSTNATAL ETHANOL-INDUCED PROTEIN CHANGES IN THE RAT PREFRONTAL CORTEX AND DORSAL HIPPOCAMPUS.

INTRODUCTION

Exposure to alcohol *in utero* induces persistent behavioural abnormalities including cognitive deficits and psychological disorders (O'Connor and Paley, 2009; Kable et al., 2016). More specifically, individuals with FASD exhibit deficits in executive function, mediated by the PFC, such as working memory, planning, problem solving and inhibitory control (Khoury et al., 2015; Kable et al., 2016). In addition, deficits in spatial memory, which relies on the functionality of the DH (Broadbent et al., 2004), are commonly observed in individuals with FASD (O'Connor and Paley, 2009; Kable et al., 2016). The molecular mechanisms underlying the observed behavioural deficits are largely unknown.

During early development, ethanol exposure has been shown to reduce cell proliferation and induce wide-spread apoptosis in the brain (Ikonomidou et al., 2000; Clements et al., 2012; Sadrian et al., 2012) In addition, early developmental-ethanol exposure may also induce persistent molecular changes, possibly through epigenetic alterations (Kaminen-Ahola et al., 2010), which influence the long-term functionality of neuronal networks and subsequently behaviour. These persistent molecular changes go beyond the intracellular signalling pathways described in *Chapter 2*. Early-postnatal ethanol-induced molecular changes in neuronal and glial cells may be apparent at the protein level and therefore can be measured with high throughput proteomic profiling techniques (Aggarwal et al., 2006).

In this study, ethanol was administered to rat pups during the early-postnatal period (P0 - P10). This is equivalent to ethanol exposure during the third trimester developmental stage of human gestation (Dobbing and Sands, 1979) during the brain growth spurt in which the neuronal networks are highly vulnerable to the toxic effects of ethanol. iTRAQ and LC-MS was then performed using PFC and DH tissue from adolescent naïve-rats (experimental rats that did not undergo behavioural testing) to observe the effects of early-postnatal ethanol exposure on a wide range of proteins in the brain. This study, therefore, examined long-term early-postnatal ethanol-induced changes in the proteomic profiles of the rat PFC and DH without the added

influence of behavioural testing (handling) on protein expression (Bohacek et al., 2015; Deutsch-Feldman et al., 2015)

To our knowledge, this is the first study to utilize iTRAQ and LC-MS to simultaneously identify and quantify large-scale, ethanol-induced protein changes in the PFC and DH of adolescent rats exposed to ethanol during the early-postnatal period. Therefore, the observed early-postnatal ethanol-induced changes in proteins related to cellular processes involved in energy metabolism, neurotransmitter signalling, redox regulation, protein metabolism and cytoskeletal structure provided valuable insight into the long-term ethanol-induced molecular changes in neurons and glial cells in the PFC and DH of the rat brain.

METHODS

ANIMALS

As described in *Chapter 2* (p.36)

EARLY-POSTNATAL ETHANOL EXPOSURE

As described in *Chapter 2* (p.36). Whole litters were randomly assigned to either an ethanol-exposed group or a control group. From P4 to P9, ethanol-pups were administered 4 g/kg/day i.p. of ethanol (12 % v/v) (*EtOH*) and control pups were administered volume controlled saline (*control*) (**Figure 4.1**). Rats in this study did not undergo treatment or behavioural testing.

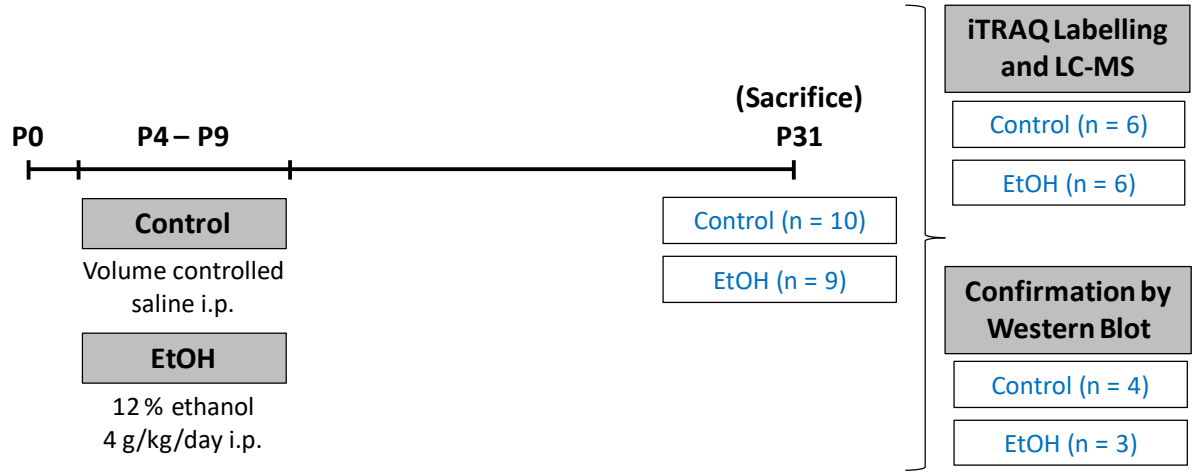

Figure 4.1: Experimental timeline

From P4 to P9 whole litters were administered 12% ethanol (4 g/kg/day i.p.) (*EtOH*) or volume controlled saline (*control*). Rats were sacrificed on P31. Six animals per group were used for iTRAQ labeling and LC-MS. The remaining rats were used to confirm proteomic results by Western blot (Control n = 4; EtOH n = 3).

SACRIFICE

As described in *Chapter 2* (p.41)

Six samples from each group were weighed and pooled together accordingly. Samples were then sonicated with triethylammonium bicarbonate (TEAB) and Na_2CO_3 buffer (1M TEAB and 20 mM Na_2CO_3), lysozyme (100 pmol/µl) and protease inhibitor cocktail (Halt^{TM} Protease & Phosphatase Inhibitor Cocktail, ThermoScientific). Following sonication, samples were incubated on ice for 1 hour and then centrifuged for 30 minutes at 17 200 g at 4 °C. The supernatant was then removed and centrifuged a second time as before. The supernatant was then removed and kept on ice. Samples were thoroughly vortexed and split into technical duplicates and labeled 1 - 8 (**Figure 4.2**). Samples were then transported on ice to the Central Analytics Facility at Tygerberg Medical Campus, University of Stellenbosch, for iTRAQ labeling and LC-MS by Dr Maré Vlok.

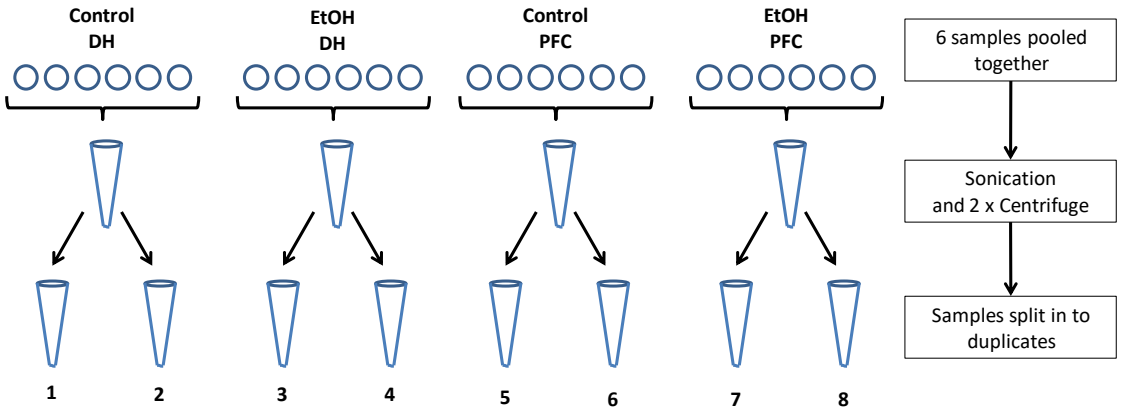

Figure 4.2: Sample preparation

The PFC and DH were analyzed separately. Six samples from each experimental group were pooled together. Pooled samples were sonicated and centrifuged twice (17 200 *g*, 4 °C). The supernatant was then vortexed and split in half. These technical duplicates were then used for iTRAQ labeling and LC-MS.

Received samples were precipitated overnight with ice-cold acetone (1:5 acetone ratio) before centrifugation at 12 000 *g* for 10 minutes. The supernatant was removed and discarded. The remaining pellet was left to air dry at room temperature and then dissolved in 100 mM diluted TEAB containing 4 M guanidine-HCl and 1 % octylgluco-mano-pyranoside, prior to protein concentration determination using a nanodrop spectrophotometer (abs 280 nm).

IN-SOLUTION DIGEST

Reduction occurred by adding 50 mM tris-(2-carboxyethyl)-phosphine (TCEP, Fluka, final concentration 5mM) in 100 mM TEAB to the samples for 30 minutes at 37 °C. Cysteine residues were then blocked by adding 200 mM methyl methanethiosulfonate (MMTS, Sigma, (final concentration 20 mM) in 100 mM TEAB for 30 minutes. This was done in order to prevent the cysteine residues interfering with the enzymatic digest. Samples were then diluted with 100 mM TEAB and proteins digested using trypsin solution (1 µg/µl, 1:50, enzyme: substrate) overnight at 37°C. Samples were dried down and re-suspended in 500 mM TEAB (pH 8).

ITRAQ LABELLING

As per manufacturer's instructions samples were labeled with an iTRAQ Reagent-8-Plex One Assay Kit (Separations). iTRAQ labels were dissolved in 70 µl 2-propanol and added to the appropriate tubes. The reaction occurred for 2 hours after which 2 µl of aliquot from each sample was taken. These aliquots were then mixed together and desalted prior to quality control analysis. Two-hundred microlitres of analytical grade water (MilliQ) were added to each sample to hydrolyze excess labels for 2 hours. The samples were then subsequently reduced and the individual samples combined (**Figure 4.3**).

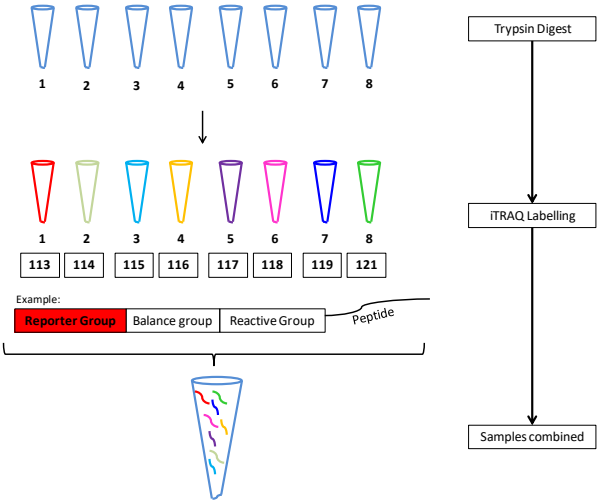

Figure 4.3: iTRAQ labeling.

After the trypsin digest, iTRAQ labels (113 - 121) were added to the respective sample (1 - 8). Isobaric tags included a reporter group, a balance group and a reactive group. Samples were then combined.

DESALTING

Residual digest reagents were removed using an in-house manufactured C18 stage tip (Empore Octadecyl C_{18} extraction discs; Supelco). The samples were loaded onto the stage tip after activating the C_{18} membrane with methanol (Sigma) and equilibrated with 2 % acetonitrile (ACN): 0.05 % trifluoroacetic acid (TFA) in analytical grade water. The bound sample was washed with 2 % ACN: 0.05 % TFA before elution with 50 % ACN: 0.05 % TFA. The eluate was evaporated to dryness. The dried peptides were dissolved in 2 % ACN: 0.01 % TFA in analytical grade water for LC-MS analysis.

LIQUID CHROMATOGRAPHY

Liquid chromatography was performed on a Thermo Scientific Ultimate 3000 RSLC equipped with a C_{18} trap column (2 cm x 100 µm) and a C_{18} analytical column (Luna C18, 5 µm, Phenomenex). The solvents employed were the loading solvent (2 % ACN: 0.1 % TFA in analytical grade water), solvent A (2 % ACN: 0.1 % TFA in analytical grade water) and solvent B (100 % ACN in analytical grade water). The samples were loaded onto the trap column using the loading solvent at a flow rate of 5 µL/min from a temperature-controlled auto-sampler set at 7 °C. Loading was performed for 10 minutes before the sample was eluted onto the analytical column. The flow rate was set to 300 nL/min and the gradient was generated as follows: 2 % solvent A for 6 minutes, 35 % solvent B from 6 - 140 minutes using Chromeleon non-linear gradient 7, 35-50 % solvent B from 140 - 150 minutes and 50 -80 % solvent B from 150-160 minutes. Thereafter the column was washed for 10 minutes with 80 % solvent B followed by equilibration. Chromatography was performed at 50 °C and the outflow delivered to the mass spectrometer through a stainless steel nano-bore emitter.

MASS SPECTROMETRY

Mass spectrometry was performed using a Thermo Scientific Fusion mass spectrometer equipped with a Nanospray Flex ionization source. The sample was introduced through a stainless steel nano-bore emitter. Data were collected in positive mode with spray voltage set to 1.9 kV and ion transfer capillary set to 275 °C. Spectra were internally calibrated using polysiloxane ions at m/z = 445.12 and 371.10. MS^1 scans were performed using the orbitrap detector set at 120 000 resolution over the scan range 350-1650 with AGC target at 2E5 and maximum injection time of 50 milliseconds. Data were acquired in profile mode. MS^2

acquisitions were performed using monoisotopic precursor selection for ion with charges +2 - +7 with error tolerance set to ± 10 ppm. Precursor ions were excluded from fragmentation once for a period of 45 seconds. Precursor ions were selected for fragmentation in HCD mode using the quadruple mass analyzer with HCD energy set to 35 %. Fragment ions were detected in the ion trap mass analyzer using rapid scan rate. The AGC target was set to 5E4 and the maximum injection time to 50 milliseconds. The data were acquired in centroid mode. MS^3 acquisitions were performed on MS^2 fragments over the range *m/z* = 100-500 with detection in the orbitrap mass analyzer at 30 000 resolution. Fragmentation mode was set to HCD at 65 % with a maximum fill time of 100 milliseconds.

DATA ANALYSIS

The raw files generated by the mass spectrometer were imported into Proteome Discoverer v1.4 (Thermo Scientific) and processed using the Mascot (Matrix Science) and SequestHT algorithms. Data analysis was structured to allow for methylthio as fixed modification as well as NQ deamidation, oxidation, and N-terminal acetylation. Peptide validation was performed using the percolator node set to search against a decoy database with a strict false discovery rate (FDR) of 1 %. Database interrogation was performed against the Uniprot *R. rattus* database (2015 edition) with semi-tryptic cleavage allowing for 2 missed cleavages. Quantitation was performed in the MS^3.

A target protein was considered identified if at least two such unique peptide matches were apparent for the protein. The data sets obtained reported the fold change of identified proteins in the PFC and DH of EtOH-rats versus control rats. A fold change greater than 1.2 identified differentially expressed proteins (Seshi, 2006; Duthie et al., 2007; Ting et al., 2009; Williamson et al., 2016). In addition, a fold change greater than 2 identified a significant change in protein levels between EtOH- and control rats (Ting et al., 2009; Yang et al., 2013; Gunton et al., 2017). Differentially expressed proteins were organized into functional categories. In addition, significantly changed proteins (> 2-fold change) were analyzed collectively (per brain area) using STRING (https://string-db.org/) to identify functional protein-protein interaction networks (Szklarczyk et al., 2015).

.

WESTERN BLOT ANALYSIS

Western blot analysis was used to validate the levels of 3 selected proteins identified by iTRAQ analysis and LC-MS. In the PFC, anti-NDUFA9 antibody [EPR13061(B)] ab181381 (NDUFA9) was used to quantify NADH dehydrogenase [ubiquinone] 1 alpha, subcomplex subunit 9. In the DH, ATP5A (51): sc-136178 (ATP5A) and GSK3-β (27C10) Rabbit mAb (GSK3β) were used to validate the expression of ATP synthase subunit g and glycogen synthase kinase-3 beta (GSK3β) respectively. ATP5A and GSK3β have previously been characterized in our laboratory however, characterization of NDUFA9 is shown below.

NDUFA9 (ANTI-NADH DEHYDROGENASE) CHARACTERIZATION

PFC lysates from control (saline + DMSO) rats in Chapter 2 were used to characterize NDUFA9. Sample preparation is described in *Chapter 2* (p. 42 and 45). To determine the optimal amount of protein, 20 µg, 30 µg, 40 µg, and 50 µg (loaded into lanes 1 - 4 and duplicated in lanes 5 - 8) of protein was electrophoresed on 12 % SDS-polyacrylamide gels for 1 hour 10 minutes (150 V) and then transferred for 1 hour (100 V) onto a Hybond nitrocellulose membrane (GE Healthcare, U.K.). The membranes were blocked for 1 hour in 5 % milk PBS-T then incubated with the primary antibody (Anti-NDUFA9 antibody [EPR13061(B)] ab181381, 1 : 5 000) overnight at 4°C in 5 % milk PBS-T. Following 3 x 10 minute washes with PBS-T, membranes were incubated for 2 hours with the secondary HRP-conjugated antibody in 5 % milk PBS-T (Goat Anti-Rabbit (GAR) IgG (H+L)-HRP Conjugate, #170-6515, BioRad,1 : 10 000). Membranes were then incubated with Clarity ^{TM} Western ECL Substrate (#170-5060, BioRad) and exposed to X-ray film (Medical X-Ray Film Blue, AGFA) to quantify the protein present. The density of each band was determined using UN-SCAN-IT Software Version 7.0 (Silk Scientific Inc, Utah, USA). A linear graph of protein content (µg) versus pixel density percentage was constructed to determine the optimal amount of protein needed to quantify NDUFA9 in the PFC (**Figure 4.4**). **Figure 4.4** illustrates that 35 µg of protein are needed to accurately quantify NDUFA9 in the PFC because the respective pixel density percentage falls within a section of the linear curve with a high gradient which enabled the identification of subtle differences between experimental groups.

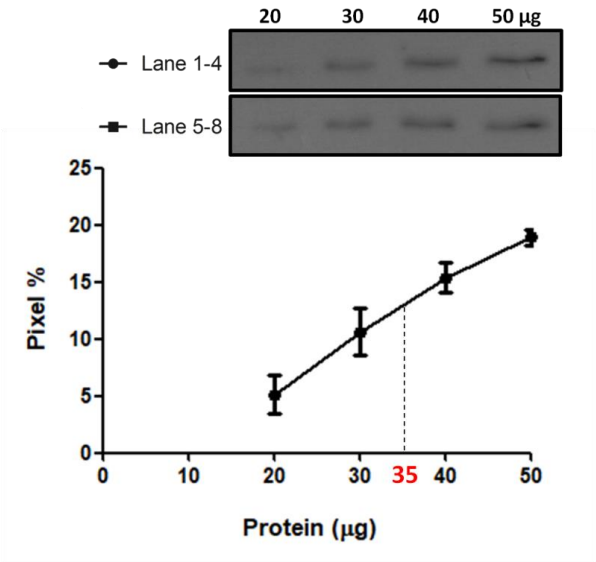

Figure 4.4: Characterization of anti-NDUFA9 antibody.

A graph of pixel density percentage (pixel %) versus protein concentration (µg) to determine the optimal amount of protein required to accurately quantify NDUFA9 in the PFC. The graph represents the mean and range of the duplicate bands. It was decided to load 35 µg of protein per well because the respective pixel density parentage falls on a section of the linear curve with a high gradient [primary antibody (anti-NDUFA9) 1: 500; secondary antibody (GAR) 1: 10 000].

EXPERIMENTAL WESTERN BLOTS

PFC and DH brain tissue samples from male **control** (n = 4) and **EtOH- (**n = 3) rats that did not undergo behavioural testing or treatment in Chapter 2 were sonicated for 10 seconds in RIPA buffer (5 M NaCl; 1% Triton X-100; 0.1% SDS; 20 mM Tris (pH 7.5); 1% sodium deoxycholate) with protease and phosphatase inhibitor cocktail (Halt™ Protease & Phosphatase Inhibitor Cocktail, ThermoScientific). Samples were then centrifuged at 17 200 x g for 30 minutes at 4 °C. The supernatants were collected and protein concentration was determined using the Pierce™ BCA Protein Assay Kit (#23225, Thermo Scientific, Rockford, U.S.A.). Loading samples contained bromophenol blue sodium (Sigma-Aldrich), dithiothreitol (Promega, Madison, USA), RIPA buffer and the respective lysate. Loading samples were boiled for 4 minutes at 95 °C, stored at -20 °C and re-boiled (4 minutes at 95 °C) then centrifuged briefly on the desk mini-centrifuge (Tomos, Laboratory Products) before use. The optimal amount of protein (NDUFA9 - 35 µg; ATP5A - 20 µg; GSK3β - 20 µg) determined during characterization was electrophoresed (150 V) on 12% SDS-polyacrylamide gels for 1 hour 10 minutes and then transferred (100 V) for 1 hour onto a Hybond nitrocellulose membrane (GE Healthcare, U.K.). The membranes were blocked overnight with 5 % BSA or

5 % milk and then immunolabelled with primary antibodies against proteins of interest **(Table 4.1** anti-NDUFA9 antibody [EPR13061(B)] ab181381, Abcam, RRID AB_2150762 (NDUFA9) - PFC 1 : 5 000; ATP5A (51) sc-136178, Santa Cruz Biotechnology, RRID AB_2061764 (ATP5A) - DH 1 : 5 000; and GSK-3β (27C10) Rabbit mAb, Cell Signalling, RRID AB_ 490890 (GSK3β) - DH 1 : 2 000). Membranes were then incubated with the appropriate secondary HRP-conjugated antibodies, goat anti-rabbit IgG (H+L)-HRP conjugate, #170-6515, BioRad (GAR) or goat anti-mouse IgG (H+L)-HRP conjugate, #170-6515, Biorad (GAM). Membranes were stripped with 0.2 M NaOH for 5 minutes and immunolabelled for the loading control monoclonal anti-alpha-tubulin antibody produced in mouse, T5168, Sigma-Aldrich, RRID AB_ 477579 (α-tubulin) 1 : 3000. Membranes were incubated with Clarity ™ Western ECL Substrate (#170-5060, BioRad) and exposed to X-ray film (Medical X-Ray Film Blue, AGFA) to quantify the protein present. The density of each band was determined using UN-SCAN-IT Software Version 7.0 (Silk Scientific Inc, Utah, USA). The density of each band was expressed as a percentage of the mean density of all the bands representing the protein of interest on the X-ray film (pixel density percentage). The pixel density percentage of each band was then normalized to the pixel density percentage of its respective reference protein (pixel %).

Table 4.1: Antibodies used in Western Blot analysis to confirm proteomics results

Antibody	Abbreviation	Identifiers	MW	Dilution
Anti-NDUFA9 antibody [EPR13061(B)] ab181381	NDUFA9	Abcam; Cat# ab181381; RRID: AB_2150762; rabbit, monoclonal	35 kDa	1 : 5 000
ATP5A (51): sc-136178	ATP5A	Santa Cruz Biotechnology; Cat# sc-136178; RRID: AB_2061764; mouse, monoclonal.	60 kDa	1 : 5 000
GSK-3β (27C10) Rabbit mAb	GSK3β	Cell Signalling; Cat# 9315; RRID: AB_490890; rabbit, monoclonal.	46 kDa	1 : 2 000
Monoclonal Anti-α-tubulin antibody	α-tubulin	Sigma-Aldrich; Cat# T5168; RRIDD: AB_477579; mouse, monoclonal.	50 kDa	1 : 3 000

STATISTICS

Western blot data were analyzed in Statistica version 13 (StatSoft, Tulsa, OK). The Shapiro-Wilk test (SW) for normality showed that all Western blot data (pixel density percentage) were normally distributed. The data were analyzed using the Student's t-tests. The data are presented as the mean ± SEM.

PROTEOMICS

PROTEINS ALTERED BY EARLY-POSTNATAL ETHANOL EXPOSURE IN THE PREFRONTAL CORTEX

iTRAQ and LC-MS identified 1 456 proteins. Of these, 61 proteins differed by 20 % (fold change greater than 1.2) in the PFC of EtOH-rats versus control rats. Thirty-one of the altered proteins were downregulated (**Figure 4.5**). Five proteins out of the 61 proteins were found to differ by a fold change greater than 2 (**Figure 4.6**). For example, *NADH dehydrogenase [ubiquinone] 1 alpha, subcomplex subunit 9 (mitochondrial)* and *dynactin* were upregulated by a fold change greater than 2 in the PFC of EtOH-rats compared to controls. Network analysis of these 5 proteins did not identify any significant protein-protein interactions (**Appendix A4.1**). **Table 4.2** lists the 61 early-postnatal ethanol-induced protein changes (fold change > 1.2) organized into functional categories.

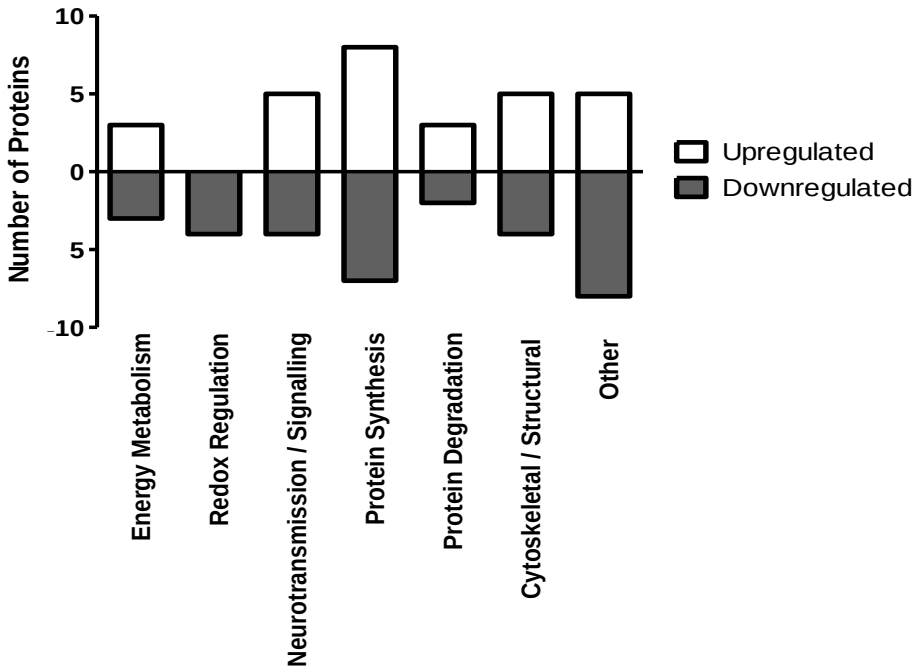

Figure 4.5: Differentially expressed (> 1.2-fold△) proteins in the *prefrontal cortex* of EtOH-rats compared to control rats.

Categorically organized ethanol-induced protein changes (> 1.2-fold△) in the PFC of EtOH-rats compared to control rats. Thirty-three out of the 61 identified proteins were upregulated. The remaining 28 proteins were downregulated.

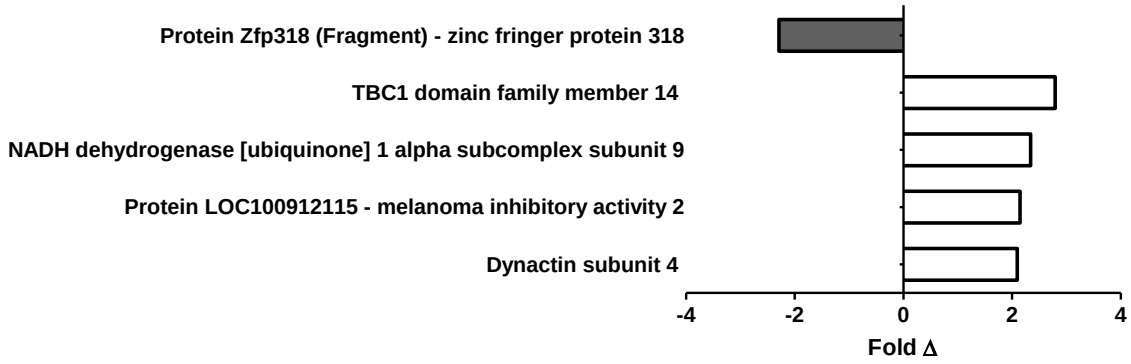

Figure 4.6: Differentially expressed (> 2-fold△) proteins in the *prefrontal cortex* of EtOH-rats compared to control rats.

Proteins identified in the PFC of EtOH-rats that were significantly changed from control rats by a fold change greater than 2. [A downregulated protein is represented by a negative value]

In the PFC, 6 energy metabolism-related proteins were identified. Levels *NADH dehydrogenase [ubiquinone] 1 alpha subcomplex subunit 9 (mitochondrial)* were increased by a fold change greater than 2 in EtOH-rats compared to control rats, while *succinate dehydrogenase [ubiquinone] flavoprotein subunit (mitochondrial)* and *cytochrome c oxidase subunit 2* were increased by a fold change greater than 1.2. However, *NADH dehyrodogenase [ubiquinone] 1 beta subcomplex, 5* was decreased in the PFC of EtOH-rats compared to control rats. In addition, proteins involved in redox regulation, such as *glutathione reductase* and *S-formylglutathione hydrolase* were downregulated in the PFC of EtOH-rats compared to controls.

Proteins related to neurotransmission and cellular signalling were both upregulated and downregulated in the PFC of EtOH-rats compared to controls (fold change greater than 1.2). *Guanine nucleotide-binding protein G(z) subunit alpha* and *protein kinase, cAMP-dependent regulatory type 2 alpha* were upregulated whereas *glutamate decarboxylase 2, ADP-ribosylation factor-like protein 3* and *isoform 4 of discs large homolog 2* were downregulated in the PFC EtOH-rats in comparison to control rats.

Nineteen proteins related to protein metabolism (synthesis and degradation) differed by more than 20 % (>1.2-fold change) between EtOH-rats and control rats in the PFC. *Protein LOC100912115 (melanoma inhibitory activity 2)* and *TBC1 domain family member 14* were upregulated and the *protein Zfp318 (zinc finger protein 318)* was downregulated by a fold change greater than 2 in the PFC of EtOH-rats versus controls (**Figure 4.6**). In addition, levels *CREB3* and *eukaryotic translation initiation factor 4H* were increased in the PFC of EtOH-rats compared to controls.

Several cytoskeletal and structural proteins were shown to have been altered by early-postnatal ethanol exposure in the PFC. *Dynactin subunit 4* was upregulated by a fold change greater than 2 in the PFC of EtOH-rats. In addition, *neural cell adhesion molecule 1* and *myosin regulatory light chain 12B* were increased and *oligodendrocyte-myelin glycoprotein* was decreased by a fold change more than 1.2 in the PFC of EtOH-rats versus controls.

Table 4.2: Proteins with a fold change > 1.2 in the *prefrontal cortex* of EtOH-rats versus control rats

PFC Category	Protein	Accession no.	Cov (%)	Pep	EtOH: Control	Fold △	
Energy Metabolism	**NADH dehydrogenase [ubiquinone] 1 alpha subcomplex subunit 9, mitochondrial**	**Q5BK63**	**29**	**13**	**2.342**	**2.342**	↑
	Cytochrome c oxidase subunit 2	B0FTB8	42	10	1.536	1.536	↑
	Succinate dehydrogenase [ubiquinone] flavoprotein subunit, mitochondrial	Q920L2	35	32	1.397	1.397	↑
	NADH dehydrogenase (Ubiquinone) 1 beta subcomplex, 5 (Predicted), isoform CRA_b	D4A565	17	6	0.696	1.438	↓
	3-ketoacyl-CoA thiolase, mitochondrial	G3V9U2	34	23	0.768	1.302	↓
	Acyl carrier protein	D3ZF13	29	6	0.785	1.274	↓
Redox Regulation	Glutathione reductase (Fragment)	P70619	19	14	0.609	1.641	↓
	Electron transfer flavoprotein-ubiquinone oxidoreductase, mitochondrial	Q66HF3	28	27	0.715	1.400	↓
	S-formylglutathione hydrolase	B0BNE5	23	9	0.772	1.296	↓
	Isoform 2 of Dehydrogenase/reductase SDR family member 7B	Q5RJY4-2	39	17	0.775	1.290	↓
Neurotransmission / Signalling	Guanine nucleotide-binding protein G(z) subunit alpha	P19627	27	11	1.711	1.711	↑
	Phosphoserine aminotransferase	E9PSV5	58	33	1.210	1.210	↑
	Protein kinase, cAMP-dependent, regulatory, type 2, alpha, isoform CRA_a	G3V8Q6	30	15	1.209	1.209	↑
	ATPase, H transporting, lysosomal V1 subunit G1	B2GUV5	35	5	1.205	1.205	↑
	Glutamate decarboxylase 2	Q05683	33	25	0.681	1.468	↓
	FXYD domain-containing ion transport regulator 7	P59649	55	7	0.760	1.315	↓
	ADP-ribosylation factor-like protein 3	P37996	51	14	0.761	1.314	↓
	Isoform 4 of Disks large homolog 2	Q63622-4	28	30	0.761	1.314	↓
Protein Synthesis	**Protein LOC100912115 - Melanoma inhibitory activity 2**	**D3ZVL1**	**27**	**30**	**2.147**	**2.147**	↑
	Transcription factor COE1	Q63398	18	13	1.685	1.685	↑
	CREB3	A0A075FKQ4	9	4	1.435	1.435	↑

PFC	Category	Protein	Accession no.	Cov (%)	Pep	EtOH: Control	Fold △	
		Eukaryotic translation initiation factor 4H	Q5XI72	48	16	1.355	1.355	↑
Protein Synthesis (cont.)		Heat shock factor-binding protein 1	Q8K3X8	55	5	1.320	1.320	↑
		Protein LOC100912427 - Nuclease-sensitive element-binding protein 1	D3ZEV0	46	14	1.235	1.235	↑
		Peptidyl-prolyl cis-trans isomerase FKBP1A	Q62658	37	7	1.234	1.234	↑
		60S ribosomal protein L10	Q6PDV7	23	6	1.221	1.221	↑
		Protein Zfp318 (Fragment) - Zinc finger protein 318	**F1M0H0**	**19**	**45**	**0.437**	**2.291**	↓
		Hepatoma-derived growth factor-related protein 3	Q923W4	8	2	0.548	1.826	↓
		Rps2r1 - RNA binding, ribosomal protein	O35805	25	6	0.621	1.610	↓
		Transferrin receptor protein 1	G3V679	25	24	0.712	1.405	↓
		Protein Hnrnpul2 - Heterogeneous Nuclear Ribonucleoprotein U-Like 2	D4ABT8	19	20	0.714	1.402	↓
		Protein Srsf3 - Serine/arginine-rich splicing factor 3	Q0ZFS8	23	8	0.767	1.305	↓
		Ribosomal protein L11	Q4V8I6	12	3	0.767	1.304	↓
Protein Degradation		**TBC1 domain family member 14**	**Q5CD77**	**20**	**17**	**2.792**	**2.792**	↑
		Lon protease homolog, mitochondrial	Q924S5	26	24	1.914	1.914	↑
		E3 ubiquitin-protein ligase HUWE1 (Fragment)	P51593	9	3	1.314	1.314	↑
		UV excision repair protein RAD23 homolog B	Q4KMA2	52	20	0.753	1.328	↓
		Proteasome subunit alpha type-2	P17220	38	8	0.756	1.323	↓
Cytoskeletal / Structural		**Dynactin subunit 4**	**Q9QUR2**	**33**	**18**	**2.097**	**2.097**	↑
		Inter-alpha-trypsin inhibitor heavy chain H3	Q63416	21	24	1.299	1.299	↑
		Myosin regulatory light chain 12B	P18666	47	9	1.222	1.222	↑
		Cell division control protein 42 homolog	Q8CFN2	40	10	1.213	1.213	↑
		Wiskott-Aldrich syndrome protein family member 1	Q5BJU7	25	19	1.211	1.211	↑
		Neural cell adhesion molecule L1	D3ZPC4	22	29	1.942	1.942	↑
		Oligodendrocyte-myelin glycoprotein	Q7TNM3	36	17	0.789	1.268	↓

PFC	Category	Protein	Accession no.	Cov (%)	Pep	EtOH: Control	Fold △	
Other		Protein LRRGT00178 (submitted name, UniProt)	Q6QI30	39	7	1.958	1.958	↑
		Ribonuclease inhibitor	E2RUH2	22	11	1.776	1.776	↑
		Proliferation-associated 2G4	Q6AYD3	37	19	1.256	1.256	↑
		Bleomycin hydrolase	P70645	29	15	1.240	1.240	↑
		DEAD (Asp-Glu-Ala-Asp) box polypeptide 5	Q6AYI1	44	31	1.238	1.238	↑
		Protein Fam83d - Family with sequence similarity 83 member D	D4ABG0	34	23	0.692	1.445	↓
		Protein RGD1309783 - Anykrin repeat domain 30A	F1M1U8	16	7	0.693	1.442	↓
		Protein Fam184a (Fragment)	F1LW90	19	27	0.727	1.376	↓
		Uncharacterized protein (Fragment)	F1M024	29	27	0.743	1.347	↓
		EF-hand domain-containing protein D2	Q4FZY0	51	17	0.763	1.311	↓
		Pyridoxal kinase	G3V647	38	13	0.782	1.279	↓
		Protein RGD1563220 (Fragment) - 60S ribosomal protein L7a	F1M1M2	40	17	0.793	1.261	↓

[The coverage percentage (Cov %) indicates the number of identified amino acids associated with that protein represented as a percentage of the total number of amino acids in that protein. The number of exclusive unique peptides (Pep) represents the number of unique peptide sequences associated with that protein. Note: Keratin, type II 75, 6A (> 2-fold change) and keratin type 1 (> 1.2-fold change) were identified and appeared to be downregulated in EtOH-rats compared to control rats. This may have been due to contamination].

PROTEINS ALTERED BY EARLY-POSTNATAL ETHANOL EXPOSURE IN THE DORSAL HIPPOCAMPUS

Of the 1456 proteins identified by iTRAQ and LC-MS, 126 proteins differed by 20 % (fold change greater than 1.2) in the DH of EtOH-rats versus control rats. Ninety-nine of the altered proteins were downregulated (**Figure 4.7**). Seven proteins out of the 126 proteins were found to differ by a fold change greater than 2 (**Figure 4.6**). For example, *ATP synthase subunit g (mitochondrial)* and *glycogen synthase kinase-3 beta* were downregulated by a fold change greater than 2 in the DH of EtOH-rats compared to controls. Network analysis of these 7 proteins did not identify any significant protein-protein interactions (**Appendix A4.2**). **Table 4.3** lists the 126 proteins (fold change > 1.2) organized into functional categories.

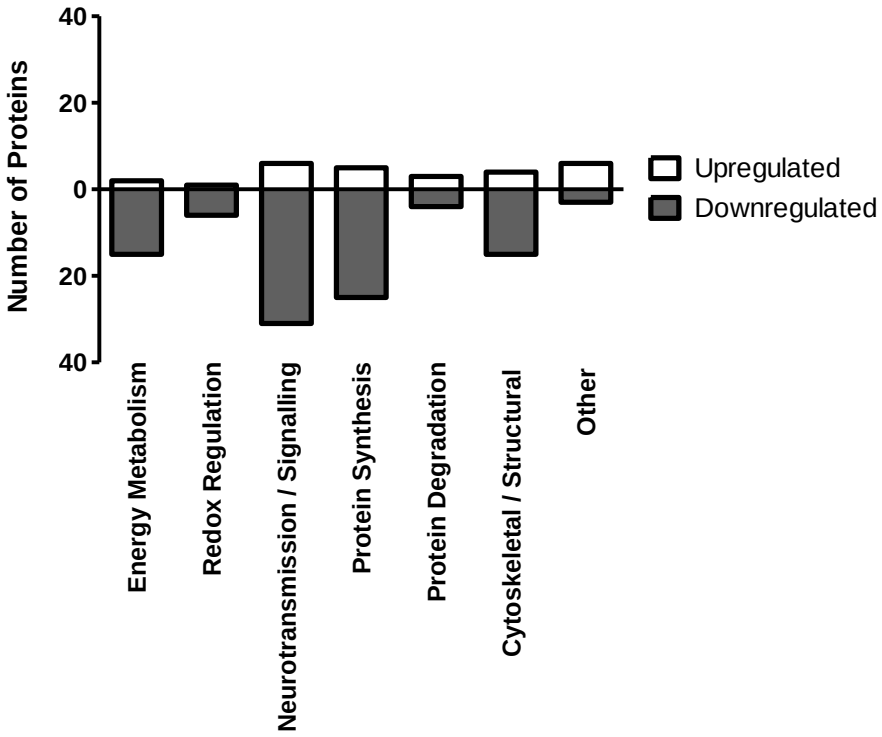

Figure 4.7: Differentially expressed (> 1.2-fold△) proteins in the *dorsal hippocampus* of EtOH-rats compared to control rats.

Categorically organized ethanol-induced protein changes (> 1.2-fold△) in the DH of EtOH-rats compared to control rats. Ninety-nine out of the 126 identified proteins were downregulated. The remaining 27 proteins were upregulated.

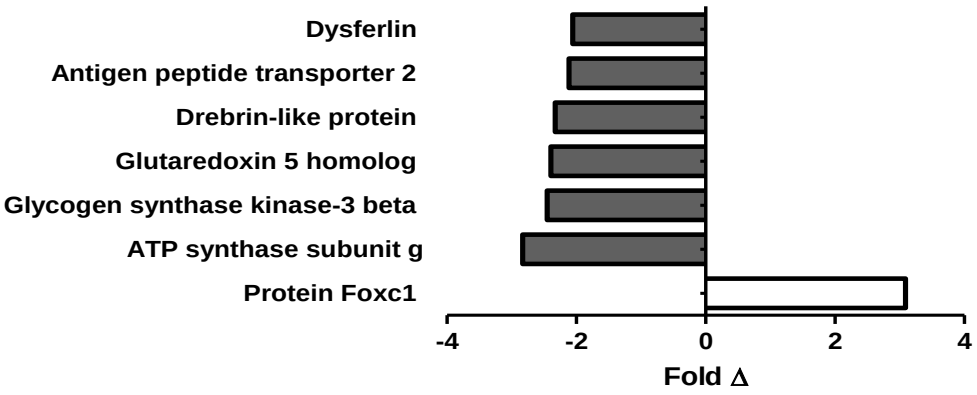

Figure 4.8: Significantly changed (> 2-fold△) proteins in the *dorsal hippocampus* of EtOH-rats compared to controls.

Proteins identified in the DH of EtOH-rats that differentiated from control rats by a fold change greater than 2. [A downregulated protein is represented by a negative value].

In the DH of rats exposed to ethanol during the early-postnatal period (EtOH-rats), several proteins related to energy metabolism were downregulated by more than 20 % compared to control rats. *ATP synthase subunit g (mitochondrial)* was downregulated by a fold change greater than 2 and *ATP synthase subunits beta, alpha and gamma* were decreased by a fold change more than 1.2 in the DH of EtOH-rats compared to controls. Further, *NADH dehydrogenase [ubiquinone] Fe-S protein 8* and *cytochrome c oxidase subunits 58* and 7C were decreased in the DH of EtOH-rats. In addition, *glutaredoxin 5 homolog*, *thioredoxin (fragment)* and *aldehyde dehydrogenase (mitochondrial))*, redox-related proteins were decreased in the DH of EtOH-rats compared to controls. However, thioredoxin-like protein 1 was increased in the DH of EtOH-rats.

In the DH, 31 proteins related to neurotransmission and cellular signalling were lower in EtOH-rats than control rats. *GSK3β* and *dysferlin* were decreased by a fold change greater than 2. In addition, *protein kinase C*, *protein kinase C beta*, *glutamate receptor 3*, *protein kinase cAMP-dependent regulatory type 2 alpha* and *calmodulin* were decreased in the DH of EtOH-rats.

Similarly, 27 proteins related to protein metabolism were downregulated in the DH of EtOH-rats compared to controls. These include *histone proteins H3, H4, H2B, H1.4 and H2A.* However, the *protein FOXC1* was increased in the DH of EtOH-rats compared to controls. In addition, cytoskeletal proteins such as *debrin-like protein*, *thymosin beta-4*, *myelin basic*

protein transcript variant N (fragment) and *myelin proteolipid protein* were downregulated in the DH of EtOH-rats compared to controls.

Table 4.3: Proteins with a fold change > 1.2 in the *dorsal hippocampus* of EtOH-rats versus control rats

DH	Category	Protein	Accession no.	Cov (%)	Pep	EtOH: Control	Fold △	
Energy Metabolism		NADH dehydrogenase (Ubiquinone) Fe-S protein 3 (Predicted), isoform CRA_c	D3ZG43	32	12	1.358	1.358	↑
		Guanidinoacetate N-methyltransferase	G3V960	41	14	1.204	1.204	↑
		ATP synthase subunit g, mitochondrial	**Q6PDU7**	**58**	**7**	**0.354**	**2.827**	↓
		Slc25a3 protein - Phosphate carrier protein	Q6IRH6	48	28	0.573	1.745	↓
		Ethylmalonic encephalopathy 1	B0BNJ4	29	6	0.607	1.649	↓
		ATP synthase subunit beta, mitochondrial	P10719	78	69	0.650	1.538	↓
		NADH dehydrogenase (Ubiquinone) Fe-S protein 8 (Predicted), isoform CRA_a	B0BNE6	17	3	0.682	1.466	↓
		Acyl carrier protein	D3ZF13	29	6	0.687	1.455	↓
		ATP synthase subunit alpha, mitochondrial	P15999	72	62	0.690	1.450	↓
		Protein RGD1562433 - Similar to ubiquilin 1 isoform 2	A0JPP0	44	22	0.710	1.409	↓
		ATP synthase F(0) complex subunit B1, mitochondrial	P19511	43	17	0.719	1.391	↓
		Dihydrolipoyllysine	P08461	46	36	0.724	1.382	↓
		Cytochrome c oxidase subunit 5B, mitochondrial	P12075	53	10	0.724	1.381	↓
		Acetyl-CoA acetyltransferase, mitochondrial	P17764	62	35	0.731	1.368	↓
		2-oxoglutarate dehydrogenase, mitochondrial	Q5XI78	36	35	0.733	1.364	↓
		Cytochrome c oxidase subunit 7C, mitochondrial	P80432	24	2	0.746	1.341	↓
		Dihydrolipoyllysine-residue succinyltransferase component of 2-oxoglutarate dehydrogenase complex, mitochondrial	Q01205	32	19	0.749	1.335	↓
		ATP synthase subunit gamma, mitochondrial	P35435	36	17	0.784	1.275	↓
Redox Regulation		Thioredoxin-like protein 1	Q920J4	34	12	1.229	1.229	↑
		Glutaredoxin 5 homolog (S. cerevisiae) (Predicted), isoform CRA_b	**D4ADD7**	**60**	**22**	**0.418**	**2.393**	↓
		Prenylcysteine oxidase	Q99ML5	28	19	0.619	1.616	↓
		Aldehyde dehydrogenase, mitochondrial	P11884	34	24	0.646	1.548	↓

DH	Category	Protein	Accession no.	Cov (%)	Pep	EtOH: Control	Fold △	
Redox Regulation (cont.)		Protein Tmx1 - Thioredoxin domain containing 1	Q52KJ9	13	9	0.718	1.393	↓
		Isovaleryl-CoA dehydrogenase, mitochondrial	P12007	40	23	0.768	1.303	↓
		Thioredoxin (Fragment)	R4GNK3	32	8	0.799	1.252	↓
Neurotransmission / Signalling		Ras-related protein Rap-2b	P61227	37	12	1.721	1.721	↑
		Neuronal calcium binding protein NECAB2	Q9ESB4	38	15	1.633	1.633	↑
		Glutamine synthetase	P09606	71	40	1.591	1.591	↑
		ADP-ribosylation factor-like protein 3	P37996	51	14	1.345	1.345	↑
		Phosphoserine aminotransferase	E9PSV5	58	33	1.292	1.292	↑
		Ryanodine receptor 1	F1LMY4	27	176	1.278	1.278	↑
		Glycogen synthase kinase-3 beta	**P18266**	**26**	**13**	**0.408**	**2.450**	↓
		Casein kinase II subunit alpha	P19139	36	13	0.574	1.742	↓
		Protein kinase C	F1M2P8	17	15	0.623	1.604	↓
		Protein kinase C beta type	P68403	23	25	0.623	1.604	↓
		Isoform XA of Plasma membrane calcium-transporting ATPase 4	Q64542-2	24	41	0.654	1.530	↓
		Olfactory receptor	M0RBF6	35	14	0.665	1.504	↓
		Protein Nbeal1 - Neurobeachin-like protein 1	F1M6V0	25	74	0.681	1.469	↓
		Protein Dmxl2 (Fragment) - Dmx-like 2	F1M164	32	86	0.694	1.440	↓
		Excitatory amino acid transporter 2	P31596	41	30	0.700	1.428	↓
		Plasma membrane calcium-transporting ATPase 1	P11505	38	67	0.704	1.420	↓
		Glutamate receptor 3	G3V6Z5	27	27	0.712	1.405	↓
		Protein Eea1 (Fragment) - Early endosome antigen 1	F1LUA1	23	44	0.724	1.380	↓
		Plasma membrane calcium-transporting ATPase 2	P11506	35	57	0.726	1.377	↓
		Growth factor receptor-bound protein 2	P62994	33	7	0.727	1.376	↓
		Isoform 2 of Mitogen-activated protein kinase 3	P21708-2	36	21	0.728	1.374	↓
		Sodium/potassium-transporting ATPase subunit beta-1	P07340	49	27	0.739	1.353	↓

DH	Category	Protein	Accession no.	Cov (%)	Pep	EtOH: Control	Fold △	
	Neurotransmission / Signalling (cont.)	Protein kinase, cAMP-dependent, regulatory, type 2, alpha, isoform CRA_a	G3V8Q6	30	15	0.742	1.348	↓
		Neuromodulin	P07936	67	14	0.749	1.335	↓
		Guanine nucleotide-binding protein G(o) subunit alpha	P59215	56	31	0.754	1.326	↓
		Sodium/potassium-transporting ATPase subunit alpha-2	P06686	53	81	0.755	1.325	↓
		GTPase NRas	Q04970	49	13	0.757	1.321	↓
		Guanine nucleotide-binding protein G(i) subunit alpha-1	P10824	41	25	0.758	1.319	↓
		Guanine nucleotide-binding protein G(i) subunit alpha-2	P04897	45	23	0.758	1.319	↓
		Sodium/potassium-transporting ATPase subunit alpha-3	P06687	53	84	0.763	1.311	↓
		CDP-diacylglycerol--inositol 3-phosphatidyltransferase	P70500	43	13	0.769	1.300	↓
		Calmodulin	P62161	89	25	0.778	1.285	↓
		Guanine nucleotide-binding protein subunit gamma (Fragment)	Q45QK6	57	3	0.782	1.279	↓
		Protein kinase C epsilon type	P09216	17	16	0.787	1.271	↓
		Caspase	Q3MHS1	14	8	0.789	1.268	↓
		V-type proton ATPase subunit F	P50408	68	8	0.791	1.265	↓
		Voltage-dependent anion-selective channel protein 1	Q9Z2L0	65	21	0.792	1.263	↓
	Protein Synthesis	**Protein Foxc1**	**M0RCA0**	**39**	**23**	**3.093**	**3.093**	↑
		Protein Snrpd3 - Small nuclear ribonucleoprotein D3	M0R907	27	5	1.488	1.488	↑
		Tumor protein D54	Q6PCT3	30	8	1.400	1.400	↑
		Transcription factor COE1	Q63398	18	13	1.241	1.241	↑
		60S acidic ribosomal protein P1	P19944	28	3	1.202	1.202	↑
		Protein Dhx57 - Dex-H-box helicase 57	F1LSC4	29	56	0.578	1.730	↓
		Protein disulfide-isomerase A6	Q63081	23	11	0.583	1.716	↓
		Prohibitin-2	Q5XIH7	46	21	0.608	1.646	↓

DH	Category	Protein	Accession no.	Cov (%)	Pep	EtOH: Control	Fold △	
	---	40S ribosomal protein S28	P62859	57	4	0.609	1.642	↓
Protein Synthesis (cont.)		Histone H3	D3ZQN4	57	14	0.613	1.631	↓
		Protein Sf3b3 - Splicing factor 3b subunit 3	E9PT66	24	37	0.621	1.611	↓
		RNA transcription, translation and transport factor	Q6QI16	50	21	0.621	1.610	↓
		Protein Tcerg1 - Transcription elongation regulator 1	D3ZTL0	16	19	0.650	1.539	↓
		Histone H4	P62804	68	19	0.704	1.421	↓
		Protein Purg - Purine rich element binding protein G	D3ZYS1	48	27	0.715	1.398	↓
		Protein Rnf14 - Ring finger protein 14	Q3ZAU6	25	16	0.724	1.382	↓
		Histone H2B	G3V8B3	72	25	0.735	1.360	↓
		60 kDa heat shock protein, mitochondrial	P63039	67	51	0.737	1.357	↓
		60S ribosomal protein L7	B0K031	29	10	0.761	1.314	↓
		Lupus La protein homolog	P38656	26	16	0.764	1.308	↓
		Brain acid soluble protein 1	Q05175	72	21	0.771	1.297	↓
		10 kDa heat shock protein, mitochondrial	P26772	93	18	0.778	1.286	↓
		Histone H1.4	P15865	48	16	0.785	1.275	↓
		Rps16 protein (Fragment)	Q5XFV9	44	13	0.790	1.267	↓
		Heterogeneous nuclear ribonucleoproteins A2/B1 (Fragment)	F1LNF1	74	45	0.796	1.257	↓
		Endoplasmin	Q66HD0	46	42	0.798	1.253	↓
		Ribosomal protein S11	Q6PDV9	51	9	0.798	1.253	↓
		Protein LOC684828 - similar to H1.2	M0R7B4	36	14	0.799	1.252	↓
		Histone H2A	D3ZWE0	60	13	0.800	1.250	↓
Protein Degradation		Protein Sacs - Sacsin is a Hsp70 co-chaperone	D4A1D3	21	118	1.316	1.316	↑
		Small ubiquitin-related modifier 3	Q5XIF4	38	5	1.214	1.214	↑
		Ubiquitin carboxyl-terminal hydrolase	F1LSM0	25	83	1.421	1.421	↑

DH	Category	Protein	Accession no.	Cov (%)	Pep	EtOH: Control	Fold △	
		26S protease regulatory subunit 6A	Q63569	45	22	0.682	1.465	↓
	Protein degradation (cont.)	Protein Tmprss2 - Transmembrane protease, serine 2	Q6P7D7	28	14	0.730	1.369	↓
		Protein Mmp25 (Fragment) O - Matrix metallopeptidase 25	F1M4E8	25	18	0.738	1.355	↓
		Cullin 2 (Predicted), isoform CRA_a	D4A0H4	27	23	0.791	1.264	↓
	Cytoskeletal / Structural	Cell adhesion molecule 3	Q1WIM3	21	10	1.485	1.485	↑
		AP-3 complex subunit beta	D4AE00	37	52	1.249	1.249	↑
		Isoform 2 of Actin-related protein 2/3 complex subunit 5-like protein	A1L108-2	32	5	1.210	1.210	↑
		Gamma-adducin	Q62847	28	22	1.201	1.201	↑
		Drebrin-like protein	**Q9JHL4**	**29**	**15**	**0.430**	**2.325**	↓
		Dysferlin (Predicted), isoform CRA_a	**D4A6X1**	**22**	**57**	**0.487**	**2.055**	↓
		Tropomodulin-2	P70566	40	18	0.631	1.585	↓
		Isoform 2 of Limbic system-associated membrane protein	Q62813-2	53	26	0.673	1.485	↓
		Thymosin beta-4	P62329	68	5	0.686	1.458	↓
		Myristoylated alanine-rich C-kinase substrate (MARCKS)	F1LMW7	55	19	0.707	1.414	↓
		Myelin basic protein transcript variant N (Fragment)	I7EFB0	62	19	0.711	1.407	↓
		MARCKS-related protein	Q9EPH2	19	4	0.719	1.391	↓
		Neurotrimin	Q62718	35	17	0.747	1.339	↓
		Cell cycle exit and neuronal differentiation protein 1	Q5FVI4	38	7	0.747	1.338	↓
		Myelin proteolipid protein	P60203	25	11	0.751	1.331	↓
		Cell division control protein 42 homolog	Q8CFN2	40	10	0.773	1.294	↓
		Opioid-binding protein/cell adhesion molecule	P32736	43	17	0.780	1.282	↓
		Neurofascin	D3ZW56	33	41	0.785	1.273	↓
		Beta-adducin	F8WFS9	29	25	0.795	1.258	↓

DH	Category	Protein	Accession no.	Cov (%)	Pep	EtOH: Control	Fold △	
Cytoskeletal / Structural (cont.)		Microtubule-associated protein 6	Q63560	47	56	0.795	1.258	↓
Other		Ribonuclease inhibitor	E2RUH2	22	11	1.719	1.719	↑
		Purine nucleoside phosphorylase (Fragment)	D3ZXK9	47	15	1.428	1.428	↑
		3'(2'),5'-bisphosphate nucleotidase 1	Q9Z1N4	51	23	1.423	1.423	↑
		Protein Gm960 (Fragment)	F1M172	36	20	1.299	1.299	↑
		Protein Gramd2 - GRAM domain-containing protein 2	D3ZIZ1	28	12	1.213	1.213	↑
		Protein Rpl34l1 - ribosomal protein L34-like1	D3ZHM1	38	6	1.203	1.203	↑
		Antigen peptide transporter 2	**Q6MGA3**	**35**	**38**	**0.473**	**2.113**	↓
		Uncharacterized protein (Fragment)	M0RA48	53	16	0.763	1.310	↓

[The coverage percentage (Cov %) indicates the number of identified amino acids associated with that protein represented as a percentage of the total number of amino acids in that protein. The number of exclusive unique peptides (Pep) represents the number of unique peptide sequences associated with that protein.]

WESTERN BLOT CONFIRMATION

In the PFC the Student t-test showed no significant difference in the levels of NDUFA9 (NADH dehydrogenase subunit 9) between control and EtOH-rats. However, the result tended to be in the same direction as the proteomic analysis. Levels of NDUFA9 tended to be greater in EtOH-rats ($t_{(5)} = -2.215$, $p = 0.078$, **Figure 4.9**). Using the acquired results as preliminary data, power analysis showed that a sample size of 11 rats per group was needed for a significant result (**Appendix A4.4**). However, we used the maximum number of rats we had available to us to perform these western blot experiments. Levels of ATP5A and GSK3β were not significantly different between control and EtOH-rats in the DH as shown by Western blot analysis (Student t-test, **Figure 4.10** & **4.11**)

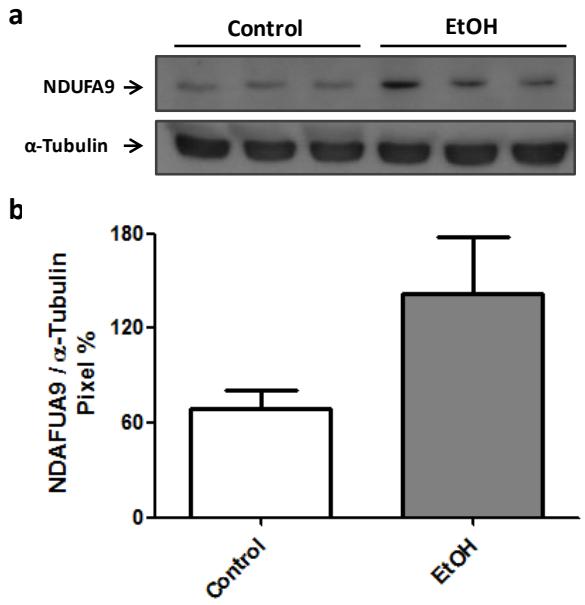

Figure 4.9: Western blot analysis of NDUFA9 in the prefrontal cortex.

(***a***) Western blot of NDUFA9 in the PFC. (***b***) Levels of NDUFA9 tended to be greater in EtOH-rats (t-test, $p = 0.07$). The data were normally distributed (SW, $p > 0.05$). The data represent the mean ± SEM. [Control, n = 4; EtOH, n = 3].

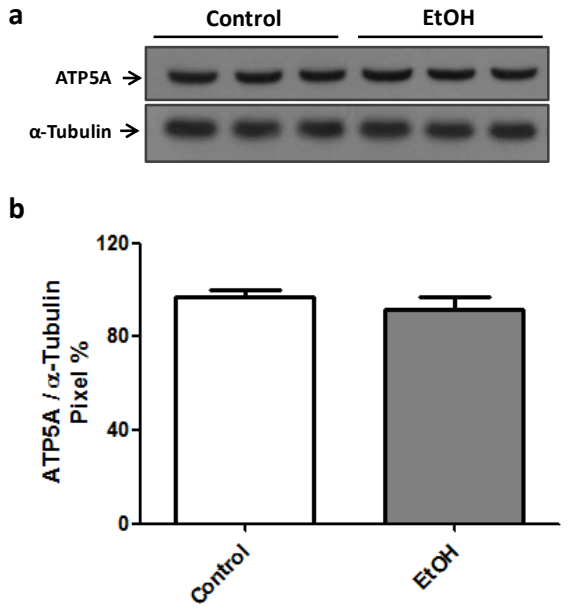

Figure 4.10: Western blot analysis of ATP5A in the dorsal hippocampus.

(***a***) Western blot analysis of ATP5A in the DH. (***b***) Student t-test revealed no significant difference in the level of ATP5A between control and EtOH-rats measured by Western blot. The data are normally distributed (SW, $p > 0.05$). The data represent the mean ± SEM. [Control, n = 4; EtOH, n = 3]

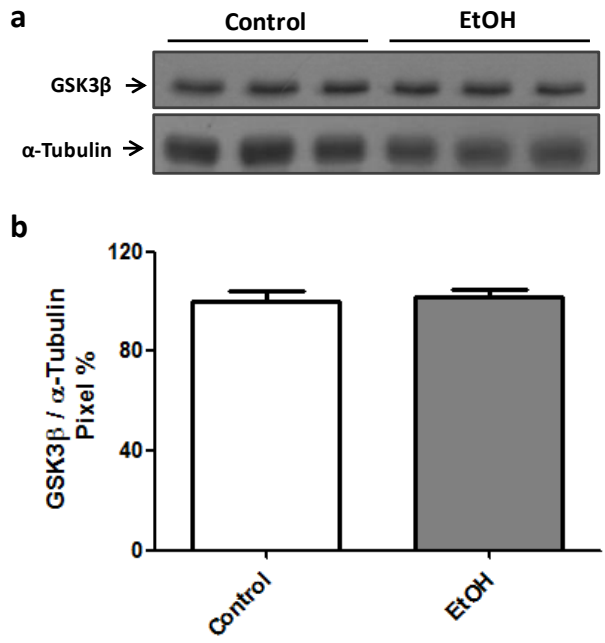

Figure 4.11: Western blot analysis of GSK3β in the dorsal hippocampus.

(***a***) Western blot analysis of GSK3β in the DH. (***b***) Student t-test revealed no significant difference in the level of GSK3β between control and EtOH-rats measured by Western blot. The data are normally distributed (SW, $p > 0.05$). The data represent the mean ± SEM. [Control, n = 4; EtOH, n = 3]

DISCUSSION

The aim of the present study was to identify the proteins altered by early-postnatal ethanol exposure in the rat PFC and DH using iTRAQ and LC-MS. The main findings of this study include a significant ethanol-induced upregulation of proteins related to energy metabolism in the PFC. However, the opposite was observed in the DH. Further, significantly more proteins were altered by early-postnatal ethanol exposure in the DH than in the PFC. These changes involved a downregulation of numerous proteins related to energy, redox regulation, neurotransmission, protein metabolism and cytoskeletal structure.

Adolescent rats exposed to early-postnatal ethanol, during the third trimester equivalent developmental stage showed an increased capacity for oxidative phosphorylation of ADP to produce ATP in the PFC. This was suggested by increased levels of NADH dehydrogenase [ubiquinone] 1 alpha subcomplex subunit 9 (mitochondrial) (NDUFA9), succinate dehydrogenase [ubiquinone] flavoprotein subunit (mitochondrial) and cytochrome *c* oxidase subunit 2 in the PFC compared to control rats. These proteins are components of Complex I, II and IV of the electron transport chain respectively (Hüttemann et al., 2012). Specifically, subunit 2 of cytochrome *c* oxidase is part of the catalytic core of the enzyme which mediates ATP synthesis (Srinivasan and Avadhani, 2012). These results suggest an increased capacity for energy production in the PFC.

The molecular effects of early-postnatal ethanol exposure are largely unexplored in the literature. However, ethanol administered prenatally has been shown to decrease the number of mitochondria and activity of the respiratory chain in the cerebrum of mice exposed to prenatal-ethanol from GD6 - GD15 (Xu et al., 2005). Further, whole foetal mice brains exposed to prenatal ethanol (25 % ethanol-derived calorie liquid diet) from GD7 - GD13, showed decreased NDUFA9 (Sari et al., 2010b). The opposing results may be due to the timing of ethanol exposure, age at sacrifice and brain area analyzed. The previous studies investigated the short-term effects of prenatal-ethanol exposure on whole brains whereas the present study separately investigated long-term effects of early-postnatal ethanol exposure on the PFC and DH. Irrespective of timing and route of administration, previous studies, in conjunction with findings in the present study demonstrated the susceptibility of mitochondrial function to ethanol-induced changes.

The suggested increase in capacity for energy production via mitochondrial oxidative phosphorylation in the PFC may result in increased mitochondrial reactive oxygen species production which may potentially lead to oxidative stress (Hüttemann et al., 2012). In addition, several proteins related to redox regulation were downregulated in the PFC of EtOH-rats compared to controls. For example, glutathione reductase and S-formylglutathione hydrolase were decreased in the PFC after early-postnatal ethanol exposure. Both these enzymes increase levels of glutathione (GSH) (Dringen, 2000; Haslam et al., 2002). Therefore, decreased levels of glutathione reductase and S-formylglutathione hydrolase may indicate decreased GSH production. These results show a decreased antioxidant capacity in the PFC after exposure to ethanol during the early-postnatal period and increased vulnerability to oxidative stress. This is in agreement with previous studies which showed decreased levels of GSH in whole embryo cultures obtained from SD dams after gestational alcohol exposure (Jilek et al., 2015) as well as in adult SD rats exposed to prenatal-ethanol (Patten et al., 2013b) compared to controls.
These results, in addition to the suggested increase in capacity for energy production and reactive oxygen species, indicate a possible shift from the normal redox environment and the potential for oxidative stress in the PFC after early-postnatal ethanol exposure. This is in agreement with Brocardo *et al*. (2011) who suggested the shift from the normal intracellular redox state may be as an indirect result of ethanol-induced dysregulation of mitochondrial function.

In the PFC of EtOH-rats there were lower levels of glutamate decarboxylase and discs large homolog 2 (isoform 4). Glutamate decarboxylase 2 (also known as glutamic acid decarboxylase 2, GAD2), synthesizes the inhibitory neurotransmitter GABA from glutamate. A previous study indicated a decreased number of GABAergic neurons in the cortex of both C57BL/6Y and BALB/CJ mouse strains exposed to 2 doses of ethanol (2.5 g/kg) via subcutaneous injections on P7 (Smiley et al., 2015). C57BL/6J mice also had a decreased number of GABAergic neurons in the medial PFC after early-postnatal ethanol exposure on P5, P7 and P9 (2 x 5 g/kg/day) (Hamilton et al., 2017). However, when ethanol was administered prenatally (35.5 % ethanol-derived calorie liquid diet, GD1 - GD22) there was no difference in the levels of glutamate decarboxylase between SD control rats and rats exposed to prenatal-ethanol (Sickmann et al., 2014). This difference may be due to the timing of ethanol exposure

(prenatal- versus postnatal-ethanol exposure). Decreased levels of glutamate decarboxylase suggests decreased levels of GABA and hence a decreased capacity for inhibitory control in the PFC of rats exposed to early-postnatal ethanol compared to controls.

Lower levels of discs large homolog 2 (isoform 4), also known as PSD-95 (Hunt et al., 1996; Maiya et al., 2012), were observed in the PFC of EtOH-rats relative to controls. PSD-95 has previously been measured in animal models of FASD when ethanol has been administered prenatally however the results are variable. In the hippocampus of adolescent Wistar rats (P30) exposed to prenatal-ethanol (6 g/kg, GD7 - GD21), PSD-95 was found not to differ from control rats (Elibol-Can et al., 2014) . Further, PSD-95 was shown to be increased in the cerebral cortex of adult rats exposed to prenatal-ethanol (2 - 4 g/kg/day, 25 % ethanol, GD7 - GD16) (Kim et al., 2010). Our results add to the varying literature regarding PSD-95 and developmental-ethanol exposure. These differences may be due to the timing and amount of ethanol exposure as well as the difference in age of the rats at which the analysis was conducted. Moreover, PSD-95 is susceptible to early-postnatal ethanol-induced changes and may parallel long-term disruptions in neuronal spine development.

In addition, rats exposed to early-postnatal ethanol had higher levels of neural cell adhesion molecule 1in the PFC compared to control rats. Neural cell adhesion molecule 1 functions at the synapse and may play a role in synaptogenesis, neuroplasticity and LTP by facilitating contact between two synapses (Dalva et al., 2007). This may suggest a compensatory mechanism to mitigate early-postnatal ethanol-induced changes in synaptic plasticity and LTP represented by decreased levels of PSD-95.

In the PFC of EtOH-rats, cytoskeletal components were altered by early-postnatal ethanol exposure. Oligodendrocyte-myelin glycoprotein levels were decreased in the PFC of rats exposed to early-postnatal ethanol. Johns & Bernard (1999) proposed 3 possible functions of myelin-oligodendroctye glycoprotein: cellular adhesion, oligodendrocyte microtubule stability and mediating the interaction between myelin and the immune system (Johns and Bernard, 1999). EtOH-rats had greater levels of dynactin in the PFC compared to control rats. Dynactin forms a complex with and activates cytoplasmic dynein, a major neuronal transporting molecule (Hirokawa et al., 2010). The dynactin-dynein complex plays a role in retrograde transport of neurotrophins, neurofilaments and misfolded or degraded proteins from the periphery towards the cell body (Levy and Holzbaur, 2006). Microtubules, actin filaments and neurofilaments are components of the neuronal cytoskeleton (Levy and Holzbaur, 2006) and

are important for maintaining cellular extensions such as axons and dendrites. A disruption in cytoskeletal proteins may indicate impaired functionality of neuronal cells

In the DH, a decreased capacity for ATP production was observed in adolescent rats exposed to early-postnatal ethanol. This was indicated by a significant decrease in ATP synthase subunits g, alpha, beta and gamma as well as cytochrome *c* oxidase subunits 5B and 7C and NADH dehydrogenase [ubiquinone] Fe-S protein 8. ATP synthase produces ATP as a result of the proton motive force generated by the electron transport chain of which cytochrome *c* oxidase and NADH dehydrogenase are major components (Hüttemann et al., 2012). Similar to that of the PFC, early-postnatal ethanol-induced molecular changes in the DH are largely unexplored in the literature. However, the observed early-postnatal ethanol-induced reduction in the capacity for energy production in the DH is in agreement with previous studies in which alcohol was administered prenatally. Studies have indicated a reduction in respiratory chain activity and decreased ATP synthase in the cerebrum of mice foetuses exposed to ethanol from GD6 to GD15 (Xu et al., 2005). ATP synthase and NADH dehydrogenase were also shown to be downregulated in foetal brains of Balb/c mice exposed to prenatal-ethanol (GD6 - GD15) (Xu et al., 2005). In addition, foetal brains of C57BL/6 mice exposed to prenatal-ethanol (25 % ethanol derived liquid diet) from embryonic day 7 to 13 had lower levels of ATP synthase compared to control mice (Sari et al., 2010b). Further, lower levels of mRNA encoding for complex IV (cyctochrome *c* oxidase) and decreased ATP production was observed in cultured cerebellar neurons obtained from P1 Long-Evans rat pups exposed to gestational alcohol (Chu et al., 2007). These studies highlight the short-term vulnerability of mitochondria to ethanol exposure during early-development in whole foetal brains. Therefore, results from the present study suggest that early-postnatal ethanol exposure may cause persistent deficits in mitochondrial function and decrease the capacity for energy production specifically in the DH.

In the DH of EtOH-rats, several redox-regulating proteins were downregulated compared to control rats. For example, glutaredoxin 5 (homolog), and thioredoxin (fragment) were decreased in adolescent rats exposed to early-postnatal ethanol. These results are similar to a previous study in which 2D SDS page-based proteomic analysis showed decreased thioredoxin, in the cerebral cortex of P21 SD rats exposed to prenatal-ethanol (36% ethanol-derived liquid diet) (Canales et al., 2013). Glutaredoxin and thioredoxin are enzymes involved in regulating

redox cell signaling via redox-sensitive posttranslational modifications. Specifically, glutaredoxin catalyzes the removal of GSH from target proteins (de-glutathionylation) (Xiong et al., 2011). Decreased levels of glutaredoxin and thioredoxin may indicate a greater number of S-glutathionylated and S-nitrosylated proteins respectively (Anand and Stamler, 2012) since these redox-sensitive enzymes reverse these processes (Xiong et al., 2011). These results may indicate decreased antioxidant capacity in the DH due to decreased ability to remove GSH from S-glutathionylated proteins. Moreover, increased levels of S-glutathionylated proteins may significantly alter signal transduction pathways since the addition of GSH to target proteins can alter the structure, function and cellular location of proteins (Xiong et al., 2011). Target proteins include kinases, phosphatases and transcription factors, hence S-glutathionylation may serve as an additional moderator of signal transduction (Xiong et al., 2011). Specifically, S-glutathionylation of PKA and Ras, upstream regulators of ERK1/2-signaling, decreases and increases their activity respectively (Xiong et al., 2011). Inactivation of PKA, will limit transcription and the potential for neural plasticity, whereas increased Ras activity may promote ERK1/2 activity (Xiong et al., 2011). Interestingly, *Chapter 2* described experiments in which rats exposed to early-postnatal ethanol had a greater P-ERK1/2 to ERK1/2 ratio in the DH. This could have resulted from the observed ethanol-induced decrease in glutaredoxin in the present study, leading to increased Ras activity due to continual S-glutathionylation. In addition, aldehyde dehydrogenase was decreased in the DH of adolescent rats exposed to early-postnatal ethanol. Aldehyde dehydrogenase is an important enzyme in the metabolism of acetaldehyde which is formed during alcohol metabolism (Tong et al., 2011). The downregulation of aldehyde dehydrogenase might lead to an accumulation of aldehydes which may cause cell damage (Wenzel et al., 2007) and impair the functionality of the DH. In the present study, both the PFC and DH showed decreased antioxidant capacity and are therefore susceptible to oxidative stress. Further, in the DH cell signaling may have been altered by S-glutathionylation.

In the DH, more signalling-related proteins were altered by early-postnatal ethanol exposure than in the PFC of these rats. For example, glutamine synthetase was increased in the DH. Glutamine synthetase, converts excess glutamate to glutamine (Suárez et al., 2002) while consuming a lot of energy in the form of ATP (Magistretti and Allaman, 2015). Increased glutamine synthetase may put further strain on energy production in the DH. In addition, increased levels of glutamine synthetase may indicate decreased levels of glutamate in the

synaptic cleft and changes in glutamate recycling (Stobart and Anderson, 2013) which may lead to impaired signalling in the DH. This may be supported by the observed decrease in glutamate receptor 3 in the DH of these rats. Further, downstream of glutamate, we observed decreased levels of calmodulin, protein kinase C and GSK3β in the DH of rats exposed to early-postnatal ethanol. Calmodulin is a major calcium-binding protein involved in multiple intracellular signalling processes (Xia and Storm, 2005). Upon calcium entry, calmodulin activates adenylyl cyclase which then leads to the activation of PKA and phosphorylation of GSK3β. Further, protein kinase C may also phosphorylate GSK3β (Kaytor and Orr, 2002). Phosphorylation of GSK3β inactivates its kinase activity (Li and Jope, 2010). Hence, results in the present study suggest decreased phosphorylation of GSK3β and hence increased activity of GSK3β in the DH of rats exposed to early-postnatal ethanol. However, we have previously observed increased levels of P-GSK3β in the DH of rats exposed to early-postnatal ethanol (*Chapter 2*). This difference may be due to the treatment and stress of behavioural testing of the rats in *Chapter 2*, whereas in the present study rats were left undisturbed until sacrifice. This highlights the importance of measuring the effects of early-postnatal ethanol-induced changes in rats that have not been subjected to prior handling-induced stress (Bohacek et al., 2015; Deutsch-Feldman et al., 2015).

In the DH, protein foxc1, a transcription factor belonging to the forkhead box family of transcription factors, was increased in EtOH-rats compared to controls. Activated ERK1/2 has been shown to promote the stability of FOXC1 (Berry et al., 2006). The > 2-fold increase in FOXC1 in the DH of EtOH-exposed rats correlates with the increased P-ERK1/2 to ERK1/2 ratio in the DH after early-postnatal ethanol exposure shown in *Chapter 2*.

Further in the DH, histone proteins H3, H4, H2B, H1.4 and H2A were downregulated in EtOH-rats compared to controls. Decreased histone proteins may be as a result of ethanol-induced DNA damage. Further, these results suggest ethanol-induced epigenetic changes. Epigenetic mechanisms may contribute to the persistent effects of ethanol exposure (Ungerer et al., 2013). Previous studies have shown ethanol-induced histone modifications. For example, when ethanol was administered prenatally, Bekdash *et al*. (2013) showed that prenatal-ethanol exposure results in histone modifications and DNA methylation in the hypothalamus of adult rats. Further, adult C57BL/6J mice exposed to early-postnatal ethanol on P4 and P7 (2 x 2.5 g/kg/day) showed altered methylation and gene expression patterns (Chater-diehl et al., 2016).

Our results, in agreement with previous studies, suggest that developmental-ethanol exposure may permanently alter genetic components.

Early-postnatal ethanol exposure induced changes in cytoskeletal proteins in the DH. For example, debrin-like protein, dysferlin and thymosin β-4 were decreased compared to control rats. Dysferlin is found in vascular endothelial cells and is associated with disruption in the blood-brain-barrier during inflammation (Hochmeister et al., 2006). Thymosin β-4 regulates actin and plays a role in cellular repair mechanisms in addition to many other structural processes such as angiogenesis, migration, differentiation and survival (Crockford et al., 2010). Further, myelin basic protein (transcript variant N) and myelin proteolipid protein were decreased in the DH of rats exposed to early-postnatal ethanol. Myelin has previously been shown to be susceptible to ethanol-induced changes. SD rats exposed to 15 % ethanol (3 g/kg/day, i.p) for 14 days had decreased levels of myelin proteolipid protein in the hippocampus compared to saline-control rats (Lee et al., 2010). Decreased myelin in the DH of rats exposed to early-postnatal ethanol suggests decreased integrity of the myelin sheath and hence decreased signal conduction. In addition, decreased myelination may further constrain cellular energetics in the DH since unmyelinated axons require more energy for signal transduction (Bercury and Macklin, 2015).

Western blot analysis of NDUFA9 (anti-NADH dehydrogenase 1 alpha subcomplex subunit 9) in the PFC and ATP5A and GSK3β in the DH did not confirm or contradict the proteomic findings. Levels of protein quantified by Western blot were in the same direction as the proteomic result. A larger sample size may have been needed due to the insensitivity of the Western blotting technique. However, we used the maximum number of rats available to us to perform the Western Blot experiments. Although, with regards to NDUFA9, the antibody used for detection (NDUFA9 (ab181381)) was recently discontinued because non-specific binding occurred in NDUFA9 knockout mice. Therefore, non-specific binding in the Western blot may have masked the early-postnatal ethanol-induced effect observed using proteomic analysis.

In summary, our results suggest increased activity of the respiratory chain in the PFC which may result in an increased production of reactive oxygen species and the potential for oxidative stress-induced damage in adolescent rats exposed to early-postnatal ethanol. Further, our

results suggest decreased inhibitory control in the PFC after early-postnatal ethanol exposure. Together these results suggest a deficit in the functionality of the PFC after early-postnatal ethanol exposure and therefore a lack of top-down control may contribute to the observed inattentiveness, learning and psychological deficits reported in the literature.

In the DH, we observed a decreased capacity for energy production after early-postnatal ethanol exposure as well as a decreased capacity to protect against oxidative stress. Further constraint on the capacity for energy production was suggested by increased levels of glutamine synthetase and decreased levels of myelin-related proteins in the DH. These results may contribute to understanding the impairments in learning and memory processes reported the in the literature by impairing the functionality of the DH. In addition, we observed changes in histone-related proteins in the DH of EtOH-rats which suggests early-postnatal ethanol may alter genetic components which may contribute to the persistent effects of ethanol exposure.

Further, in this study the PFC and DH were analyzed separately. Our results indicate region-specific effects of early-postnatal ethanol exposure on the brain since we observed opposing results regarding neuronal energetics in the PFC and DH. In addition, a greater number of proteins were shown to be altered by early-postnatal ethanol exposure in the DH compared to the PFC. This may indicate that the DH is more susceptible to the detrimental effects of early-postnatal ethanol exposure. These proteomic profiles have contributed valuable insight into the long-term early-postnatal ethanol-induced changes in protein levels in the PFC and DH.

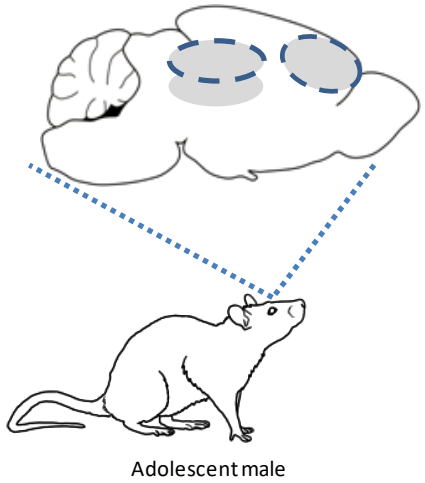

	Energy Metabolism	Redox Regulation	Signaling	Structural
Prefrontal Cortex	↑ oxidative phosphorylation	↓ protection against oxidative stress	↓ inhibitory control	↓ cytoskeletal - proteins
Dorsal Hippocampus	↓ ATP production	↓ protection against oxidative stress	↓ glutamate recycling ↓ calmodulin-dependent signaling	↓ myelination

Figure 4.12: Summary of proteomic results in the *prefrontal cortex* and *dorsal hippocampus* after early-postnatal ethanol exposure

CHAPTER 5: THE EFFECTS OF PRENATAL-ETHANOL EXPOSURE COUPLED WITH MATERNAL SEPARATION STRESS ON THE RAT BRAIN.

INTRODUCTION

In addition to cognitive deficits, individuals exposed to alcohol *in utero* are more likely to have psychological disorders, such as anxiety and depression, attention deficits and a lack of impulse control (O'Connor and Paley, 2009; Kable et al., 2016). The neurochemistry underlying FASD is still unknown and there is currently no treatment for FASD therefore the neurobehavioural deficits and FASD-associated psychological disorders usually persist into adulthood (Famy et al., 1998; Streissguth et al., 2004; Rangmar et al., 2015a, 2015b). Further, FASD is highly prevalent in low-socioeconomic rural areas in which alcohol is heavily abused. Consequently, children born with FASD may face further adverse childhood experiences when living with alcohol-abusing parent/s (Anda et al., 2002). It has been shown that exposure to childhood adversities *alone* can lead to the development of psychological disorders later in adulthood (Mullen et al., 1996; Heim and Nemeroff, 2001; Carr et al., 2013; Grasso et al., 2013). Therefore, early-life adversities may contribute to the development of FASD-associated psychological disorders and cognitive deficits. However, the interaction between alcohol exposure *in utero* and exposure to childhood adversities and its effects on the adult brain have not been fully investigated.

Animal studies have taken into account the timing, quantity and manner of alcohol consumption during pregnancy when choosing animal models of FASD (Patten et al., 2014). However, childhood adversity is a factor which has not been included in animal models of FASD. Therefore, the interaction between exposure to ethanol *in utero* and early-life adversity on the developing brain needs to be investigated. Researchers are able to model childhood adversity using a well characterized animal model of early-life stress, maternal separation (Daniels et al., 2004; Ladd et al., 2004). The maternal separation model has been used to study the development of brain and behavioural disorders in adulthood after exposure to adverse environmental experiences early in life. For example, adult rats exposed to 3 hours of daily maternal separation from P2 - P14 exhibit anxiety- and depression-like behaviour in the EPM and FST respectively (Daniels et al., 2004; Dimatelis et al., 2012; Makena et al., 2012). Further,

maternally separated rats displayed increased number and duration of 22 kHz ultrasonic vocalizations (Dimatelis et al., 2012) which is indicative of a depressive-phenotype (Portfors, 2007).

Therefore, modeling early-life adversity in animal models of FASD can be achieved by coupling prenatal-ethanol with the maternal separation model of early-life stress. Hence, in the present study, in addition to prenatal-ethanol exposure (10 % ethanol solution sweetened with 0.066 % saccharin), rat pups were subsequently exposed to maternal separation for 3 hours/day from P2 to P14. The combination of prenatal-ethanol and maternal separation in an animal model may be a better representation of the etiology of FASD and the associated-psychological deficits. To behaviourally characterize this model, a battery of behavioural tests were used. These tests included measures of cognitive function, hyperactivity and anxiety-like behaviour as in *Chapter 2*, and additional tests such as the EPM, FST and the recording of ultrasonic vocalizations to assesses anxiety- and depression-like behaviour (Ennaceur and Delacour, 1988; Portfors, 2007; Walf and Frye, 2007; Castagné et al., 2010; Slattery and Cryan, 2012). However, instead of the MWM, the NOT was used to asses cognitive function in order to minimize stress to the animals because the NOT relies on spontaneous exploratory behaviour and therefore there is no extensive training and/or exposure to aversive stimuli (Ennaceur and Delacour, 1988; Bevins and Besheer, 2006; Antunes and Biala, 2012; Cohen and Stackman, 2015). Our research group has previously used these behavioural tests to measure, cognitive function, anxiety- and depression-like behaviour in rats (Makena et al., 2012; McFie et al., 2012; Dimatelis et al., 2016; van Zyl et al., 2016).

ERK1/2 and GSK3β are converging points for many signalling cascades that are involved in neurogenesis, differentiation, migration and survival (Moors et al., 2007). Significant components of these signalling cascades are vulnerable to ethanol exposure and dysregulation of these kinases may underlie the observed deficits in neural plasticity and consequently neurotransmission and learning and memory (Lee and Son, 2009; Schmitt et al., 2009; Peng et al., 2010; Chen et al., 2013; Goggin et al., 2014). However, the long-term *in vivo* ethanol-induced molecular changes in ERK1/2 and GSK3β are relatively unexplored in the literature. Hence, in *Chapter 2* we investigated early-postnatal ethanol-induced changes in components of these signalling cascades in adolescent rats exposed to ethanol during the third trimester equivalent developmental stage. In this chapter, we explored prenatal-ethanol exposure-

induced changes in ERK1/2 and GSK3β signalling in adult rats. Importantly, dysregulation of ERK1/2 and GSK3β would influence the functionality of their downstream substrates. For instance, CREB is a transcription factor downstream of both ERK1/2 and GSK3β signalling (Kaidanovich-Beilin and Woodgett, 2011; Bradley et al., 2012; Beurel et al., 2015). Therefore, disruption of ERK1/2 and GSK3β signalling may lead to the irregular expression of some plasticity-related proteins. For example, synaptophysin, a synaptic vesicle-related protein can be used to indirectly measure synaptic density and identify deficits in neural plasticity as a consequence of prenatal-ethanol exposure (Elibol-Can et al., 2014). Further, based on observations made in *Chapter 4* in which energy-related proteins were significantly down regulated in the brain of adolescent rats exposed to ethanol during the early-postnatal period, this chapter investigated ethanol-induced changes in ATP synthase in the PFC and DH of adult rats exposed to prenatal-ethanol.

ERK1/2 and GSK3β signalling dysfunction has also been implicated in maternal separation models of early-life stress in which animals presented with anxiety- and depression-like behaviour (Lippmann et al., 2007; Makena et al., 2012; Mozzaquatro et al., 2014; Dimatelis et al., 2015). For example, adult SD maternally separated rats (P2 - P14, 3 hours/day) showed impaired exercise-induced ERK1/2 activation and spent less time in the open arms of the EPM compared to non-separated rats demonstrating anxiety-like behaviour (Makena et al., 2012). Further, mice exposed to 3 hours/day of maternal separation stress showed increased immobility time in the FST as well as decreased phosphorylation of GSK3β in the hippocampus (Bian et al., 2015). Therefore, decreased phosphorylation of ERK1/2 and GSK3β may play a role in anxiety- and depression-like behaviour observed after maternal separation stress. Similarly, maternal separation stress decreased energy-related proteins in the PFC of rats exposed to 3 hours of daily maternal separation from P2 - P14 (Dimatelis et al., 2013). Hence, both the ERK1/2- and GSK3β-signalling cascades and energy-related proteins have been implicated in models of prenatal-ethanol as well as models of early-life stress, this further highlights the need to investigate the interaction between exposure to ethanol *in utero* and postnatal-environmental adversities on the developing brain. In addition to the effects of prenatal-ethanol and maternal separation stress on the developing brain this chapter also investigated the possible differential effects of these developmental insults on male and female rats.

By coupling prenatal-ethanol with maternal separation stress we hoped to provide a more representative model of FASD in which the possible effect of childhood adversities are accounted for. These tests included the NOT to measure short-term memory function (Ennaceur and Delacour, 1988), the recording of ultrasonic vocalizations (Portfors, 2007) and the EPM (Walf and Frye, 2007) to assess anxiety-like behaviour, the OFT to measure activity and the FST to measure depression-like behaviour (Castagné et al., 2010; Slattery and Cryan, 2012; Dimatelis et al., 2015). In addition, we further aimed to investigate long-term prenatal-ethanol and early-life stress-induced changes in the ERK1/2- and GSK3β-signalling cascades in order to provide insight into the molecular mechanisms underlying cognitive deficits in FASD and the associated-psychological disorders.

METHODS

ANIMALS

Adult male and female SD rats were obtained from the University of Cape Town, Faculty of Health Sciences Animal Unit and housed in a nearby Satellite Facility in the Anatomy Building. Animals were housed in a 12 hour: 12 hour light/dark cycle (lights on at 06:00) with *ad libitum* access to food and water. The temperature was maintained at 23 ± 1 °C and the light intensity at 120 - 150 lux. There was no source of environmental enrichment present in the home cage because it has previously been shown to reduce the effects of prenatal-ethanol exposure and early-life stress (Hannigan et al., 1993; Francis et al., 2002). Ethics approval was obtained from The University of Cape Town Animal Ethics Committee [015/004]. All experimental procedures aimed to minimize the pain and suffering of the animals used and adhered to the guidelines set out in the South African National Standard: The Care and Use of Animals for Scientific Purpose (2008).

PRENATAL-ETHANOL EXPOSURE

Adult female SD rats were introduced to a 0.066 % saccharin solution with the choice of water for 24 hours. The following day the water bottle was removed. Saccharin-control dams continued to have *ad libitum* access to 0.066 % saccharin solution. Ethanol-treated dams however, were trained to voluntarily consume a 0.066 % saccharin-sweetened ethanol solution. Ethanol-treated dams were introduced to a 10 % ethanol solution in a step wise manner (0 %, 2 %, 5 %, 10 %) every second day. Ethanol-treated dams had *ad libitum* access to 10 % ethanol for 10 days to establish a stable drinking pattern (**Figure 5.1).** In previous studies, the blood alcohol levels were measured and found to be 80 – 90 mg/dl (Brady et al., 2012; Marquardt et al., 2014). These are considered to be moderate levels of intoxication (Marquardt and Brigman, 2016). Once a stable drinking pattern was established, vaginal smears were performed (Marcondes et al., 2002) before male rats were paired with the adult females for breeding. Males and females were paired for the duration of the estrus cycle or until the presence of a vaginal plug. This was considered GD0. The adult male rats were not habituated to 0.066 % saccharin or 10 % ethanol, therefore during pairing an additional bottle containing H_2O was present. After the male rat was removed, a red plastic tube and nesting material (tissue paper and shredded paper) were placed in the cage with the dam throughout gestation (**Figure 5.1**). The 0.066 % saccharin and 10 % ethanol bottles were weighed daily throughout gestation to

determine how much alcohol was consumed during pregnancy. Around the expected DOB, females were monitored twice daily for the presence of pups. The DOB was designated as P0. On P2, litters were sexed and culled to a maximum of 10 pups with a minimum of 2 female pups per litter in order to promote equal nourishment and nurturing of pups (Alleva et al., 1989; Agnish and Kellert, 1997). Further on P2, the red tube and nesting material were removed from the cage to avoid any effect of environmental enrichment on the pups. The ethanol concentration was then decreased in a stepwise manner (10 %, 5 %, 2 %, 0 %) every 2 days in order to minimize the effects of ethanol withdrawal. Therefore, by P6 ethanol-treated dams had *ad libitum* access to 0.066% saccharin.

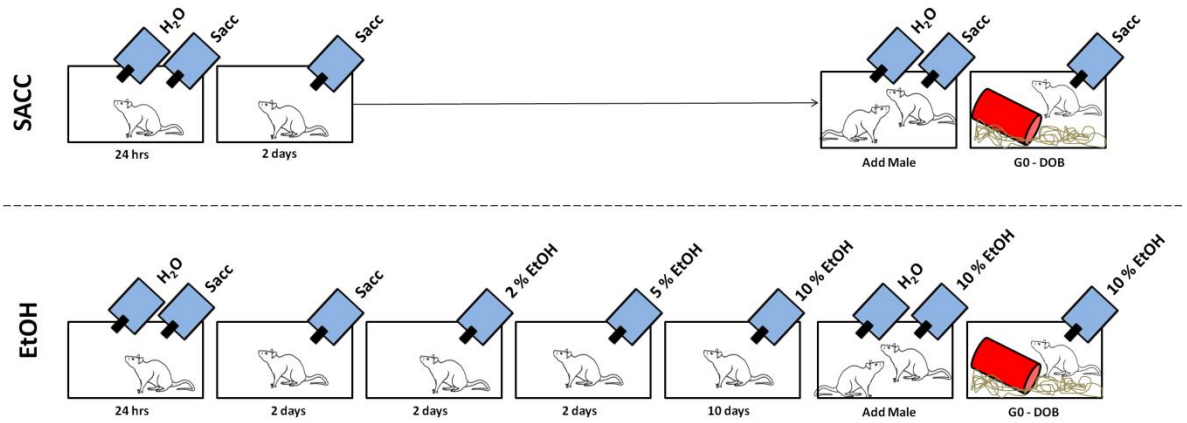

Figure 5.1: Prenatal -ethanol exposure paradigm.

All dams were given the choice of H_2O or 0.066% saccharin (sacc) for 24 hours. Saccharin-control dams continued to have *ad libitum* access to 0.066% saccharin. Whereas, ethanol-treated dams were introduced to a 10 % ethanol saccharin-sweetened solution. The ethanol concentration was increased every second day (0 %, 2 %, 5 %, 10 %). In order to achieve a stable drinking pattern ethanol-treated dams had *ad libitum* access to 10 % ethanol for 10 days before the addition of the male rat. Male and female rats were paired for the duration of the estrus cycle or until the presence of a vaginal plug. During this time an H_2O bottle was placed in the cage because the male rat was not habituated to either 0.066 % saccharin or 10 % ethanol. After the removal of the male rat a red tube and nesting material were added to the cage. The saccharin-control and ethanol-treated dams continued to have *ad libitum* access to either 0.066 % saccharin or 10 % ethanol respectively throughout gestation (GD0 - DOB).

MATERNAL SEPARATION

Whole-litters were chosen at random to undergo maternal separation (MS) from P2 to P14 for 3 hours/day (09:00 - 12:00) while control litters were left undisturbed (nMS). Pups were carefully removed from their home cage and placed in a separate clean cage. Pups were then taken to a separate room to prevent communication between the pups and the dam by ultrasonic

vocalizations (Portfors, 2007). Cages were placed under infrared lighting (± 30 °C) with the lids removed. After 3 hours, pups were returned to the dam in their home cage.

All pups were weighed on P2, P8, P15 and P21 to monitor the effects of prenatal-ethanol and maternal separation on body weight. On P21, all rat pups were weaned from the dam. Pups from the same litter were separated by sex and housed in groups of 2 - 3 rats per cage.

EXPERIMENTAL GROUPS

Prenatal-ethanol exposure coupled with early-life stress resulted in 4 experimental groups: **control** (sacc + nMS); **MS** (sacc + MS); **EtOH** (ethanol + nMS) and **EtOH+MS** (ethanol + MS). A maximum of 2 rats per litter were used in the same experimental group to minimize litter effects. Randomly selected male rats (control, n = 11; MS, n = 7; EtOH, n = 7; EtOH+MS, n = 8) underwent behavioural testing from P57 to P62 while the remaining rats were left undisturbed. All rats were sacrificed on P63. Brain tissue from male and female naïve-rats (experimental rats that did not undergo behavioural testing) were used in Western Blot analysis (male: control, n = 8; MS, n = 8; EtOH, n = 8; EtOH+MS, n = 8 and female: control, n = 8; MS, n = 8; EtOH, n = 8; EtOH+MS, n = 8) (**Figure 5.2**).

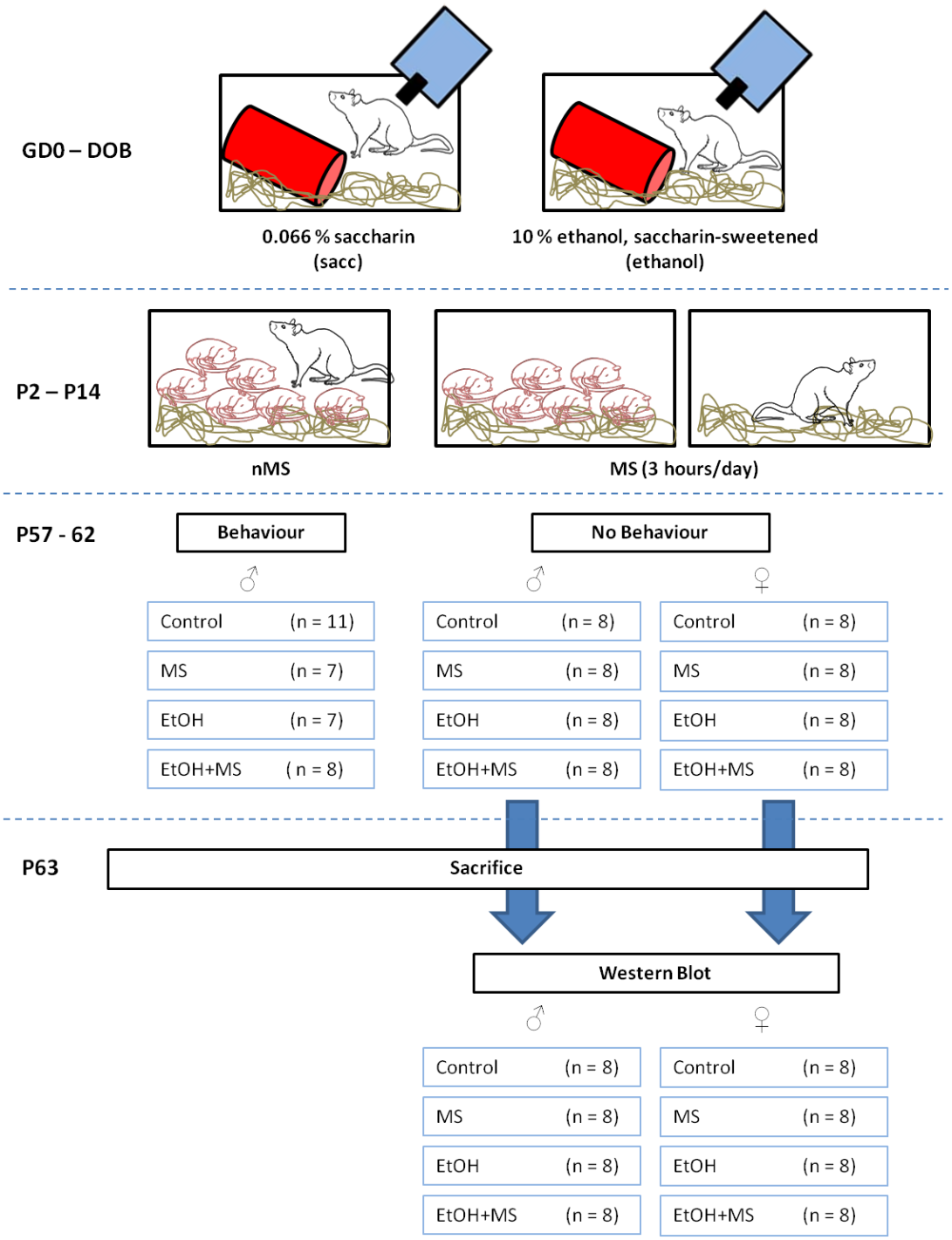

Figure 5.2: Experimental groups.

Dams were exposed to either a 0.066% saccharin solution or a 10% ethanol saccharin-sweetened solution throughout gestation (GD0 - DOB). Whole-litters were then subjected to early-life stress (maternal separation, MS) or were left undisturbed (nMS) from P2 to P14. This resulted in 4 experimental groups for behavioural analysis from P57 to P62 (**control**, sacc + nMS, n = 11; **MS**, sacc + MS, n = 7; **EtOH**, EtOH + nMS, n = 7 and **EtOH+MS**, n = 8) and Western Blot analysis (male: control, n = 8; MS, n = 8; EtOH, n = 8; EtOH+MS, n = 8 and female: control, n = 8; MS, n = 8; EtOH, n = 8; EtOH+MS, n = 8).

BEHAVIOUR

Randomly selected male rats (**control** (n = 11); **MS** (n = 7); **EtOH** (n= 7); **EtOH+MS**, (n = 8)) underwent behavioural testing from P57 to P62 (**Figure 5.3**) during the light phase (08:00 - 10:00). All rats were habituated to the behavioural testing area one hour before the start of each test to decrease the stress due to the exposure to a novel environment as this would have a confounding effect on the behavioural outcome. The behavioural equipment was cleaned with 70 % ethanol and water between behavioural tests to prevent the detection of another rat's scent on the apparatus which could affect the behavioural results. Behaviour was recorded on a video camera (Sony Handycam; DCR-SX83E; Tokyo, Japan) mounted approximately 1 m above the behavioural apparatus. Behavioural videos were later analyzed with Ethovision version 7.0 (Noldus Information Technology, Netherlands).

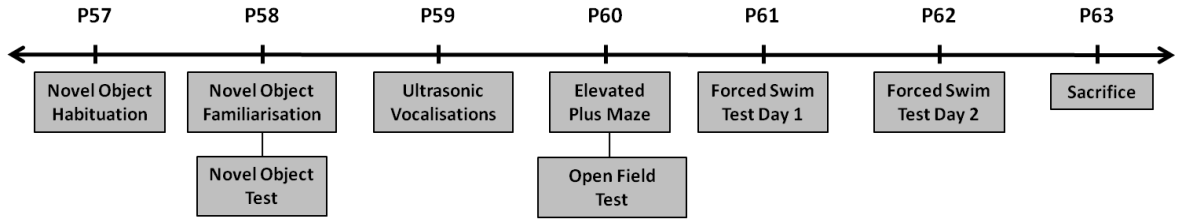

Figure 5.3: Behavioural timeline.

Behavioural testing took place from P57 - P62. Habituation to the novel object test arena took place on P57 followed by the novel object familiarization trial and novel object test trial on P58. The recording of ultrasonic vocalizations occurred on P59. On P60, the elevated plus maze was immediately followed by the open field test. The forced swim test habituation swim and test swim took place on P61 and P62 respectively. All rats were sacrificed on P63.

NOVEL OBJECT TEST

The NOT was used to assess short-term memory on P57 and P58 (Ennaceur and Delacour, 1988). Habituation to the NOT arena took place on P57. Rats were individually placed in the NOT arena (60 cm x 60 cm) and left to explore the environment for 10 minutes. Twenty-four hours later, on P58, rats were familiarized with 2 identical green objects which were screwed into place in the arena. Rats were individually placed in the bottom right hand corner opposite the objects then left to explore the arena for 10 minutes. Rats were then returned to their home cage for 1 hour. For the test trial the top right hand object was replaced with a yellow cylindrical object (novel object). Rats were then individually placed in the NOT arena in the same manner and left to explore the environment for 5 minutes (**Figure 5.4**). The distance travelled and time

spent with each object during habituation, familiarization and the test trial were measured using Ethovision software.

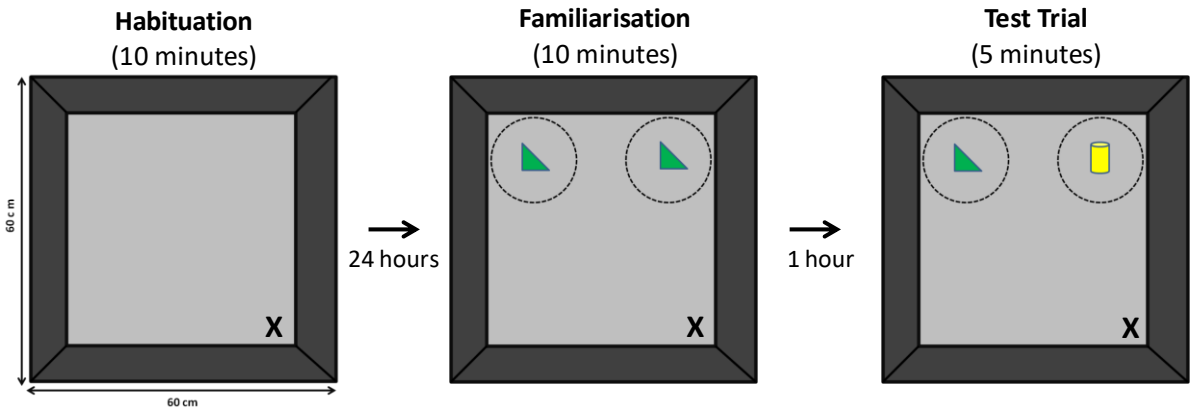

Figure 5.4: Novel object test.

On P57 rats (**control**, n = 11; **MS**, n = 7; **EtOH**, n = 7; **EtOH+MS**, n = 8) were individually placed (**X**) in the novel object arena (60 cm x 60 cm) to habituate to the environment for 10 minutes. On P58, 24 hours later, rats were familiarized with 2 identical green objects for 10 minutes then returned to their home cage. The top right hand object was then replaced with a yellow cylinder (novel object) and after 1 hour rats were again placed in the arena for a 5-minute test trial. The distance travelled and the time spent with each object during habituation, familiarization and the test trial were determined with Ethovision software.

ULTRASONIC VOCALISATIONS

Ultrasonic vocalizations were recorded on P59. Cage mates were individually placed in adjacent Plexiglas cylinders lined with sawdust. This allowed for visualization of the other rat and communication via ultrasonic vocalizations in an environment similar to that of their home cage. Direction sensitive bat detectors were centrally placed over each cylinder and set to detect ultrasonic vocalizations of 22 kHz (**Figure 5.5**). Vocalizations were recorded for 10 minutes and the duration (milliseconds) and number of 22 kHz calls were measured as well as the latency to the first call (milliseconds) using UltraVox software (Noldus Information Technology, Wageningen, Netherlands). Ultrasonic vocalizations ranging from 300 - 4000 milliseconds were used for analysis (Portfors, 2007). Cylinders were cleaned with 70 % ethanol and water, and fresh sawdust added to each cylinder between recordings.

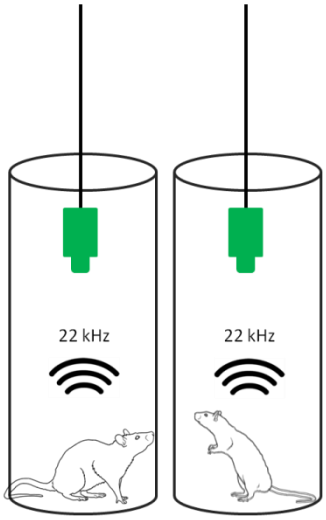

Figure 5.5: The recording of ultrasonic vocalizations

On P59, cage mates were individually placed in separate Plexiglas cylinders lined with sawdust. Bat detectors were centrally placed over each cylinder. The duration (milliseconds) and number of ultrasonic vocalizations of 22 kHz as well as the latency (milliseconds) to the first 22 kHz vocalization were recorded during a 10-minute period.

ELEVATED PLUS MAZE

The EPM was conducted on P60 in a temperature controlled room (23 ± 1°C; 50 ± 20 lux). The EPM consisted of 2 open arms and 2 closed arms linked via a centre zone. Rats were placed in the centre of the maze facing the open arms and left to explore the arena for 5 minutes (**Figure 5.6**). The time spent in the open arms, closed arms and centre zone as well as the distance travelled was measured using Ethovision software.

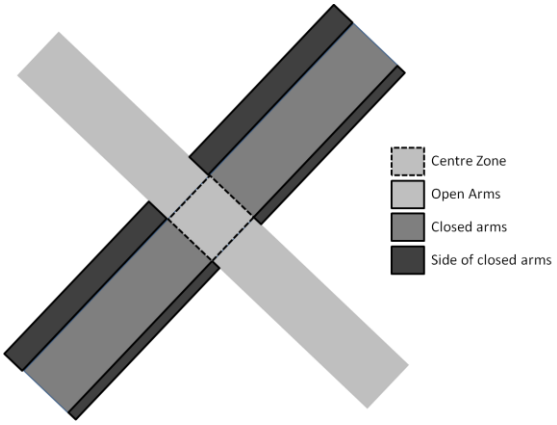

Figure 5.6: Elevated plus maze.

The EPM consisted on 2 open arms and 2 closed arms linked via a centre zone. On P60, rats were individually placed in the centre zone facing the open arms and left to explore the maze for 5 minutes.

OPEN FIELD TEST

On P60, immediately after the EPM rats underwent a 5-minute trial in the open field as described in *Chapter 2* (p.38).

FORCED SWIM TEST

The FST took place on P61 and P62. Cylinders were filled with water (23 ± 1°C) to a height of 30 cm and separated by sheets of cardboard (**Figure 5.7**). The FST consists of two trials: the habituation swim and the test swim. The habituation swim is conducted in order for the rat to learn that this is an inescapable task and therefore immobility behaviour is accentuated during the test trial the following day (Castagné et al., 2010; Slattery and Cryan, 2012; Dimatelis et al., 2015). On P61, rats were individually placed in separate Plexiglass cylinders and allowed to swim for 15 minutes (habituation). The test swim took place on P62 (24 hours later), during which, rats were again individually placed in separate cylinders and allowed to swim for 5 minutes (Castagné et al., 2010; Slattery and Cryan, 2012; Dimatelis et al., 2015). Rats were briefly towel dried before being returned to the satellite animal facility then placed into clean cages with their original cage mates. Cylinders were emptied then cleaned with 70 % ethanol and wiped down with dH_2O before being refilled with water after every rat. The time spent swimming, immobile and climbing, as well as the latency to the first bout of immobility were manually determined during later video analysis.

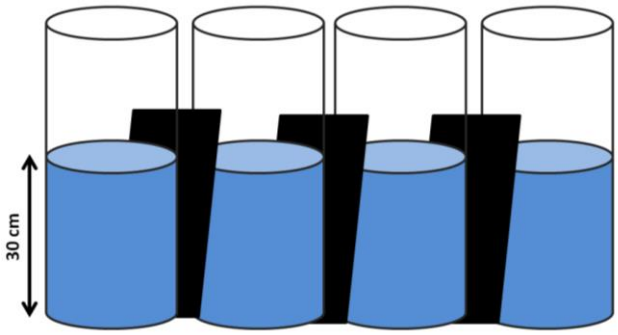

Figure 5.7: The forced swim test.

On P61 rats were exposed to a 10-minute habituation swim in individual cylinders. Cylinders were filled with water (23 ± 1 °C) to a height of 30 cm and separated by sheets of cardboard. A 5-minute swim took place 24 hours later on P62 in the same manner.

SACRIFICE

On P63 rats were habituated to a closed room adjacent to the decapitation area 1 hour before sacrifice took place to decrease stress due to exposure to a novel environment. Rats were then swiftly sacrificed using a rat guillotine, without anaesthesia between 08:00 and 10:00. The blood odour was eliminated by thoroughly cleaning the equipment (the guillotine and dissection tools) with 70 % ethanol after each decapitation. Immediately after decapitation the whole-head was briefly submerged in liquid nitrogen to preserve phosphorylated proteins in the brain (Makena et al., 2012). The PFC and DH were rapidly removed and stored in liquid nitrogen until they were needed. The PFC and DH from naïve male and female control, MS, EtOH and EtOH+MS rat groups were used for Western blot analysis in this chapter. The PFC and DH from the remaining naïve-rats were used for proteomics analysis which is described in *Chapter 6* (p.192).

WESTERN BLOT ANALYSIS

PFC and DH brain tissue samples from male and female **control** (♂ n = 8; ♀ n = 8), **MS-** (♂ n = 8; ♀ n = 8), **EtOH-** (♂ n = 8; ♀ n = 8) and **EtOH+MS-** (♂ n = 8; ♀ n = 8) rats that *did not undergo behavioural testing* were sonicated for 10 seconds in RIPA buffer (5 M NaCl; 1% Triton X-100; 0.1 % SDS; 20 mM Tris (pH 7.5); 1% Deoxycholate) with protease and phosphatase inhibitor cocktail (Halt™ Protease & Phosphatase Inhibitor Cocktail, ThermoScientific). Samples were then centrifuged at 17 200 *x* g for 30 minutes at 4°C. The supernatants were collected and protein concentration was determined using the Pierce™ BCA Protein Assay Kit (#23225, Thermo Scientific, Rockford, U.S.A.). Loading samples contained bromophenol blue sodium (Sigma-Aldrich), dithiothreitol (Promega, Madison, USA), RIPA buffer and the respective lysate. Loading samples were boiled for 4 minutes at 95 °C and stored at -20 °C. Samples were re-boiled (4 minutes at 95 °C) and centrifuged briefly on the desk mini-centrifuge (Tomos, Laboratory Products) before use.

The optimal amount of protein (20 µg) determined during characterization was electrophoresed on 12% SDS-polyacrylamide gels for 1 hour 15 minutes (150 V) and then transferred (100 V) for 1 hour onto a hybond nitrocellulose membrane (GE Healthcare, U.K.). The membranes were blocked for 1 hour with 5 % bovine serum albumin (BSA) or 5 % milk and then

immunolabelled overnight with primary antibodies **(Table 5.1:** Phospho-p44/42 MAPK (Thr202/Tyr204) Rabbit mAb #4370, Cell Signalling, RRID AB_ 10234795 (**P-ERK1/2**): PFC 1 : 4 000 and DH 1 : 7 000; Phospho-GSK-3Beta (Ser 9)(5B3) Rabbit mAb, Cell Signalling, RRID AB_ 2115201 (**P-GSK3β**): PFC 1 : 4 000 and DH 1 : 2 000; Phospho-CREB (Ser133) (87G3) Rabbit mAb, Cell Signalling, Cat# 9198, RRID: AB_2561044 (**P-CREB**): PFC 1 : 2 000 and DH 1 : 2 000; Mouse monoclonal anti-synaptophysin, Abcam SY38 ab8049, RRID AB_444181 (**Synaptophysin**): PFC 1 : 60 000 and DH 1 : 60 000; and ATP5A (51): sc-136178, Santa Cruz Biotechnology, RRID AB_2061764 (**ATP5A**): PFC 1 : 5 000 and DH 1 : 5 000) against proteins of interest. Membranes were then incubated with the appropriate secondary HRP-conjugated antibodies (Goat Anti-Rabbit IgG (H+L)-HRP Conjugate, #170-6515, BioRad (**GAR**): P-ERK1/2, PFC 1 : 12 000, DH 1 : 14 000; P-GSK3β, PFC 1 : 10 000, DH 1 : 10 000; P-CREB, PFC 1 : 10 000, DH 1 : 10 000 and Goat Anti-Mouse IgG (H+L)-HRP conjugate, #170-6515, Biorad (**GAM**): synaptophysin and ATP5A, PFC 1 : 10 000, DH 1 : 10 000). Membranes were stripped with 0.2 M NaOH for 5 minutes and immunolabelled with antibody to the respective reference protein **(Table 5.1:** p44/42 MAPK (ERK1/2) Antibody, Cell Signalling, RRID AB_ 823494 (**ERK1/2**): PFC 1 : 2 000 and DH 1 : 2 000; GSK-3β (27C10) Rabbit mAb, Cell Signalling, RRID AB_ 490890 (**GSK3β**): PFC 1 : 8 000 and DH 1 : 8 000; CREB (48H2) Rabbit mAb, Cell Signalling; Cat# 9197, RRID: AB_331277, (**CREB**): PFC 1 : 2 000 and DH 1 : 2 000 and Monoclonal Anti-alpha-tubulin antibody produced in mouse, T5168, Sigma-Aldrich, RRID AB_ 477579 (**α-tubulin**): PFC 1 : 3 000 and DH 1 : 3 000**)**. Secondary antibodies for the reference proteins were GAR: ERK1/2: PFC 1 : 10 000, DH 1 : 10 000; GSK3β: PFC 1 : 14 000; DH 1 : 14 000; CREB: PFC : 10 000, DH 1 : 10 000 and GAM: α-Tubulin: PFC1 : 10 000 and DH 1 : 10 000. Membranes were then incubated with Clarity ™ Western ECL Substrate (#170-5060, BioRad) and exposed to X-ray film (Medical X-Ray Film Blue, AGFA) to quantify the protein present. The density of each band was determined using UN-SCAN-IT Software Version 7.0 (Silk Scientific Inc, Utah, USA). The density of each band was calculated as a percentage of the mean density of all the bands representing the protein of interest on the X-ray film (pixel density percentage). The pixel density percentage of each band of interest was then normalized to the pixel density percentage of its respective reference protein (*Pixel %*).

Table 5.1: Primary antibodies used for Western blot analysis.

Antibody	Abbreviation	Identifiers	MW	Dilution	
				PFC	DH
Phospho-p44/42 MAPK (Erk1/2) (Thr202/Tyr204) (D13.14.4E) XP® Rabbit mAb	P-ERK1/2	Cell Signalling; Cat# 4370; RRID: AB_10234795; rabbit; monoclonal.	44 / 42 kDa	1 : 7000	1 : 4000
p44/42 MAPK (ERK1/2) Antibody	ERK1/2	Cell Signalling; Cat# 9102; RRID: AB_823494; rabbit, polyclonal.	44 / 42 kDa	1 : 2000	1 : 2000
Phospho-GSK-3β (Ser 9)(5B3) Rabbit mAb	P-GSK3β	Cell Signalling; Cat# 9323; RRID: AB_2115201; rabbit; monoclonal.	46 kDa	1 : 4000	1 : 2000
GSK-3β (27C10) Rabbit mAb	GSK3β	Cell Signalling; Cat# 9315; RRID: AB_490890; rabbit; monoclonal.	46 kDa	1 : 8000	1 : 8000
Phospho-CREB (Ser133) (87G3) Rabbit mAb	P-CREB	Cell Signalling; Cat# 9198; RRID: AB_2561044; rabbit monoclonal.	43 kDa	1 : 2000	1 :2000
CREB (48H2) Rabbit mAb	CREB	Cell Signalling; Cat# 9197; RRID: AB_331277; rabbit monoclonal.	43 kDa	1 : 2000	1 : 2000
Mouse monoclonal [4E206] to Synaptophysin	Synaptophysin	Abcam; Cat# ab18008; RRID: AB_444181; mouse; monoclonal.	38 kDa	1 : 60000	1 : 60000
ATPA (51): sc-136178	ATP5A	Santa Cruz Biotechnology; #136178; RRID: AB_2061764; mouse; monoclonal	51 kDa	1 : 5000	1 : 10000
Monoclonal Anti-α-Tubulin antibody	α-Tubulin	Sigma-Aldrich; Cat# T5168; RRIDD: AB_477579; mouse; monoclonal.	50 kDa	1: 3000	1 : 3000

STATISTICS

Data collected from behavioural analysis and Western blot experiments were tested for normality using the Shapiro-Wilk test (SW). Depending on the spread of the data, normally distributed data, SW $p > 0.05$, **(**Weight of female rats on P15, P21, P57 and P63; distance travelled during the novel object habituation, familiarisation and test trial; object duration during the familiarization trial, object duration during the NOT trial; number and duration of 22 kHz ultrasonic vocalizations; distance travelled in the EPM; closed arm duration; centre zone duration; total number of entries into the open arms of the EPM; distance travelled in the OFT; time spent immobile, swimming and climbing in the FST; levels of P-ERK1/2, P-ERK1/2 to total ERK, P-GSK3β, GSK3β , P-GSK3β to GSK3β, P-CREB, CREB, P-CREB/CREB, synaptophysin in the PFC of male rats; levels of P-ERK1/2, ERK, P-ERK1/2 to total ERK1/2 ratio, P-GSK3β, GSK3β , P-GSK3β/GSK3β, P-CREB, CREB, synaptophysin and ATP5A in the DH of male rats; levels of ERK, P-ERK1/2 to total ERK1/2 ratio, P-GSK3β, GSK3β, P-GSK3β/GSK3β, P-CREB and synaptophysin in the PFC of female rats and the levels of P-ERK1/2, ERK, P-ERK1/2 to total ERK1/2 ratio, P-GSK3β, GSK3β , P-GSK3β/GSK3β, P-CREB, CREB, synaptophysin and ATP5A in the DH of female rats**)** were analyzed using parametric tests, which included repeated-measures ANOVA and Student t-tests followed by Duncan's post-hoc test when appropriate. If the data were not normally distributed, SW $p < 0.05$, **(**weight of male rats; latency to reach the objects and object frequency during novel object familiarization and test trial; latency to first 22 kHz ultrasonic vocalization; number of entries made into the arms of the EPM; open arm duration; latency to enter the open arms and closed arms respectively; number of entries into the open arms per minute; inner duration of OFT; frequency to enter the inner zone duration of the OFT; latency to enter the inner zone of the OFT; levels of ATP5A in the PFC of male rats; P-CREB to CREB ratio in the DH of male rats; levels of P-ERK1/2, total CREB, P-CREB/CREB ratio and ATP5A in the PFC of female rats and levels of total CREB in the DH of female rats**)** non-parametric tests such as the Kruskal-Wallis tests, Friedman and Wilcoxon matched-pairs test, followed by Bonferroni correction, were used when applicable. In addition, exploratory pairwise correlations between behavioural outcomes and neurochemical analyses were not conducted in this study because the neurochemical analyses were performed on rats that did not undergo behavioural testing. However, we did perform exploratory pairwise correlations within behavioural measures and within neurochemical analyses (**Appendix A5**). Parametric data were represented by the mean ± standard error of the mean (SEM) whereas non-parametric data were represented by the

median and inter-quartile range (IQR). All data were analyzed in Statistica version 12 (StatSoft, Tulsa, OK). A significant effect was identified with a *p*-value less than 0.05 (**Appendix A5**, p.297).

RESULTS

DEVELOPMENTAL DATA

Developmental data (liquid consumption during gestation, litter size and weight of pups on P2 are shown in **Table 5.2**. Saccharin-control dams consumed an average of 65.47 ± 7.31 *ml* per day of a 0.066% saccharin solution during gestation. Ethanol-treated dams consumed an average of 20.31 ± 1.02 *ml* per day of a saccharin-sweetened 10 % ethanol solution throughout gestation. Ethanol-treated dams gave birth to significantly fewer pups than saccharin-control dams (Student t-test, $p < 0.05$). Further, on P2, male pups exposed to prenatal-ethanol weighed significantly less than male saccharin-control pups (Student t-test, $p < 0.05$). There was no difference in body weight between female saccharin-control pups and female prenatal-ethanol exposed pups on P2 (Student t-test).

Table 5.2: Developmental data

	Saccharin-control dams	**Ethanol-treated dams**
Liquid consumption (*ml*) (GD0 - DOB)	65.47 ± 7.31 (n = 11 dams)	20.31 ± 1.02 (n = 11 dams)
Litter size on P2 (no. of pups)	14.09 ± 1.14 (n = 11 litters)	10.36 ± 1.07 * (n = 11 litters)
	Saccharin-control pups	**Ethanol-exposed pups**
Weight (g) on P2 - *Male pups*	7.03 ± 0.09 (n = 86)	6.47 ± 0.12 * (n = 64)
Weight (g) on P2 - *Female pups*	6.70 ± 0.09 (n = 65)	6.62 ± 0.14 (n = 47)

Ethanol-treated dams gave birth to fewer pups than saccharin-control dams (Student t-test, $*p < 0.05$). On P2 male pups exposed to prenatal-ethanol weighed significantly less than control pups (Student t-test, $*p < 0.05$). There was no significant difference in body weight between saccharin-control and ethanol-exposed female pups on P2 (t-test). The data represent the mean ± SEM.

WEIGHT ANALYSIS

All rats were weighed on P8 (one week into maternal separation stress), P15 (day after the last session of maternal separation), P21 (at weaning), P57 (the start of behavioural analysis) and P63 (the day of sacrifice). Weight data of **control** (sacc + nMS), **MS-** (sacc + MS), **EtOH-** (EtOH + nMS) and **EtOH+MS-** (EtOH + MS) rats are represented in **Figure 5.8.**

On P8, male EtOH-rats weighed significantly less than control rats (Kruskal-Wallis, $H_{(3, N = 113)} = 50.50$, $p < 0.05$, **Figure 5.8a**). Similarly, on P15, EtOH-rats weighed significantly less than control rats, however EtOH+MS-rats weighed more than EtOH-rats (Kruskal-Wallis, $H_{(3, N = 99)} = 23.03$, $p < 0.001$, **Figure 5.8b**). When rats were weaned from the dam on P21, EtOH-rats weighed less than control rats (Kruskal-Wallis, $H_{(3, N = 100)} = 33.98$, $p < 0.001$, **Figure 5.8c**). **Figure 5.8d**, shows that EtOH-rats continued to weigh less than control rats on P57 (Kruskal-Wallis, $H_{(3, N = 100)} = 13.52$, $p < 0.01$). However, on P63 before rats were sacrificed, there was no significant weight difference between experimental groups (Kruskal-Wallis, **Figure 5.8e**).

On P8 female EtOH-rats weighed less than control and EtOH+MS-rats (Kruskal-Wallis, $H_{(3, N = 47)} = 10.98$, $p < 0.05$, **Figure 5.8f**). Two-way ANOVA (*treatment x stress*) revealed a significant treatment effect on body weight in female rats on P15 ($F_{(1, 33)} = 4.59$, $p < 0.05$). Further, post-hoc analysis showed that female EtOH-rats weighed less than control and EtOH-rats on P15 (Duncan's post-hoc test, $p < 0.05$, **Figure 5.8g**). Two-way ANOVA (*treatment x stress*) showed a tendency towards a main effect of treatment on body weight on P21 and P57 ($F_{(1, 40)} = 2.93$, $p = 0.09$ and $F_{(1, 40)} = 3.63$, $p = 0.06$ respectively, **Figures 5.8h and 5.8i**). Further, there was an interaction between treatment and stress on body weight on P21 and P57 that was tending towards significance ($F_{(1, 40)} = 3.88$, $p = 0.06$ and $F_{(1, 40)} = 3.54$, $p = 0.07$, respectively, **Figures 5.8h and 5.8i**). On P63, two-way ANOVA (*treatment x stress*) revealed a main effect of treatment on body weight ($F_{(1, 31)} = 4.23$, $p < 0.05$). Post-hoc analysis revealed that female EtOH-rats weighed less than control rats on the day of sacrifice (Duncan's post-hoc test, $p < 0.05$, **Figure 5.8j**).

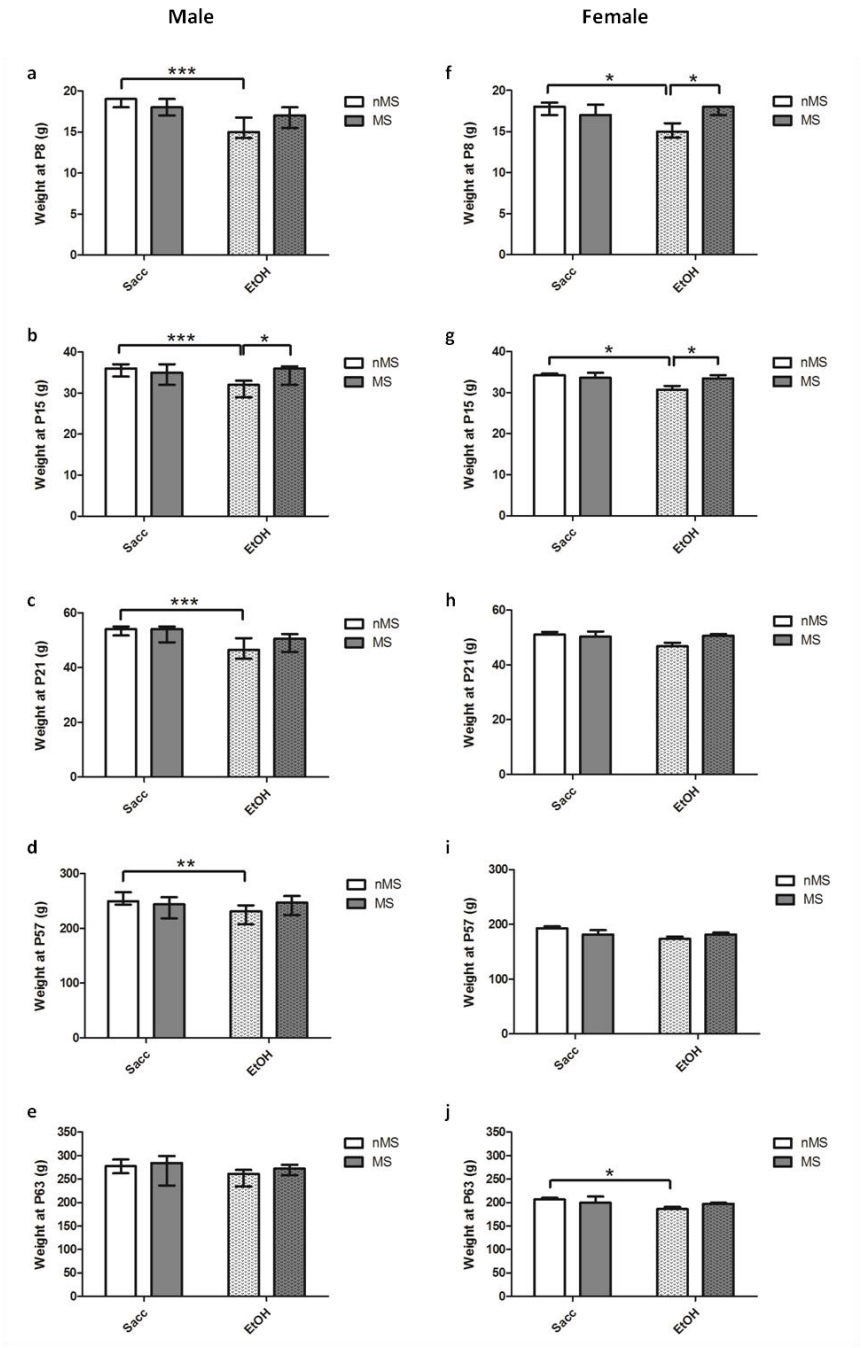

Figure 5.8: Body weight of male and female rats on postnatal days 8, 15, 21, 57 and 63.

(***a-e***) Body weight of *male* rats on P8, P15, P21, P57 and P63 respectively. (***a***) On P8, male EtOH-rats weighed significantly less than control rats (Kruskal Wallis, ***$p < 0.001$). (***b***) Male EtOH-rats weighed less than control and EtOH+MS-rats on P15 (Kruskal-Wallis, * $p < 0.05$; *** $p < 0.001$). (***c***) On P21, male EtOH-rats weighed significantly less than control rats (Kruskal-Wallis, * $p < 0.05$; *** $p < 0.001$). (***d***) EtOH-rats weighed less than control rats on P57 (Kruskal-Wallis, ** $p < 0.01$). (***e***) However on the day of sacrifice, P63, there were no significant differences between experimental groups (Kruskal-Wallis). ***(f-j)*** Body weight of *female* rats on P8, 15, 21, 57 and 63. (***f***) On P8, female EtOH-rats weighed significantly less than control rats and EtOH+MS-rats (Kruskal-Wallis, * $p < 0.05$). (***g***) Duncan's post-hoc test showed that female EtOH-rats weighed less than female controls and EtOH+MS-rats on P15 (* $p < 0.05$). (***h-i***) On P21 and P57, there were no significant differences between experimental groups. However, a main effect of treatment and the interaction between treatment and stress on body weight tended to be significant (two-way ANOVA, $0.1 > p > 0.05$). (**j**) On P63, female EtOH-rats weighed less than female control rats (Duncan's post-hoc test, * $p < 0.05$). The data in graphs ***a-f*** are not normally distributed (SW, $p < 0.05$) and the graphs represent the median and IQR. However, the data in graphs ***g-i*** are normally distributed (SW, $p > 0.05$) and represent the mean ± SEM. [**control**, sacc + nMS; **MS**, sacc + MS; **EtOH**, ethanol + nMS; **EtOH+MS**].

BEHAVIOUR

NOVEL OBJECT TEST

Figures 5.9-5.15 depict the data obtained from the novel object habituation trial, the novel object familiarization trial and the novel object test trial.

HABITUATION

Distance travelled during the habituation trial of the NOT was analyzed to measure the exploratory activity of **control** (sacc + nMS, n = 11), **MS-** (sacc + MS, n = 7), **EtOH-** (ethanol + nMS, n = 7) and **EtOH+MS-** (ethanol + MS, n = 8) rats at the start of behavioural testing on P57.

The distance travelled during the full 10-minute trial is represented in **Figure 5.9a-b**. Two-way ANOVA (*treatment x stress*) revealed a significant interaction between treatment and stress ($F_{(1, 29)} = 12.41$, $p < 0.01$). Maternal separation increased distance travelled in saccharin-rats whereas maternal separation stress decreased distance travelled in rats exposed to prenatal-ethanol (**Figure 5.9a**). Further post-hoc analysis showed that MS-rats travelled significantly further than control rats; and EtOH+MS-rats travelled less than EtOH-rats during the habituation trial (Duncan's post-hoc test, $p < 0.05$).

Repeated-measures ANOVA (*treatment x stress x minute*) was used to analyze the distance travelled per minute of the habituation trial. There was a significant interaction between treatment and stress ($F_{(1,29)} = 12.41$, $p < 0.01$) and a significant main effect of time ($F_{(9,261)} = 35.09$, $p < 0.001$) on the distance travelled (**Figure 5.9b**). Post-hoc analysis showed that MS- and EtOH-rats travelled a greater distance per minute than control and EtOH+MS-rats respectively (Duncan post-hoc test, $p < 0.05$). Distance travelled per minute decreased over the 10-minute trial (Duncan post-hoc test, $p < 0.001$).

Analysis of the first 5 minutes of the habituation trial is shown in **Figure 5.9c-d**. Two-way ANOVA (*treatment x stress*) identified a significant interaction between treatment and stress in the total distance travelled during the first 5 minutes of the habituation trial ($F_{(1,29)} = 12.15$, $p < 0.01$). MS-rats travelled a greater distance than control rats whereas EtOH+MS-rats travelled less than the EtOH-rats (**Figure 5.9c**). Post-hoc analysis showed that MS- and EtOH-rats travelled a greater distance than control and EtOH+MS-rats respectively during the first 5 minutes (Duncan's post-hoc test, $p < 0.05$).

Repeated-measures ANOVA (*treatment x stress x minute*) showed a significant interaction between treatment and stress ($F_{(1, 29)} = 12.15$, $p < 0.0.1$) as well a significant main effect of time ($F_{(4, 116)} = 6.34$, $p < 0.001$) on the distance travelled during the first 5 minutes of the habituation trial (**Figure 5.9d**). Post-hoc analysis showed that MS- and EtOH-rats travelled a greater distance than control and EtOH+MS-rats respectively (Duncan's post-hoc test, $p < 0.05$). Distance travelled per minute decreased over the first 5 minutes of the habituation trial (Duncan's post-hoc test, $p < 0.01$).

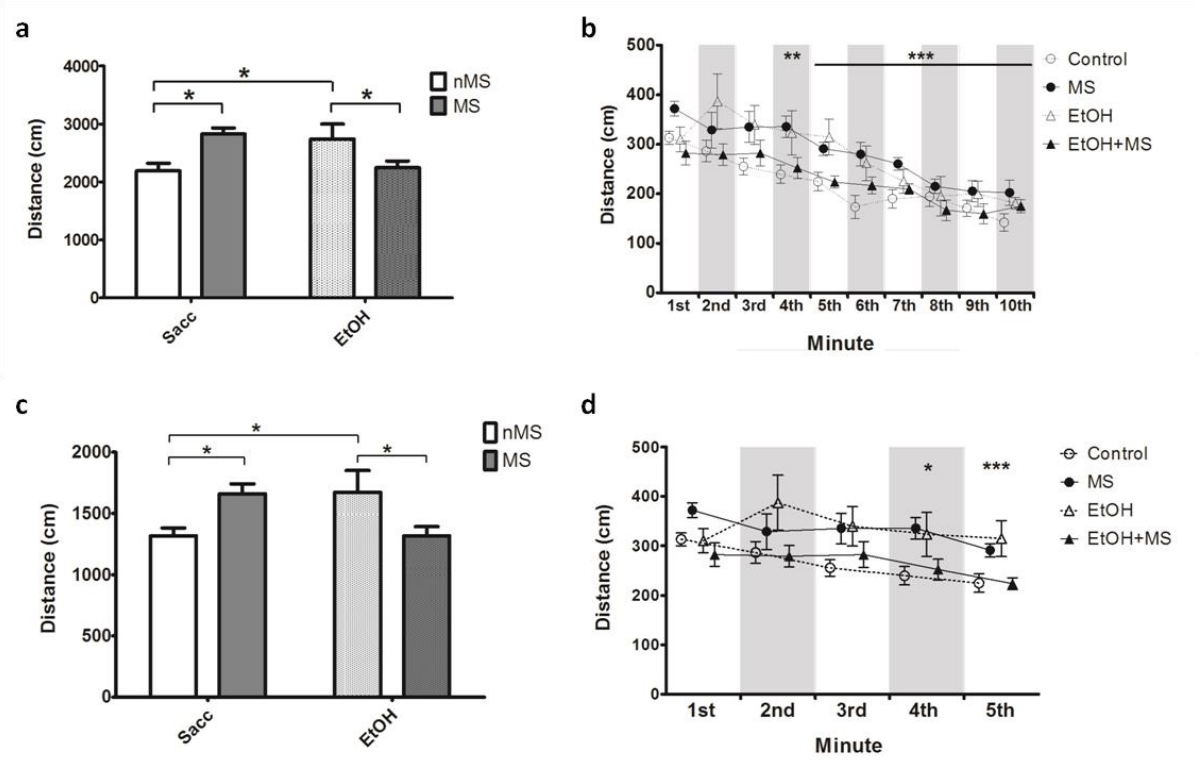

Figure 5.9: Distance travelled during habituation to the novel object test arena (no objects present).

(***a***) Distance travelled during the full 10-minute habitation trial. MS- and EtOH- rats travelled a greater distance than control rats (Duncan's post-hoc test, * $p < 0.05$) and EtOH+MS-rats travelled less than EtOH-rats (Duncan's post-hoc test, * $p < 0.05$). (***b***) Distance travelled per minute across the full 10-minute trial. The distance travelled in the 4th-minute and all subsequent minutes was less than the distance travelled during the 1st-minute (Duncan's post-hoc test, ** $p < 0.01$, *** $p < 0.001$). (***c***) Distance travelled during the first 5 minutes of the habituation trial. Again, MS- and EtOH-rats travelled a greater distance than control rats (Duncan's post-hoc test, * $p < 0.05$) and EtOH+MS-rats travelled less than EtOH-rats (Duncan's post-hoc test, * $p < 0.05$). (***d***) Distance travelled per min for the first 5 minutes of the habituation trial. The distance travelled in the 4th-minute and all subsequent minutes was less than the distance travelled during the 1st-minute (Duncan's Post-hoc test, ** $p < 0.01$, *** $p < 0.001$). The data are normally distributed (SW, $p > 0.05$). The graphs represent the mean ± SEM. [**Control**, sacc + nMS (n = 11); **MS**, sacc + MS (n = 7); **EtOH**, ethanol + nMS (n = 7); **EtOH+MS** (n = 8)].

OBJECT FAMILIARISATION

On P58, two identical objects were placed in the NOT arena. The distance travelled (**Figure 5.10**), the time spent with the objects (duration) (**Figure 5.11**) as well as the frequency and latency to approach the objects (**Figure 5.12**) were measured during a 10-minute recording of **control** (sacc + nMS, n = 11), **MS-** (sacc + MS, n = 7), **EtOH-** (ethanol + nMS, n = 7) and **EtOH+MS-** (n = 8) rats.

During familiarization there were no significant differences between experimental groups in the distance travelled during the full 10-minute trial (**Figure 5.10a**, Two-way ANOVA). Repeated-measures ANOVA (*treatment x stress x minute*) for the distance travelled per minute for the full 10-minute trial showed a significant main effect of time ($F_{(9, 252)} = 24.09$, $p < 0.001$). Distance travelled per minute decreased over the 10-minute trial (**Figure 5.10b**, Duncan's post-hoc test, $p < 0.05$).

Similarly, in **Figure 5.10c**, analysis of the first 5 minutes of the familiarization trial revealed no significant effect of stress or treatment on the distance travelled (Two-way ANOVA, $p > 0.05$). Repeated-measures ANOVA (*treatment x stress x minute*) showed a significant main effect of time ($F_{(4,112)} = 12.82$, $p < 0.001$) and a significant interaction between treatment, stress and time ($F_{(4,112)} = 2.80$, $p < 0.05$) on the distance travelled per minute during the first 5 minutes of the familiarization trial. Distance travelled per minute decreased over the 5-minute trial (Duncan's post-hoc test, $p < 0.05$). The distance travelled by control and MS-rats during the 4th- and 5th-minute was significantly less than the distance travelled during the 1st-minute (Duncan's post-hoc test, $p < 0.05$). Whereas, the distance travelled by EtOH- and EtOH+MS-rats during the 3rd-, 4th- and 5th-minute was significantly less than the distance travelled during the 1st-minute (Duncan's post-hoc test, $p < 0.05$) (**Figure 5.10d**).

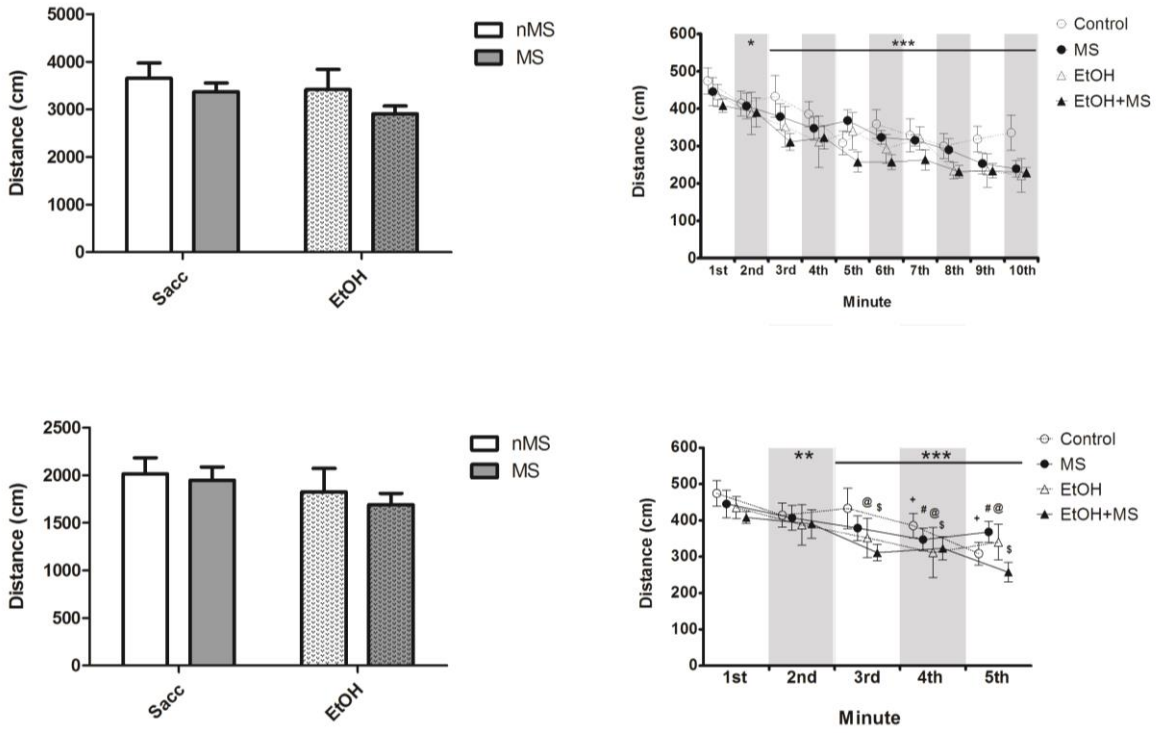

Figure 5.10: Distance travelled during the familiarization trial.

(***a***) Total distance travelled during the 10-minute familiarization trial. There were no significant differences between experimental groups (two-way ANOVA). (***b***) Distance travelled per minute of the full 10-minute familiarization trial. Distance travelled in the 2nd-minute and all subsequent minutes was significantly less than the distance travelled during the 1st-minute period (Duncan's post-hoc test * $p < 0.05$, ***$p < 0.001$). (***c***) Total distance travelled during the first 5 minutes of the familiarization trial. There was no significant effect of treatment or stress on the distance travelled (two-way ANOVA). (***d***) Distance travelled per minute for the first 5 minutes of the familiarization trial. Distance travelled in the 2nd-minute and all subsequent minutes was significantly less than the distance travelled during the 1st-minute period (Duncan's post-hoc test, * $p < 0.05$, ***$p < 0.001$). The distance travelled by control and MS-rats during the 4th- and 5th-minute was significantly less than the distance travelled during the 1st-minute (Duncan's post-hoc test, $^{+}$ $p < 0.05$ and $^{\#}$ $p < 0.05$ respectively). The distance travelled by EtOH- and EtOH+MS-rats during the 3rd-, 4th- and 5th-minute was significantly less than the distance travelled during the 1st-minute (Duncan's post-hoc test, $^{@}$ $p < 0.05$ and $^{\$}$ $p < 0.05$ respectively). The data are normally distributed (SW, $p > 0.05$). The graphs represent the mean ± SEM. [**control**, sacc + nMS (n = 11); **MS**, sacc + MS (n = 7); **EtOH**, ethanol + nMS (n = 7); **EtOH+MS**, (n = 8)].

Figure 5.11 shows the interaction with the two identical objects during the 10-minute familiarization trial on P58. The time spent with the left and right object (uncorrected duration) is represented in **Figure 5.11a**. Repeated-measures ANOVA (*treatment x stress x object*) revealed a significant main effect of treatment ($F_{(1,29)} = 6.67$, $p < 0.05$) and a significant interaction between stress and object ($F_{(1,29)} = 4.68$, $p < 0.05$). Further post-hoc analysis showed that saccharin-rats spent more time with the objects than rats exposed to prenatal-ethanol (Duncan's post-hoc test, $p < 0.05$). Importantly control rats spent significantly more time with the right object than with the left object, indicating a preference for one of the two identical

objects (Duncan's post-hoc test, $p < 0.05$). This preference needed to be taken into account for the novel object test trial. Hence, a correction factor was determined by dividing the time spent with the right object by the time spent with the left object. The corrected data were created by multiplying the time spent with the left object by the correction factor. Therefore **Figure 5.11b** represents the corrected left and right object duration. Repeated-measures ANOVA (*treatment x stress x object*) still showed a significant main effect of treatment on object duration ($F_{(1,29)} = 8.97$, $p < 0.01$). Saccharin-rats spent more time with the two identical objects than rats exposed to prenatal-ethanol (Duncan's post-hoc test, $p < 0.01$).

The total object duration (time spent with the left object and right object) is shown in **Figures 5.11c-d**. Again, two-way ANOVA (*treatment x stress*) revealed a significant main effect of treatment on total object duration ($F_{(1,29)} = 6.67$, $p < 0.05$). Saccharin-rats spent more time with the two identical objects than rats exposed to prenatal-ethanol (Duncan's post-hoc test, $p < 0.05$). **Figure 5.11d** takes into account the preference indicated in **Figure 5.11a**. Two-way ANOVA (*treatment x stress*) of the corrected total object time shows a significant main effect of treatment ($F_{(1,29)} = 8.97$, $p < 0.1$). Saccharin-rats spent more time with the objects than rats exposed to prenatal-ethanol (Duncan's post-hoc test, $p < 0.01$).

Figure 5.11e shows the percentage of total object time spent with the right object. Two-way ANOVA (*treatment x stress*) indicates a significant main effect of stress on the percentage object time spent with the right object ($F_{(1,29)} = 4.34$, $p < 0.05$). Rats that underwent maternal separation stress spent less time with the right object than non-maternally separated rats (Duncan's post-hoc test, $p < 0.05$). There were no significant differences between experimental groups after the preference for the right object was accounted for. This is shown in **Figure 5.11f** (two-way ANOVA).

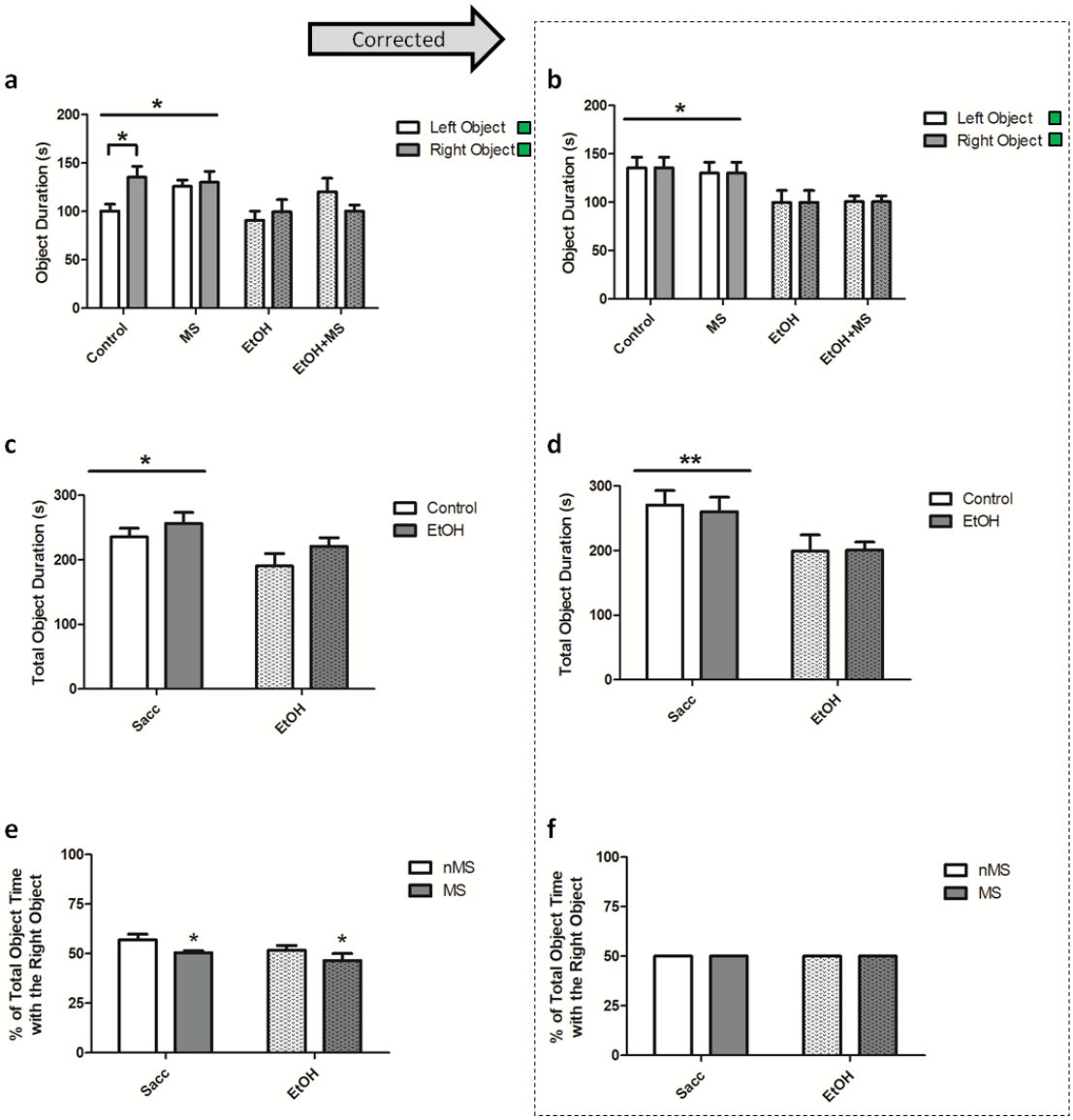

Figure 5.11: Interaction with the two identical objects during the familiarization trial of the novel object test.

(***a***) Left and right object duration (s). Saccharin-rats spent more time with the objects than rats exposed to prenatal-ethanol (Duncan's post-hoc test, * $p < 0.05$). Further, control rats spent more time with the right object versus the left object (Duncan's post-hoc test, * $p < 0.05$). This indicates a preference for one of the identical objects. Therefore, a correction factor was applied to the data represented in graphs ***b***, ***e*** and ***f***. The correction factor was determined by dividing the time spent with the right object by the time spent with the left object. The corrected data were created by multiplying the time spent with the left object by the correction factor. (***b***) Corrected left and right object duration. Saccharin-rats spent more time with the objects than rats exposed to prenatal-ethanol (Duncan's post-hoc test, * $p < 0.05$). However, there was no longer an object preference in any of the experimental groups. (***c***) Total object duration. Saccharin-rats spent more time with the objects than rats exposed to prenatal-ethanol (Duncan's post-hoc test, * $p < 0.05$) (***d***) Corrected total object duration. After correction, saccharin-rats spent more time with the objects than prenatal-ethanol exposed-exposed (Duncan's post-hoc test, ** $p < 0.01$) (***e***) Percentage of total object time spent with the right object. Rats that underwent maternal separation stress spent less time with the right object than non-maternally separated rats (Duncan's post-hoc test, * $p < 0.05$). (***f***). Corrected percentage of the total object time spent with the right object. There were no significant differences between experimental groups (two-way ANOVA). The data are normally distributed (SW, $p > 0.05$). The graphs represent the mean ± SEM [**Control**, sacc + nMS (n = 11); **MS**, sacc + MS (n = 7); **EtOH**, ethanol + nMS (n = 7); **EtOH+MS** (n = 8)].

Latency to approach the objects and frequency of approaches are shown in **Figure 5.12**. Friedman ANOVA indicated a significant difference between left and right object latency ($p < 0.001$). Post-hoc analysis revealed that both control and EtOH-rats took longer to reach the right object (Wilcoxon Matched Pairs, $p < 0.05$, **Figure 5.12a**) whereas there was no significant difference in latency to reach the objects in MS- and EtOH+MS-rats. This difference in latency to reach the object was corrected and depicted in **Figure 5.12b**.

Friedman ANOVA showed that there was a significant difference in frequency to approach the two identical objects ($p < 0.01$). Further post-hoc analysis revealed that control rats visited the right object with greater frequency than the left object (**Figure 5.12c**, Wilcoxon Matched Pairs test, $p < 0.01$). This preference was corrected and the result is shown in **Figure 5.12d**.

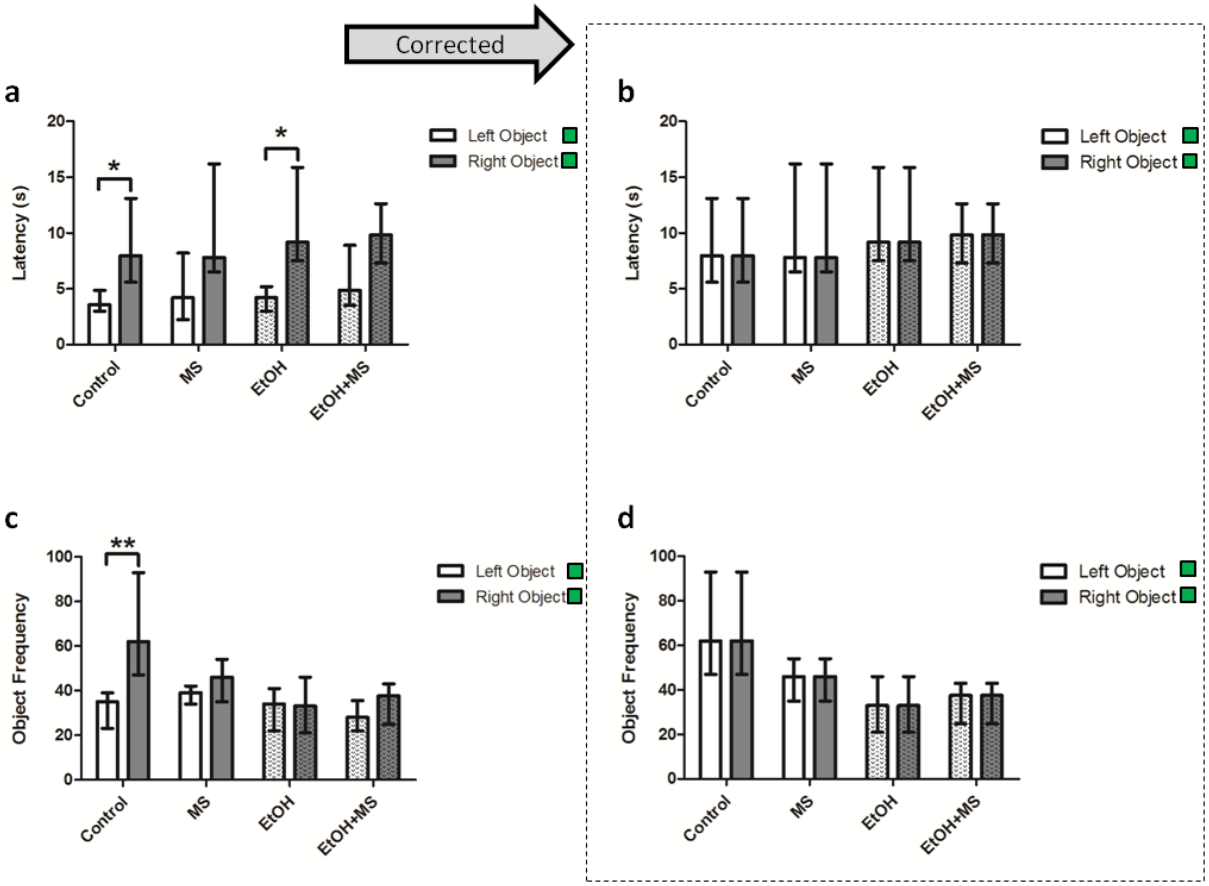

Figure 5.12: Latency to approach the objects and frequency of approaches during the familiarization trial.

(***a***) Latency to approach the left and right object. Both control and EtOH-rats took longer to reach the right object than the left object (Wilcoxon Matched Pairs test, * $p < 0.05$). (***b***) Corrected latencies to reach the left and right object. There were no significant differences between experimental groups (Friedman ANOVA). (***c***) Object frequency. Control rats approached the right object with greater frequency than the left object (Wilcoxon Matched Pairs, ** $p < 0.01$), indicating a preference for the right object. (***d***) Corrected object frequency. There were no significant differences between experimental groups (Friedman ANOVA).The data are not normally distributed (SW, $p > 0.05$). The graphs represent the median and IQR [**Control**, sacc + nMS (n = 11); **MS**, sacc + MS (n = 7); **EtOH**, ethanol + nMS (n = 7); **EtOH+MS** (n = 8)].

NOVEL OBJECT TEST

One hour after the familiarization test, the right object was replaced with a novel object. Rats were placed back in the novel object test arena and the data obtained from the 5-minute recording are represented in **Figures 5.13-5.15.** There were no significant differences between experimental groups in the total distance travelled during the 5-minute novel object test trial (**Figure 5.13a**, Two-way ANOVA). However, repeated-measures ANOVA (*treatment x stress x minute*) showed a significant main effect of time on the distance travelled per minute ($F_{(4,116)}$

= 3.30, $p < 0.001$). Distance travelled per minute decreased over the 5-minute trial (**Figure 5.13b**, Duncan's post-hoc test, $p < 0.001$).

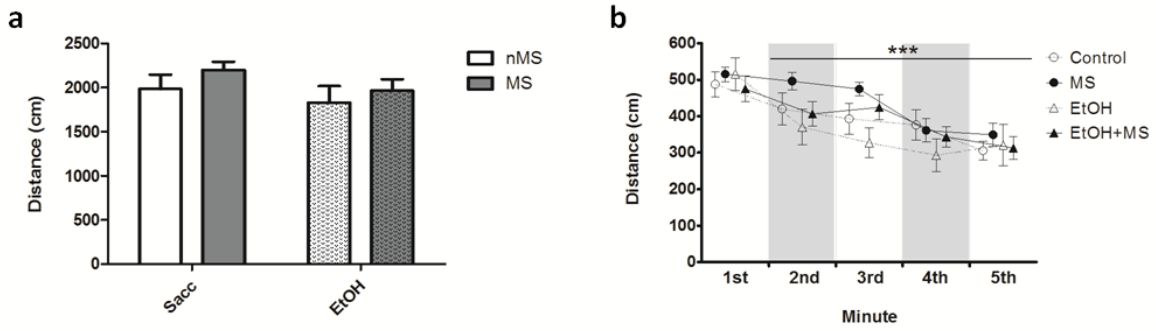

Figure 5.13: Distance travelled during the test trial.

(***a***) Total distance travelled during the 5-minute novel object test trial. There were no significant differences between experimental groups (two-way ANOVA). (***b***). Distance travelled in the 2nd-minute and all subsequent minutes was significantly less than the distance travelled during the 1st-minute (Duncan post-hoc test, *** $p < 0.001$). The data are normally distributed (SW, $p > 0.05$). The graphs represent the mean ± SEM [**Control**, sacc + nMS (n = 11); **MS**, sacc+MS (n = 7); **EtOH**, ethanol + nMS (n = 7): **EtOH+MS** (n = 8)].

Figure 5.14 shows the interaction with the novel object. **Figure 5.14a, c, e** represent the uncorrected data whereas **Figure 5.14b, d, f** show the data after correction for the object preference identified during the familiarization trial (i.e. after multiplying the time spent with the left object by the correction factor described in **Figure 5.11**). In **Figure 5.14a**, repeated-measures ANOVA (*treatment x stress x object*) showed a significant main effect of object on object duration ($F_{(1,29)} = 4.57$, $p < 0.05$). All experimental groups spent more time with the novel object than the familiar object (Duncan's post-hoc test, $p < 0.05$). However, the corrected data show that there are no significant differences in time spent with the objects for all experimental groups (**Figure 5.14b**, Friedman ANOVA). Total object duration was not significantly different between experimental groups (**Figure 5.14c**, Two-way ANOVA) but Kruskal-Wallis analysis of the corrected total object duration data showed that EtOH+MS-rats spent less time with the objects than control rats ($p < 0.05$). Two-way ANOVA (*treatment x stress*) of both the corrected and uncorrected data representing the percentage of total object time spent with the novel object showed that there were no significant differences between experimental groups (**Figure 5.14e and f**).

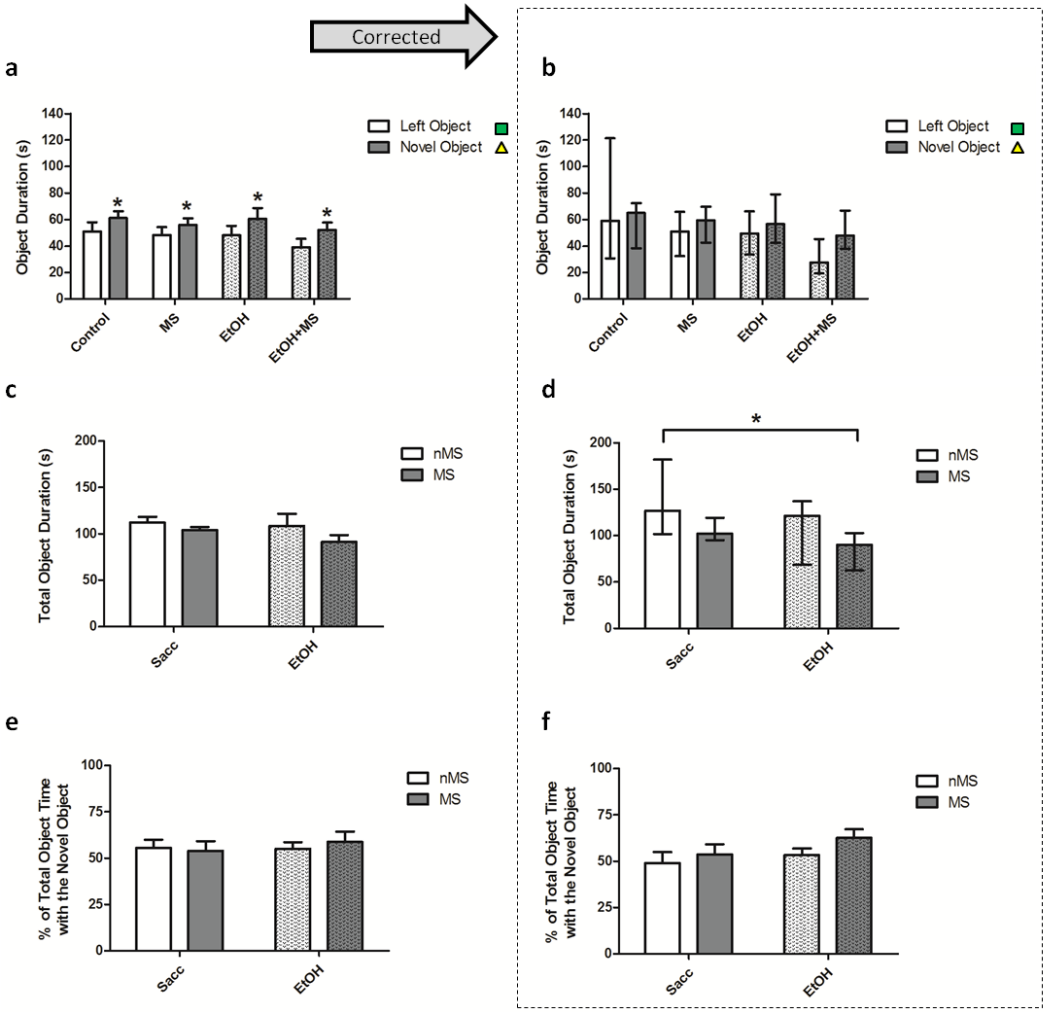

Figure 5.14: Object duration during the test trial (novel object).

(***a***) Left and right object duration (s). All experimental groups spent more time with the novel object than the familiar object (Duncan's post-hoc test, * $p < 0.05$). The correction factor calculated from the familiarization trial was applied to the data represented in graphs ***b***, ***e*** and ***f***. (***b***) Corrected left and right object duration. There were no significant differences between experimental groups (Friedman ANOVA). (***c***) Total object duration. There were no significant differences between experimental groups (Duncan's post-hoc test) (***d***) Corrected total object duration. EtOH+MS-rats spent less time with the objects than control rats (Duncan's post-hoc test, * $p < 0.05$) (***e***) Percentage of total object time spent with the right object. (***f***). Corrected percentage of the total object time spent with the right object. There were no significant differences between experimental groups (Two-way ANOVA). The data in graphs ***a, c, e*** and **f** are normally distributed (SW, $p > 0.05$) and the graphs represent the mean ± SEM. The data shown in **b** and **d** are not normally distributed (SW, $p < 0.05$) and the data represent the median and IQR. [**Control**, sacc + nMS (n = 11); **MS**, sacc + MS (n = 7); **EtOH**, ethanol + nMS (n = 7); **EtOH+MS** (n = 8)].

Latencies to approach the objects and frequency of approaches during the novel object test trial are shown in **Figure 5.15**. Friedman ANOVA showed no significant differences between experimental groups for the latency to approach the left object and the novel object. After the correction factor, calculated from the familiarization trial, Friedman ANOVA showed that there was a significant difference between the latency to reach the left object and the novel

object ($p < 0.001$). Post-hoc testing revealed that both MS- and EtOH-rats took longer to reach the left object than the novel object (Wilcoxon Matches Pairs test, $p < 0.05$).

Friedman ANOVA of the uncorrected object frequency during the novel object test trial identified a difference between left and novel object frequency ($p < 0.001$). Control, MS- and EtOH-rats showed a greater frequency to approach the novel object than the familiar object (Wilcoxon Matched Pairs, $p < 0.05$, $p < 0.01$). However, analysis of the corrected object frequency revealed no significant group differences (Friedman ANOVA).

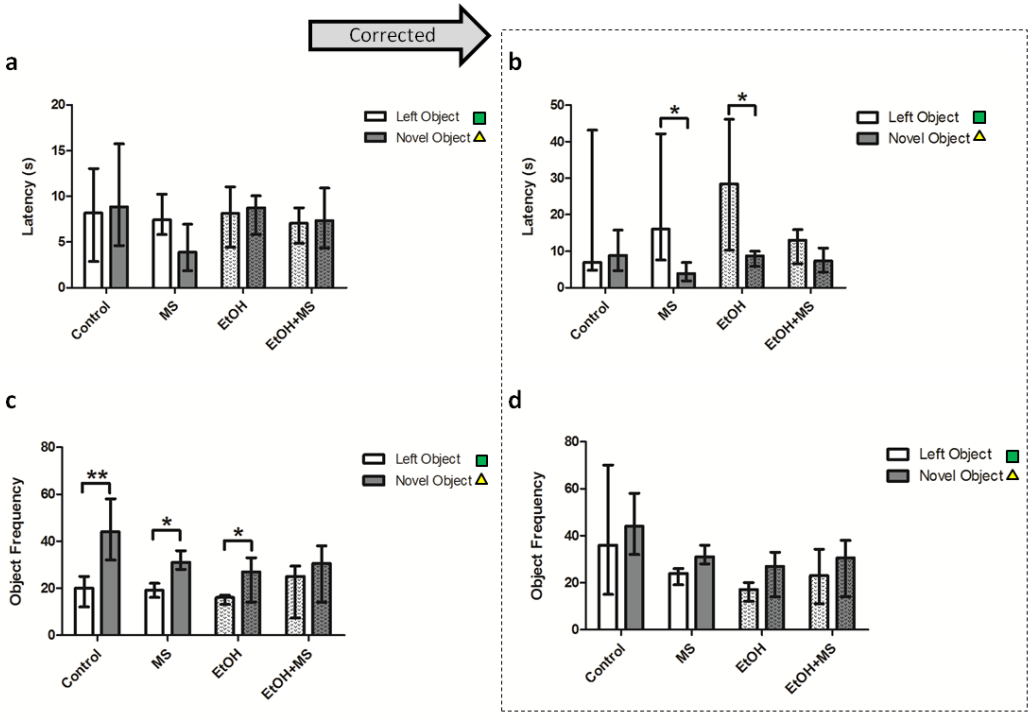

Figure 5.15: Latency to approach the objects and frequency of approaches during the test trial.

(***a***) Latency to approach the left object and the novel object. There were no significant differences between experimental groups (Friedman ANOVA). (***b***) Corrected latency to approach the left and novel objects. MS- and EtOH-rats took longer to reach the left object than the novel object (Wilcoxon Matched Pairs test, $p < 0.05$) (***c***) Object frequency. Control, MS- and EtOH-rats approached the novel object more frequently than the left object (Wilcoxon Matched Pairs, * $p < 0.05$, ** $p < 0.01$). (***d***) Corrected object frequency. There were no significant differences between experimental groups (Friedman ANOVA). The data are not normally distributed (SW, $p > 0.05$). The graphs represent the median and IQR [**Control**, sacc + nMS (n = 11); **MS**, sacc + MS (n = 7); **EtOH**, ethanol + nMS (n = 7); **EtOH+MS** (n = 8)].

ULTRASONIC VOCALIZATIONS

The recording of 22 kHz ultrasonic vocalizations took place on P59. **Figure 5.16** represents the number of calls, the average call duration and the latency to the first call in **control** (sacc + nMS, n = 11), **MS-** (sacc + MS, n = 7), **EtOH-** (ethanol+ nMS, n = 7) and **EtOH+MS-** (n = 8) rats.

Two-way ANOVA (*treatment x stress*) showed a main effect of stress on the number of 22 kHz calls ($F_{(1, 29)} = 12.56$, $p < 0.01$) and a main effect of treatment on the number of 22 kHz calls tended to be significant ($F_{(1, 29)} = 12.56$, $p = 0.06$, **Figure 5.16a**). Post-hoc analysis revealed that MS-rats as well as EtOH-rats made significantly more calls than control rats during the 10-minute recording period (Duncan's post-hoc test, * $p < 0.05$, ** $p < 0.01$).

Two-way ANOVA (*treatment x stress*) showed a main effect of treatment ($F_{(1, 29)} = 6.69$, $p < 0.05$) and stress ($F_{(1, 29)} = 11.61$, $p < 0.01$) on the average duration (milliseconds) of 22 kHz ultrasonic vocalizations. Post-hoc analysis showed that both MS-and EtOH-rats made calls of a longer duration than control rats. (**Figure 5.16b**, Duncan's post-hoc test $p < 0.01$). **Figure 5.16c** indicates that control rats tended to have a longer latency to the first 22 kHz call than MS-rats (Kruskal-Wallis, $p = 0.052$).

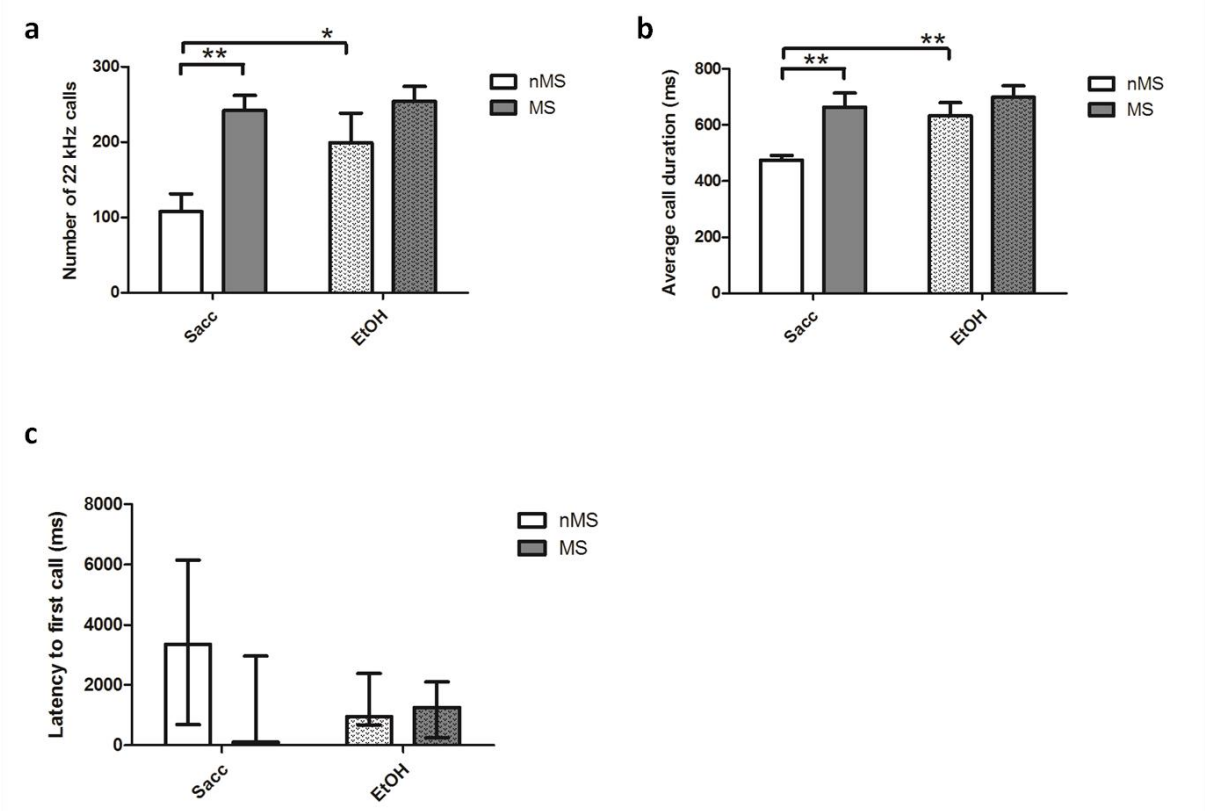

Figure 5.16: Ultrasonic Vocalizations.

(***a***) Number of 22 kHz calls made during a 10-minute recording of ultrasonic vocalizations. MS-rats as well as EtOH-rats made significantly more calls than control rats (Duncan's post-hoc test, * $p < 0.05$, ** $p < 0.01$). (***b***) The average duration (ms) of 22 kHz calls. Both EtOH-rats and MS-rats made longer calls of 22 kHz than control rats (Duncan's post-hoc test, ** $p < 0.01$). The data are normally distributed (SW, $p > 0.05$). The graphs represent the mean ± SEM. (***c***) Latency to the first 22 kHz vocalization. There are no differences between experimental groups however, analysis shows that results tended to be different (Kruskal-Wallis, $p = 0.052$). The data are not normally distributed (SW, $p < 0.05$). The data represent the median and IQR. [**Control**, sacc + nMS (n = 11); **MS**, sacc + MS (n = 7), **EtOH**, ethanol + nMS (n = 7), **EtOH + MS**, (n = 8)].

ELEVATED PLUS MAZE

Anxiety-like behaviour and exploratory activity of **control** (sacc + nMS, n = 11), **MS-** (sacc + MS, n = 7), **EtOH-** (EtOH + nMS, n = 7) and **EtOH+MS-** (n = 8) rats were measured on P60 during a 5-minute session in the EPM.

The distance travelled and the number of entries made into the arms of the EPM are depicted in **Figure 5.17**. Two-way ANOVA (*treatment x stress*) of the total distance travelled during the 5-minute trial showed no significant differences between experimental groups. Repeated-measures ANOVA (*treatment x stress x minute*) revealed a significant main effect of time on the distance travelled per minute ($F_{(4,116)} = 9.44$, $p < 0.001$). Distance travelled per minute decreased over the 5-minute trial (Duncan's post-hoc test, $p < 0.05$, **Figure 5.17b**).

The total number of entries made into the arms (open and closed) of the EPM were not significantly different between experimental groups (Kruskal-Wallis, **Figure 5.17c**). Repeated-measures ANOVA (*treatment x stress x minute*) showed no significant difference in the number of entries made per minute into the arms of the EPM over the 5-minute trial (**Figure 5.17d**).

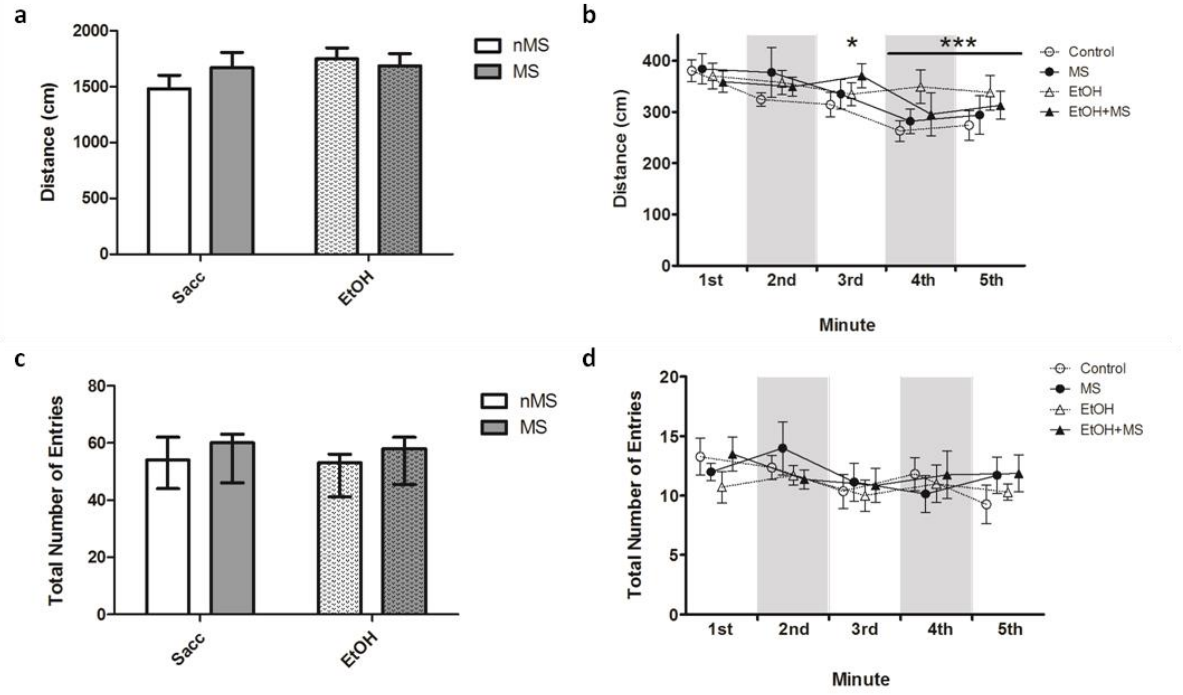

Figure 5.17: Distance travelled and the number of entries made during the Elevated Plus Maze (EPM).

(***a***) Total distance travelled in the EPM. There were no significant differences between experimental groups (two-way ANOVA). (***b***) Distance travelled per minute in the EPM. Distance travelled during the 3rd-minute and all subsequent minutes was significantly less than the distance travelled during the 1st-minute (Duncan's post-hoc test, * $p < 0.05$, *** $p < 0.001$). (***c***) Total number of entries into the open and closed arms of the EPM. There were no significant differences between experimental groups (Kruskal-Wallis). The data were not normally distributed (SW, $p < 0.05$). The data represent the median and IQR. (***d***) The number of entries made into the open and closed arms of the EPM per minute. There were no significant differences between experimental groups over the 5-minute trial (Repeated-measures ANOVA). The data are normally distributed (***a, b, d***; SW, $p > 0.05$). The data represent the mean ± SEM. [**Control**, sacc + nMS (n = 11); **MS**, sacc + MS (n = 7), **EtOH**, ethanol + nMS (n = 7), **EtOH + MS** (n = 8)].

Figure 5.18a-f shows the time spent in the open arms, closed arms and centre zone of the EPM. Two-way ANOVA (*treatment x stress*) showed no significant difference between experimental groups in the time spent in the open arms of the EPM (**Figure 5.18a**). Friedman ANOVA revealed a significant effect of time on open arm duration ($p < 0.001$). Time spent in the open arms per minute decreased over the 5-minute trial in the EPM (Wilcoxon Matches Pairs test, $p < 0.01$, **Figure 5.18b**). Total time spent in the closed arms of the EPM was not significantly

different between experimental groups (two-way ANOVA, **Figure 5.18c**). Repeated-measures ANOVA (*treatment x stress x minute*) showed a significant main effect of time on the time spent in the closed arms of the EPM ($F_{(4, 116)} = 6.65$, $p < 0.01$, **Figure 5.18d**). Time spent in the closed arms per minute of the EPM increased over the 5-minute trial (Duncan's post-hoc test, $p < 0.01$). Two-way ANOVA (*treatment x stress*) showed a significant main effect of stress on the time spent in the centre zone of the EPM ($F_{(1, 29)} = 4.58$, $p < 0.05$). MS- and EtOH+MS-rats spent more time in the centre zone of the EPM than control and EtOH-rats (Duncan's post-hoc test, $p = 0.05$, **Figure 5.18e**). Repeated-measures ANOVA (*treatment x stress x minute*) showed a significant main effect of time on centre zone duration ($F_{(4, 116)} = 2.99$, $p < 0.05$). Time spent in the centre zone of the EPM increased between the 1st-minute and 2nd-minute then decreased during the 3rd-minute of the 5-minute trial (Duncan's post-hoc test, $p < 0.05$, **Figure 5.18f**).

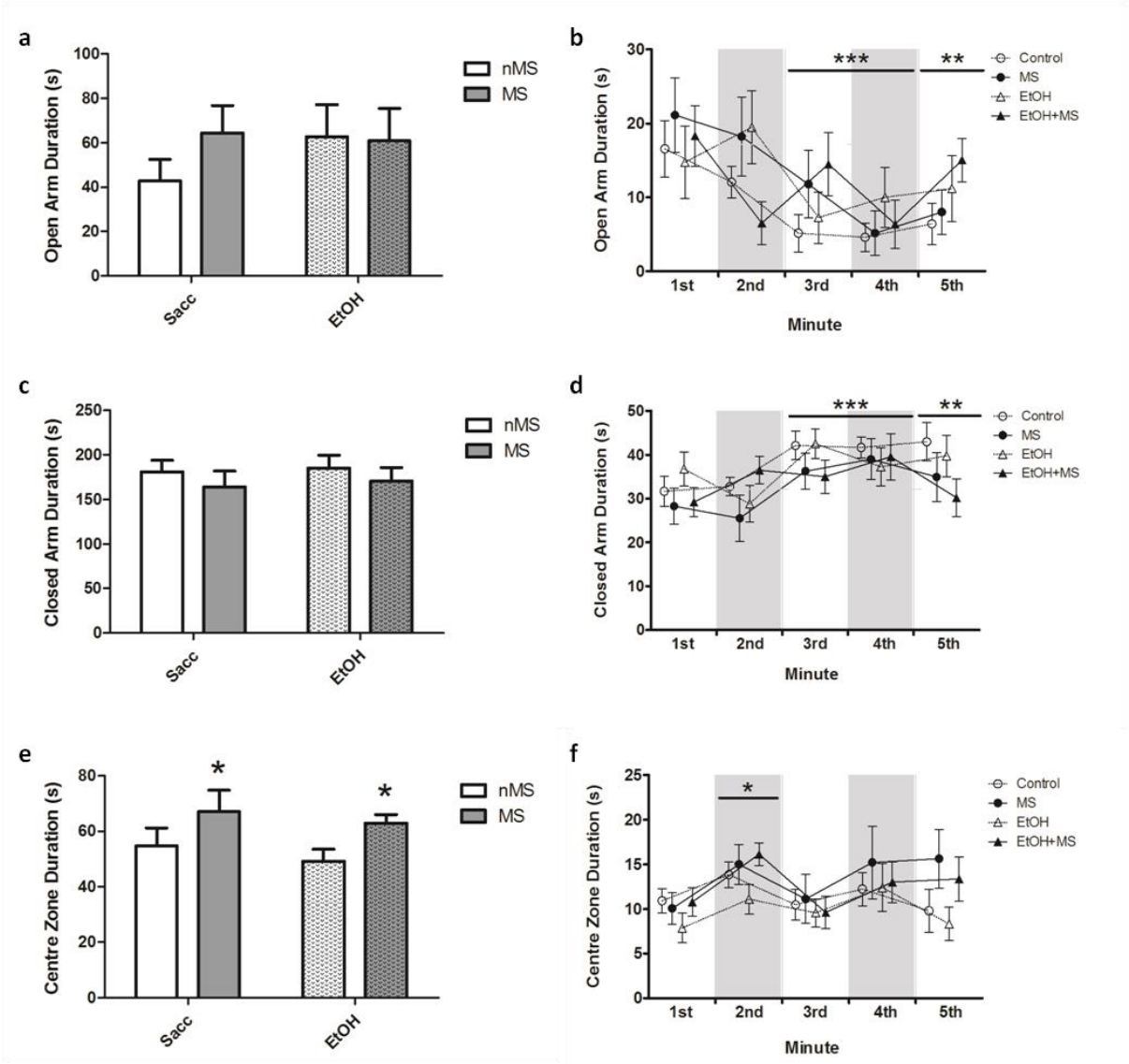

Figure 5.18: Time spent in the open arms, closed arms and centre zone of the Elevated Plus Maze (EPM).

(***a***) Open arm duration. There were no significant differences between experimental groups in the time spent in the open arms (two-way ANOVA). (***b***) Time spent in the open arms of the EPM per minute. Time spent per minute in the open arms decreased from the 3rd-minute onwards (Wilcoxon Matched Pairs test, ** $p < 0.01$, *** $p < 0.001$). The data are not normally distributed (SW, $p < 0.05$). The graph represents the median and IQR. (***c***) Closed arm duration. There was no significant difference between experimental groups in the time spent in the closed arms of the EPM (two-way ANOVA). (***d***) Time spent per minute in the closed arms of the EPM. Time spent per minute in the closed arms increased from the 3rd-minute onwards (Duncan's post-hoc test, ** $p < 0.01$, *** $p < 0.001$). (***e***) Centre zone duration. MS- and EtOH+MS-rats spent more time in the centre zone of the EPM than control and EtOH-rats (Duncan's post-hoc test, * $p = 0.05$). (***f***) Time spent per minute in the centre zone of the EPM increased between the 1st- and 2nd-minute then decreased during the 3rd-minute of the 5-minute trial (Duncan's post-hoc test, * $p < 0.05$). The data are normally distributed (***a, c-f***; SW, $p > 0.05$). The data represent the mean ± SEM. [**Control**, sacc + nMS (n = 11); **MS**, sacc + MS (n = 7), **EtOH**, ethanol + nMS (n = 7), **EtOH + MS** (n = 8)].

The latency to enter the open and closed arms of the EPM is shown in **Figure 5.19a-b**. There were no significant differences between experimental groups in the latency to enter the open arms or the closed arms of the EPM (Kruskal-Wallis). However, the latency to enter the closed arms tended towards a significant increase in MS-rats (Kruskal-Wallis, $p = 0.052$, **Figure 5.19b**).

The total number of entries into the open arms of the EPM and the number of entries made into the open arms of the EPM per minute of the 5-minute trial are shown in **Figure 5.19c-d**. Two-way ANOVA (*treatment x stress*) revealed no significant differences between experimental groups in the total number of entries made into the open arms of the EPM. Friedman ANOVA showed a significant effect of time on the number of entries made into the open arms of the EPM ($p < 0.001$). The number of entries made into the open arms of the EPM decreased over the 5-minute trial (Wilcoxon Matched Pairs test, $p < 0.01$, **Figure 5.19d**).

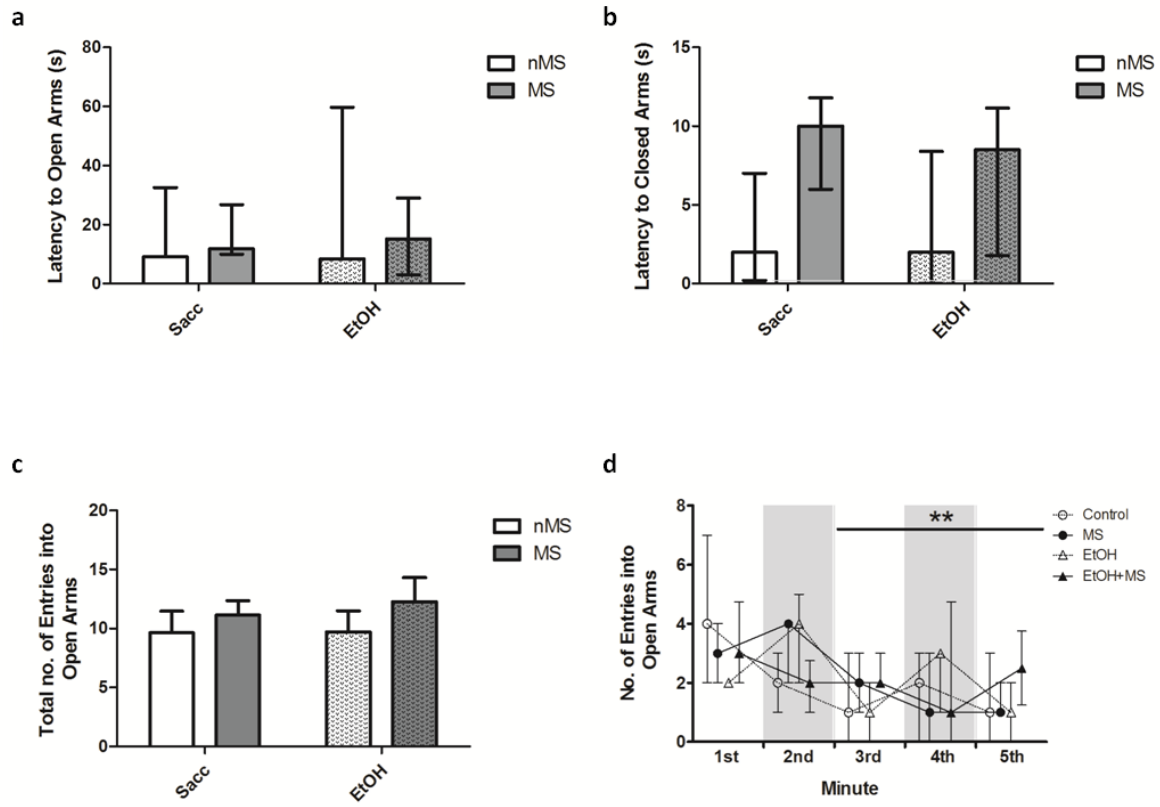

Figure 5.19: Latency to enter the open and closed arms as well as the number of entries made into the open arms of the Elevated Plus Maze (EPM)

(***a***) Latency to enter the open arms of the EPM. There was no significant difference between experimental groups (Kruskal-Wallis). (***b***) Latency to enter the closed arms of the EPM was tending towards significance (Kruskal-Wallis, $p = 0.052$). (***c***) Total number of entries into the open arms. There was no significant difference between experimental groups (two-way ANOVA). The data are normally distributed (SW, $p > 0.05$). The graph represents the mean ± SEM. (***d***) The number of entries per minute made into the open arms of the EPM decreased from the 3rd-minute onwards (Wilcoxon Matched Pairs test, ** $p < 0.01$). The data are not normally distributed (SW, $p < 0.05$). The graphs (***a, b, d***) represent the median and IQR. [**Control**, sacc + nMS (n = 11); **MS**, sacc + MS (n = 7), **EtOH**, ethanol + nMS (n = 7), **EtOH + MS** (n = 8)].

OPEN FIELD TEST

The OFT took place immediately after the EPM on P60. Locomotor activity and anxiety-like behaviour of **control** (sacc + nMS, n = 11), **MS-** (sacc + MS, n = 7), **EtOH-** (EtOH + nMS, n = 7) and **EtOH+MS-** (EtOH + MS, n = 8) rats were measured.

The distance travelled during the 5-minute trial is depicted in **Figure 5.20**. Two-way ANOVA (*treatment x stress*) showed no significant differences between experimental groups in the distance travelled during the OFT. Repeated-measures ANOVA (*treatment x stress x minute*)

revealed a significant main effect of time on distance travelled per minute in the OFT ($F_{(4,116)}$ = 30.15, $p < 0.001$). Distance travelled per minute decreased over the 5-minute trial (Duncan's post-hoc test, $p < 0.001$).

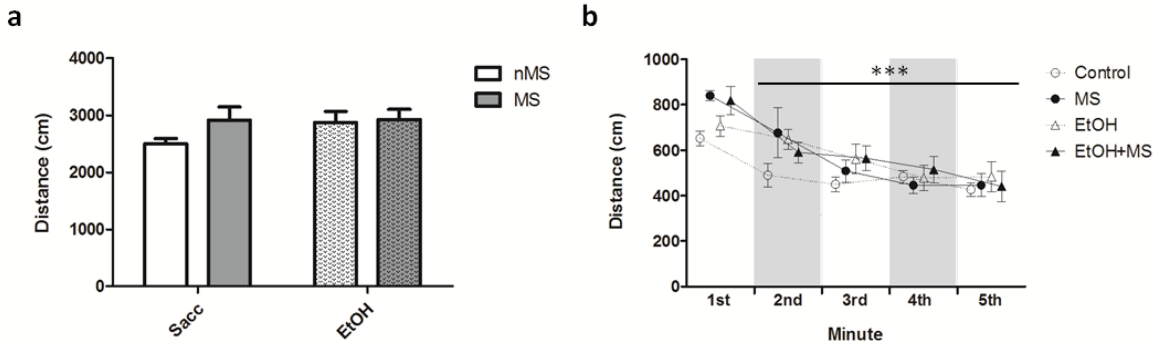

Figure 5.20: Distance Travelled during the Open Field Test (OFT)

(***a***) Total distance travelled during the OFT. There were no significant differences between experimental groups (two-way ANOVA, $p > 0.1$). (***b***) Distance travelled per minute decreased over the 5-minute trial (Duncan's post-hoc test, $p < 0.05$). The data were normally distributed (SW, $p > 0.05$). The data represent the mean ± SEM. [**Control**, Sacc + nMS (n = 11); **MS**, Sacc + MS (n = 7), **EtOH**, EtOH + nMS (n = 7), **EtOH + MS** (n = 8)].

Two-way ANOVA (*treatment x stress*) showed a significant main effect of treatment on the time spent in the inner zone of the open field arena ($F_{(1, 29)}$ = 4.89, $p < 0.05$, **Figure 5.21a**). Post-hoc analysis showed that EtOH-rats spent more time in the inner zone of the open field than control rats (Duncan's post-hoc test, $p < 0.05$). There were no significant differences between experimental groups for time spent per minute in the inner zone of the open field (Friedman ANOVA, **Figure 5.21b**). Two-way ANOVA (*treatment x stress*) showed a significant main effect of treatment on the frequency of entries into the inner zone of the open field ($F_{(1, 29)}$ = 8.23, $p < 0.01$). EtOH-rats entered the inner zone of the open field arena more frequently than control rats (Duncan's post-hoc test $p < 0.05$, **Figure 5.21c**). However, the frequency to enter the inner zone of the open field arena per minute did not differ between experimental groups (Friedman ANOVA, **Figure 5.21d**). Latency to enter the inner zone of the open field arena did not differ between experimental groups (Kruskal-Wallis, **Figure 5.21e**).

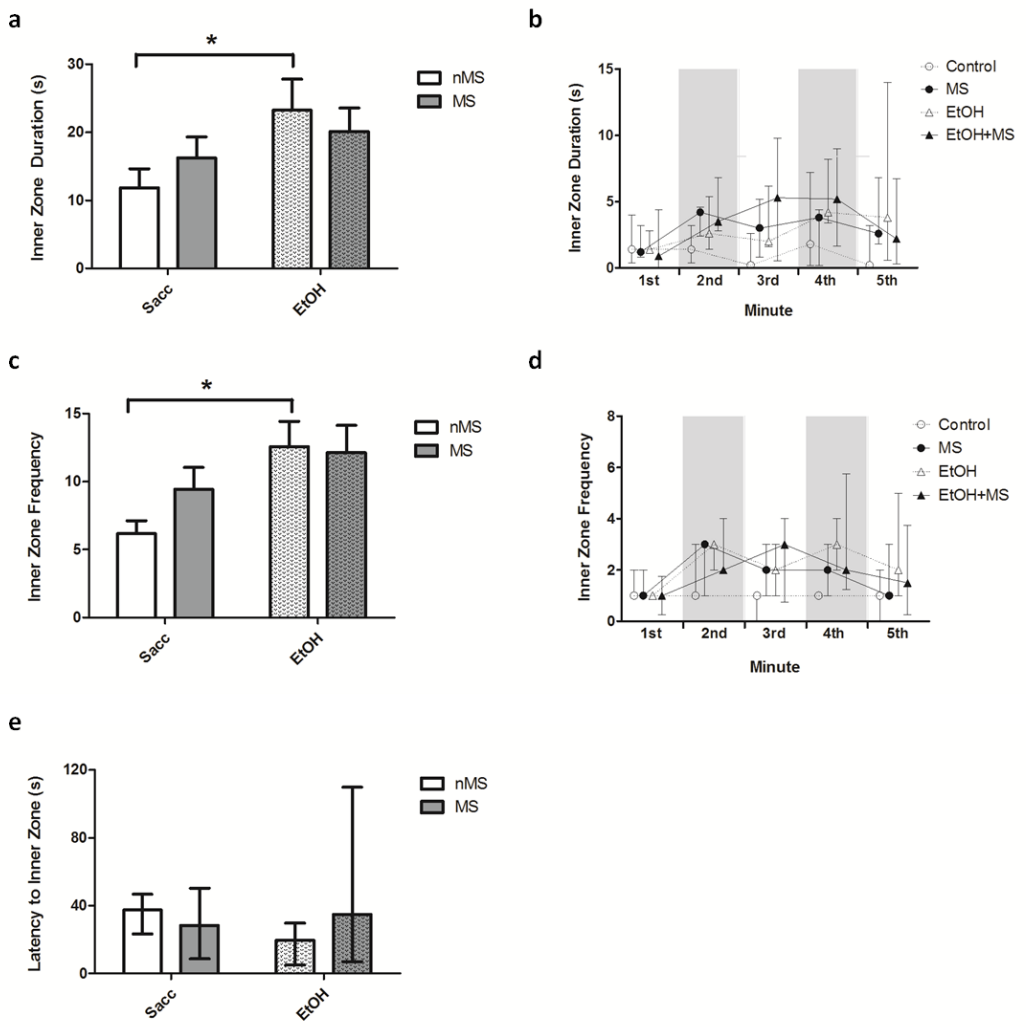

Figure 5.21: Inner zone duration, number of entries and latency to enter the inner zone of the open field.

(***a***) Inner zone duration. EtOH-rats spent more time in the inner zone of the open field than control rats (Duncan's post-hoc test, * $p < 0.05$). (**b**) The time spent per minute in the inner zone of the open field did not differ between experimental groups (Friedman ANOVA,) (**c**) The number of entries into the inner zone of the open field arena. EtOH-rats entered the inner zone more frequently than control rats (Duncan's post-hoc test, * $p < 0.05$). (**d**) The number of entries made per minute into the inner zone of the open field did not differ between experimental groups (Friedman ANOVA). (***e***) There were no significant differences between experimental groups in time taken to enter the inner zone of the open field arena (Kruskal-Wallis). The data represented in graphs ***a*** and ***c*** are normally distributed (SW, $p > 0.05$) and represent the mean ± SEM. The data represented in graphs ***b, d***, and ***e*** are not normally distributed (SW, $p < 0.05$) and represent the median and IQR. [**Control**, sacc + nMS (n = 11); **MS**, sacc + MS (n = 7), **EtOH**, ethanol + nMS (n = 7), **EtOH + MS** (n = 8)].

FORCED SWIM TEST

On P62, 24 hours after the habituation swim, **control** (n = 11), **MS-** (n = 7), **EtOH-** (n = 7) and **EtOH+MS-** (EtOH+MS) rats were placed back into the cylinders and allowed to swim for 5 minutes. Time spent immobile, swimming and climbing, and the latency to reach immobility

were measured. Two-way ANOVA (*treatment x stress*) revealed a significant main effect of stress on the time spent immobile in the FST ($F_{(1, 29)} = 5.01$, $^*p < 0.05$). Rats exposed to 3 hours of maternal separation stress spent less time immobile than nMS-rats (Duncan's post-hoc test, $p < 0.05$, **Figure 5.22a**). A main effect of stress was observed on the time spent swimming during the FST (two-way ANOVA, $F_{(1, 29)} = 5.58$, $p < 0.05$). Maternally separated rats spent more time swimming than non-stressed rats (Duncan's post-hoc test, $p < 0.05$ **Figure 5.22b**). There was no significant difference between experimental groups in the time spent climbing (two-way ANOVA, **Figure 5.22c**) or in the latency to reach immobility during the FST (Kruskal-Wallis, **Figure 5.22d**).

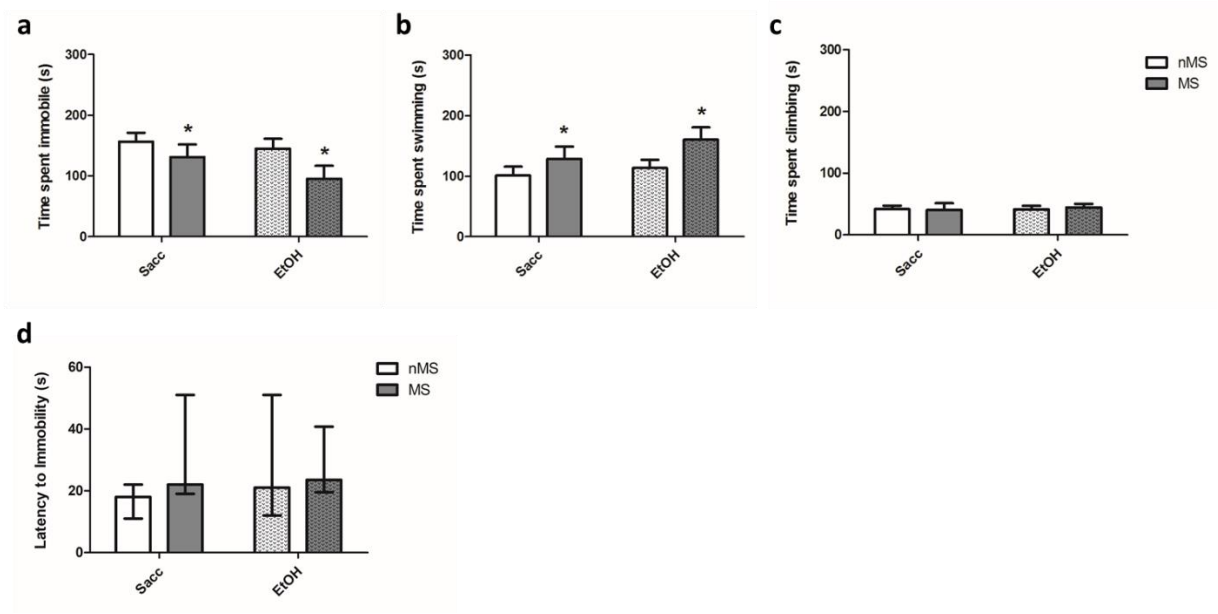

Figure 5.22: Forced Swim Test

(***a***) Rats exposed to maternal separation stress spent less time immobile (***b***) and more time swimming than nMS-rats (Duncan's post-hoc test, * $p < 0.05$). (***c***) There was no significant difference in the time spent climbing during the FST (two-way ANOVA). The data are normally distributed (SW, $p > 0.05$). The graphs represent the mean ± SEM. (***d***) There was no significant difference between groups for the latency to reach immobility (Kruskal-Wallis). These data were not normally distributed (SW, $p < 0.05$) and the data represent the median and IQR. [**Control**, sacc + nMS (n = 11); **MS**, sacc + MS (n = 7), **EtOH**, ethanol + nMS (n = 7), **EtOH + MS** (n = 8)].

WESTERN BLOT

WESTERN BLOT ANALYSIS OF MALE RATS

There were no significant differences between experimental groups in the levels of P-ERK1/2 (two-way ANOVA) and ERK1/2 (Kruskal-Wallis analysis, $p > 0.1$) in the PFC of male rats (**Figure 5.23b and c**). There was a significant interaction between the factors treatment and stress on the P-ERK1/2 to ERK1/2 ratio in the PFC of male rats ($F_{(1, 28)} = 5.75$, $p < 0.05$). The ratio of P-ERK1/2 to ERK1/2 tended to be greater in MS-rats versus control rats whereas the P-ERK1/2 to ERK1/2 ratio tended to be lower in EtOH+MS-rats compared to EtOH-rats. The ratio of P-ERK1/2 to ERK1/2 was significantly increased in the PFC of male EtOH-rats compared to control rats (Duncan's post-hoc test, $p < 0.05$, **Figure 5.23d**). In the DH of male rats there were no significant differences between experimental groups in the levels of P-ERK1/2 and ERK1/2 (two-way ANOVA). The interaction between the factors treatment and stress on the P-ERK1/2 to ERK1/2 ratio tended towards significance in the DH of male rats ($F_{(1,28)} = 3.20$, $p = 0.08$, **Figure 5.23h**). The pattern was similar to that of the PFC

Two-way ANOVA (*treatment x stress*) revealed a significant treatment effect on the levels of P-GSK3β in the PFC of male rats ($F_{(1,28)} = 6.08$, $p < 0.05$). P-GSK3β was significantly increased in the PFC of male rats exposed to prenatal-ethanol (Duncan's post-hoc test, $p < 0.05$, **Figure 5.24b**). Total GSK3β and the ratio of P-GSK3β to GSK3β in the PFC of male rats were not significantly different between experimental groups (two-way ANOVA). In the DH, the levels of P-GSK3β, GSK3β and the ratio of P-GSK3β to GSK3β were not significantly different between experimental groups (two-way ANOVA, **Figure 5.24f-h**).

The levels of P-CREB, CREB and the ratio of P-CREB to total CREB were not significantly different between experimental groups in both the PFC and DH of male rats (Two-way ANOVA; Kruskal-Wallis, **Figure 5.25**).

Two-way ANOVA (*treatment x stress*) of synaptophysin in both the PFC and DH of male rats revealed no significant differences between experimental groups (**Figure 5.26**).

The levels ATP5A were not significantly different between experimental groups in both the PFC (Kruskal-Wallis) and DH (two-way ANOVA) of male rats (**Figure 5.27**).

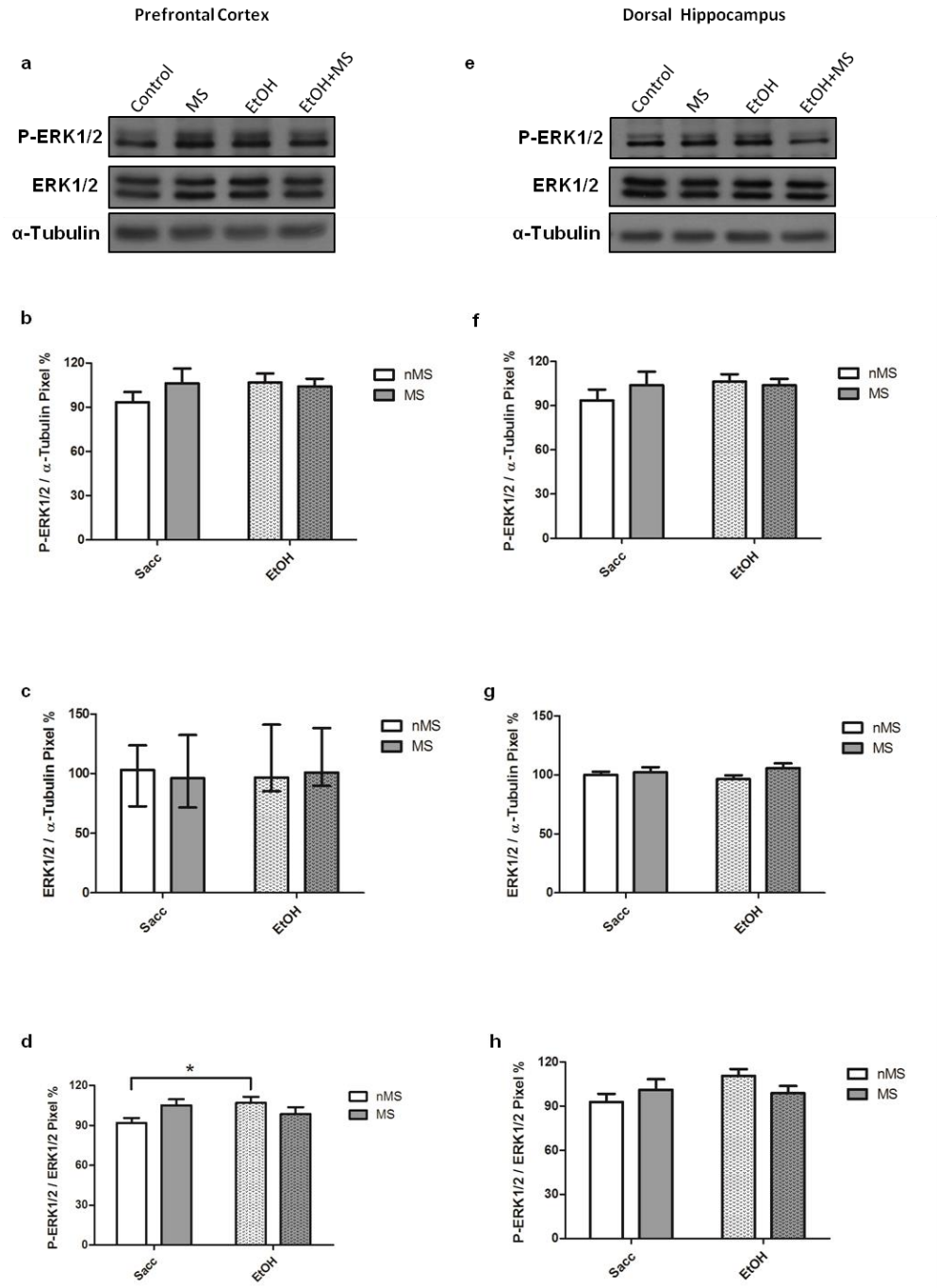

Figure 5.23: Western blot analysis of P-ERK1/2 and ERK1/2 in the prefrontal cortex and dorsal hippocampus of adult *male* rats.

(***a***) Western blot of P-ERK1/2, ERK1/2 and the corresponding reference protein, α-tubulin, in the PFC (***b***) P-ERK1/2 / α-tubulin in the PFC is not significantly different between experimental groups (two-way ANOVA). (***c***) ERK1/2 / α-tubulin in the PFC is not significantly different between groups (Kruskal-Wallis, $p > 0.1$). The data are not normally distributed (SW, $p < 0.05$) and the graph represents the median and IQR. (***d***) The P-ERK1/2 to ERK1/2 ratio in the PFC is significantly increased in EtOH-rats versus control rats (Duncan's post-hoc test * $p < 0.05$). (***e***) Western blot of P-ERK1/2, ERK1/2 and the reference protein, α-tubulin, in the DH (***f*** and ***g***) P-ERK1/2 and ERK1/2 in the DH is not significantly different between experimental groups (two-way ANOVA). (***h***) P-ERK1/2 to ERK1/2 ratio in the DH. The interaction between the factors treatment and stress tended to be significant (two-way ANOVA, p = 0.08). The data are normally distributed (SW, $p > 0.05$) and graphs represent the mean ± SEM, except for those represented in ***c***. [**Control**, sacc + nMS (n = 8); **MS**, sacc + MS (n = 8), **EtOH**, ethanol + nMS (n = 8), **EtOH+MS**, (n = 8)].

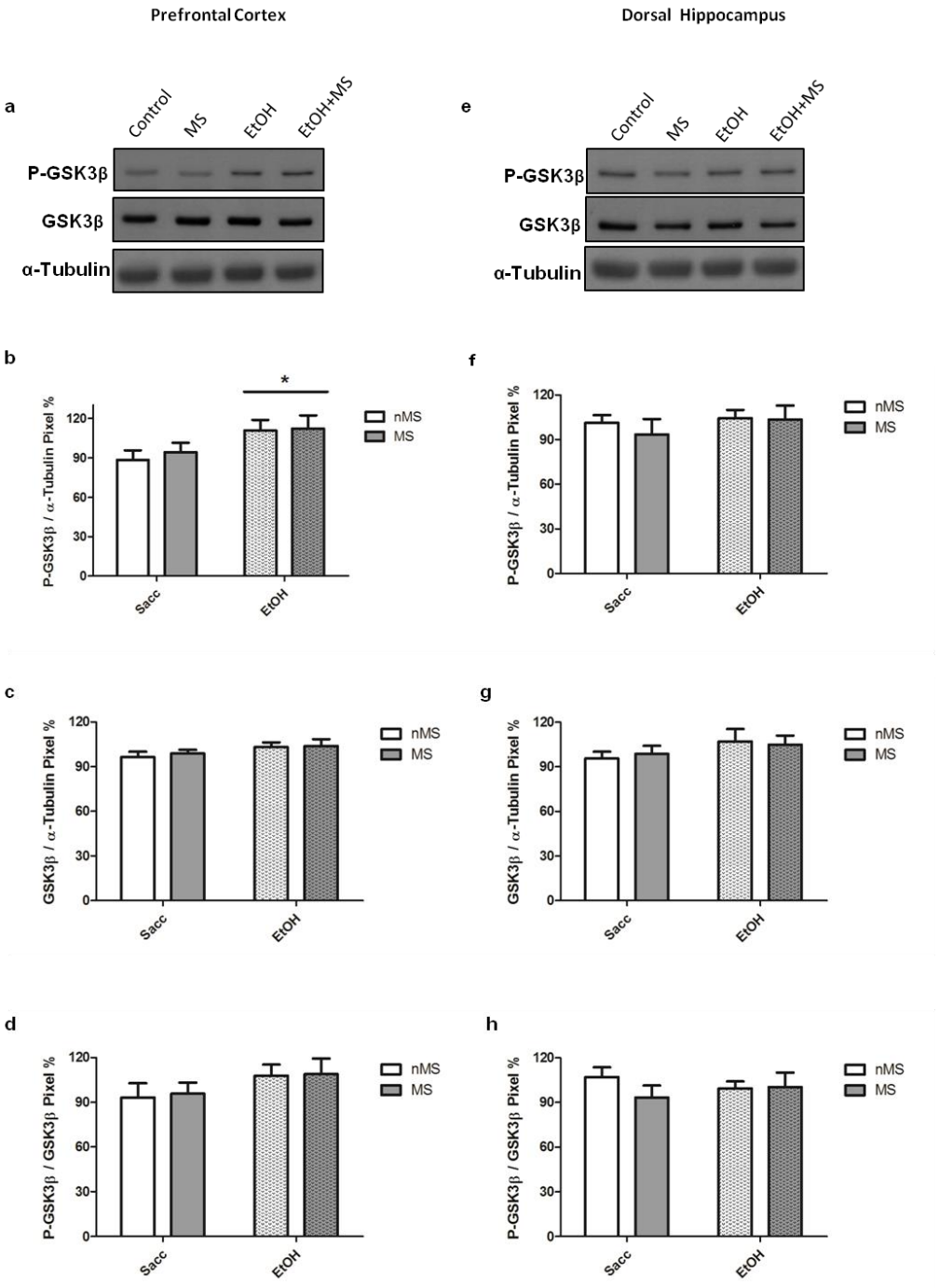

Figure 5.24: Western blot analysis of P-GSK3β and GSK3β in the prefrontal cortex and dorsal hippocampus of adult *male* rats.

(***a***) Western blot of P-GSK3β, GSK3β and the reference protein, α-tubulin, in the PFC of male rats. (***b***) P-GSK3β / α-tubulin was significantly higher in the PFC of rats exposed to prenatal-ethanol (Duncan post-hoc test, * $p < 0.05$). (***c*** and ***d***) The pixel density percentage of GSK3β / α-tubulin and the ratio of P-GSK3β to GSK3β were not significantly different between experimental groups (two-way ANOVA). (***e***) Western blot of P-GSK3β, GSK3β and the reference protein, α-tubulin, in the DH of male rats. (***f*** - ***h***)There were no significant differences between experimental groups in P-GSK3β / α-tubulin, GSK3β / α-tubulin and the ratio of P-GSK3β to GSK3β (two-way ANOVA).The data were normally distributed (SW, $p > 0.05$) and represent the mean ± SEM. [**Control**, sacc + nMS (n = 8); **MS**, sacc + MS (n = 8), **EtOH**, ethanol + nMS (n = 8), **EtOH+MS**, (n = 8)].

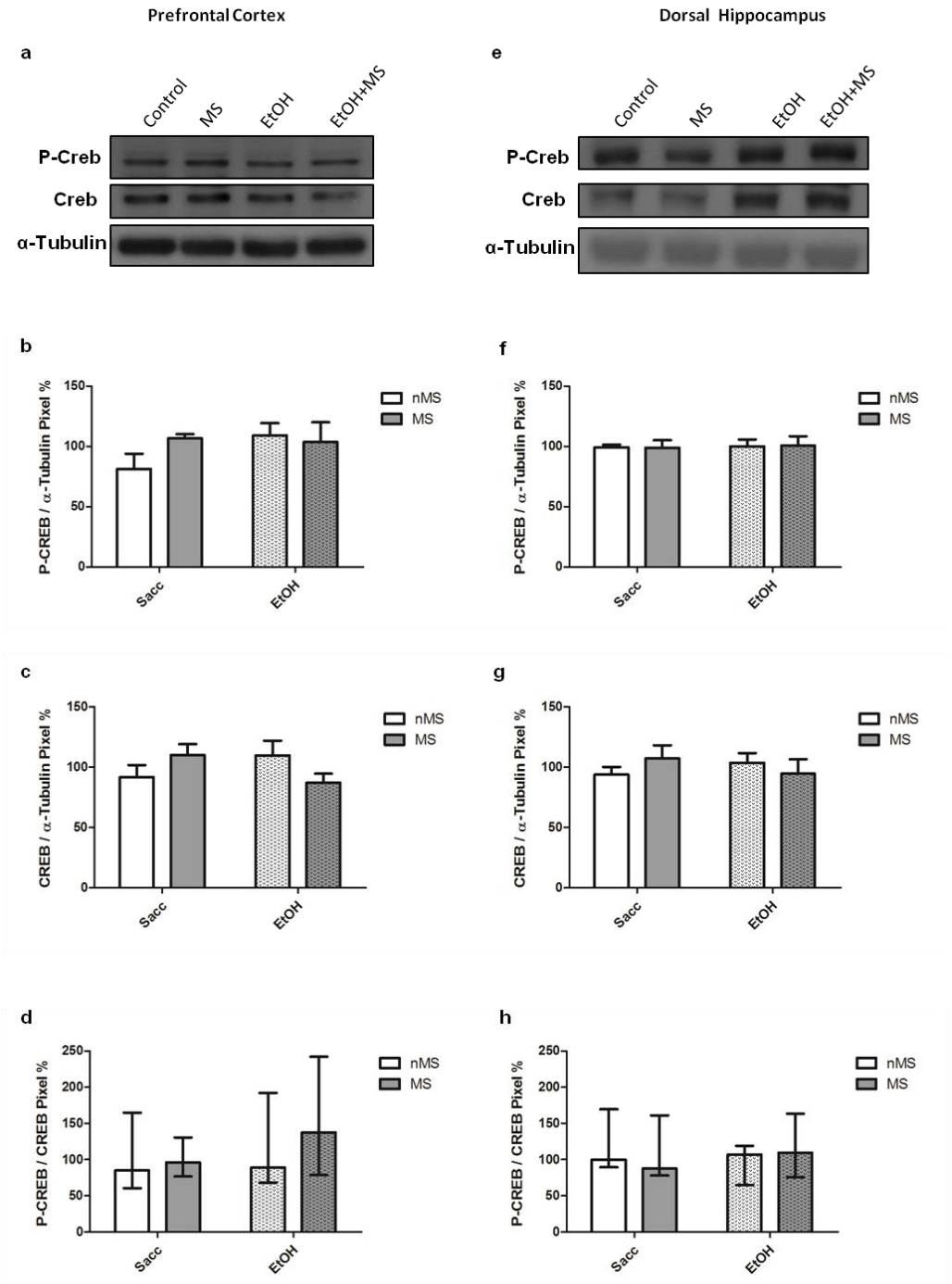

Figure 5.25: Western Blot analysis of P-CREB and CREB in the prefrontal cortex and dorsal hippocampus of adult *male* rats.

(***a***) Western blot analysis of P-CREB, CREB and the reference protein, α-tubulin, in the PFC of male rats. (***b*** - ***d***) There were no significant differences between experimental groups in the pixel density percentage of P-CREB / α-tubulin, CREB / α-tubulin (two-way ANOVA) and the ratio of P-CREB to CREB (Kruskal-Wallis) in the PFC of male rats. (***e***) Western blot analysis of P-CREB, CREB and the reference protein, α-tubulin, in the DH of male rats. (***f*** - ***h***) There were no significant differences between experimental groups in the levels of P-CREB / α-tubulin, CREB / α-tubulin (two-way ANOVA) and the ratio of P-CREB to CREB (Kruskal-Wallis) in the DH of male rats. The data are normally distributed (SW, $p > 0.05$) and the graphs represent the mean ± SEM, except for those represented in ***d*** and ***h***. The data in ***d*** and ***h*** are not normally distributed (SW, $p < 0.05$) and represent the median and IQR. [**Control**, sacc + nMS (n = 8); **MS**, sacc + MS (n = 8), **EtOH**, ethanol + nMS (n = 8), **EtOH+MS** (n = 8)].

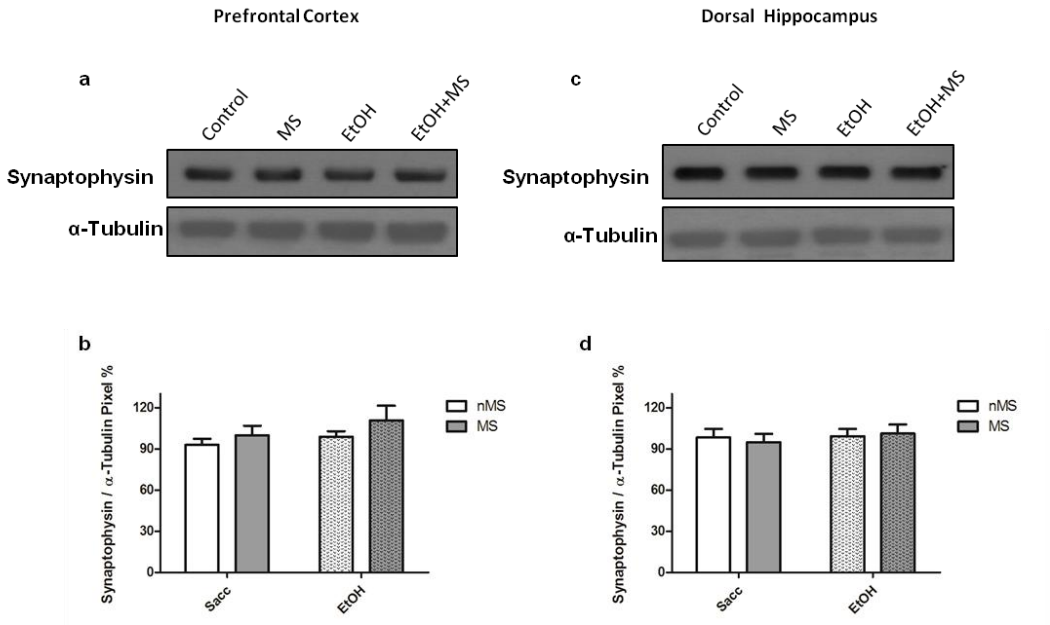

Figure 5.26: Western blot analysis of synaptophysin in the prefrontal cortex and dorsal hippocampus of adult *male* rats.

(***a***) Western Blot of synaptophysin and the reference protein, α-tubulin, in the PFC of male rats. (***b***) Two-way ANOVA showed no significant differences between experimental groups in the levels of synaptophysin in the PFC of male rats. (***c***) Western Blot of synaptophysin and the reference protein, α-tubulin, in the DH of male rats. (***d***) There were no significant differences between experimental groups in the levels of synaptophysin in the DH of male rats (two-way ANOVA). The data were normally distributed (SW, $p > 0.05$). The graphs represent the mean ± SEM. [**Control**, sacc + nMS (n = 8); **MS**, sacc + MS (n = 8), **EtOH**, ethanol + nMS (n = 8), **EtOH+MS** (n = 8)].

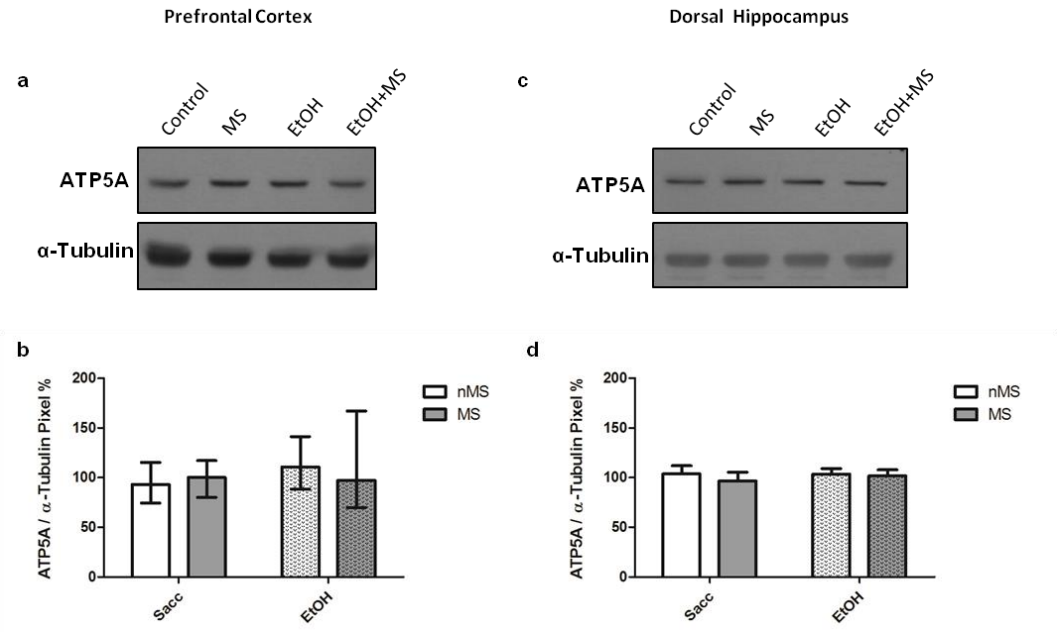

Figure 5.27: Western blot analysis of ATP5A in the prefrontal cortex and dorsal hippocampus of adult *male* rats.

(***a***) Western blot of ATP5A and the reference protein, α-tubulin, in the PFC of male rats (***b***) ATP5A / α-tubulin did not differ between experimental groups (Kruskal-Wallis). The data were not normally distributed (SW, $p < 0.05$) and the graph represents the median and IQR. (***c***) Western blot of ATP5A and the reference protein, α-tubulin, in the DH of male rats. (***d***) There were no significant differences between experimental groups in the levels of ATP5A / α-tubulin in the DH of male rats (two-way ANOVA). The data were normally distributed (SW, $p > 0.05$) and the graph represents the mean ± SEM. [**Control**, sacc + nMS (n = 8); **MS**, sacc + MS (n = 8), **EtOH**, ethanol + nMS (n = 8), **EtOH+MS** (n = 8)].

WESTERN BLOT ANALYSIS OF FEMALE RATS

Levels of P-ERK1/2 and ERK1/2 in the PFC of female rats were not significantly different between experimental groups (Kruskal-Wallis). Two-way ANOVA (*treatment x stress*) revealed a significant interaction between the two factors on the P-ERK1/2 to ERK1/2 ratio in the PFC of female rats. Levels of P-ERK1/2 to ERK1/2 were increased in MS-rats whereas the P-ERK1/2 to ERK1/2 ratio was decreased in EtOH+MS-rats ($F_{(1,27)} = 4.24$, $p < 0.05$). Duncan's post-hoc analysis only revealed group differences between control and EtOH-rats in the PFC of female rats that tended to be significant ($p = 0.052$, **Figure 5.28d**). Similarly, in the DH, the levels of P-ERK1/2 and ERK1/2 were not significantly different between experimental groups (two-way ANOVA). Two-way ANOVA (*treatment x stress*) showed a significant interaction between treatment and stress on the P-ERK1/2 to total ERK1/2 ratio in the DH ($F_{(1, 28)} = 4.77$, $p < 0.05$). MS-rats had greater levels of P-ERK1/2 to ERK1/2 compared to controls where as EtOH+MS-rats had lower levels of P-ERK1/2 to ERK1/2 compared to EtOH-rats. Post-hoc

testing only revealed group differences that tended to be significant (Duncan post-hoc test, p = 0.09, **Figure 5.28h**).

Levels of P-GSK3β and GSK3β in both the PFC and DH of female rats were not significantly different between experimental groups (two-way ANOVA, **Figure 5.29**). Two-way ANOVA (*treatment x stress*) of P-GSK3β to total GSK3β in the PFC of female rats revealed a significant treatment effect ($F_{(1, 28)}$ = 5.4, $p < 0.05$). Female rats exposed to prenatal-ethanol had a greater level of P-GSK3β to total GSK3β than saccharin-control rats (Duncan's post-hoc test, $p < 0.05$, **Figure 5.29d**). The P-GSK3β to total GSK3β ratio in the DH was not significantly different between experimental groups (two-way ANOVA). However, the main effect of stress on the P-GSK3β to total GSK3β ratio in the DH tended to be significant ($F_{(1, 28)}$ = 3.90, p = 0.058, **Figure 5.29h**).

There were no significant differences in the levels of P-CREB, CREB and the ratio of P-CREB to total CREB in the PFC of female rats (two-way ANOVA and Kruskal-Wallis, **Figure 5.30b-d**). In the DH, two-way ANOVA (*treatment x stress*) showed a significant interaction between treatment and stress on the levels of P-CREB ($p < 0.05$). Levels of P-CREB were tending to be increased in the DH of MS-rats versus control rats, whereas levels of P-CREB were tending to be decreased in the DH of EtOH+MS-rats versus EtOH-rats (**Figure 5.30f**). There were no significant differences in the levels of CREB (two-way ANOVA) and the P-CREB to CREB ratio (Kruskal-Wallis) in the DH of female rats (**Figure 5.30g-h**).

Two-way ANOVA (*treatment x stress*) showed a significant interaction between treatment and stress ($F_{(1,28)}$ = 5.82, $p < 0.05$) on synaptophysin levels in the PFC of female rats. Maternal separation stress in sacc-control rats decreased synaptophysin where as maternal separation coupled with prenatal-ethanol increased synaptophysin levels in the PFC of female rats. Post-hoc analysis showed that MS-rats had significantly lower levels of synaptophysin than EtOH+MS-rats (Duncan's post-hoc test, $p < 0.05$, **Figure 5.31a**). Two-way ANOVA (*treatment x stress*) of synaptophysin in the DH of female rats revealed no significant differences between experimental groups.

The levels ATP5A were not significantly different between experimental groups in both the PFC (Kruskal-Wallis) and DH (two-way ANOVA) of female rats (**Figure 5.32**).

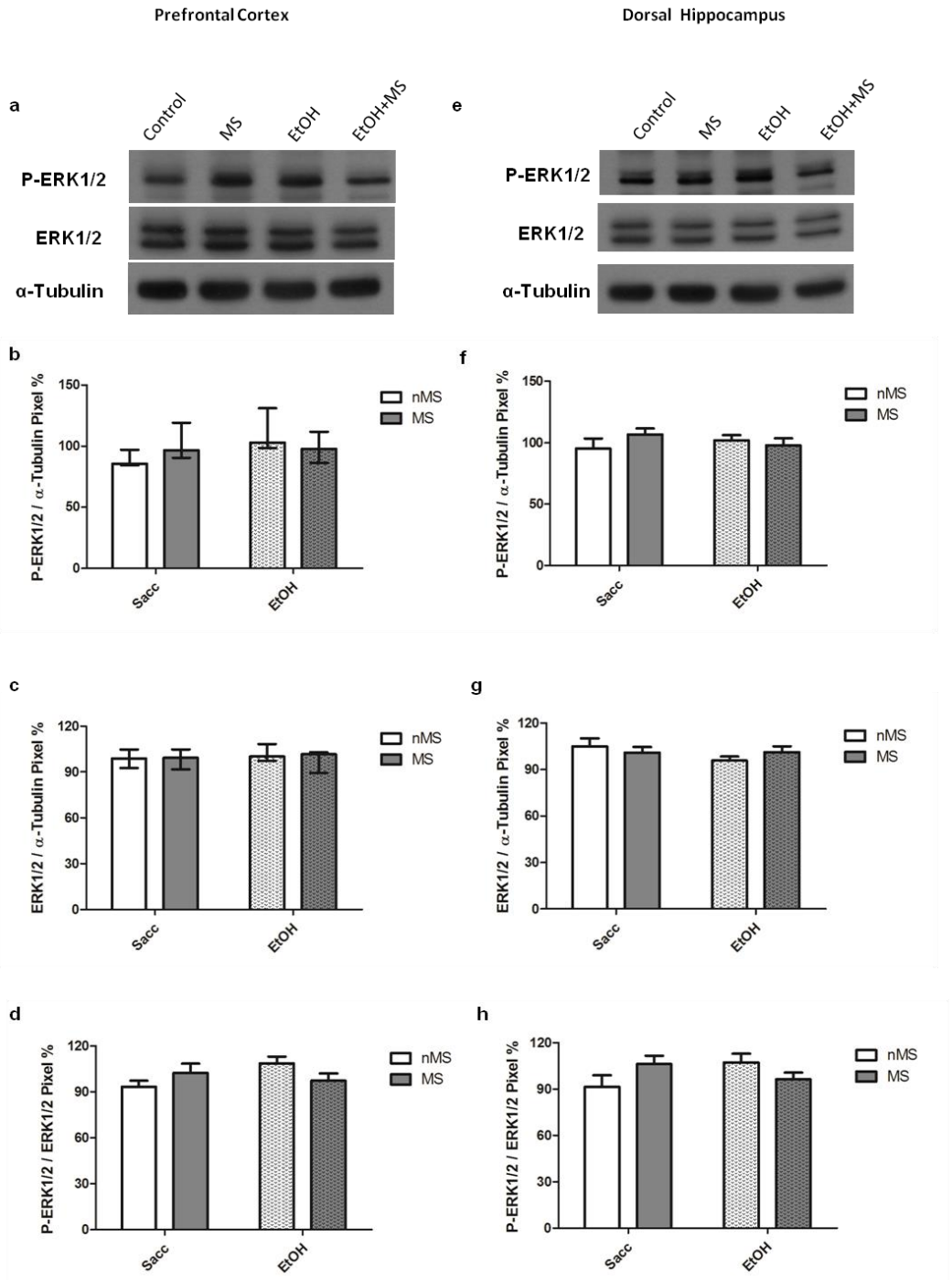

Figure 5.28: Western Blot of P-ERK1/2 and ERK1/2 in the prefrontal cortex and dorsal hippocampus of adult female rats.

(***a***) Western blot of P-ERK1/2, ERK1/2 and the reference protein, α-tubulin, in the PFC of female rats. (***b-c***) Levels of P-ERK1/2 / α-tubulin and ERK1/2 / α-tubulin were not significantly different between experimental groups (Kruskal-Wallis). The data are not normally distributed (SW, $p < 0.05$) and the graphs represent the median and IQR. (***d***) There was a significant interaction between the factors treatment and stress on the P-ERK1/2 to ERK1/2 ratio in the PFC. Duncan's post-hoc analysis revealed group differences that tended to be significant ($p = 0.052$). (***e***) Western blot of P-ERK1/2, ERK1/2 and the reference protein, α-tubulin, in the DH of female rats. (***f*** and ***g***) The pixel density percentages of P-ERK1/2 / α-tubulin and ERK1/2 / α-tubulin in the DH were not significantly different between experimental groups (two-way ANOVA). (***h***) There was a significant interaction between treatment and stress on the P-ERK1/2 to ERK1/2 ratio in the DH. Duncan's post-hoc analysis revealed group difference that tended to be significant ($p = 0.09$). The data were normally distributed (**d, f-g**; SW, $p > 0.05$) and graphs represent the mean ± SEM. [**Control**, sacc + nMS (n = 8); **MS**, sacc + MS (n = 8), **EtOH**, ethanol + nMS (n = 8), **EtOH+MS**, (n = 8)].

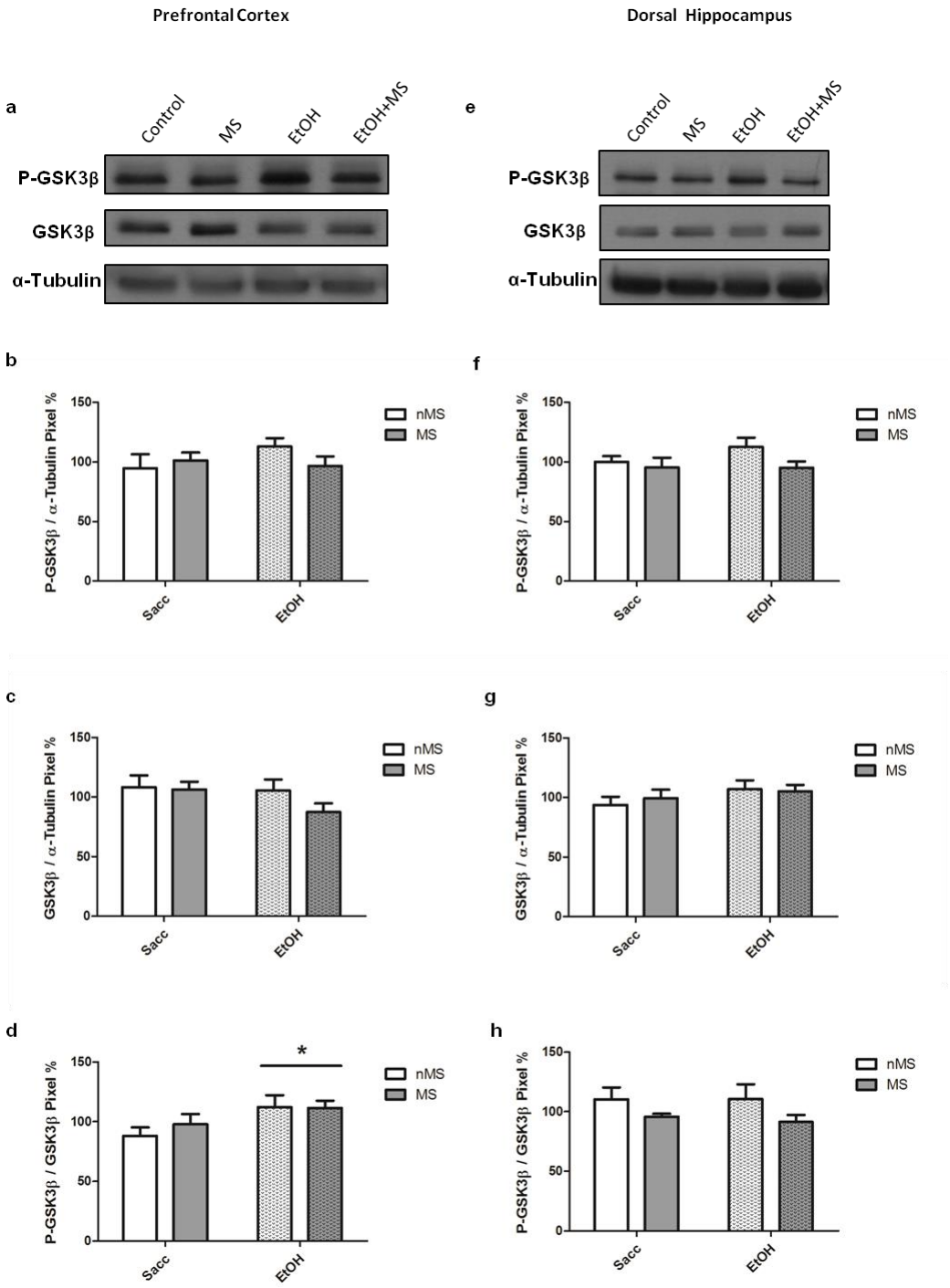

Figure 5.29: Western blot analysis of P-GSK3β and GSK3β in the prefrontal cortex and dorsal hippocampus of adult *female rats.*

(***a***) Western blot of P-GSK3β, GSK3β and the reference protein, α-tubulin, in the PFC of female rats. (***b-c***) P-GSK3β / α-tubulin and GSK3β / α-tubulin in the PFC were not significantly different between experimental groups (two-way ANOVA). (***d***) The ratio of P-GSK3β to GSK3β was significantly higher in the PFC of rats exposed to prenatal-ethanol (Duncan's post-hoc test * $p < 0.05$). (***e***) Western blot of P-GSK3β, GSK3β and the reference protein, α-tubulin, in the DH of female rats. (***f-h***). There were no significant differences between experimental groups in the levels of P-GSK3β / α-tubulin, GSK3β / α-tubulin and the ratio of P-GSK3β to GSK3β in the DH (two-way ANOVA). The data were normally distributed (SW, $p > 0.05$) and the graphs represent the mean ± SEM. [**Control**, sacc + nMS (n = 8); **MS**, sacc + MS (n = 8), **EtOH**, ethanol + nMS (n = 8), **EtOH+MS**, (n = 8)].

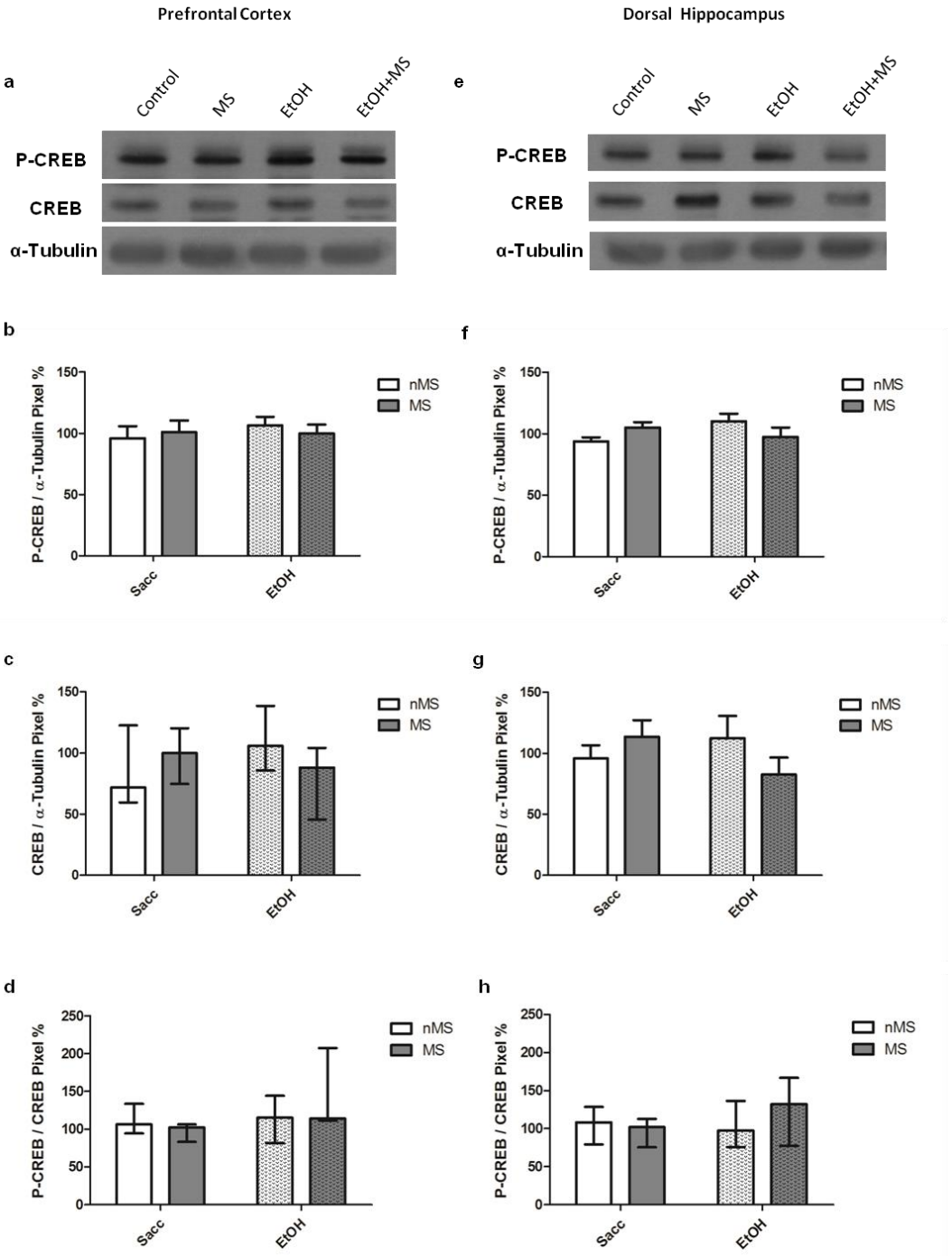

Figure 5.30: Western Blot of P-CREB and CREB in the prefrontal cortex and dorsal hippocampus of adult *female* rats.

(***a***) A Western blot of P-CREB, CREB and the reference protein α-tubulin in the PFC of female rats. (***b-d***) There were no significant differences in the levels of P-CREB, CREB and the ratio of P-CREB to CREB (two-way ANOVA and Kruskal-Wallis) in the PFC. (***e***) A Western blot of P-CREB, CREB and the reference protein α-tubulin in the DH of female rats. (***f***) There was a significant interaction between the factors treatment and stress on the levels of P-CREB in the DH of female rats (two-way ANOVA, $p < 0.05$). EtOH-rats tended to have greater levels of P-CREB than control rats (Duncan's post-hoc test, $p = 0.07$). (**g**) Levels of total CREB were not significantly different between experimental groups (two-way ANOVA). (**h**) Levels of P-CREB / CREB were not significantly different between groups (Kruskal-Wallis). The data represented in b, f and g are normally distributed (SW, $p > 0.05$) and the graphs represent the mean ± SEM. The data in c, d and h are not normally distributed (SW, $p < 0.05$). These graphs represent the median and IQR. [**Control**, sacc + nMS (n = 8); **MS**, sacc + MS (n = 8), **EtOH**, ethanol + nMS (n = 8), **EtOH+MS**, (n = 8)].

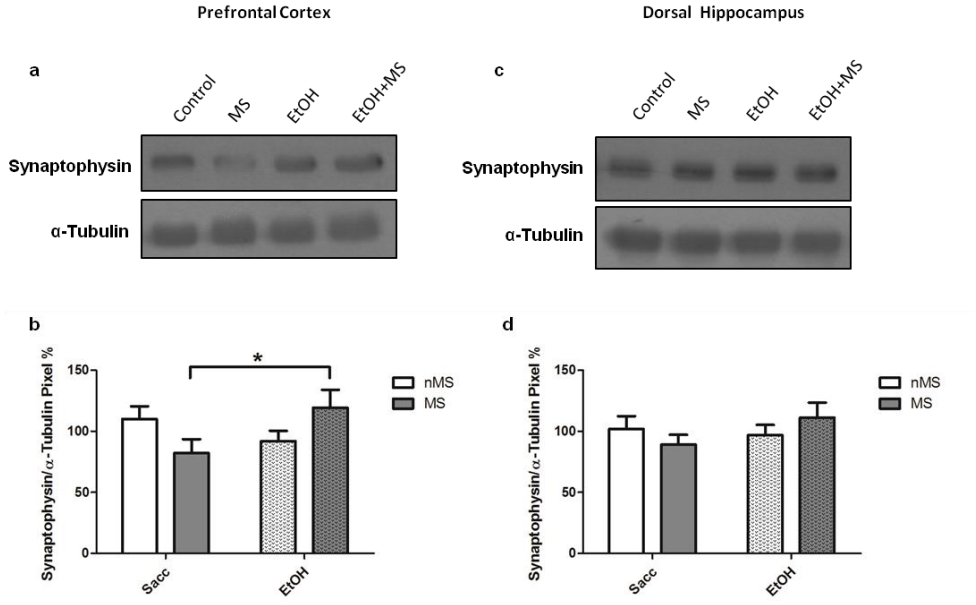

Figure 5.31: Western blot analysis of synaptophysin in the prefrontal cortex and dorsal hippocampus of adult *female* rats.

(***a***) Western blot of synaptophysin and the reference protein, α-tubulin, in the PFC of female rats. (***b***) The levels of synaptophysin / α-tubulin was significantly lower in MS-rats than EtOH+MS-rats (Duncan's post-hoc test, * $p < 0.05$) (***c***) Western blot of synaptophysin and the reference protein, α-tubulin, in the DH of female rats. (***d***) There were no significant differences between experimental groups (two-way ANOVA). The data are normally distributed (SW, $p > 0.05$). The graphs represent the mean ± SEM. [**Control**, sacc + nMS (n = 8); **MS**, sacc + MS (n = 8), **EtOH**, ethanol + nMS (n = 8), **EtOH+MS** (n = 8)].

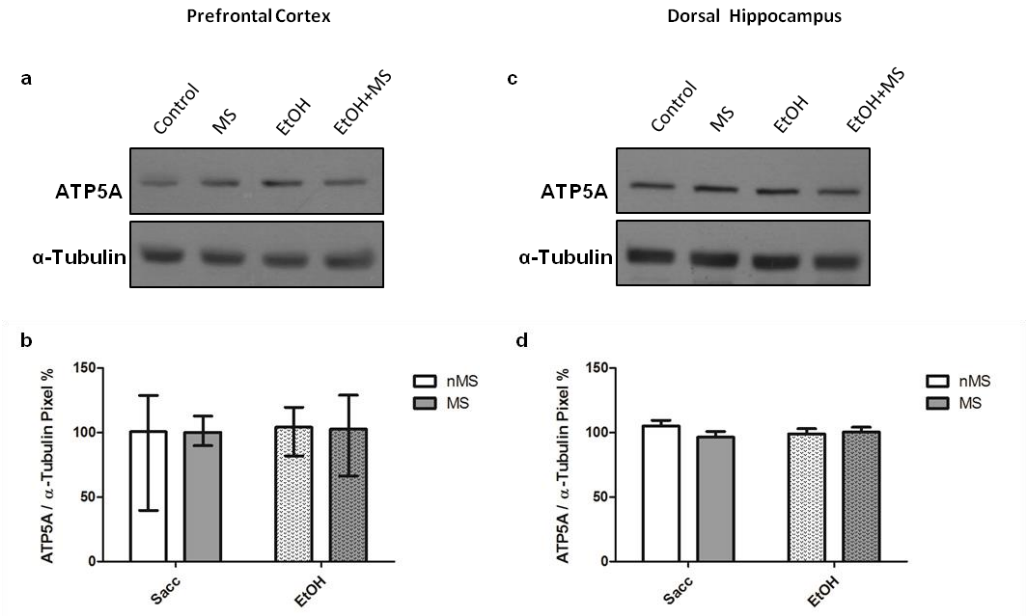

Figure 5.32: Western blot analysis of ATP5A in the prefrontal cortex and dorsal hippocampus of adult *female* rats.

a) Western blot of ATP5A and the reference protein, α-tubulin, in the PFC of female rats (***b***) Levels of ATP5A / α-tubulin did not differ between experimental groups (Kruskal-Wallis). The data were not normally distributed (SW, $p < 0.05$) and the graph represents the median and IQR. (***c***) Western blot of ATP5A and the reference protein, α-tubulin, in the DH of female rats. (***d***) There are no significant differences between experimental groups in the levels of ATP5A / α-tubulin in the DH of female rats (two-way ANOVA). The data are normally distributed (SW, $p > 0.05$) and the graph represents the mean ± SEM. [**Control**, sacc + nMS (n = 8); **MS**, sacc + MS (n = 8), **EtOH**, ethanol + nMS (n = 8), **EtOH+MS** (n = 8)].

DISCUSSION

A major finding in this chapter was that both prenatal-ethanol exposure and early-life stress, increased exploratory activity and the P-ERK1/2 to ERK1/2 ratio in the PFC and DH of adult male rats. However, the combination of prenatal-ethanol exposure with maternal separation decreased exploratory activity and the P-ERK1/2 to ERK1/2 ratio in the PFC and DH to that of control rats. A similar change in P-ERK1/2 activity was observed in the PFC and DH of adult female rats after prenatal-ethanol exposure and the combination of prenatal-ethanol and maternal separation. These results suggest that 3 hours of daily maternal separation stress reduced the effects of prenatal-ethanol exposure on behaviour and the brain and may implicate P-ERK1/2 signalling in exploratory behaviour. Further, compared to control rats, MS- and EtOH-rats showed an increased number and duration of 22 kHz ultrasonic vocalizations indicating a negative emotional state (Portfors, 2007). However, the combination of prenatal-ethanol and maternal separation stress did not decrease the observed increase in number and duration of 22 kHz ultrasonic vocalizations. These results suggest that maternal separation stress reduces the effects of prenatal-ethanol exposure in a behavioural-dependent manner, i.e. maternal separation stress reduced the prenatal-ethanol-induced increase in exploratory behaviour but did not reduce the observed negative emotional state.

In the present study, the animal model of FASD was characterized by fewer pups being born to ethanol-treated dams compared to saccharin-control dams and on P2, male ethanol-exposed pups weighed significantly less than saccharin-control pups. This model of FASD was further characterized by significant deficits in weight gain. Both male and female EtOH-rats weighed less (or tended to weigh less) than control rats throughout different stages of development (P8, P15, P21, P57 and P63). These results are in agreement with Brys *et al*. (2014) who observed a significant number of still-born pups born to Wistar dams that were fed a 10 % and a 35 % ethanol liquid-diet throughout gestation compared to control dams. In addition, from P7 - P40 male and female Wistar rats exposed to prenatal-ethanol (35 % ethanol liquid-diet) gained less weight compared to control rats (Brys et al., 2014). However, studies have also observed no differences in the number of pups born to ethanol-treated mouse dams (saccharin-sweetened, 10 % ethanol solution, 4 hours/day throughout gestation) compared to control-dams and no difference in weight gain was observed between experimental groups at any time point (P7, P14 and P23) (Brady *et al*., 2013). Further, there was no difference in weight gain from P8 -

P21 observed between SD control rats and rats exposed to both prenatal- and early-postnatal ethanol (Barbier et al., 2008). The differences in developmental data may be due to the different species and prenatal-ethanol exposure paradigms used. Further, in the present study, EtOH-dams consumed a third of the amount of liquid consumed by saccharin-dams and this could have further influenced the developmental data.

MS-rats and control rats did not differ in body weight at any time point in the present study. This is in agreement with previous studies in which there was no difference in body weight between maternally separated Wistar rats and control rats after 3 hours/day of repeated maternal separation stress from P2 - P15 (Hulshof et al., 2011) and similarly there was no difference between adult SD rats maternally separated from P2 - P14 (3 hours/day) versus control rats (Makena et al., 2012). However, previous studies have shown that both male and female Long-Evans rats that were maternally separated (3 hours /day, P2 - P14) weighed less than control rats on P14 (Kalinichev et al., 2002) and C57BL/6N mice that were separated for 3 hours/day from P2 - P21 weighed less than control mice on P14 and P28 (Bian et al., 2015). Interestingly on P8 (female rats) and P15 (male rats), EtOH+MS-rats weighed more than EtOH-rats. This was the first indication that maternal separation was possibly reducing the effects of prenatal-ethanol exposure during the early-stages of development. However, this weight-reducing effect of ethanol was not reversed by maternal separation in adulthood as there was no difference in body weight between EtOH- and EtOH+MS-rats at P57 and P63.

On the first day of behavioural testing, when rats were first introduced to a novel environment, MS- and EtOH- rats showed greater exploratory activity than control rats as shown by the increased distance travelled during the novel object habituation trial. This is similar to a previous study in which ethanol was administered during the early-postnatal period (P4 - P9, 5.25 mg/kg/day) and in adolescence the ethanol exposed SD rats (P30) were more exploratory on the first day of behavioural testing in the open field compared to non-exposed controls (Monk et al., 2012). However, maternal separation (3 hours/day, P2 - P15) has been shown to have no effect on exploratory behaviour of Wistar rats introduced to the open field arena in adulthood (Hulshof et al., 2011). In addition, on day one of behavioural testing, the combination of prenatal-ethanol and maternal separation stress reduced exploratory levels to that of control rats reflecting a significant interaction between early-life stress and prenatal-ethanol exposure on exploratory behaviour. Again, this result suggests that maternal separation reduced the effects of prenatal-ethanol exposure. This result does not agree with a previous

study in which there was no interaction between prenatal-ethanol and early-life stress on activity levels in a novel open field environment (Alberry and Singh, 2016). Alberry and Singh. (2016) also investigated the effects of prenatal-ethanol coupled with additional early-life stress. However, there were significant methodological differences: a continuous preference drinking model was used with B6 mice in which ethanol-treated dams had access to both water and a 10 % ethanol solution but maternal separation took place for 3 hours a day from P2 - P14 in a similar manner as in the present study (Alberry and Singh, 2016). This suggests that the interaction between prenatal-ethanol exposure and early-life stress on exploratory behaviour may be further dependent on species and ethanol exposure paradigm.

In contrast, during the familiarization trial of the NOT, ethanol-exposed rats (EtOH- and EtOH+MS-rats) spent less time investigating the 2 identical objects than the saccharin-only rats (control and MS-rats). This result demonstrated differential effects of prenatal-ethanol exposure and early-life stress on exploratory behaviour compared to the first day of behavioural testing. The NOT protocol used involved habituating the rats with the novel object arena and behavioural testing room for 10 minutes, 24 hours prior to the familiarization trial (2 identical objects) in order to prevent environmental exploration interfering with object interaction (Bevins and Besheer, 2006). However, in the present study, ethanol-exposed rats (EtOH- and EtOH+MS-rats) appeared to have been exploring the environment rather than investigating the novel objects during the familiarization trial. Ethanol-exposed rats were not stationary during this time since the distance travelled between experimental groups was similar.

There was no difference in locomotor activity between experimental groups in subsequent behavioural tests such as during the familiarization and test trial of the NOT and further during the EPM and OFT on the 2nd and 4th day of behavioural testing respectively (locomotor activity was not measured on the 3rd day). Previous studies have shown that prenatal-ethanol exposed (Brocardo et al., 2012; Brys et al., 2014) and maternally separated rats (Shalev and Kafkafi, 2002; Dimatelis et al., 2012) had similar levels of locomotor activity to that of control rats. In addition, C57BL/6J mice exposed to the combination of prenatal-ethanol and maternal separation (3 hours/day), also showed no difference in the distance travelled during the OFT (Alberry and Singh, 2016). Further, when ethanol was administered during the early-postnatal period (P4 - P9, 5.25 mg/kg/day), the distance travelled by adolescent SD rats decreased per day (P30 - P33) (Monk et al., 2012). More so, within each behavioural test, the distance travelled per minute (time-bin) decreased over time in the present study. Taken together these

results indicate a decreased response to novelty and eliminates differences in activity as a confounding factor in behavioural tests of learning and memory, anxiety- and depression-like behaviour.

However, these results also indicate that none of the behavioural groups demonstrated hyperactive (or hypoactive) behaviour. Prenatal-ethanol exposure (4-6 g/kg/day 25 % ethanol) has previously-been shown to induce hyperactivity in 5-week old SD rats in the OFT (Kim *et al*., 2013) whereas maternal separation stress (3 hours/day, P2 - P14) has been shown to decrease activity in the open field in adult Long-Evans rats (Lippmann et al., 2007). In the present study, the open field test took place on the 4th day of behavioural testing and therefore differences in activity levels could have been masked by the decreased innate response to novelty. However, the increased distance travelled in the novel object arena on day one of behavioural testing may also be interpreted as increased hyperactivity in response to a novel environment in EtOH- and MS-rats.

During the NOT, all rats spent more time investigating the novel object versus the familiar object. However, after the data were corrected for the object preference identified during the familiarization trial all experimental groups spent a similar amount of time with each object. This indicates that there were no differences in capacity for learning and memory between experimental groups. This is in agreement with a previous study in male which C57BL6/J mice exposed to prenatal-ethanol (*ad libitum* access to 5 % ethanol in water throughout gestation) and control mice did not distinguish between the novel and familiar object (Fidalgo et al., 2017). Further, in previous studies in which ethanol was administered during the early-postnatal period, juvenile Long-Evans rats exposed to early-postnatal ethanol (5.25 g/kg/day of 23.93 % ethanol, P7 - P9) did not show learning and memory impairments in the NOT (Jablonski et al., 2013) but adult Long-Evans rats exposed to early-postnatal ethanol (5 g/kg/day, P4 - P9) showed impaired object recognition memory in the NOT by spending less time investigating the novel object compared to controls (MacIlvane et al., 2016). MacIlvane *et al*. (2016) employed a different protocol to the one used in the present study which consisted of a 20-minute delay instead of a 1-hour delay as in the present method.

Likewise, adult Wistar rats exposed to 3 hours/day of maternal separation stress during the first 2 postnatal weeks showed impaired object recognition in the NOT compared to control rats (Hulshof et al., 2011). Non-maternally separated Wistar rats spent more time with the novel object whereas the maternally separated rats spent an equal time with both objects (Hulshof et

al., 2011). However, the NOT protocol used by Hulshof *et al*. (2011) differed from the present study since all 3 trials (habituation, familiarization and test trial) occurred on the same day and were separated by a 5-minute interval. In addition, adult Wistar maternally separated rats (3 hours/day, P2 - P21) showed impaired performance in learning and memory in the NOT with a protocol that encompassed a 30-minute habituation trial followed by a 5-minute familiarization trial with 2 identical objects 24 hours later and then a 5-minute test trial after a 1-hour delay (Aisa *et al*., 2007). Therefore, the differences in results may be due to the different time-intervals between and duration of the habituation, familiarization and novel object test trials. Specifically, the retention interval (time between the familiarization trial and test trial), was 1 hour in this protocol. Hence, the results demonstrate the effects of prenatal-ethanol and maternal separation stress on short-term object recognition memory. Increasing this interval may reveal an effect on long-term memory (Cohen and Stackman, 2015). In addition to no overt learning and memory impairments observed in EtOH- and MS-rats, there was no evidence for impaired object recognition in rats exposed to both prenatal-ethanol and maternal-separation stress. However, excitotoxic lesions in the DH of naive mice did not impair object recognition memory when the memory load was low (number of novel objects = 1) whereas in the case of high memory load (number of novel objects = 4 - 6) object recognition memory was significantly impaired (Sannino et al., 2012). Therefore, increasing the complexity of the NOT may expose learning and memory deficits induced by prenatal-ethanol exposure and/or maternal separation stress. Further, the NOT relies heavily on spontaneous exploratory behaviour which can be highly variable (Antunes and Biala, 2012; Lyon et al., 2012) and, as shown in this study, altered by prenatal-ethanol and/or early-life stress. Therefore, a word of caution is needed when reporting prenatal-ethanol- and/or maternal separation stress-induced cognitive deficits in the NOT.

On day 3 of behavioural testing, MS-, EtOH- and EtOH+MS-rats exhibited a greater number and duration of vocalizations than control rats. Ultrasonic vocalizations at 22 kHz are associated with a negative emotional state (Portfors, 2007). Therefore, a supporting result is that the control rats tended to take longer to generate negative emotional state-related 22 kHz vocalizations. The recording of ultrasonic vocalizations in adult rats exposed to prenatal-ethanol is largely unexplored in the literature. However, ultrasonic vocalizations recorded from juvenile (P14) Long-Evans rats exposed to prenatal-ethanol throughout gestation (11.5 - 35% ethanol derived liquid-diet) demonstrated a greater latency to emit and decreased number of

isolation-induced ultrasonic vocalizations of 40 kHz (Wellmann et al., 2015). This is in agreement with the present study since ultrasonic vocalizations of 40 kHz are associated with positive-affective state (Portfors, 2007). Conversely, adolescent (P28 and P42) Long-Evans rats exposed to a 11.5 - 35 % ethanol-calorie derived liquid-diet throughout gestation did not differ in latency or number of 22 kHz or 50 kHz ultrasonic vocalizations compared to controls rats recorded during play behaviour (Waddell et al., 2016). To our knowledge this is the first study to demonstrate increased number and duration of 22 kHz ultrasonic vocalizations in adult SD rats exposed to prenatal-ethanol.

In addition, our results are in agreement with previous studies in which maternally separated rats (3 hours/day, P2 - P14) have previously exhibited longer and more ultrasonic vocalizations of 22 kHz (Dimatelis et al., 2012, 2015). Further, male Long-Evans maternally separated rats emitted more 20 - 28 kHz ultrasonic vocalizations in response to a loud auditory startle stimulus compared to control rats (Kalinichev et al., 2002) indicating a greater negative affective response. However, the additional maternal separation stress did not reduce the prenatal-ethanol-induced increase in 22 kHz ultrasonic vocalizations as with exploratory behaviour. Twenty-two kilohertz vocalizations have not been measured in adult rats exposed to the combination of prenatal-ethanol and maternal separation stress therefore, this is an additional novel demonstration.

The negative affect state indicated by longer and more ultrasonic vocalizations of 22 kHz was not observed in subsequent behavioural tests for anxiety- and depression-like behaviour. During the recording of ultrasonic vocalizations in the present study, rat pairs were able to visualize each other through the Plexiglas cylinders and therefore, increased 22 kHz vocalizations may be an indication of increased *communication* of negative affective state whereas the EPM, OFT and FST make use of rodents innate response to open spaces and inescapable conditions (Brudzynski, 2005; Portfors, 2007; Walf and Frye, 2007; Slattery and Cryan, 2012; Wöhr and Schwarting, 2013). Ultrasonic vocalizations were recorded on the 3rd day of behavioural testing and the EPM, OFT and FST took place on the 4th, 5th and 6th day of behavioural testing. Therefore, behaviour in these subsequent tasks may have been influenced by previous behavioural tests and handling, thereby masking/reducing anxiety- and depression-like behaviour (Blokland et al., 2012; Bohacek et al., 2015; Deutsch-Feldman et al., 2015).

EtOH- and MS-rats did not show anxiety-like behaviour in the EPM or OFT. All groups spent a similar amount of time in the open arms of the EPM. However, EtOH-rats spent more time

in the inner zone of the OFT compared to controls which suggests an induced anxiolytic effect. This was not the expected result since prenatal-ethanol and maternal separation stress have previously been shown to induce anxiety-like behaviour in the EPM and OFT (Lee et al., 2007; Makena et al., 2012). The EPM and OFT took place consecutively on the 4th day of behavioural testing, therefore behavioural results may have been influenced by the handling and behavioural testing on days 1-3. These include the NOT and the recording of ultrasonic vocalizations. In addition, contrary to previous studies in which maternal separation stress has been shown to induce depression-like behaviour (Lee *et al.*, 2007), maternally-separated rats (MS- and EtOH+MS-) spent more time swimming during the FST than nMS rats, which is not indicative of despair-like behaviour. However, behavioural results induced by maternal separation stress are variable. Wistar rats exposed to 3 hours per day of maternal separation stress during the first 2 postnatal weeks did not show changes in anxiety-like and exploratory behaviour in adulthood (Hulshof et al., 2011) and adult maternally separated rats have been shown to have spent more time in the open arms of the EPM compared to control rats (Dimatelis et al., 2012). Further, SD female maternally separated (3 hours of daily-repeated maternal separation from P2 - P14) rats have been shown to be resistant to developing the maternal separation-induced depression-like phenotype (Dimatelis et al., 2016). Further, as mentioned above, rats were tested in a battery of behavioural tests and therefore results could have been influenced by handling and multiple testing (Blokland et al., 2012; Bohacek et al., 2015; Deutsch-Feldman et al., 2015). For this reason, Aisa *et al.* (2007) proposed using a different cohort of animals for each behavioural test. However, we used the maximum number of rats available to us which did not allow for multiple cohorts.

Our results add to the varying maternal separation-induced behavioural changes in anxiety- and depression-like. Importantly, the combination of prenatal-ethanol exposure and maternal separation stress did not enhance (or reduce) the behaviour of EtOH- and MS-rats in the EPM, OFT and FST, as hypothesized, however again indicating the specificity of the reducing effect of subsequent maternal separation stress after prenatal-ethanol exposure on exploratory behaviour.

In summary, EtOH-rats showed significant deficits in weight gain throughout development, increased exploratory activity in a novel environment and a heightened negative emotional state which are in line with the phenotypic characterizations of animal models of FASD. Additionally, MS-rats showed a negative emotional state during recording of 22 kHz ultrasonic

vocalizations. However, MS-rats did not fully display the depressive-phenotype as shown by increased exploratory behaviour and decreased despair in the FST. The behavioural inconsistencies may be due to previous behavioural tests influencing the results of subsequent behaviour since rats underwent behavioural testing in a of battery tests. In order to avoid this, some studies used a different cohort of animals for each behavioural test (Aisa et al., 2007) or only used one behavioural test in the study (Desbonnet et al., 2010). In addition, maternal separation is thought to sensitize the brain to stressful events and hence trigger the onset of anxiety- and depression-like behaviors, therefore additional chronic stress in adulthood can induce depression-like behaviour in the FST whereas maternal separation alone is insufficient (Marais et al., 2008). However, the effects of maternal separation are non-linear and in some instances it has been thought that early-life stress may optimally program the brain to adapt to stressful events in adulthood (Oomen et al., 2010).

The combination of prenatal-ethanol exposure and early-life stress did not enhance the behaviour induced by either developmental insult. Instead, EtOH+MS-rats tended to weigh more than EtOH-rats and showed reduced exploratory behaviour compared to EtOH- and MS-rats. These results indicate that additional maternal separation stress may reduce specific prenatal-ethanol-induced changes in body weight and behaviour.

Western blot analysis was performed using the PFC and DH of both male *and female* rats that *did not undergo* behavioural testing. This is a significant advantage since previous studies have suggested that behavioural testing and handling may alter protein changes in the brain (Bohacek et al., 2015; Deutsch-Feldman et al., 2015). Therefore in the present study we present protein changes induced primarily by the effects of prenatal-ethanol exposure, early-life stress or the combination of both insults without the added influence of prior repeated behavioural tests.

A consistent finding in this study was a significant interaction between prenatal-ethanol exposure and early-life stress, in the form of maternal separation (3 hours/day P2 - P14) on the levels of P-ERK1/2 to ERK1/2 in male and female rats in both the PFC and DH. Maternal separation stress increased the P-ERK1/2 to ERK1/2 ratio in saccharin-rats whereas maternal separation stress decreased the P-ERK1/2 to ERK1/2 ratio in rats exposed to prenatal-ethanol. Further, the P-ERK1/2 to ERK1/2 ratio was increased in the PFC of male EtOH-rats compared

to control rats. This result tended to be significant in the PFC and DH of female EtOH-rats. These results indicate increased activity of P-ERK1/2 signalling in both male and female adult rats exposed to prenatal-ethanol or maternal separation stress and a reduction in P-ERK 1/2 signalling in rats exposed to both developmental insults. These results also demonstrate that the effects of prenatal-ethanol and maternal separation as well as the combination of both insults on ERK1/2 activity are common between brain regions and male and female rats.

The long-term molecular effects of prenatal-ethanol on the ERK1/2 signalling are largely unknown and relatively unexplored in the literature. In addition, when ethanol was administered during the early-postnatal period (2 x 2.5 g/kg, on P7), C57BL/6J mice sacrificed within 24 hours of ethanol exposure, had unchanged levels of total ERK1/2 and impaired phosphorylation of ERK1/2 in cortical cytosolic extracts and the hippocampus compared to control mice (Subbanna et al., 2013). However, a long-term study in which ERK1 and ERK2 were analyzed separately in the dentate gyrus of adult C57BL/6J mice exposed to prenatal-ethanol (5 % ethanol sweetened with 0.066 % saccharin) demonstrated that levels of P-ERK2 relative to total ERK2 were decreased compared to control rats (Samudio-Ruiz et al., 2009). This result does not agree with the present study and this may be due to the separate analysis of ERK1 and ERK2.

In the present study ethanol appeared to affect the PFC and DH in a similar manner by increasing the levels of P-ERK1/2 to ERK1/2 compared to controls in both brain regions, whereas we have previously observed opposing effects of ethanol exposure when ethanol was administered during the early-postnatal period (*Chapter 2*). In Chapter 2, early-postnatal ethanol exposure decreased P-ERK1/2 relative to ERK1/2 in the PFC and increased the ratio in the DH of adolescent rats. This differential effect of ethanol exposure on ERK1/2 phosphorylation may be due to the different stages of development and periods of ethanol exposure as well as the age at which rats were sacrificed. An additional reason for the observed differential effects of ethanol exposure on the levels of P-ERK1/2 in previous studies may be attributed to the time of day at which animals were sacrificed. Lower levels of P-ERK1/2 were observed in SD rats sacrificed in the morning (9 am) compared to those sacrificed in the evening (6 pm) (Musazzi et al., 2014). In the present study rats were sacrificed in the morning, therefore control rats may have had reduced levels of P-ERK1/2 whereas prenatal-ethanol exposure and maternal separation may have impaired the circadian-rhythm regulation of ERK1/2 phosphorylation.

Maternal separation stress has previously been shown to influence P-ERK1/2 signalling in the brain. However, our results do not agree with previous studies in which SD rats exposed to 3 hours/day of maternal separation stress from P2 - P14 showed no difference in levels of P-ERK1/2 to ERK1/2 in the hippocampus (Makena et al., 2012) and adult (P100) female rats had decreased levels of P-ERK1/2 to ERK1/2 in the VH rats compared to controls (Dimatelis et al., 2016). These opposing results may be due to the affects of behavioural testing in the OFT, EPM and NOT (Makena et al., 2012) and FST (Dimatelis et al., 2016) prior to sacrifice in the previous studies. Whereas in the present study, Western blot analysis was performed on brain tissue obtained from naïve-rats and therefore increased levels of P-ERK1/2 relative to ERK1/2 in MS-rats was not a result of repeated behavioural testing or handling. However, prolonged maternal separation stress (6 hours/day from P2 - P21) resulted in decreased phosphorylation of ERK1/2 on P7 and a tendency for increased levels of P-ERK1/2 in the hippocampus of naïve-rats on P21 (Ohta et al., 2017). This result indicates transient phosphorylation of ERK1/2 that depends on the age at analysis.

Importantly, increased P-ERK1/2 activity in naïve MS- and EtOH-rats mirrored the increase in exploratory behaviour observed in MS- and EtOH-behavioural rats. Similarly, maternal separation stress subsequent to prenatal-ethanol exposure reduced P-ERK1/2 activity and exploratory behaviour in adult naïve-rats and behavioural MS- and EtOH-rats (both male and female) respectively. This robust result may implicate P-ERK1/2 signalling in exploratory behaviour in response to a novel environment.

Downstream of P-ERK1/2 signalling, in both the PFC and DH of male and female rats, the levels of P-CREB relative to CREB did not mirror the observed interaction of prenatal-ethanol exposure and maternal separation stress on P-ERK1/2 signalling. However, in agreement with previous studies the levels of total CREB remained unchanged by prenatal-ethanol exposure and maternal separation stress (Lippmann et al., 2007; Bian et al., 2015). Further, the combination of prenatal-ethanol exposure and maternal separation stress did not alter the levels of P-CREB, CREB or the ratio of P-CREB to CREB. However, ethanol exposure has been shown to decrease the capacity of CREB to bind to DNA (Soares-Simi et al., 2013). Therefore, even though we did not observe prenatal ethanol-induced changes in CREB activation, CREB-mediated transcription may still be impaired due to inefficient binding of CREB to DNA. In addition, CREB-mediated transcription depends on the co-operation of many upstream

signalling pathways and co-factors (Medina, 2011; Marsden, 2013) which may be susceptible to developmental insults.

The GSK3β signalling pathway also influences CREB activity (Kaidanovich-Beilin and Woodgett, 2011; Bradley et al., 2012; Beurel et al., 2015). Therefore, the expected changes in CREB activity as a consequence of maternal separation stress- and prenatal-ethanol-induced changes in ERK1/2-signalling may have been compensated for or masked by GSK3β-signalling. Male rats exposed to prenatal-ethanol had increased levels of P-GSK3β in the PFC compared to saccharin-only rats whereas female rats exposed to prenatal-ethanol had increased levels of P-GSK3β to total GSK3β in the PFC compared to saccharin-only rats. This indicates that prenatal-ethanol exposure induced changes that lead to *reduced activity* (Polter et al., 2010) of GSK3β signalling in the PFC whereas prenatal-ethanol exposure did not alter GSK3β signalling in the DH. Total levels of GSK3β, were unchanged by prenatal-ethanol which does not agree with a previous study, in which C57BL/6J mice (P40 - P50) exposed to a 10% ethanol solution sweetened with 0.066% saccharin for 4 hours per day throughout gestation had decreased total levels of GSK3β and increased GSK3β phosphorylation (serine 9) in the hippocampus (Goggin et al., 2014). These differences may be due to the different species, or ethanol exposure paradigm used as well as the age of the animal at the time of tissue analysis. In contrast to previous studies, maternal separation stress did not alter levels of P-GSK3β or total GSK3β in the present study. For instance, C57BL/6N mice exposed to 3 hours/day of maternal separation stress (P2 - P21) had increased levels of total GSK3β and less P-GSK3β relative to GSK3β in the hippocampus compared to non-separated mice (Bian et al., 2015). Increased levels of GSK3β and decreased levels of P-GSK3β (*inactive*) are associated with depression-like behaviour (Marsden, 2013). This is in agreement with the observed behavioural results since male behavioural MS-rats did not exhibit depression-like behaviour in the FST. In addition, the combination of prenatal-ethanol exposure did not enhance or reduce GSK3βsignalling in the PFC or DH in adult male and female rats.

Levels of the synaptosomal marker, synaptophysin, were decreased in the PFC of female saccharin-rats exposed to maternal separation whereas levels of synaptophysin were increased in the PFC of female ethanol-rats exposed to maternal separation. Interestingly, this interaction is in the opposite direction to the effects of prenatal-ethanol exposure and maternal separation stress on P-ERK1/2 activity and exploratory behaviour. Previously, synaptophysin knockout

mice were shown to be more exploratory than the wild type control mice (Schmitt et al., 2009). This finding is in agreement with the present study since MS- and EtOH-rats tended to have less synaptophysin and were more exploratory on day 1 of behavioural testing compared to control and EtOH+MS-rats. However, decreased synaptophysin was observed in naïve *female* MS- and EtOH-rats whereas the increased exploratory activity was observed in *male behavioural* MS- and EtOH-rats. Further, there were no differences in synaptophysin levels observed in male naïve-rats. Therefore, this result must be interpreted with caution.

In *Chapter 3* and *Chapter 4*, ethanol exposure during the third trimester equivalent developmental stage (early-postnatal ethanol exposure) decreased the capacity for energy production in the VH and DH and increased the capacity in the PFC of adolescent rats compared to controls. Specifically, proteomic analysis revealed that naïve adolescent rats exposed to early-postnatal ethanol exposure had less ATP synthase (mitochondrial subunits g, alpha, beta and gamma) than control rats in the DH (*Chapter 4*). However, in the present study the levels of ATP5A (ATP synthase alpha chain) were unchanged by maternal separation, prenatal-ethanol exposure and the combination of both developmental insults in the PFC and DH of both male and female naïve rats. ATP synthase has previously been shown to be decreased in foetal mice brains exposed to prenatal-ethanol (Xu et al., 2005; Sari et al., 2010b) which highlighted the short-term effects of gestational ethanol exposure on the capacity for energy production. Further, maternal separation has been shown to decrease the capacity for energy production in the PFC of adult SD rats (Dimatelis et al., 2013). In contrast, the present study suggests no prenatal-ethanol or early-life stress-induced long-term changes in energy production in adult rats. However, in the present study, ATP5A represents the alpha chain of the enzyme and hence there may be deficits in other subunits, as suggested by observations in *Chapter 4*, but that was beyond the scope of this chapter.

In this chapter adult rats exposed to prenatal-ethanol showed significant deficits in weight gain throughout development, increased exploratory activity in a novel environment and a heightened negative emotional state which are in line with the phenotypic characterizations of FASD. In addition, maternally separated rats demonstrated a negative affective state during the recording of ultrasonic vocalizations which is characteristic of a depressive-phenotype. Interestingly, additional maternal separation stress reduced prenatal-ethanol-induced changes

in weight and exploratory activity therefore highlighting a significant interaction between prenatal-ethanol exposure and early-life stress. In parallel with behavioural results the combination of prenatal-ethanol exposure and maternal separation stress reduced the activity of the P-ERK1/2-signalling pathway to levels similar to that of control rats in both the PFC and DH of male and female rats. However, this interaction was not observed in GSK3β signalling as well as downstream of these signalling kinases as shown by levels of P-CREB and CREB.

To our knowledge, this is the first study to investigate components of the ERK- and GSK3β-signalling cascades in adult rats exposed to prenatal-ethanol and subsequent early-life stress in the form of maternal separation (3 hours/day, P2 - P14). Our results highlight a significant interaction between prenatal-ethanol exposure and maternal separation stress on exploratory behaviour in response to a novel environment and P-ERK-signalling in the PFC and DH of adult male and female SD rats. This interaction demonstrates the need to account for early-life stress in animal models of FASD. However, the various behavioural and neurochemical changes in the brain induced by prenatal-ethanol exposure and maternal separation described in the literature and as shown in the present study highlights the difficulty in developing an animal of FASD that encompasses early-life stress. Moreover, this study shows the importance of creating a robust animal model of FASD in which the possible effect of childhood adversities are accounted for in order to investigate prenatal-ethanol exposure-induced changes in the brain and how these changes relate to the cognitive and psychological deficits observed in FASD.

CHAPTER 6: THE EFFECTS OF PRENATAL-ETHANOL EXPOSURE COUPLED WITH MATERNAL SEPARATION STRESS ON THE ADULT RAT BRAIN: A PROTEOMICS STUDY

INTRODUCTION

Exposure to alcohol *in utero* induces persistent behavioural abnormalities including cognitive deficits and psychological disorders such as anxiety and depression (O'Connor and Paley, 2009; Kable et al., 2016) which suggests dysfunction in the PFC and DH (Broadbent et al., 2004; Khoury et al., 2015). However, the underlying neurochemistry is still unknown and there are currently no treatments for FASD. Therefore, the neurobehavioural deficits and FASD-associated psychological disorders may persist into adulthood (Famy et al., 1998; Streissguth et al., 2004; Rangmar et al., 2015b)

In addition to *in utero* alcohol exposure, children born with FASD may face further adverse childhood experiences when living with alcohol-abusing parent/s (Anda et al., 2002) such as child abuse and neglect. It has been shown that exposure to childhood adversities *alone* can lead to the development of psychological disorders and cognitive deficits later in adulthood (Mullen et al., 1996; Heim and Nemeroff, 2001; Carr et al., 2013; Grasso et al., 2013). Therefore, in conjunction with the timing, quantity and pattern of prenatal-alcohol exposure, early-life environmental stress may contribute to the development of FASD. However, the interaction between *in utero* alcohol exposure and early-life stress is largely unexplored in the literature because childhood adversity is a factor which has not been included in the design of animal models of FASD.

In *Chapter 5*, we described the result of prenatal-ethanol exposure with coupled a well characterized model of early life-stress, maternal separation stress (3 hours/day, P2 - P14) (Daniels et al., 2004; Ladd et al., 2004). Maternal separation stress reduced prenatal-ethanol-induced changes in weight and exploratory activity. Further, in parallel with behavioural results the combination of prenatal-ethanol exposure and maternal separation stress reduced the activity of the P-ERK1/2-signalling pathway to levels similar to that of control rats. This result highlighted a significant interaction between prenatal-ethanol exposure and maternal separation stress on behaviour and the adult rat brain.

The present study further investigated the effects of prenatal-ethanol exposure coupled with maternal separation stress by using high throughput proteomic profiling techniques, iTRAQ labeling and LC-MS, to simultaneously identify and quantify protein expression in the PFC and DH of adult MS-, EtOH- and EtOH+MS-rats. Hence, the observed prenatal-ethanol and early-life stress-induced changes in proteins related to cellular processes involved in energy metabolism, neurotransmitter signalling, redox regulation, protein metabolism and cytoskeletal structure may provide valuable insight into the long-term molecular changes in neuronal cells involved in FASD and the associated psychological deficits.

METHODS

ANIMALS

As described in *Chapter 5* (p.130)

PRENATA-ETHANOL EXPOSURE

As described in *Chapter 5* (p.130)

MATERNAL SEPARATION

As described in *Chapter 5* (p.131)

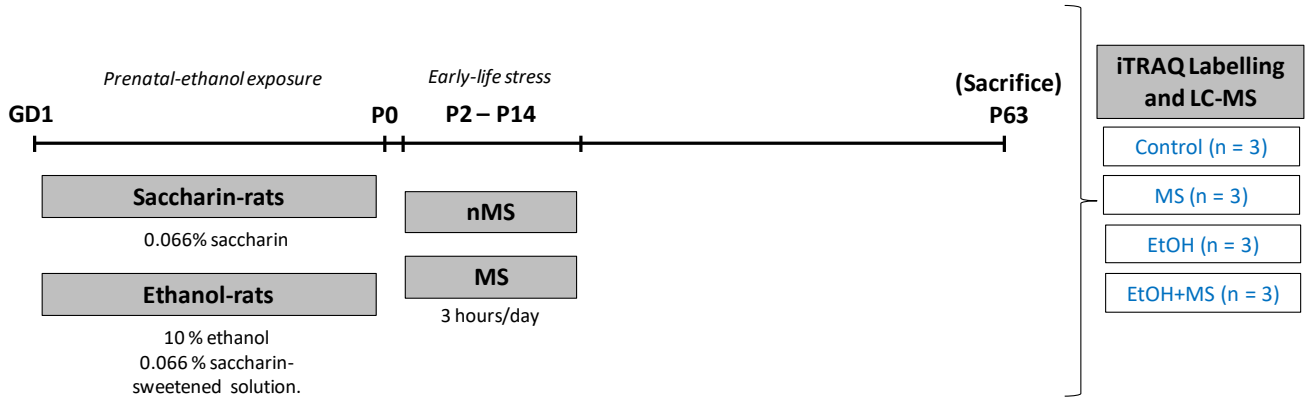

Figure 6.1: Experimental timeline

Ethanol-rats were exposed to saccharin-sweetened ethanol throughout gestation (gestational day 1 (GD1) to the date of birth, postnatal day 0 (P0)) whereas saccharin-rats were exposed to saccharin only. Whole-litters were exposed to maternal separation (MS) from P2 - P14 for 3 hours/day while control litters were left undisturbed (nMS). This resulted in 4 experimental groups: **Control**, (sacc + nMS); **MS**, (sacc + MS); **EtOH**, (ethanol + nMS); **EtOH + MS** (ethanol + MS). Rats were sacrificed on P63. Three rats per group were used in iTRAQ and LC-MS analysis of the PFC and DH. The PFC and DH were analyzed separately.

SACRIFICE

As described in *Chapter 5* (p.138). The PFC and DH of *naïve*, *male* control, MS-, EtOH- and EtOH+MS-rats were stored in liquid nitrogen until use in iTRAQ labeling and LC-MS.

PROTEOMICS

Three samples from each experimental group were weighed and pooled together accordingly (**PFC**: control, n = 3; MS, n = 3; EtOH, n = 3; EtOH+MS, n = 3; **DH**: control, n = 3; MS, n = 3; EtOH, n = 3; EtOH+MS, n = 3). Samples were then sonicated in triethylammonium bicarbonate (TEAB) and Na_2CO_3 buffer (1 M TEAB and 20 mM Na_2CO_3) with added protease inhibitor cocktail (Halt™ Protease & Phosphatase Inhibitor Cocktail, ThermoScientific). Following sonication, samples were incubated on ice for 1 hour and then centrifuged for 30 minutes at 17 200 *g* at 4 °C. The supernatant was removed and centrifuged a second time as before. Following the second 30 minutes in the centrifuge the supernatant was removed and thoroughly vortexed. Samples were then transported on ice to the Central Analytical Facility, Tygerberg Medical Campus, University of Stellenbosch and handed over to Dr Maré Vlok who performed the procedures described below.

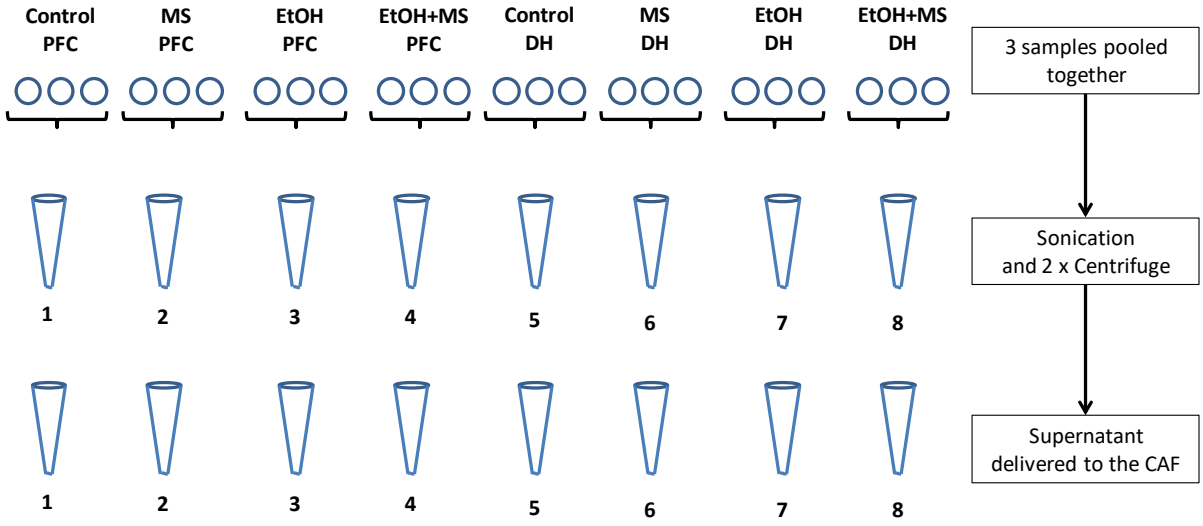

Figure 6.2: Sample preparation

The PFC and DH were analyzed separately. Three samples from each experimental group were pooled together. Pooled samples were sonicated and centrifuged twice (17 200 *g*, 4°C). The supernatant was then delivered the Central Analytics Facility (CAF) for iTRAQ labeling and LC-MS.

The received samples were precipitated overnight with ice-cold acetone (1:5 sample to acetone ratio). Precipitated proteins were pelleted by centrifugation at 12 000 *g* for 10 minutes. The supernatant was removed and the remaining pellet was dissolved in 100 mM TEAB, 4 M guanidine-HCL and 0.1 % octylgluco-mano-pyranoside, prior to protein concentration determination.

IN-SOLUTION DIGEST

Samples were reduced by adding 50 mM triscarboxyethyl phosphine (TCEP; Fluka) in 100 mM TEAB for 60 minutes at 37 °C. Cysteine residues were blocked by adding 200 mM methane methylthiosulphonate (MMTS; Sigma) in 100 mM TEAB for 30 minutes. Samples were then diluted with 100 mM TEAB. Proteins were digested by adding 10 µl trypsin solution (1 µg/µl) (Promega) overnight at 37 °C.

ITRAQ LABELLING

The digested samples were evaporated to dryness and re-suspended in 20 µl of 300 mM TEAB. iTRAQ labels were dissolved in 70 µl 2-propanol before being combined with the respective sample. The labeling reaction proceeded for 2 hours before excess labels were hydrolysed by the addition of 100 µl analytical grade water. The samples were then evaporated to dryness.

FIRST DIMENSION CHROMATOGRAPHY

First dimension chromatography was performed using batch-wise elution from an in-house manufactured C18 SPE device. The sample was dissolved in 2 % acetonitrile (ACN) in 100 mM TEAB (pH 8) and eluted with 5 %, 7.5 %, 10 %, 12.5 %, 15 %, 20 %, 25 %, 30 %, 40 % and 50 % ACN in 100 mM TEAB. The fractions were evaporated to dryness prior to LC- MS analysis.

LIQUID CHROMATOGRAPHY

Liquid chromatography was performed on a Thermo Scientific Ultimate 3000 RSLC equipped with a C18 trap column (2 cm x 100 µm) and an in-house manufactured C18 analytical column (35 cm x 75 µm) (Luna C18, 5µm; Phenomenex). The solvents employed were the loading solvent (2 % ACN: 0.1 % FA in analytical grade water), Solvent A (2 % ACN: 0.1% FA in analytical grade water) and Solvent B (100 % ACN in analytical grade water). The samples were loaded onto the trap column using the loading solvent at a flow rate of 5 µL/min from a temperature controlled (7 °C) auto-sampler. Loading was performed for 10 minutes before the sample was eluted onto the analytical column. The flow rate was set to 350 nL/minute and the was gradient generated as follows: 2 % solvent A for 5 minutes; 2 % - 35 % solvent B from 5

- 70 minutes using Chromeleon non-linear gradient 7 and 35 % - 50 % from 70 - 75 minutes. Thereafter the column was washed for 10 minutes with 80 % solvent B followed by equilibration. Chromatography was performed at 50 °C and the outflow delivered to the mass spectrometer through a stainless steel nano-bore emitter.

MASS SPECTROMETRY

Mass spectrometry was performed using a Thermo Scientific Fusion mass spectrometer equipped with a Nanospray Flex ionization source. The sample was introduced through a stainless steel emitter. Data was collected in positive mode with spray voltage set to 2.1 kV and ion transfer capillary set to 275 °C. Spectra were internally calibrated using polysiloxane ions at *m/z* = 445.12 and 371.10024. MS^1 scans were performed using the orbitrap detector set at 12 000 resolution over the scan range 350 - 1650 with AGC target at 2E5 and maximum injection time of 40 milliseconds. Data were acquired in profile mode. MS^2 acquisitions were performed using monoisotopic precursor selection for ion with charges +2 - +6 with error tolerance set to ±10 ppm. Precursor ions were excluded from fragmentation once for a period of 30 seconds. Precursor ions were selected for fragmentation in HCD mode using the quadrupole mass analyzer with HCD energy set ± 50 % from 32.5 %. Fragment ions were detected in the orbitrap mass analyzer at 60 000 resolution. The AGC target was set to 1E4 and the maximum injection time to 45 milliseconds. The data were acquired in centroid mode.

DATA ANALYSIS

The raw files generated by the mass spectrometers were imported into Proteome Discoverer version 1.4 (Thermo Scientific) and processed using the SequestHT algorithm. Data analysis was structured to allow for iTRAQ 8-plex on N-terminal and K as well methylthio as a fixed modification. Deamidation (NQ) and oxidation (M) were set as variable modifications. Peptide validation was performed using the percolator node set to search against a decoy database with a strict FDR of 1 %. Database interrogation was performed against the Uniprot *R. rattus* database (2015 edition) with semi-tryptic cleavage allowing for 2 missed cleavages. Quantitation was performed in Scaffold Q+ (Proteome Software) and the data imported validated using the X!Tandem algorithm included in Scaffold Q+.

A target protein was considered identified if at least two such unique peptide matches were apparent for the protein. Data were represented as a fold change relative to the control group.

A fold change greater than 1.2 identified differentially expressed proteins (Seshi, 2006; Unwin et al., 2006; Duthie et al., 2007; Ting et al., 2009; Williamson et al., 2016). A fold change greater than 2 identified a significant change (Ting et al., 2009; Yang et al., 2013; Gunton et al., 2017) in protein levels in MS-, EtOH- and EtOH+MS-rat tissue relative to control rats. Differentially expressed proteins were organized into functional categories. In addition, significantly changed proteins (> 2-fold change) were collectively analyzed using STRING (https://string-db.org/) to identify functional protein-protein interaction networks (Szklarczyk et al., 2015).

iTRAQ and LC-MS identified 1 104 proteins and generated 6 proteomic profiles. These were the proteomic profiles of **MS**-, **EtOH**- and **EtOH+MS**-rats relative to control rats in both the **PFC** and **DH.**

PROTEINS ALTERED BY PRENATAL-ETHANOL EXPOSURE AND/OR MATERNAL SEPARATION IN PREFRONTAL CORTEX

Of the 1 104 proteins identified by iTRAQ and LC-MS, 140 proteins were altered in the PFC of MS-, EtOH- and EtOH+MS-rats by a fold change greater than 1.2 (20 %). Forty-six of these proteins were altered in MS-rats, 19 proteins were altered in EtOH-rats and 117 were altered in the PFC of EtOH+MS-rats (**Figure 6.3**).

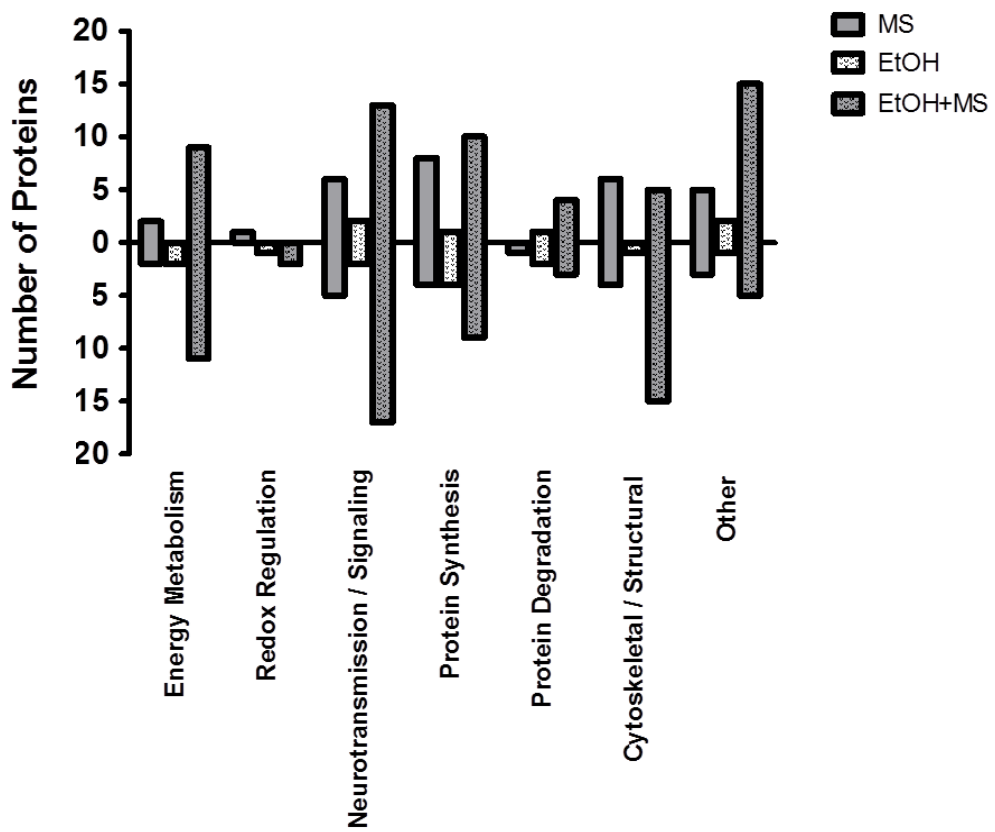

Figure 6.3: Number of differentially expressed (>1.2-fold △) proteins in the *prefrontal cortex* of MS-, EtOH- and EtOH+MS-rats compared to control rats.

Categorically organized differentially expressed proteins in the PFC of MS-, EtOH- and EtOH+MS-rats compared to control rats.

In the PFC of MS-rats there were no proteins altered by maternal separation stress that differed by a fold change greater than 2. However, 46 proteins differed by more than 20% in the PFC of MS-rats compared to control rats (**Table 6.1**). Energy-related proteins *phosphoenolpyruvate carboxykinase* and *NADH ubiquinone oxidoreductase subunit 10 (NDUFB10)* were increased while, *pyruvate kinase* was decreased in the PFC of MS-rats relative to controls. The redox-related protein *microsomal glutathione S-transferase 3* was increased in the PFC of MS-rats. Signalling-related proteins *β-arrestin-1* and *neuroplastin* were decreased in the PFC of MS-rats. Further, *prohibitin* and *eukaryotic translation initiation factor 3 subunit B* were increased while *eukaryotic initiation factor 4A-II* and *histone H4* were decreased in the PFC of MS-rats relative to controls. Structural proteins such as *isoform 3 of dynamin-like protein (mitochondrial)* was increased while *C-fos induced growth factor (isoform CRA_b), isoform 2 of dynamin-2* and *isoform 2 of myelin basic protein* were decreased in the PFC of MS-rats.

In the PFC of EtOH-rats, 4 proteins differed by a fold change greater than 2 relative to control rats (**Figure 6.4**). These included *ring finger protein 217, transcription initiation factor TFIID subunit 9B* and *xanthine dehydrogenase/oxidase* which were decreased and *immunoglobulin-like domain-containing receptor 2* which was increased (**Figure 6.4**). Network analysis of these 2 proteins did not identify any significant interactions (**Appendix A6.1**). Further, 19 proteins were altered by prenatal-ethanol exposure in the PFC of EtOH-rats by more than 20% (**Table 6.2**). For example, *NADH ubiquinone oxidoreductase subunit 7 (NDUFA7), β-arrestin-1, c-fos induced growth factor (isoform CRA-b)* and *isoform 2 of dynamin-2* were decreased in the PFC of EtOH-rats compared to controls.

In the PFC of EtOH+MS-rats, 117 proteins were differentially expressed from control rats by a fold change greater than 1.2 (**Table 6.3**). Of these, 7 were altered by a fold change greater than 2. These include *transcription initiation factor TFIID subunit 9B, transcription elongation factor A-like 5, ubiquitin-40S ribosomal protein, tubulin α-1A chain* and *isoform 2 of dynamin-2* which were decreased while *immunoglobulin-like domain-containing receptor 2* was increased relative to control rats (**Figure 6.5**). Network analysis of these 7 proteins did not identify any significant interactions (**Appendix A6.2**).The remaining proteins that differed by more than 20 % in the PFC of EtOH+MS-rats relative to control rats include the energy-related proteins *phosphoglucomutase 2-like 1, glycogenin -1 phosphophenolpyruvate carboxykinase, mitochondrial 2-oxoglutarate/malate carrier protein* and *ATP subunit alpha* which were increased while *citrate synthase, pyruvate kinase, creatine kinase B-type* and *NADH*

ubiquinone oxidoreductase subunit 7 (NDUFA7) were decreased. In addition, *superoxide dismutase* and *peroxiredoxn-6* were decreased in the PFC of EtOH+MS-rats relative to controls. Further, , *glutamine synthetase*, *β-arrestin-1*, *α-synuclein*, *synapsin-2*, *eukaryotic initiation, factor 4A-II*, *2',3'-cyclic-nucleotide 3'-phosphodiesterase (CNPase)* and *c-fos induced growth factor (isoform CRA-b)* were decreased while *disks large homolog 4 (PSD-95)*, *prohibitin*, and *isoform 3 dynamin-like protein (mitochondrial)* were increased in the PFC of EtOH+MS-rats (**Table 6.3**).

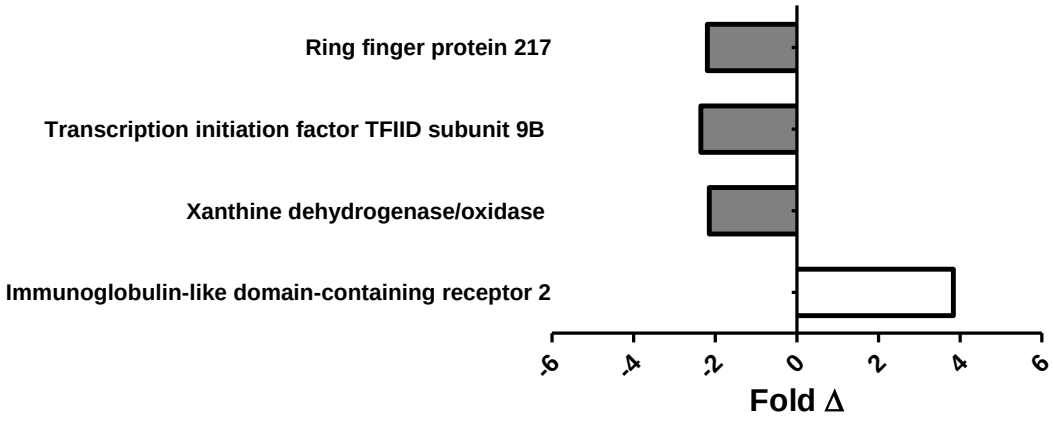

Figure 6.4: Significantly changed proteins (> 2-fold△) in the *prefrontal cortex* of EtOH-rats compared control rats.

Proteins identified in the PFC of EtOH-rats that differed from control rats by a fold change greater than 2. [A downregulated protein is represented by a negative value]

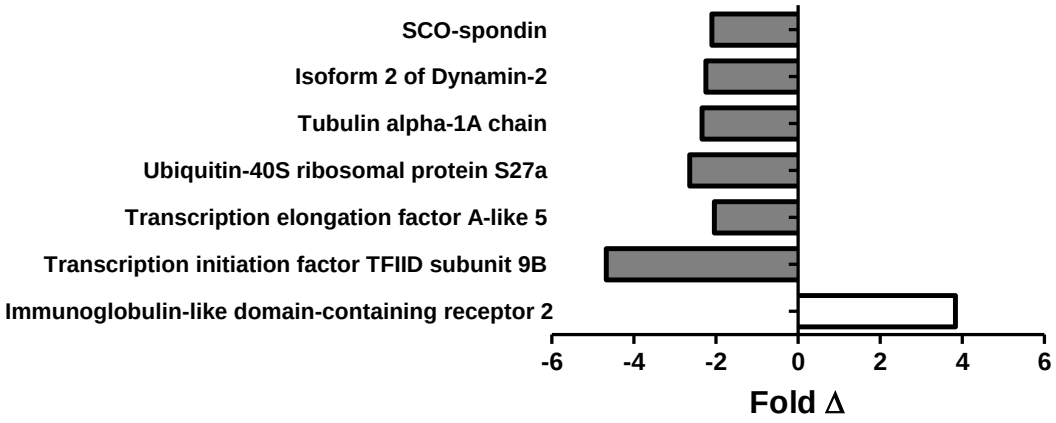

Figure 6.5: Significantly changed proteins (> 2-fold△) in the *prefrontal cortex* of EtOH+MS-rats compared control rats.

Proteins identified in the PFC of EtOH+MS-rats that differed from control rats by a fold change greater than 2. [A downregulated protein is represented by a negative value].

Table 6.1: Proteins with a fold change > 1.2 in the *prefrontal cortex* of MS-rats compared to control rats.

PFC Category	Protein	Accession no.	Cov (%)	Pep	Control : Control	MS : Control	Fold △	
Energy metabolism	Pck2 protein (Fragment) - Phosphoenolpyruvate carboxykinase	B2RYG2_RAT	6.79	4	1.000	1.227	1.227	↑
	Protein Ndufb10 - NADH ubiquinone oxidoreductase subunit B10	D4A0T0_RAT	14.77	2	1.000	1.205	1.205	↑
	Pyruvate kinase PKM	KPYM_RAT	59.51	85	1.000	0.731	1.369	↓
	Fatty acid-binding protein	FABPH_RAT	61.65	10	1.000	0.767	1.304	↓
Redox regulation	Protein Mgst3 - Microsomal glutathione S-transferase 3	D4ADS4_RAT	17.76	2	1.000	1.419	1.419	↑
Neurotransmission/ Signalling	Protein Rasal1 - RAS protein activator like 1 (GAP1 like) (Predicted)	D3ZHY9_RAT	3.50	2	1.000	1.735	1.735	↑
	Low-density lipoprotein receptor-related protein 4	LRP4_RAT	0.94	4	1.000	1.269	1.269	↑
	Caskin-1	D3ZE17_RAT	2.38	2	1.000	1.248	1.248	↑
	Protein Tnik - Similar to Traf2 and NCK interacting kinase, splice variant 4 (Predicted), isoform CRA_a	D3ZZQ0_RAT	3.10	3	1.000	1.245	1.245	↑
	Epidermal growth factor receptor pathway substrate 15-like 1	D3ZJR1_RAT	3.08	2	1.000	1.225	1.225	↑
	Beta-arrestin-1	ARRB1_RAT	10.53	5	1.000	0.665	1.504	↓
	Neuroplastin	NPTN_RAT	11.96	7	1.000	0.759	1.318	↓
	Sn1-specific diacylglycerol lipase beta	DGLB_RAT	2.10	2	1.000	0.763	1.311	↓
	ADP-ribosylation factor 6	ARF6_RAT	17.14	2	1.000	0.800	1.250	↓
Protein synthesis	Prohibitin	PHB_RAT	6.62	2	1.000	1.388	1.388	↑
	B-cell CLL/lymphoma 6	B2GUV8_RAT	2.26	2	1.000	1.308	1.308	↑
	LOC687565 - density regulated protein	B0BNB2_RAT	13.40	2	1.000	1.302	1.302	↑
	Ilf2 protein	B2RZC6_RAT	15.64	4	1.000	1.288	1.288	↑
	Protein Nars - Asparaginyl-tRNA synthetase	F1LPV0_RAT	7.35	3	1.000	1.284	1.284	↑
	Eukaryotic translation initiation factor 3 subunit B	EIF3B_RAT	3.26	2	1.000	1.248	1.248	↑
	Translin	Q71SY3_RAT	12.28	3	1.000	1.230	1.230	↑
	60S ribosomal protein L24	RL24_RAT	13.38	2	1.000	1.220	1.220	↑
	Protein Cct7 - Chaperonin-containing TCP1 subunit 7	D4AC23_RAT	14.71	7	1.000	0.632	1.583	↓
	Protein Tceal5	M0RDJ7_RAT	20.00	4	1.000	0.640	1.563	↓
	Histone H4	H4_RAT	63.11	30	1.000	0.653	1.531	↓
	Eukaryotic initiation factor 4A-II	IF4A2_RAT	35.87	18	1.000	0.692	1.446	↓

PFC	Category	Protein	Accession no.	Cov (%)	Pep	Control : Control	MS : Control	Fold △	
Protein degradation		Ubiquitin-40S ribosomal protein S27a	RS27A_RAT	19.23	4	1.000	0.664	1.507	↓
Cytoskeletal / Structural		Protein Krtap9-1 - Keratin-associated protein 9-1	D3ZD90_RAT	33.33	2	1.000	1.344	1.344	↑
		Isoform 3 of Dynamin-like 120 kDa protein, mitochondrial	OPA1_RAT	2.91	2	1.000	1.294	1.294	↑
		Actin-related protein 2/3 complex subunit 5-like protein	ARP5L_RAT	12.42	4	1.000	1.268	1.268	↑
		Radixin	Q5PQK5_RAT	11.66	2	1.000	1.206	1.206	↑
		Tropomyosin alpha-1 chain	TPM1_RAT	32.04	3	1.000	1.203	1.203	↑
		C-fos induced growth factor, isoform CRA_b	G3V9S8_RAT	5.83	2	1.000	0.556	1.798	↓
		Isoform 2 of Dynamin-2	DYN2_RAT	13.91	4	1.000	0.601	1.664	↓
		Tubulin alpha-1A chain	TBA1A_RAT	75.17	11	1.000	0.749	1.336	↓
		Twinfilin-1	TWF1_RAT	7.43	3	1.000	0.754	1.327	↓
		Isoform 2 of Myelin basic protein	MBP_RAT	40.24	19	1.000	0.778	1.285	↓
Other		Uncharacterized protein	D3Z9X6_RAT	14.15	3	1.000	1.417	1.417	↑
		Prefoldin 1 (Predicted)	D3ZX38_RAT	23.77	3	1.000	1.351	1.351	↑
		Annexin	Q6IMZ3_RAT	8.77	5	1.000	1.308	1.308	↑
		GDP-mannose pyrophosphorylase B (Predicted), isoform CRA_a	D4A746_RAT	7.22	2	1.000	1.223	1.223	↑
		Annexin A3	ANXA3_RAT	17.28	5	1.000	1.204	1.204	↑
		Ferritin (Fragment)	A0JPM7_RAT	10.13	2	1.000	1.202	1.202	↑
		Protein Serpinb9	Q6AYF8_RAT	6.15	3	1.000	0.601	1.663	↓
		SCO-spondin	SSPO_RAT	0.37	2	1.000	0.703	1.423	↓
		Hemoglobin subunit alpha-1/2	HBA_RAT	72.54	50	1.000	0.748	1.337	↓

[The coverage percentage (**Cov %**) indicates the number of identified amino acids associated with that protein represented as a percentage of the total number of amino acids in that protein. The number of exclusive unique peptides (**Pep**) represents the number of unique peptide sequences associated with that protein].

Table 6.2: Proteins with a fold change > 1.2 in the *prefrontal cortex* of EtOH-rats compared to control rats.

PFC Category	Protein	Accession no.	Cov (%)	Pep	Control : Control	EtOH : Control	Fold△	
Energy metabolism	Ndufa7 protein (NADH ubiquinone oxidoreductase subunit A7)	A9UMV9_RAT	19.64	2	1.000	0.798	1.253	↓
Neurotransmission/ Signalling	Protein Rasal1 - RAS protein activator like 1 (GAP1 like) (Predicted)	D3ZHY9_RAT	3.50	2	1.000	1.295	1.295	↑
	Low-density lipoprotein receptor-related protein 4	LRP4_RAT	0.94	4	1.000	1.203	1.203	↑
	Beta-arrestin-1	ARRB1_RAT	10.53	5	1.000	0.713	1.403	↓
	RCG56371 - Sepiapterin reductase - 7,8-dihydrobiopterin:NADP oxidoreductase	B2RYK3_RAT	13.74	2	1.000	0.777	1.288	↓
Protein synthesis	Ring finger and SPRY domain containing 1	A1L1K9_RAT	2.43	2	1.000	1.267	1.267	↑
	Transcription initiation factor TFIID subunit 9B	**TAF9B_RAT**	**6.20**	**2**	**1.000**	**0.426**	**2.348**	↓
	Protein Tceal5 - Transcription elongation factor A-like5, isoform CRA_a	M0RDJ7_RAT	20.00	4	1.000	0.730	1.370	↓
	AXIN1 up-regulated 1 (Predicted)	D4AAK3_RAT	0.00	3	1.000	0.751	1.332	↓
	Protein Aimp1 - Aminoacyl tRNA synthetase complex-interacting multifunctional protein 1	Q4G079_RAT	10.79	2	1.000	0.797	1.255	↓
Protein degradation	Ubiquilin-1	UBQL1_RAT	11.00	4	1.000	1.202	1.202	↑
	Ring finger protein 217	**D4ABK2_RAT**	**5.99**	**3**	**1.000**	**0.456**	**2.193**	↓
	Clusterin	CLUS_RAT	9.62	3	1.000	0.791	1.265	↓
Cytoskeletal / Structural	C-fos induced growth factor, isoform CRA_b	G3V9S8_RAT	5.83	2	1.000	0.519	1.928	↓
	Isoform 2 of Dynamin-2	DYN2_RAT	13.91	4	1.000	0.781	1.280	↓
Other	**Protein Ildr2 (Fragment) - Immunoglobulin-like domain-containing receptor 2**	**F1M2C7_RAT**	**0.00**	**2**	**1.000**	**3.838**	**3.838**	↑
	Ferritin (Fragment)	A0JPM7_RAT	10.13	2	1.000	1.316	1.316	↑
	Xanthine dehydrogenase/oxidase	**XDH_RAT**	**1.20**	**2**	**1.000**	**0.466**	**2.146**	↓
	SCO-spondin	SSPO_RAT	0.37	2	1.000	0.746	1.341	↓

The coverage percentage (**Cov %**) indicates the number of identified amino acids associated with that protein represented as a percentage of the total number of amino acids in that protein. The number of exclusive unique peptides (**Pep**) represents the number of unique peptide sequences associated with that protein.]

Table 6.3: Proteins with a fold change >1.2 in the *prefrontal cortex* of EtOH+MS-rats compared to control rats.

PFC Category	Protein	Accession no.	Cov (%)	Pep	Control : Control	EtOH+MS : Control	Fold △	
Energy metabolism	NADH dehydrogenase (Ubiquinone) Fe-S protein 3 (Predicted), isoform CRA_c	D3ZG43_RAT	22.73	6	1.000	1.436	1.436	↑
	Mitochondrial 2-oxoglutarate/malate carrier protein	G3V6H5_RAT	22.61	5	1.000	1.287	1.287	↑
	Protein Pgm2l1 - Phosphoglucomutase 2-like 1	D3Z955_RAT	9.18	5	1.000	1.239	1.239	↑
	Glycogenin-1 (Fragment)	F8WFR6_RAT	7.25	2	1.000	1.228	1.228	↑
	Pck2 protein (Fragment) - Phosphoenolpyruvate carboxykinase	B2RYG2_RAT	6.79	4	1.000	1.228	1.228	↑
	ATP synthase subunit alpha	F1LP05_RAT	48.82	45	1.000	1.205	1.205	↑
	NADH dehydrogenase (Ubiquinone) Fe-S protein 8 (Predicted), isoform CRA_a	B0BNE6_RAT	9.43	2	1.000	1.201	1.201	↑
	Citrate synthase	G3V936_RAT	41.20	32	1.000	0.673	1.486	↓
	Fatty acid-binding protein	FABPH_RAT	61.65	10	1.000	0.721	1.388	↓
	Pyruvate kinase PKM	KPYM_RAT	59.51	85	1.000	0.744	1.344	↓
	Fructose-bisphosphate aldolase C	ALDOC_RAT	75.48	42	1.000	0.760	1.316	↓
	Isocitrate dehydrogenase [NAD] subunit alpha, mitochondrial	F1M294_RAT	20.75	4	1.000	0.761	1.315	↓
	Pyruvate dehydrogenase E1 component subunit alpha	D4A5G8_RAT	34.35	13	1.000	0.783	1.278	↓
	Alpha glucosidase 2 alpha neutral subunit (Predicted)	D3ZAN3_RAT	8.28	6	1.000	0.791	1.264	↓
	Creatine kinase B-type	KCRB_RAT	64.04	79	1.000	0.792	1.262	↓
	Ndufa7 protein (NADH ubiquinone oxidoreductase subunit A7)	A9UMV9_RAT	19.64	2	1.000	0.795	1.258	↓
Redox regulation	Superoxide dismutase [Cu-Zn]	Q6LDS4_RAT	32.89	7	1.000	0.759	1.318	↓
	Peroxiredoxin-6	PRDX6_RAT	75.89	27	1.000	0.787	1.270	↓
Neurotransmission/ Signalling	Low-density lipoprotein receptor-related protein 4	LRP4_RAT	0.94	4	1.000	1.298	1.298	↑
	Caskin-1	D3ZE17_RAT	2.38	2	1.000	1.255	1.255	↑
	GRIP1-associated protein 1	GRAP1_RAT	6.93	6	1.000	1.251	1.251	↑
	Sideroflexin 3	G3V804_RAT	9.35	2	1.000	1.242	1.242	↑
	Protein transport protein Sec31A	SC31A_RAT	2.64	2	1.000	1.235	1.235	↑
	Ankyrin repeat and sterile alpha motif domain-containing protein 1B	ANS1B_RAT	1.59	2	1.000	1.234	1.234	↑
	Disks large homolog 4	DLG4_RAT	4.56	2	1.000	1.232	1.232	↑
	Adenosylhomocysteinase	SAHH_RAT	30.56	14	1.000	1.212	1.212	↑
	Sideroflexin-5	SFXN5_RAT	5.56	2	1.000	1.210	1.210	↑

PFC	Category	Protein	Accession no.	Cov (%)	Pep	Control : Control	EtOH+MS : Control	Fold △	
	Neurotransmission/ signalling (cont.)	Protein Neurobeachin (Fragment)	F1LXU4_RAT	1.59	2	1.000	1.207	1.207	↑
		Epidermal growth factor receptor pathway substrate 15-like 1	D3ZJR1_RAT	3.08	2	1.000	1.201	1.201	↑
		Protein Prkcsh - Protein kinase C substrate 80K-H	B1WC34_RAT	8.57	6	1.000	1.201	1.201	↑
		Sn1-specific diacylglycerol lipase beta	DGLB_RAT	2.10	2	1.000	0.677	1.478	↓
		Septin 7	A2VCW8_RAT	34.10	22	1.000	0.699	1.430	↓
		Glutamine synthetase	GLNA_RAT	19.03	15	1.000	0.708	1.413	↓
		Beta-arrestin-1	ARRB1_RAT	10.53	5	1.000	0.727	1.375	↓
		Alpha-synuclein	SYUA_RAT	60.00	22	1.000	0.734	1.363	↓
		MAP2K4delta	S4VP54_RAT	5.39	2	1.000	0.741	1.350	↓
		Protein Arhgap1 - Rho GTPase-activating protein 1	D4A6C5_RAT	18.68	7	1.000	0.741	1.350	↓
		Protein Pgp - Glycerol-3-phosphate phosphatase	D3ZDK7_RAT	8.72	2	1.000	0.747	1.339	↓
		Synapsin-2	SYN2_RAT	52.22	45	1.000	0.751	1.332	↓
		Serine/threonine-protein phosphatase 2A activator	B2RYQ2_RAT	23.53	7	1.000	0.763	1.311	↓
		Phosphatidylethanolamine-binding protein 1	PEBP1_RAT	47.59	31	1.000	0.776	1.289	↓
		Protein Ahcyl1 - S-adenosylhomocysteine hydrolase-like protein 1	D4A5X8_RAT	14.74	6	1.000	0.780	1.283	↓
		14-3-3 protein epsilon	1433E_RAT	74.51	59	1.000	0.784	1.276	↓
		Synaptic vesicle glycoprotein 2A	SV2A_RAT	10.65	9	1.000	0.793	1.261	↓
		Centaurin alpha	Q63629_RAT	13.84	8	1.000	0.794	1.260	↓
		Opioid-binding protein/cell adhesion molecule	OPCM_RAT	17.39	11	1.000	0.800	1.250	↓
	Protein synthesis	Prohibitin	PHB_RAT	6.62	2	1.000	1.334	1.334	↑
		60S ribosomal protein L24	RL24_RAT	13.38	2	1.000	1.311	1.311	↑
		40S ribosomal protein S12	RS12_RAT	6.06	2	1.000	1.285	1.285	↑
		60S ribosomal protein L6	H7C5Y5_RAT	22.22	8	1.000	1.282	1.282	↑
		Peptidyl-prolyl cis-trans isomerase	D3ZZR9_RAT	19.29	2	1.000	1.274	1.274	↑
		Eukaryotic translation initiation factor 2 subunit 3	IF2G_RAT	6.99	2	1.000	1.257	1.257	↑
		Protein Hnrnpab - Heterogeneous nuclear ribonucleoprotein A/B	Q9QX81_RAT	18.37	8	1.000	1.250	1.250	↑
		RNA-binding motif protein, X chromosome retrogene-like	RMXRL_RAT	14.43	7	1.000	1.220	1.220	↑
		Protein LOC100912027 - 60S ribosomal protein L27-like	M0R7P0_RAT	22.06	3	1.000	1.209	1.209	↑

PFC	Category	Protein	Accession no.	Cov (%)	Pep	Control : Control	EtOH+MS : Control	Fold △	
Protein synthesis(cont.)		Hepatoma-derived growth factor-related protein 3	F1LPC7_RAT	20.86	2	1.000	1.205	1.205	↑
		Transcription initiation factor TFIID subunit 9B	**TAF9B_RAT**	**6.20**	**2**	**1.000**	**0.214**	**4.673**	↓
		Protein Tceal5 - Transcription elongation factor A-like 5	**M0RDJ7_RAT**	**20.00**	**4**	**1.000**	**0.492**	**2.035**	↓
		C-terminal-binding protein 1	CTBP1_RAT	6.74	2	1.000	0.517	1.934	↓
		Eukaryotic initiation factor 4A-II	IF4A2_RAT	35.87	18	1.000	0.524	1.908	↓
		B-cell CLL/lymphoma 6	B2GUV8_RAT	2.26	2	1.000	0.555	1.802	↓
		Histone H4	H4_RAT	63.11	30	1.000	0.674	1.484	↓
		Protein Cct7 - Chaperonin-containing TCP1 subunit 7	D4AC23_RAT	14.71	7	1.000	0.685	1.459	↓
		60S ribosomal protein L18	RL18_RAT	13.83	3	1.000	0.748	1.337	↓
		Reticulon-1	RTN1_RAT	17.37	10	1.000	0.784	1.276	↓
Protein degradation		Ubiquilin-1	UBQL1_RAT	11.00	4	1.000	1.305	1.305	↑
		26S proteasome non-ATPase regulatory subunit 13	PSD13_RAT	4.26	2	1.000	1.205	1.205	↑
		Proteasome (Prosome, macropain) 26S subunit, non-ATPase, 3	Q5U2S7_RAT	4.53	3	1.000	1.246	1.246	↑
		Proteasome subunit beta type-4	PSB4_RAT	28.90	5	1.000	1.212	1.212	↑
		Ubiquitin-40S ribosomal protein S27a	**RS27A_RAT**	**19.23**	**4**	**1.000**	**0.379**	**2.637**	↓
		Clusterin	CLUS_RAT	9.62	3	1.000	0.745	1.342	↓
		Protein Ubqln2 - Ubiquilin 2	D4AA63_RAT	11.13	7	1.000	0.780	1.283	↓
Cytoskeletal / Structural		Protein Krtap9-1 - Keratin-associated protein 9-1	D3ZD90_RAT	33.33	2	1.000	1.810	1.810	↑
		Isoform 3 of Dynamin-like 120 kDa protein, mitochondrial	OPA1_RAT	2.91	2	1.000	1.391	1.391	↑
		Actin-related protein 2/3 complex subunit 5-like protein	ARP5L_RAT	12.42	4	1.000	1.387	1.387	↑
		Tripartite motif-containing protein 3	TRIM3_RAT	2.42	2	1.000	1.367	1.367	↑
		Tubulin alpha-8 chain	TBA8_RAT	44.77	2	1.000	1.213	1.213	↑
		Tubulin alpha-1A chain	**TBA1A_RAT**	**75.17**	**11**	**1.000**	**0.427**	**2.340**	↓
		Isoform 2 of Dynamin-2	**DYN2_RAT**	**13.91**	**4**	**1.000**	**0.446**	**2.243**	↓
		C-fos induced growth factor, isoform CRA_b	G3V9S8_RAT	5.83	2	1.000	0.519	1.928	↓
		Protein Tln2 - Talin 2	D3ZA84_RAT	1.94	3	1.000	0.558	1.791	↓
		Twinfilin-1	TWF1_RAT	7.43	3	1.000	0.571	1.753	↓
		Brevican, isoform CRA_a	G3V8G4_RAT	9.85	8	1.000	0.593	1.687	↓
		Neuronal membrane glycoprotein M6-a	GPM6A_RAT	8.99	2	1.000	0.595	1.680	↓

PFC	Category	Protein	Accession no.	Cov (%)	Pep	Control : Control	EtOH+MS : Control	Fold △	
Cytoskeletal / Structural (cont.)		Tubulin alpha-4A chain	TBA4A_RAT	66.29	12	1.000	0.658	1.520	↓
		Pls3 protein - plastin 3 (Fragment)	Q562B2_RAT	6.46	3	1.000	0.679	1.474	↓
		Clathrin light chain A	CLCA_RAT	22.18	9	1.000	0.740	1.351	↓
		Actin, cytoplasmic 2	ACTG_RAT	70.40	95	1.000	0.746	1.341	↓
		Tropomyosin 5	P97726_9MURI	38.31	22	1.000	0.755	1.324	↓
		Isoform 2 of Myelin basic protein	MBP_RAT	40.24	19	1.000	0.769	1.300	↓
		Protein Tubb6 - Tubulin beta chain	Q4QQV0_RAT	48.77	11	1.000	0.770	1.299	↓
		Protein Ank2 (Fragment) - Ankyrin 2	F1M9N9_RAT	10.97	3	1.000	0.775	1.290	↓
		2',3'-cyclic-nucleotide 3'-phosphodiesterase	CN37_RAT	39.52	23	1.000	0.787	1.270	↓
		Endophilin-A1 (Fragment)	F1LQ05_RAT	38.46	26	1.000	0.794	1.260	↓
Other		**Protein Ildr2 (Fragment) - Immunoglobulin-like domain-containing receptor 2**	**F1M2C7_RAT**	**0.00**	**2**	**1.000**	**3.838**	**3.838**	↑
		COP9 (Constitutive photomorphogenic) homolog, subunit 5 (Arabidopsis thaliana)	Q4KM69_RAT	5.69	2	1.000	1.485	1.485	↑
		Alpha globin	Q63910_RAT	19.72	3	1.000	1.391	1.391	↑
		Ferritin (Fragment)	A0JPM7_RAT	10.13	2	1.000	1.353	1.353	↑
		Annexin	Q6IMZ3_RAT	8.77	5	1.000	1.349	1.349	↑
		Uncharacterized protein	D3Z9X6_RAT	14.15	3	1.000	1.326	1.326	↑
		Protein tfg - TRK fused gene	Q6AYR1_RAT	9.05	2	1.000	1.322	1.322	↑
		Protein - heterogeneous nuclear ribonucleoprotein A0	F1M3H8_RAT	7.26	3	1.000	1.290	1.290	↑
		Uncharacterized protein	Q6P769_RAT	19.44	5	1.000	1.270	1.270	↑
		Hemopexin	HEMO_RAT	5.00	2	1.000	1.260	1.260	↑
		Protein Sec23a - SEC23A (S. cerevisiae) (Predicted)	B5DFC3_RAT	4.05	2	1.000	1.249	1.249	↑
		Selenium-binding protein 1	SBP1_RAT	6.78	2	1.000	1.235	1.235	↑
		Protein Timm8a1 - Uncharacterized protein	F1LP21_RAT	22.68	2	1.000	1.221	1.221	↑
		Protein Vat1l - Vesicle amine transport 1-like	D3ZE32_RAT	8.41	3	1.000	1.214	1.214	↑
		Carbonic anhydrase 1 O	CAH1_RAT	19.92	7	1.000	1.212	1.212	↑
		Mitochondrial import receptor subunit TOM70	R9PXR4_RAT	4.64	2	1.000	1.210	1.210	↑
		Protein Eea1 (Fragment) - Early endosome antigen 1	F1LUA1_RAT	3.40	5	1.000	1.203	1.203	↑
		SCO-spondin	**SSPO_RAT**	**0.37**	**2**	**1.000**	**0.477**	**2.099**	↓
		C38 protein	B7X6I3_RAT	14.77	4	1.000	0.690	1.449	↓

PFC	Category	Protein	Accession no.	Cov (%)	Pep	Control : Control	EtOH+MS : Control	Fold △	
	Other (cont.)	Protein RGD1559864 -Uncharacterized protein	D3ZBS6_RAT	23.25	11	1.000	0.770	1.299	↓
		Protein Serpinb9	Q6AYF8_RAT	6.15	3	1.000	0.711	1.406	↓
		Xanthine dehydrogenase/oxidase	XDH_RAT	1.20	2	1.000	0.720	1.388	↓
		Importin subunit beta-1	F2Z3Q8_RAT	10.39	7	1.000	0.734	1.363	↓

[The coverage percentage (**Cov %**) indicates the number of identified amino acids associated with that protein represented as a percentage of the total number of amino acids in that protein. The number of exclusive unique peptides (**Pep**) represents the number of unique peptide sequences associated with that protein].

PROTEINS ALTERED BY PRENATAL-ETHANOL EXPOSURE AND/OR MATERNAL SEPARATION IN THE DORSAL HIPPOCAMPUS

Of the 1 104 proteins identified by iTRAQ and LC-MS, 377 of these proteins differed in the DH of MS-, EtOH- and EtOH+MS-rats by more than 20 % (fold change greater than 1.2) compared to control rats. Forty-six were altered in MS-rats, 333 were altered in EtOH-rats and 49 proteins were altered in EtOH+MS-rats in the DH (**Figure 6.6**).

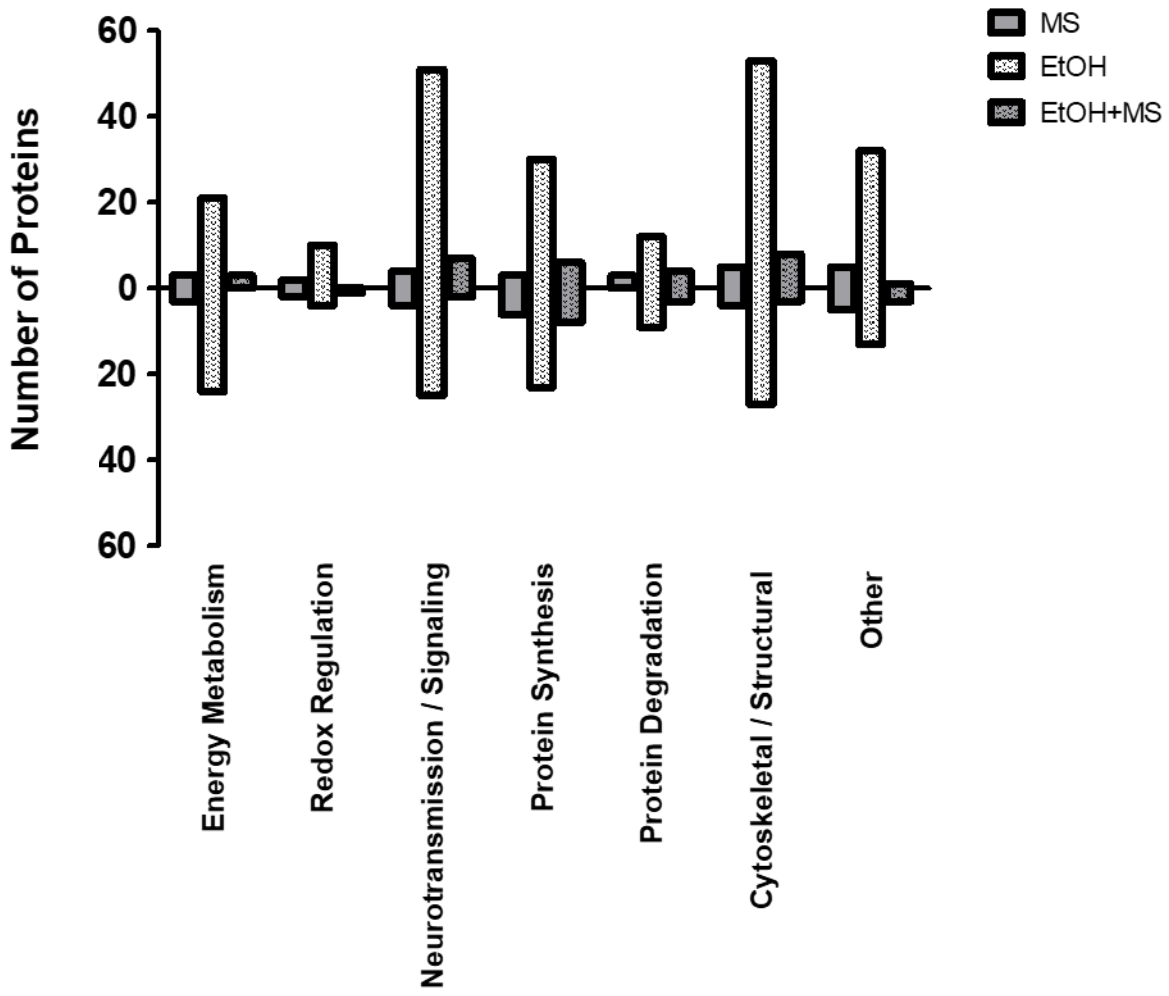

Figure 6.6: Number of differentially expressed proteins (> 1.2-fold △) in the *dorsal hippocampus* of MS-, EtOH- and EtOH+MS-rats compared to control rats.

Categorically organized differentially expressed proteins in the DH of MS-, EtOH- and EtOH+MS-rats compared to control rats.

In the DH of MS-rats, *ring finger and SPRY domain containing 1* and *laminin, alpha 5 (isoform CRA_a)* were altered by a fold change greater than 2 relative to control rats (**Figure 6.7**). Network analysis of these 2 proteins did not identify any significant interactions (**Appendix A6.3**). An additional 44 proteins were altered by a fold change greater than 1.2 in the DH of MS-rats relative to control rats (**Table 6.4**). These include *hexokinase-1, glycerol-3-phoshphate dehydrogenase [NAD(+)], cytochrome c oxidase subunit 2, ADP/ATP translocase, PSD-95, glutamate receptor 1, CNPase, prohibitin-2* and *myelin proteolipid protein* which were decreased while *β-arrestin-1* and *clathrin-light chain A* were increased.

In the DH of EtOH-rats, 333 proteins were altered by prenatal-ethanol exposure with a fold change greater than 1.2 (**Appendix A6**). Of these, 29 were significantly changed by a fold change greater than 2 (**Figure 6.8**). Network analysis of these proteins detected significant enrichment (STRING p = 0.000518), indicating that they interact amongst each other more than what would be expected per chance and therefore may be partially biologically connected as a group (**Figure 6.9)**. Identified processes involved *sulfur metabolism* (GO.00006790: acyl-CoA-binding protein, lactoglutathione lyase, hemoglobin beta-1, superoxide dismutase [Cu-Zn], superoxide dismutase mitochondrial and thioredoxin), *glutathione metabolism* (GO.0006749: lactoglutathione lyase, superoxide dismutase [Cu-Zn] and superoxide dismutase mitochondrial), *oxygen transport* (GO.0015671: hemoglobin subunit beta-1, hemoglobin subunit beta-2 and hemoglobin subunit alpha1/2) and *peptide metabolism* (GO.0006518: lactoglutathione lyase, hemoglobin beta-1, 60S ribosomal protein L18, superoxide dismutase [Cu-Zn] and superoxide dismutase mitochondrial) (**Figure 6.9**). **Table 6.5** presents the proteins altered by prenatal-ethanol exposure in the DH that differed by a fold change greater than 1.5. For example, *ATP synthase subunit delta, mitochondrial; cytochrome c (somatic), acyl carrier protein, acyl-CoA-binding protein, superoxide dismutase, thioredoxin (fragment), histone H4, microtubule-associated protein 4* and *clathrin light chain A* were upregulated in the DH of EtOH-rats while *transcription initiation factor TFIID subunit 9B* and *tubulin α-1A* chain were downregulated. Proteins that differed by more than 50 % in the DH of EtOH-rats relative to control rats include energy-related proteins such as *L-lactate dehydrogenase, glucose-6-phosphate isomerase, glyceraldehyde-3-phosphate dehydrogenase, phosphoglycerate kinase 1, creatine kinase B-type* and *pyruvate kinase were decreased.*

Further, signalling-related proteins such as *calretinin, calbindin* and *calmodulin,* were increased while *β-arrestin* was decreased in the DH of EtOH-rats relative to controls. *Histones*

H3, *H1.5*, and *H1.0* were increased while transcription initiation factor TFIID subunit 9B was decreased in the DH of EtOH-rats compared to controls.

Structural proteins such as *β-synuclein*, *microtubule-associated proteins (Q63724_RATRT, D3ZNA6_RAT)*, and *myelin proteolipid protein* were increased in the DH of EtOH-rats relative to controls. Further, *tubulin α-1A chain* and *actin cytoplasmic 2* were decreased in the DH of EtOH-rats relative to control rats.

Forty-nine proteins were differentially expressed in the DH by the combination of prenatal-ethanol exposure and maternal separation compared to controls. Only 2 of these proteins differed by a fold change greater than 2, *ring finger protein 217* and *laminin, alpha 5 (isoform CRA-a)*, relative to control rats (**Figure 6.10**). Network analysis of these 2 proteins did not identify significant protein-protein interactions (**Appendix A6.4**). The remaining proteins differed by a fold change greater than 1.2. For example, *NDUFA7*, *glucose-6-phosphate isomerase*, *β-arrestin* and *isoform2 of dynamin-2* were increased while *thioredoxin* and *synaptic vesicle glycoprotein 2B* were decreased in the DH of EtOH+MS-rats relative to controls.

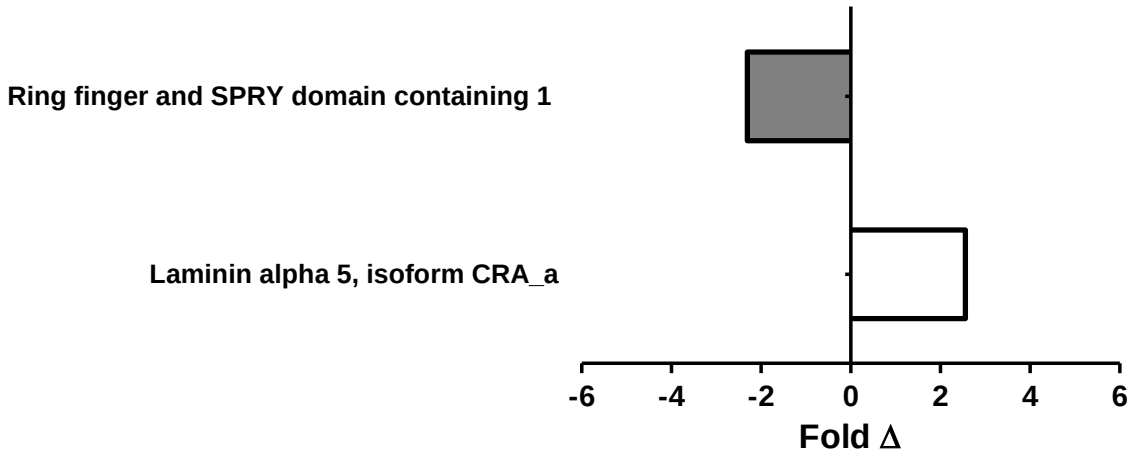

Figure 6.7: Significantly changed proteins (> 2-fold △) in the *dorsal hippocampus* of MS-rats compared control rats.

Proteins identified in the DH of MS-rats that differed from control rats by a fold change greater than 2. [A downregulated protein is represented by a negative value].

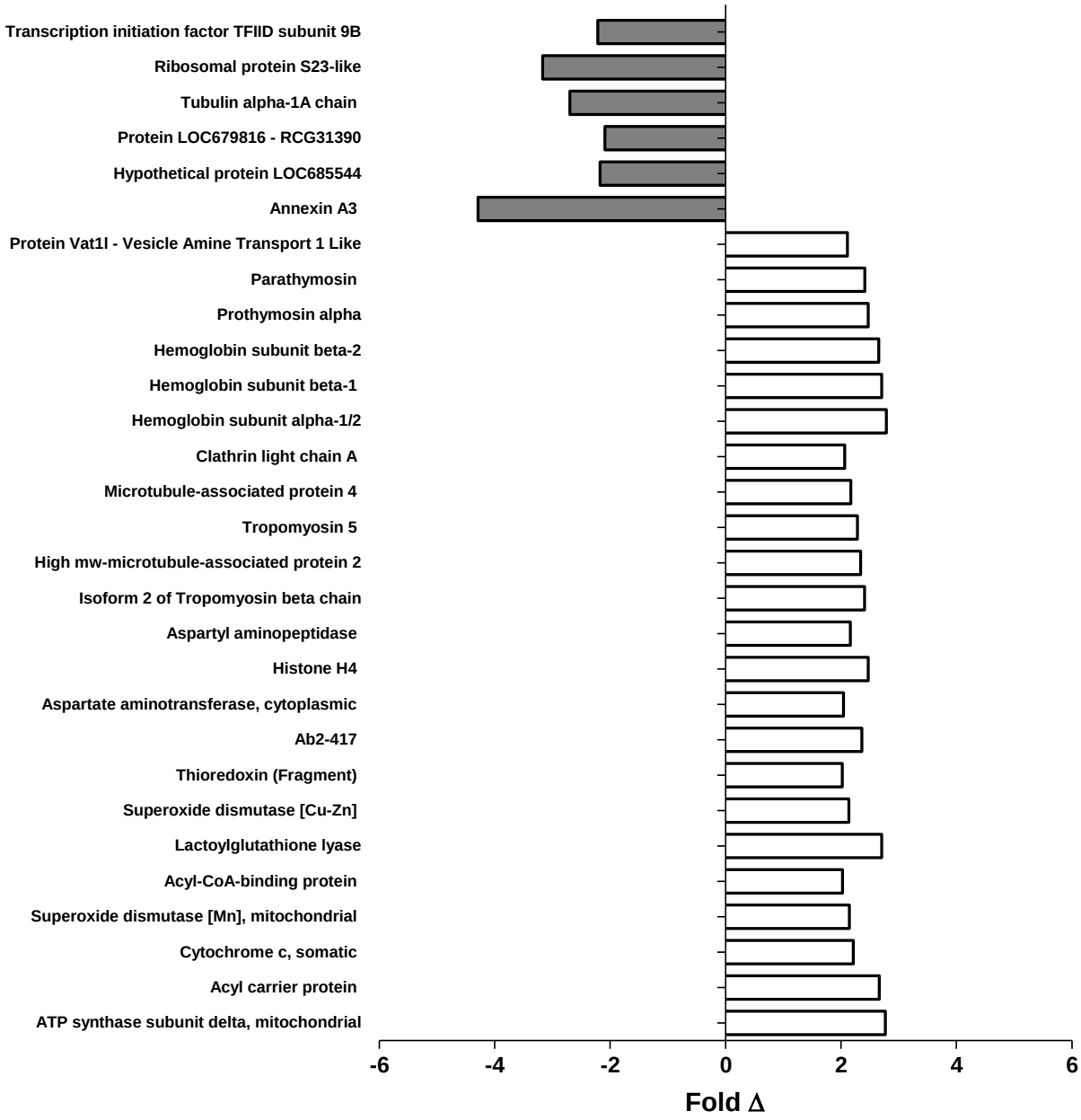

Figure 6.8: Significantly changed proteins (> 2-fold △) in the *dorsal hippocampus* of EtOH-rats compared control rats.

Proteins identified in the DH of EtOH-rats that differed from control rats by a fold change greater than 2. In addition, 60S ribosomal protein L18 was decreased by a fold change of 26.17. [A downregulated protein is represented by a negative value].

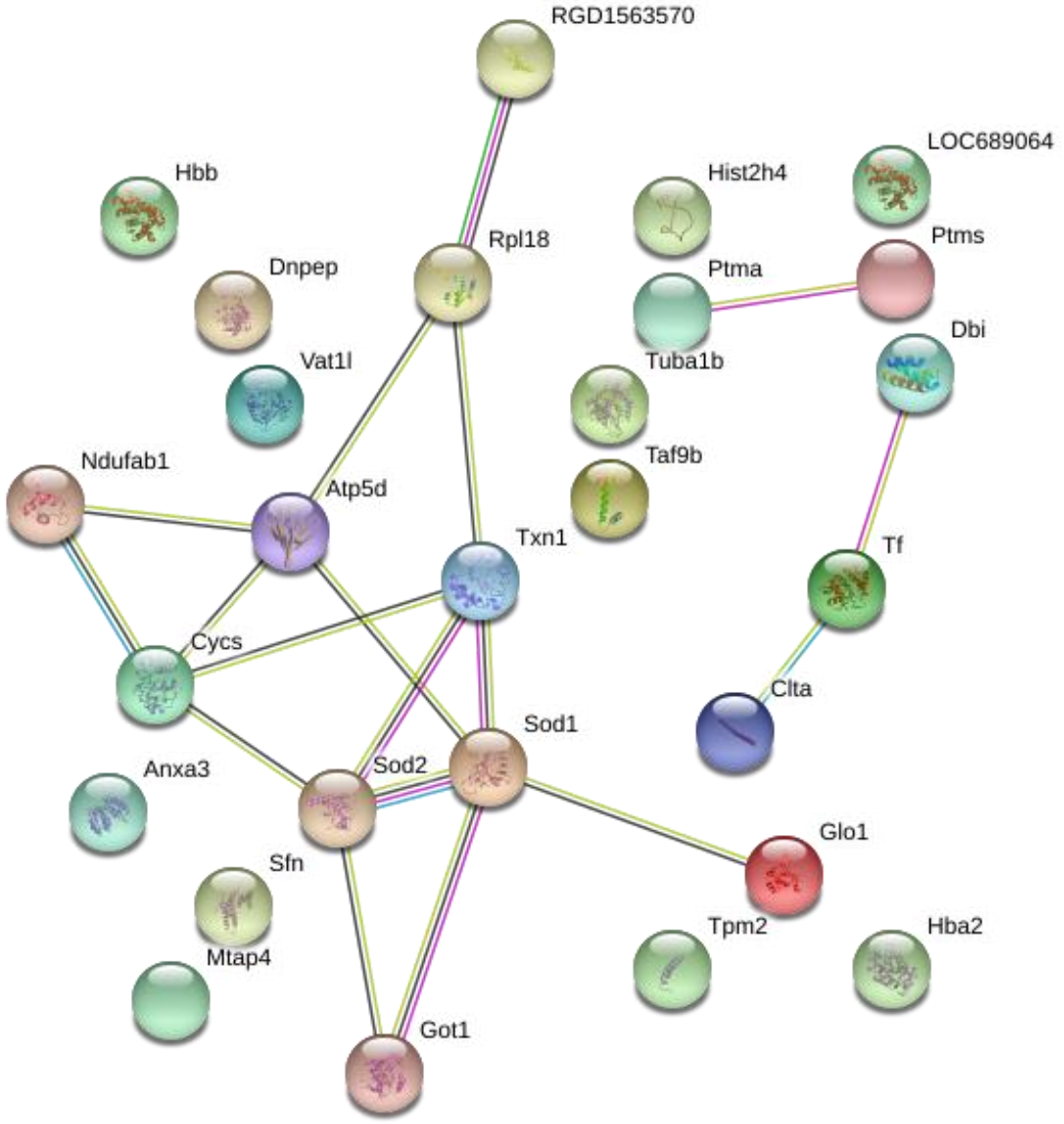

Figure 6.9: Network analysis of significantly changed proteins (>2-fold△) in the *dorsal hippocampus* of EtOH-rats relative to control rats

Significant enrichment was detected amongst the 29 significantly changed proteins in the DH of EtOH-rats versus controls indicating that these proteins have more interactions among themselves than would be expected by random chance (STRING, p = 0,000518). [RGD1563570: Ribosomal protein S23-like, Rpla8: 60S Ribsomal protein L18, Atp5d: ATP synthase subunit delta, Ndufab1: Acyl carrier protein, Cycs: Cytochrome C, Sod1: Superoxide dismutase[Cu-Zn], Sod2: Superoxide dismutase [Mn], Txn1: Thioredoxin (fragment), Got1: Asparate aminotransferase, Glo1: Lactoglutathione Lyase, Hbb: Hemoglobin subunit beta-1, Dnpep: Aspartyl aminopeptidase, Vat1l: Vesicle amine transport-like 1, Anxa3: Annexin A3, Sfn: Mtap1: Microtubule-associated protein 4, Hist2h4: Histone H4, LOC689064: Hemoglobin subunit beta-2, Ptma: Prothymosinalpha, Ptms: Parathymosin, Tuba1b: Tubulin alpha-1A chain, Taf9b:Transcription initiation factor TFFIID subunit 9B, Dbi: Acyl-CoA binding protein, Tf: Ab2-417 (serotransferrin), Clta: Calthrin light chain A, Tpm2: Isoform 2 of tropomyosin beta chain, Hba2: Hemoglobin subunit alpha-1/2]

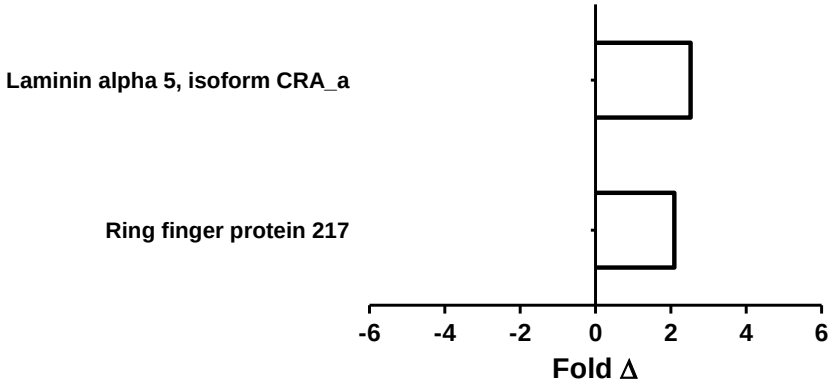

Figure 6.10: Significantly changed proteins (> 2-fold △) in the *dorsal hippocampus* of EtOH+MS-rats compared control rats.

Proteins identified in the DH of EtOH+MS-rats that differed from control rats by a fold change greater than 2. [A downregulated protein is represented by a negative value].

Table 6.4: Proteins with a fold change > 1.2 in the *dorsal hippocampus* of MS-rats compared to control rats.

DH Category	Protein	Accession no.	Cov (%)	Pep	Control : Control	MS : Control	Fold △	
Energy metabolism	Malate dehydrogenase, cytoplasmic	MDHC_RAT	34.13	2	1.000	1.277	1.277	↑
	Aspartate aminotransferase, mitochondrial	AATM_RAT	46.28	46	1.000	1.218	1.218	↑
	Hexokinase-1	HXK1_RAT	22.88	30	1.000	0.687	1.456	↓
	Glycerol-3-phosphate dehydrogenase [NAD(+)], cytoplasmic	GPDA_RAT	11.46	4	1.000	0.771	1.298	↓
	Cytochrome c oxidase subunit 2	B0FTB8_RATLE	17.62	4	1.000	0.778	1.286	↓
	ADP/ATP translocase 1	Q6P9Y4_RAT	36.91	23	1.000	0.787	1.271	↓
Redox regulation	Glutathione S-transferase alpha-3	GSTA3_RAT	34.39	9	1.000	1.234	1.234	↑
	Protein Mgst3 - Microsomal glutathione S-transferase 3	D4ADS4_RAT	17.76	2	1.000	0.668	1.497	↓
Neurotransmission / signalling	B-cell CLL/lymphoma 6	B2GUV8_RAT	2.26	2	1.000	1.387	1.387	↑
	Centaurin alpha	Q63629_RAT	13.84	8	1.000	1.309	1.309	↑
	Beta-arrestin-1	ARRB1_RAT	10.53	5	1.000	1.252	1.252	↑
	ADP-ribosylation factor 6	ARF6_RAT	17.14	2	1.000	1.246	1.246	↑
	Disks large homolog 4	DLG4_RAT	4.56	2	1.000	0.743	1.345	↓
	Glutamate receptor 1	M0R9A7_RAT	5.52	3	1.000	0.781	1.281	↓
Protein synthesis	Protein Tceal5 - RCG20041, isoform CRA_a	M0RDJ7_RAT	20.00	4	1.000	1.229	1.229	↑
	60S ribosomal protein L24	RL24_RAT	13.38	2	1.000	1.227	1.227	↑
	Eukaryotic translation initiation factor 3 subunit B	EIF3B_RAT	3.26	2	1.000	1.203	1.203	↑
	Ring finger and SPRY domain containing 1	**A1L1K9_RAT**	**2.43**	**2**	**1.000**	**0.434**	**2.304**	↓
	Peptidyl-prolyl cis-trans isomerase B	PPIB_RAT	12.96	3	1.000	0.616	1.624	↓
	Protein Ddx6 - dead-box helicase 6	D3ZD73_RAT	7.45	3	1.000	0.780	1.281	↓
	Prohibitin-2	PHB2_RAT	22.07	5	1.000	0.781	1.281	↓
	Protein LZIC - Leucine zipper and CTNNBIP1 domain containing	LZIC_RAT	17.37	2	1.000	0.791	1.264	↓
	Protein Scai - suppressor of cancer cell invasion	F1M3P6_RAT	12.71	8	1.000	0.795	1.258	↓
Protein degradation	IBR domain containing 1 (Predicted) - Ring finger protein 217	D4ABK2_RAT	5.99	3	1.000	1.983	1.983	↑
	Proteasome (Prosome, macropain) 26S subunit, non-ATPase, 7 (Predicted)	D4AEH3_RAT	13.75	4	1.000	1.284	1.284	↑
	Protein Ube2o (Fragment) - Ubiquitin-conjugating enzyme E2O	F1M403_RAT	2.33	2	1.000	1.250	1.250	↑

DH	Category	Protein	Accession no.	Cov (%)	Pep	Control : Control	MS : Control	Fold △	
		Laminin, alpha 5, isoform CRA_a	**F1MAN8_RAT**	**0.51**	**3**	**1.000**	**2.556**	**2.556**	↑
	Cytoskeletal / structural	Protein Krtap9-1 - Keratin-associated protein 9-1	D3ZD90_RAT	20.75	4	1.000	1.257	1.257	↑
		Clathrin light chain A	CLCA_RAT	22.18	9	1.000	1.250	1.250	↑
		Protein transport protein Sec31A	SC31A_RAT	2.64	2	1.000	1.221	1.221	↑
		Tripartite motif-containing protein 3	TRIM3_RAT	2.42	2	1.000	0.615	1.626	↓
		Myelin proteolipid protein	MYPR_RAT	14.08	10	1.000	0.711	1.406	↓
		C38 protein	B7X6I3_RAT	14.77	4	1.000	0.770	1.299	↓
		2',3'-cyclic-nucleotide 3'-phosphodiesterase	CN37_RAT	39.52	23	1.000	0.787	1.271	↓
		Cul1 protein	B1WBY1_RAT	3.09	2	1.000	0.799	1.251	↓
	Other	Serum albumin	ALBU_RAT	24.84	42	1.000	1.383	1.383	↑
		Alpha globin	Q63910_RAT	19.72	3	1.000	1.334	1.334	↑
		Hemoglobin subunit alpha-1/2	HBA_RAT	72.54	50	1.000	1.291	1.291	↑
		Protein Wdr47 - WD repeat-containing protein 47	G3V9M3_RAT	3.15	3	1.000	1.280	1.280	↑
		Carbonic anhydrase 1	CAH1_RAT	19.92	7	1.000	1.239	1.239	↑
		Sulfated glycoprotein 1	SAP_RAT	8.48	10	1.000	1.234	1.234	↑
		Prion protein (Fragment)	A0A075TCV0_RATNI	10.57	3	1.000	0.735	1.360	↓
		Uncharacterized protein	F1M2D3_RAT	38.30	2	1.000	0.764	1.308	↓
		Annexin A3	ANXA3_RAT	17.28	5	1.000	0.766	1.306	↓
		Protein LOC100911918 (Fragment) - Microtubule-associated protein RP/EB family member 2	M0R7M8_RAT	15.85	2	1.000	0.768	1.302	↓
		Mitochondrial import receptor subunit TOM70	R9PXR4_RAT	4.64	2	1.000	0.793	1.260	↓

[The coverage percentage (**Cov %**) indicates the number of identified amino acids associated with that protein represented as a percentage of the total number of amino acids in that protein. The number of exclusive unique peptides (**Pep**) represents the number of unique peptide sequences associated with that protein]

Table 6.5: Proteins with a fold change > 1.5 in the *dorsal hippocampus* of EtOH-rats compared to control rats.

DH Category	Protein	Accession no.	Cov(%)	Pep	Control : Control	EtOH : Control	Fold △	
Energy metabolism	**ATP synthase subunit delta, mitochondrial**	**G3V7Y3_RAT**	**48.81**	**11**	**1.000**	**2.769**	**2.769**	↑
	Acyl carrier protein	**D3ZF13_RAT**	**13.46**	**3**	**1.000**	**2.661**	**2.661**	↑
	Cytochrome c, somatic	**CYC_RAT**	**69.52**	**32**	**1.000**	**2.211**	**2.211**	↑
	Acyl-CoA-binding protein	**Q6TXF3_RAT**	**6.00**	**11**	**1.000**	**2.027**	**2.027**	↑
	Gene - DLST - dihydrolipoamide S-succinyltransferase	Q8CJG5_RAT	23.13	16	1.000	1.886	1.886	↑
	Gamma-enolase	ENOG_RAT	63.36	66	1.000	1.770	1.770	↑
	Transketolase	TKT_RAT	49.12	40	1.000	1.674	1.674	↑
	L-lactate dehydrogenase	B5DEN4_RAT	48.49	35	1.000	0.506	1.977	↓
	Glucose-6-phosphate isomerase	G6PI_RAT	18.10	3	1.000	0.537	1.862	↓
	Creatine kinase B-type	KCRB_RAT	64.04	79	1.000	0.621	1.609	↓
	Glyceraldehyde-3-phosphate dehydrogenase	G3P_RAT	58.26	54	1.000	0.625	1.599	↓
	Phosphoglycerate kinase 1	PGK1_RAT	57.79	72	1.000	0.640	1.563	↓
	Pyruvate kinase PKM	KPYM_RAT	59.51	85	1.000	0.645	1.551	↓
	Glycerol-3-phosphate dehydrogenase [NAD(+)], cytoplasmic	GPDA_RAT	11.46	4	1.000	0.649	1.541	↓
Redox regulation	**Lactoylglutathione lyase**	**LGUL_RAT**	**52.72**	**11**	**1.000**	**2.703**	**2.703**	↑
	Superoxide dismutase [Mn], mitochondrial	**SODM_RAT**	**52.25**	**21**	**1.000**	**2.147**	**2.147**	↑
	Superoxide dismutase [Cu-Zn]	**Q6LDS4_RAT**	**32.89**	**7**	**1.000**	**2.137**	**2.137**	↑
	Thioredoxin (Fragment)	**R4GNK3_RAT**	**31.73**	**12**	**1.000**	**2.024**	**2.024**	↑
	Ac1002	Q7TQ90_RAT	8.03	8	1.000	1.730	1.730	↑
	Peroxiredoxin-2	PRDX2_RAT	18.69	8	1.000	1.668	1.668	↑
	Copper transport protein ATOX1	ATOX1_RAT	32.35	4	1.000	1.657	1.657	↑
	Glutathione S-transferase omega 1	B6DYQ5_RAT	26.97	10	1.000	1.559	1.559	↑
Neurotransmission / signalling	**Aspartate aminotransferase, cytoplasmic**	**AATC_RAT**	**64.65**	**57**	**1.000**	**2.045**	**2.045**	↑
	Complexin-1	CPLX1_RAT	39.55	12	1.000	1.978	1.978	↑
	Protein S100-B	S100B_RAT	40.22	22	1.000	1.961	1.961	↑
	Na(+)/H(+) exchange regulatory cofactor NHE-RF1	NHRF1_RAT	10.39	4	1.000	1.946	1.946	↑
	Protein Pkn3 - Protein kinase N3	D3ZC07_RAT	6.89	5	1.000	1.849	1.849	↑

DH	Category	Protein	Accession no.	Cov(%)	Pep	Control : Control	EtOH : Control	Fold △	
	Neurotransmission / signalling (cont.)	Receptor-type tyrosine-protein phosphatase zeta	PTPRZ_RAT	9.28	27	1.000	1.767	1.767	↑
		Neurogranin	NEUG_RAT	55.13	8	1.000	1.730	1.730	↑
		Voltage-gated potassium channel subunit beta-2	KCAB2_RAT	20.16	6	1.000	1.730	1.730	↑
		Protein Pgp - Glycerol-3-phosphate phosphatase	D3ZDK7_RAT	8.72	2	1.000	1.700	1.700	↑
		Adenine phosphoribosyltransferase	APT_RAT	30.00	6	1.000	1.668	1.668	↑
		Calretinin	CALB2_RAT	15.50	2	1.000	1.659	1.659	↑
		Astrocytic phosphoprotein PEA-15	PEA15_RAT	44.62	11	1.000	1.644	1.644	↑
		EF-hand domain-containing protein D2	EFHD2_RAT	41.00	12	1.000	1.604	1.604	↑
		Calbindin	CALB1_RAT	49.04	15	1.000	1.571	1.571	↑
		Isoform 2 of Alpha-endosulfine	ENSA_RAT	53.85	5	1.000	1.571	1.571	↑
		Calmodulin	CALM_RAT	69.13	35	1.000	1.538	1.538	↑
		Neuromodulin	NEUM_RAT	71.68	22	1.000	1.531	1.531	↑
		Myristoylated alanine-rich C-kinase substrate	MARCS_RAT	44.98	12	1.000	1.515	1.515	↑
		Protein Nbea - neurobeachin (Fragment)	F1LXU4_RAT	1.59	2	1.000	0.611	1.638	↓
		Protein Atp6v1h - ATPase H+-transporting V1 subunit H	E9PTI1_RAT	24.04	12	1.000	0.614	1.629	↓
		Serine/threonine-protein phosphatase 2A activator	B2RYQ2_RAT	23.53	7	1.000	0.632	1.582	↓
		14-3-3 protein theta	1433T_RAT	48.98	21	1.000	0.644	1.554	↓
		Calcium/calmodulin-dependent protein kinase type II subunit beta	F1LNI8_RAT	26.83	14	1.000	0.649	1.542	↓
		UDP-N-acetylglucosamine--peptide N-acetylglucosaminyltransferase 110 kDa subunit	OGT1_RAT	4.05	3	1.000	0.653	1.531	↓
		Vacuolar protein sorting-associated protein 35	G3V8A5_RAT	17.96	11	1.000	0.662	1.511	↓
		Beta-arrestin-1	ARRB1_RAT	10.53	5	1.000	0.663	1.508	↓
		14-3-3 protein beta/alpha	1433B_RAT	67.89	25	1.000	0.665	1.504	↓
	Protein synthesis	**Histone H4**	**H4_RAT**	**63.11**	**30**	**1.000**	**2.473**	**2.473**	↑
		Protein Hnrnpab - Heterogeneous nuclear ribonucleoprotein A/B	Q9QX81_RAT	18.37	8	1.000	1.940	1.940	↑
		Protein Tceal5 - transcription elongation factor A-like 5, isoform CRA_a	M0RDJ7_RAT	20.00	4	1.000	1.868	1.868	↑
		Ubiquitin-40S ribosomal protein S27a	RS27A_RAT	19.23	4	1.000	1.864	1.864	↑
		Histone H3	D3ZJ08_RAT	23.53	4	1.000	1.820	1.820	↑

DH	Category	Protein	Accession no.	Cov(%)	Pep	Control : Control	EtOH : Control	Fold △	
	Protein synthesis (cont.)	Far upstream element-binding protein 2	M0R961_RAT	8.60	4	1.000	1.783	1.783	↑
		Protein RCG45259 - Histone H1/H5 family	M0R7B4_RAT	17.39	8	1.000	1.766	1.766	↑
		Brain acid soluble protein 1	BASP1_RAT	68.64	37	1.000	1.762	1.762	↑
		Caprin-1	CAPR1_RAT	2.69	3	1.000	1.708	1.708	↑
		Hepatoma-derived growth factor	F1LPC7_RAT	20.86	2	1.000	1.702	1.702	↑
		RNA-binding motif protein, X chromosome retrogene-like	RMXRL_RAT	14.43	7	1.000	1.701	1.701	↑
		Nucleobindin-1	NUCB1_RAT	12.42	4	1.000	1.664	1.664	↑
		Single-stranded DNA-binding protein	G3V7K6_RAT	22.30	2	1.000	1.632	1.632	↑
		Psip1 protein - PC4 and SFRS1-interacting protein	Q566D6_RAT	12.08	2	1.000	1.583	1.583	↑
		Histone H1.5	H15_RAT	18.47	4	1.000	1.529	1.529	↑
		Histone H1.0	H10_RAT	11.86	2	1.000	1.521	1.521	↑
		60S ribosomal protein L18	**RL18_RAT**	**13.83**	**3**	**1.000**	**0.038**	**26.17**	↓
		Protein RGD1563570 -ribosomal protein S23-like	**D3Z9X6_RAT**	**14.15**	**3**	**1.000**	**0.316**	**3.168**	↓
		Transcription initiation factor TFIID subunit 9B	**TAF9B_RAT**	**6.20**	**2**	**1.000**	**0.452**	**2.214**	↓
		Peptidyl-prolyl cis-trans isomerase B	PPIB_RAT	12.96	3	1.000	0.567	1.765	↓
		Profilin	D3ZDU5_RAT	48.65	17	1.000	0.613	1.630	↓
		Profilin-1	PROF1_RAT	65.00	26	1.000	0.651	1.536	↓
		Protein Cct7 - Chaperonin-containing TCP1 subunit 7	D4AC23_RAT	14.71	7	1.000	0.664	1.507	↓
	Protein degradation	**Aspartyl aminopeptidase**	**Q4V8H5_RAT**	**7.58**	**4**	**1.000**	**2.161**	**2.161**	↑
		Calpastatin	D3ZL24_RAT	11.03	4	1.000	1.592	1.592	↑
		Cytosolic non-specific dipeptidase	CNDP2_RAT	26.74	15	1.000	1.565	1.565	↑
		Aminoacylase-1A	ACY1A_RAT	16.18	5	1.000	1.539	1.539	↑
		Protein Serpinb9	Q6AYF8_RAT	6.15	3	1.000	0.588	1.701	↓
	Cytoskeletal / structural	**Isoform 2 of Tropomyosin beta chain**	**TPM2_RAT**	**17.61**	**3**	**1.000**	**2.406**	**2.406**	↑
		HMW-MAP2 (Fragment) - High molecular weight - microtubule-associated protein	**P70652_9MURI**	**57.30**	**8**	**1.000**	**2.342**	**2.342**	↑
		Tropomyosin 5	**P97726_9MURI**	**38.31**	**22**	**1.000**	**2.284**	**2.284**	↑
		Microtubule-associated protein 4	**MAP4_RAT**	**4.26**	**3**	**1.000**	**2.169**	**2.169**	↑
		Clathrin light chain A	**CLCA_RAT**	**22.18**	**9**	**1.000**	**2.066**	**2.066**	↑

DH	Category	Protein	Accession no.	Cov(%)	Pep	Control : Control	EtOH : Control	Fold △	
	Cytoskeletal / structural (cont.)	Microtubule-associated protein	Q63724_RATRT	57.11	180	1.000	1.983	1.983	↑
		Isoform 5 of Tropomyosin alpha-1 chain	TPM1_RAT	38.78	10	1.000	1.942	1.942	↑
		Nucleolin	NUCL_RAT	19.64	18	1.000	1.932	1.932	↑
		Protein Krtap9-1 - Keratin-associated protein 9-1	F1M294_RAT	33.33	2	1.000	1.887	1.887	↑
		Neuronal membrane glycoprotein M6-a	GPM6A_RAT	8.99	2	1.000	1.735	1.735	↑
		Beta-synuclein	SYUB_RAT	53.28	43	1.000	1.723	1.723	↑
		Spna2 protein - Spectrin alpha chain, non-erythrocytic 1	Q6IRK8_RAT	60.07	256	1.000	1.689	1.689	↑
		Stathmin	STMN1_RAT	52.35	21	1.000	1.684	1.684	↑
		Myelin proteolipid protein	MYPR_RAT	14.08	10	1.000	1.675	1.675	↑
		Mammalian ependymin-related protein 1	EPDR1_RAT	8.93	2	1.000	1.657	1.657	↑
		Clathrin light chain B	CLCB_RAT	23.14	10	1.000	1.644	1.644	↑
		Laminin, alpha 5, isoform CRA_a	F1MAN8_RAT	0.51	3	1.000	1.617	1.617	↑
		Protein piccolo	PCLO_RAT	4.09	13	1.000	1.577	1.577	↑
		Microtubule-associated protein	D3ZNA6_RAT	25.68	25	1.000	1.572	1.572	↑
		Neurofilament medium polypeptide	NFM_RAT	27.19	33	1.000	1.563	1.563	↑
		Drebrin	DREB_RAT	31.68	29	1.000	1.563	1.563	↑
		Protein Clip1 - CAP-Gly domain-containing linker protein 1	F1MAH8_RAT	2.20	2	1.000	1.559	1.559	↑
		ERC protein 2	ERC2_RAT	9.51	10	1.000	1.525	1.525	↑
		Microtubule-associated protein 6	MAP6_RAT	32.56	35	1.000	1.509	1.509	↑
		Tubulin alpha-1A chain	**TBA1A_RAT**	**75.17**	**11**	**1.000**	**0.371**	**2.697**	↓
		Actin, aortic smooth muscle	ACTA_RAT	43.50	6	1.000	0.529	1.891	↓
		Actin, cytoplasmic 2	ACTG_RAT	70.40	95	1.000	0.613	1.632	↓
		Septin 8 (Predicted)	G3V9Z6_RAT	15.38	5	1.000	0.631	1.585	↓
		Prelamin-A/C	LMNA_RAT	3.46	2	1.000	0.658	1.520	↓
	Other	**Hemoglobin subunit alpha-1/2**	**HBA_RAT**	**72.54**	**50**	**1.000**	**2.787**	**2.787**	↑
		Hemoglobin subunit beta-1	**HBB1_RAT**	**89.12**	**72**	**1.000**	**2.706**	**2.706**	↑
		Hemoglobin subunit beta-2	**HBB2_RAT**	**78.91**	**12**	**1.000**	**2.653**	**2.653**	↑
		Prothymosin alpha	**PTMA_RAT**	**34.82**	**6**	**1.000**	**2.471**	**2.471**	↑
	Other (cont.)	**Parathymosin**	**PTMS_RAT**	**22.55**	**5**	**1.000**	**2.414**	**2.414**	↑

DH	Category	Protein	Accession no.	Cov(%)	Pep	Control : Control	EtOH : Control	Fold △	
		Ab2-417	**Q7TMC7_RAT**	**11.75**	**10**	**1.000**	**2.360**	**2.360**	↑
		Protein Vat1l - Vesicle Amine Transport 1 Like	**D3ZE32_RAT**	**8.41**	**3**	**1.000**	**2.111**	**2.111**	↑
		ATP-dependent (S)-NAD(P)H-hydrate dehydratase	D3ZLK9_RAT	12.84	3	1.000	1.970	1.970	↑
		Pyridoxal kinase	G3V647_RAT	41.03	12	1.000	1.968	1.968	↑
		Pdxp protein - pyridoxal phosphatase	B2GV79_RAT	24.66	6	1.000	1.948	1.948	↑
		SCO-spondin	SSPO_RAT	0.37	2	1.000	1.934	1.934	↑
		D-dopachrome decarboxylase	DOPD_RAT	50.85	9	1.000	1.889	1.889	↑
		Sulfated glycoprotein 1	SAP_RAT	8.48	10	1.000	1.799	1.799	↑
		Protein LOC100912106 - Programmed cell death 5	D4ADF5_RAT	28.80	7	1.000	1.781	1.781	↑
		Protein LOC100909983 - Acidic leucine-rich nuclear phosphoprotein 32 family member A	M0R9D0_RAT	17.96	6	1.000	1.763	1.763	↑
		Uncharacterized protein	D3ZWT8_RAT	29.92	3	1.000	1.735	1.735	↑
		Zero beta-globin (Fragment)	Q63011_RAT	81.51	22	1.000	1.727	1.727	↑
		Hemopexin	HEMO_RAT	5.00	2	1.000	1.724	1.724	↑
		Reticulocalbin-2	RCN2_RAT	29.38	11	1.000	1.687	1.687	↑
		Protein RGD1310819 - Similar to putative protein (5S487)	D3ZEA1_RAT	14.95	3	1.000	1.640	1.640	↑
		Ribonuclease UK114	UK114_RAT	67.15	13	1.000	1.625	1.625	↑
		Protein Naca - Nascent polypeptide-associated complex alpha subunit	M0R9L0_RAT	1.94	6	1.000	1.605	1.605	↑
		Cortactin	Q66HL2_RAT	19.25	17	1.000	1.510	1.510	↑
		Annexin A3	**ANXA3_RAT**	**17.28**	**5**	**1.000**	**0.233**	**4.286**	↓
		Protein LOC685544 - Hypothetical protein LOC685544	**D3ZQT2_RAT**	**0.00**	**2**	**1.000**	**0.460**	**2.175**	↓
		Protein RCG31390 (submitted name, UniProt)	**G3V9A3_RAT**	**23.79**	**3**	**1.000**	**0.479**	**2.089**	↓
		LOC681996 protein - Activator of Hsp90 ATPase activity 1	B0BN63_RAT	9.76	3	1.000	0.502	1.992	↓
		Uncharacterized protein	M0RCB1_RAT	8.33	2	1.000	0.565	1.769	↓

[The coverage percentage (**Cov %**) indicates the number of identified amino acids associated with that protein represented as a percentage of the total number of amino acids in that protein. The number of exclusive unique peptides (**Pep**) represents the number of unique peptide sequences associated with that protein

Table 6.6: Proteins with a fold change > 1.2 in the *dorsal hippocampus* of EtOH+MS-rats compared to control rats.

DH Category	Protein	Accession no.	Cov (%)	Pep	Control : Control	EtOH+MS : Control	Fold △	
Energy metabolism	Long-chain-fatty-acid--CoA ligase ACSBG1	ACBG1_RAT	4.44	3	1.000	1.392	1.392	↑
	Ndufa7 protein	A9UMV9_RAT	19.64	2	1.000	1.319	1.319	↑
	Glucose-6-phosphate isomerase	G6PI_RAT	18.10	3	1.000	1.256	1.256	↑
Redox regulation	Thioredoxin (Fragment)	R4GNK3_RAT	31.73	12	1.000	0.624	1.602	↓
Neurotransmission / signalling	Centaurin alpha	Q63629_RAT	13.84	8	1.000	1.335	1.335	↑
	Beta-arrestin-1	ARRB1_RAT	10.53	5	1.000	1.324	1.324	↑
	COP9 signalosome complex subunit 8	CSN8_RAT	23.44	3	1.000	1.277	1.277	↑
	Protein Nbea - neurobeachin (Fragment)	F1LXU4_RAT	1.59	2	1.000	1.260	1.260	↑
	Protein Rasal1 - RAS protein activator like 1 (GAP1 like) (Predicted)	D3ZHY9_RAT	3.50	2	1.000	1.215	1.215	↑
	Catenin beta-1	CTNB1_RAT	3.46	2	1.000	1.201	1.201	↑
	Synaptic vesicle glycoprotein 2B	SV2B_RAT	4.98	5	1.000	0.545	1.835	↓
	Serine/threonine-protein phosphatase PP1-gamma catalytic subunit	PP1G_RAT	23.84	6	1.000	0.675	1.481	↓
Protein synthesis	AXIN1 up-regulated 1 (Predicted)	D4AAK3_RAT	0.00	3	1.000	1.516	1.516	↑
	40S ribosomal protein S9	RS9_RAT	8.25	2	1.000	1.274	1.274	↑
	C-terminal-binding protein 1	CTBP1_RAT	6.74	2	1.000	1.272	1.272	↑
	60S ribosomal protein L31	RL31_RAT	31.20	4	1.000	1.262	1.262	↑
	Elongation factor 1-gamma	EF1G_RAT	20.37	12	1.000	1.250	1.250	↑
	Protein LOC683961 - similar to ribosomal protein S13	M0RCY2_RAT	18.06	2	1.000	1.206	1.206	↑
	Protein Srsf3 - Putative uncharacterized protein	Q0ZFS8_RAT	20.73	4	1.000	0.630	1.587	↓
	Protein Nars - Asparaginyl-tRNA synthetase	F1LPV0_RAT	7.35	3	1.000	0.634	1.578	↓
	Ring finger and SPRY domain containing 1	A1L1K9_RAT	2.43	2	1.000	0.692	1.445	↓
	Protein LZIC - Leucine zipper and CTNNBIP1 domain containing	LZIC_RAT	17.37	2	1.000	0.711	1.407	↓
	40S ribosomal protein S12	RS12_RAT	6.06	2	1.000	0.746	1.340	↓
	Protein Tardbp - Tar DNA binding protein	I6L9G6_RAT	8.07	3	1.000	0.748	1.338	↓
	Lupus La protein homolog	Q66HM7_RAT	5.78	2	1.000	0.752	1.331	↓
	Transcription initiation factor TFIID subunit 9B	TAF9B_RAT	6.20	2	1.000	0.776	1.289	↓

DH Category	Protein	Accession no.	Cov (%)	Pep	Control : Control	EtOH+MS : Control	Fold △	
Protein degradation	**IBR domain containing 1 (Predicted) - Ring finger protein 217**	**D4ABK2_RAT**	**5.99**	**3**	**1.000**	**2.097**	**2.097**	↑
	Proteasome (Prosome, macropain) 26S subunit, non-ATPase, 7 (Predicted)	D4AEH3_RAT	13.75	4	1.000	1.379	1.379	↑
	Protein Ube2o (Fragment) - Ubiquitin-conjugating enzyme E2O	F1M403_RAT	2.33	2	1.000	1.336	1.336	↑
	Proteasome subunit beta type-7	PSB7_RAT	14.08	6	1.000	1.207	1.207	↑
	Cystatin-B	CYTB_RAT	18.37	3	1.000	0.753	1.328	↓
	Ubiquilin-1	UBQL1_RAT	11.00	4	1.000	0.766	1.306	↓
	Charged multivesicular body protein 5	CHMP5_RAT	15.53	3	1.000	0.782	1.278	↓
Cytoskeletal / structural	**Laminin, alpha 5, isoform CRA_a**	**F1MAN8_RAT**	**0.51**	**3**	**1.000**	**2.528**	**2.528**	↑
	Isoform 2 of Dynamin-2	DYN2_RAT	13.91	4	1.000	1.538	1.538	↑
	Protein Abi2 - ABI interactor 2	F1LYA6_RAT	8.80	4	1.000	1.332	1.332	↑
	Tubulin alpha-1A chain	TBA1A_RAT	75.17	11	1.000	1.282	1.282	↑
	Kinesin heavy chain isoform 5A	F1M8F2_RAT	3.99	2	1.000	1.256	1.256	↑
	Protein Krtap9-1 - Keratin-associated protein 9-1	F1M294_RAT	33.33	2	1.000	1.250	1.250	↑
	Isoform 5 of Tropomyosin alpha-1 chain	TPM1_RAT	38.78	10	1.000	1.232	1.232	↑
	Actin-related protein 2/3 complex subunit 5-like protein	ARP5L_RAT	12.42	4	1.000	1.229	1.229	↑
	Transgelin	TAGL_RAT	16.42	2	1.000	0.736	1.359	↓
	Vimentin	G3V8C3_RAT	19.53	7	1.000	0.744	1.344	↓
	Kinesin-1 heavy chain	KINH_RAT	2.91	2	1.000	0.787	1.271	↓
Other	Protein Wdr47 - WD repeat-containing protein 47	G3V9M3_RAT	3.15	3	1.000	1.289	1.289	↑
	SCO-spondin	SSPO_RAT	0.37	2	1.000	1.279	1.279	↑
	Serum albumin	ALBU_RAT	24.84	42	1.000	0.799	1.251	↓
	Annexin A3	ANXA3_RAT	17.28	5	1.000	0.784	1.276	↓
	Protein Vat1l - Vesicle amine transport 1-like	D3ZE32_RAT	8.41	3	1.000	0.724	1.381	↓

[The coverage percentage (**Cov %**) indicates the number of identified amino acids associated with that protein represented as a percentage of the total number of amino acids in that protein. The number of exclusive unique peptides (**Pep**) represents the number of unique peptide sequences associated with that protein].

DISCUSSION

To our knowledge, this is the first study to use high throughput proteomic profiling techniques to identify and quantify proteins in the PFC and DH of adult SD rats subjected to prenatal-ethanol exposure. In addition, this is the first study to use iTRAQ and LC-MS to investigate protein changes in the rat brain after exposure to the combination of prenatal-ethanol exposure and early-life stress in the form of repeated maternal separation (3 hours/day, P2 - P14).

In the PFC the possibility of an additive effect of prenatal-ethanol exposure and maternal separation was suggested by the greater number of proteins that were differentially expressed in the PFC of EtOH+MS-rats relative to controls, compared to the PFC of MS- and EtOH-rats. In contrast, a greater number of proteins were altered in the DH of EtOH-rats relative to controls, compared to the DH of MS- and EtOH+MS-rat groups, indicating the possibility that maternal separation stress reduced the effects of prenatal-ethanol exposure on the DH.

In the PFC, early-life stress appeared to cause a downregulation of glycolysis and an upregulation of gluconeogenesis. Pyruvate kinase was decreased in the PFC of MS-rats relative to control rats. Pyruvate kinase converts phosphoenolpyruvate to pyruvate during the final step of glycolysis. Further, in the PFC of MS-rats, phosphoenolpyruvate carboxykinase was increased compared to controls. Phosphoenolpyruvate carboxykinase plays a significant role in gluconeogenesis by converting oxaloacetate to phosphoenolpyruvate. This result suggests a decreased capacity for glycolysis and an increased capacity for gluconeogenesis in the PFC of rats exposed to maternal separation (3 hours/day, P2 - P14). Gluconeogenesis in astrocytes provides an alternative source of glucose under times of stress and other pathological conditions (Yip et al., 2017). The observed increase in levels of NADH ubiquinone oxidoreductase subunit B10 (NDUFB10), a subunit of Complex I of the mitochondrial respiratory chain, in the PFC of MS-rats may represent increased capacity for mitochondrial oxidative phosphorylation.

The maternal separation model of depression has previously been shown to have decreased energy-related proteins in the PFC of adult male SD rats (Dimatelis et al., 2013). For example, creatine kinase B-type, aconitate hydratase, malate dehydrogenase and glucose-6-phosphate isomerase were downregulated in the PFC of adult SD rat exposed to repeated maternal separation stress (3 hours/day, P2 - P14) (Dimatelis et al., 2013). These differences may be due

to the age and treatment of the rats. In the present study rats underwent repeated maternal separation stress (3 hours/day, P2 - P14) and were then left undisturbed until sacrifice at P63. Whereas in the previous study rats exposed to maternal separation stress were treated with saline injections from P68 to P100 and sacrificed on P101 (Dimatelis et al., 2013). Again, this highlights the need to study neurochemistry on rats that have not been subjected to prior stress other than the model being investigated.

In EtOH-rats, NADH ubiquinone oxidoreductase subunit A7 (NDUFA7), a subunit of Complex I of the mitochondrial respiratory chain, was decreased in the PFC. This result is in agreement with previous studies in which a decreased capacity for ATP production was observed shortly after ethanol exposure (Xu et al., 2005; Chu et al., 2007; Sari et al., 2010b). A decreased number and volume of mitochondria as well as a reduction in respiratory chain activity was observed in the cerebrum of mice foetuses exposed to ethanol from GD6 to GD15 (Xu et al., 2005) and decreased ATP production was observed in cultured cerebellar neurons obtained from P1 Long-Evans rat pups exposed to gestational alcohol (Chu et al., 2007). Further, a proteomics study showed decreased levels of NADH dehydrogenase (ubiquinone) 1 alpha subcomplex subunit 9 (NDUFA9) and NADH-ubiquinone oxidoreductase 20 kDA subunit in whole foetal brains exposed to a 25 % ethanol-derived calorie liquid diet from GD7 - GD13. Our results demonstrate a long-term decrease in capacity for energy production in the PFC of rats exposed to prenatal-ethanol.

A greater number of energy-related proteins were altered in the PFC of EtOH+MS-rats than in the PFC of MS- and EtOH-rats. Citrate synthase and creatine kinase B-type were decreased in EtOH+MS-rats compared to controls. Citrate synthase is involved in the first step of the tricarboxylic acid cycle and creatine kinase produces phosphocreatine which can be used to generate ATP. Further, we observed greater levels of mitochondrial 2-oxoglutarate/malate carrier protein, and ATP synthase subunit alpha in the PFC of EtOH+MS-rats. This could represent increased capacity for mitochondrial oxidative phosphorylation of ADP and the production of reactive oxygen species in the PFC of rats exposed to the combination of prenatal-ethanol and maternal separation stress.

We also observed increased levels of phosphoglucomutase 2-like 1 and glycogenin in the PFC of EtOH+MS-rats. This may indicate increased energy storage in the form of glycogen in astrocytes and therefore represent resilience in the form of an energy buffer. Further, and

similar to the PFC of MS-rats, EtOH+MS-rats had decreased levels of pyruvate kinase and increased phosphoenolpyruvate carboxykinase, hence limiting the production of pyruvate from phosphoenolpyruvate and favoring gluconeogenesis (Magistretti and Allaman, 2015). In addition, similar to the PFC of EtOH-rats, EtOH+MS-rats had decreased levels of NDUFA7 in the PFC. These results demonstrate the combined effect of prenatal-ethanol exposure and maternal separation stress on the adult rat PFC.

Our results suggest a decreased capacity for glycolysis and an increased capacity for mitochondrial oxidative phosphorylation in the PFC of rats exposed to maternal separation stress. This may produce reactive oxygen species (Hüttemann et al., 2012; Magistretti and Allaman, 2015) and may lead to oxidative stress in the PFC of MS-rats. In addition, increased levels of microsomal glutathione S-transferase were observed in the PFC of these rats. Microsomal glutathione S-transferase decreases levels of GSH through the process of S-glutathionylation, a posttranslational modification, in response to oxidative stress to protect against further oxidative stress-induced damage (Townsend et al., 2009). However, an imbalance in enzymes towards favoring S-glutathionylation may suggest a decreased capacity to protect against oxidative stress due to continual depletion of GSH. Our results are similar to a previous study in which 2D electrophoreses and MALDI-TOF mass spectrometry analysis of the PFC of adult SD rats exposed to chronic unpredictable stress showed a dysregulation of energy and glutathione metabolism, including an increase in glutathione S-transferase, compared to controls (Yang et al., 2013). Our results, in conjunction with this previous study, suggest that the capacity to protect against oxidative stress in the PFC may be compromised in animal models of depression. In addition, increased levels of glutathione S-transferase may suggest increased levels of S-glutathionylated proteins in the PFC of rats exposed to maternal separation stress. S-glutathionylation results in the conjugation of GSH to target proteins which can alter their structure, function and cellular location (Xiong et al., 2011). Therefore, S-glutathionylation of kinases, phosphatases and transcription factors can change cell signalling processes and may serve as a regulator of signal transduction pathways (Xiong et al., 2011).

In the PFC of adult rats exposed to prenatal-ethanol we did not observe altered redox-regulating proteins. However, adult rats exposed to the combination of prenatal-ethanol and maternal

separation stress had a decreased capacity to protect against oxidative stress in the PFC due to low levels of superoxide dismutase and peroxiredoxin-6. Mitochondrial enzymes produce superoxide which can be converted to hydrogen peroxide by superoxide dismutase then reduced to water by peroxiredoxin (Fukai and Ushio-Fukai, 2011). EtOH+MS-rats had greater levels of ATP synthase subunit alpha, suggesting an increased capacity for mitochondrial oxidative phosphorylation and hence increased production of reactive oxygen species. Therefore, our results suggest that the PFC of rats exposed to both prenatal-ethanol and early-life stress may also be susceptible to oxidative stress-induced cell damage.

Several proteins related to neurotransmission or signalling were shown to be differentially expressed in the PFC of MS-rats relative to controls. For example, β-arrestin-1 and neuroplastin were decreased in the PFC of MS-rats. β-arrestin has been shown to facilitate G-protein coupled receptor- (GPCR) stimulation of the mitogen activated protein kinase- (MAPK) signalling pathway (Tohgo et al., 2002) and to facilitate the internalization of β-adrenergic receptors (Nygaard et al., 2013). Neuroplastin is a cell adhesion molecule involved in several neuronal processes, specifically the trafficking of signalling partners (Beesley et al., 2014). Lower levels of β-arrestin in the PFC of MS-rats may indicate an increased number of β-adrenergic receptors in the cellular membrane. β-adrenergic receptors may have become insensitive to the stress hormone norepinephrine. Therefore, less internalization of β-adrenergic receptors may represent a compensatory mechanism in order to mitigate the insensitivity of these receptors. Further, norepinephrine can stimulate glycogenolysis in astrocytes to provide lactate for neurons (Magistretti and Allaman, 2015). Hence, an increased number of β-adrenergic receptors at the cellular membrane my also indicate a mechanism by which glycogen storage is used to generate energy for neurons since our results suggest a decreased capacity for glycolysis in the PFC of these rats.

Only 4 proteins related to neurotransmission or signalling were shown to be differentially expressed in the PFC of EtOH-rats compared to controls. EtOH-rats had decreased levels of sepiapterin reductase in the PFC. Sepiaterin reductase is involved in the final step of tetrahydrobiopterin (BH_4) production. Sepiaterin reductase deficient mice have been shown to have lower levels of the neurotransmitters DA, norepinephrine and serotonin (Yang et al., 2006). Decreased levels of sepiaterin reductase therefore suggests decreased levels of

dopamine, norepineprhine and serotonin in the PFC of EtOH-rats which is similar to Sari *et al*. (2010) who found decreased levels of DA in mice foetuses on GD13 after exposure to prenatal-ethanol (25 % ethanol-calorie derived liquid-diet) from GD7 - GD13.

In the PFC of EtOH+MS-rats, levels of α-synuclein and synapsin 2 were decreased while levels of disks large homolog 4 (PSD-95) were increased in the PFC of EtOH+MS-rats. These findings are in agreement with previous studies in which maternal separation (3 hours/day, P2 - P14) alone decreased synapsin 1 in the PFC of adult SD rats (Dimatelis et al., 2013) and prenatal-ethanol was shown to increase PSD-95 in the cerebral cortex of SD rats (6 weeks of age) exposed to prenatal-ethanol (2 - 4 g/kg/day, 25 v/v %) from GD7 to GD16 (Kim et al., 2010). In addition, glutamine synthetase was decreased in the PFC of EtOH+MS-rats. This is in agreement with a previous study in which decreased glutamine synthetase activity was observed in hippocampal slices obtained from P21 Wistar rats after exposure to ethanol throughout gestation and lactation via the dams drinking water (2.5 - 20 % ethanol, GD5 - P0 - P21) (Cesconetto et al., 2016). Glutamine synthetase is found in astrocytes and protects against excitotoxicity by converting excess glutamate to glutamine (Suárez et al., 2002). Glutamine is then shuttled to neurons and converted back to glutamate to replenish vesicular stores (Magistretti and Allaman, 2015). Therefore, decreased levels of glutamine synthetase may suggest lower levels of glutamine and impaired recycling of glutamate. Further, glutamine synthetase is inactivated by oxidative stress which may occur after prenatal ethanol exposure (Brocardo et al., 2011, 2012). In the present study we observed an increased capacity for oxidative phosphorylation of ADP in the PFC of these rats and hence increased production of reactive oxygen species in conjunction with a decreased capacity to protect against oxidative stress. Therefore, decreased glutamine synthetase and further potential inactivation by oxidative stress may indicate an increased susceptibility of PFC neurons in EtOH+MS-rats to excitation- and oxidative stress-induced neuronal damage and impaired glutamate recycling. This is consistent with Brolese *et al*. (2015) who showed decreased glutamate uptake and lower levels of GSH in juvenile Wistar rats exposed to prenatal-ethanol (10 % v/v beer solution). In the present study we observed a similar result in rats exposed to prenatal-ethanol in addition to maternal separation stress.

In addition to the above signalling related proteins, β-arrestin-1 was decreased in the PFC of EtOH+MS-rats as in the PFC of MS- and EtOH-rats. This result further highlights the combined effect of maternal separation stress and prenatal-ethanol exposure in the PFC.

Dynamin isoforms were altered by repeated maternal separation stress in the PFC. Isoform 3 of dynamin-like 120 kDa protein was increased in the PFC of MS-rats whereas isoform 2 of dynamin was decreased relative to controls. Dynamin plays a role in the fission step of clathrin-mediated synaptic vesicle endocytosis and therefore, dynamin is crucial for normal synaptic transmission (Raimondi et al., 2011). Our results are in agreement with previous studies in which dynamin has been shown to be altered by chronic mild stress and antidepressant treatment (Carboni, 2015). Dynamin 1 has been shown to be decreased in the hippocampus of adult male Flinders resistant line rats after repeated maternal separation (3 hours/day, P2 - P14) (Piubelli et al., 2011). Changes in dynamin may indicate impaired synaptic vesicle cycling and altered neurotransmission signalling in the PFC of MS-rats.

In addition, *c*-fos-induced growth factor (vascular endothelial growth factor D, VEGF-D), tubulin alpha-1A and myelin basic protein isoform 2 were decreased in the PFC of MS-rats. Our results are in agreement with 2 previous studies: C57BL/6J mice that were separated from the dam for 4 hours/day from P2 - P5, 8 hours/day from P6 - P16 and weaned on P17 showed decreased myelination and white matter integrity in the PFC relative to control mice (not separated and weaned in P23) at 30 days of age (Carlyle et al., 2017). Myelin basic protein was decreased in the PFC of SD rats on P21 and P60 after 3 weeks of maternal separation (3 hours/day, P3 - P21) (Yang et al., 2017). The early-postnatal period, during which maternal separation stress occurred, is characterized by increased neuronal growth and myelination (Dobbing and Sands, 1979). The mechanism of myelination may be significantly altered during this period and these results suggest that deficits in the myelination process persist into adulthood since a difference in myelination markers occurs after rats have been returned to a normal environment. Recent findings suggest that oxidative stress impairs the maturation and proliferation of oligodendrocytes which leads to a decrease in myelination (Monin et al., 2015; Maas et al., 2017). Mice with genetically-induced decreased levels of GSH and hence decreased antioxidant capacity had lower levels of myelin basic protein (Monin et al., 2015). Our results are in agreement with these previous findings. Our results suggest an increased production of reactive oxygen species and a decreased capacity to protect against oxidative stress which may have lead to deficits in oligodendrocyte maturation and hypomyelination as suggested by lower levels of myelin basic protein in the PFC of MS-rats relative to control rats. Decreased myelination may be indicative of impaired signal conduction (Douglas Fields, 2015)

and increased energy requirement of the neuronal networks in the PFC which may lead to further production of reactive oxygen species. Further, myelin may also provide metabolic support in the form of aerobic glycolysis and lactate to sections of the axon (Bercury and Macklin, 2015). Therefore, hypomyelination may indicate decreased metabolic support which may further impair signal conduction in the PFC of MS-rats.

In the PFC of EtOH-rats, iTRAQ and LC-MS identified VEGF-D and isoform 2 of dynamin to be decreased relative to control rats. VEGF-D is involved in angiogenesis (Marconcini et al., 1999). Ethanol exposure during early development has previously been shown to alter the vasculature in the brain (Jégou et al., 2012). Whole foetal brains of mice exposed to prenatal ethanol (9 %, 0.5 - 3 g/kg) from GD13 - GD19 had altered cortical microvasculature organization and decreased levels of VEGF and VEGF receptors (Jégou et al., 2012). Micro-hemorrhages and neuronal cell death have also been observed in the cerebral cortex when ethanol was administered to SD rats during the early-postnatal period (P3 - P5) via ethanol inhalation chambers (± 8 g/dl, 3 hours/day) (Welch et al., 2017).

In the PFC of rats exposed to the combination of prenatal-ethanol and maternal separation stress we observed a decrease in endocytosis- and myelin-related proteins. Levels of clathrin light chain A and isoform 2 of dynamin 2 were decreased in the PFC of EtOH+MS-rats. These proteins are involved in clathrin-mediated endocytosis of synaptic vesicles (Raimondi et al., 2011). These results suggest impaired synaptic vesicle recycling which may indicate improper neurotransmission. In addition, lower levels of the myelin-associated proteins, myelin basic protein and 2',3'-cyclic-nucleotide 3'-phosphodiesterase (CNPase), suggest further impairments in mechanisms of signal transduction.

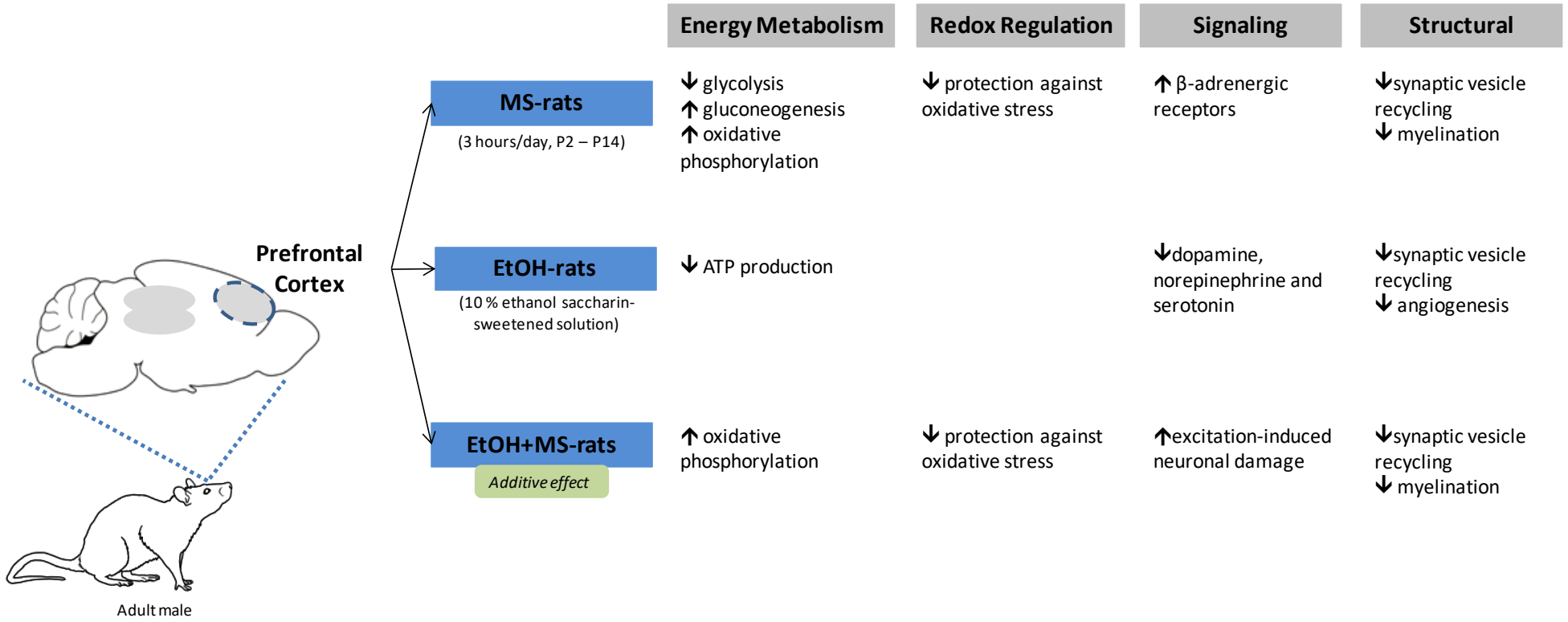

Figure 6.10: Summary of proteomic results in the *prefrontal cortex* after maternal separation stress, prenatal-ethanol exposure and the combination of both insults.

A large number of proteins were identified to be differentially expressed in the DH of EtOH-rats compared to the DH of MS- and EtOH-rats. Therefore, with regards to the proteins identified in the DH of EtOH-rats, the discussion will focus on proteins that differed by a fold change greater than 1.5.

In the DH of MS-rats we observed decreased levels of hexokinase-1, glycerol-3-phosphate dehydrogenase [NAD(+)] (cytoplasmic), ADP/ATP translocase and cytochrome *c* oxidase subunit 2. Hexokinase converts glucose to glucose-6-phosphate, therefore our results suggest there is decreased glycolytic activity in the DH. Further, decreased levels of glycerol-3-phosphate dehydrogenase [NAD(+)] (cytoplasmic), a component of the electron transport chain and cytochrome *c* oxidase subunit 2, the catalytic core of cytochrome *c* oxidase which mediates ATP synthesis (Srinivasan and Avadhani, 2012) suggests a decreased capacity for ATP production. Moreover, less ATP is transported out of the mitochondria due to decreased levels of ADP/ATP translocase. These results suggest a decreased capacity for energy production in the DH of rats exposed to maternal separation stress. Our results do not agree with a previous study in which maternal separation was shown to increase energy-related proteins in the ventral regions of the hippocampus (Marais et al., 2009). For example, ATP synthase subunit alpha and subunit d were increased in the VH of adult SD rats exposed to repeated maternal separation (3 hours/day, P2 - P14) (Marais et al., 2009). However, in this previous study the VH was analyzed and rats underwent daily saline-injections from P40 - P82 , the stress of which may account for the differential results.

In the DH of EtOH-rats, glucose-6-phosphate isomerase (phosphohexose isomerase), glyceraldehyde-3-phosphate dehydrogenase (GAPDH), phosphoglycerate kinase-1 and pyruvate kinase were decreased compared to controls rats. Further, lactate dehydrogenase, which converts pyruvate to lactate, was decreased in the DH of EtOH-rats. Our results indicate decreased capacity for glycolysis in the DH of adult rats exposed to prenatal-ethanol. Our results are in agreement with Tan *et al*. (2013) who found decreased activity of hexokinase, pyruvate kinase and lactate dehydrogenase in the whole brains of chicken embryos exposed to ethanol. However, acyl carrier, acyl-CoA binding protein and ATP synthase subunit delta were increased in the DH of EtOH-rats. This result suggests an increased capacity for ATP production via lipid metabolism after prenatal-ethanol.

Fewer energy-related proteins were differentially expressed in the DH of EtOH+MS-rats compared the number of proteins identified in the DH of EtOH-rats. NDUFA7, long chain fatty acid-CoA ligase and glucose-6-phosphate isomerase (phosphohexose isomerase) were increased in the DH of rats exposed to both prenatal-ethanol and maternal separation. Greater levels of NDUFA7 suggest increased oxidative phosphorylation which agrees with results found in the DH of EtOH-rats. However, our results also suggest increased glycolytic capacity in the DH of EtOH+MS-rats which is opposite to the suggested result in the DH of MS- and EtOH-rats. This result may indicate a possible reducing effect of maternal separation stress when coupled with prenatal-ethanol exposure.

In the DH of rats exposed to 3 hours of daily maternal separation stress from P2 - P14 our results suggest an increased capacity to protect against oxidative stress. Levels of glutathione S-transferase alpha-3 were greater in the DH of MS-rats compared to controls. Glutathione S-transferase alpha-3 belongs to the major cytosolic subfamily of transferases and aids in detoxification by binding GSH to electrophilic target compounds and therefore reduces oxidative stress (Laborde, 2010). This is in agreement with a previous study in which redox-related proteins were increased in the ventral portion of the hippocampus of adult SD rats exposed to maternal separation stress (3 hours/day, P2 - P14) (Marais et al., 2009). However, we also observed decreased levels of microsomal gluthathione S-transferase in the DH of these rats relative to controls. Microsomal glutathione S-transferase is part of the smaller membrane-associated proteins in eicosanoid and glutathione metabolism (MAPEG) subfamily of glutathione transferase (Hayes et al., 2005) and is membrane-bound (Nebert and Vasiliou, 2004). The different cellular locations, cytosolic versus membrane-bound, may contribute to the opposing result.

Several proteins relating to redox regulation were upregulated in the DH of EtOH-rats compared to controls. For example, lactoglutathione lyase, superoxide dismutase, thioredoxin and peroxiredoxin-2 were increased in the DH of these rats. Network analysis of protein-protein interactions identified sulfur metabolism and glutathione metabolism as significantly enriched processes. Therefore, our results suggests increased capacity for S-glutathionylation and GSH production (Townsend et al., 2009; Xiong et al., 2011). Superoxide dismutase and peroxiredoxin decrease levels of superoxide which is produced by mitochondrial enzymes

(Fukai and Ushio-Fukai, 2011) and thioredoxin is an important antioxidant (Arnér and Holmgren, 2000). Therefore, our results suggest an increased capacity to protect against oxidative stress in the DH of adult rats exposed to prenatal-ethanol. However, when prenatal-ethanol exposure was coupled with maternal separation stress we observed lower levels of thioredoxin in the DH of EtOH+MS-rats compared to controls. Decreased levels of thioredoxin suggest a decreased capacity to protect against oxidative stress-induced damage (Arnér and Holmgren, 2000) in the DH of adult rats exposed to both prenatal-ethanol and early-life stress in the form of repeated maternal separation.

In the DH of MS-rats, β-arrestin-1 was increased compared to control rats. Over expression of β-arrestin leads to increased P-ERK1/2 bound to β-arrestin in the cytosol thus decreasing translocation of P-ERK1/2 to the nucleus (Tohgo et al., 2002). In addition, glutamate receptor 1 and PSD-95 were decreased in the DH of MS-rats relative to controls. PSD-95 is a major postsynaptic density protein which has previously been shown to be altered by maternal separation stress. Our results agree with a study in which 21 day old SD rats separated twice daily for 3 hours from P2 - P21 had decreased levels of PSD-95 as well as decreased spine density in hippocampal neurons (Ohta et al., 2017). Our results suggest that this disruption in neuronal spine development in the hippocampus may persist into adulthood.

In the DH of EtOH-rats more proteins related to neurotransmission and signalling were differentially expressed from control rats compared to the number of proteins identified in the PFC of these rats. We observed increased levels of calmodulin, neuromodulin, neurogranin and calcineurin (> 1.2 fold change) and decreased levels of calcium/calmodulin-dependent kinase II. Calcium enters neurons through glutamate-mediated activation of NMDA receptors or voltage-gated calcium channels and can bind to calmodulin, a calcium-binding protein. Calcium induces a conformational change in calmodulin which enables it to activate calcium/calmodulin-dependent kinase II, adenylyl cyclase and calcineurin. Neuromodulin and neurogranin regulate levels of calmodulin under basal conditions and release calmodulin upon increased intracellular concentration of calcium (Xia and Storm, 2005). In the present study, increased levels of calmodulin suggest increased activity of adenylyl cyclase and therefore increased activity of ERK1/2 via RAS-1 and 2 (Xia and Storm, 2005). Therefore, this result is

in agreement with *Chapter 5*, in which we observed increased levels of P-ERK1/2 to ERK1/2 in the DH of male EtOH-rats.

Further, in the DH of EtOH-rats we also observed increased levels of calbindin and calretinin and decreased levels of β-arrestin-1 compared to control rats. Calbindin and calretinin are calcium-binding proteins found in GABAergic neurons (Finesmith and Favero, 2014; Smiley et al., 2015). These results differ to previous findings which showed that Swiss Webster mice (P0) exposed to prenatal-ethanol from GD7 till the DOB had lower levels of calbindin in the cerebellum compared to control rats (Finesmith and Favero, 2014). In addition, a reduction in calretinin-labelled neurons (subtype of GABAergic neurons) was observed in the cortex of adult mice exposed to 2 doses of ethanol (2.5 g/kg) on P7 (Smiley et al., 2015). These differences may be due to the different species of rodent and brain area investigated. However, these results in addition to the findings in the present study demonstrate the susceptibility of these calcium-binding proteins to prenatal-ethanol exposure.

β-arrestin and neurobeachin were decreased in the DH of EtOH-rats. However, the combination of prenatal-ethanol exposure and maternal separation stress increased levels of β-arrestin and neurobeachin in the DH of EtOH+MS-rats relative to controls. This result demonstrates the possibility that maternal separation stress may reduce the effects of prenatal-ethanol exposure on the DH.

In the DH of MS-rats, laminin alpha 5 (isoform CRA_a) and clathrin light chain A were increased relative to control rats. In addition myelin proteolipid protein and CNPase were decreased in the DH of these rats. CNPase is a myelin-associated enzyme and a marker of mature-oligodendrocytes (Myllykoski et al., 2016). Escitalopram (anti-depressant) treatment of rats exposed to 3 hours/day of maternal separation stress (P2 - P14) increased levels of CNPase relative to vehicle-treated controls (Dimatelis et al., 2013). These results implicate CNPase in the mechanism of antidepressant-treatment and therefore suggest the involvement of CNPase in the mechanisms of early-life stress. This is supported by the decreased levels of myelin-associated proteins observed in the DH of MS-rats in the study. However, in contrast to the PFC of MS-rats, we observed an increased capacity to protect against oxidative stress in the DH of these rats. Hence early-life stress-induced deficits in markers of myelination in the DH may be due to mechanisms other than redox imbalance impairing oligodendrocytes. However, similar to the PFC of MS-rats, decreased markers of myelination may suggested

impaired conduction velocity and altered timing of signal transmission (Douglas Fields, 2015) in the DH of rats exposed to 3 hours/day of maternal separation stress from P2 - P14.

In the DH of EtOH-rats we observed a greater number of structural proteins altered by prenatal-ethanol than in the PFC of these rats. For example, high molecular weight-microtubule-associated protein and microtubule-associated proteins 4 and 6 were increased in the DH of EtOH-rats. Further, tubulin alpha-1A, and actin cytoplasmic 2 were decreased in the DH of EtOH-rats relative to control rats. Decreased levels of total actin and tubulin have been observed in primary cultures of hippocampal neurons obtained from rat embryos on GD16 that were then exposed to 30 mM ethanol for 14 days (Romero et al., 2010). This result agrees with the results found in the present study. Prenatal-ethanol exposure induces persistent changes in cytoskeletal-related proteins which may indicate dysfunction in neuronal structure and therefore impaired neuronal function.
Further, clathrin light chains A and B were increased in the DH of EtOH-rats. Clathrin light chains produce the clathrin-coat surrounding synaptic vesicles and therefore function in endocytosis and synaptic vesicle recycling. Clathrin was decreased in cultured adult hippocampal rat neurons after chronic ethanol exposure demonstrating the susceptibility of clathrin to ethanol (Marín et al., 2010).

Another endocytosis-related protein, isoform 2 of dynamin was increased in the DH of EtOH+MS-rats, along with tubulin alpha-1A. Dynamin is involved in the fission step of clathrin-mediated endocytosis (Raimondi et al., 2011) Therefore, changes in dynamin may indicate impaired synaptic vesicle cycling and altered neurotransmission signalling in the PFC of EtOH+MS-rats.

This study highlights the multifaceted effects of maternal separation stress and prenatal-ethanol exposure on the developing brain. Proteins involved in mechanisms of glycolysis, gluconeogenesis, antioxidant capacity, endocytosis, vesicle recycling and myelination were implicated. Further, our results suggest that these early-developmental insults have differential effects on the PFC and DH. In the PFC, we observed an additive effect of the combination of prenatal-ethanol and maternal separation. Whereas in the DH, this combination appeared to reduce the prenatal-ethanol-induced protein changes. These proteomic profiles provide

valuable insight into the long-term effects of early-life stress and prenatal-ethanol exposure and suggest that no single mechanism can account for the behavioural deficits observed in FASD and the associated-psychological deficits.

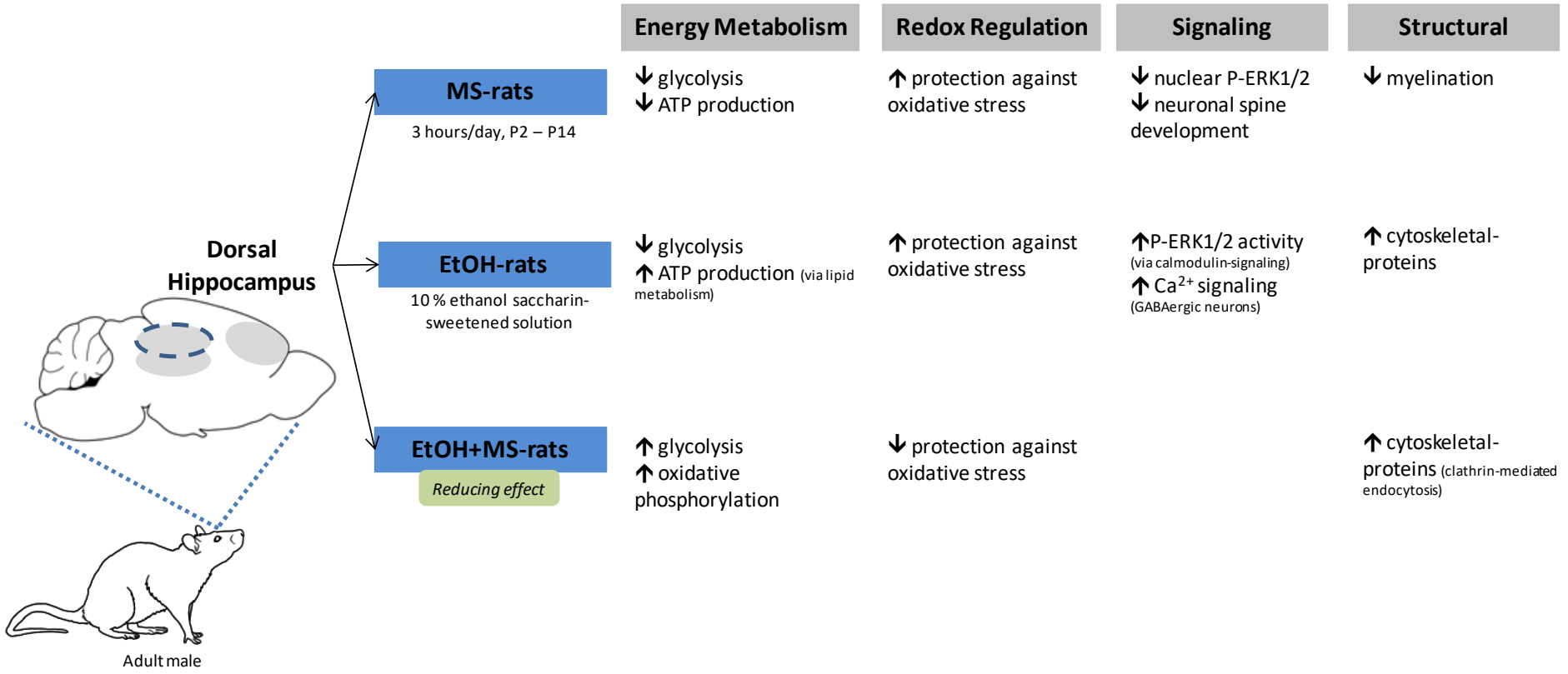

Figure 6.11: Summary of proteomic results in the *dorsal hippocampus* after maternal separation stress, prenatal-ethanol exposure and the combination of both insults.

CHAPTER 7: OVERALL DISCUSSION AND CONCLUSION

The work presented in this thesis investigated the long-term effects of ethanol exposure during early development on the rat brain and behaviour using 2 animal models of FASD. We utilized, for the first time, high throughput proteomic techniques to investigate protein changes in adolescent and adult rat brains exposed to ethanol during early development. Moreover, the brain regions of interest, the PFC, DH and VH, were analyzed separately and therefore the proteomic profiles obtained provide invaluable insight into the long-term effects of ethanol exposure on protein changes in these functionally distinct brain regions. We further utilized a PDE1 inhibitor, vinpocetine, to further investigate the mechanism of action of this drug and its effects on neural plasticity-related proteins, such as components of the ERK1/2- and GSK3β-signalling cascades. We showed that vinpocetine treatment has the potential to restore early-postnatal ethanol-induced protein changes and that these changes extend beyond neural plasticity. Additional maternal separation stress was incorporated into an animal model of FASD to account for the likelihood of experiencing further early-life adversity after *in utero* alcohol exposure. This showed a significant and specific interaction between prenatal-ethanol exposure and maternal separation stress on the rat brain and behaviour and highlights the importance of accounting for possible early-life stress in animal models of FASD. This thesis described novel approaches to investigating the effects of *in utero* alcohol exposure on the brain and in addition, highlights methodological complexities when modelling FASD in rodents.

EARLY-POSTNATAL ETHANOL EXPOSURE

In *Experiments 1 and 2*, we investigated the effects of ethanol exposure on the developing brain during the third trimester equivalent developmental stage using an animal model of FASD. We hypothesized that adolescent rats exposed to early-postnatal ethanol would take longer to find the hidden platform in the MWM and have reduced levels of neural plasticity-related proteins, specifically components of the ERK1/2- and GSK3β-signalling cascades, in the PFC and DH. Adolescent rats exposed to ethanol during the early-postnatal period did not show overt behavioural impairments such as hyperactivity in the OFT or spatial learning and memory deficits in the MWM and therefore did not phenotypically represent FASD. This may have been due to the presence of environmental enrichment which has previously been shown to

reduced ethanol-induced changes (Hannigan et al., 1993; Francis et al., 2002). However, Sluyter et al. (2005) did not observe learning and memory deficits in mice exposed to ethanol during the early stages of development. This was accompanied by a lack of structural changes in the hippocampus identified by West, (1981) and West & Hamre, (1985) who demonstrated massive sprouting of the mossy fibre terminals after early-postnatal ethanol exposure (7 – 7.5 g/kg/day, P1 – P10). Therefore, it would have been interesting to measure structural changes in order to visualize deficits in neural plasticity on a structural level and further to establish whether the lack of cognitive deficits observed in these studies were accompanied by a lack of ethanol-induced structural changes in the rat brain. However, early-postnatal ethanol exposure had significant effects on protein levels in the adolescent rat brain that included those related to neural plasticity in addition to proteins related to energy metabolism and redox regulation. These results highlight the broad effects of early-postnatal ethanol exposure on the brain despite the lack of overt behavioural deficits in the behavioural tests used. Further, our results provide insight into the region-specific early-postnatal ethanol-induced protein changes in the brain. For example, we found that levels of P-ERK1/2 were decreased in the PFC and elevated in the DH of rats exposed to early-postnatal ethanol. Further, proteomic analysis of the VH demonstrated that exposure to ethanol during the early-postnatal period decreased the expression of proteins related to energy metabolism, redox regulation, signalling, protein metabolism and cytoskeletal structure compared to non-exposed control rats. These results showed a decreased capacity for energy production in the VH which is in agreement with previous studies that reported decreased activity of the respiratory chain when investigating the *short-term* effects of *prenatal-ethanol* exposure on cultured neuronal cells and foetuses (Xu et al., 2005; Chu et al., 2007; Sari et al., 2010b). Our results suggest that early-postnatal ethanol exposure induces persistent effects that may reduce the capacity for energy production in the long-term. Further, early-postnatal ethanol exposure decreased proteins involved in redox regulation thereby decreasing the capacity to protect against oxidative stress. These results indicate an increased susceptibility to oxidative stress-induced damage and a shift from the normal cellular redox-state after early-postnatal ethanol exposure in the VH. Prenatal-ethanol exposure paradigms have indicated the potential for oxidative stress (Patten et al., 2013b) and this may be as an indirect result of ethanol-induced dysregulation of mitochondrial function (Brocardo et al., 2011). In addition, early-postnatal ethanol exposure decreased levels of myelin proteolipid protein which could lead to ethanol-induced impairments in myelination. Myelination of axons is essential for rapid conduction of electrical signals necessary for

optimal functioning. Importantly, myelin provides metabolic support and decreases the energy-cost of signal transduction (Bercury and Macklin, 2015). A compensatory mechanism may be evidenced by the early-postnatal ethanol-induced increase in several beneficial proteins such as those involved in taurine production, structural integrity and cell migration, differentiation and survival. Our results clearly demonstrate that early-postnatal ethanol exposure can induce significant protein changes in the PFC and hippocampus, which span a wide range of functional categories. The lack of behavioural deficits made it impossible to describe the neurochemistry in terms of behavioural phenotype. However, ethanol exposure during early development can result in a spectrum of changes ranging from mild to severe, and there can also be environmental factors that contribute to the absence of behavioural deficits. Therefore, the lack of overt behavioural deficits may be due factors such as environmental enrichment, choice of behavioural tests, repeated behavioural testing and handling which could have masked behavioural deficits (Blokland et al., 2012; Bohacek et al., 2015; Deutsch-Feldman et al., 2015). Therefore, the ethanol-induced protein changes in the brain may be of significance and be more pronounced in animals that do display behavioural deficits.

We further investigated the effects of early-postnatal ethanol exposure on the PFC and DH of rats that did not undergo treatment or behavioural testing. Therefore, the second novel proteomic profile obtained was not influenced by the stress of handling during treatment and behavioural testing (Bohacek et al., 2015; Deutsch-Feldman et al., 2015) and largely represents the effects of ethanol exposure during the third trimester equivalent developmental stage on proteins in the PFC and DH. We again observed region-specific effects of early-postnatal ethanol exposure. In the PFC there was an increased capacity for energy production whereas in the DH, energy-related proteins were decreased compared to non-exposed controls. Further, a greater number of proteins were altered by early-postnatal ethanol exposure in the DH compared to the PFC which suggests the DH might be more susceptible to the detrimental effects of early-postnatal ethanol exposure. More specifically, the PFC of rats exposed to early-postnatal ethanol that did not undergo behavioural testing, was characterized by an increased capacity for oxidative phosphorylation coupled with a decreased antioxidant capacity which suggests a greater potential for oxidative stress-induced damage. However, previous studies, in which ethanol was administered *prenatally* and the *short-term* effects of ethanol exposure were investigated using neuronal cultures and foetuses, demonstrated a decreased capacity for energy production (Xu et al., 2005; Chu et al., 2007; Sari et al., 2010b). However, decreased

capacity to protect against oxidative stress after ethanol exposure during early development agrees with previous studies (Brocardo et al., 2011). Further, our results suggest decreased inhibitory control and long-term impairments in neuronal spine development, as suggested by decreased levels of glutamate decarboxylase 2 and PSD-95 respectively, in the PFC after early-postnatal ethanol exposure. The DH of rats exposed to early-postnatal ethanol was characterized by a decreased capacity for ATP production, and similar to the PFC, a decreased capacity to protect against oxidative stress due to reduced capacity to remove GSH from S-glutathionylated proteins (de-glutathionylation), as suggested by decreased levels of glutaredoxin. Moreover, increased levels of S-glutathionylated proteins, may have significantly altered signal transduction pathways since the addition of GSH to target proteins can alter the structure, function and cellular location of proteins (Xiong et al., 2011). In addition, there was evidence that could lead to altered levels of glutamate, impaired intracellular signalling and changes in genetic components as shown by increased glutamine synthetase, decreased calmodulin and protein kinase C, and downregulated histone proteins, respectively, in the DH of rats exposed to early-postnatal ethanol. These ethanol-induced protein changes could lead to a deficit in the functionality of both the PFC and DH after early-postnatal ethanol exposure and therefore these alterations may contribute to the observed inattentiveness, learning and psychological deficits reported in the literature.

VINPOCETINE

In *Experiment 1*, rats were exposed to ethanol during the early-postnatal period and treated with the PDE1 inhibitor, vinpocetine, in order to investigate the mechanism of vinpocetine action and its potential to restore ethanol-induced behavioural and neural plasticity changes via the ERK1/2- and GSK3β-signalling pathways. Further, we described the wide-range of proteins altered by vinpocetine treatment of early-postnatal ethanol-exposed adolescent rats in order to elucidate molecular mechanisms underlying the long-term effects of early-postnatal ethanol exposure and PDE1 inhibition that go beyond the neural plasticity proteins related to ERK1/2- and GSK3β-signalling.

In this study, adolescent rats exposed to early-postnatal ethanol did not show overt behavioural deficits however, there were significant ethanol-induced protein changes in the PFC, DH and VH. Importantly, vinpocetine treatment of rats exposed to early-postnatal ethanol reversed the ethanol-induced decrease in levels of P-ERK1/2 and increased the amount of MKP-1 in the

PFC compared to controls. Further, vinpocetine reduced the ethanol-induced increase in P-PERK1/2 activity and reduced the inhibitory activity of GSK3β in the DH. The synaptosomal marker, synaptophysin, was also increased in the DH of ethanol-exposed rats treated with vinpocetine. Vinpocetine treatment further restored several proteins in the VH of rats exposed to early-postnatal ethanol. For example, myelin proteolipid protein and several signalling-related proteins were increased in rats treated with vinpocetine. These results point towards restored signal conduction and intracellular-signalling. In addition, protein synthesizing proteins were also increased by vinpocetine treatment compared to non-treated ethanol-exposed rats. Our results are in agreement with previous studies in which vinpocetine was suggested to increase levels of cAMP and cGMP via PDE inhibition thereby activating intracellular-signalling cascades and subsequently transcription factors such as CREB and the serum response factor (SRF) (Medina, 2011) therefore increasing protein synthesis. However, our results were limited by the number of differentially expressed proteins identified by iTRAQ and LC-MS. Vinpocetine has previously been shown to increase blood flow and metabolic activity, as well as protect against reactive oxygen species (Nivison-Smith *et al*., 2017). However, proteomic analysis did not provide enough evidence to demonstrate these specific effects of PDE1 inhibition or clarify a mechanism independent of PDE inhibition. A second limitation, although in line with the aim of this study, there was no experimental group consisting of saline-control rats treated with vinpocetine. This additional experimental group would have made it possible to distinguish the effects of early-postnatal ethanol exposure from vinpocetine treatment on the observed protein changes. Therefore, the protein alterations observed in rats exposed to early-postnatal ethanol and treated with vinpocetine must be interpreted with caution. In addition, further investigation is necessary because the rats used in the study did not display overt behavioural deficits even though early-postnatal ethanol exposure and treatment with vinpocetine altered proteins closely related to learning and memory.

Our results provide insight into the mechanism of vinpocetine action in that it reversed early-postnatal ethanol exposure-induced changes in the rat brain. The mechanism of vinpocetine action involves proteins closely related to neural plasticity however, proteomic analysis demonstrated the wide-range of protein alterations that go beyond the ERK1/2 and GSK3β signaling pathways. Therefore, vinpocetine treatment of rats exposed to early-postnatal ethanol in conjunction with proteomic analysis has the potential to identify novel treatment targets to reduce the effects of ethanol exposure during early development on the brain.

PRENATAL-ETHANOL EXPOSURE

A voluntary drinking paradigm was used for the second animal model of FASD (*Experiments 3 and 4)*) in order to investigate the effects of prenatal-ethanol exposure on behaviour and neural plasticity-related proteins involved in P-ERK1/2 and GSK3β-signalling in adult rats. We did not observe overt learning and memory deficits using this prenatal-ethanol exposure model of FASD (*ad libitum* access to a 10 % ethanol saccharin-sweetened solution, throughout gestation). The lack of behavioural deficits may be due to the timing, pattern and quantity ethanol exposure. Further, with specific reference to the NOT, the difference in behavioural outcomes between our results and previous studies may be attributed to the different time-intervals between, and duration of, the habituation, familiarization and novel object test trials. Further, increasing the complexity of the NOT may expose learning and memory deficits induced by prenatal-ethanol exposure since object recognition has been shown to be impaired with increase memory load (4 - 6 novel objects) (Sannino et al., 2012). Further, the NOT relies heavily on spontaneous exploratory behaviour (Ennaceur and Delacour, 1988) which was affected by prenatal-ethanol and maternal separation stress. Therefore, the use of the NOT as a test of cognition may have not been appropriate in this study and a word of caution must be added when reporting prenatal-ethanol- and/or maternal separation stress-induced cognitive deficits with the NOT. However, this model of FASD was otherwise characterized by deficits in weight gain throughout development, increased exploratory activity in a novel environment and a heightened negative emotional state and therefore demonstrated some of the phenotypic characteristics of FASD. To our knowledge this is the first study to demonstrate increased number and duration of 22 kHz ultrasonic vocalizations in adult SD rats exposed to prenatal-ethanol.

Prenatal-ethanol exposure similarly increased the ratio of P-ERK1/2 to ERK1/2 in the PFC and DH of adult rats However, in contrast, early-postnatal ethanol reduced ERK1/2 activity in the PFC and increased ERK1/2 activity in the DH. This result highlights the differential effects of ethanol exposure on the same protein in different brain regions. This difference may be due to a number of different factors such as age of the animals at tissue collection (adolescent vs. adult) and ethanol-exposure paradigm (prenatal- vs. early-postnatal ethanol exposure). Moreover, rats in the early-postnatal study had increased ERK1/2 activity in the DH, this may have been due to the fact that these rats had undergone a week of training in the MWM prior

to tissue collection. This result highlights the possible effects of behavioural tests on neurochemistry (behavioural testing vs. naïve-rats).

Proteomic analysis revealed brain region-specific prenatal-ethanol-induced protein changes. Proteomic analysis of the PFC of male (naïve) rats exposed to prenatal-ethanol showed evidence of decreased energy production and impaired synaptic-vesicle cycling. The DH of these rats had a decreased capacity for glycolytic activity, increased protection against oxidative stress and evidence for increased P-ERK1/2 activity via calmodulin-signalling (which is in agreement with the Western blot results). These results demonstrate the wide-range of effects of prenatal-ethanol and highlight different proteins in distinct brain areas. It is important to separately analyze brain areas because distinct brain regions have different protein expression profiles due to their different functional roles (Peterson *et al.,* 2015) Therefore, the same protein may be differentially expressed in distinct regions (Sharma *et al.,* 2015). Further, processes regulating protein expression may be differentially susceptible to ethanol- and stress-induced changes depending on brain region which will influence levels of the same proteins between brain areas. In addition, these proteins changes largely reflect prenatal-ethanol-induced alterations in the brain since Western blot and proteomic analysis was conducted on naïve-rats and therefore the results were not influenced by handling- and behavioural test-induced stress.

PRENATAL-ETHANOL EXPOSURE AND MATERNAL SEPARATION

To account for possible early-life adversity after *in utero* alcohol exposure, we investigated the effects of additional maternal separation stress (3 hours/day, P2 -P14) after prenatal-ethanol exposure. In agreement with previous studies rats exposed to maternal separation stress exhibited a negative emotional state by emitting longer and more 22 kHz ultrasonic vocalizations (Portfors, 2007; Dimatelis et al., 2012, 2015). In addition, maternally separated rats showed increased exploratory behaviour in response to a novel environment and increased levels of P-ERK1/2 in the PFC and DH, in parallel to rats exposed to prenatal-ethanol. Further, the PFC of maternally separated rats was characterized by an increased capacity for oxidative phosphorylation of ADP but a decreased capacity to protect against oxidative stress. This increased susceptibility towards oxidative stress-induced damage may have impaired oligodendrocyte function and contributed to the evidence for decreased myelination in the PFC

of these rats. An opposite result was observed in the DH of maternally separated rats, indicating region-specific effects of maternal separation stress on the brain. The DH of maternally separated rats was characterized by a decreased capacity for ATP production and an increased antioxidant capacity. However, there was also evidence that could lead to impaired myelination in the DH as shown by decreased levels of myelin proteolipid protein. Therefore, myelination may have been impaired by a mechanism other than oxidative stress-induced damage to oligodendrocytes. In addition, proteomic analysis suggested impaired spine development and decreased nuclear levels of P-ERK1/2 in the DH of these rats. Therefore, even though Western blot analysis indicated increased levels of P-ERK1/2 it may not translocate to the nucleus to activate downstream transcription factors. These protein changes may have impaired the functionality of the PFC and DH and contributed towards the negative affective state observed in MS-rats.

Interestingly, subsequent maternal separation stress after prenatal-ethanol exposure increased prenatal-ethanol-induced weight loss and reduced exploratory activity and P-ERK1/2 to levels similar to that of control rats. Therefore, indicating that maternal separation stress reduced the effects of prenatal-ethanol exposure. However, additional maternal separation stress did not reduce the observed heightened negative emotional state since rats exposed to the combination of prenatal-ethanol and maternal separation stress also exhibited more and longer 22 kHz ultrasonic vocalizations. Twenty-two kilohertz vocalizations have not been measured in adult rats exposed to the combination of prenatal-ethanol and maternal separation stress therefore, this is an additional novel demonstration. This result suggests that maternal separation stress reduces the effects of prenatal-ethanol exposure in a behavioural-dependent manner. Therefore, indicating a significant *and specific* interaction between prenatal-ethanol exposure and maternal separation stress on behaviour. In support of this *specific* interaction, the combination of prenatal-ethanol exposure and maternal separation stress did not enhance (or reduce) the behaviour of EtOH- and MS-rats in the EPM, OFT and FST, as hypothesized. Western blot analysis demonstrated a similar interaction between maternal separation stress and prenatal-ethanol exposure on the P-ERK1/2 to ERK1/2 ratio. Subsequent maternal separation reduced the prenatal-ethanol-induced increase in P-ERK1/2 in both the PFC and DH of male and female naïve-rats. Maternal separation stress has previously been shown to interact with P-ERK1/2 and specifically, maternal separation stress prevented exercise-induced increase in P-ERK1/2 activity (Makena et al., 2012). Therefore, maternal separation stress subsequent to prenatal-

ethanol exposure may similarly prevent the prenatal-ethanol-induced increase in P-ERK1/2 activity. However, the basis for this interaction deserves further investigation since the interaction between prenatal-ethanol exposure and maternal separation was opposite to the effect on levels of the synaptosomal marker, synaptophysin, in the PFC of adult female rats. In these rats, P-ERK1/2 activity may have been increased due to a compensatory mechanism in order to increase signaling capacity in the presence of reduced structural integrity.

Proteomic analysis showed and additive effect of the developmental insults on proteins changes in the PFC and a reducing effect on protein changes in the DH. More specifically, the PFC of rats exposed to both prenatal-ethanol and maternal separation stress had an increased capacity for oxidative phosphorylation but a decreased capability to protect against oxidative stress. There was also additional evidence that could lead to decreased myelination, impaired synaptic vesicle recycling and increased susceptibility to excitation-induced neuronal damage, as shown by decreased levels of myelin basic protein and CNPase, clathrin and dynamin, and glutamine synthetase respectively, in the PFC of these rats. The DH of rats exposed to both prenatal-ethanol and maternal separation stress was characterized an increased capacity for oxidative phosphorylation and a decreased capacity to protect against oxidative stress. Therefore, suggesting the potential for oxidative stress-induced damage in both brain regions.

Our results highlight a significant interaction between prenatal-ethanol exposure and early-life stress on the brain and behaviour. More specifically, maternal separation stress reduced the effects of prenatal-ethanol exposure. However, future investigations may wish to further develop prenatal-ethanol exposure coupled with maternal separation stress as a model of FASD, with particular focus, and possible manipulation of, P-ERK1/2 signaling in the brain.

FUTURE CONSIDERATIONS

During these experiments there were several experimental limitations which should be taken into consideration when pursuing future investigations into the effects of ethanol exposure during early-development on the brain. Specifically, the experimental design lacked focus and multiple variables were manipulated which made it challenging to compare results between the early-postnatal and prenatal-ethanol exposure paradigms. Although, this highlighted the difficulty in modelling the multifaceted disorder, FASD. Future studies should develop one paradigm of ethanol-exposure, specifically prenatal-ethanol exposure coupled with additional early-life stress, since the results presented clearly indicate the need to account for early-life

adversity in animal models of FASD. In addition, although performing neurochemical analyses in naïve-rats is beneficial, in that the results largely represent the model being tested because there are no additional effects of behavioural tests and handling, it can be difficult to describe neurochemical changes in terms of behaviour. Therefore, if possible future studies should perform neurochemical analyses on both naïve- and behavioural animals. And importantly, male and female rats should be used throughout all the experiments. Further, the results presented in this thesis provide evidence for altered P-ERK1/2 activity after ethanol-exposure during early-development and an interaction between prenatal-ethanol exposure and maternal separation stress on P-ERK1/2 activity and synaptophysin levels. Therefore, in order to provide insight into the basis of this interaction future studies may focus on this signaling pathway and in addition measure structural changes at the synaptic level. In addition, future studies may choose to perform neurochemical analyses on brain regions other than the hippocampus and prefrontal cortex, such as the striatum, in order to broaden the investigation into the effects of ethanol exposure during early development on the brain. Further it is important to note that different brain regions, in particular the prefrontal cortex, have multiple and sometimes antagonistic functions. Therefore, it is important to investigate wide spread ethanol-induced changes and investigate the brain as a whole in order to fully understand the mechanisms underlying the persistent deficits observed after *in utero* alcohol exposure.

CONCLUSION

Our results highlight the wide-spread differential effects of ethanol exposure during early-development on the brain and behaviour. These studies highlight the importance of timing, quantity and pattern of ethanol exposure as well as the importance of age at behavioural testing and tissue analysis, therefore demonstrating the difficulty and complexity of modeling FASD. In addition, our results highlight the importance of performing neurochemical analysis on rats that have not been subjected to prior stressors (injections, behavioural tests, handling), other than the model being investigated and further, to separately analyze functionally distinct brain regions.

Ethanol exposure during early development induced a wide-range of protein changes in the rat brain that may potentially underlie the observed behavioural deficits. These proteins include those closely-related to neural plasticity such as ERK1/2 and GSK3β, as well as proteins

involved in mechanisms of energy metabolism, redox regulation, redox signaling, cell signalling and cytoskeletal structure. The novel proteomic profiles depicted in these studies provide valuable insight into the long-term wide-spread effects of ethanol exposure during early development on the brain.

We showed that the mechanism of vinpocetine treatment does involve proteins closely related to neural plasticity however proteomic analysis demonstrates additional protein changes that go beyond the P-ERK1/2- and GSK3β-signalling cascades. These results provide a better understanding of the mechanisms of vinpocetine treatment. In addition, the use of vinpocetine, a PDE1 inhibitor, in conjunction with large-scale proteomic analysis has the potential to identify novel targets to reduce the effects of ethanol exposure during early-development on the brain.

We demonstrated, for the first time, an interaction between prenatal-ethanol exposure and early-life stress (maternal separation) on exploratory behaviour in response to a novel environment and the levels of P-ERK1/2 in the PFC and DH of adult rats. Subsequent maternal separation stress reduced prenatal-ethanol-induced changes in exploratory behaviour and levels of P-ERK1/2. However, this interaction was not observed with anxiety- and depression-like behaviours. This highlights a significant and specific interaction between prenatal-ethanol exposure and maternal separation on the brain and behaviour. More importantly, this interaction highlights the importance of accounting for the possible effects of early-life adversity when modeling FASD.

This thesis provides a better understanding of the effects of ethanol exposure during early development on the brain. The results presented in this thesis contribute valuable insight to the field of FASD and the animal models used to study this multifaceted disorder.

ETHICAL APPROVAL

Ethics authorization was obtained from the University of Cape, the Faculty of Health Sciences Animal Research Ethics Committee [Project numbers: 014/002 and 015/004].

All experimental procedures aimed to minimize the pain and suffering of the animals used and adhered to the guideline set out in the South African National Standard: The Care and Use of Animals for Scientific Purpose (2008).

We were certified by the South African Veterinary Council (SAVC) to monitor all animals under our care and perform the necessary procedures.

REFERENCES

Adinoff B (2004) Neurobiologic processes in drug reward and addiction. Harv Rev Psychiatry 12:305–320.

Adnams CM, Kodituwakku PW, Hay A, Molteno CD, Viljoen D, May PA (2001) Patterns of Cognitive-Motor Development in Children With Fetal Alcohol Syndrome From a Community in South Africa. Alcohol Clin Exp Res 25:557–562.

Aggarwal K, Choe LH, Lee KH (2006) Shotgun proteomics using the iTRAQ isobaric tags. Briefings Funct Genomics Proteomics 5:112–120.

Agnish ND, Kellert KA (1997) The Rationale for Culling of Rodent Litters. Fundam Appl Toxicol 38:2–6.

Agoglia AE, Sharko AC, Psilos KE, Holstein SE, Reid GT, Hodge CW (2015) Alcohol alters the activation of ERK1/2, a functional regulator of binge alcohol drinking in adult C57BL/6J mice. Alcohol Clin Exp Res 39:463–475.

Aisa B, Tordera R, Lasheras B, Del Río J, Ramírez MJ (2007) Cognitive impairment associated to HPA axis hyperactivity after maternal separation in rats. Psychoneuroendocrinology 32:256–266.

Akbarian S, Davis RJ (2010) Keep the “phospho” on MAPK, be happy. Nat Med 16:1187–1188.

Alberry B, Singh SM (2016) Developmental and behavioral consequences of early life maternal separation stress in a mouse model of fetal alcohol spectrum disorder. Behav Brain Res 308:94–103.

Alleva E, Caprioli A, Laviola G, Superiore I (1989) Litter Gender Composition Affects Maternal Behavior of the Primiparous Mouse Dam (Mus musculus). J Comp Psychol 103:83–87.

An L, Yang Z, Zhang T (2013) Imbalanced Synaptic Plasticity Induced Spatial Cognition Impairment in Male Offspring Rats Treated with Chronic Prenatal Ethanol Exposure. Alcohol Clin Exp Res 37:763–770.

An L, Zhang T (2013) Spatial cognition and sexually dimorphic synaptic plasticity balance impairment in rats with chronic prenatal ethanol exposure. Behav Brain Res 256:564–574.

An L, Zhang T (2015) Prenatal ethanol exposure impairs spatial cognition and synaptic plasticity in female rats. Alcohol 49:581–588.

Anand P, Stamler JS (2012) Enzymatic mechanisms regulating protein S-nitrosylation : implications in health and disease. J Mol Med 90:233–244.

Anda RF, Whitfield CL, Felitti VJ, Chapman D, Edwards VJ, Dube SR, Williamson DF (2002) Adverse Childhood Experiences, Alcoholic Parents, and Later Risk of Alcoholism and Depression. Psychiatr Serv 53:1–9.

Andersen SL, Teicher MH (2000) Sex differences in dopamine receptors and their relevance to ADHD. Neurosci Biobehav Rev 24:137–141.

Antunes M, Biala G (2012) The novel object recognition memory: Neurobiology, test procedure, and its modifications. Cogn Process 13:93–110.

Arnér ESJ, Holmgren A (2000) Physiological functions of thioredoxin and thioredoxin reductase. Eur J Biochem 267:6102–6109.

Bailey BN, Delaney-Black V, Covington CY, Ager J, Janisse J, Hannigan JH, Sokol RJ (2004) Prenatal exposure to binge drinking and cognitive and behavioral outcomes at age 7 years. Am J Obstet Gynecol 191:1037–1043.

Banuelos C, Ryan J G, Montgomery KS, Fincher AS, Wang H, Frye GD, Setlow B, Bizon JL (2012) Altered spatial learning and delay discounting in a rat model of human third trimester binge ethanol exposure. Behav Pharmacol 23:54–65.

Barbier E, Pierrefiche O, Vaudry D, Vaudry H, Daoust M, Naassila M (2008) Long-term alterations in vulnerability to addiction to drugs of abuse and in brain gene expression after early life ethanol exposure. Neuropharmacology 55:1199–1211.

Beesley PW, Herrera-Molina R, Smalla KH, Seidenbecher C (2014) The Neuroplastin adhesion molecules: Key regulators of neuronal plasticity and synaptic function. J Neurochem 131:268–283.

Bekdash RA, Zhang C, Sarkar DK (2013) Gestational Choline Supplementation Normalized Fetal Alcohol-Induced Alterations in Histone Modifications , Gene Expression in b -Endorphin-Producing POMC Neurons of the Hypothalamus. Alcohol Clin Exp Res 37:1133–1142.

Bercury KK, Macklin WB (2015) Dynamics and mechanisms of CNS myelination. Dev Cell 32:447–458.

Berry FB, Mirzayans F, Walter MA (2006) Regulation of FOXC1 Stability and Transcriptional Activity by an Epidermal Growth Factor-activated Mitogen-activated Protein Kinase Signaling Cascade. 281:10098–10104.

Bessa JM (2009) A trans-dimensional approach to the behavioral aspects of depression. Front Behav Neurosci 3:1–7.

Beurel E, Grieco SF, Jope RS (2015) Glycogen synthase kinase-3 (GSK3): Regulation, actions, and diseases. Pharmacol Ther 148:114–131.

Bevins RA, Besheer J (2006) Object recognition in rats and mice: a one-trial non-matching-to-sample learning task to study "recognition memory." Nat Protoc 1:1306–1311.

Bian Y, Yang L, Wang Z, Wang Q, Zeng L, Xu G (2015) Repeated three-hour maternal separation induces depression-like behavior and affects the expression of hippocampal plasticity-related proteins in C57BL/6N mice. Neural Plast 2015.

Blokland A, Ten Oever S, van Gorp D, van Draanen M, Schmidt T, Nguyen E, Krugliak A, Napoletano A, Keuter S, Klinkenberg I (2012) The use of a test battery assessing affective behavior in rats: order effects. Behav Brain Res 228:16–21.

Boehme F, Gil-Mohapel J, Cox A, Patten A, Giles E, Brocardo PS, Christie BR (2011) Voluntary exercise induces adult hippocampal neurogenesis and BDNF expression in a rodent model of fetal alcohol spectrum disorders. Eur J Neurosci 33:1799–1811.

Bohacek J, Manuella F, Roszkowski M, Mansuy IM (2015) Hippocampal gene expression induced by cold swim stress depends on sex and handling. Psychoneuroendocrinology 52:1–12.

Boschen KE, Criss KJ, Palamarchouk V, Roth TL, Klintsova AY (2015) Effects of developmental alcohol exposure vs. intubation stress on BDNF and TrkB expression in the hippocampus and frontal cortex of neonatal rats. Int J Dev Neurosci 43:16–24.

Bradley CA, Peineau S, Taghibiglou C, Nicolas CS, Whitcomb DJ, Bortolotto ZA, Kaang B-K, Cho K, Wang YT, Collingridge GL (2012) A pivotal role of GSK-3 in synaptic plasticity. Front Mol Neurosci 5:1–11.

Brady ML, Allan AM, Caldwell KK (2012) A Limited Access Mouse Model of Prenatal Alcohol Exposure that Produces Long-Lasting Deficits in Hippocampal-Dependent Learning and Memory. Alcohol Clin Exp Res 36:457–466.

Brady ML, Diaz MR, Iuso A, Everett JC, Valenzuela CF, Caldwell KK (2013) Moderate Prenatal Alcohol Exposure Reduces Plasticity and Alters NMDA Receptor Subunit Composition in the Dentate Gyrus. J Neurosci 33:1062–1067.

Broadbent NJ, Squire LR, Clark RE (2004) Spatial memory, recognition memory, and the hippocampus. Proc Natl Acad Sci U S A 101:14515–14520.

Brocardo PS, Boehme F, Patten A, Cox A, Gil-Mohapel J, Christie BR (2012) Anxiety- and depression-like behaviors are accompanied by an increase in oxidative stress in a rat model of fetal alcohol spectrum

disorders: Protective effects of voluntary physical exercise. Neuropharmacology 62:1607–1618.

Brocardo PS, Gil-Mohapel J, Christie BR (2011) The role of oxidative stress in fetal alcohol spectrum disorders. Brain Res Rev 67:209–225.

Brolese G, Lunardi P, De Souza DF, Lopes FM, Leite MC, Gonçalves CA (2015) Pre-and postnatal exposure to moderate levels of ethanol can have long-lasting effects on hippocampal glutamate uptake in adolescent offspring. PLoS One 10:1–13.

Brudzynski SM (2005) Principles of rat communication: Quantitative parameters of ultrasonic calls in rats. Behav Genet 35:85–92.

Brys I, Pupe S, Bizarro L (2014) Attention, locomotor activity and developmental milestones in rats prenatally exposed to ethanol. Int J Dev Neurosci 38:161–168.

Burd L, Blair J, Dropps K (2012) Prenatal alcohol exposure, blood alcohol concentrations and alcohol elimination rates for the mother, fetus and newborn. J Perinatol 32:652–659.

Burden MJ, Andrew C, Saint-amour D, Meintjes EM, Molteno CD, Hoyme HE, Robinson LK, Khaole N, Nelson CA, Jacobson JL, Jacobson SW (2009) The Effects of Fetal Alcohol Syndrome on Response Execution and Inhibition : An Event-Related Potential Study. 33:1994–2004.

Canales L, Gambrell C, Chen J, Neal RE (2013) Prenatal alcohol exposure alters the cerebral cortex proteome in weanling rats. Reprod Toxicol 39:69–75.

Caprara DL, Klein J, Koren G (2006) Diagnosis of fetal alcohol spectrum disorder (FASD): Fatty acid ethyl esters and neonatal hair analysis. Ann Ist Super Sanita 42:39–45.

Carboni L (2015) The contribution of proteomic studies in humans , animal models , and after antidepressant treatments to investigate the molecular neurobiology of major depression. :889–898.

Carlyle BC, Duque A, Kitchen RR, Bordner KA (2017) Maternal separation with early weaning : A rodent model providing novel insights into neglect associated developmental deficits. 24:1401–1416.

Carr CP, Martins CMS, Stingel AM, Lemgruber VB, Juruena MF (2013) The Role of Early Life Stress in Adult Psychiatric Disorders. J Nerv Ment Dis 201:1007–1020.

Castagné V, Moser P, Roux S, Porsolt RD (2010) Rodent models of depression: forced swim and tail suspension behavioral despair tests in rats and mice. Curr Protoc Pharmacol Chapter 5:Unit 5.8.

Cesconetto PA, Andrade CM, Cattani D, Domingues JT, Parisotto EB, Filho DW, Zamoner A (2016) Maternal Exposure to Ethanol During Pregnancy and Lactation Affects Glutamatergic System and Induces Oxidative Stress in Offspring Hippocampus. Alcohol Clin Exp Res 40:52–61.

Chao M V. (2003) Neurotrophins and their receptors: A convergence point for many signalling pathways. Nat Rev Neurosci 4:299–309.

Chater-diehl EJ, Laufer BI, Castellani CA, Alberry BL (2016) Alteration of Gene Expression, DNA Methylation, and Histone Methylation in Free Radical Scavenging Networks in Adult Mouse Hippocampus following Fetal Alcohol Exposure. PLoS One 11:1–25.

Chen M-F, Huang T-Y, Kuo Y-M, Yu L, Chen H, Jen CJ (2013) Early postinjury exercise reverses memory deficits and retards the progression of closed-head injury in mice. J Physiol 591:985–1000.

Chen Y, Baram TZ (2016) Toward Understanding How Early-Life Stress Reprograms Cognitive and Emotional Brain Networks. Neuropsychopharmacology 41:197–206.

Choi KW, Watt MH, Skinner D, Kalichman SC (2015) “Wine you get every day, but a child you can’t replace”: The perceived impact of parental drinking on child outcomes in a South African township. J Child Adolesc Ment Heal 27:173–187.

Chu J, Tong M, Monte SM (2007) Chronic ethanol exposure causes mitochondrial dysfunction and oxidative

stress in immature central nervous system neurons. Acta Neuropathol 113:659–673.

Clements KM, Smith LM, Reynolds JNJ, Overton PG, Thomas JD, Napper RM (2012) Early postnatal ethanol exposure: Glutamatergic excitotoxic cell death during acute withdrawal. Neurophysiology 44:376–386.

Cohen SJ, Stackman RW (2015) Assessing rodent hippocampal involvement in the novel object recognition task . A review. Behav Brain Res 285:105–117.

Converse AK, Moore CF, Holden JE, Ahlers EO, Moirano JM, Larson JA, Resch LM, DeJesus OT, Barnhart TE, Nickles RJ, Murali D, Christian BT, Schneider ML (2014) Moderate-Level Prenatal Alcohol Exposure Induces Sex Differences in Dopamine D1 Receptor Binding in Adult Rhesus Monkeys. Alcohol Clin Exp Res 38:2934–2943.

Creeley CE, Dikranian KT, Johnson SA, Farber NB, Olney JW (2013) Alcohol-induced apoptosis of oligodendrocytes in the fetal macaque brain. Acta Neuropathol Commun 1:1–11.

Crockford D, Turjman N, Allan C, Angel J (2010) Thymosin B4: Structure, function, and biological properties supporting current and future clinical applications. Ann N Y Acad Sci 1194:179–189.

Cullen CL, Burne THJ, Lavidis N a., Moritz KM (2014) Low Dose Prenatal Alcohol Exposure Does Not Impair Spatial Learning and Memory in Two Tests in Adult and Aged Rats. PLoS One 9:1–9.

Cullen CL, Burne THJ, Lavidis NA, Moritz KM (2013) Low Dose Prenatal Ethanol Exposure Induces Anxiety-Like Behaviour and Alters Dendritic Morphology in the Basolateral Amygdala of Rat Offspring. PLoS One 8:1–12.

Dalva MB, McClelland AC, Kayser MS (2007) Cell adhesion molecules: signalling functions at the synapse. Nat Rev Neurosci 8:206–220.

Daniels WMU, Pietersen CY, Carstens ME, Stein DJ (2004) Maternal separation in rats leads to anxiety-like behavior and a blunted ACTH response and altered neurotransmitter levels in response to a subsequent stressor. Metab Brain Dis 19:3–14.

Daskalakis NP, Kloet ER De, Yehuda R, Malaspina D, Kranz TM (2015) Early Life Stress Effects on Glucocorticoid - BDNF Interplay in the Hippocampus. Front Mol Neurosci 8:1–13.

Davis S, Vanhoutte P, Pages C, Caboche J, Laroche S (2000) The MAPK/ERK cascade targets both Elk-1 and cAMP response element-binding protein to control long-term potentiation-dependent gene expression in the dentate gyrus in vivo. J Neurosci 20:4563–4572.

Desbonnet L, Garrett L, Clarke G, Kiely B, Cryan JF, Dinan TG (2010) Effects of the probiotic Bifidobacterium infantis in the maternal separation model of depression. Neuroscience 170:1179–1188.

Deutsch-Feldman M, Picetti R, Seip-Cammack K, Zhou Y, Kreek MJ (2015) Effects of handling and vehicle injections on adrenocorticotropic and corticosterone concentrations in Sprague-Dawley compared with Lewis rats. J Am Assoc Lab Anim Sci 54:35–39.

Dimatelis JJ, Stein DJ, Russell VA (2012) Behavioral changes after maternal separation are reversed by chronic constant light treatment. Brain Res 1480:61–71.

Dimatelis JJ, Stein DJ, Russell VA (2013) Chronic exposure to light reverses the effect of maternal separation on proteins in the prefrontal cortex. J Mol Neurosci 51:835–843.

Dimatelis JJ, Vermeulen IM, Bugarith K, Stein DJ, Russell VA (2015) Female rats are resistant to developing the depressive phenotype induced by maternal separation stress. Metab Brain Dis.

Dimatelis JJ, Vermeulen IM, Bugarith K, Stein DJ, Russell VA (2016) Female rats are resistant to developing the depressive phenotype induced by maternal separation stress. Metab Brain Dis 31:109–119.

Dobbing J, Sands J (1979) Comparative aspects of the brain growth spurt. Early Hum Dev 311:79–83.

Donald KA, Eastman E, Howells FM, Adnams C, Riley EP, Woods RP, Narr KL, Stein DJ (2015a) Neuroimaging

effects of prenatal alcohol exposure on the developing human brain: a magnetic resonance imaging review. Acta Neuropsychiatr 27:251–269.

Donald KA, Roos A, Fouche J-P, Koen N, Howells FM, Woods RP, Zar HJ, Narr KL, Stein DJ (2015b) A study of the effects of prenatal alcohol exposure on white matter microstructural integrity at birth. Acta Neuropsychiatr 27:197–205.

Douglas Fields R (2015) A new mechanism of nervous system plasticity: activity-dependent myelination. Nat Rev Neurosci 16:756–767.

Dringen R (2000) Metabolism and functions of glutathione in brain. Prog Neurobiol 62:649–671.

DuPont CM, Coppola JJ, Kaercher RM, Lindquist DH (2014) Impaired trace fear conditioning and diminished ERK1/2 phosphorylation in the dorsal hippocampus of adult rats administered alcohol as neonates. Behav Neurosci 128:187–198.

Duthie KA, Osborne LC, Foster LJ, Abraham N (2007) Proteomics Analysis of Interleukin (IL)-7-induced Signaling Effectors Shows Selective Changes in IL-7R 449F Knock-in T Cell Progenitors. Mol Cell proteomics 6:1700–1710.

El Khoury A, Gruber SHM, Mørk A, Mathé A a (2006) Adult life behavioral consequences of early maternal separation are alleviated by escitalopram treatment in a rat model of depression. Prog Neuropsychopharmacol Biol Psychiatry 30:535–540.

Elibol-Can B, Kilic E, Yuruker S, Jakubowska-Dogru E (2014) Investigation into the effects of prenatal alcohol exposure on postnatal spine development and expression of synaptophysin and PSD95 in rat hippocampus. Int J Dev Neurosci 33:106–114.

Ennaceur A, Delacour J (1988) A new one-trial test for neurobiological studies of memory in rats . 1: Behavioral data. Behav Brain Res 31:47–59.

Fabricius K, Wörtwein G, Pakkenberg B (2008) The impact of maternal separation on adult mouse behaviour and on the total neuron number in the mouse hippocampus. Brain Struct Funct 212:403–416.

Famy C, Streissguth AP, Unis AS (1998) Mental illness in adults with fetal alcohol syndrome or fetal alcohol effects. Am J Psychiatry 155:552–554.

Fanselow MS, Dong H (2010) Are the Dorsal and Ventral Hippocampus Functionally Distinct Structures? Neuron 65:7–19.

Faravelli C (2012) Childhood stressful events, HPA axis and anxiety disorders. World J Psychiatry 2:13–25.

Feldmann A, Amphornrat J, Schönherr M, Winterstein C, Möbius W, Ruhwedel T, Danglot L, Nave K-A, Galli T, Bruns D, Trotter J, Krämer-Albers E-M (2011) Transport of the major myelin proteolipid protein is directed by VAMP3 and VAMP7. J Neurosci 31:5659–5672.

Fidalgo S, Skipper C, Takyi A, McIver A, Tsiligkaridis T, Quadir A, Gard PR (2017) Low-dose chronic prenatal alcohol exposure abolishes the pro-cognitive effects of angiotensin IV. Behav Brain Res 329:140–147.

Filgueiras CC, Krahe TE, Medina AE (2010) Phosphodiesterase type 1 inhibition improves learning in rats exposed to alcohol during the third trimester equivalent of human gestation. Neurosci Lett 473:202–207.

Finesmith D, Favero C (2014) Prenatal ethanol exposure affects calbindin expression in an FASD mouse model. J Young Investig 26:17–23.

Flak AL, Su S, Bertrand J, Denny CH, Kesmodel US, Cogswell ME (2014) The Association of Mild, Moderate, and Binge Prenatal Alcohol Exposure and Child Neuropsychological Outcomes: A Meta-Analysis. Alcohol Clin Exp Res 38:214–226.

Francis DD, Diorio J, Plotsky PM, Meaney MJ (2002) Environmental enrichment reverses the effects of maternal separation on stress reactivity. J Neurosci 22:7840–7843.

Fuglestad AJ, Whitley ML, Carlson SM, Boys CJ, Eckerle JK, Fink BA, Wozniak JR (2015) Executive functioning deficits in preschool children with Fetal Alcohol Spectrum Disorders. Child Neuropsychol 21:716–731.

Fukai T, Ushio-Fukai M (2011) Superoxide dismutases: role in redox signaling, vascular function, and diseases. AntioxidRedox Signal 15:1583–1606.

Gil-Mohapel J, Boehme F, Patten A, Cox A, Kainer L, Giles E, Brocardo PS, Christie BR (2011) Altered adult hippocampal neuronal maturation in a rat model of fetal alcohol syndrome. Brain Res 1384:29–41.

Godin EA, O'Leary-Moore SK, Khan AA, Parnell SE, Ament JJ, Dehart DB, Johnson BW, Allan Johnson G, Styner MA, Sulik KK (2010) Magnetic resonance microscopy defines ethanol-induced brain abnormalities in prenatal mice: Effects of acute insult on gestational day 7. Alcohol Clin Exp Res 34:98–111.

Goggin SL, Caldwell KK, Cunningham LA, Allan AM (2014) Prenatal alcohol exposure alters p35, CDK5 and GSK3β in the medial frontal cortex and hippocampus of adolescent mice. Toxicol Reports 1:544–553.

Goodlett CR, Peterson SD (1995) Sex differences in vulnerability to developmental spatial learning deficits induced by limited binge alcohol exposure in neonatal rats. Neurobiol Learn Mem 64:265–275.

Granato A, Palmer LM, De Giorgio A, Tavian D, Larkum ME (2012) Early exposure to alcohol leads to permanent impairment of dendritic excitability in neocortical pyramidal neurons. J Neurosci 32:1377–1382.

Grasso DJ, Ford JD, Briggs-Gowan MJ (2013) Early life trauma exposure and stress sensitivity in young children. J Pediatr Psychol 38:94–103.

Gunton AN, Sanchez-arias JC, Carmona-wagner EO, Wicki-stordeur LE, Swayne LA (2017) Upregulation of inflammatory mediators in the ventricular zone after cortical stroke. 1600092:9–10.

Hamilton GF, Hernandez IJ, Krebs CP, Bucko PJ, Rhodes JS (2017) Neonatal alcohol exposure reduces number of parvalbumin-positive interneurons in the medial prefrontal cortex and impairs passive avoidance acquisition in mice deficits not rescued from exercise. Neuroscience 352:52–63.

Hamilton GF, Jablonski SA, Schiffino FL, St. Cyr SA, Stanton ME, Klintsova AY (2014) Exercise and environment as an intervention for neonatal alcohol effects on hippocampal adult neurogenesis and learning. Neuroscience 265:274–290.

Hamilton GF, Whitcher LT, Klintsova AY (2010) Postnatal binge-like alcohol exposure decreases dendritic complexity while increasing the density of mature spines in mPFC layer II/III pyramidal neurons. Synapse 64:127–135.

Hannigan J, Berman R, Zajac C (1993) Environmental enrichment and the behavioral effects of prenatal exposure to alcohol in rats. Neurotoxicol Teratol 15:261–266.

Haslam R, Rust S, Pallett K, Cole D, Coleman J (2002) Cloning and characterisation of S-formylglutathione hydrolase from Arabidopsis thaliana: A pathway for formaldehyde detoxification. Plant Physiol Biochem 40:281–288.

Hausknecht K, Acheson A (2005) Prenatal alcohol exposure causes attention deficits in male rats. Behav Neurosci 119:302–310.

Hayes JD, Flanagan JU, Jowsey IR (2005) Glutathione Transferases. Annu Rev Pharmacol Toxicol 45:51–88.

Heim C, Nemeroff CB (2001) The role of childhood trauma in the neurobiology of mood and anxiety disorders: preclinical and clinical studies. Biol Psychiatry 49:1023–1039.

Hendrickson TJ, Mueller BA, Sowell ER, Mattson SN, Coles CD, Kable JA, Jones KL, Boys CJ, Lim KO, Riley EP, Wozniak JR (2017) Cortical gyrification is abnormal in children with prenatal alcohol exposure. NeuroImage Clin 15:391–400.

Hirokawa N, Niwa S, Tanaka Y (2010) Molecular motors in neurons: Transport mechanisms and roles in brain function, development, and disease. Neuron 68:610–638.

Hochmeister S, Grundtner R, Bauer J, Engelhardt B, Lyck R, Gordon G, Korosec T, Kutzelnigg A, Berger JJ, Bradl M, Bittner RE, Lassmann H (2006) Dysferlin is a new marker for leaky brain blood vessels in multiple sclerosis. J Neuropathol Exp Neurol 65:855–865.

Hoyme HE et al. (2016) Updated Clinical Guidelines for Diagnosing Fetal Alcohol Spectrum Disorders. Pediatrics 138:e20154256.

Hulshof HJ, Novati A, Sgoifo A, Luiten PGM, den Boer JA, Meerlo P (2011) Maternal separation decreases adult hippocampal cell proliferation and impairs cognitive performance but has little effect on stress sensitivity and anxiety in adult Wistar rats. Behav Brain Res 216:552–560.

Hunt CA, Schenker LJ, Kennedy MB (1996) PSD-95 is associated with the postsynaptic density and not with the presynaptic membrane at forebrain synapses. J Neurosci 16:1380–1388.

Hüttemann M, Helling S, Sanderson TH, Sinkler C, Samavati L, Mahapatra G, Varughese A, Lu G, Liu J, Ramzan R, Vogt S, Grossman LI, Doan JW, Marcus K, Lee I (2012) Regulation of mitochondrial respiration and apoptosis through cell signaling: Cytochrome c oxidase and cytochrome c in ischemia/reperfusion injury and inflammation. Biochim Biophys Acta - Bioenerg 1817:598–609.

Ikonomidou C, Bittigau P, Ishimaru MJ, Wozniak DF, Koch C, Genz K, Price MT, Stefovska V, Hörster F, Tenkova T, Dikranian K, Olney JW (2000) Ethanol-induced apoptotic neurodegeneration and fetal alcohol syndrome. Science (80-) 287:1056–1060.

Incerti M, Vink J (2010) Reversal of Alcohol-Induced Learning Deficits in the Young Adult in a Model of Fetal Alcohol Syndrome. Obstet Gynecol 115:350–356.

Ishii A, Fyffe-Maricich SL, Furusho M, Miller RH, Bansal R (2012) ERK1/ERK2 MAPK Signaling is Required to Increase Myelin Thickness Independent of Oligodendrocyte Differentiation and Initiation of Myelination. J Neurosci 32:8855–8864.

Jablonski SA, Schreiber WB, Westbrook SR, Brennan LE, Stanton ME (2013) Determinants of novel object and location recognition during development. Behav Brain Res 256:140–150.

Jégou S, El Ghazi F, De Lendeu PK, Marret S, Laudenbach V, Uguen A, Marcorelles P, Roy V, Laquerrière A, Gonzalez BJ (2012) Prenatal alcohol exposure affects vasculature development in the neonatal brain. Ann Neurol 72:952–960.

Jeon K-I, Xu X, Aizawa T, Lim JH, Jono H, Kwon D-S, Abe J-I, Berk BC, Li J-D, Yan C (2010) Vinpocetine inhibits NF-kappaB-dependent inflammation via an IKK-dependent but PDE-independent mechanism. Proc Natl Acad Sci U S A 107:9795–9800.

Jilek JL, Sant KE, Cho KH, Reed MS, Pohl J, Hansen JM, Harris C (2015) Ethanol Attenuates Histiotrophic Nutrition Pathways and Alters the Intracellular Redox Environment and Thiol Proteome during Rat Organogenesis. 147:475–489.

Johns TG, Bernard CCA (1999) The structure and function of myelin oligodendrocyte glycoprotein. J Neurochem 72:1–9.

Jones KL (2011) The effects of alcohol on fetal development. Birth Defects Res C Embryo Today 93:3–11.

Kable JA, Connor MJO, Carmichael H, Paley B, Mattson SN, Anderson SM, Riley EP (2016) Neurobehavioral Disorder Associated with Prenatal Alcohol Exposure (ND-PAE): Proposed DSM-5 Diagnosis. Child Psychiatry Hum Dev 47:335–346.

Kaidanovich-Beilin O, Woodgett JR (2011) GSK-3: Functional Insights from Cell Biology and Animal Models. Front Mol Neurosci 4:40.

Kalinichev M, Easterling KW, Plotsky PM, Holtzman SG (2002) Long-lasting changes in stress-induced corticosterone response and anxiety-like behaviors as a consequence of neonatal maternal separation in Long-Evans rats. Pharmacol Biochem Behav 73:131–140.

Kaminen-Ahola N, Ahola A, Maga M, Mallitt KA, Fahey P, Cox TC, Whitelaw E, Chong S (2010) Maternal ethanol consumption alters the epigenotype and the phenotype of offspring in a mouse model. PLoS Genet 6:1–10.

Kandel ER, Dudai Y, Mayford MR (2014) The molecular and systems biology of memory. Cell 157:163–186.

Kaytor MD, Orr HT (2002) The GSKB signaling cascade and neurodegenerative disease. Curr Opin Neurobiol 12:275–278.

Kelly SJ, Day N, Streissguth AP (2000) Effects of prenatal alcohol exposure on social behavior in humans and other species. Neurotoxicol Teratol 22:143–149.

Khoury JE, Milligan K, Girard TA (2015) Executive Functioning in Children and Adolescents Prenatally Exposed to Alcohol: A Meta-Analytic Review. Neuropsychol Rev 25:149–170.

Kim J-E, Ji E-S, Seo J-H, Lee M-H, Cho S, Pak YK, Seo T-B, Kim C-J (2012) Alcohol exposure induces depression-like behavior by decreasing hippocampal neuronal proliferation through inhibition of the BDNF-ERK pathway in gerbils. Animal Cells Syst (Seoul) 16:190–197.

Kim KC, Go HS, Bak HR, Choi CS, Choi I, Kim P, Han S-H, Han SM, Shin CY, Ko KH (2010) Prenatal exposure of ethanol induces increased glutamatergic neuronal differentiation of neural progenitor cells. J Biomed Sci 17:1–9.

Kim P, Park J, Choi C, Choi I, Joo S (2013) Effects of Ethanol Exposure During Early Pregnancy in Hyperactive, Inattentive and Impulsive Behaviors and MeCP2 Expression in Rodent Offspring. Neurochem Res 38:620–631.

Kleiber ML, Mantha K, Stringer RL, Singh SM (2013) Neurodevelopmental alcohol exposure elicits long-term changes to gene expression that alter distinct molecular pathways dependent on timing of exposure. J Neurodev Disord 5:1–19.

Kodituwakku PW (2007) Defining the behavioral phenotype in children with fetal alcohol spectrum disorders: A review. Neurosci Biobehav Rev 31:192–201.

Krahe TE, Paul AP, Medina AE (2010) Phosphodiesterase Type 4 Inhibition Does Not Restore Ocular Dominance Plasticity in a Ferret Model of Fetal Alcohol Spectrum Disorders. Alcohol Cinical Exp Res 34:493–498.

Krahe TE, Wang W, Medina AE (2009) Phosphodiesterase inhibition increases CREB phosphorylation and restores orientation selectivity in a model of fetal alcohol spectrum disorders. PLoS One 4:1–13.

Kruger NJ, Von Schaewen A (2003) The oxidative pentose phosphate pathway: Structure and organisation. Curr Opin Plant Biol 6:236–246.

Laborde E (2010) Glutathione transferases as mediators of signaling pathways involved in cell proliferation and cell death. Cell Death Differ 17:1373–1380.

Ladd CO, Huot RL, Thrivikraman K V, Nemeroff CB, Plotsky PM (2004) Long-term adaptations in glucocorticoid receptor and mineralocorticoid receptor mRNA and negative feedback on the hypothalamo-pituitary-adrenal axis following neonatal maternal separation. Biol Psychiatry 55:367–375.

Lantz CL, Wang W, Medina AE (2012) Early alcohol exposure disrupts visual cortex plasticity in mice. Int J Dev Neurosci 30:351–357.

Lebel C, Mattson SN, Riley EP, Jones KL, Adnams CM, May PA, Bookheimer SY, O'Connor MJ, Narr KL, Kan E, Abaryan Z, Sowell ER (2012) A Longitudinal Study of the Long-Term Consequences of Drinking during Pregnancy: Heavy In Utero Alcohol Exposure Disrupts the Normal Processes of Brain Development. J Neurosci 32:15243–15251.

Lee DH, Jeong JY, Kim YS, Kim JS, Cho YW, Roh GS, Kim HJ, Kang SS, Cho GJ, Choi WS (2010) Ethanol down regulates the expression of myelin proteolipid protein in the rat hippocampus. Anat Cell Biol 43:194–200.

Lee DH, Moon J, Ryu J, Jeong JY, Roh GS, Kim HJ, Cho GJ, Choi WS, Kang SS (2015) Effects of postnatal alcohol exposure on hippocampal gene expression and learning in adult mice. Genes Genet Syst 90:335–342.

Lee E, Son H (2009) Adult hippocampal neurogenesis and related neurotrophic factors. BMB Rep 42:239–244.

Lee J-H, Kim HJ, Kim JG, Ryu V, Kim B-T, Kang D-W, Jahng JW (2007) Depressive behaviors and decreased expression of serotonin reuptake transporter in rats that experienced neonatal maternal separation. Neurosci Res 58:32–39.

Lei W, Omotade OF, Myers KR, Zheng JQ (2016) Actin cytoskeleton in dendritic spine development and plasticity. Curr Opin Neurobiol 39:86–92.

Levy JR, Holzbaur ELF (2006) Cytoplasmic dynein/dynactin function and dysfunction in motor neurons. Int J Dev Neurosci 24:103–111.

Lewis SJ, Zuccolo L, Davey Smith G, Macleod J, Rodriguez S, Draper ES, Barrow M, Alati R, Sayal K, Ring S, Golding J, Gray R (2012) Fetal Alcohol Exposure and IQ at Age 8: Evidence from a Population-Based Birth-Cohort Study. PLoS One 7:1–8.

Li X, Jope RS (2010) Is Glycogen Synthase Kinase-3 a Central Modulator in Mood Regulation? Neuropsychopharmacology 35:2143–2154.

Liesi P (1997) Ethanol-exposed central neurons fail to migrate and undergo apoptosis. J Neurosci Res 48:439–448.

Lipinski RJ, Hammond P, O'Leary-Moore SK, Ament JJ, Pecevich SJ, Jiang Y, Budin F, Parnell SE, Suttie M, Godin EA, Everson JL, Dehart DB, Oguz I, Holloway HT, Styner MA, Johnson GA, Sulik KK (2012) Ethanol-induced face-brain dysmorphology patterns are correlative and exposure-stage dependent. PLoS One 7:1–10.

Lippmann M, Bress A, Nemeroff CB, Plotsky PM, Monteggia LM (2007) Long-term behavioural and molecular alterations associated with maternal separation in rats. Eur J Neurosci 25:3091–3098.

Livy D., Miller EK, Maier SE, West JR (2003) Fetal alcohol exposure and temporal vulnerability: effects of binge-like alcohol exposure on the developing rat hippocampus. Neurotoxicol Teratol 25:447–458.

Lyon L, Saksida LM, Bussey TJ (2012) Spontaneous object recognition and its relevance to schizophrenia : a review of findings from pharmacological , genetic , lesion and developmental rodent models. :647–672.

Maas DA, Vallès A, Martens GJM (2017) Oxidative stress, prefrontal cortex hypomyelination and cognitive symptoms in schizophrenia. Transl Psychiatry 7:1–10.

MacIlvane NM, Pochiro JM, Hurwitz NR, Goodfellow MJ, Lindquist DH (2016) Recognition memory is selectively impaired in adult rats exposed to binge-like doses of ethanol during early postnatal life. Alcohol 57:55–63.

Magistretti PJ, Allaman I (2015) A Cellular Perspective on Brain Energy Metabolism and Functional Imaging. Neuron 86:883–901.

Mai L, Jope RS, Li X (2002) BDNF-mediated signal transduction is modulated by GSK3B and mood stabilizing agents. J Neurochem 82:75–83.

Maiya R, Lee S, Berger KH, Kong EC, Slawson JB, Griffith LC, Takamiya K, Huganir RL, Margolis B, Heberlein U (2012) DlgS97/SAP97, a Neuronal Isoform of Discs Large, Regulates Ethanol Tolerance. PLoS One 7.

Makena N, Bugarith K, Russell VA (2012) Maternal separation enhances object location memory and prevents exercise-induced MAPK/ERK signalling in adult Sprague-Dawley rats. Metab Brain Dis 27:377–385.

Mantha K (2013) Neurodevelopmental Timing of Ethanol Exposure May Contribute to Observed Heterogeneity of Behavioral Deficits in a Mouse Model of Fetal Alcohol Spectrum Disorder (FASD). J Behav Brain Sci 3:85–99.

Marais L, Hattingh SM, Stein DJ, Daniels WMU (2009) A proteomic analysis of the ventral hippocampus of rats subjected to maternal separation and escitalopram treatment. Metab Brain Dis 24:569–586.

Marais L, van Rensburg SJ, van Zyl JM, Stein DJ, Daniels WMU (2008) Maternal separation of rat pups increases the risk of developing depressive-like behavior after subsequent chronic stress by altering corticosterone and neurotrophin levels in the hippocampus. Neurosci Res 61:106–112.

Marconcini L, Marchio S, Morbidelli L, Cartocci E, Albini A, Ziche M, Bussolino F, Oliviero S (1999) c-fos-induced growth factor/vascular endothelial growth factor D induces angiogenesis in vivo and in vitro. Proc Natl Acad Sci U S A 96:9671–9676.

Marcondes F, Bianchi F, Tanno A (2002) Determination of the estrous cycle phases of rats: some helpful considerations. Braz J Biol 62:609–614.

Marín MP, Esteban-Pretel G, Ponsoda X, Romero AM, Ballestín R, López C, Megías L, Timoneda J, Molowny A, Canales JJ, Renau-Piqueras J (2010) Endocytosis in cultured neurons is altered by chronic alcohol exposure. Toxicol Sci 115:202–213.

Marquardt K, Brigman JL (2016) The impact of prenatal alcohol exposure on social , cognitive and affective behavioral domains : Insights from rodent models. 51:1–15.

Marquardt K, Sigdel R, Caldwell K, Brigman JL (2014) Prenatal ethanol exposure impairs executive function in mice into adulthood. Alcohol Clin Exp Res 38:2962–2968.

Marsden WN (2013) Synaptic plasticity in depression: Molecular, cellular and functional correlates. Prog Neuro-Psychopharmacology Biol Psychiatry 43:168–184.

Martinowich K, Manji H, Lu B (2007) New insights into BDNF function in depression and anxiety. Nat Neurosci 10:1089–1093.

May PA, Blankenship J, Marais A-S, Gossage JP, Kalberg WO, Barnard R, De Vries M, Robinson LK, Adnams CM, Buckley D, Manning M, Jones KL, Parry C, Hoyme HE, Seedat S (2013a) Approaching the prevalence of the full spectrum of fetal alcohol spectrum disorders in a South African population-based study. Alcohol Cinical Exp Res 37:818–830.

May PA, Blankenship J, Marais AS, Gossage JP, Kalberg WO, Joubert B, Cloete M, Barnard R, De Vries M, Hasken J, Robinson LK, Adnams CM, Buckley D, Manning M, Parry CDH, Hoyme HE, Tabachnick B, Seedat S (2013b) Maternal alcohol consumption producing fetal alcohol spectrum disorders (FASD): Quantity, frequency, and timing of drinking. Drug Alcohol Depend 133:502–512.

May PA, Gossage JP (2011) Maternal risk factors for fetal alcohol spectrum disorders: not as simple as it might seem. Alcohol Res Health 34:15–26.

May PA, Tabachnick B, Hasken JM, Marais A-S, de Vries MM, Barnard R, Joubert B, Cloete M, Botha I, Kalberg WO, Buckley D, Burroughs ZR, Bezuidenhout H, Robinson LK, Manning MA, Adnams CM, Seedat S, Parry CDH, Hoyme HE (2017) Who is most affected by prenatal alcohol exposure: Boys or girls? Drug Alcohol Depend 177:258–267.

May PA, Vries MM De, Marais A, Kalberg WO, Adnams CM, Hasken JM, Tabachnick B, Robinson LK, Manning MA, Lyons K, Hoyme D, Seedat S, Parry CDH, Hoyme HE (2016) The continuum of fetal alcohol spectrum disorders in four rural communities in south africa : Prevalence and characteristics. 159:207–218.

McFie S, Sterley T-L, Howells FM, Russell V a (2012) Clozapine decreases exploratory activity and increases anxiety-like behaviour in the Wistar-Kyoto rat but not the spontaneously hypertensive rat model of attention-deficit/hyperactivity disorder. Brain Res 1467:91–103.

McLaughlin KA, Conron KJ, Koenen KC, Gilman SE (2010) Childhood adversity, adult stressful life events, and risk of past-year psychiatric disorder: a test of the stress sensitization hypothesis in a population-based sample of adults. Psychol Med 40:1647–1658.

Medina AE (2011) Fetal alcohol spectrum disorders and abnormal neuronal plasticity. Neuroscientist 17:274–

287.

Medina AE, Krahe TE, Ramoa AS (2006) Restoration of neuronal plasticity by a phosphodiesterase type 1 inhibitor in a model of fetal alcohol exposure. J Neurosci 26:1057–1060.

Meintjes EM, Jacobson JL, Molteno CD, Gatenby JC, Warton C, Cannistraci CJ, Hoyme HE, Robinson LK, Khaole N, Gore JC, Jacobson SW (2010) An fMRI Study of Number Processing in Children With Fetal Alcohol Syndrome. 34:1450–1464.

Mick E, Biederman J, Faraone S V, Sayer J, Kleinman S (2002) Case-control study of attention-deficit hyperactivity disorder and maternal smoking, alcohol use, and drug use during pregnancy. J Am Acad Child Adolesc Psychiatry 41:378–385.

Miki T, Kuma H, Yokoyama T, Sumitani K, Matsumoto Y, Kusaka T, Warita K, Wang Z-Y, Hosomi N, Imagawa T, S Bedi K, Itoh S, Nakamura Y, Takeuchi Y (2008) Early postnatal ethanol exposure induces fluctuation in the expression of BDNF mRNA in the developing rat hippocampus. Acta Neurobiol Exp (Wars) 68:484–493.

Monin A, Baumann PS, Griffa A, Xin L, Mekle R, Fournier M, Butticaz C, Klaey M, Cabungcal JH, Steullet P, Ferrari C, Cuenod M, Gruetter R, Thiran JP, Hagmann P, Conus P, Do KQ (2015) Glutathione deficit impairs myelin maturation: relevance for white matter integrity in schizophrenia patients. Mol Psychiatry 20:827–838.

Monk BR, Leslie FM, Thomas JD (2012) The Effects of Perinatal Choline Supplementation on Hippocampal Cholinergic Development in Rats Exposed to Alcohol During the Brain Growth Spurt. Hippocampus 1757:1750–1757.

Moors M, Cline JE, Abel J, Fritsche E (2007) ERK-dependent and -independent pathways trigger human neural progenitor cell migration. Toxicol Appl Pharmacol 221:57–67.

Möykkynen T, Korpi ER (2012) Acute effects of ethanol on glutamate receptors. Basic Clin Pharmacol Toxicol 111:4–13.

Mozzaquatro B, Domenica M, Luiz A, Zeni G, Galeotti N, Wayne C (2014) ERK1/2 phosphorylation is involved in the antidepressant-like action of 2, 5-diphenyl-3-(4- fluorophenylseleno)-selenophene in mice. Eur J Pharmacol 736:44–54.

Muggli E, Matthews H, Penington A, Claes P, O'Leary C, Forster D, Donath S, Anderson PJ, Lewis S, Nagle C, Craig JM, White SM, Elliott EJ, Halliday J (2017) Association Between Prenatal Alcohol Exposure and Craniofacial Shape of Children at 12 Months of Age. JAMA Pediatr 171:771–780.

Mullen PE, Martin JL, Anderson JC, Romans SE, Herbison GP (1996) The long-term impact of the physical, emotional, and sexual abuse of children: a community study. Child Abuse Negl 20:7–21.

Musazzi L, Seguini M, Mallei A, Treccani G, Pelizzari M, Tornese P, Racagni G, Tardito D (2014) Time-dependent activation of MAPK/Erk1/2 and Akt/GSK3 cascades: modulation by agomelatine. 15:1–12.

Mustroph ML, Chen S, Desai SC, Cay EB, DeYoung EK, Rhodes JS (2012) Aerobic exercise is the critical variable in an enriched environment that increases hippocampal neurogenesis and water maze learning in male C57BL/6J mice. Neuroscience 219:62–71.

Myllykoski M, Seidel L, Muruganandam G, Raasakka A, Torda AE, Kursula P (2016) Structural and functional evolution of 2',3'-cyclic nucleotide 3'-phosphodiesterase. Brain Res 1641:64–78.

Nardelli A, Lebel C, Rasmussen C, Andrew G, Beaulieu C (2011) Extensive deep gray matter volume reductions in children and adolescents with fetal alcohol spectrum disorders. Alcohol Clin Exp Res 35:1404–1417.

Nebert DW, Vasiliou V (2004) Analysis of the glutathione S-transferase (GST) gene family. Hum Genomics 1:60–64.

Nesvizhskii AI, Keller A, Kolker E, Aebersold R (2003) A statistical model for identifying proteins by tandem

mass spectrometry. Anal Chem 75:4646–4658.

Newville J, Valenzuela CF, Li L, Jantzie LL, Cunningham LA (2017) Acute oligodendrocyte loss with persistent white matter injury in a third trimester equivalent mouse model of fetal alcohol spectrum disorder. Glia 65:1317–1332.

Nilsson M, Perfilieva E, Johansson U, Orwar O, Eriksson PS (1999) Enriched environment increases neurogenesis in the adult rat dentate gyrus and improves spatial memory. J Neurobiol 39:569–578.

Nishi M, Horii-Hayashi N, Sasagawa T (2014) Effects of early life adverse experiences on the brain: Implications from maternal separation models in rodents. Front Neurosci 8:1–6.

Nunes F, Ferreira-Rosa K, Pereira MDS, Kubrusly RC, Manhães AC, Abreu-Villaça Y, Filgueiras CC (2011) Acute administration of vinpocetine, a phosphodiesterase type 1 inhibitor, ameliorates hyperactivity in a mice model of fetal alcohol spectrum disorder. Drug Alcohol Depend 119:81–87.

Nygaard R, Zou Y, Dror RO, Mildorf TJ, Arlow DH, Manglik A, Pan AC, Liu CW, Fung JJ, Bokoch MP, Thian FS, Kobilka TS, Shaw DE, Mueller L, Prosser RS, Kobilka BK (2013) The dynamic process of β2-adrenergic receptor activation. Cell 152:532–542.

O'Connor MJ, Paley B (2009) Psychiatric conditions associated with prenatal alcohol exposure. Dev Disabil Res Rev 15:225–234.

O'Leary-Moore SK, Parnell SE, Lipinski RJ, Sulik KK (2011) Magnetic resonance-based imaging in animal models of fetal alcohol spectrum disorder. Neuropsychol Rev 21:167–185.

O'Leary CM, Bower C, Zubrick SR, Geelhoed E, Kurinczuk JJ, Nassar N (2010a) A new method of prenatal alcohol classification accounting for dose, pattern and timing of exposure: improving our ability to examine fetal effects from low to moderate alcohol. J Epidemiol Community Heal 64:956–962.

O'Leary CM, Nassar N, Kurinczuk JJ, de Klerk N, Geelhoed E, Elliott EJ, Bower C (2010b) Prenatal Alcohol Exposure and Risk of Birth Defects. Pediatrics 126:843–850.

Ohta KI, Suzuki S, Warita K, Kaji T, Kusaka T, Miki T (2017) Prolonged maternal separation attenuates BDNF-ERK signaling correlated with spine formation in the hippocampus during early brain development. J Neurochem 141:179–194.

Oktyabrsky ON, Smirnova G V (2007) Redox Regulation of Cellular Functions. Biochem 72:132–145.

Olivier L, Curfs LMG, Viljoen DL (2016) Fetal alcohol spectrum disorders: Prevalence rates in South Africa. South African Med J 106:S103–S106.

Olney JW, Wozniak DF, Jevtovic-Todorovic V, Farber NB, Bittigau P, Ikonomidou C (2002) Glutamate and GABA receptor dysfunction in the fetal alcohol syndrome. Neurotox Res 4:315–325.

Olson HC, Feldman JJ, Streissguth AP, Sampson PD, Bookstein FL (1998) Neuropsychological deficits in adolescents with fetal alcohol syndrome: clinical findings. Alcohol Clin Exp Res 22:1998–2012.

Oomen CA, Soeters H, Audureau N, Vermunt L, van Hasselt FN, Manders EMM, Joëls M, Lucassen PJ, Krugers H (2010) Severe early life stress hampers spatial learning and neurogenesis, but improves hippocampal synaptic plasticity and emotional learning under high-stress conditions in adulthood. J Neurosci 30:6635–6645.

Oshiro WM, Beasley TE, McDaniel KL, Taylor MM, Evansky P, Moser VC, Gilbert ME, Bushnell PJ (2014) Selective cognitive deficits in adult rats after prenatal exposure to inhaled ethanol. Neurotoxicol Teratol 45:44–58.

Owens DM, Keyse SM (2007) Differential regulation of MAP kinase signalling by dual-specificity protein phosphatases. Oncogene 26:3203–3213.

Park J, Gupta RS (2013) Adenosine Metabolism, Adenosine Kinase, and Evolution. In: Adenosine: A Key Link between Metabolism and Brain Activity, Adenosine: (Masino S, Boison D, eds), pp 23–55. New York:

Springer.

Patten A, Gil-Mohapel J, Wortman R, Noonan A, Brocardo P, Christie B (2013a) Effects of Ethanol Exposure during Distinct Periods of Brain Development on Hippocampal Synaptic Plasticity. Brain Sci 3:1076–1094.

Patten AR, Brocardo PS, Christie BR (2013b) Omega-3 supplementation can restore glutathione levels and prevent oxidative damage caused by prenatal ethanol exposure. J Nutr Biochem 24:760–769.

Patten AR, Fontaine CJ, Christie BR (2014) A Comparison of the Different Animal Models of Fetal Alcohol Spectrum Disorders and Their Use in Studying Complex Behaviors. Front Pediatr 2:1–19.

Paul AP, Pohl-Guimaraes F, Krahe TE, Filgueiras CC, Lantz CL, Colello RJ, Wang W, Medina AE (2010) Overexpression of serum response factor restores ocular dominance plasticity in a model of fetal alcohol spectrum disorders. J Neurosci 30:2513–2520.

Pei J, Job J, Kully-Martens K, Rasmussen C (2011) Executive function and memory in children with Fetal Alcohol Spectrum Disorder. Child Neuropsychol 17:290–309.

Peng S, Zhang Y, Zhang J, Wang H, Ren B (2010) ERK in learning and memory: A review of recent research. Int J Mol Sci 11:222–232.

Phillips D., Krueger S., Rydquist J. (1991) Short- and long-term effects of combined pre- and postnatal ethanol exposure (three trimester equivalency) on the development of myelin and axons in rat optic nerve. Int J Dev Neurosci 9:631–647.

Piubelli C, Carboni L, Becchi S, Mathé AA, Domenici E (2011) Regulation of cytoskeleton machinery, neurogenesis and energy metabolism pathways in a rat gene-environment model of depression revealed by proteomic analysis. Neuroscience 176:349–380.

Plotsky PM, Thrivikraman K V, Nemeroff CB, Caldji C, Sharma S, Meaney MJ (2005) Long-Term Consequences of Neonatal Rearing on Central Corticotropin-Releasing Factor Systems in Adult Male Rat Offspring. Neuropsychopharmacology 30:2192–2204.

Polter A, Beurel E, Yang S, Garner R, Song L, Miller CA, Sweatt JD, McMahon L, Bartolucci AA, Li X, Jope RS (2010) Deficiency in the inhibitory serine-phosphorylation of glycogen synthase kinase-3 increases sensitivity to mood disturbances. Neuropsychopharmacology 35:1761–1774.

Portfors C V (2007) Types and functions of ultrasonic vocalizations in laboratory rats and mice. J Am Assoc Lab Anim Sci 46:28–34.

Puglia MP, Valenzuela CF (2010) Repeated third trimester-equivalent ethanol exposure inhibits long-term potentiation in the hippocampal CA1 region of neonatal rats. Alcohol 44:283–290.

Raimondi A, Ferguson SM, Lou X, Armbruster M, Paradise S, Giovedi S, Messa M, Kono N, Takasaki J, Cappello V, O'Toole E, Ryan TA, De Camilli P (2011) Overlapping Role of Dynamin Isoforms in Synaptic Vesicle Endocytosis. Neuron 70:1100–1114.

Rangmar J, Hjern A, Vinnerljung B, Stromland K, Aronson M, Fahlke C (2015a) Psychosocial Outcomes of Fetal Alcohol Syndrome in Adulthood. Pediatrics 135:52–58.

Rangmar J, Sandberg AD, Aronson M, Fahlke C (2015b) Cognitive and executive functions, social cognition and sense of coherence in adults with fetal alcohol syndrome. Nord J Psychiatry 69:1754–1760.

Resendiz M, Mason S, Lo CL, Zhou FC (2014) Epigenetic regulation of the neural transcriptome and alcohol interference during development. Front Genet 5:1–15.

Ripps H, Shen W (2012) Review: taurine: a "very essential" amino acid. Mol Vis 18:2673–2686.

Robertson FC, Narr KL, Molteno CD, Jacobson JL, Jacobson SW, Meintjes EM (2016) Prenatal Alcohol Exposure is Associated with Regionally Thinner Cortex During the Preadolescent Period. 26:3083–3095.

Robinson M, Oddy WH, McLean NJ, Jacoby P, Pennell CE, De Klerk NH, Zubrick SR, Stanley FJ, Newnham JP

(2010) Low-moderate prenatal alcohol exposure and risk to child behavioural development: A prospective cohort study. An Int J Obstet Gynaecol 117:1139–1150.

Rojas-Mayorquín AE, Padilla-Velarde E, Ortuño-Sahagún D (2016) Prenatal alcohol exposure in rodents as a promising model for the study of ADHD molecular basis. Front Neurosci 10:1–10.

Romero AM, Esteban-pretel G, Marı P (2010) Chronic Ethanol Exposure Alters the Levels, Assembly, and Cellular Organization of the Actin Cytoskeleton and Microtubules in Hippocampal Neurons in Primary Culture. Toxicol Sci 118:602–612.

Rubert G, Minana R, Pascual M, Guerri C (2006) Ethanol Exposure During Embryogenesis Decreases the Radial Glial Progenitor Pool and Affects the Generation of Neurons and Astrocytes. J Neurosci Res 84:483–496.

Russell VA (2003) In vitro glutamate-stimulated release of dopamine from nucleus accumbens core and shell of spontaneously hypertensive rats. Metab Brain Dis 18:161–168.

Russell V, De Villiers A, Sagvolden T, Lamm M, Taljaard J (1998) Differences between electrically-, ritalin- and D-amphetamine-stimulated release of [3H]dopamine from brain slices suggest impaired vesicular storage of dopamine in an animal model of Attention-Deficit Hyperactivity Disorder. Behav Brain Res 94:163–171.

Sadrian B, Subbanna S, Wilson DA, Basavarajappa BS, Saito M (2012) Lithium prevents long-term neural and behavioral pathology induced by early alcohol exposure. Neuroscience 206:122–135.

Sagvolden T (2000) Behavioral validation of the spontaneously hypertensive rat (SHR) as an animal model of attention-deficit/hyperactivity disorder (AD/HD). Neurosci Biobehav Rev 24:31–39.

Sakai R, Ukai W, Sohma H, Hashimoto E (2005) Attenuation of brain derived neurotrophic factor (BDNF) by ethanol and cytoprotective effect of exogenous BDNF against ethanol damage in neuronal cells. :1005–1013.

Saleh A, Potter GG, McQuoid DR, Boyd B, Turner R, MacFall JR, Taylor WD (2017) Effects of early life stress on depression, cognitive performance and brain morphology. Psychol Med 47:171–181.

Samudio-Ruiz SL, Allan AM, Valenzuela CF, Perrone-Bizzozero NI, Caldwell KK (2009) Prenatal ethanol exposure persistently impairs NMDA receptor-dependent activation of extracellular signal-regulated kinase in the mouse dentate gyrus. J Neurochem 109:1311–1323.

Sannino S, Russo F, Torromino G, Pendolino V, Calabresi P, De Leonibus E (2012) Role of the dorsal hippocampus in object memory load. Learn Mem 19:211–218.

Sari Y, Hammad LA, Saleh MM, Rebec G V., Mechref Y (2010a) Alteration of selective neurotransmitters in fetal brains of prenatally alcohol-treated C57BL/6 mice: Quantitative analysis using liquid chromatography/tandem mass spectrometry. Int J Dev Neurosci 28:263–269.

Sari Y, Zhang M, Mechref Y (2010b) Differential expression of proteins in fetal brains of alcohol-treated prenatally C57BL/6 mice: a proteomic investigation. Electrophoresis 31:483–496.

Sayal K, Heron J, Golding J, Alati R, Smith GD, Gray R, Emond A (2009) Binge Pattern of Alcohol Consumption During Pregnancy and Childhood Mental Health Outcomes: Longitudinal Population-Based Study. Pediatrics 123:289–296.

Schmitt U, Tanimoto N, Seeliger M, Schaeffel F, Leube RE (2009) Detection of behavioral alterations and learning deficits in mice lacking synaptophysin. Neuroscience 162:234–243.

Schneider ML, Moore CF, Adkins MM (2011) The effects of prenatal alcohol exposure on behavior: rodent and primate studies. Neuropsychol Rev 21:186–203.

Schneider ML, Moore CF, Barnhart TE, Larson J a, DeJesus OT, Mukherjee J, Nickles RJ, Converse AK, Roberts AD, Kraemer GW (2005) Moderate-level prenatal alcohol exposure alters striatal dopamine system function in rhesus monkeys. Alcohol Clin Exp Res 29:1685–1697.

Seshi B (2006) An integrated approach to mapping the proteome of the human bone marrow stromal cell.

Proteomics 6:5169–5182.

Shalev U, Kafkafi N (2002) Repeated maternal separation does not alter sucrose-reinforced and open-field behaviors. Pharmacol Biochem Behav 73:115–122.

Shenolikar S, Cohen PTW, Cohen P, Nairn AC, Perry SV (1979) The Role of Calmodulin in the Structure and Regulation of Phosphorylase Kinase from Rabbit Skeletal Muscle. Eur J Biochem 100:329–337.

Sickmann HM, Patten a R, Morch K, Sawchuk S, Zhang C, Parton R, Szlavik L, Christie BR (2014) Prenatal ethanol exposure has sex-specific effects on hippocampal long-term potentiation. Hippocampus 24:54–64.

Sinning A, Liebmann L, Kougioumtzes A, Westermann M, Bruehl C, Hu CA (2011) Synaptic Glutamate Release Is Modulated by the Na+ Driven Cl-/ HCO3- Exchanger Slc4a8. J Neurosci 31:7300–7311.

Slattery DA, Cryan JF (2012) Using the rat forced swim test to assess antidepressant-like activity in rodents. Nat Protoc 7:1009–1014.

Smiley JF, Saito M, Bleiwas C, Masiello K, Ardekani B, Guilfoyle DN, Gerum S, Wilson DA, Vadasz C (2015) Selective reduction of cerebral cortex GABA neurons in a late gestation model of fetal alcohol spectrum disorder. Alcohol 49:571–580.

Soares-Simi SL, Pastrello DM, Ferreira ZS, Yonamine M, Marcourakis T, Scavone C, Camarini R (2013) Changes in CREB activation in the prefrontal cortex and hippocampus blunt ethanol-induced behavioral sensitization in adolescent mice. Front Integr Neurosci 7:1–12.

Sokol RJ, Delaney-Black V, Nordstrom B (2003) Fetal Alcohol Spectrum Disorder. Am Med Assoc 290:2996–2999.

Sousa VC, Vital J, Costenla AR, Batalha VL, Sebastião AM, Ribeiro JA, Lopes L V (2014) Maternal separation impairs long term-potentiation in CA1-CA3 synapses and hippocampal-dependent memory in old rats. Neurobiol Aging 35:1680–1685.

Spohr HL, Willms J, Steinhausen HC (2007) Fetal alcohol spectrum disorders in young adulthood. J Pediatr 150:175–179.

Srinivasan S, Avadhani NG (2012) Cytochrome c oxidase dysfunction in oxidative stress. Free Radic Biol Med 53:1252–1263.

Stobart JL, Anderson CM (2013) Multifunctional role of astrocytes as gatekeepers of neuronal energy supply. Front Cell Neurosci 7:1–21.

Streissguth AP, Bookstein FL, Barr HM, Sampson PD, O'Malley K, Young JK (2004) Risk factors for adverse life outcomes in fetal alcohol syndrome and fetal alcohol effects. J Dev Behav Pediatr 25:228–238.

Suárez I, Bodega G, Fernández B (2002) Glutamine synthetase in brain: Effect of ammonia. Neurochem Int 41:123–142.

Subbanna S, Shivakumar M, Psychoyos D, Xie S, Basavarajappa BS (2013) Anandamide-CB1 Receptor Signaling Contributes to Postnatal Ethanol-Induced Neonatal Neurodegeneration, Adult Synaptic, and Memory Deficits. J Neurosci 33:6350–6366.

Suttie AM, Foroud T (2013) Facial Dysmorphism Across the Fetal Alcohol Spectrum. 131:779–788.

Swart PC, Currin CB, Russell VA, Dimatelis JJ (2017) Early Ethanol Exposure and Vinpocetine Treatment Alter Learning- and Memory- Related Proteins in the Rat Hippocampus and Prefrontal Cortex. J Neurosci Res 95:1204–1215.

Szklarczyk D, Franceschini A, Wyder S, Forslund K, Heller D, Huerta-cepas J, Simonovic M, Roth A, Santos A, Tsafou KP, Kuhn M, Bork P, Jensen LJ, Mering C Von (2015) STRING v10 : protein – protein interaction networks , integrated over the tree of life. 43:447–452.

Tan RR, Li YF, Zhang XT, Huang YH, Wu YP, Ouyang SH, Tsoi B, Yi RN, Yang X, Kurihara H, He RR (2013)

Glucose metabolism disorder is a risk factor in ethanol exposure induced malformation in embryonic brain. Food Chem Toxicol 60:238–245.

Tarr B a., Kellaway L a., Gibson a. SC, Russell V a. (2004) Voluntary running distance is negatively correlated with striatal dopamine release in untrained rats. Behav Brain Res 154:493–499.

Thomas JD, Idrus NM, Monk BR, Dominguez HD (2010) Prenatal choline supplementation mitigates behavioral alterations associated with prenatal alcohol exposure in rats. Birth Defects Res Part A Clin Mol Teratol 88:827–837.

Ting L, Cowley MJ, Hoon SL, Guilhaus M, Raftery MJ, Cavicchioli R (2009) Normalization and Statistical Analysis of Quantitative Proteomics Data Generated by Metabolic Labeling. Mol Cell proteomics 8:2227–2242.

Tiwari V, Chopra K (2011) Resveratrol prevents alcohol-induced cognitive deficits and brain damage by blocking inflammatory signaling and cell death cascade in neonatal rat brain. J Neurochem 117:678–690.

Tohgo A, Pierce KL, Choy EW, Lefkowitz RJ, Luttrell LM (2002) β-arrestin scaffolding of the ERK cascade enhances cytosolic ERK activity but inhibits ERK-mediated transcription following angiotensin AT1a receptor stimulation. J Biol Chem 277:9429–9436.

Tong M, Longato L, Nguyen QG, Chen WC, Spaisman A, De La Monte SM (2011) Acetaldehyde-mediated neurotoxicity: Relevance to fetal alcohol spectrum disorders. Oxid Med Cell Longev 2011:1–13.

Townsend DM, Manevich Y, He L, Hutchens S, Pazoles CJ, Tew KD (2009) Novel Role for Glutathione S - Transferase Pi REGULATOR OF PROTEIN S-GLUTATHIONYLATION FOLLOWING OXIDATIVE AND. J Biol Chem 284:436–445.

Treit S, Zhou D, Lebel C, Rasmussen C, Andrew G, Beaulieu C (2014) Longitudinal MRI reveals impaired cortical thinning in children and adolescents prenatally exposed to alcohol. Hum Brain Mapp 35:4892–4903.

Tripp G, Wickens JR (2009) Neurobiology of ADHD. Neuropharmacology 57:579–589.

Tsai G, Coyle JT (1998) The role of glutamatergic neurotransmission in the pathophysiology of alcoholism. Annu Rev Med 49:173–184.

Ungerer M, Knezovich J, Ramsay M (2013) In utero alcohol exposure, epigenetic changes, and their consequences. Alcohol Res 35.

Unwin RD, Smith DL, Blinco D, Wilson CL, Miller CJ, Evans CA, Jaworska E, Baldwin SA, Barnes K, Pierce A, Spooncer E, Whetton AD (2006) Quantitative proteomics reveals posttranslational control as a regulatory factor in primary hematopoietic stem cells. Blood 107:4687–4695.

van Zyl PJ, Dimatelis JJ, Russell VA (2016) Behavioural and biochemical changes in maternally separated Sprague–Dawley rats exposed to restraint stress. Metab Brain Dis 31:121–133.

Vink J, Auth J, Abebe DT, Brenneman DE, Spong CY (2005) Novel peptides prevent alcohol-induced spatial learning deficits and proinflammatory cytokine release in a mouse model of fetal alcohol syndrome. Am J Obstet Gynecol 193:825–829.

Voorhees JL, Tarr AJ, Wohleb ES, Godbout JP, Mo X, Sheridan JF, Eubank TD, Marsh CB (2013) Prolonged restraint stress increases IL-6, reduces IL-10, and causes persistent depressive-like behavior that is reversed by recombinant IL-10. PLoS One 8:1–11.

Vorhees C V, Williams MT (2006) Morris water maze: procedures for assessing spatial and related forms of learning and memory. Nat Protoc 1:848–858.

Waddell J, Yang T, Ho E, Wellmann K, Mooney S (2016) Prenatal Ethanol Exposure and Whisker Clipping Disrupt Ultrasonic Vocalizations and Play Behavior in Adolescent Rats. Brain Sci 6:1–11.

Walf AA, Frye CA (2007) The use of the elevated plus maze as an assay of anxiety-related behavior in rodents.

Nat Protoc 2:322–328.

Warton FL, Howells FM, Russell VA (2009) Increased glutamate-stimulated release of dopamine in substantia nigra of a rat model for attention-deficit/hyperactivity disorder-lack of effect of methylphenidate. Metab Brain Dis 24:599–613.

Welch JH, Mayfield JJ, Leibowitz AL, Baculis BC, Fernando C (2017) Third trimester-equivalent ethanol exposure causes micro-hemorrhages in the rat brain. Neuroscience 324:107–118.

Wellmann KA, George F, Brnouti F, Mooney SM (2015) Docosahexaenoic acid partially ameliorates deficits in social behavior and ultrasonic vocalizations caused by prenatal ethanol exposure. Behav Brain Res 286:201–211.

Wenzel P, Hink U, Oelze M, Schuppan S, Schaeuble K, Schildknecht S, Ho KK, Weiner H, Bachschmid M, Münzel T, Daiber A (2007) Role of reduced lipoic acid in the redox regulation of mitochondrial aldehyde dehydrogenase (ALDH-2) activity: Implications for mitochondrial oxidative stress and nitrate tolerance. J Biol Chem 282:792–799.

West JR, Hamre KM (1985) Effects of alcohol exposure during different periods of development: changes in hippocampal mossy fibers. Dev Brain Res 17:280–284.

West JR, Hodges CA, Black AC (1981) Prenatal exposure to ethanol alters the organization of hippocampal mossy fibers in rats. Science 211:957–959.

Weyrauch D, Schwartz M, Hart B, Klug MG, Burd L (2017) Comorbid Mental Disorders in Fetal Alcohol Spectrum Disorders. J Dev Behav Pediatr 38:283–291.

Williams L, Jackson CPT, Choe N, Pelland L, Scott SH, Reynolds JN (2014) Sensory-Motor Deficits in Children with Fetal Alcohol Spectrum Disorder Assessed Using a Robotic Virtual Reality Platform. Alcohol Clin Exp Res 38:116–125.

Williamson JC, Edwards AVG, Verano-braga T, Kjeldsen F, Jensen ON, Larsen MR (2016) High-performance hybrid Orbitrap mass spectrometers for quantitative proteome analysis : Observations and implications. Proteomics 16:907–914.

Willoughby K a, Sheard ED, Nash K, Rovet J (2008) Effects of prenatal alcohol exposure on hippocampal volume, verbal learning, and verbal and spatial recall in late childhood. J Int Neuropsychol Soc 14:1022–1033.

Wöhr M, Schwarting RKW (2013) Affective communication in rodents : ultrasonic vocalizations as a tool for research on emotion and motivation. cell Tissue Res 354:81–97.

Womersley JS, Hsieh JH, Kellaway LA, Gerhardt GA, Russell VA (2011) Maternal separation affects dopamine transporter function in the spontaneously hypertensive rat: an in vivo electrochemical study. Behav Brain Funct 7:1–11.

Wouters FS, Bastiaens PIH, Wirtz KWA, Jovin TM (1998) FRET microscopy demonstrates molecular association of non-specific lipid transfer protein (nsL-TP) with fatty acid oxidation enzymes in peroxisomes. 17:7179–7189.

Wozniak JR, Mueller BA, Bell CJ, Muetzel RL, Hoecker HL, Boys CJ, Lim KO (2013) Global Functional Connectivity Abnormalities in Children with Fetal Alcohol Spectrum Disorders. Alcohol Clin Exp Res 37:748–756.

Xia Z, Storm DR (2005) The role of calmodulin as a signal integrator for synaptic plasticity. Nat Rev Neurosci 6:267–276.

Xiong Y, Uys JD, Tew KD, Townsend DM (2011) S-glutathionylation: From Molecular Mechanisms to Health Outcomes. AntioxidRedox Signal 15.

Xu Y, Liu P, Li Y (2005) Impaired development of mitochondria plays a role in the central nervous system defects of fetal alcohol syndrome. Birth Defects Res (Part A) Clin Mol Teratol 73:83–91.

Yang S, Lee YJ, Kim J-M, Park S, Peris J, Laipis P, Park YS, Chung JH, Oh SP (2006) A murine model for human sepiapterin-reductase deficiency. Am J Hum Genet 78:575–587.

Yang Y, Cheng Z, Tang H, Jiao H, Sun X, Cui Q (2017) Neonatal Maternal Separation Impairs Prefrontal Cortical Myelination and Cognitive Functions in Rats Through Activation of Wnt Signaling. Cereb Cortex 27:2871–2884.

Yang Y, Yang D, Tang G, Zhou C, Cheng K, Zhou J, Wu B, Peng Y, Liu C, Zhan Y, Chen J, Chen G, Xie P (2013) Proteomics reveals energy and glutathione metabolic dysregulation in the prefrontal cortex of a rat model of depression. Neuroscience 247:191–200.

Yip J, Geng X, Shen J, Ding Y (2017) Cerebral Gluconeogenesis and Diseases. Front Pharmacol 7:1–12.

Zhang J, Wu J, Zeng W, Yao K, Zu H, Zhao Y (2016) Function of Thymosin Beta-4 in Ethanol-Induced Microglial Activation. Cell Physiol Biochem 38:2230–2238.

Zhou D, Lebel C, Lepage C, Rasmussen C, Evans A, Wyper K, Pei J, Andrew G, Massey A, Massey D, Beaulieu C (2011) Developmental cortical thinning in fetal alcohol spectrum disorders. Neuroimage 58:16–25.

Zhou R, Wang S, Zhu X (2010) Prenatal ethanol exposure attenuates GABAergic inhibition in basolateral amygdala leading to neuronal hyperexcitability and anxiety-like behavior of adult rat offspring. Neuroscience 170:749–757.

APPENDICES: RAW DATA AND STATISTICAL ANALYSES

A2: CHAPTER 2

WEIGHT ANALYSIS

Table A2.1: Body weight of saline-control and ethanol-exposed rat pups from P4 - P9 (raw data)

Body Weight (g)						
Litter	**P4**	**P5**	**P6**	**P7**	**P8**	**P9**
Saline	10	14	14	16	20	20
Saline	12	14	15	17	20	22
Saline	10	12	13	15	17	19
Saline	10	12	14	16	19	22
Saline	10	12	14	15	18	21
Saline	9	11	11	13	15	17
Saline	9	11	12	13	17	17
Saline	11	13	14	15	17	19
Saline	12	14	15	17	19	21
EtOH	13	13	16	18	17	21
EtOH	9	12	13	14	17	20
EtOH	11	12	12	15	16	16
EtOH	11	12	13	16	17	19
EtOH	12	13	16	17	18	20
EtOH	11	12	15	16	18	20
EtOH	11	12	14	17	19	22
EtOH	9	10	12	13	15	18

Table A2.2: Body weight of control, EtOH- and vinp-rats from P25 - P31 (raw data)

Body Weight (g)								
Rat Number	**Group**	**P25**	**P26**	**P27**	**P28**	**P29**	**P30**	**P31**
78	Control	61	65	70	74	79	82	88
79	Control	68	73	77	80	85	91	98
104	Control	67	71	76	78	82	87	93
105	Control	70	72	76	81	86	91	97
106	Control	63	65	69	74	79	83	89
107	Control	69	72	76	80	85	91	97
140	Control	67	70	74	78	83	87	93
141	Control	68	70	75	78	83	88	91
175	Control	50	56	60	64	66	73	77
176	Control	40	49	53	56	58	65	70
177	Control	51	57	59	65	68	74	79
150	Control	63	66	70	73	77	84	88
151	Control	62	63	66	68	72	76	82
197	Control	66	69	73	78	84	87	96
198	Control	63	66	71	75	78	83	90
202	Control	70	72	78	82	88	93	101
203	Control	66	69	74	78	83	88	95
56	EtOH	65	71	74	80	84	90	99
57	EtOH	62	70	72	77	81	89	97
64	EtOH	51	55	60	65	70	74	78
38	EtOH	62	68	72	78	85	91	99
45	EtOH	68	71	75	80	85	90	98
46	EtOH	68	70	74	79	85	90	95
132	EtOH	77	80	87	89	94	100	105
186	EtOH	41	45	50	53	56	61	65
187	EtOH	55	59	64	66	71	75	80
166	EtOH	74	78	82	86	89	98	103
167	EtOH	62	66	68	72	76	82	88
54	Vinp	67	72	78	83	90	95	103
55	Vinp	57	62	66	70	73	78	86
63	Vinp	55	58	60	66	70	74	80
37	Vinp	65	67	74	81	83	91	96
43	Vinp	67	70	76	79	84	91	95
44	Vinp	71	73	78	81	85	93	99
130	Vinp	75	78	84	88	91	97	104
131	Vinp	73	75	76	82	88	95	99
184	Vinp	53	59	64	68	71	75	81
185	Vinp	48	51	57	59	62	68	74
165	Vinp	76	79	83	89	92	100	106

Table A2.3: Shapiro-Wilk test results for body weight from P4 - P9 and P25 - P31.

Weight on Postnatal Day (P)	Shapiro-Wilk, W	*P* Value
P4	0,952	0,482
P5	0,949	0,436
P6	0,962	0,684
P7	0,922	0,163
P8	0,961	0,642
P9	0,959	0,606
P25	0,931	0,021
P26	0,939	0,037
P27	0,954	0,109
P28	0,938	0,034
P29	0,927	0,015
P30	0,943	0,047
P31	0,939	0,035

Table A2.4: Repeated-measures ANOVA and Duncan's post-hoc test for the average body weight of saline-control and ethanol exposed rat pups per litter from P4 - P9.

Repeated Measures Analysis of Variance (Spreadsheet7)
Sigma-restricted parameterization
Effective hypothesis decomposition

Effect	SS	Degr. of Freedom	MS	F	p
Intercept	22489,08	1	22489,08	2272,155	0,000000
Treatment	0,00	1	0,00	0,000	0,997934
Error	148,47	15	9,90		
DAY	995,33	5	199,07	326,599	0,000000
DAY*Treatment	7,34	5	1,47	2,409	0,044160
Error	45,71	75	0,61		

Duncan test; variable DV_1 (Spreadsheet7)
Approximate Probabilities for Post Hoc Tests
Error: Between; Within; Pooled MS = 2,1575, df = 25,182

Cell No.	Treatment	DAY	{1} 10,220	{2} 12,433	{3} 13,519	{4} 15,174	{5} 18,030	{6} 19,874	{7} 10,913	{8} 11,950	{9} 13,830	{10} 15,696	{11} 17,282	{12} 19,570
1	Saline	P4		0,000050	0,000031	0,000021	0,000018	0,000011	0,341301	0,029202	0,000104	0,000021	0,000019	0,000019
2	Saline	P5	0,000050		0,005590	0,000050	0,000021	0,000017	0,053325	0,504603	0,074793	0,000271	0,000028	0,000021
3	Saline	P6	0,000031	0,005590		0,000109	0,000025	0,000017	0,002089	0,046598	0,666760	0,008638	0,000072	0,000024
4	Saline	P7	0,000021	0,000050	0,000109		0,000050	0,000025	0,000033	0,000309	0,071339	0,471615	0,008993	0,000037
5	Saline	P8	0,000018	0,000021	0,000025	0,000050		0,000063	0,000019	0,000021	0,000041	0,004281	0,305041	0,040808
6	Saline	P9	0,000011	0,000017	0,000017	0,000025	0,000063		0,000019	0,000018	0,000024	0,000041	0,002194	0,673459
7	EtOH	P4	0,341301	0,053325	0,002089	0,000033	0,000019	0,000019		0,007905	0,000031	0,000021	0,000017	0,000018
8	EtOH	P5	0,029202	0,504603	0,046598	0,000309	0,000021	0,000018	0,007905		0,000056	0,000025	0,000021	0,000017
9	EtOH	P6	0,000104	0,074793	0,666760	0,071339	0,000041	0,000024	0,000031	0,000056		0,000061	0,000050	0,000025
10	EtOH	P7	0,000021	0,000271	0,008638	0,471615	0,004281	0,000041	0,000021	0,000025	0,000061		0,000187	0,000050
11	EtOH	P8	0,000019	0,000028	0,000072	0,008993	0,305041	0,002194	0,000017	0,000021	0,000050	0,000187		0,000055
12	EtOH	P9	0,000019	0,000021	0,000024	0,000037	0,040808	0,673459	0,000018	0,000017	0,000025	0,000050	0,000055	

Duncan test; variable DV_1 (Spreadsheet7)
Approximate Probabilities for Post Hoc Tests
Error: Within MS = ,60951, df = 75,000

Cell No.	DAY	{1} 10,546	{2} 12,206	{3} 13,665	{4} 15,420	{5} 17,678	{6} 19,731
1	P4		0,000114	0,000055	0,000050	0,000031	0,000025
2	P5	0,000114		0,000115	0,000055	0,000050	0,000031
3	P6	0,000055	0,000115		0,000114	0,000055	0,000050
4	P7	0,000050	0,000055	0,000114		0,000114	0,000055
5	P8	0,000031	0,000050	0,000055	0,000114		0,000114
6	P9	0,000025	0,000031	0,000050	0,000055	0,000114	

Table A2.5: Friedman ANOVA of body weight of control, EtOH- and vinp-rats from P25 - P30

All Groups
Friedman ANOVA and Kendall Coeff. of Concordance (Spreadsheet20)
ANOVA Chi Sqr. (N = 39, df = 5) = 195,0000 p =0,00000
Coeff. of Concordance = 1,0000 Aver. rank r = 1,0000

Variable	Average Rank	Sum of Ranks	Mean	Std.Dev.
P25	1,00000(	39,000(	62,9743(	9,010191
P26	2,00000(	78,000(	66,7179[illegible]	8,23966[illegible]
P27	3,00000(	117,000(	71,0512[illegible]	8,44782[illegible]
P28	4,00000(	156,000(	75,2051[illegible]	8,67901[illegible]
P29	5,00000(	195,000(	79,5128[illegible]	9,27041[illegible]
P30	6,00000(	234,000(	85,12821	9,67410[illegible]

Aggregate Results
Friedman ANOVA and Kendall Coeff. of Concordance (Spreadsheet20)

Coeff. of Concordance = 1,0000 Aver. rank r = 1,0000

Variable	Group	Average Rank	Sum of Ranks	Mean	Std.Dev.
P25	Contro	1,00000(	17,000(	62,5882[illegible]	8,20867[illegible]
P26	Contro	2,00000(	34,000(	66,1764[illegible]	6,67303[illegible]
P27	Contro	3,00000(	51,000(	70,4117[illegible]	7,12441[illegible]
P28	Contro	4,00000(	68,000(	74,2352[illegible]	7,10219[illegible]
P29	Contro	5,00000(	85,000(	78,5882[illegible]	8,16286[illegible]
P30	Contro	6,00000(	102,000(	83,7058[illegible]	7,65477[illegible]
P25	EtOH	1,00000(	11,0000(	62,2727[illegible]	10,2965[illegible]
P26	EtOH	2,00000(	22,0000(	66,6363[illegible]	10,1614[illegible]
P27	EtOH	3,00000(	33,0000(	70,7272[illegible]	10,1596[illegible]
P28	EtOH	4,00000(	44,0000(	75,0000(	10,3440[illegible]
P29	EtOH	5,00000(	55,0000(	79,6363[illegible]	10,6796[illegible]
P30	EtOH	6,00000(	66,0000(	85,4545[illegible]	11,5096[illegible]
P25	Vinp	1,00000(	11,0000(	64,2727[illegible]	9,59261
P26	Vinp	2,00000(	22,0000(	67,6363[illegible]	9,0584(
P27	Vinp	3,00000(	33,0000(	72,3636[illegible]	9,16813
P28	Vinp	4,00000(	44,0000(	76,9090[illegible]	9,67941
P29	Vinp	5,00000(	55,0000(	80,8181[illegible]	10,1273[illegible]
P30	Vinp	6,00000(	66,0000(	87,0000(	11,0453[illegible]

Table A2.6: Kruskal-Wallis analysis of body weight on P31.

Multiple Comparisons p values (2-tailed); P31 (Spreadsheet20)
Independent (grouping) variable: Group
Kruskal-Wallis test: H (2, N= 39) =1,895616 p =,3876

Depend.: P31	Control R:17,176	EtOH R:21,682	Vinp R:22,682
Control		0,92152(	0,63628[illegible]
EtOH	0,92152(		1,00000(
Vinp	0,63628[illegible]	1,00000(	

OPEN FIELD TEST

Table A2.7: Open field test (raw data)

		Distance (cm)						
Rat number	Group	0 - 1 min	1 - 2 min	2 - 3 min	3 - 4 min	4 - 5 min	Total Distance (cm)	Total Inner Zone Duration (s)
78	Control	697,91	707,50	595,22	468,03	598,07	3066,85	27,20
79	Control	668,19	764,52	795,34	478,88	611,75	3318,82	15,20
104	Control	281,43	47,93	323,77	326,68	22,40	1002,23	0,00
105	Control	673,60	453,71	294,70	258,07	91,15	1771,38	4,80
106	Control	392,18	332,74	598,98	446,85	113,78	1884,53	0,00
107	Control	927,36	663,43	718,67	572,07	300,32	3190,81	24,00
140	Control	459,69	409,60	344,34	194,59	342,63	1751,20	0,00
141	Control	663,60	742,42	537,63	682,99	546,21	3176,10	13,80
150	Control	537,72	281,48	496,78	681,09	153,63	2150,76	6,80
151	Control	538,26	415,74	196,52	227,79	375,30	1753,61	0,20
175	Control	795,42	243,24	281,92	54,13	236,42	1617,95	0,40
176	Control	670,85	579,38	885,71	808,63	475,73	3420,46	26,40
177	Control	423,31	680,46	692,67	657,48	114,19	2570,24	16,60
197	Control	633,36	433,01	555,61	604,53	140,35	2367,06	8,40
198	Control	967,58	698,08	841,96	519,15	720,55	3747,94	28,60
202	Control	922,11	508,83	401,49	424,38	39,41	2296,39	0,80
203	Control	514,85	779,95	258,58	550,10	258,50	2361,99	1,60
56	EtOH	805,98	535,60	740,72	455,47	634,98	3177,94	11,20
57	EtOH	752,00	493,46	732,62	586,43	519,86	3090,34	13,60
64	EtOH	516,75	430,91	488,77	415,75	349,31	2202,93	4,00
38	EtOH	736,42	693,12	725,26	579,02	370,51	3104,47	18,20
45	EtOH	538,59	410,99	393,08	265,45	188,24	1796,53	0,00
46	EtOH	429,95	249,66	365,16	629,92	346,93	2022,94	1,40
132	EtOH	738,66	560,28	671,03	595,65	63,09	2629,13	10,20
166	EtOH	519,09	674,26	457,68	833,09	422,26	2906,55	17,20
167	EtOH	954,89	651,42	849,53	834,92	311,66	3602,45	8,40
186	EtOH	633,49	421,91	509,45	274,95	641,07	2488,87	4,60
187	EtOH	626,33	541,09	413,72	684,74	746,67	3012,69	22,80
54	Vinp	609,73	467,67	616,21	383,85	452,74	2530,22	4,60
55	Vinp	812,05	502,91	434,63	432,77	55,75	2238,13	2,40
63	Vinp	195,13	35,27	21,63	584,45	532,53	1369,27	0,00
37	Vinp	848,17	655,97	391,16	616,10	432,29	2943,87	9,60
43	Vinp	654,39	484,99	102,11	57,60	666,95	1966,32	0,00
44	Vinp	554,47	306,62	111,17	580,64	476,59	2029,76	0,00
130	Vinp	745,57	648,20	509,90	473,50	739,19	3117,29	2,80
131	Vinp	626,35	699,81	525,15	777,03	633,68	3263,31	23,00
165	Vinp	880,58	504,90	710,12	347,77	149,08	2592,96	2,40
184	Vinp	694,36	448,77	209,12	570,15	343,55	2266,05	2,00
185	Vinp	923,42	658,44	466,95	640,51	611,05	3300,39	5,20

Table A2.8: Shapiro-Wilk test results for the variables measured in the OFT

Variable	Shapiro-Wilk, W	*P* Value
Total Distance(cm)	0,970	0,374
Distance (0-1)	0,977	0,605
Distance (1-2)	0,940	0,037
Distance (2-3)	0,982	0,778
Distance (3-4)	0,967	0,292
Distance (4-5)	0,950	0,083
Inner Zone Duration (s)	0,855	0,000

Table A2.9: One-way ANOVA test results for the total distance travelled in the OFT between control, EtOH- and vinp-rats.

Effect	Univariate Tests of Significance for Distance (cm) (Spreadsheet1) Sigma-restricted parameterization Effective hypothesis decomposition SS	Degr. of Freedom	MS	F	p
Intercept	24505765	1	24505765	541,318	0,000000
Group	584742	2	292371	0,6458	0,530192
Error	1629737	36	45270		

Table A2.10: Repeated-measures ANOVA and Duncan's post-hoc analysis of the distance travelled per minute for the first 5 minutes of the OFT between control, EtOH- and vinp-rats.

Effect	Repeated Measures Analysis of Variance (Spreadsheet31) Sigma-restricted parameterization Effective hypothesis decomposition SS	Degr. of Freedom	MS	F	p
Intercept	4896295	1	4896295	541,2007	0,000000
Group	116208	2	58104	0,6422	0,532033
Error	3256955	36	90471		
MINUTE	1351689	4	337922	12,5979	0,000000
MINUTE*Group	405167	8	5064	1,8881	0,066125
Error	3862615	144	26824		

Cell No.	Duncan test; variable DV_1 (Spreadsheet31) Approximate Probabilities for Post Hoc Tests Error: Within MS = 26824,, df = 144,00 MINUTE	{1} 655,48	{2} 508,16	{3} 493,98	{4} 501,93	{5} 380,21
1	0 - 1 min		0,000079	0,000028	0,000060	0,000004
2	1 - 2 min	0,000079		0,721684	0,866541	0,001054
3	2 - 3 min	0,000028	0,721684		0,830250	0,002164
4	3 - 4 min	0,000060	0,866541	0,830250		0,001487
5	4 - 5 min	0,000004	0,001054	0,002164	0,001487	

Table A2.11: Kruskal-Wallis analysis of the time spent in the inner zone of the OFT between control, EtOH- and vinp-rats.

Depend.: Time (sec)	Multiple Comparisons p values (2-tailed); Time (sec) (Spreadsheet20) Independent (grouping) variable: Group Kruskal-Wallis test: H (2, N= 39) =2,731284 p =,2552 Saline+DMSO R:20,971	EtOH+DMSO R:23,091	EtOH+Vinp R:15,409
Saline+DMSO		1,000000	0,622408
EtOH+DMSO	1,000000		0,342279
EtOH+Vinp	0,622408	0,342279	

EXPOSURE TO A NOVEL OBJECT

Table A2.12: Exposure to a novel object (cone) test (raw data).

Rat Number	Exp. Group	Distance (cm)	Novel Object Duration (s)	Frequency	Latency to first
78	Control	2541,16	42	11	39,4
79	Control	1857,14	79,8	13	135
104	Control	152,97	0	0	0
105	Control	113,48	0	0	0
106	Control	1676,91	22,4	10	139,8
107	Control	1683,20	23	7	104,6
140	Control	2147,52	21,8	5	145,8
141	Control	308,43	0	0	0
150	Control	347,77	0	0	0
151	Control	713,30	0	0	0
175	Control	2321,38	34,2	9	130,8
176	Control	263,10	0	0	0
177	Control	142,45	0	0	0
197	Control	1489,51	25,2	9	185,8
198	Control	1186,80	23	5	213,6
202	Control	743,87	0	0	0
203	Control	841,25	18	3	152,6
56	EtOH	1965,18	47,8	10	96
57	EtOH	1590,49	59,6	10	189
64	EtOH	605,09	0	0	0
38	EtOH	297,87	0	0	0
45	EtOH	426,60	0	0	0
46	EtOH	1188,82	15	3	98,4
132	EtOH	312,81	0	0	0
166	EtOH	1578,32	35,8	7	151,4
167	EtOH	2014,17	24,2	8	75
186	EtOH	335,42	0	0	0
187	EtOH	233,39	0	0	0
54	Vinp	388,71	0	0	0
55	Vinp	655,57	0	0	0
63	Vinp	420,28	0	0	0
37	Vinp	538,42	0	0	0
43	Vinp	432,28	0	0	0
44	Vinp	157,39	0	0	0
130	Vinp	210,00	0	0	0
131	Vinp	272,02	0	0	0
165	Vinp	231,27	0	0	0
184	Vinp	888,76	0,2	1	114,4
185	Vinp	1131,11	1,2	4	126,6

Table A2.13: Shapiro-Wilk test results for the variables measured in the exposure to a novel object (cone) test.

Variable	Shapiro-Wilk, W	*P* value
Distance	0,867	0,002
NO duration	0,687	0
Frequency to NO	0,714	0
Latency to NO	0,741	0

Table A2.14: Kruskal-Wallis test results for the distance travelled in the novel object (cone) test).

	Multiple Comparisons p values (2-tailed); Distance (cm) (Spreadsheet53) Independent (grouping) variable: Exp. Group Kruskal-Wallis test: H (2, N= 39) =3,064912 p =,2160		
Depend.: Distance (cm)	Control R:22,176	EtOH R:21,727	Vinp R:14,909
Control		1,000000	0,298547
EtOH	1,000000		0,482369
Vinp	0,298547	0,482369	

Table A2.15: Kruskal-Wallis test results for the duration spent in the cone zone in the novel object (cone) test).

	Multiple Comparisons p values (2-tailed); Novel Object Duration (s) (Spreadsheet53) Independent (grouping) variable: Exp. Group Kruskal-Wallis test: H (2, N= 39) =4,895218 p =,0865		
Depend.: Novel Object Duration (s)	Control R:22,529	EtOH R:21,818	Vinp R:14,273
Control		1,000000	0,183853
EtOH	1,000000		0,361978
Vinp	0,183853	0,361978	

Table A2.16: Kruskal-Wallis test result for the latency to reach the novel object (cone).

	Multiple Comparisons p values (2-tailed); Latency to first (Spreadsheet53) Independent (grouping) variable: Exp. Group Kruskal-Wallis test: H (2, N= 39) =3,901004 p =,1422		
Depend.: Latency to first	Control R:22,941	EtOH R:20,273	Vinp R:15,182
Control		1,000000	0,235877
EtOH	1,000000		0,885104
Vinp	0,235877	0,885104	

Table A2.17: Kruskal-Wallis test results for the frequency to enter the cone zone in the novel object (cone) test).

	Multiple Comparisons p values (2-tailed); Frequency (Spreadsheet53) Independent (grouping) variable: Exp. Group Kruskal-Wallis test: H (2, N= 39) =4,770326 p =,0921		
Depend.: Frequency	Control R:22,882	EtOH R:21,091	Vinp R:14,455
Control		1,000000	0,168312
EtOH	1,000000		0,516738
Vinp	0,168312	0,516738	

MORRIS WATER MAZE

Table A2.18: Morris Water Maze (raw data).

	Av. Latency to reach the platform (s)				% Time spent in the platform quadrant
Group	Day 1	Day 2	Day 3	Day 4	
Control	119	49	27	33	23,07
Control	49	14	11	9	44,47
Control	105	56	10	14	41,23
Control	81	77	68	35	12,93
Control	57	35	11	41	43,95
Control	79	68	19	19	24,87
Control	96	68	31	37	17,15
Control	83	20	19	41	48,73
Control	120	45	24	22	19,17
Control	104	117	119	32	28,11
Control	73	72	16	9	29,66
Control	85	53	24	47	20,43
Control	91	69	49	20	18,21
Control	59	12	31	11	41,04
Control	65	35	35	37	27,44
Control	25	23	18	23	22,80
Control	64	25	28	20	8,68
EtOH	119	101	82	27	27,60
EtOH	107	26	46	28	40,50
EtOH	82	28	24	14	35,60
EtOH	74	21	27	11	39,10
EtOH	101	44	15	14	35,84
EtOH	95	75	85	64	21,55
EtOH	63	29	19	12	32,84
EtOH	54	46	17	6	53,21
EtOH	118	76	65	71	15,17
EtOH	42	65	51	25	31,74
EtOH	96	45	48	41	29,95
Vinp	120	49	49	56	43,21
Vinp	90	73	92	90	23,08
Vinp	86	33	22	15	46,18
Vinp	91	60	16	16	29,46
Vinp	92	50	10	22	36,30
Vinp	95	23	11	56	20,08
Vinp	53	39	17	9	27,73
Vinp	95	48	18	40	14,30
Vinp	87	91	51	43	32,80
Vinp	104	42	41	43	36,00
Vinp	77	38	21	30	25,30

Table A2.19: Shapiro-Wilk test results for the variables measured in the MWM.

Variable	Shapiro-Wilk, W	*P* value
Av. Latency to reach the platform on Day 1	0,966	0,277
Av. Latency to reach the platform on Day 2	0,958	0,153
Av. Latency to reach the platform on Day 3	0,827	0
Av. Latency to reach the platform on Day 4	0,912	0,004
% Time spent in the platform quadrant	0,986	0,898

Table A2.20: Repeated-measures ANOVA and Duncan's post-hoc test results for the average latency to reach the platform during training in the MWM between control, EtOH- and vinp-rats.

Effect	Repeated Measures Analysis of Variance (Spreadsheet1) Sigma-restricted parameterization Effective hypothesis decomposition SS	Degr. of Freedom	MS	F	p
Intercept	381177,2	1	381177,2	291,4655	0,000000
Group	1154,8	2	577,4	0,4415	0,646505
Error	47080,6	36	1307,8		
DAY	67992,6	3	22664,2	77,1530	0,000000
DAY*Group	1684,3	6	280,7	0,9556	0,458924
Error	31725,7	108	293,8		

Cell No.	Duncan test; variable DV_1 (Spreadsheet1) Approximate Probabilities for Post Hoc Tests Error: Within MS = 293,76, df = 108,00 DAY	{1} 84,532	{2} 49,735	{3} 35,011	{4} 30,381
1	Day 1		0,000105	0,000057	0,000046
2	Day 2	0,000105		0,000342	0,000060
3	Day 3	0,000057	0,000342		0,235534
4	Day 4	0,000046	0,000060	0,235534	

Table A2.21: One-way ANOVA of the percentage time spent in the platform quadrant during the probe trial.

Effect	Univariate Tests of Significance for % Time spent in the platform quadrant (Spreadsheet1) Sigma-restricted parameterization Effective hypothesis decomposition SS	Degr. of Freedom	MS	F	p
Intercept	34544,49	1	34544,49	292,0839	0,000000
Group	186,49	2	93,25	0,7884	0,462249
Error	4257,69	36	118,27		

Table A2.22: Raw absorbance values from the spectrophotometer for PFC samples

Raw Data: BDNF ELISA PFC

Date 27.01.2015 17:46:54
Plate form 96 Wells

Absorbance's Filter 1: 450nm

	1	2	3	4	5	6	7	8	9	10	11	12
A	0,171	0,164	0,161	0,151	0,161	0,161	0,162	0,153	0,141	0,152	1,163	1,171
B	0,15	0,152	0,150	0,156	0,145	0,144	0,133	0,150	0,144	0,152	0,642	0,819
C	0,159	0,149	0,151	0,160	0,150	0,150	0,154	0,155	0,150	0,146	0,389	0,415
D	0,168	0,164	0,152	0,147	0,152	0,178	0,147	0,144	0,140	0,143	0,255	0,279
E	0,167	0,158	0,145	0,150	0,150	0,155	0,150	0,150	0,155	0,158	0,180	0,196
F	0,165	0,14	0,154	0,148	0,146	0,149	0,154	0,158	0,147	0,147	0,141	0,157
G	0,217	0,163	0,157	0,158	0,152	0,156	0,155	0,162	0,142	0,151	0,135	0,150
H	0,205	0,174	0,172	0,145	0,169	0,159	0,164	0,159	0,174	0,153	0,111	0,137

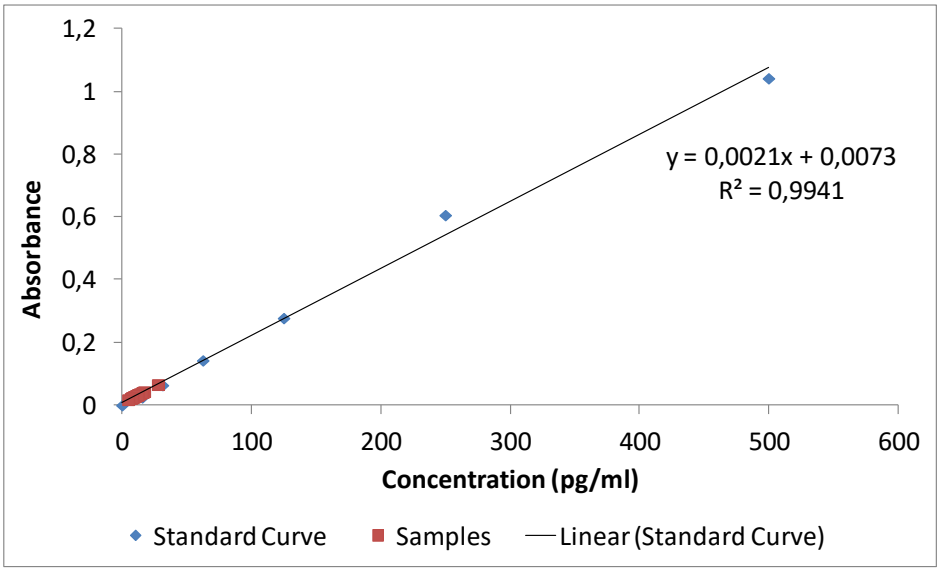

Figure A2.1: Standard curve used to calculate BDNF concentration in the PFC

Table A2.23: Raw absorbance values from the spectrophotometer for DH samples

Raw Data - BDNF DH

Date 28.11.2014 16:04:48
Plate format: 96 Wells

Absorbances Filter 1: 450nm

	1	2	3	4	5	6	7	8	9	10	11	12
A	0,278	0,266	0,267	0,267	0,257	0,235	0,234	0,238	0,242	0,237	1,190	1,153
B	0,281	0,253	0,240	0,235	0,238	0,223	0,231	0,236	0,244	0,225	0,618	0,660
C	0,258	0,251	0,250	0,265	0,257	0,246	0,233	0,237	0,236	0,248	0,360	0,395
D	0,259	0,214	0,214	0,218	0,240	0,233	0,222	0,230	0,237	0,244	0,237	0,267
E	0,249	0,236	0,244	0,255	0,238	0,249	0,227	0,248	0,236	0,243	0,180	0,201
F	0,239	0,238	0,246	0,255	0,255	0,260	0,191	0,189	0,225	0,147	0,152	0,162
G	0,283	0,269	0,251	0,249	0,254	0,270	0,250	0,254	0,143	0,161	0,139	0,146
H	0,273	0,268	0,254	0,256	0,237	0,237	0,262	0,241	0,164	0,154	0,134	0,133

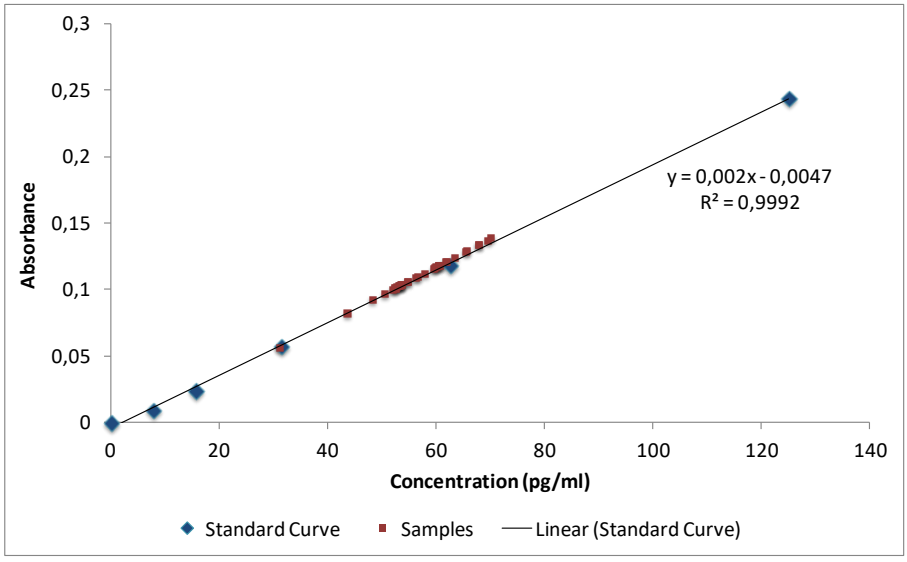

Figure A2.2: Standard curve used to calculate BDNF concentration in the DH

Table A2.24: BDNF concentration in the PFC and DH calculated from the standard curves above (raw data).

PFC				DH			
Rat Number	Group	BDNF Concentration (pg/ml)	BDNF Concentration (pg/mg)	Rat Number	Group	BNDF Concentration (pg/ml)	BDNF Concentration (pg/mg)
78	Control	11,76	0,24	78	Control	67,81	1,36
79	Control	10,10	0,20	79	Control	52,33	1,05
104	Control	10,33	0,21	105	Control	53,29	1,07
105	Control	10,81	0,22	106	Control	69,48	1,39
106	Control	13,98	0,28	106	Control	53,76	1,08
140	Control	14,14	0,28	140	Control	59,48	1,19
141	Control	15,57	0,31	141	Control	70,19	1,40
150	Control	8,90	0,18	150	Control	52,10	1,04
151	Control	9,22	0,18	151	Control	56,14	1,12
175	Control	9,38	0,19	151	Control	54,71	1,09
177	Control	17,24	0,34	175	Control	65,75	1,31
197	Control	11,52	0,23	176	Control	67,81	1,36
202	Control	16,52	0,33	177	Control	43,52	0,87
38	EtOH	11,60	0,23	197	Control	61,86	1,24
45	EtOH	12,48	0,25	202	Control	61,78	1,24
46	EtOH	9,38	0,19	38	EtOH	65,43	1,31
56	EtOH	12,95	0,26	45	EtOH	59,95	1,20
57	EtOH	7,32	0,15	46	EtOH	60,35	1,21
64	EtOH	16,05	0,32	56	EtOH	57,81	1,16
166	EtOH	10,10	0,20	57	EtOH	50,43	1,01
167	EtOH	12,48	0,25	64	EtOH	59,71	1,19
186	EtOH	7,71	0,15	132	EtOH	60,43	1,21
187	EtOH	7,71	0,15	166	EtOH	53,29	1,07
37	Vinp	12,08	0,24	167	EtOH	56,62	1,13
43	Vinp	11,13	0,22	186	EtOH	53,52	1,07
44	Vinp	12,08	0,24	187	EtOH	63,29	1,27
54	Vinp	4,86	0,10	37	Vinp	53,05	1,06
55	Vinp	7,95	0,16	43	Vinp	60,67	1,21
63	Vinp	7,95	0,16	44	Vinp	60,43	1,21
130	Vinp	6,76	0,14	54	Vinp	52,41	1,05
131	Vinp	4,86	0,10	55	Vinp	52,57	1,05
165	Vinp	8,90	0,18	130	Vinp	48,29	0,97
184	Vinp	7,24	0,14	184	Vinp	53,76	1,08
185	Vinp	11,13	0,22	185	Vinp	54,71	1,09

Table A2.25: Shapiro-Wilk test results for the BDNF concentration (pg/mg) in the PFC and DH.

	Shapiro-Wilk, W	*P* Value
PFC - BNDF Concentration (pg/mg)	0,977	0,691
DH - BNDF Concentration (pg/mg)	0,961	0,364

Table A2.26: One-way ANOVA and Duncan's post-hoc test result for BDNF in the PFC

Univariate Tests of Significance for Concentration (pg/ml) (Spreadsheet14)
Sigma-restricted parameterization
Effective hypothesis decomposition

Effect	SS	Degr. of Freedom	MS	F	p
Intercept	3746,49	1	3746,49	476,422	0,00000
Group	79,080	2	39,540	5,0281	0,01284
Error	243,778	31	7,864		

Duncan test; variable Concentration (pg/ml) (Spreadsheet14)
Approximate Probabilities for Post Hoc Tests
Error: Between MS = 7,8638, df = 31,000

Cell No.	Group	{1} 12,269	{2} 10,778	{3} 8,6306
1	Saline+DMSO		0,21785	0,00604
2	EtOH+DMSO	0,21785		0,07981
3	EtOH+Vinp	0,00604	0,07981	

Table A2.27: One-way ANOVA result for BDNF in the DH

Univariate Tests of Significance for Concentration (pg/ml) (Spreadsheet21)
Sigma-restricted parameterization
Effective hypothesis decomposition

Effect	SS	Degr. of Freedom	MS	F	p
Intercept	104787,0	1	104787,0	2722,74	0,00000
Group	125,3	2	62,7	1,629	0,21256
Error	1193,1	31	38,5		

Table A2.28: Raw pixel density percentages for the proteins quantified using Western blot analysis in the PFC of control, EtOH- and vinp-rats.

	Prefrontal Cortex							
Group	MKP-1	P-ERK	ERK	P-ERK / ERK	P-GSK3β	GSK3β	P-GSK3β / GSK3β	Synaptophysin
Control	131,05	17,08	8,02	212,97	6,74	9,97	67,60	161,46
Control	87,06	10,76	10,18	105,70	7,36	5,92	124,32	103,29
Control	78,99	8,93	9,31	95,92	16,45	9,32	176,50	60,11
Control	79,48	13,15	11,33	116,06	7,89	11,67	67,61	132,94
Control	89,28	11,69	10,62	110,08	12,77	11,66	109,52	110,30
Control	63,19	11,81	9,08	130,07	9,99	9,36	106,73	45,30
Control	82,65	11,19	10,47	106,88	6,47	11,11	58,24	136,00
Control	90,81	12,02	9,65	124,56	6,27	9,12	68,75	127,78
Control	75,75	11,71	10,55	111,00	9,52	10,67	89,22	117,35
Control	81,50	8,99	11,85	75,86	6,16	10,42	59,12	93,39
Control	58,58	11,53	9,37	123,05	5,82	7,73	75,29	46,65
Control	-	10,27	11,03	93,11	8,92	10,26	86,94	64,51
Control	-	13,27	12,79	103,75	15,48	12,07	128,25	144,64
Control	-	9,68	10,32	93,80	12,77	11,55	110,56	-
EtOH	75,05	10,17	12,45	81,69	10,93	10,14	107,79	51,42
EtOH	85,57	9,23	11,64	79,30	8,12	9,95	81,61	100,66
EtOH	107,36	11,66	12,63	92,32	8,53	12,33	69,18	84,59
EtOH	112,31	7,06	9,14	77,24	5,89	10,06	58,55	107,33
EtOH	80,42	10,23	13,06	78,33	8,62	12,79	67,40	104,52
EtOH	47,52	9,95	10,80	92,13	14,90	11,79	126,38	106,52
EtOH	70,95	7,13	10,60	67,26	13,55	11,54	117,42	87,64
EtOH	127,74	7,53	11,86	63,49	17,67	14,30	123,57	62,59
EtOH	153,71	14,24	10,81	131,73	9,49	9,70	97,84	52,68
EtOH	110,47	10,48	10,75	97,49	13,66	7,86	173,79	154,26
EtOH	-	9,79	12,02	81,45	6,95	14,27	48,70	35,43
Vinp	139,12	11,09	12,98	85,44	14,46	13,99	103,36	129,92
Vinp	110,53	12,18	11,22	108,56	15,45	12,13	127,37	126,75
Vinp	78,66	8,89	11,58	76,77	11,95	16,25	73,54	121,84
Vinp	156,39	11,22	10,76	104,28	12,82	9,62	133,26	78,59
Vinp	114,65	10,83	13,41	80,76	11,92	11,19	106,52	113,28
Vinp	107,55	14,06	11,80	119,15	15,20	11,86	128,16	119,42
Vinp	103,01	8,18	11,35	72,07	14,28	11,48	124,39	102,46
Vinp	145,29	12,12	10,95	110,68	8,27	9,16	90,28	81,36
Vinp	132,27	15,86	13,76	115,26	14,49	12,93	112,06	118,92
Vinp	101,98	13,67	11,40	119,91	17,07	12,90	132,33	113,89
Vinp	135,69	12,32	10,47	117,67	13,18	12,95	101,78	-

Table A2.29: Raw pixel density percentages for the proteins quantified using Western blot analysis in the DH of control, EtOH- and vinp-rats.

	Dorsal Hippocampus							
Group	**MKP-1**	**P-ERK**	**ERK**	**P-ERK / ERK**	**P-GSK3β**	**GSK3β**	**P-GSK3β / GSK3β**	**Synaptophysin**
Control	70,63	18,50	17,52	105,59	12,32	11,14	110,59	89,17
Control	91,26	18,70	14,54	128,61	14,31	10,87	131,65	72,98
Control	107,66	10,00	11,93	83,82	12,60	11,28	111,70	66,30
Control	96,35	16,22	12,60	128,73	7,74	11,45	67,60	103,33
Control	88,38	4,10	9,38	43,71	7,85	10,47	74,98	119,06
Control	99,73	2,82	12,07	23,36	3,50	8,83	39,64	79,44
Control	91,53	2,53	11,30	22,39	10,40	11,72	88,74	121,51
Control	101,92	8,25	9,54	86,48	8,87	10,33	85,87	126,91
Control	82,93	1,78	7,40	24,05	7,98	10,19	78,31	123,75
Control	62,27	12,14	11,22	108,20	1,70	8,43	20,17	91,54
Control	-	14,59	13,38	109,04	1,29	10,58	12,19	76,62
Control	-	14,46	13,94	103,73	5,45	11,39	47,85	74,48
Control	-	5,68	11,98	47,41	10,34	10,83	95,48	78,39
Control	-	-	-	-	4,87	11,42	42,64	90,43
EtOH	146,26	19,07	15,30	124,64	7,95	9,69	82,04	38,21
EtOH	109,04	11,45	11,13	102,88	7,47	10,39	71,90	86,36
EtOH	85,48	8,78	11,71	74,98	10,37	12,28	84,45	110,87
EtOH	112,93	18,77	10,11	185,66	6,67	9,68	68,90	50,10
EtOH	58,97	14,15	12,20	115,98	7,02	11,48	61,15	85,79
EtOH	82,61	18,89	9,53	198,22	12,77	12,01	106,33	110,78
EtOH	85,27	12,66	14,15	89,47	11,68	9,62	121,41	89,30
EtOH	145,53	11,75	8,85	132,77	10,35	11,68	88,61	52,25
EtOH	116,13	-	-	-	14,34	12,08	118,71	38,80
EtOH	-	-	-	-	20,11	13,18	152,58	85,91
EtOH	-	-	-	-	16,31	11,97	136,26	131,69
Vinp	110,82	20,49	20,02	102,35	10,74	9,95	107,94	143,76
Vinp	82,09	15,74	17,26	91,19	11,07	11,69	94,70	166,38
Vinp	70,94	7,49	15,37	48,73	13,17	12,72	103,54	128,43
Vinp	97,00	18,68	15,05	124,12	20,72	14,26	145,30	141,60
Vinp	43,07	16,77	15,91	105,41	15,73	10,93	143,92	135,65
Vinp	123,66	13,99	12,28	113,93	18,00	10,89	165,29	71,93
Vinp	91,28	7,21	12,12	59,49	11,88	11,31	105,04	88,62
Vinp	141,86	8,02	11,46	69,98	10,53	11,34	92,86	106,81
Vinp	102,60	19,37	11,66	166,12	13,97	11,72	119,20	146,89
Vinp	-	15,21	9,15	166,23	21,25	11,82	179,78	139,85
Vinp	-	11,74	9,94	118,11	18,68	10,38	179,96	135,88

Table A2.30: Shapiro-Wilk test results for the variables measured in Western blot experiments.

Brain Area	Variable	Shapiro-Wilk, W	*P* Value
PFC	MKP-1	0,962	0,316
PFC	P-ERK1/2	0,971	0,447
PFC	ERK1/2	0,966	0,327
PFC	P-ERK1/2 / ERK	0,840	0,001
PFC	P-GSK3β	0,936	0,039
PFC	GSK3β	0,986	0,913
PFC	P-GSK3β / GSK3β	0,950	0,104
PFC	Synaptophysin	0,966	0,358
DH	MKP-1	0,972	0,623
DH	P-ERK1/2	0,940	0,074
DH	ERK1/2	0,961	0,306
DH	P-ERK1/2 / ERK	0,965	0,375
DH	P-GSK3β	0,978	0,692
DH	GSK3β	0,979	0,707
DH	P-GSK3β / GSK3β	0,986	0,922
DH	Synaptophysin	0,972	0,473

Table A2.31: One-way ANOVA and Duncan's post-hoc test of MKP-1 in the PFC of control, EtOH- and vinp-rats.

Univariate Tests of Significance for MKP-1/P38 Pixel Density (%) (Spreadsh
Sigma-restricted parameterization
Effective hypothesis decomposition

Effect	SS	Degr. of Freedom	MS	F	p
Intercept	321623,8	1	321623,8	532,5358	0,000000
Groups	7685,1	2	3842,5	6,3624	0,005118
Error	17514,5	29	603,9		

Duncan test; variable MKP-1/P38 Pixel Density (%) (Spreadsheet1)
Approximate Probabilities for Post Hoc Tests
Error: Between MS = 603,95, df = 29,000

Cell No.	Groups	{1} 83,486	{2} 97,110	{3} 120,47
1	Contro		0,211172	0,002318
2	EtOH	0,211172		0,036610
3	Vinp	0,002318	0,036610	

Table A2.32: One-way ANOVA of MKP-1 in the DH of control, EtOH- and vinp-rats.

Univariate Tests of Significance for MKP-1/a-tubulin Pixel Density (%) (Spreadsheet14)
Sigma-restricted parameterization
Effective hypothesis decomposition

Effect	SS	Degr. of Freedom	MS	F	p
Intercept	260787,0	1	260787,0	420,6277	0,000000
Groups	1129,5	2	564,7	0,9109	0,415106
Error	15499,9	25	620,0		

Table A2.33: One-way ANOVA of P-ERK1/2 in the PFC of control, EtOH- and vinp-rats.

Univariate Tests of Significance for Pixel Total % (Spreadsheet1)
Sigma-restricted parameterization
Effective hypothesis decomposition

Effect	SS	Degr. of Freedom	MS	F	p
Intercept	4353,354	1	4353,354	965,8593	0,000000
"Var1"	28,934	2	14,467	3,2098	0,053240
Error	148,739	33	4,507		

Table A2.34: One-way ANOVA of ERK1/2 in the PFC of control, EtOH- and vinp-rats.

Univariate Tests of Significance for Pixel Total % (Spreadsheet1)
Sigma-restricted parameterization
Effective hypothesis decomposition

Effect	SS	Degr. of Freedom	MS	F	p
Intercept	4444,222	1	4444,222	3304,208	0,000000
Group	14,814	2	7,407	5,507	0,008634
Error	44,386	33	1,345		

Duncan test; variable Pixel Total % (Spreadsheet1)
Approximate Probabilities for Post Hoc Tests
Error: Between MS = 1,3450, df = 33,000

Cell No.	Group	{1} 10,326	{2} 11,433	{3} 11,789
1	Saline+DMSO		0,026688	0,005855
2	EtOH+DMSO	0,026688		0,459997
3	EtOH+Vinp	0,005855	0,459997	

Table A2.35: Kruskal-Wallis analysis of P-ERK1/2 to ERK1/2 in the PFC of control, EtOH- and vinp-rats.

Multiple Comparisons p values (2-tailed); Pixel Total % (Spreadsheet1)
Independent (grouping) variable: Group
Kruskal-Wallis test: H (2, N= 36) =8,112730 p =,0173

Depend.: Pixel Total %	Saline+DMSO R:23,357	EtOH+DMSO R:11,364	EtOH+Vinp R:19,455
Saline+DMSO		0,014168	1,000000
EtOH+DMSO	0,014168		0,215102
EtOH+Vinp	1,000000	0,215102	

Table A2.36: One-way ANOVA of P-ERK1/2 in the DH of control, EtOH- and vinp-rats.

Univariate Tests of Significance for Pixel Total % (Spreadsheet6)
Sigma-restricted parameterization
Effective hypothesis decomposition

Effect	SS	Degr. of Freedom	MS	F	p
Intercept	5058,317	1	5058,317	181,2337	0,000000
Group	139,439	2	69,719	2,4980	0,097895
Error	809,403	29	27,910		

Table A2.37: One-way ANOVA of ERK1/2 in the DH of control, EtOH- and vinp-rats.

Univariate Tests of Significance for Pixel Total % (Spreadsheet10)
Sigma-restricted parameterization
Effective hypothesis decomposition

Effect	SS	Degr. of Freedom	MS	F	p
Intercept	4761,450	1	4761,450	617,6593	0,000000
Group	23,368	2	11,684	1,5157	0,236554
Error	223,557	29	7,709		

Table A2.38: One-way ANOVA and Duncan's post-hoc test for P-ERK1/2 to ERK1/2 in the DH of control, EtOH- and vinp-rats.

Univariate Tests of Significance for Pixel Total % (Spreadsheet1) Sigma-restricted parameterization Effective hypothesis decomposition					
Effect	SS	Degr. of Freedom	MS	F	p
Intercept	332699,4	1	332699,4	202,0471	0,000000
"Var1"	12938,1	2	6469,1	3,9286	0,030916
Error	47752,6	29	1646,6		

Duncan test; variable Pixel Total % (Spreadsheet1) Approximate Probabilities for Post Hoc Tests Error: Between MS = 1646,6, df = 29,000				
Cell No.	Var1	{1} 78,088	{2} 128,07	{3} 105,97
1	Saline-DMSO		0,012323	0,130916
2	EtoH-DMSO	0,012323		0,227633
3	EtOH-Vinp	0,130916	0,227633	

Table A2.39: Kruskal-Wallis analysis of P-GSK3β in the PFC of control, EtOH- and vinp-rats.

Multiple Comparisons p values (2-tailed); Pixel Total % (Spreadsheet2) Independent (grouping) variable: Group Kruskal-Wallis test: H (2, N= 36) =7,546484 p =,0230			
Depend.: Pixel Total %	Saline+DMSO R:13,786	EtOH+DMSO R:17,636	EtOH+Vinp R:25,364
Saline+DMSO		1,000000	0,019147
EtOH+DMSO	1,000000		0,256259
EtOH+Vinp	0,019147	0,256259	

Table A2.40: One-way ANOVA and Duncan post-hoc analysis of GSK3β in the PFC of control, EtOH- and vinp-rats.

Univariate Tests of Significance for Pixel Total % (Spreadsheet1) Sigma-restricted parameterization Effective hypothesis decomposition					
Effect	SS	Degr. of Freedom	MS	F	p
Intercept	4463,788	1	4463,788	1261,397	0,000000
Group	29,675	2	14,838	4,193	0,023847
Error	116,779	33	3,539		

Duncan test; variable Pixel Total % (Spreadsheet1) Approximate Probabilities for Post Hoc Tests Error: Between MS = 3,5388, df = 33,000				
Cell No.	Group	{1} 10,059	{2} 11,339	{3} 12,224
1	Saline+DMSO		0,107392	0,011345
2	EtOH+DMSO	0,107392		0,260808
3	EtOH+Vinp	0,011345	0,260808	

Table A2.41: One-way ANOVA of P-GSK3β to GSK3β in the PFC of control, EtOH- and vinp-rats.

Univariate Tests of Significance for Pixel Total % (Spreadsheet1) Sigma-restricted parameterization Effective hypothesis decomposition					
Effect	SS	Degr. of Freedom	MS	F	p
Intercept	36,60654	1	36,60654	378,8501	0,000000
Group	0,20112	2	0,10056	1,0407	0,364500
Error	3,18864	33	0,09663		

Table A2.42: Kruskal-Wallis analysis of P-GSK3β in the DH of control, EtOH- and vinp-rats.

Univariate Tests of Significance for Pixel Total % (Spreadsheet28) Sigma-restricted parameterization Effective hypothesis decomposition					
Effect	SS	Degr. of Freedom	MS	F	p
Intercept	4628,30(	1	4628,30(	274,412{	0,00000(
"Var1"	326,241	2	163,121	9,6715	0,00049{
Error	556,58{	33	16,866		

Duncan test; variable Pixel Total % (Spreadsheet28) Approximate Probabilities for Post Hoc Tests Error: Between MS = 16,866, df = 33,000				
Cell No.	Var1	{1} 7,8014	{2} 11,367	{3} 15,067
1	Saline-DMSO		0,04233(	0,000253
2	EtOH-DMSO	0,04233(		0,035594
3	EtOH-Vinp	0,000253	0,035594	

Table A2.43: One-way ANOVA of GSK3β in the DH of control, EtOH- and vinp-rats.

Univariate Tests of Significance for Pixel Total % (Spreadsheet50) Sigma-restricted parameterization Effective hypothesis decomposition					
Effect	SS	Degr. of Freedom	MS	F	p
Intercept	4421,507	1	4421,507	3557,65{	0,00000(
Group	5,527	2	2,763	2,223	0,12420(
Error	41,013	33	1,243		

Table A2.44: One-way ANOVA and Duncan's post-hoc test for P-GSK3β to GSK3β in the DH of control, EtOH- and vinp-rats.

Univariate Tests of Significance for Pixel Total % (Spreadsheet1) Sigma-restricted parameterization Effective hypothesis decomposition					
Effect	SS	Degr. of Freedom	MS	F	p
Intercept	360005,3	1	360005,3	325,054(	0,00000(
"Var1"	21261,9	2	10631,(	9,598{	0,00051{
Error	36548,2	33	1107,5		

Duncan test; variable Pixel Total % (Spreadsheet1) Approximate Probabilities for Post Hoc Tests Error: Between MS = 1107,5, df = 33,000				
Cell No.	Var1	{1} 71,957	{2} 99,304	{3} 130,68
1	Saline-DMSO		0,05391(	0,00025{
2	EtOH-DMSO	0,05391(		0,028351
3	EtOH-Vinp	0,00025{	0,028351	

Table A2.45: One-way ANOVA of synaptophysin in the PFC of control, EtOH- and vinp-rats.

Univariate Tests of Significance for Synaptophysin/P38 Pixel Density (%) (Spreadsheet23) Sigma-restricted parameterization Effective hypothesis decomposition					
Effect	SS	Degr. of Freedom	MS	F	p
Intercept	336383,2	1	336383,2	322,775{	0,00000(
Groups	3389,5	2	1694,7	1,6262	0,21301{
Error	32306,9	31	1042,2		

Table A2.46: One-way ANOVA and Duncan's post-hoc test for synaptophysin in the DH of control, EtOH- and vinp-rats.

Univariate Tests of Significance for Synaptophysin/a-tubulin Pixel Density (%) (Spreadsheet32)
Sigma-restricted parameterization
Effective hypothesis decomposition

Effect	SS	Degr. of Freedom	MS	F	p
Intercept	359319,4	1	359319,4	507,3326	0,000000
Groups	13428,4	2	6714,2	9,4799	0,000558
Error	23372,3	33	708,3		

Duncan test; variable Synaptophysin/a-tubulin Pixel Density (%) (Spreadsheet32)
Approximate Probabilities for Post Hoc Tests
Error: Between MS = 708,25, df = 33,000

Cell No.	Groups	{1} 93,851	{2} 80,005	{3} 127,80
1	Contro		0,214444	0,004040
2	EtOH	0,214444		0,000220
3	Vinp	0,004040	0,000220	

Table A2.47: Glutamate- and potassium-stimulated release of [^{3}H]-DA (raw data)

Rat Number	Exp. Group	Treatment	Sex	Glutamate	Potassium
80	Control Male	Control	Male	0,237	2,951
81	Control Male	Control	Male	0,228	3,414
90	Control Male	Control	Male	0,515	6,480
91	Control Male	Control	Male	0,251	3,168
152	Control Male	Control	Male	0,529	9,063
173	Control Male	Control	Male	0,309	4,443
174	Control Male	Control	Male	0,364	3,258
195	Control Male	Control	Male	0,268	4,208
196	Control Male	Control	Male	0,162	3,144
204	Control Male	Control	Male	0,309	6,671
205	Control Male	Control	Male	0,345	6,066
182	Control Male	Control	Male	0,311	5,762
58	EtOH Male	EtOH	Male	0,247	4,262
59	EtOH Male	EtOH	Male	0,252	3,920
65	EtOH Male	EtOH	Male	0,389	4,527
66	EtOH Male	EtOH	Male	0,313	4,936
34	EtOH Male	EtOH	Male	0,328	5,209
35	EtOH Male	EtOH	Male	0,164	4,067
47	EtOH Male	EtOH	Male	0,384	4,489
48	EtOH Male	EtOH	Male	0,286	3,163
183	EtOH Male	EtOH	Male	0,321	7,043
163	EtOH Male	EtOH	Male	0,542	6,976
164	EtOH Male	EtOH	Male	0,464	4,903
82	Control Female	Control	Female	0,203	3,996
83	Control Female	Control	Female	0,167	3,424
92	Control Female	Control	Female	0,372	4,268
93	Control Female	Control	Female	0,210	3,785
153	Control Female	Control	Female	0,291	8,520
154	Control Female	Control	Female	0,294	7,563
155	Control Female	Control	Female	0,260	6,726
170	Control Female	Control	Female	0,252	3,672
171	Control Female	Control	Female	0,317	3,846
190	Control Female	Control	Female	0,155	4,057
191	Control Female	Control	Female	0,129	4,455
61	EtOH Female	EtOH	Female	0,115	2,550
62	EtOH Female	EtOH	Female	0,190	5,469
68	EtOH Female	EtOH	Female	0,211	6,371
69	EtOH Female	EtOH	Female	0,250	4,858
30	EtOH Female	EtOH	Female	0,204	2,419
31	EtOH Female	EtOH	Female	0,254	3,589
41	EtOH Female	EtOH	Female	0,306	3,363
42	EtOH Female	EtOH	Female	0,269	4,211
180	EtOH Female	EtOH	Female	0,153	5,462
181	EtOH Female	EtOH	Female	0,349	7,234
160	EtOH Female	EtOH	Female	0,495	6,559
161	EtOH Female	EtOH	Female	0,309	5,243

Table A2.48: Shapiro-Wilk Test results for the variables measured in the *in vitro* superfusion experiments

Variable	Shapiro-Wilk, W	*P* value
Glutamate stimulation	0,943	0,027
Potassium stimulation	0,942	0,023

Table A2.49: Kruskal-Wallis multiple comparisons test of glutamate-stimulated release of [^{3}H]-DA.

	Multiple Comparisons p values (2-tailed); Glutamate (Spreadsheet1) Independent (grouping) variable: Exp. Group Kruskal-Wallis test: H (3, N= 46) =6,919887 p =,0745			
Depend.: Glutamate	Control Male R:26,917	EtOH Male R:30,318	Control Female R:17,773	EtOH Female R:19,083
Control Male		1,00000(	0,61608	0,91715
EtOH Male	1,00000(		0,17029	0,26966
Control Female	0,61608	0,17029		1,00000(
EtOH Female	0,91715	0,26966	1,00000(	

Table A2.50: Kruskal-Wallis multiple comparisons test of potassium-stimulated release of [^{3}H]-DA.

	Multiple Comparisons p values (2-tailed); Potassium (Spreadsheet1) Independent (grouping) variable: Exp. Group Kruskal-Wallis test: H (3, N= 46) =,4193928 p =,9362			
Depend.: Potassium	Control Male R:21,833	EtOH Male R:25,455	Control Female R:23,364	EtOH Female R:23,500
Control Male		1,00000(	1,00000(	1,00000(
EtOH Male	1,00000(		1,00000(	1,00000(
Control Female	1,00000(	1,00000(		1,00000(
EtOH Female	1,00000(	1,00000(	1,00000(	

Table A2.51: Kruskal-Wallis multiple comparisons test of glutamate-stimulated release of [^{3}H]-DA between male and female rats.

	Multiple Comparisons p values (2-tailed); Glutamate (Spreadsheet1) Independent (grouping) variable: Sex Kruskal-Wallis test: H (1, N= 46) =6,496473 p =,0108	
Depend.: Glutamate	Male R:28,543	Female R:18,457
Male		0,010821
Female	0,010821	

Table A2.52: Kruskal-Wallis multiple comparisons test of potassium-stimulated release of [^{3}H]-DA between male and female rats.

	Multiple Comparisons p values (2-tailed); Potassium (Spreadsheet1) Independent (grouping) variable: Sex Kruskal-Wallis test: H (1, N= 46) =,0010860 p =,9737	
Depend.: Potassium	Male R:23,565	Female R:23,435
Male		0,973711
Female	0,973711	

EXPLORATORY PAIRWISE CORRELATIONS

Table A2.53: Exploratory pairwise correlations between behavioural and neurochemical measures.

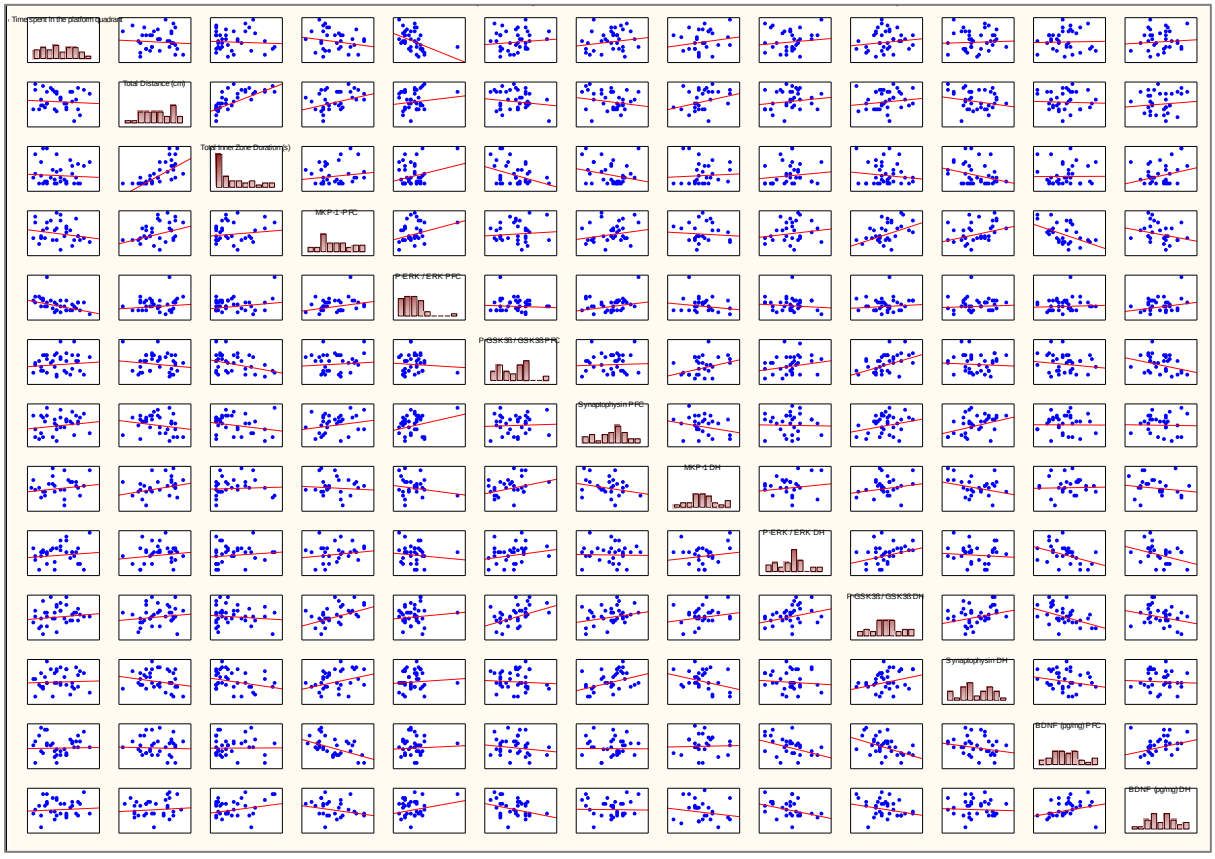

NETWORK ANALYSIS OF SIGNIFICANTLY CHANGED PROTIENS(> 2-FOLD)

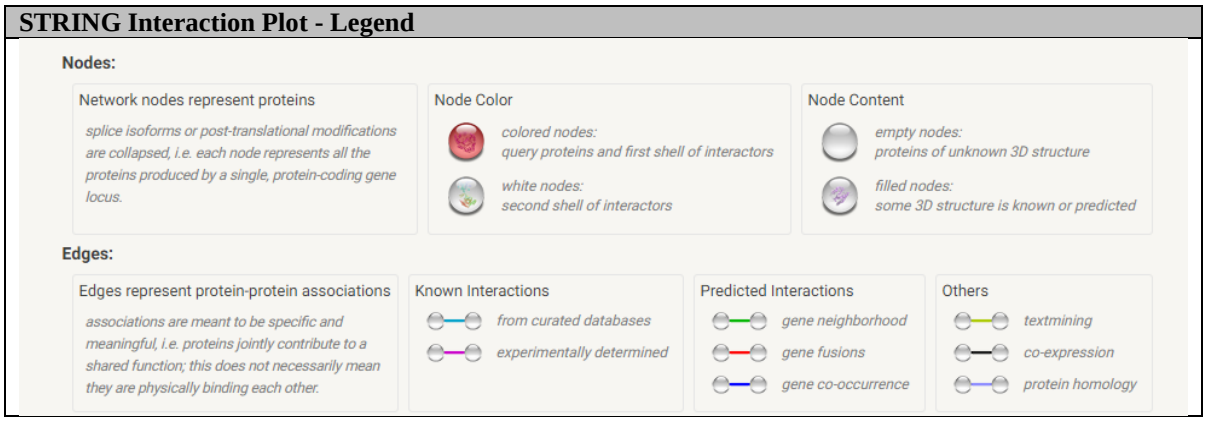

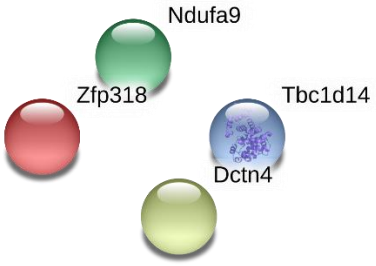

Figure A4.1: Network analysis of significantly changed proteins (>2-fold change) in the PFC of EtOH-rats relative to controls. There were no significant interactions within this set of proteins.

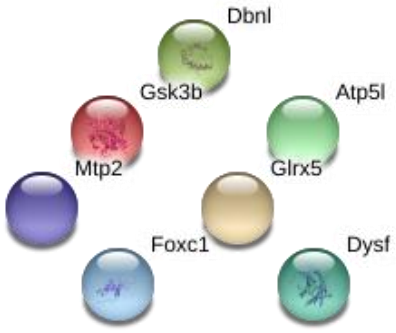

Figure A4.2: Network analysis of significantly changed proteins (>2-fold change) in the DH of EtOH-rats compared to controls. There were no significant interactions between the significantly changed proteins.

WESTERN BLOT CONFIRMATION

Table A4.1: Raw data (pixel density percentage) used for confirmation by Western blot

		Pixel Total %		
Rat Number	**Group**	**NDAFUA9/α-Tubulin**	**ATP5A / α-Tubulin**	**GSK3β / α-Tubulin**
122	Control	51,176	89,678	98,738
102	Control	63,955	92,453	89,262
121	Control	58,116	100,195	112,246
143	Control	102,574	104,682	98,595
114	EtOH	213,075	101,143	96,192
133	EtOH	115,474	92,243	102,336
115	EtOH	97,503	81,275	106,661

Table A4.2: Shapiro-Wilk test results for the variables measured using Western blot analysis

	Shapiro-Wilk, W	***P* value**
NDAFUA9 /α-Tubulin	0,828	0,077
ATP5A / α-Tubulin	0,949	0,721
GSK3β / α-Tubulin	0,981	0,967

Table A4.3: Student t-test analysis of NDUFA9/α-tubulin in the PFC

	T-tests; Grouping: Group (Spreadsheet1) Group 1: Control Group 2: EtOH										
Variable	Mean Control	Mean EtOH	t-value	df	p	Valid N Control	Valid N EtOH	Std.Dev. Control	Std.Dev. EtOH	F-ratio Variances	p Variances
NDAFUA9/AlphaTubulin	68,95534	142,0174	-2,21522	5	0,077594	4	3	23,01280	62,19038	7,303104	0,140674

Table A4.4: Power Analysis of NDUFA9/α-tubulin in the PFC

Breakdown Table of Descriptive Statistics (Spreadsheet1) N=7 (No missing data in dep. var. list)				
Group	NDAFUA9/AlphaTubulin Means	NDAFUA9/AlphaTubulin N	NDAFUA9/AlphaTubulin Std.Dev.	NDAFUA9/AlphaTubulin Std.Err.
Control	68,9553	4	23,0128(	11,5064(
EtOH	142,017	3	62,1903	35,9056
All Grps	100,267	7	55,4902	20,9733

	Power Calculation (Spreadsheet1) Two Means, t-Test, Ind. Samples H0: Mu1 = Mu2
	Value
Population Mean Mu1	142,020(
Population Mean Mu2	68,960(
Population S.D. (Sigma)	55,490(
Standardized Effect (Es)	1,3166
Sample Size N1	3,000(
Sample Size N2	4,000(
Type I Error Rate (Alpha)	0,050(
Critical Value of t	2,570
Power	0,2892

	Sample Size Calculation (Spreadsheet1) Two Means, t-Test, Ind. Samples H0: Mu1 = Mu2
	Value
Population Mean Mu1	142,020(
Population Mean Mu2	68,960(
Population S.D. (Sigma)	55,490(
Standardized Effect (Es)	1,3166
Type I Error Rate (Alpha)	0,050(
Critical Value of t	2,086(
Power Goal	0,800(
Actual Power for Required N	0,8356
Required N (per group)	11,000(

Table A4.5: Student t-test analysis of ATP5A/α-tubulin in the DH

Variable	T-tests; Grouping: Exp Group (Spreadsheet1) Group 1: Control Group 2: EtOH Mean Control	Mean EtOH	t-value	df	p	Valid N Control	Valid N EtOH	Std.Dev. Control	Std.Dev. EtOH	F-ratio Variances	p Variances
Pixel Total (%)	96,7519	91,5534	0,82380	5	0,44755	4	3	6,91010	9,95193	2,07417	0,54375

Table A4.6: Student t-test analysis of GSK3β/α-tubulin in the DH

Variable	T-tests; Grouping: Group (Spreadsheet1) Group 1: Control Group 2: EtOH Mean Control	Mean EtOH	t-value	df	p	Valid N Control	Valid N EtOH	Std.Dev. Control	Std.Dev. EtOH	F-ratio Variances	p Variances
GSK3B / Alpha Tubulin	99,7101	101,729	-0,3285	5	0,75581	4	3	9,46026	5,26105	3,23340	0,49022

DEVELOPMENTAL DATA

Table A5.1: Average daily liquid consumption (ml) per dam

Treatment	GD0	GD1	GD2	GD3	GD4	GD5	GD6	GD7	GD8	GD9	GD10	GD11	GD12	GD13	GD14	GD15	GD16	GD17	GD18	GD19	GD20	GD21	GD22	Average (ml)
Saccharin-control	50	49	53	42	63	52	57	53	53	51	41	81	60	48	50	53	58	48	41	50	43	53	62	53
Saccharin-control	40	35	44	35	29	32	42	29	31	25	27	30	26	27	34	38	28	35	31	34	45	29	33	33
Saccharin-control	44	44	45	39	35	45	33	39	40	53	33	49	33	56	31	45	58	33	33	40	53	56	29	42
Saccharin-control	77	97	85	81	101	90	52	105	45	48	52	61	47	64	77	85	130	123	109	108	76	25	62	78
Saccharin-control	39	39	40	40	39	34	29	40	30	38	31	45	27	30	44	45	68	66	60	65	49	14	43	42
Saccharin-control	-	45	62	71	60	51	61	80	40	83	81	81	60	85	77	75	97	82	78	95	83	30	49	69
Saccharin-control	80	85	66	69	101	129	84	70	100	84	95	64	58	95	83	94	-	24	144	76	32	-	-	82
Saccharin-control	108	97	55	63	80	102	62	71	95	110	92	59	79	82	104	144	-	136	141	115	49	-	-	92
Saccharin-control	32	47	34	41	43	61	72	48	51	60	47	43	36	45	49	50	68	30	45	51	42	54	54	48
Saccharin-control	44	104	110	111	86	137	123	121	95	120	126	141	169	111	111	165	150	159	186	196	86	98	-	125
Saccharin-control	48	88	91	87	83	92	80	87	80	80	81	80	79	58	69	115	124	113	128	98	88	27	-	85
Saccharin-control	50	53	36	37	25	30	25	34	28	49	30	27	29	36	43	51	58	77	66	-	-	-	-	41
Saccharin-control	71	93	68	58	41	44	48	60	49	70	64	50	51	53	74	70	70	83	74	30	-	-	-	61
Ethanol-treated	19	16	16	16	14	18	14	16	14	11	14	16	14	15	14	13	14	22	11	16	24	20	14	16
Ethanol-treated	6	16	13	20	17	18	15	13	16	14	17	11	18	24	12	24	65	23	19	25	25	25	28	20
Ethanol-treated	13	19	16	24	24	21	15	16	20	17	29	17	21	32	23	28	29	27	35	41	29	43	-	25
Ethanol-treated	6	16	20	12	19	12	11	18	15	15	19	18	17	15	32	24	25	25	26	29	10	13	-	18
Ethanol-treated	14	18	20	13	22	14	20	25	11	15	21	25	15	19	25	20	25	26	25	27	23	4	25	20
Ethanol-treated	16	19	20	16	17	25	17	25	18	17	20	20	23	36	22	28	29	21	37	83	9	-	-	25
Ethanol-treated	18	22	25	16	19	23	16	19	38	20	19	21	20	29	29	30	38	30	46	3	6	-	-	23
Ethanol-treated	8	24	19	17	17	19	20	16	22	21	15	20	24	28	31	31	29	20	22	22	7	19	-	21
Ethanol-treated	19	22	9	19	18	14	15	22	15	22	22	23	27	30	41	35	28	25	12	-	-	-	-	22
Ethanol-treated	19	26	11	20	26	19	10	23	14	25	22	15	19	19	23	23	22	26	35	18	-	-	-	21
Ethanol-treated	16	10	17	16	9	13	19	13	14	*	13	13	15	10	15	13	14	15	14	16	22	13	12	14

Breakdown Table of Descriptive Statistics (Spreadsheet1)
N=24 (No missing data in dep. var. list)

Treatment	Average daily consumption (ml) Means	Average daily consumption (ml) N	Average daily consumption (ml) Std.Dev.	Average daily consumption (ml) Std.Err.	Average daily consumption (ml) Minimum	Average daily consumption (ml) Maximum	Average daily consumption (ml) Q25	Average daily consumption (ml) Median	Average daily consumption (ml) Q75
Saccharin-control	65,47272	13	26,36411	7,31209(	33,00000	124,9545	42,00000	61,05000	81,65000
Ethanol-treated	20,30510	11	3,35180	1,01060!	14,18182	24,6667	18,04545	20,50000	23,19048
All Grps	44,77090	24	29,93385	6,11022:	14,18182	124,9545	20,62500	37,13158	65,20682

Table A5.2: Raw data - Litter size on P2

Litter #	Treatment	Total no. pups at P2	No. male pups at P2	No. female pups at P2
8	Saccharin-control	16	11	5
11	Saccharin-control	14	6	8
12	Saccharin-control	4	3	1
15	Saccharin-control	15	7	8
16	Saccharin-control	13	8	5
4	Saccharin-control	15	9	6
19	Saccharin-control	15	9	6
20	Saccharin-control	19	12	7
23	Saccharin-control	13	6	7
24	Saccharin-control	17	9	8
28	Saccharin-control	14	9	5
6	Ethanol-exposed	10	6	4
9	Ethanol-exposed	16	9	7
10	Ethanol-exposed	9	5	4
13	Ethanol-exposed	12	7	5
14	Ethanol-exposed	12	6	6
2	Ethanol-exposed	14	11	3
1	Ethanol-exposed	9	6	3
17	Ethanol-exposed	8	2	6
21	Ethanol-exposed	8	6	2
22	Ethanol-exposed	13	6	7
26	Ethanol-exposed	3	1	2

Table A5.3: Litter size on P2

T-tests; Grouping: Treatment (Spreadsheet1)
Group 1: Sacc
Group 2: EtOH

Variable	Mean Sacc	Mean EtOH	t-value	df	p	Valid N Sacc	Valid N EtOH	Std.Dev. Sacc	Std.Dev. EtOH	F-ratio Variances	p Variances
Total #Pups at P2	14,0909:	10,3636-	2,381468	20	0,027292	11	11	3,780332	3,557323	1,129310	0,851283

Table A5.4: Raw data - Body weight of male rats on P8, P15, P21, P57 and P63

Weight (g) - Male Rats							
Group	Treatment	Stress	P8	P15	P21	P57	P63
Control	Sacc	nMS	21	37	53	250	276
Control	Sacc	nMS	19	37	55	242	263
Control	Sacc	nMS	19	35	53	244	262
Control	Sacc	nMS	19	36	54	240	258
Control	Sacc	nMS	19	35	55	245	270
Control	Sacc	nMS	19	36	49	240	263
Control	Sacc	nMS	18	36	54	246	276
Control	Sacc	nMS	19	37	52	149	196
Control	Sacc	nMS	20	36	59	245	197
Control	Sacc	nMS	19	34	55	266	303
Control	Sacc	nMS	20	37	55	278	312
Control	Sacc	nMS	17	34	58	227	279
Control	Sacc	nMS	19	37	51	273	292
Control	Sacc	nMS	18	36	54	246	291
Control	Sacc	nMS	17	38	56	249	282
Control	Sacc	nMS	17	37	54	297	315
Control	Sacc	nMS	19	36	54	261	291
Control	Sacc	nMS	19	37	55	275	308
Control	Sacc	nMS	18	34	53	263	288
Control	Sacc	nMS	19	32	56	262	276
Control	Sacc	nMS	19	32	53	246	258
Control	Sacc	nMS	19	33	56	278	284
Control	Sacc	nMS	19	33	57	258	292
Control	Sacc	nMS	19	34	53	273	244
Control	Sacc	nMS	19	39	49	266	
Control	Sacc	nMS	19	38	51	244	
Control	Sacc	nMS	15	37	49	238	
Control	Sacc	nMS	19	38	47	253	
Control	Sacc	nMS	19	37	51	263	
Control	Sacc	nMS	18	36	52	215	
MS	Sacc	MS	17	32	53	244	299
MS	Sacc	MS	19	29	54	234	295
MS	Sacc	MS	16	28	53	253	309
MS	Sacc	MS	15	32	53	231	287
MS	Sacc	MS	19	31	56	219	339
MS	Sacc	MS	17	30	55	199	299
MS	Sacc	MS	19	36	47	174	241
MS	Sacc	MS	21	36	48	165	222
MS	Sacc	MS	19	35	42	217	206
MS	Sacc	MS	19	37	47	197	199
MS	Sacc	MS	19	37	47	266	243
MS	Sacc	MS	19	39	43	266	222
MS	Sacc	MS	19	36	54	226	283
MS	Sacc	MS	19	34	58	244	280
MS	Sacc	MS	18	34	55	267	303
MS	Sacc	MS	17	35	55	250	294
MS	Sacc	MS	19	32	54	255	285
MS	Sacc	MS	19	33	54	252	276
MS	Sacc	MS	17	37	53	278	
MS	Sacc	MS	17	34	57	263	
MS	Sacc	MS	15	37	55	254	
MS	Sacc	MS	17	38	55	238	
MS	Sacc	MS	17	36	55		
MS	Sacc	MS	17	37	55		
MS	Sacc	MS	19				
MS	Sacc	MS	18				
MS	Sacc	MS	17				
MS	Sacc	MS	17				
MS	Sacc	MS	18				
MS	Sacc	MS	16				

Weight (g) - Male Rats							
Group	Treatment	Stress	P8	P15	P21	P57	P63
EtOH	EtOH	nMS	16	26	47	254	287
EtOH	EtOH	nMS	15	33	49	209	242
EtOH	EtOH	nMS	15	32	47	181	224
EtOH	EtOH	nMS	15	32	40	223	263
EtOH	EtOH	nMS	12	31	49	153	202
EtOH	EtOH	nMS	15	32	46	233	268
EtOH	EtOH	nMS	17	39	52	220	259
EtOH	EtOH	nMS	18	38	51	202	295
EtOH	EtOH	nMS	15	33	53	241	260
EtOH	EtOH	nMS	15	34	53	242	235
EtOH	EtOH	nMS	17	34	51	252	226
EtOH	EtOH	nMS	17	33	50	220	262
EtOH	EtOH	nMS	13	28	51	230	272
EtOH	EtOH	nMS	16	29	45	271	232
EtOH	EtOH	nMS	16	34	42	236	240
EtOH	EtOH	nMS	13	26	43	204	264
EtOH	EtOH	nMS	11	29	43	199	269
EtOH	EtOH	nMS	15	33	42	240	275
EtOH	EtOH	nMS	17	32	45	265	
EtOH	EtOH	nMS	13	29	47	207	
EtOH	EtOH	nMS	17	30	45	221	
EtOH	EtOH	nMS	15	30	44	235	
EtOH	EtOH	nMS	14	30	43	242	
EtOH	EtOH	nMS	15	29	46	251	
EtOH+MS	EtOH	MS	17	28	49	232	260
EtOH+MS	EtOH	MS	17	31	45	249	272
EtOH+MS	EtOH	MS	13	32	47	215	254
EtOH+MS	EtOH	MS	17	30	43	206	240
EtOH+MS	EtOH	MS	18	32	45	243	281
EtOH+MS	EtOH	MS	15	28	49	245	280
EtOH+MS	EtOH	MS	17	38	52	204	257
EtOH+MS	EtOH	MS	17	36	53	253	286
EtOH+MS	EtOH	MS	19	36	52	222	303
EtOH+MS	EtOH	MS	16	36	51	211	278
EtOH+MS	EtOH	MS	16	37	51	197	258
EtOH+MS	EtOH	MS	18	37	54	238	274
EtOH+MS	EtOH	MS	18	36	52	240	259
EtOH+MS	EtOH	MS	18	36	56	272	294
EtOH+MS	EtOH	MS	15	38	52	248	270
EtOH+MS	EtOH	MS	19	35	58	254	271
EtOH+MS	EtOH	MS	19	38	44	272	272
EtOH+MS	EtOH	MS	16	33	50	261	
EtOH+MS	EtOH	MS	15	34	46	273	
EtOH+MS	EtOH	MS	15	36	43	251	
EtOH+MS	EtOH	MS	13	36	55	291	
EtOH+MS	EtOH	MS	20		46	270	
EtOH+MS	EtOH	MS	17			246	
EtOH+MS	EtOH	MS	18			253	
EtOH+MS	EtOH	MS	18				
EtOH+MS	EtOH	MS	16				
EtOH+MS	EtOH	MS	17				
EtOH+MS	EtOH	MS	16				
EtOH+MS	EtOH	MS	12				

Table A5.5: Raw data - Body weight of female rats on P8. P15, P21, 57 and P63

Weight (g) - Female Rats							
Group	**Treatment**	**Stress**	**P8**	**P15**	**P21**	**P57**	**P63**
Control	Sacc	nMS	17	32	49	194	208
Control	Sacc	nMS	20	35	54	191	204
Control	Sacc	nMS	18	34	50	163	188
Control	Sacc	nMS	18	35	47	184	206
Control	Sacc	nMS	17	36	51	203	215
Control	Sacc	nMS	17	36	51	203	216
Control	Sacc	nMS	18	34	56	199	215
Control	Sacc	nMS	18	32	55	204	202
Control	Sacc	nMS	16	34	48	200	
Control	Sacc	nMS	20	34	50	189	
MS	Sacc	MS	17	29	52	184	205
MS	Sacc	MS	17	29	51	185	208
MS	Sacc	MS	19	36	42	188	148
MS	Sacc	MS	18	34	44	173	177
MS	Sacc	MS	17	32	51	158	240
MS	Sacc	MS	18	34	51	129	218
MS	Sacc	MS	19	39	51	186	
MS	Sacc	MS	17	36	60	194	
MS	Sacc	MS	17			224	
MS	Sacc	MS	17			194	
EtOH	EtOH	nMS	14	31	45	154	177
EtOH	EtOH	nMS	15	28	45	177	192
EtOH	EtOH	nMS	16	34	51	180	201
EtOH	EtOH	nMS	16	35	48	187	191
EtOH	EtOH	nMS	15	30	47	188	182
EtOH	EtOH	nMS	19	28	53	175	173
EtOH	EtOH	nMS	15	30	43	169	
EtOH	EtOH	nMS	14	30	42	159	
EtOH+MS	EtOH	MS	15	31	49	186	204
EtOH+MS	EtOH	MS	17	30	44	170	185
EtOH+MS	EtOH	MS	17	33	49	161	195
EtOH+MS	EtOH	MS	18	36	52	150	181
EtOH+MS	EtOH	MS	17	36	51	169	199
EtOH+MS	EtOH	MS	18	37	55	198	204
EtOH+MS	EtOH	MS	17	36	51	203	207
EtOH+MS	EtOH	MS	14	33	55	179	211
EtOH+MS	EtOH	MS	18	34	46	188	194
EtOH+MS	EtOH	MS	17	30	47	186	190
EtOH+MS	EtOH	MS	18	32	50	180	195
EtOH+MS	EtOH	MS	20		49	184	195
EtOH+MS	EtOH	MS	19		51	186	193
EtOH+MS	EtOH	MS	18		53	182	200
EtOH+MS	EtOH	MS	21		49	185	204
EtOH+MS	EtOH	MS	19		51	195	
EtOH+MS	EtOH	MS	18		53		
EtOH+MS	EtOH	MS	17		55		
EtOH+MS	EtOH	MS	17				

Table A5.6: Shapiro-Wilk test results for body weight analysis on P8, P15, P21, P57 and P63 in male and female rats.

Sex	Age	Shapiro-Wilk, W	*P* value
Male	P2	0,859	0
Male	P8	0,918	0,000
Male	P15	0,937	0,000
Male	P21	0,946	0,000
Male	P57	0,944	0,000
Male	P63	0,962	0,020
Female	P2	0,869	0,000
Female	P8	0,941	0,020
Female	P15	0,953	0,122
Female	P21	0,970	0,299
Female	P57	0,955	0,082
Female	P63	0,956	0,173

Table 5A.7: Student t-test result for body weight analysis of male rats on P2

	T-tests; Grouping: Treatment (Spreadsheet44) Group 1: Sacc Group 2: EtOH										
Variable	Mean Sacc	Mean EtOH	t-value	df	p	Valid N Sacc	Valid N EtOH	Std.Dev. Sacc	Std.Dev. EtOH	F-ratio Variances	p Variances
Weight (g)	7,03488	6,46875	3,96286	148	0,00011	86	64	0,80363	0,94228	1,37482	0,17103

Table A5.8: Student t-test result for body weight analysis of female rats on P2

	T-tests; Grouping: Treatment (Spreadsheet50) Group 1: Sacc Group 2: EtOH										
Variable	Mean Sacc	Mean EtOH	t-value	df	p	Valid N Sacc	Valid N EtOH	Std.Dev. Sacc	Std.Dev. EtOH	F-ratio Variances	p Variances
Weight (g)	6,707692	6,617021	0,575215	110	0,566321	65	47	0,722908	0,945313	1,709957	0,047083

Table A5.9: Kruskal-Wallis test of body weight of male rats on P8.

	Multiple Comparisons p values (2-tailed); Weight (g) (Spreadsheet10) Independent (grouping) variable: Group Kruskal-Wallis test: H (3, N= 113) =50,50376 p =,0000			
Depend.: Weight (g)	Control R:83,417	MS R:66,300	EtOH R:24,458	EtOH+MS R:46,983
Control		0,258243	0,000000	0,000117
MS	0,258243		0,000019	0,141442
EtOH	0,000000	0,000019		0,076374
EtOH+MS	0,000117	0,141442	0,076374	

Table A5.10: Kruskal-Wallis test of body weight of male rats on P15.

	Multiple Comparisons p values (2-tailed); Weight (g) (Spreadsheet28) Independent (grouping) variable: Group Kruskal-Wallis test: H (3, N= 99) =23,03420 p =,0000			
Depend.: Weight (g)	Control R:64,783	MS R:51,583	EtOH R:27,667	EtOH+MS R:52,595
Control		0,559972	0,000014	0,815140
MS	0,559972		0,023525	1,000000
EtOH	0,000014	0,023525		0,022067
EtOH+MS	0,815140	1,000000	0,022067	

Table A5.11: Kruskal-Wallis test of body weight of male rats on P21.

	Multiple Comparisons p values (2-tailed); Weight (g) (Spreadsheet17) Independent (grouping) variable: Group Kruskal-Wallis test: H (3, N= 100) =33,98262 p =,0000			
Depend.: Weight (g)	Control R:66,817	MS R:62,979	EtOH R:25,438	EtOH+MS R:41,977
Control		1,000000	0,000001	0,013717
MS	1,000000		0,000044	0,085097
EtOH	0,000001	0,000044		0,320518
EtOH+MS	0,013717	0,085097	0,320518	

Table A5.12: Kruskal-Wallis test of body weight of male rats on P57.

	Multiple Comparisons p values (2-tailed); Weight (g) (Spreadsheet41) Independent (grouping) variable: Group Kruskal-Wallis test: H (3, N= 100) =13,52235 p =,0036			
Depend.: Weight (g)	Contol R:63,167	MS R:47,977	EtOH R:34,354	EtOH+MS R:53,125
Contol		0,372865	0,001724	1,000000
MS	0,372865		0,669786	1,000000
EtOH	0,001724	0,669786		0,150032
EtOH+MS	1,000000	1,000000	0,150032	

TableA5.13: Kruskal-Wallis test of body weight of male rats on P63.

	Multiple Comparisons p values (2-tailed); Weight (g) (Spreadsheet30) Independent (grouping) variable: Group Kruskal-Wallis test: H (3, N= 77) =8,122643 p =,0435			
Depend.: Weight (g)	Control R:44,688	MS R:44,472	EtOH R:26,667	EtOH+MS R:38,235
Control		1,000000	0,058701	1,000000
MS	1,000000		0,101733	1,000000
EtOH	0,058701	0,101733		0,757592
EtOH+MS	1,000000	1,000000	0,757592	

Table A5.14: Kruskal-Wallis test of body weight of female rats on P8.

	Multiple Comparisons p values (2-tailed); Weight (g) (Spreadsheet63) Independent (grouping) variable: Group Kruskal-Wallis test: H (3, N= 47) =10,98055 p =,0118			
Depend.: Weight (g)	Control R:28,450	MS R:25,800	EtOH R:9,9375	EtOH+MS R:26,632
Control		1,000000	0,026531	1,000000
MS	1,000000		0,088382	1,000000
EtOH	0,026531	0,088382		0,023200
EtOH+MS	1,000000	1,000000	0,023200	

Table A5.15: Two-way ANOVA and Duncan's post-hoc test of body weight of female rats on P15.

Univariate Tests of Significance for Weight (g) (Spreadsheet75) Sigma-restricted parameterization Effective hypothesis decomposition					
Effect	SS	Degr. of Freedom	MS	F	p
Intercept	39536,04	1	39536,04	6105,173	0,000000
Treatment	29,73	1	29,73	4,591	0,039614
Stress	10,29	1	10,29	1,588	0,216410
Treatment*Stress	24,39	1	24,39	3,767	0,060858
Error	213,70	33	6,48		

Duncan test; variable Weight (g) (Spreadsheet19) Approximate Probabilities for Post Hoc Tests Error: Between MS = 6,4758, df = 33,000			
Cell No.	Treatment	{1} 33,944	{2} 32,316
1	Sacc		0,060362
2	EtOH	0,060362	

Duncan test; variable Weight (g) (Spreadsheet19) Approximate Probabilities for Post Hoc Tests Error: Between MS = 6,4758, df = 33,000						
Cell No.	Treatment	Stress	{1} 34,200	{2} 33,625	{3} 30,750	{4} 33,455
1	Sacc	Contro		0,633648	0,011080	0,562063
2	Sacc	MS	0,633648		0,028207	0,887536
3	EtOH	Contro	0,011080	0,028207		0,030412
4	EtOH	MS	0,562063	0,887536	0,030412	

Table A5.16: Two-way ANOVA of body weight of female rats on P21.

Univariate Tests of Significance for Weight (g) (Spreadsheet97) Sigma-restricted parameterization Effective hypothesis decomposition					
Effect	SS	Degr. of Freedom	MS	F	p
Intercept	97308,57	1	97308,57	7072,557	0,000000
Treatment	40,33	1	40,33	2,932	0,094609
Stress	21,54	1	21,54	1,566	0,218130
Treatment*Stress	53,44	1	53,44	3,884	0,055685
Error	550,34	40	13,76		

Table A5.17: Two-way ANOVA of body weight of female rats on P57.

Univariate Tests of Significance for Weight (g) (Spreadsheet106) Sigma-restricted parameterization Effective hypothesis decomposition					
Effect	SS	Degr. of Freedom	MS	F	p
Intercept	1373343	1	1373343	5088,280	0,000000
Treatment	981	1	981	3,636	0,063753
Stress	36	1	36	0,134	0,715788
Treatment*Stress	956	1	956	3,543	0,067083
Error	10796	40	270		

Table A5.18: Two-way ANOVA and Duncan's post-hoc test of body weight of female rats on P63.

Univariate Tests of Significance for Weight (g) (Spreadsheet115) Sigma-restricted parameterization Effective hypothesis decomposition					
Effect	SS	Degr. of Freedom	MS	F	p
Intercept	118640(	1	118640(	5008,953	0,00000(
Treatment	1003	1	1003	4,236	0,04807!
Stress	26	1	26	0,111	0,74115!
Treatment*Stress	655	1	655	2,767	0,10629!
Error	7343	31	237		

Duncan test; variable Weight (g) (Spreadsheet115) Approximate Probabilities for Post Hoc Tests Error: Between MS = 236,86, df = 31,000						
Cell No.	Treatment	Stress	{1} 206,75	{2} 199,33	{3} 186,00	{4} 197,13
1	Sacc	Contro		0,354324	0,020465	0,258988
2	Sacc	MS	0,354324		0,119509	0,782211
3	EtOH	Contro	0,020465	0,119509		0,168061
4	EtOH	MS	0,258988	0,782211	0,168061	

NOVEL OBJECT TEST - HABITUATION TRIAL

Table A5.19: Raw data - Novel object habituation trial

				Distance Travelled (cm) per minute											
Rat Number	Group	Treatment	Stress	0-1 min	1-2 min	2-3 min	3-4 min	4-5min	5-6 min	6-7 min	7-8 min	8-9 min	9-10 min	Total Distance (cm) in 5 min	Total Distance (cm) in 10 min
80	Control	Sacc	nMS	391,76	298,50	246,34	159,47	180,43	174,80	207,51	168,65	138,83	178,75	1276,51	2145,06
81	Control	Sacc	nMS	268,22	228,28	224,38	319,49	217,35	100,67	158,03	157,79	150,62	73,92	1257,72	1898,75
180	Control	Sacc	nMS	304,61	270,11	229,88	236,86	184,46	215,04	240,20	153,47	200,86	207,91	1225,92	2243,40
181	Control	Sacc	nMS	328,42	309,64	207,59	250,32	238,57	253,37	242,45	199,84	208,45	186,44	1334,55	2425,10
182	Control	Sacc	nMS	308,57	277,43	287,74	327,20	259,44	84,86	222,83	250,95	199,18	156,40	1460,37	2374,59
200	Control	Sacc	nMS	324,40	310,51	355,37	265,60	323,44	310,01	211,90	296,99	224,92	161,83	1579,32	2784,98
201	Control	Sacc	nMS	366,18	367,29	329,09	255,98	278,74	161,70	155,14	277,12	229,05	100,72	1597,28	2521,01
202	Control	Sacc	nMS	301,54	422,93	314,94	270,07	255,84	201,32	295,88	249,13	219,96	184,31	1565,32	2715,92
210	Control	Sacc	nMS	233,15	164,53	183,59	155,65	249,47	166,04	122,64	150,37	141,40	165,39	986,40	1732,25
211	Control	Sacc	nMS	291,73	192,26	219,41	242,97	186,96	202,93	141,18	134,96	77,24	141,34	1133,33	1830,98
212	Control	Sacc	nMS	324,94	306,67	209,61	149,07	95,10	34,21	91,79	100,52	91,55	6,00	1085,39	1409,46
50	MS	Sacc	MS	324,32	248,49	223,58	288,47	302,00	157,05	246,13	287,70	180,78	117,00	1386,86	2375,51
51	MS	Sacc	MS	411,85	254,92	306,42	367,81	250,62	291,22	245,85	169,90	272,81	221,12	1591,62	2792,53
150	MS	Sacc	MS	357,84	301,55	371,63	308,02	255,57	345,28	286,41	228,21	136,26	311,06	1594,61	2901,82
151	MS	Sacc	MS	385,84	218,58	279,21	300,42	278,37	326,78	202,37	181,96	261,91	123,14	1462,43	2558,59
170	MS	Sacc	MS	366,97	411,98	313,97	431,64	288,46	234,05	280,08	216,15	153,94	186,15	1813,01	2883,38
171	MS	Sacc	MS	326,98	445,05	476,28	375,01	349,69	302,92	307,99	199,22	181,07	223,91	1973,00	3188,12
172	MS	Sacc	MS	428,73	420,17	374,91	276,73	312,09	301,97	253,10	221,92	249,38	231,85	1812,63	3070,84
60	EtOH	EtOH	nMS	273,37	169,84	223,80	113,06	131,99	206,55	144,58	107,91	116,96	176,02	912,06	1664,08
61	EtOH	EtOH	nMS	261,36	276,16	211,35	269,41	242,95	154,23	178,16	20,48	230,94	153,25	1261,22	1998,28
130	EtOH	EtOH	nMS	248,49	454,99	272,09	282,80	393,64	338,60	184,54	203,17	267,22	234,28	1652,00	2879,83
131	EtOH	EtOH	nMS	257,63	380,67	363,51	347,80	385,23	284,66	255,98	315,82	195,17	205,77	1734,85	2992,25
190	EtOH	EtOH	nMS	408,17	324,69	388,09	353,56	321,84	217,04	242,84	273,00	270,79	161,93	1796,35	2961,95
191	EtOH	EtOH	nMS	351,77	495,19	438,75	414,07	355,34	210,85	233,38	171,81	101,11	188,99	2055,13	2961,28
192	EtOH	EtOH	nMS	370,14	608,57	478,12	481,42	371,05	419,61	337,87	276,66	218,70	147,88	2309,30	3710,02
41	EtOH+MS	EtOH	MS	396,56	304,15	288,27	337,99	278,21	292,62	190,85	188,56	132,18	223,02	1605,19	2632,42
70	EtOH+MS	EtOH	MS	203,74	279,09	281,69	223,45	187,33	242,92	190,78	178,94	204,75	130,65	1175,30	2123,34
71	EtOH+MS	EtOH	MS	234,25	285,33	250,00	215,14	222,76	232,54	175,48	149,77	110,13	134,26	1207,49	2009,65
140	EtOH+MS	EtOH	MS	266,30	352,95	347,95	357,53	268,60	220,19	232,90	293,59	209,67	190,94	1593,33	2740,62
141	EtOH+MS	EtOH	MS	339,84	358,30	329,14	222,48	196,19	230,46	246,35	121,46	221,00	162,68	1445,95	2427,88
160	EtOH+MS	EtOH	MS	321,49	238,68	119,93	213,88	219,38	164,19	241,50	158,43	65,42	140,19	1113,35	1883,08
161	EtOH+MS	EtOH	MS	208,44	176,06	294,30	216,93	191,46	141,44	174,51	97,29	201,59	199,45	1087,19	1901,46
40	EtOH+MS	EtOH	MS	286,69	236,43	345,87	228,34	223,09	209,66	221,12	146,37	130,30	220,54	1320,42	2248,41

Table A5.20: Shapiro-Wilk test results for the variables analyzed in the novel object habituation trial.

Test	Variable	Shapiro-Wilk, W	*P* Value
NOT Habituation Trial	Total Distance (10 min)	0,981	0,815
	Total Distance (5 min)	0,972	0,525
	Distance (0-1 min)	0,978	0,735
	Distance (1-2 min)	0,949	0,129
	Distance (2-3 min)	0,973	0,559
	Distance (3-4 min)	0,986	0,939
	Distance (4-5 min)	0,982	0,864
	Distance (5-6 min)	0,986	0,939
	Distance (6-7 min)	0,988	0,970
	Distance (7-8 min)	0,972	0,551
	Distance (8-9 min)	0,957	0,209
	Distance (9-10 min)	0,957	0,213

Table A5.21: Two-way ANOVA and Duncan's post-hoc results for the total distance travelled during the full 10-minute NOT habituation trial.

Univariate Tests of Significance for TOTAL DISTANCE (cm) (Spreadsheet18)
Sigma-restricted parameterization
Effective hypothesis decomposition

Effect	SS	Degr. of Freedom	MS	F	p
Intercept	19926212	1	19926212	975,952	0,00000
Treatment	1738	1	1738	0,0085	0,92711
Stress	40646	1	40646	0,1991	0,65878
Treatment*Stress	253451	1	253451	12,413	0,00143
Error	592098	29	20417		

Duncan test; variable Total Distance (cm) in 10 min (Spreadsheet6)
Approximate Probabilities for Post Hoc Tests
Error: Between MS = 2042E2, df = 29,000

Cell No.	Treatment	Stress	{1} 2189,2	{2} 2824,4	{3} 2738,2	{4} 2245,9
1	Sacc	nMS		0,01409	0,02791	0,80427
2	Sacc	MS	0,01409		0,70629	0,02092
3	EtOH	nMS	0,02791	0,70629		0,03797
4	EtOH	MS	0,80427	0,02092	0,03797	

Table A5.22: Repeated-measures ANOVA and Duncan's post-hoc results of the distance travelled per minute of the full 10-minute NOT habituation trial

Effect	Repeated Measures Analysis of Variance (Spreadsheet1) Sigma-restricted parameterization Effective hypothesis decomposition SS	Degr. of Freedom	MS	F	p
Intercept	1992621	1	1992621	975,9526	0,000000
Treatment	174	1	174	0,0085	0,927118
Stress	4065	1	4065	0,1991	0,658782
Treatment*Stress	253451	1	253451	12,4136	0,001434
Error	592099	29	20417		
MINUTE	908026	9	100892	35,0929	0,000000
MINUTE*Treatment	32120	9	3569	1,2414	0,269901
MINUTE*Stress	29441	9	3271	1,1378	0,336243
MINUTE*Treatment*Stress	35046	9	3894	1,3544	0,209261
Error	750373	261	2875		

Cell No.	Duncan test; variable DV_1 (Spreadsheet6) Approximate Probabilities for Post Hoc Tests Error: Between MS = 20417,, df = 29,000 Treatment	Stress	{1} 218,92	{2} 282,44	{3} 273,82	{4} 224,59
1	Sacc	nMS		0,014094	0,027910	0,804277
2	Sacc	MS	0,014094		0,706299	0,020922
3	EtOH	nMS	0,027910	0,706299		0,037975
4	EtOH	MS	0,804277	0,020922	0,037975	

Cell No.	Duncan test; variable DV_1 (Spreadsheet6) Approximate Probabilities for Post Hoc Tests Error: Within MS = 2875,0, df = 261,00 MINUTE	{1} 317,40	{2} 314,85	{3} 296,57	{4} 280,56	{5} 257,44	{6} 225,14	{7} 217,04	{8} 192,37	{9} 181,64	{10} 171,12
1	0-1 min		0,845663	0,136911	0,009086	0,000017	0,000004	0,000004	0,000005	0,000001	0,000001
2	1-2 min	0,845663		0,166159	0,012817	0,000025	0,000004	0,000004	0,000004	0,000005	0,000001
3	2-3 min	0,136911	0,166159		0,225300	0,004277	0,000003	0,000004	0,000004	0,000004	0,000005
4	3-4 min	0,009086	0,012817	0,225300		0,079866	0,000045	0,000005	0,000004	0,000004	0,000004
5	4-5min	0,000017	0,000025	0,004277	0,079866		0,014416	0,003131	0,000004	0,000004	0,000004
6	5-6 min	0,000004	0,000004	0,000003	0,000045	0,014416		0,539250	0,017548	0,001814	0,000106
7	6-7 min	0,000004	0,000004	0,000004	0,000005	0,003131	0,539250		0,061599	0,010074	0,000950
8	7-8 min	0,000005	0,000004	0,000004	0,000004	0,000004	0,017548	0,061599		0,416486	0,129181
9	8-9 min	0,000001	0,000005	0,000004	0,000004	0,000004	0,001814	0,010074	0,416486		0,425642
10	9-10 min	0,000001	0,000001	0,000005	0,000004	0,000004	0,000106	0,000950	0,129181	0,425642	

Table A5.23: Two-way ANOVA and Duncan's post-hoc results of the total distance travelled during the first 5 minutes of the NOT habituation trial

Effect	Univariate Tests of Significance for TOTAL DISTANCE (Spreadsheet26) Sigma-restricted parameterization Effective hypothesis decomposition SS	Degr. of Freedom	MS	F	p
Intercept	7113060	1	7113060	885,8488	0,000000
Treatment	314	1	314	0,0039	0,950580
Stress	299	1	299	0,0037	0,951782
Treatment*Stress	975539	1	975539	12,1492	0,001583
Error	2328600	29	80297		

Cell No.	Duncan test; variable Total Distance (cm) in 5 min (Spreadsheet6) Approximate Probabilities for Post Hoc Tests Error: Between MS = 80297,, df = 29,000 Treatment	Stress	{1} 1318,4	{2} 1662,0	{3} 1674,4	{4} 1318,5
1	Sacc	nMS		0,028188	0,027292	0,999235
2	Sacc	MS	0,028188		0,931103	0,022121
3	EtOH	nMS	0,027292	0,931103		0,023324
4	EtOH	MS	0,999235	0,022121	0,023324	

Table A5.24: Repeated-measures ANOVA and Duncan's post-hoc results of the distance travelled per minute for the first 5 minutes of the NOT habituation trial

Effect	Repeated Measures Analysis of Variance (Spreadsheet1) Sigma-restricted parameterization Effective hypothesis decomposition SS	Degr. of Freedom	MS	F	p
Intercept	1422612(	1	1422612(	885,848	0,00000(
Treatment	63	1	63	0,0039	0,95058(
Stress	60	1	60	0,0037	0,95178
Treatment*Stress	19510	1	19510	12,149	0,00158
Error	46572(	29	16059		
MINUTE	72726	4	18181	6,344(	0,00011
MINUTE*Treatment	25163	4	6291	2,195(	0,07380
MINUTE*Stress	13941	4	3485	1,2161	0,30778
MINUTE*Treatment*Stress	8015	4	2004	0,6992	0,59403
Error	33244	116	286(		

Cell No.	Duncan test; variable DV_1 (Spreadsheet6) Approximate Probabilities for Post Hoc Tests Error: Between MS = 16059,, df = 29,000 Treatment	Stress	{1} 263,67	{2} 332,40	{3} 334,88	{4} 263,71
1	Sacc	nMS		0,02818	0,02729	0,99923
2	Sacc	MS	0,02818		0,93110	0,02212
3	EtOH	nMS	0,02729	0,93110		0,02332
4	EtOH	MS	0,99923	0,02212	0,02332	

Cell No.	Duncan test; variable DV_1 (Spreadsheet6) Approximate Probabilities for Post Hoc Tests Error: Within MS = 2865,9, df = 116,00 MINUTE	{1} 317,40	{2} 314,85	{3} 296,57	{4} 280,56	{5} 257,44
1	0-1 min		0,84675	0,13869	0,01030	0,00005
2	1-2 min	0,84675		0,16822	0,01420(	0,00009
3	2-3 min	0,13869	0,16822		0,22710	0,00510
4	3-4 min	0,01030	0,01420(	0,22710		0,08214
5	4-5min	0,00005	0,00009	0,00510	0,08214	

NOVEL OBJECT TEST - FAMILIARIZATION TRIAL

Table A5.25: Raw data - Distance travelled during the 10 minute familiarization trial

				Distance (cm)											
Rat Number	Group	Treatment	Stress	0-1 min	1-2 min	2-3 min	3-4 min	4-5 min	5-6 min	6-7 min	7-8 min	8-9 min	9-10 min	Total Distance (cm) in 5 min	Total Distance (cm) in 10 min
80	Control	Sacc	nMS	315,83	257,80	175,22	206,53	144,49	157,07	124,92	181,05	196,50	176,93	1099,88	1936,35
81	Control	Sacc	nMS	321,63	251,82	307,19	274,76	143,94	200,76	190,64	201,81	201,24	141,07	1299,33	2234,85
180	Control	Sacc	nMS	413,22	350,45	328,43	377,63	362,78	392,60	206,12	291,81	374,50	297,59	1832,51	3395,12
181	Control	Sacc	nMS	516,01	397,72	308,19	313,34	255,29	218,42	224,10	197,71	258,32	325,60	1790,55	3014,70
182	Control	Sacc	nMS	579,64	610,24	819,80	560,12	358,73	356,08	629,94	574,55	317,00	667,47	2928,52	5473,56
200	Control	Sacc	nMS	419,69	390,93	495,16	390,70	370,76	311,44	413,78	324,67	430,15	289,44	2067,24	3836,72
201	Control	Sacc	nMS	423,76	436,15	379,78	369,73	252,38	489,09	326,07	223,66	216,55	199,04	1861,80	3316,21
202	Control	Sacc	nMS	401,29	411,12	290,84	307,56	378,89	357,57	339,09	296,14	564,45	357,12	1789,70	3704,08
210	Control	Sacc	nMS	565,29	392,70	652,21	453,02	264,52	453,31	351,20	313,61	371,92	278,65	2327,74	4096,43
211	Control	Sacc	nMS	578,98	539,80	512,62	413,84	394,33	557,72	501,21	377,87	226,53	446,59	2439,56	4549,48
212	Control	Sacc	nMS	682,94	518,69	491,50	572,61	467,84	449,11	306,84	317,31	348,09	509,91	2733,58	4664,83
50	MS	Sacc	MS	436,18	362,51	328,51	292,60	333,57	395,28	317,20	351,04	270,30	271,16	1753,38	3358,36
51	MS	Sacc	MS	333,01	300,62	357,27	321,46	401,48	289,03	319,71	377,59	134,89	216,71	1713,84	3051,78
150	MS	Sacc	MS	338,21	317,78	314,32	237,99	324,73	282,42	260,46	195,21	289,02	249,79	1533,03	2809,92
151	MS	Sacc	MS	387,64	387,53	269,13	348,50	235,49	297,22	309,11	209,09	170,12	185,49	1628,29	2799,32
170	MS	Sacc	MS	593,17	452,66	377,81	446,31	457,44	353,96	277,11	342,05	307,25	259,83	2327,38	3867,59
171	MS	Sacc	MS	477,76	483,55	504,93	467,56	386,03	271,97	379,17	212,75	331,75	334,27	2319,82	3849,73
172	MS	Sacc	MS	551,19	546,57	498,74	317,34	438,31	372,08	344,25	340,21	267,82	157,45	2352,15	3833,96
60	EtOH	EtOH	nMS	459,28	224,94	228,25	156,68	222,59	205,44	174,98	216,91	58,73	235,57	1291,74	2183,37
61	EtOH	EtOH	nMS	351,60	281,51	204,88	150,63	236,52	162,36	310,89	160,92	191,55	64,36	1225,14	2115,22
130	EtOH	EtOH	nMS	392,60	372,72	306,78	322,35	331,52	315,39	374,43	197,32	190,28	196,73	1725,97	3000,13
131	EtOH	EtOH	nMS	380,70	355,08	365,79	210,29	275,58	285,80	333,56	273,61	316,91	273,65	1587,44	3070,96
190	EtOH	EtOH	nMS	479,04	601,73	463,08	491,27	514,60	416,65	373,38	244,54	292,55	392,23	2549,72	4269,07
191	EtOH	EtOH	nMS	549,91	490,88	541,68	537,28	459,90	369,28	357,52	310,58	354,32	167,76	2579,65	4139,11
40	EtOH+MS	EtOH	MS	407,57	373,80	331,10	225,26	143,15	290,87	259,89	167,06	179,81	200,66	1480,89	2579,17
41	EtOH+MS	EtOH	MS	476,05	424,59	336,32	355,27	243,14	234,39	241,79	287,12	217,24	173,84	1835,37	2989,74
70	EtOH+MS	EtOH	MS	340,34	211,86	291,70	210,14	210,51	194,05	127,68	272,23	276,19	221,79	1264,55	2356,49
71	EtOH+MS	EtOH	MS	343,46	370,54	277,83	304,07	257,39	282,05	219,47	266,20	169,22	229,34	1553,29	2719,57
140	EtOH+MS	EtOH	MS	411,58	297,99	301,94	295,03	255,13	214,08	253,51	177,31	239,58	240,94	1561,68	2687,09
141	EtOH+MS	EtOH	MS	391,96	373,27	186,26	302,50	225,42	190,22	276,73	249,11	203,19	299,79	1479,41	2698,45
160	EtOH+MS	EtOH	MS	443,74	509,54	361,95	467,16	329,04	335,28	376,71	238,98	252,62	239,75	2111,43	3554,76
161	EtOH+MS	EtOH	MS	449,40	558,92	401,47	424,73	396,43	318,04	350,16	193,45	332,15	227,46	2230,96	3652,22

Table A5.26: Raw data - Object interaction during the novel object familiarization trial

Rat Number	Group	Treatment	Stress	LO Duration (s)	RO Duration (s)	Total Object Time (s)	LO%	RO%	Correction Factor	Corrected LO Duration (s)	Corrected Total Object Duration (s)	Corrected LO (%)	Corrected RO (%)
80	Control	Sacc	nMS	80,20	144,80	225,00	35,64	64,36	1,81	144,80	289,60	50,00	50,00
81	Control	Sacc	nMS	106,80	186,20	293,00	36,45	63,55	1,74	186,20	372,40	50,00	50,00
180	Control	Sacc	nMS	134,80	149,64	284,44	47,39	52,61	1,11	149,64	299,28	50,00	50,00
181	Control	Sacc	nMS	89,84	80,56	170,40	52,72	47,28	0,90	80,56	161,12	50,00	50,00
182	Control	Sacc	nMS	117,12	157,52	274,64	42,64	57,36	1,34	157,52	315,04	50,00	50,00
200	Control	Sacc	nMS	84,92	129,24	214,16	39,65	60,35	1,52	129,24	258,48	50,00	50,00
201	Control	Sacc	nMS	96,88	106,72	203,60	47,58	52,42	1,10	106,72	213,44	50,00	50,00
202	Control	Sacc	nMS	131,52	106,60	238,12	55,23	44,77	0,81	106,60	213,20	50,00	50,00
210	Control	Sacc	nMS	85,56	86,80	172,36	49,64	50,36	1,01	86,80	173,60	50,00	50,00
211	Control	Sacc	nMS	119,76	149,28	269,04	44,51	55,49	1,25	149,28	298,56	50,00	50,00
212	Control	Sacc	nMS	55,44	191,56	247,00	22,45	77,55	3,46	191,56	383,12	50,00	50,00
50	MS	Sacc	MS	128,40	124,60	253,00	50,75	49,25	0,97	124,60	249,20	50,00	50,00
51	MS	Sacc	MS	92,40	83,20	175,60	52,62	47,38	0,90	83,20	166,40	50,00	50,00
150	MS	Sacc	MS	134,20	131,40	265,60	50,53	49,47	0,98	131,40	262,80	50,00	50,00
151	MS	Sacc	MS	118,60	112,40	231,00	51,34	48,66	0,95	112,40	224,80	50,00	50,00
170	MS	Sacc	MS	126,80	129,36	256,16	49,50	50,50	1,02	129,36	258,72	50,00	50,00
171	MS	Sacc	MS	145,52	153,32	298,84	48,69	51,31	1,05	153,32	306,64	50,00	50,00
172	MS	Sacc	MS	135,56	176,76	312,32	43,40	56,60	1,30	176,76	353,52	50,00	50,00
60	EtOH	EtOH	nMS	75,60	91,40	167,00	45,27	54,73	1,21	91,40	182,80	50,00	50,00
61	EtOH	EtOH	nMS	110,00	157,80	267,80	41,08	58,92	1,43	157,80	315,60	50,00	50,00
130	EtOH	EtOH	nMS	87,40	108,80	196,20	44,55	55,45	1,24	108,80	217,60	50,00	50,00
131	EtOH	EtOH	nMS	125,80	90,80	216,60	58,08	41,92	0,72	90,80	181,60	50,00	50,00
190	EtOH	EtOH	nMS	99,04	85,16	184,20	53,77	46,23	0,86	85,16	170,32	50,00	50,00
191	EtOH	EtOH	nMS	88,72	113,68	202,40	43,83	56,17	1,28	113,68	227,36	50,00	50,00
192	EtOH	EtOH	nMS	50,24	49,00	99,24	50,62	49,38	0,98	49,00	98,00	50,00	50,00
40	EtOH+MS	EtOH	MS	109,80	125,20	235,00	46,72	53,28	1,14	125,20	250,40	50,00	50,00
41	EtOH+MS	EtOH	MS	99,00	108,00	207,00	47,83	52,17	1,09	108,00	216,00	50,00	50,00
70	EtOH+MS	EtOH	MS	92,40	116,00	208,40	44,34	55,66	1,26	116,00	232,00	50,00	50,00
71	EtOH+MS	EtOH	MS	67,60	87,40	155,00	43,61	56,39	1,29	87,40	174,80	50,00	50,00
140	EtOH+MS	EtOH	MS	166,80	73,60	240,40	69,38	30,62	0,44	73,60	147,20	50,00	50,00
141	EtOH+MS	EtOH	MS	147,00	112,40	259,40	56,67	43,33	0,76	112,40	224,80	50,00	50,00
160	EtOH+MS	EtOH	MS	101,00	92,36	193,36	52,23	47,77	0,91	92,36	184,72	50,00	50,00
161	EtOH+MS	EtOH	MS	180,28	87,72	268,00	67,27	32,73	0,49	87,72	175,44	50,00	50,00

Table A5.27: Raw data - Object frequency and latency to the objects during the novel object test familiarization trial -

Rat Number	Group	Treatment	Stress	LO Frequency	RO Frequency	Correction Factor	Corrected LO Frequency	Latency to LO (s)	Latency to RO (s)	Correction Factor	Corrected Latency to LO (s)
80	Control	Sacc	nMS	24,00	19,00	0,79	19,00	3,4	7	2,05882353	7
81	Control	Sacc	nMS	22,00	28,00	1,27	28,00	6,8	3,2	0,47058824	3,2
180	Control	Sacc	nMS	35,00	71,00	2,03	71,00	3,32	7,96	2,39759036	7,96
181	Control	Sacc	nMS	15,00	55,00	3,67	55,00	3,56	5,6	1,57303371	5,6
182	Control	Sacc	nMS	39,00	64,00	1,64	64,00	2,44	7,36	3,01639344	7,36
200	Control	Sacc	nMS	43,00	57,00	1,33	57,00	3	24,16	8,05333333	24,16
201	Control	Sacc	nMS	39,00	47,00	1,21	47,00	5,72	1,84	0,32167832	1,84
202	Control	Sacc	nMS	46,00	62,00	1,35	62,00	4,48	26,96	6,01785714	26,96
210	Control	Sacc	nMS	28,00	99,00	3,54	99,00	3,96	13,12	3,31313131	13,12
211	Control	Sacc	nMS	35,00	93,00	2,66	93,00	4,88	12,36	2,53278689	12,36
212	Control	Sacc	nMS	23,00	105,00	4,57	105,00	3	8,2	2,73333333	8,2
50	MS	Sacc	MS	53,00	46,00	0,87	46,00	3,6	7,8	2,16666667	7,8
51	MS	Sacc	MS	39,00	44,00	1,13	44,00	8,2	16,2	1,97560976	16,2
150	MS	Sacc	MS	22,00	35,00	1,59	35,00	11,8	3	0,25423729	3
151	MS	Sacc	MS	42,00	35,00	0,83	35,00	4,8	11,8	2,45833333	11,8
170	MS	Sacc	MS	34,00	48,00	1,41	48,00	2,2	6,52	2,96363636	6,52
171	MS	Sacc	MS	41,00	54,00	1,32	54,00	4,2	21,4	5,0952381	21,4
172	MS	Sacc	MS	36,00	59,00	1,64	59,00	2,24	7,76	3,46428571	7,76
60	EtOH	EtOH	nMS	22,00	21,00	0,95	21,00	3	7	2,33333333	7
61	EtOH	EtOH	nMS	22,00	19,00	0,86	19,00	5,4	9,2	1,7037037	9,2
130	EtOH	EtOH	nMS	33,00	33,00	1,00	33,00	5,2	32,2	6,19230769	32,2
131	EtOH	EtOH	nMS	41,00	30,00	0,73	30,00	4,8	7,6	1,58333333	7,6
190	EtOH	EtOH	nMS	57,00	44,00	0,77	44,00	4,2	7,52	1,79047619	7,52
191	EtOH	EtOH	nMS	37,00	77,00	2,08	77,00	2,88	12,32	4,27777778	12,32
192	EtOH	EtOH	nMS	34,00	46,00	1,35	46,00	3,68	15,88	4,31521739	15,88
40	EtOH+MS	EtOH	MS	18,00	44,00	2,44	44,00	19	13	0,68421053	13
41	EtOH+MS	EtOH	MS	34,00	38,00	1,12	38,00	9,8	11,6	1,18367347	11,6
70	EtOH+MS	EtOH	MS	22,00	27,00	1,23	27,00	6,2	8,2	1,32258065	8,2
71	EtOH+MS	EtOH	MS	24,00	24,00	1,00	24,00	3,4	7	2,05882353	7
140	EtOH+MS	EtOH	MS	47,00	23,00	0,49	23,00	2,2	6,8	3,09090909	6,8
141	EtOH+MS	EtOH	MS	22,00	40,00	1,82	40,00	3,8	10,2	2,68421053	10,2
160	EtOH+MS	EtOH	MS	32,00	37,00	1,16	37,00	4,84	9,48	1,95867769	9,48
161	EtOH+MS	EtOH	MS	36,00	46,00	1,28	46,00	4,92	14,8	3,00813008	14,8

Table A5.28: Shapiro-Wilk test results for variables analyzed in the novel object familiarization trial

Test	Variable	Shapiro-Wilk, W	*P* Value
Familiarization	Total Distance (10 min)	0,974	0,608
	Total Distance (5 min)	0,960	0,278
	Distance (0-1 min)	0,941	0,077
	Distance (1-2 min)	0,972	0,546
	Distance (2-3 min)	0,902	0,007
	Distance (3-4 min)	0,972	0,552
	Distance (4-5 min)	0,964	0,349
	Distance (5-6 min)	0,971	0,534
	Distance (6-7min)	0,939	0,069
	Distance (7-8 min)	0,880	0,002
	Distance (8-9 min)	0,960	0,282
	Distance (9-10 min)	0,877	0,002
	LO Duration (s)	0,985	0,919
	RO Duration (s)	0,968	0,419
	Corrected LO Duration (s)	0,968	0,419
	Total Object Duration (s)	0,979	0,756
	Corrected Total Object Duration (s)	0,968	0,419
	% Time with RO	0,946	0,098
	Corrected % Time with RO	NA	NA
	Latency to LO	0,684	0,000
	Latency to RO	0,851	0,000
	Corrected Latency to LO	0,851	0,000
	LO Frequency	0,958	0,226
	RO Frequency	0,912	0,011
	Corrected LO Frequency	0,912	0,011

Table A5.29: Two-way ANOVA result of the total distance travelled during the full 10 minute NOT familiarization trial

	Univariate Tests of Significance for Total Distance in 10 min (cm) (Spreadsheet1) Sigma-restricted parameterization Effective hypothesis decomposition				
Effect	SS	Degr. of Freedom	MS	F	p
Intercept	32452302	1	32452302	501,0506	0,000000
Treatment	186336	1	186336	2,8770	0,10094
Stress	50339	1	50339	0,7772	0,38549
Treatment*Stress	788	1	788	0,0122	0,91290
Error	1813518	28	64768		

Table A5.30: Repeated-measures ANOVA and Duncan's post-hoc results of the distance travelled per minute of the full 10 minute NOT familiarization trial

Effect	SS	Degr. of Freedom	MS	F	p
Intercept	3245230	1	3245230	501,050	0,00000
Treatment	186337	1	186337	2,8770	0,10094
Stress	50339	1	50339	0,7772	0,38549
Treatment*Stress	789	1	789	0,0122	0,91290
Error	181351	28	6476		
TIME	105162	9	11684	24,0994	0,00000
TIME*Treatment	19651	9	2183	0,4503	0,90632
TIME*Stress	17784	9	1976	0,4076	0,93049
TIME*Treatment*Stress	75316	9	8368	1,7260	0,08349
Error	122183	252	484		

Repeated Measures Analysis of Variance (Spreadsheet1)
Sigma-restricted parameterization
Effective hypothesis decomposition

Duncan test; variable DV_1 (Spreadsheet34)
Approximate Probabilities for Post Hoc Tests
Error: Within MS = 4848,5, df = 252,00

Cell No.	MINUTE	{1} 444,15	{2} 401,75	{3} 375,33	{4} 347,63	{5} 314,75	{6} 313,09	{7} 307,86	{8} 268,23	{9} 267,21	{10} 266,50
1	0-1 min		0,01488	0,00012	0,00000	0,00000	0,00000	0,00000	0,00000	0,00000	0,00000
2	1-2 min	0,01488		0,12914	0,00267	0,00000	0,00000	0,00000	0,00000	0,00000	0,00000
3	2-3 min	0,00012	0,12914		0,11157	0,00073	0,00066	0,00025	0,00000	0,00000	0,00000
4	3-4 min	0,00000	0,00267	0,11157		0,05887	0,05984	0,03507	0,00001	0,00001	0,00001
5	4-5 min	0,00000	0,00000	0,00073	0,05887		0,92431	0,71261	0,01276	0,01263	0,01273
6	5-6 min	0,00000	0,00000	0,00066	0,05984	0,92431		0,76383	0,01356	0,01412	0,01468
7	6-7 min	0,00000	0,00000	0,00025	0,03507	0,71261	0,76383		0,02281	0,02587	0,02800
8	7-8 min	0,00000	0,00000	0,00000	0,00001	0,01276	0,01356	0,02281		0,95318	0,92615
9	8-9 min	0,00000	0,00000	0,00000	0,00001	0,01263	0,01412	0,02587	0,95318		0,96737
10	9-10 min	0,00000	0,00000	0,00000	0,00001	0,01273	0,01468	0,02800	0,92615	0,96737	

Table A5.31: Two-way ANOVA result of the total distance travelled during the first 5 minutes of the NOT familiarization trial

Effect	SS	Degr. of Freedom	MS	F	p
Intercept	106445691	1	106445691	454,8554	0,000000
Treatment	378621	1	378621	1,6179	0,213849
Stress	80423	1	80423	0,3437	0,562423
Treatment*Stress	8869	1	8869	0,0379	0,847056
Error	6552586	28	234021		

Univariate Tests of Significance for Total Distance in 5 min (cm) (Spreadsheet1)
Sigma-restricted parameterization
Effective hypothesis decomposition

Table A5.32: Repeated-measures ANOVA and Duncan's post-hoc results for the distance travelled per minute during the first 5 minutes of the NOT familiarization trial

Repeated Measures Analysis of Variance (Spreadsheet1)
Sigma-restricted parameterization
Effective hypothesis decomposition

Effect	SS	Degr. of Freedom	MS	F	p
Intercept	2128913	1	2128913	454,855	0,00000
Treatment	75724	1	75724	1,6179	0,21384
Stress	16085	1	16085	0,3437	0,56242
Treatment*Stress	1774	1	1774	0,0379	0,84705
Error	1310517	28	46804		
TIME	282247	4	70562	18,821	0,00000
TIME*Treatment	11342	4	2835	0,7563	0,55587
TIME*Stress	9497	4	2374	0,6333	0,63976
TIME*Treatment*Stress	41917	4	10479	2,7953	0,02950
Error	419878	112	3749		

Duncan test; variable DV_1 (Spreadsheet3)
Approximate Probabilities for Post Hoc Tests
Error: Within MS = 3748,9, df = 112,00

Cell No.	TIME	{1} 444,15	{2} 401,75	{3} 375,33	{4} 347,63	{5} 314,75
1	0-1 min		0,006682	0,00007	0,00004	0,00002
2	1-2 min	0,006682		0,08726	0,00090	0,00004
3	2-3 min	0,00007	0,08726		0,07313	0,00024
4	3-4 min	0,00004	0,00090	0,07313		0,03391
5	4-5 min	0,00002	0,00004	0,00024	0,03391	

Duncan test; variable DV_1 (Spreadsheet1)
Approximate Probabilities for Post Hoc Tests
Error: Between; Within; Pooled MS = 12360,, df = 47,595

Cell No.	Treatment	Stress	TIME	{1} 474,39	{2} 414,31	{3} 432,81	{4} 385,44	{5} 308,54	{6} 445,31	{7} 407,32	{8} 378,67	{9} 347,39	{10} 368,15	{11} 435,52	{12} 387,81	{13} 351,74	{14} 311,42	{15} 340,12	{16} 408,01	{17} 390,06	{18} 311,07	{19} 323,02	{20} 257,53
1	Sacc	Control	0-1 min		0,090560	0,233274	0,016355	0,000014	0,612312	0,317964	0,166486	0,070195	0,126533	0,525796	0,205297	0,079166	0,021415	0,056474	0,316766	0,213675	0,021523	0,032111	0,002319
2	Sacc	Control	1-2 min	0,090560		0,556806	0,431659	0,004877	0,626241	0,909562	0,596470	0,330305	0,496285	0,729181	0,685058	0,359835	0,140366	0,282886	0,912561	0,703305	0,140323	0,188756	0,026421
3	Sacc	Control	2-3 min	0,233274	0,556806		0,200408	0,000808	0,838533	0,688810	0,424751	0,216663	0,344018	0,962373	0,497620	0,238495	0,083408	0,182104	0,685600	0,512165	0,083525	0,115849	0,013279
4	Sacc	Control	3-4 min	0,016355	0,431659	0,200408		0,039945	0,380912	0,731270	0,906044	0,559686	0,777871	0,460288	0,967119	0,596466	0,275067	0,494586	0,729998	0,940600	0,276527	0,352739	0,064483
5	Sacc	Control	4-5 min	0,000014	0,004877	0,000808	0,039945		0,054021	0,156788	0,304773	0,558323	0,379433	0,072697	0,251402	0,520389	0,963491	0,628456	0,155185	0,240119	0,964848	0,820649	0,375304
6	Sacc	MS	0-1 min	0,612312	0,626241	0,838533	0,380912	0,054021		0,299167	0,077327	0,008993	0,040740	0,864468	0,396556	0,178043	0,057933	0,133066	0,567450	0,410851	0,057966	0,082157	0,008312
7	Sacc	MS	1-2 min	0,317964	0,909562	0,688810	0,731270	0,156788	0,299167		0,426071	0,107108	0,284233	0,665766	0,750217	0,408053	0,165681	0,325396	0,990416	0,763503	0,166038	0,220400	0,032672
8	Sacc	MS	2-3 min	0,166486	0,596470	0,424751	0,906044	0,304773	0,077327	0,426071		0,371485	0,738213	0,405329	0,881683	0,660230	0,316646	0,554490	0,659300	0,858978	0,318894	0,401454	0,078193
9	Sacc	MS	3-4 min	0,070195	0,330305	0,216663	0,559686	0,558323	0,008993	0,107108	0,371485		0,537810	0,204411	0,542621	0,939587	0,571807	0,899067	0,374997	0,525539	0,577711	0,690729	0,180523
10	Sacc	MS	4-5 min	0,126531	0,496285	0,344018	0,777871	0,379431	0,040740	0,284232	0,738213	0,537810		0,327037	0,757787	0,774770	0,392338	0,659722	0,553293	0,737888	0,395495	0,488913	0,105419
11	EtOH	Control	0-1 min	0,525798	0,729181	0,962373	0,460288	0,072697	0,864468	0,665766	0,405329	0,204411	0,327037		0,197106	0,025473	0,000784	0,011110	0,665650	0,493258	0,077773	0,108407	0,012174
12	EtOH	Control	1-2 min	0,205297	0,685058	0,497620	0,967119	0,251402	0,396556	0,750217	0,881683	0,542621	0,757787	0,197106		0,315085	0,039615	0,197350	0,751188	0,968726	0,264454	0,339430	0,061035
13	EtOH	Control	2-3 min	0,079166	0,359835	0,238495	0,596466	0,520389	0,178043	0,408053	0,660230	0,939587	0,774770	0,025471	0,315085		0,260570	0,730420	0,406766	0,563725	0,540083	0,651883	0,164606
14	EtOH	Control	3-4 min	0,021415	0,140366	0,083408	0,275067	0,963491	0,057933	0,165681	0,316646	0,571807	0,392338	0,000784	0,039615	0,260570		0,393629	0,164510	0,252785	0,995298	0,839615	0,396774
15	EtOH	Control	4-5 min	0,056474	0,282880	0,182104	0,494586	0,628456	0,133066	0,325399	0,554490	0,899067	0,659722	0,011110	0,197350	0,730420	0,393629		0,323307	0,461537	0,648152	0,765569	0,212521
16	EtOH	MS	0-1 min	0,316766	0,912561	0,685600	0,729998	0,155185	0,567450	0,990416	0,659300	0,374997	0,553293	0,665650	0,751188	0,406766	0,164510	0,323307		0,594284	0,009765	0,023277	0,000042
17	EtOH	MS	1-2 min	0,213675	0,703309	0,512165	0,940600	0,240119	0,410851	0,763503	0,858978	0,525539	0,737888	0,493258	0,968726	0,563725	0,252789	0,461537	0,594284		0,035915	0,072965	0,000279
18	EtOH	MS	2-3 min	0,021523	0,140323	0,083525	0,276527	0,964848	0,057966	0,166038	0,318894	0,577711	0,395495	0,077773	0,264454	0,540083	0,995298	0,648152	0,009765	0,035915		0,723136	0,109745
19	EtOH	MS	3-4 min	0,032111	0,188756	0,115849	0,352739	0,820649	0,082157	0,220400	0,401454	0,690729	0,488913	0,108407	0,339430	0,651883	0,839615	0,765569	0,023277	0,072965	0,723136		0,064191
20	EtOH	MS	4-5 min	0,002319	0,026421	0,013279	0,064483	0,375304	0,008312	0,032672	0,078193	0,180523	0,105419	0,012174	0,061035	0,164606	0,396774	0,212521	0,000042	0,000279	0,109745	0,064191	

Table A5.33: Repeated-measures ANOVA and Duncan's post-hoc results for object duration during the NOT familiarization trial

Repeated Measures Analysis of Variance (Spreadsheet191)
Sigma-restricted parameterization
Effective hypothesis decomposition

Effect	SS	Degr. of Freedom	MS	F	p
Intercept	812770,6	1	812770,6	842,039	0,00000
Treatment	6439,6	1	6439,6	6,6715	0,01510
Stress	2571,1	1	2571,1	2,6637	0,11347
Treatment*Stress	97,1	1	97,1	0,1006	0,75341
Error	27992,0	29	965,2		
OBJECTS	765,9	1	765,9	1,0141	0,32224
OBJECTS*Treatment	2584,7	1	2584,7	3,4225	0,07452
OBJECTS*Stress	3537,6	1	3537,6	4,6842	0,03881
OBJECTS*Treatment*Stress	4,7	1	4,7	0,0063	0,93751
Error	21900,9	29	755,2		

Duncan test; variable DV_1 (Spreadsheet191)
Approximate Probabilities for Post Hoc Tests
Error: Between MS = 965,24, df = 29,000

Cell No.	Treatment	{1} 121,79	{2} 103,33
1	Sacc		0,023034
2	EtOH	0,023034	

Duncan test; variable DV_1 (Spreadsheet191)
Approximate Probabilities for Post Hoc Tests
Error: Between; Within; Pooled MS = 860,22, df = 57,148

Cell No.	Stress	OBJECTS	{1} 96,647	{2} 121,42	{3} 123,02	{4} 114,25
1	Contro	LO Duratior		0,019918	0,020324	0,091600
2	Contro	RO Duratior	0,019918		0,876337	0,487233
3	MS	LO Duratior	0,020324	0,876337		0,396992
4	MS	RO Duratior	0,091600	0,487233	0,396992	

Duncan test; variable DV_1 (Spreadsheet191)
Approximate Probabilities for Post Hoc Tests
Error: Between; Within; Pooled MS = 860,22, df = 57,148

Cell No.	Treatment	Stress	OBJECTS	{1} 100,26	{2} 135,36	{3} 125,93	{4} 130,15	{5} 90,971	{6} 99,520	{7} 120,49	{8} 100,33
1	Sacc	Contro	LO Duratior		0,030354	0,116052	0,073446	0,556295	0,960202	0,199783	0,995937
2	Sacc	Contro	RO Duratior	0,030354		0,550192	0,724360	0,010068	0,036822	0,364146	0,035483
3	Sacc	MS	LO Duratior	0,116052	0,550192		0,761289	0,039112	0,114446	0,712573	0,104802
4	Sacc	MS	RO Duratior	0,073446	0,724360	0,761289		0,022147	0,071414	0,540376	0,067573
5	EtOH	Contro	LO Duratior	0,556295	0,010068	0,039112	0,022147		0,539495	0,077204	0,568247
6	EtOH	Contro	RO Duratior	0,960202	0,036822	0,114446	0,071414	0,539495		0,199963	0,959890
7	EtOH	MS	LO Duratior	0,199783	0,364146	0,712573	0,540376	0,077204	0,199963		0,154070
8	EtOH	MS	RO Duratior	0,995937	0,035483	0,104802	0,067573	0,568247	0,959890	0,154070	

Table A5.34: Repeated-measures ANOVA and Duncan's post-hoc results for the corrected object duration during the NOT familiarization trial

Repeated Measures Analysis of Variance (Spreadsheet42)
Sigma-restricted parameterization
Effective hypothesis decomposition

Effect	SS	Degr. of Freedom	MS	F	p
Intercept	863436,1	1	863436,1	450,5951	0,000000
Treatment	17183,9	1	17183,9	8,9676	0,005574
Stress	76,9	1	76,9	0,0402	0,842585
Treatment*Stress	144,6	1	144,6	0,0755	0,785473
Error	55570,2	29	1916,2		
OBJECTS	0,0	1	0,0		
OBJECTS*Treatment	0,0	1	0,0		
OBJECTS*Stress	0,0	1	0,0		
OBJECTS*Treatment*Stress	0,0	1	0,0		
Error	0,0	29	0,0		

Duncan test; variable DV_1 (Spreadsheet68)
Approximate Probabilities for Post Hoc Tests
Error: Between MS = 1916,2, df = 29,000

Cell No.	Treatment	{1} 133,33	{2} 99,955
1	Sacc		0,004609
2	EtOH	0,004609	

Table A5.35: Two-way ANOVA and Duncan's post-hoc results for total object duration during the NOT familiarization trial

Univariate Tests of Significance for Total Object Time (s) (Spreadsheet18)
Sigma-restricted parameterization
Effective hypothesis decomposition

Effect	SS	Degr. of Freedom	MS	F	p
Intercept	162554	1	162554	842,0391	0,000000
Treatment	1287	1	1287	6,6715	0,015108
Stress	5142	1	5142	2,6637	0,113475
Treatment*Stress	194	1	194	0,1006	0,753413
Error	55984	29	1930		

Duncan test; variable Total Object Time (s) (Spreadsheet18)
Approximate Probabilities for Post Hoc Tests
Error: Between MS = 1930,5, df = 29,000

Cell No.	Treatment	{1} 243,57	{2} 206,67
1	Sacc		0,023034
2	EtOH	0,023034	

Table A5.36: Two-way ANOVA and Duncan's post-hoc results for the corrected total object duration during the NOT familiarization trial

Univariate Tests of Significance for Corrected Total Object Time (Spreadsheet18)
Sigma-restricted parameterization
Effective hypothesis decomposition

Effect	SS	Degr. of Freedom	MS	F	p
Intercept	172687	1	172687	450,5951	0,000000
Treatment	3436	1	3436	8,9676	0,005574
Stress	154	1	154	0,0402	0,842585
Treatment*Stress	289	1	289	0,0755	0,785473
Error	111140	29	3832		

Duncan test; variable Corrected Total Object Time (Spreadsheet18)
Approximate Probabilities for Post Hoc Tests
Error: Between MS = 3832,4, df = 29,000

Cell No.	Treatment	{1} 266,66	{2} 199,91
1	Sacc		0,004609
2	EtOH	0,004609	

Table A5.37: Two-way ANOVA and Duncan's post-hoc results for the percentage time spent with the right object during NOT familiarization trial

Univariate Tests of Significance for RO (%) (Spreadsheet78)
Sigma-restricted parameterization
Effective hypothesis decomposition

Effect	SS	Degr. of Freedom	MS	F	p
Intercept	84342,59	1	84342,59	1318,763	0,000000
Treatment	163,12	1	163,12	2,551	0,121097
Stress	277,61	1	277,61	4,341	0,046135
Treatment*Stress	2,54	1	2,54	0,040	0,843464
Error	1854,72	29	63,96		

Duncan test; variable RO (%) (Spreadsheet78)
Approximate Probabilities for Post Hoc Tests
Error: Between MS = 63,956, df = 29,000

Cell No.	Stress	{1} 54,938	{2} 48,340
1	Contro		0,025356
2	MS	0,025356	

Duncan test; variable RO (%) (Spreadsheet78)
Approximate Probabilities for Post Hoc Tests
Error: Between MS = 63,956, df = 29,000

Cell No.	Treatment	Stress	{1} 56,916	{2} 50,452	{3} 51,829	{4} 46,493
1	Sacc	Contro		0,137462	0,214242	0,022275
2	Sacc	MS	0,137462		0,733515	0,331263
3	EtOH	Contro	0,214242	0,733515		0,218523
4	EtOH	MS	0,022275	0,331263	0,218523	

Table A5.38: Two-way ANOVA results for the corrected percentage time spent with the right object during NOT familiarization trial

Univariate Tests of Significance for Corrected RO (%) (Spreadsheet42)
Sigma-restricted parameterization
Effective hypothesis decomposition

Effect	SS	Degr. of Freedom	MS	F	p
Intercept	79741,10	1	79741,10	1,309279E+34	0,000000
Treatment	0,00	1	0,00	8,833048E-02	0,768429
Stress	0,00	1	0,00	1,788692E+00	0,191481
Treatment*Stress	0,00	1	0,00	8,833048E-02	0,768429
Error	0,00	29	0,00		

Table A5.39: Friedman ANOVA repeated-measures and Wilcoxon Matched Pairs results for latency to the left object (LO) and right object (RO) during the NOT familiarization trial

All Groups
Friedman ANOVA and Kendall Coeff. of Concordance (Spreadsheet15)
ANOVA Chi Sqr. (N = 33, df = 1) = 18,93939 p = ,00001
Coeff. of Concordance = ,57392 Aver. rank r = ,56061

Variable	Average Rank	Sum of Ranks	Mean	Std.Dev.
Latency LO (s)	1,121212	37,00000	4,99758	3,284341
Latency RO (s)	1,878788	62,00000	11,06182	6,791878

All Groups
Wilcoxon Matched Pairs Test (Spreadsheet129)
Marked tests are significant at p <,05000

Pair of Variables	Valid N	T	Z	p-value
Latency to LO & Latency to RO	33	62,00000	3,904121	0,000095

Aggregate Results
Wilcoxon Matched Pairs Test (Spreadsheet1)
Marked tests are significant at p <,05000

Pair of Variables	Group	Valid N	T	Z	p-value
Latency LO (s) & Latency RO (s)	Contro	11	6,500000	2,356137	0,018467
Latency LO (s) & Latency RO (s)	MS	7	6,000000	1,352247	0,176297
Latency LO (s) & Latency RO (s)	EtOH	7	0,00	2,366432	0,017961
Latency LO (s) & Latency RO (s)	EtOH+MS	8	6,000000	1,680336	0,092933

Table A5.40: Friedman ANOVA repeated-measures and Wilcoxon Matched Pairs results for the left object (LO) and right object (RO) frequency during the NOT familiarization trial

All Groups
Friedman ANOVA and Kendall Coeff. of Concordance (Spreadsheet172)
ANOVA Chi Sqr. (N = 33, df = 1) = 7,258065 p = ,00706
Coeff. of Concordance = ,21994 Aver. rank r = ,19556

Variable	Average Rank	Sum of Ranks	Mean	Std.Dev.
LO Frequency	1,272727	42,0000(	33,24242	10,25314
RO Frequency	1,727273	57,0000(	47,57576	22,12469

All Groups
Wilcoxon Matched Pairs Test (Spreadsheet1)
Marked tests are significant at p <,05000

Pair of Variables	Valid N	T	Z	p-value
LO Frequency & RO Frequency	31	79,5000(	3,302018	0,00096(

Aggregate Results
Wilcoxon Matched Pairs Test (Spreadsheet1)
Marked tests are significant at p <,05000

Pair of Variables	Group	Valid N	T	Z	p-value
LO Frequency & RO Frequency	Contro	11	1,00000(	2,845147	0,004439
LO Frequency & RO Frequency	MS	7	5,00000(	1,521278	0,128191
LO Frequency & RO Frequency	EtOH	6	10,0000(	0,104828	0,916512
LO Frequency & RO Frequency	EtOH+MS	7	6,00000(	1,352247	0,176297

Table A5.41: Friedman ANOVA repeated-measures results for the corrected left object (LO) and right object (RO) frequency during the NOT familiarization trial

All Groups
Friedman ANOVA and Kendall Coeff. of Concordance (Spreadsheet1)
ANOVA Chi Sqr. (N = 33, df = 1) = 1,000000 p = ,31731
Coeff. of Concordance = ,03030 Aver. rank r = -,3E-7

Variable	Average Rank	Sum of Ranks	Mean	Std.Dev.
RO Frequency	1,515152	50,0000(	47,57576	22,12469
Corrected LO Frequency	1,484848	49,0000(	47,57576	22,12469

NOVEL OBJECT TEST TRIAL

Table A5.42: Raw data - Distance traveled during the novel object test trial

Distance (cm) per min									
Rat Number	**Group**	**Treatment**	**Stress**	**0-1 min**	**1-2 min**	**2-3 min**	**3-4 min**	**4-5 min**	**TOTAL DISTANCE (cm)**
80	Control	Sacc	nMS	308,97	119,09	150,76	151,18	162,86	892,87
81	Control	Sacc	nMS	363,04	283,65	234,11	269,64	195,45	1345,88
180	Control	Sacc	nMS	455,46	412,86	304,72	280,44	400,65	1854,12
181	Control	Sacc	nMS	404,81	340,60	315,66	300,74	322,63	1684,43
182	Control	Sacc	nMS	488,60	432,01	494,27	406,75	304,75	2126,36
200	Control	Sacc	nMS	546,34	552,14	637,89	696,96	334,00	2767,31
201	Control	Sacc	nMS	516,53	336,83	348,32	362,22	240,06	1803,96
202	Control	Sacc	nMS	451,19	641,43	443,74	421,65	345,10	2303,12
210	Control	Sacc	nMS	505,72	428,35	488,92	401,56	301,58	2126,12
211	Control	Sacc	nMS	700,36	531,47	409,38	401,58	449,80	2492,58
212	Control	Sacc	nMS	623,86	539,32	492,42	441,80	305,57	2402,96
50	MS	Sacc	MS	512,97	604,32	486,90	287,83	343,07	2235,09
51	MS	Sacc	MS	455,40	463,65	416,60	287,73	352,06	1975,44
150	MS	Sacc	MS	565,92	508,19	567,37	500,27	441,18	2582,93
151	MS	Sacc	MS	501,28	449,14	454,48	335,34	402,56	2142,80
170	MS	Sacc	MS	602,29	505,48	488,36	458,93	424,28	2479,34
171	MS	Sacc	MS	457,25	530,72	437,24	317,15	279,90	2022,27
172	MS	Sacc	MS	512,38	413,20	471,71	341,11	203,96	1942,37
60	EtOH	EtOH	nMS	309,67	224,80	134,52	110,78	238,76	1018,53
61	EtOH	EtOH	nMS	425,21	225,17	283,07	169,64	158,14	1261,22
130	EtOH	EtOH	nMS	511,05	436,32	406,20	332,48	576,14	2262,18
131	EtOH	EtOH	nMS	590,25	474,74	351,49	463,68	392,46	2272,62
190	EtOH	EtOH	nMS	665,02	563,68	297,86	308,81	285,10	2120,48
191	EtOH	EtOH	nMS	581,78	364,65	473,30	315,78	180,19	1915,70
192	EtOH	EtOH	nMS	526,42	302,56	344,77	347,97	416,75	1938,47
40	EtOH+MS	EtOH	MS	493,33	393,56	440,04	263,60	285,91	1876,43
41	EtOH+MS	EtOH	MS	533,59	448,27	471,77	378,13	455,97	2287,72
70	EtOH+MS	EtOH	MS	318,79	226,10	321,73	295,18	250,57	1412,36
71	EtOH+MS	EtOH	MS	316,59	347,98	288,54	282,21	203,64	1438,96
140	EtOH+MS	EtOH	MS	541,92	412,96	381,96	297,54	387,24	2021,61
141	EtOH+MS	EtOH	MS	493,94	560,37	602,29	486,19	324,71	2467,49
160	EtOH+MS	EtOH	MS	539,05	463,27	422,78	311,93	364,58	2101,61
161	EtOH+MS	EtOH	MS	562,51	398,39	466,06	433,92	229,79	2090,68

Table A5.43: Raw data - Object interaction during the novel object test trial

Rat Number	Group	Treatment	Stress	LO Duration (s)	RO Duration (s)	Total Object Duration (s)	RO (%)	Correction Factor	Corrected LO Duration (s)
80	Control	Sacc	nMS	89,60	37,00	126,60	29,23	1,81	161,77
81	Control	Sacc	nMS	59,00	79,00	138,00	57,25	1,74	102,86
180	Control	Sacc	nMS	49,08	72,44	121,52	59,61	1,11	54,48
181	Control	Sacc	nMS	34,28	35,80	70,08	51,08	0,90	30,74
182	Control	Sacc	nMS	90,20	38,36	128,56	29,84	1,34	121,31
200	Control	Sacc	nMS	38,76	65,52	104,28	62,83	1,52	58,99
201	Control	Sacc	nMS	53,76	67,92	121,68	55,82	1,10	59,22
202	Control	Sacc	nMS	24,44	63,96	88,40	72,35	0,81	19,81
210	Control	Sacc	nMS	28,36	85,92	114,28	75,18	1,01	28,77
211	Control	Sacc	nMS	31,84	62,12	93,96	66,11	1,25	39,69
212	Control	Sacc	nMS	61,28	64,88	126,16	51,43	3,46	211,74
50	MS	Sacc	MS	52,92	59,40	112,32	52,88	0,97	51,35
51	MS	Sacc	MS	56,56	35,84	92,40	38,79	0,90	50,93
150	MS	Sacc	MS	40,76	59,84	100,60	59,48	0,98	39,91
151	MS	Sacc	MS	34,20	69,72	103,92	67,09	0,95	32,41
170	MS	Sacc	MS	23,88	70,88	94,76	74,80	1,02	24,36
171	MS	Sacc	MS	62,64	53,16	115,80	45,91	1,05	66,00
172	MS	Sacc	MS	67,08	42,52	109,60	38,80	1,30	87,47
60	EtOH	EtOH	nMS	88,60	79,00	167,60	47,14	1,21	107,12
61	EtOH	EtOH	nMS	46,20	55,20	101,40	54,44	1,43	66,28
130	EtOH	EtOH	nMS	40,36	56,52	96,88	58,34	1,24	50,24
131	EtOH	EtOH	nMS	35,76	42,44	78,20	54,27	0,72	25,81
190	EtOH	EtOH	nMS	39,16	27,12	66,28	40,92	0,86	33,67
191	EtOH	EtOH	nMS	35,96	75,60	111,56	67,77	1,28	46,08
192	EtOH	EtOH	nMS	50,76	87,48	138,24	63,28	0,98	49,51
40	EtOH+MS	EtOH	MS	26,16	76,64	102,80	74,55	1,14	29,83
41	EtOH+MS	EtOH	MS	55,40	36,32	91,72	39,60	1,09	60,44
70	EtOH+MS	EtOH	MS	13,40	43,00	56,40	76,24	1,26	16,82
71	EtOH+MS	EtOH	MS	14,40	48,40	62,80	77,07	1,29	18,62
140	EtOH+MS	EtOH	MS	57,64	35,20	92,84	37,91	0,44	25,43
141	EtOH+MS	EtOH	MS	47,84	68,08	115,92	58,73	0,76	36,58
160	EtOH+MS	EtOH	MS	52,64	47,36	100,00	47,36	0,91	48,14
161	EtOH+MS	EtOH	MS	44,56	63,08	107,64	58,60	0,49	21,68

Table A5.44: Raw data - Object Frequency and latency to the objects during the novel object test trial

Rat Number	Group	Treatment	Stress	LO Frequency	RO Frequency	Correction Factor	Corrected LO Frequency	Latency to LO	Latency to RO	Correction Factor	Corrected Latency to LO
80	Control	Sacc	nMS	12	5	0,79	10	2,40	4,60	2,06	4,94
81	Control	Sacc	nMS	12	10	1,27	15	10,00	12,00	0,47	4,71
180	Control	Sacc	nMS	14	45	2,03	28	2,88	5,44	2,40	6,91
181	Control	Sacc	nMS	19	32	3,67	70	2,96	16,80	1,57	4,66
182	Control	Sacc	nMS	31	41	1,64	51	14,04	11,12	3,02	42,35
200	Control	Sacc	nMS	27	58	1,33	36	8,16	15,76	8,05	65,72
201	Control	Sacc	nMS	20	32	1,21	24	14,80	2,52	0,32	4,76
202	Control	Sacc	nMS	11	50	1,35	15	7,28	3,80	6,02	43,81
210	Control	Sacc	nMS	25	106	3,54	88	13,04	16,64	3,31	43,20
211	Control	Sacc	nMS	25	44	2,66	66	12,04	8,84	2,53	30,49
212	Control	Sacc	nMS	20	64	4,57	91	2,44	4,92	2,73	6,67
50	MS	Sacc	MS	22	32	0,87	19	7,40	3,88	2,17	16,03
51	MS	Sacc	MS	22	37	1,13	25	10,24	6,92	1,98	20,23
150	MS	Sacc	MS	19	28	1,59	30	7,24	1,48	0,25	1,84
151	MS	Sacc	MS	21	28	0,83	18	5,80	3,04	2,46	14,26
170	MS	Sacc	MS	17	36	1,41	24	2,56	4,60	2,96	7,59
171	MS	Sacc	MS	16	31	1,32	21	8,56	14,44	5,10	43,62
172	MS	Sacc	MS	16	19	1,64	26	12,16	1,84	3,46	42,13
60	EtOH	EtOH	nMS	13	14	0,95	12	4,40	9,20	2,33	10,27
61	EtOH	EtOH	nMS	8	14	0,86	7	4,20	5,80	1,70	7,16
130	EtOH	EtOH	nMS	17	33	1,00	17	11,04	13,44	6,19	68,36
131	EtOH	EtOH	nMS	17	28	0,73	12	8,12	10,04	1,58	12,86
190	EtOH	EtOH	nMS	25	27	0,77	19	24,16	4,04	1,79	43,26
191	EtOH	EtOH	nMS	16	27	2,08	33	6,64	7,88	4,28	28,40
192	EtOH	EtOH	nMS	15	40	1,35	20	10,68	8,72	4,32	46,09
40	EtOH+MS	EtOH	MS	8	38	2,44	20	8,80	3,28	0,68	6,02
41	EtOH+MS	EtOH	MS	23	44	1,12	26	6,28	7,72	1,18	7,43
70	EtOH+MS	EtOH	MS	7	13	1,23	9	8,80	17,00	1,32	11,64
71	EtOH+MS	EtOH	MS	7	11	1,00	7	7,80	4,80	2,06	16,06
140	EtOH+MS	EtOH	MS	35	28	0,49	17	4,96	11,00	3,09	15,33
141	EtOH+MS	EtOH	MS	30	38	1,82	55	8,48	10,56	2,68	22,76
160	EtOH+MS	EtOH	MS	28	17	1,16	32	3,20	4,16	1,96	6,27
161	EtOH+MS	EtOH	MS	27	33	1,28	35	4,80	6,92	3,01	14,44

Table A5.45: Shapiro-Wilk test results for the variables analyzed during the novel object test trial.

Test	Variable	Shapiro-Wilk, W	*P* Value
Novel Object Test TEST TRIAL	Total Distance (5 min)	0,944	0,091
	Distance (0-1 min)	0,956	0,198
	Distance (1-2 min)	0,973	0,576
	Distance (2-3 min)	0,967	0,393
	Distance (3-4 min)	0,943	0,082
	Distance (4-5 min)	0,975	0,639
	LO Duration (s)	0,951	0,146
	RO Duration (s)	0,959	0,243
	Corrected LO Duration (s)	0,771	0,001
	Total Object Duration (s)	0,976	0,666
	Corrected Total Object Duration (s)	0,860	0,001
	% Time with RO	0,963	0,314
	Corrected % Time with RO	0,949	0,137
	Latency to LO	0,898	0,005
	Latency to RO	0,925	0,025
	Corrected Latency to LO	0,843	0,025
	LO Frequency	0,978	0,730
	RO Frequency	0,862	0,006
	Corrected LO Frequency	0,809	0,000

Table A5.46: Two-way ANOVA result of the total distance travelled during the 5 minute novel object test trial

	Univariate Tests of Significance for Distance (cm) (Spreadsheet152) Sigma-restricted parameterization Effective hypothesis decomposition				
Effect	SS	Degr. of Freedom	MS	F	p
Intercept	12662752	1	12662752	638,5637	0,000000
Treatment	301092	1	301092	1,5184	0,227765
Stress	24425	1	24425	1,2317	0,276186
Treatment*Stress	1286	1	1286	0,0649	0,800736
Error	575071	29	19830		

Table A5.47: Repeated-measures ANOVA and Duncan's post-hoc results of the distance travelled per minute of the 5 minute novel object test trial

	Repeated Measures Analysis of Variance (Spreadsheet1) Sigma-restricted parameterization Effective hypothesis decomposition				
Effect	SS	Degr. of Freedom	MS	F	p
Intercept	2531410	1	2531410	637,619	0,000000
Treatment	60591	1	60591	1,5262	0,226601
Stress	48971	1	48971	1,2335	0,275853
Treatment*Stress	2571	1	2571	0,0648	0,800919
Error	115132	29	39701		
TIME	62147	4	15537	33,0045	0,000000
TIME*Treatment	2636	4	6591	1,4001	0,238300
TIME*Stress	4569	4	11424	2,4267	0,051815
TIME*Treatment*Stress	2444	4	6111	1,298	0,274930
Error	54607	116	4708		

	Duncan test; variable DV_1 (Spreadsheet1) Approximate Probabilities for Post Hoc Tests Error: Within MS = 4707,5, df = 116,00					
Cell No.	TIME	{1} 496,41	{2} 422,28	{3} 403,92	{4} 347,29	{5} 319,98
1	0-1 min		0,000127	0,000057	0,000046	0,000028
2	1-2 min	0,000127		0,279263	0,000084	0,000046
3	2-3 min	0,000057	0,279263		0,001193	0,000059
4	3-4 min	0,000046	0,000084	0,001193		0,108712
5	4-5 min	0,000028	0,000046	0,000059	0,108712	

Table A5.48: Repeated-measures ANOVA and Duncan's post-hoc results for object duration during the novel object test trial

Effect	SS	Degr. of Freedom	MS	F	p
Repeated Measures Analysis of Variance (Spreadsheet77) Sigma-restricted parameterization Effective hypothesis decomposition					
Intercept	172659,7	1	172659,7	662,7547	0,00000(
Treatment	270,7	1	270,7	1,0390	0,31648(
Stress	636,4	1	636,4	2,4427	0,12891(
Treatment*Stress	87,9	1	87,9	0,3374	0,56580(
Error	7555,0	29	260,5		
OBJECTS	1881,7	1	1881,7	4,5730	0,04103(
OBJECTS*Treatment	60,5	1	60,5	0,1471	0,70411(
OBJECTS*Stress	2,9	1	2,9	0,0070	0,93372(
OBJECTS*Treatment*Stress	12,1	1	12,1	0,0294	0,86507(
Error	11932,(	29	411,5		

Cell No.	OBJECTS	{1} 46,893	{2} 57,749
Duncan test; variable DV_1 (Spreadsheet77) Approximate Probabilities for Post Hoc Tests Error: Within MS = 411,48, df = 29,000			
1	LO Duration (s		0,03814(
2	RO Duration (s	0,03814(	

Table A5.49: Friedman ANOVA repeated-measures result for the corrected object duration during the novel object test trial

Variable	Average Rank	Sum of Ranks	Mean	Std.Dev.
All Groups Friedman ANOVA and Kendall Coeff. of Concordance (Spreadsheet77) ANOVA Chi Sqr. (N = 33, df = 1) = 2,454545 p = ,11719 Coeff. of Concordance = ,07438 Aver. rank r = ,04545				
RO Duration (s)	1,63636(	54,0000(	57,7490(	16,5686(
Corrected LO Duration (s)	1,36363(	45,0000(	56,9108(	42,6826(

Table A5.50: Two-way ANOVA result for total object duration during the novel object test trial

Effect	SS	Degr. of Freedom	MS	F	p
Univariate Tests of Significance for Total Object Duration (s) (Spreadsheet77) Sigma-restricted parameterization Effective hypothesis decomposition					
Intercept	345319,(	1	345319,(	662,754(	0,00000(
Treatment	541,4	1	541,4	1,039(	0,31648(
Stress	1272,8	1	1272,8	2,4427	0,12891(
Treatment*Stress	175,8	1	175,8	0,3374	0,56580(
Error	15110,1	29	521,(		

Table A5.51: Kruskal-Wallis test with Bonferroni corrections for multiple comparisons for the corrected total object duration during the novel object test trial

Depend.: Corrected Total Object Duration (s)	Control R:22,182	MS R:16,286	EtOH R:18,714	EtOH+MS R:9,0000
Multiple Comparisons p values (2-tailed); Corrected Total Object Duration (s) (Spreadsheet77) Independent (grouping) variable: Group Kruskal-Wallis test: H (3, N= 33) =8,893118 p =,0307				
Control		1,00000(	1,00000(	0,02008(
MS	1,00000(		1,00000(	0,87261(
EtOH	1,00000(	1,00000(		0,31345(
EtOH+MS	0,02008(	0,87261(	0,31345(	

Table A5.52: Two-way ANOVA result for the percentage time spent with the right object during novel object test trial

Effect	Univariate Tests of Significance for RO (%) (Spreadsheet77) Sigma-restricted parameterization Effective hypothesis decomposition SS	Degr. of Freedom	MS	F	p
Intercept	99499,34	1	99499,34	503,4291	0,000000
Treatment	39,26	1	39,26	0,1987	0,659115
Stress	8,27	1	8,27	0,0419	0,839310
Treatment*Stress	52,91	1	52,91	0,2677	0,608806
Error	5731,65	29	197,64		

Table A5.53: Two-way ANOVA results for the corrected percentage time spent with the right object during novel object test trial

Effect	Univariate Tests of Significance for Corrected RO% (Spreadsheet77) Sigma-restricted parameterization Effective hypothesis decomposition SS	Degr. of Freedom	MS	F	p
Intercept	95178,83	1	95178,83	392,7852	0,000000
Treatment	359,39	1	359,39	1,4831	0,233103
Stress	379,93	1	379,93	1,5679	0,220516
Treatment*Stress	42,78	1	42,78	0,1765	0,677466
Error	7027,21	29	242,32		

Table A5.54: Friedman ANOVA repeated-measures result for latency to the left object (LO) and right object (RO) during the novel object test trial

Variable	All Groups Friedman ANOVA and Kendall Coeff. of Concordance (Spreadsheet35) ANOVA Chi Sqr. (N = 33, df = 1) = 1,484848 p = ,22302 Coeff. of Concordance = ,04500 Aver. rank r = ,01515 Average Rank	Sum of Ranks	Mean	Std.Dev.
Latency to LO	1,393939	46,0000	8,071515	4,522795
Latency to RO	1,606061	53,0000	7,975758	4,648730

Table A5.55: Friedman ANOVA repeated-measures and Wilcoxon Matched Pairs test results for the corrected latency to the objects during the novel object test trial

Variable	All Groups Friedman ANOVA and Kendall Coeff. of Concordance (Spreadsheet60) ANOVA Chi Sqr. (N = 33, df = 1) = 18,93939 p = ,00001 Coeff. of Concordance = ,57392 Aver. rank r = ,56061 Average Rank	Sum of Ranks	Mean	Std.Dev.
Corrected Latency to LO	1,878788	62,0000	21,82561	18,69302
Latency to RO	1,121212	37,0000	7,97576	4,64873

Pair of Variables	Aggregate Results Wilcoxon Matched Pairs Test (Spreadsheet60) Marked tests are significant at p <,05000 Group	Valid N	T	Z	p-value
Corrected Latency to LO & Latency to RO	Contro	11	11,0000	1,956039	0,050461
Corrected Latency to LO & Latency to RO	MS	7	0,00	2,366432	0,017961
Corrected Latency to LO & Latency to RO	EtOH	7	0,00	2,366432	0,017961
Corrected Latency to LO & Latency to RO	EtOH+MS	8	6,0000	1,680336	0,092893

Table A5.56: Friedman ANOVA repeated-measures and Wilcoxon Matched Pairs results for the left object (LO) and right object (RO) frequency during the novel object test trial

All Groups
Friedman ANOVA and Kendall Coeff. of Concordance (Spreadsheet30)
ANOVA Chi Sqr. (N = 33, df = 1) = 18,93939 p = ,00001
Coeff. of Concordance = ,57392 Aver. rank r = ,56061

Variable	Average Rank	Sum of Ranks	Mean	Std.Dev.
LO Frequency	1,121212	37,00000	18,93939	7,25835
RO Frequency	1,878788	62,00000	33,42424	18,80995

Aggregate Results
Wilcoxon Matched Pairs Test (Spreadsheet1)
Marked tests are significant at p <,05000

Pair of Variables	Group	Valid N	T	Z	p-value
LO Frequency & RO Frequency	Contro	11	3,000000	2,667325	0,007646
LO Frequency & RO Frequency	MS	7	0,00	2,366432	0,017961
LO Frequency & RO Frequency	EtOH	7	0,00	2,366432	0,017961
LO Frequency & RO Frequency	EtOH+MS	8	10,00000	1,120224	0,262619

Table A5.57: Friedman ANOVA repeated-measures result for the corrected left object (LO) and right object (RO) frequency during the novel object test trial

All Groups
Friedman ANOVA and Kendall Coeff. of Concordance (Spreadsheet1)
ANOVA Chi Sqr. (N = 33, df = 1) = 2,454545 p = ,11719
Coeff. of Concordance = ,07438 Aver. rank r = ,04545

Variable	Average Rank	Sum of Ranks	Mean	Std.Dev.
Corrected LO Frequency	1,363636	45,00000	29,65276	21,87960
RO Frequency	1,636364	54,00000	33,42424	18,80995

ULTRASONIC VOCALIZATIONS

Table A5.58: Raw data - Ultrasonic vocalizations

Rat #	Group	Treatment	Stress	Number of Calls	Av. Call Duration	Latency to First Call
80	Control	Sacc	nMS	197	501,75	687
81	Control	Sacc	nMS	97	465,22	5567
180	Control	Sacc	nMS	15	383,27	15862
181	Control	Sacc	nMS	252	590,09	669
182	Control	Sacc	nMS	11	441,36	6151
200	Control	Sacc	nMS	100	454,05	5238
201	Control	Sacc	nMS	195	526,42	550
202	Control	Sacc	nMS	83	432,35	2043
210	Control	Sacc	nMS	91	492,21	7023
211	Control	Sacc	nMS	108	483,26	3347
212	Control	Sacc	nMS	35	453,97	2780
50	MS	Sacc	MS	284	686,63	727
51	MS	Sacc	MS	185	551,19	2963
150	MS	Sacc	MS	332	920	115
151	MS	Sacc	MS	255	744,37	0
170	MS	Sacc	MS	205	563,38	0
171	MS	Sacc	MS	200	561,71	0
172	MS	Sacc	MS	232	612,49	3050
60	EtOH	EtOH	nMS	152	593,4	956
61	EtOH	EtOH	nMS	111	648,34	3636
130	EtOH	EtOH	nMS	370	849,75	683
131	EtOH	EtOH	nMS	251	702,62	848
190	EtOH	EtOH	nMS	236	584,39	1043
191	EtOH	EtOH	nMS	220	604,54	0
192	EtOH	EtOH	nMS	52	442,61	2390
40	EtOH+MS	EtOH	MS	234	610,29	1504
41	EtOH+MS	EtOH	MS	173	642,63	3564
70	EtOH+MS	EtOH	MS	331	834,21	203
71	EtOH+MS	EtOH	MS	245	704,077	423
140	EtOH+MS	EtOH	MS	289	667,55	1201
141	EtOH+MS	EtOH	MS	186	591,17	1313
160	EtOH+MS	EtOH	MS	310	909,43	0
161	EtOH+MS	EtOH	MS	262	629,19	2303

Table A5.59: Shapiro-Wilk test results for variables analyzed during the recording of 22 kHz ultrasonic vocalizations.

Variable	Shapiro-Wilk, W	*P* Value
Number of calls	0,967	0,412
Average call duration (ms)	0,942	0,078
Latency to first call (ms)	0,695	0,000

Table A5.60: Two-way ANOVA and Duncan's post-hoc test for the number of 22 kHz ultrasonic vocalizations

Univariate Tests of Significance for Number of Calls (Spreadsheet9)
Sigma-restricted parameterization
Effective hypothesis decomposition

Effect	SS	Degr. of Freedom	MS	F	p
Intercept	128256	1	128256	226,021	0,00000
Stress	71296	1	71296	12,5643	0,00135
Treatment	21196	1	21196	3,7353	0,06309
Stress*Treatment	12545	1	12545	2,2108	0,14784
Error	164562	29	5675		

Duncan test; variable Number of Calls (Spreadsheet1)
Approximate Probabilities for Post Hoc Tests
Error: Between MS = 5674,5, df = 29,000

Cell No.	Stress	{1} 143,11	{2} 248,20
1	nMS		0,00053
2	MS	0,00053	

Duncan test; variable Number of Calls (Spreadsheet1)
Approximate Probabilities for Post Hoc Tests
Error: Between MS = 5674,5, df = 29,000

Cell No.	Treatment	Stress	{1} 107,64	{2} 241,86	{3} 198,86	{4} 253,75
1	Sacc	nMS		0,00186	0,02224	0,00103
2	Sacc	MS	0,00186		0,26382	0,75496
3	EtOH	nMS	0,02224	0,26382		0,17965
4	EtOH	MS	0,00103	0,75496	0,17965	

Table A5.61: Two-way ANOVA and Duncan's post-hoc test for the average duration of 22 kHz ultrasonic vocalizations

Univariate Tests of Significance for Av. Call Duration (Spreadsheet9)
Sigma-restricted parameterization
Effective hypothesis decomposition

Effect	SS	Degr. of Freedom	MS	F	p
Intercept	1214786	1	1214786	1094,23	0,00000
Treatment	74315	1	74315	6,694	0,01495
Stress	128870	1	128870	11,608	0,00194
Treatment*Stress	29471	1	29471	2,655	0,11406
Error	321948	29	11102		

Duncan test; variable Av. Call Duration (Spreadsheet1)
Approximate Probabilities for Post Hoc Tests
Error: Between MS = 11102,, df = 29,000

Cell No.	Treatment	{1} 547,98	{2} 667,61
1	Sacc		0,00307
2	EtOH	0,00307	

Duncan test; variable Av. Call Duration (Spreadsheet1)
Approximate Probabilities for Post Hoc Tests
Error: Between MS = 11102,, df = 29,000

Cell No.	Stress	{1} 536,09	{2} 681,89
1	nMS		0,00057
2	MS	0,00057	

Duncan test; variable Av. Call Duration (Spreadsheet1)
Approximate Probabilities for Post Hoc Tests
Error: Between MS = 11102,, df = 29,000

Cell No.	Treatment	Stress	{1} 474,90	{2} 662,82	{3} 632,24	{4} 698,57
1	Sacc	nMS		0,00185	0,00591	0,00041
2	Sacc	MS	0,00185		0,56673	0,50366
3	EtOH	nMS	0,00591	0,56673		0,24524
4	EtOH	MS	0,00041	0,50366	0,24524	

Table A5.62: Kruskal-Wallis test of the latency to the first 22 kHz ultrasonic vocalization

Multiple Comparisons p values (2-tailed); Latency (ms) (Spreadsheet1)
Independent (grouping) variable: Group
Kruskal-Wallis test: H (3, N= 33) =7,711864 p =,0524

Depend.: Latency (ms)	Control R:23,182	MS R:11,000	EtOH R:15,571	EtOH+MS R:15,000
Control		0,05502	0,62136	0,41164
MS	0,05502		1,00000	1,00000
EtOH	0,62136	1,00000		1,00000
EtOH+MS	0,41164	1,00000	1,00000	

Table A5.63: Raw data - Distance and number of entries in the Elevated Plus Maze -

				Distance (cm)						Number Entries					
Rat Number	Group	Treatment	Stress	0-1 min	1-2 min	2-3 min	3-4 min	4-5 min	Total Distance (cm)	0-1 min	1-2 min	2-3 min	3-4 min	4-5 min	Total Entries
80	Control	Sacc	nMS	394,28	342,23	399,82	325,25	349,52	1811,25	17	14	13	5	15	60
81	Control	Sacc	nMS	404,23	273,30	440,16	245,97	376,34	1743,15	18	9	16	6	16	62
180	Control	Sacc	nMS	326,20	338,37	313,83	340,20	329,76	1648,43	11	9	11	10	17	54
181	Control	Sacc	nMS	329,11	282,76	318,32	300,03	270,98	1501,95	10	14	8	13	12	53
182	Control	Sacc	nMS	318,11	347,47	334,25	326,25	361,74	1688,24	8	15	8	11	9	47
200	Control	Sacc	nMS	368,26	350,43	357,36	310,93	374,64	1761,88	10	16	11	11	9	54
201	Control	Sacc	nMS	447,23	343,87	220,80	197,98	135,65	1345,53	24	14	8	18	4	64
202	Control	Sacc	nMS	447,23	343,87	220,80	197,98	135,65	1751,73	8	8	2	18	4	70
210	Control	Sacc	nMS	439,40	380,33	383,10	297,62	250,05	965,78	14	14	18	18	10	44
211	Control	Sacc	nMS	242,69	235,62	195,20	136,30	155,14	1556,22	9	16	14	8	1	42
212	Control	Sacc	nMS	468,96	327,85	272,73	213,67	272,96	531,21	17	7	5	12	5	16
50	MS	Sacc	MS	270,75	237,83	308,22	211,41	155,70	1184,12	11	5	15	6	8	41
51	MS	Sacc	MS	457,21	319,21	202,61	183,28	199,62	1363,20	10	21	6	11	16	60
150	MS	Sacc	MS	285,60	271,61	337,39	287,84	333,91	1517,97	15	9	6	11	8	46
151	MS	Sacc	MS	445,85	506,89	358,44	346,13	236,41	1894,07	12	17	17	16	8	66
170	MS	Sacc	MS	379,07	284,64	295,09	285,17	340,37	1584,74	12	20	11	5	18	63
171	MS	Sacc	MS	452,75	469,89	409,01	316,93	361,13	2009,85	10	11	10	8	13	48
172	MS	Sacc	MS	396,86	549,36	433,62	341,36	431,05	2155,30	14	15	13	14	11	63
60	EtOH	EtOH	nMS	459,33	318,03	218,73	237,80	173,70	1407,87	7	14	4	7	8	36
61	EtOH	EtOH	nMS	373,84	369,15	327,61	364,75	294,18	1729,97	9	14	14	14	9	56
130	EtOH	EtOH	nMS	266,72	395,77	409,47	320,26	330,81	1723,37	8	9	10	17	13	53
131	EtOH	EtOH	nMS	398,83	416,08	322,41	412,15	382,35	1934,29	13	13	11	13	10	56
190	EtOH	EtOH	nMS	329,91	254,47	334,36	284,36	325,76	1528,87	12	9	7	5	12	41
191	EtOH	EtOH	nMS	332,91	319,93	347,48	324,55	412,30	1737,39	17	11	11	9	9	53
192	EtOH	EtOH	nMS	429,76	427,69	379,98	499,94	444,45	2183,71	9	12	13	12	11	53
40	EtOH+MS	EtOH	MS	271,32	291,82	316,12	109,23	218,26	1207,40	10	8	12	5	7	38
41	EtOH+MS	EtOH	MS	373,37	277,23	267,36	274,71	283,10	1475,84	15	13	3	6	9	42
70	EtOH+MS	EtOH	MS	385,35	364,40	432,57	261,41	411,71	1856,26	14	10	13	13	16	62
71	EtOH+MS	EtOH	MS	437,02	434,76	442,89	513,35	417,83	2246,14	9	13	14	23	15	70
140	EtOH+MS	EtOH	MS	349,63	341,73	323,49	249,37	241,62	1505,90	10	12	9	12	18	58
141	EtOH+MS	EtOH	MS	412,38	404,70	374,37	272,95	357,38	1821,87	18	10	12	11	9	58
160	EtOH+MS	EtOH	MS	270,49	344,82	446,96	279,26	258,23	1602,48	12	15	16	9	14	62
161	EtOH+MS	EtOH	MS	371,54	333,75	361,88	402,94	314,41	1784,61	20	10	8	15	7	56

Table A5.64: Raw data - Variables used to determine anxiety levels in the Elevated Plus Maze

				Open Arm Duration						Closed Arm Duration						Centre Zone Duration						Latency		Number of Entries into the Open Arms					
Rat Number	Group	Treatment	Stress	0-1 min	1-2 min	2-3 min	3-4 min	4-5 min	Total Open Arm Duration (s)	0-1 min	1-2 min	2-3 min	3-4 min	4-5 min	Total Closed Arm Duration (s)	0-1 min	1-2 min	2-3 min	3-4 min	4-5 min	Total Centre Zone Duration (s)	To Open Arms	To Closed Arms	0-1 min	1-2 min	2-3 min	3-4 min	4-5 min	Total Entries into Open Arms
80,00	Control	Sacc	nMS	10,0	15,6	1,4	0,0	6,0	33,2	40,2	27,6	44,8	44,4	40,8	197,8	9,6	15,0	8,0	15,6	11,2	59,4	0,0	0,0	7	2	1	0	2	11
81,00	Control	Sacc	nMS	9,0	15,8	0,8	14,4	9,8	49,8	36,6	36,8	50,4	42,2	45,6	211,8	13,6	7,8	7,2	3,2	3,4	35,2	0,2	0,2	6	3	2	2	5	18
180,00	Control	Sacc	nMS	12,6	5,6	16,6	0,0	6,0	40,8	35,8	44,8	21,4	44,6	38,8	185,6	10,8	9,2	22,0	14,6	13,0	69,6	15,4	9,0	2	1	4	0	3	9
181,00	Control	Sacc	nMS	12,6	6,8	0,0	3,4	0,0	22,8	38,6	29,0	46,6	38,6	48,4	201,4	8,6	24,2	12,8	18,0	10,0	73,6	12,4	7,0	2	3	0	2	0	7
182,00	Control	Sacc	nMS	40,2	16,8	4,6	19,2	2,4	83,2	12,0	23,0	41,4	25,0	44,4	145,8	7,2	19,0	13,8	13,2	12,6	66,0	0,2	0,2	2	4	3	2	1	10
200,00	Control	Sacc	nMS	41,8	7,0	25,2	4,2	28,2	106,4	13,6	36,4	26,0	47,4	18,6	142,0	4,6	14,6	7,4	6,8	13,0	46,6	0,0	0,0	4	3	3	1	2	11
201,00	Control	Sacc	nMS	15,2	13,4	0,0	4,4	0,0	33,0	24,4	34,2	52,6	42,8	59,2	213,4	18,4	10,8	4,6	10,6	0,4	44,8	3,6	3,6	9	2	0	4	0	15
202,00	Control	Sacc	nMS	15,2	13,4	0,0	4,4	0,0	69,0	24,4	34,2	52,6	42,8	59,2	147,4	18,4	10,8	4,6	10,6	0,4	75,4	25,4	19,0	9	2	0	4	0	19
210,00	Control	Sacc	nMS	15,2	26,6	8,2	0,8	18,2	2,2	36,8	21,2	33,0	38,0	18,4	254,2	7,8	11,2	15,0	17,6	23,6	31,2	22,0	1,0	4	6	5	3	3	1
211,00	Control	Sacc	nMS	2,2	0,0	0,0	0,0	0,0	19,8	49,2	37,6	50,4	56,8	60,0	191,2	8,0	16,8	3,8	2,6	0,0	83,8	9,2	3,0	1	0	0	0	0	3
212,00	Control	Sacc	nMS	8,2	11,6	0,0	0,0	0,0	10,4	36,6	35,6	44,0	35,6	39,4	101,0	13,0	12,8	16,0	21,6	20,2	16,0	32,6	2,0	2	1	0	0	0	2
50,00	MS	Sacc	MS	43,0	23,2	2,2	0,0	15,0	83,6	8,0	17,2	37,8	21,4	21,2	105,6	9,2	19,4	18,2	37,6	23,0	107,4	11,2	10,0	4	1	4	0	1	10
51,00	MS	Sacc	MS	36,2	11,2	34,4	6,6	1,8	90,4	19,4	21,2	23,4	37,2	31,4	132,6	4,0	26,2	1,8	15,0	23,2	70,2	11,8	11,8	3	8	2	3	1	15
150,00	MS	Sacc	MS	10,0	5,0	9,4	3,6	0,0	28,0	31,6	45,2	46,6	42,0	55,2	220,8	19,0	10,0	3,6	15,2	4,2	52,0	14,4	9,0	4	2	1	3	0	9
151,00	MS	Sacc	MS	22,2	15,8	3,4	1,6	0,6	43,6	30,2	32,2	38,2	47,4	54,4	202,6	7,6	10,4	17,4	10,0	3,0	48,4	26,8	11,0	3	4	3	1	1	11
170,00	MS	Sacc	MS	12,0	3,4	0,0	0,0	5,0	20,4	32,4	36,4	52,0	56,8	37,6	215,4	11,8	13,8	6,4	2,8	15,0	49,8	10,0	6,0	2	3	0	0	1	6
171,00	MS	Sacc	MS	11,8	44,4	16,8	2,0	15,6	90,8	40,2	2,0	32,0	43,2	22,8	140,2	7,8	13,8	11,2	14,6	21,2	68,6	1,6	1,6	1	4	2	1	4	12
172,00	MS	Sacc	MS	12,8	24,6	16,4	22,4	18,2	94,6	36,0	24,4	23,8	25,0	22,0	131,2	11,0	11,4	19,2	11,2	19,8	72,6	42,4	15,0	4	4	3	3	2	15
60,00	EtOH	EtOH	nMS	36,4	24,6	0,0	7,0	3,4	71,4	20,4	24,4	52,2	30,8	36,6	164,4	3,2	9,6	7,8	21,4	18,4	60,6	0,0	0,0	2	4	0	1	1	8
61,00	EtOH	EtOH	nMS	23,2	15,6	0,8	5,4	30,0	75,0	27,6	25,6	43,4	43,0	19,0	158,6	9,0	18,2	12,6	11,0	10,0	61,0	0,0	0,0	2	4	1	3	2	12
130,00	EtOH	EtOH	nMS	6,6	22,2	10,6	8,0	0,0	47,4	42,4	26,0	36,2	30,4	53,2	188,4	10,4	11,8	12,8	21,2	5,0	61,2	47,4	10,0	2	2	1	5	0	10
131,00	EtOH	EtOH	nMS	21,4	26,2	25,0	17,6	24,0	114,4	31,4	21,2	30,0	31,6	28,4	142,6	5,6	12,0	5,8	10,8	7,2	41,4	8,4	8,4	3	5	5	3	3	17
190,00	EtOH	EtOH	nMS	0,2	5,2	0,0	0,0	0,0	5,4	43,0	42,4	56,0	57,4	50,6	249,6	15,6	11,6	3,6	2,6	8,6	42,0	59,8	2,0	1	2	0	0	0	2
191,00	EtOH	EtOH	nMS	2,8	2,4	11,4	1,4	10,2	28,2	48,4	45,8	39,4	44,2	46,4	224,4	7,8	11,2	8,8	14,0	3,4	45,2	27,0	7,0	2	1	2	1	1	7
192,00	EtOH	EtOH	nMS	12,6	40,2	3,0	30,6	10,6	97,0	44,2	16,2	40,6	23,2	44,0	168,4	3,4	3,2	15,4	5,8	5,6	33,4	0,0	0,0	2	5	1	3	2	12
40,00	EtOH+MS	EtOH	MS	9,8	1,0	4,0	0,0	1,4	16,2	41,8	40,4	38,8	44,6	54,6	220,4	6,0	18,2	17,0	14,2	1,2	56,6	18,8	6,0	2	2	2	0	1	6
41,00	EtOH+MS	EtOH	MS	6,6	5,4	0,0	0,0	7,6	19,6	38,0	32,4	56,0	53,4	42,0	222,0	12,4	22,2	1,8	5,8	8,8	51,0	28,0	7,0	3	3	0	0	1	7
70,00	EtOH+MS	EtOH	MS	29,2	5,4	27,0	15,4	13,6	90,6	20,4	40,8	27,8	24,8	28,0	142,0	9,8	13,8	5,0	19,6	17,0	65,2	11,4	11,4	4	2	5	5	2	17
71,00	EtOH+MS	EtOH	MS	35,4	23,0	23,0	23,2	20,6	125,2	19,8	22,0	27,4	11,2	18,0	98,4	2,8	14,8	9,0	25,0	22,0	73,8	11,2	11,2	3	4	3	9	6	24
140,00	EtOH+MS	EtOH	MS	3,4	0,4	0,6	0,2	10,6	15,2	40,2	41,2	43,8	51,0	27,8	204,0	16,8	17,6	15,0	8,0	20,0	77,6	29,4	10,0	2	1	2	1	4	10
141,00	EtOH+MS	EtOH	MS	25,8	14,4	9,8	0,0	25,6	75,8	20,6	26,0	34,6	45,2	26,6	153,0	11,8	18,0	13,4	10,8	8,0	62,0	0,4	0,4	5	1	2	0	3	11
160,00	EtOH+MS	EtOH	MS	13,6	0,8	22,4	0,2	17,2	54,2	27,6	46,8	27,6	51,4	23,6	177,2	15,2	10,6	8,6	8,2	15,6	58,2	37,6	11,0	2	2	3	1	3	11
161,00	EtOH+MS	EtOH	MS	22,8	1,8	29,0	12,0	23,8	89,6	25,2	42,6	24,0	34,6	21,2	147,6	11,4	13,8	7,0	12,4	14,2	58,8	0,4	0,4	5	1	2	4	2	12

Table A5.65: Shapiro-Wilk test results for the variables measured in the elevated plus maze

	Variable	Shapiro-Wilk, W	*P* Value
Elevated Plus Maze	Total Distance	0,943	0,875
	Distance (0-1 min)	0,937	0,056
	Distance (1-2 min)	0,945	0,096
	Distance (2-3 min)	0,951	0,142
	Distance (3-4 min)	0,964	0,344
	Distance (4-5 min)	0,954	0,173
	Total Entries	0,928	0,031
	No. Entries (0-1 min)	0,919	0,018
	No. Entries (1-2min)	0,971	0,507
	No. Entries (2-3 min)	0,978	0,726
	No. Entries (3-4 min)	0,952	0,154
	No. Entries (4-5 min)	0,967	0,406
	Open Arm Duration (s)	0,939	0,065
	Open Arm Duration (0-1 min)	0,906	0,007
	Open Arm Duration (1-2 min)	0,909	0,009
	Open Arm Duration (2-3 min)	0,827	0,000
	Open Arm Duration (3-4 min)	0,775	0,000
	Open Arm Duration (4-5 min)	0,885	0,002
	Closed Arm Duration (s)	0,963	0,318
	Closed Arm Duration (0-1 min)	0,964	0,340
	Closed Arm Duration (1-2 min)	0,952	0,162
	Closed Arm Duration (2-3 min)	0,950	0,129
	Closed Arm Duration (3-4 min)	0,959	0,237
	Closed Arm Duration (4-5 min)	0,925	0,026
	Centre Zone Duration (s)	0,980	0,793
	Centre Zone Duration (s) (0-1 min)	0,963	0,318
	Centre Zone Duration (s) (1-2 min)	0,956	0,201
	Centre Zone Duration (s) (2-3 min)	0,956	0,204
	Centre Zone Duration (s) (3-4 min)	0,926	0,027
	Centre Zone Duration (s) (4-5 min)	0,942	0,077
	Latency to Open Arms	0,882	0,002
	Latency to Closed Arms	0,909	0,005
	No. Entries into Open Arms	0,970	0,486
	No. Entries into Open Arms (0-1 min)	0,817	0,000
	No. Entries into Open Arms (1-2 min)	0,916	0,014
	No. Entries into Open Arms (2-3 min)	0,897	0,004
	No. Entries into Open Arms (3-4min)	0,844	0,002
	No. Entries into Open Arms (4-5 min)	0,892	0,003

Table A5.66: Two-way ANOVA result for the distance travelled during the Elevated Plus Maze

	Univariate Tests of Significance for Distance (cm) (Spreadsheet253) Sigma-restricted parameterization Effective hypothesis decomposition				
Effect	SS	Degr. of Freedom	MS	F	p
Intercept	8662697	1	8662697	732,941	0,00000
Treatment	158377	1	158377	1,340	0,25647
Stress	32995	1	32995	0,2792	0,60127
Treatment*Stress	126835	1	126835	1,0731	0,30879
Error	3427536	29	118191		

Table A5.67: Repeated-measures two-way ANOVA and Duncan's post-hoc test results for the distance travelled per minute during the Elevated Plus Maze

	Repeated Measures Analysis of Variance (Spreadsheet326) Sigma-restricted parameterization Effective hypothesis decomposition				
Effect	SS	Degr. of Freedom	MS	F	p
Intercept	1770055	1	1770055	1036,152	0,00000
Treatment	1726	1	1726	1,01	0,32313
Stress	1182	1	1182	0,069	0,79434
Treatment*Stress	1257	1	1257	0,736	0,39787
Error	49540	29	1708		
TIME	13087	4	3272	9,44	0,00000
TIME*Treatment	2499	4	625	1,803	0,13290
TIME*Stress	1190	4	297	0,858	0,49129
TIME*Treatment*Stress	1029	4	257	0,743	0,56484
Error	40206	116	346		

	Duncan test; variable DV_1 (Spreadsheet1) Approximate Probabilities for Post Hoc Tests Error: Within MS = 3466,0, df = 116,00					
Cell No.	MINUTE	{1} 373,82	{2} 348,48	{3} 336,56	{4} 293,07	{5} 301,11
1	0-1 min		0,08311	0,01537	0,00002	0,00004
2	1-2 min	0,08311		0,41255	0,00043	0,00206
3	2-3 min	0,01537	0,41255		0,00465	0,01605
4	3-4 min	0,00002	0,00043	0,00465		0,58023
5	4-5 min	0,00004	0,00206	0,01605	0,58023	

Table A5.68: Kruskal-Wallis test result for the number of entries made during the Elevated Plus Maze

	Multiple Comparisons p values (2-tailed); TOTAL ENTRIES (Spreadsheet36) Independent (grouping) variable: Group Kruskal-Wallis test: H (3, N= 33) =2,762845 p =,4297			
Depend.: TOTAL ENTRIES	Control R:16,727	MS R:19,429	EtOH R:12,143	EtOH+MS R:19,500
Control		1,00000	1,00000	1,00000
MS	1,00000		0,95192	1,00000
EtOH	1,00000	0,95192		0,84918
EtOH+MS	1,00000	1,00000	0,84918	

Table A5.69: Repeated-measures two-way ANOVA result for the number of entries made per minute during the Elevated Plus Maze

	Repeated Measures Analysis of Variance (Spreadsheet1) Sigma-restricted parameterization Effective hypothesis decomposition				
Effect	SS	Degr. of Freedom	MS	F	p
Intercept	20941,4	1	20941,4	1078,22	0,00000
Treatment	3,59	1	3,59	0,185	0,67032
Stress	22,85	1	22,85	1,176	0,28704
Treatment*Stress	5,61	1	5,61	0,289	0,59500
Error	563,24	29	19,42		
MINUTE	93,37	4	23,34	1,348	0,25634
MINUTE*Treatment	24,80	4	6,20	0,358	0,83798
MINUTE*Stress	24,62	4	6,16	0,356	0,83972
MINUTE*Treatment*Stress	48,20	4	12,05	0,696	0,59625
Error	2008,4	116	17,31		

Table A5.70: Two-way ANOVA result for the time spent in the open arms of the Elevated Plus Maze

	Univariate Tests of Significance for Open Arm Duration (s) (Spreadsheet10) Sigma-restricted parameterization Effective hypothesis decomposition				
Effect	SS	Degr. of Freedom	MS	F	p
Intercept	106149,5	1	106149,5	82,6123	0,00000
Treatment	524,4	1	524,4	0,4080	0,52795
Stress	783,0	1	783,0	0,6093	0,44135
Treatment*Stress	1109,3	1	1109,3	0,8633	0,36047
Error	37262,4	29	1284,9		

Table A5.71: Friedman ANOVA and Wilcoxon Matched Pairs test results for the time spent in the open arms per minute of the Elevated Plus Maze

All Groups
Wilcoxon Matched Pairs Test (Spreadsheet9)
Marked tests are significant at p <,05000

Pair of Variables	Valid N	T	Z	p-value
0-1 min & 0-1 min				
0-1 min & 1-2 min	33	179,500(	1,804651	0,071130
0-1 min & 2-3 min	33	96,000(	3,296614	0,000979
0-1 min & 3-4 min	33	48,000(	4,154270	0,000033
0-1 min & 4-5 min	33	116,000(	2,939258	0,003290
1-2 min & 0-1 min	33	179,500(	1,804651	0,071130
1-2 min & 1-2 min				
1-2 min & 2-3 min	31	161,000(	1,704899	0,088214
1-2 min & 3-4 min	32	53,500(	3,936127	0,000083
1-2 min & 4-5 min	32	179,000(	1,589410	0,111969
2-3 min & 0-1 min	33	96,000(	3,296614	0,000979
2-3 min & 1-2 min	31	161,000(	1,704899	0,088214
2-3 min & 2-3 min				
2-3 min & 3-4 min	28	133,000(	1,594000	0,110937
2-3 min & 4-5 min	27	171,000(	0,432450	0,665415
3-4 min & 0-1 min	33	48,000(	4,154270	0,000033
3-4 min & 1-2 min	32	53,500(	3,936127	0,000083
3-4 min & 2-3 min	28	133,000(	1,594000	0,110937
3-4 min & 3-4 min				
3-4 min & 4-5 min	30	145,000(	1,799730	0,071904
4-5 min & 0-1 min	33	116,000(	2,939258	0,003290
4-5 min & 1-2 min	32	179,000(	1,589410	0,111969
4-5 min & 2-3 min	27	171,000(	0,432450	0,665415
4-5 min & 3-4 min	30	145,000(	1,799730	0,071904
4-5 min & 4-5 min				

All Groups
Friedman ANOVA and Kendall Coeff. of Concordance (Spreadsheet46)
ANOVA Chi Sqr. (N = 33, df = 4) = 29,62893 p = ,00001
Coeff. of Concordance = ,22446 Aver. rank r = ,20023

Variable	Average Rank	Sum of Ranks	Mean	Std.Dev.
0-1 min	4,000000	132,000(	17,57576	12,23619
1-2 min	3,454545	114,000(	13,60000	11,18336
2-3 min	2,712121	89,500(	9,27273	10,59715
3-4 min	2,106061	69,500(	6,30303	8,30679
4-5 min	2,727273	90,000(	9,86061	9,55713

Table A5.72: Two-way ANOVA result for the time spent in the closed arms of the Elevated Plus Maze

Univariate Tests of Significance for Closed Arm Duration (s) (Spreadsheet10)
Sigma-restricted parameterization
Effective hypothesis decomposition

Effect	SS	Degr. of Freedom	MS	F	p
Intercept	979304,7	1	979304,7	526,4273	0,000000
Treatment	226,7	1	226,7	0,1219	0,729558
Stress	1993,5	1	1993,5	1,0716	0,309140
Treatment*Stress	11,2	1	11,2	0,0060	0,938630
Error	53948,3	29	1860,3		

Table A5.73: Repeated-measures two-way ANOVA and Duncan's post-hoc test results for the time spent per minute in the closed arms during the Elevated Plus Maze

Repeated Measures Analysis of Variance (Spreadsheet90)
Sigma-restricted parameterization
Effective hypothesis decomposition

Effect	SS	Degr. of Freedom	MS	F	p
Intercept	201381,6	1	201381,6	617,8875	0,000000
Treatment	0,1	1	0,1	0,0002	0,988224
Stress	696,7	1	696,7	2,1377	0,154466
Treatment*Stress	63,1	1	63,1	0,1936	0,663162
Error	9451,7	29	325,9		
MINUTE	2120,5	4	530,1	6,6518	0,000074
MINUTE*Treatment	330,0	4	82,5	1,0353	0,392152
MINUTE*Stress	516,0	4	129,0	1,6186	0,174220
MINUTE*Treatment*Stress	477,6	4	119,4	1,4980	0,207325
Error	9244,8	116	79,7		

Duncan test; variable DV_1 (Spreadsheet90)
Approximate Probabilities for Post Hoc Tests
Error: Within MS = 79,697, df = 116,00

Cell No.	MINUTE	{1} 31,424	{2} 31,297	{3} 39,236	{4} 39,636	{5} 37,497
1	0-1 min		0,954007	0,000840	0,000578	0,006771
2	1-2 min	0,954007		0,000867	0,000571	0,007805
3	2-3 min	0,000840	0,000867		0,855996	0,430437
4	3-4 min	0,000578	0,000571	0,855996		0,363725
5	4-5 min	0,006771	0,007805	0,430437	0,363725	

Table A5.74: Two-way ANOVA and Duncan's post-hoc results for the time spent in the centre zone of the Elevated Plus Maze

Univariate Tests of Significance for Centre Zone Duration (s) (Spreadsheet10)
Sigma-restricted parameterization
Effective hypothesis decomposition

Effect	SS	Degr. of Freedom	MS	F	p
Intercept	109015,9	1	109015,9	372,2025	0,000000
Treatment	181,2	1	181,2	0,6186	0,437932
Stress	1342,6	1	1342,6	4,5841	0,040805
Treatment*Stress	3,5	1	3,5	0,0121	0,913139
Error	8493,9	29	292,9		

Duncan test; variable Centre Zone Duration (s) (Spreadsheet10)
Approximate Probabilities for Post Hoc Tests
Error: Between MS = 292,89, df = 29,000

Cell No.	Stress	{1} 64,813	{2} 52,578
1	MS		0,050140
2	nMS	0,050140	

Table A5.75: Repeated-measures Two-way ANOVA and Duncan's post-hoc test results for the time spent per minute in the centre zone of the Elevated Plus Maze

Repeated Measures Analysis of Variance (Spreadsheet24)
Sigma-restricted parameterization
Effective hypothesis decomposition

Effect	SS	Degr. of Freedom	MS	F	p
Intercept	22260,22	1	22260,22	462,2216	0,000000
Treatment	59,21	1	59,21	1,2295	0,276620
Stress	218,57	1	218,57	4,5385	0,041749
Treatment*Stress	6,02	1	6,02	0,1250	0,726186
Error	1396,62	29	48,16		
MINUTE	417,60	4	104,40	2,9895	0,021680
MINUTE*Treatment	5,20	4	1,30	0,0372	0,997326
MINUTE*Stress	128,49	4	32,12	0,9199	0,454953
MINUTE*Treatment*Stress	65,50	4	16,37	0,4689	0,758466
Error	4050,92	116	34,92		

Duncan test; variable DV_1 (Spreadsheet24)
Approximate Probabilities for Post Hoc Tests
Error: Within MS = 34,922, df = 116,00

Cell No.	MINUTE	{1} 10,048	{2} 14,055	{3} 10,200	{4} 13,079	{5} 11,582
1	0-1 min		0,013369	0,917326	0,058285	0,325177
2	1-2 min	0,013369		0,015197	0,503866	0,111035
3	2-3 min	0,917326	0,015197		0,063049	0,344282
4	3-4 min	0,058285	0,503866	0,063049		0,305717
5	4-5 min	0,325177	0,111035	0,344282	0,305717	

Table A5.76: Kruskal-Wallis test result for the latency to enter the open arms during the Elevated Plus Maze

Multiple Comparisons p values (2-tailed); Latency to Open Arms (s) (Spreadsheet285)
Independent (grouping) variable: Group
Kruskal-Wallis test: H (3, N= 33) =1,726848 p =,6310

Depend.: Latency to Open Arms (s)	Control R:14,455	MS R:19,071	EtOH R:16,000	EtOH+MS R:19,563
Control		1,000000	1,000000	1,000000
MS	1,000000		1,000000	1,000000
EtOH	1,000000	1,000000		1,000000
EtOH+MS	1,000000	1,000000	1,000000	

Table A5.77: Kruskal-Wallis test result for the latency to enter the closed arms during the Elevated Plus Maze

Multiple Comparisons p values (2-tailed); Latency to Closed Arms (s) (Spreadsheet1)
Independent (grouping) variable: Group
Kruskal-Wallis test: H (3, N= 33) =7,724632 p =,0521

Depend.: Latency to Closed Arms (s)	Control R:13,182	MS R:23,643	EtOH R:12,357	EtOH+MS R:20,500
Control		0,151492	1,000000	0,620160
MS	0,151492		0,173985	1,000000
EtOH	1,000000	0,173985		0,622271
EtOH+MS	0,620160	1,000000	0,622271	

Table A5.78: Two-way ANOVA and Duncan's post-hoc results for the number of entries into the open arms of the Elevated Plus Maze

Univariate Tests of Significance for Open Arm Entries (Spreadsheet32)
Sigma-restricted parameterization
Effective hypothesis decomposition

Effect	SS	Degr. of Freedom	MS	F	p
Intercept	3642,189	1	3642,189	130,9927	0,000000
Treatment	2,800	1	2,800	0,1007	0,753275
Stress	32,573	1	32,573	1,1715	0,288010
Treatment*Stress	2,112	1	2,112	0,0759	0,784818
Error	806,331	29	27,805		

Table A5.79: Friedman ANOVA and Wilcoxon Matched Pairs test results for the number of entries made into the open arms per minute of the Elevated Plus Maze

All Groups
Friedman ANOVA and Kendall Coeff. of Concordance (Spreadsheet103)
ANOVA Chi Sqr. (N = 33, df = 4) = 25,12269 p = ,00005
Coeff. of Concordance = ,19032 Aver. rank r = ,16502

Variable	Average Rank	Sum of Ranks	Mean	Std.Dev.
0-1 min	3,803030	125,5000	3,303030	2,038456
1-2 min	3,606061	119,0000	2,787879	1,709488
2-3 min	2,696970	89,0000	1,878788	1,596042
3-4 min	2,454545	81,0000	1,969697	2,038456
4-5 min	2,439394	80,5000	1,727273	1,546624

All Groups
Wilcoxon Matched Pairs Test (Spreadsheet103)
Marked tests are significant at p <,05000

Pair of Variables	Valid N	T	Z	p-value
0-1 min & 0-1 min				
0-1 min & 1-2 min	28	171,5000	0,717300	0,473190
0-1 min & 2-3 min	27	68,0000	2,907025	0,003649
0-1 min & 3-4 min	28	68,0000	3,074142	0,002111
0-1 min & 4-5 min	30	78,0000	3,177808	0,001484
1-2 min & 0-1 min	28	171,5000	0,717300	0,473190
1-2 min & 1-2 min				
1-2 min & 2-3 min	29	109,0000	2,346117	0,018971
1-2 min & 3-4 min	30	137,0000	1,964276	0,049495
1-2 min & 4-5 min	27	79,0000	2,642750	0,008224
2-3 min & 0-1 min	27	68,0000	2,907025	0,003649
2-3 min & 1-2 min	29	109,0000	2,346117	0,018971
2-3 min & 2-3 min				
2-3 min & 3-4 min	25	158,5000	0,107628	0,914291
2-3 min & 4-5 min	25	140,0000	0,605406	0,544910
3-4 min & 0-1 min	28	68,0000	3,074142	0,002111
3-4 min & 1-2 min	30	137,0000	1,964276	0,049495
3-4 min & 2-3 min	25	158,5000	0,107628	0,914291
3-4 min & 3-4 min				
3-4 min & 4-5 min	25	141,5000	0,565045	0,572043
4-5 min & 0-1 min	30	78,0000	3,177808	0,001484
4-5 min & 1-2 min	27	79,0000	2,642750	0,008224
4-5 min & 2-3 min	25	140,0000	0,605406	0,544910
4-5 min & 3-4 min	25	141,5000	0,565045	0,572043
4-5 min & 4-5 min				

OPEN FIELD TEST

Table: A5.80: Raw data - Open Field Test

				Distance (cm) per min						Inner Zone Duration (s) per min						Inner Zone Frequency						
Rat Number	Group	Treatment	Stress	0-1 min	1-2 min	2-3 min	3-4 min	4-5 min	Total Distance (cm)	0-1 min	1-2 min	2-3 min	3-4 min	4-5 min	Total Inner Zone Duration (s)	0-1 min	1-2 min	2-3 min	3-4 min	4-5 min	Total Entries into Inner Zone	Latency to Inner Zone (s)
80	Control	Sacc	nMS	637,36	89,60	357,61	555,22	552,25	2192,24	1,4	0	0	0	2,6	4,00	1	0	0	0	2	3	23,40
81	Control	Sacc	nMS	730,03	579,60	526,90	643,52	258,59	2740,56	4	1,4	6,8	14,4	0	26,60	2	1	4	4	0	10	30,80
180	Control	Sacc	nMS	566,05	506,47	477,31	429,23	436,93	2416,95	0	0	0	2,6	0	2,60	0	0	0	1	0	1	190,60
181	Control	Sacc	nMS	492,38	537,17	295,83	511,46	374,68	2215,51	1,2	3,2	0	7,2	3,2	14,80	1	2	0	2	2	7	44,00
182	Control	Sacc	nMS	567,51	646,20	601,01	368,55	371,10	2554,50	2,6	4,8	8	7,4	0,2	23,00	2	4	4	1	1	11	25,40
200	Control	Sacc	nMS	687,61	477,75	426,44	492,35	515,29	2600,12	4,8	0,4	0,2	1	1,8	8,20	1	1	1	1	1	5	37,60
201	Control	Sacc	nMS	785,77	483,97	306,37	572,31	519,46	2667,89	0,4	5,2	0	4,4	15	25,00	1	2	0	1	5	9	53,80
202	Control	Sacc	nMS	588,29	693,33	631,60	507,36	499,89	2920,54	4,2	3,2	0,2	0,2	0,2	8,00	1	3	1	1	1	7	37,40
210	Control	Sacc	nMS	562,47	327,10	390,19	346,74	315,22	1942,29	0,6	1,4	1,6	0	0	3,60	1	1	1	0	0	3	5,20
211	Control	Sacc	nMS	758,58	400,53	487,37	364,13	328,60	2339,24	2,2	0,6	2,6	1,8	4,8	12,00	2	1	1	1	2	7	10,60
212	Control	Sacc	nMS	792,42	646,37	447,92	523,37	517,09	2927,47	0,4	1,8	0	0,4	0	2,60	1	3	0	1	0	5	46,80
50	MS	Sacc	MS	819,96	144,82	263,68	287,18	430,57	1946,53	1,2	0	0	0	6,8	8,00	2	0	0	0	3	5	28,60
51	MS	Sacc	MS	768,01	431,07	464,86	435,43	181,83	2281,25	0,4	4,2	0,8	2,4	0	7,80	1	1	1	1	0	4	50,20
150	MS	Sacc	MS	796,94	900,55	575,66	401,68	490,50	3165,70	3,2	4,6	3,6	0,2	1,8	13,40	3	3	1	1	1	9	8,60
151	MS	Sacc	MS	908,41	927,29	637,75	611,32	590,04	3675,24	1	4,2	3	7,4	2,4	18,00	1	3	3	5	1	13	22,40
170	MS	Sacc	MS	816,93	677,25	569,62	448,01	489,84	3002,23	2,8	2,4	7	3,8	12,4	28,40	1	3	5	2	5	16	28,20
171	MS	Sacc	MS	847,18	845,71	611,94	463,44	393,86	3169,70	5	5,8	5,2	3,8	5,4	25,20	1	3	3	3	2	11	47,60
172	MS	Sacc	MS	923,35	806,28	435,71	474,20	544,84	3188,78	0,8	2,6	2,6	4,4	2,6	13,00	1	2	2	2	1	8	20,00
60	EtOH	EtOH	nMS	666,43	529,22	526,49	221,48	206,37	2150,14	0,8	2,6	6	3,4	0,6	13,40	1	3	3	1	2	10	4,80
61	EtOH	EtOH	nMS	842,66	585,49	384,97	404,36	436,79	2655,39	1,2	3,2	1,6	21,6	0,8	28,40	1	2	1	4	2	9	7,40
130	EtOH	EtOH	nMS	842,30	819,62	929,23	645,25	555,19	3791,95	2,4	6,8	12,4	2,6	21,8	46,00	3	4	7	4	5	22	30,80
131	EtOH	EtOH	nMS	537,41	800,16	592,59	589,54	563,15	3083,19	1,4	5,4	6,2	4,2	4,6	21,80	1	3	3	2	5	14	4,60
190	EtOH	EtOH	nMS	701,67	633,27	484,72	606,31	470,25	2897,29	1,2	2	1,4	8,2	3,8	16,60	1	3	2	3	1	10	19,60
191	EtOH	EtOH	nMS	583,67	630,96	506,79	461,59	771,49	2955,67	2,8	0,2	1,8	7,6	14	26,40	1	1	1	4	8	15	29,60
192	EtOH	EtOH	nMS	773,35	537,53	507,63	418,77	377,90	2615,84	2,8	1,4	2	3,8	0,2	10,20	1	2	2	3	1	8	27,20
40	EtOH+MS	EtOH	MS	770,46	410,26	429,70	327,13	143,14	2080,75	0,4	0	0	1,2	0	1,60	1	0	0	1	0	2	35,40
41	EtOH+MS	EtOH	MS	628,04	493,08	468,13	492,53	429,83	2511,78	0	3,4	6	6,4	1,8	17,60	0	2	4	2	1	9	69,80
70	EtOH+MS	EtOH	MS	964,01	696,70	384,03	297,54	631,66	2974,49	1,4	3,8	0	1	9,2	15,40	1	4	0	1	7	13	10,60
71	EtOH+MS	EtOH	MS	947,43	725,53	593,42	744,76	339,02	3350,99	7,6	3,6	10,4	7,8	1,2	30,60	6	4	5	5	1	20	6,80
140	EtOH+MS	EtOH	MS	783,01	455,80	531,07	439,82	484,68	2695,58	5,4	2,8	12	4	2,6	26,80	2	2	3	2	2	11	14,80
141	EtOH+MS	EtOH	MS	533,06	743,56	877,54	715,21	749,03	3618,79	0	2,8	2,2	9,6	3	17,60	0	2	3	6	4	15	109,80
161	EtOH+MS	EtOH	MS	882,08	617,13	587,62	497,87	298,53	2886,42	0,2	9,2	8	3	0	20,40	1	2	4	2	0	9	34,20
160	EtOH+MS	EtOH	MS	1041,17	583,88	641,42	603,54	443,97	3315,23	1,4	7,8	4,6	9,4	8	31,20	1	5	3	6	3	18	40,00

Table A5.81: Shapiro-Wilk test results for the variables analyzed during the Open Field Test

Variable	Shapiro-Wilk, W	*P* Value
Total Distance (cm)	0,978	0,710
Distance (0-1 min)	0,969	0,447
Distance (1-2 min)	0,968	0,434
Distance (2-3 min)	0,931	0,038
Distance (3-4 min)	0,991	0,993
Distance (4-5 min)	0,980	0,787
Total Inner Zone Duration (s)	0,957	0,219
Inner Zone Duration (0-1 min)	0,873	0,001
Inner Zone Duration (1-2 min)	0,947	0,100
Inner Zone Duration (2-3 min)	0,862	0,001
Inner Zone Duration (3-4 min)	0,834	0,000
Inner Zone Duration (4-5 min)	0,756	0,000
Inner Zone Frequency	0,970	0,474
Inner Zone Frequency (0-1 min)	0,643	0,000
Inner Zone Frequency (1-2 min)	0,938	0,062
Inner Zone Frequency (2-3 min)	0,900	0,006
Inner Zone Frequency (3-4 min)	0,880	0,002
Inner Zone Frequency (4-5 min)	0,838	0,002
Latency to Inner Zone (s)	0,682	0,000

Table A5.82: Two-way ANOVA result for the distance travelled during the Open Field Test

	Univariate Tests of Significance for Distance (cm) (Spreadsheet1) Sigma-restricted parameterization Effective hypothesis decomposition				
Effect	SS	Degr. of Freedom	MS	F	p
Intercept	25131150	1	25131150	1140,05	0,00000
Treatment	29962	1	299624	1,359	0,25317
Stress	43601	1	436019	1,978	0,17023
Treatment*Stress	26727	1	267273	1,212	0,27990
Error	639269	29	22043		

Table A5.83: Repeated-measures two-way ANOVA result for the distance travelled per minute during the Open Field Test

	Repeated Measures Analysis of Variance (Spreadsheet1) Sigma-restricted parameterization Effective hypothesis decomposition				
Effect	SS	Degr. of Freedom	MS	F	p
Intercept	5022281	1	5022281	1140,167	0,00000
Treatment	6026	1	60269	1,368	0,25163
Stress	8667	1	86679	1,968	0,17129
Treatment*Stress	5319	1	53195	1,208	0,28083
Error	127741	29	44049		
MINUTE	19025	4	47563	30,151	0,00000
MINUTE*Treatment	2183	4	5458	0,346	0,84635
MINUTE*Stress	13478	4	33696	2,136	0,08071
MINUTE*Treatment*Stress	10180	4	25451	1,613	0,17556
Error	182990	116	15775		

	Duncan test; variable DV_1 (Spreadsheet2) Approximate Probabilities for Post Hoc Tests Error: Within MS = 15775,, df = 116,00					
Cell No.	MINUTE	{1} 743,82	{2} 587,37	{3} 513,73	{4} 481,85	{5} 445,81
1	0--1 min		0,00010	0,00005	0,00004	0,00002
2	1--2 min	0,00010		0,01895	0,00132	0,00006
3	2--3 min	0,00005	0,01895		0,30480	0,03877
4	3--4 min	0,00004	0,00132	0,30480		0,24613
5	4--5 min	0,00002	0,00006	0,03877	0,24613	

Table A5.84: Two-way ANOVA and Duncan's post-hoc test results for the time spent in the inner zone during the Open Field Test

Univariate Tests of Significance for Inner Zone Duration (s) (Spreadsheet1)
Sigma-restricted parameterization
Effective hypothesis decomposition

Effect	SS	Degr. of Freedom	MS	F	p
Intercept	10196,78	1	10196,78	106,9718	0,000000
Treatment	466,39	1	466,39	4,8928	0,035004
Stress	3,35	1	3,35	0,0351	0,852697
Treatment*Stress	112,43	1	112,43	1,1794	0,286414
Error	2764,34	29	95,32		

Duncan test; variable Inner Zone Duration (s) (Spreadsheet1)
Approximate Probabilities for Post Hoc Tests
Error: Between MS = 95,322, df = 29,000

Cell No.	Treatment	{1} 13,567	{2} 21,600
1	Sacc		0,025710
2	EtOH	0,025710	

Duncan test; variable Inner Zone Duration (s) (Spreadsheet1)
Approximate Probabilities for Post Hoc Tests
Error: Between MS = 95,322, df = 29,000

Cell No.	Treatment	Stress	{1} 11,855	{2} 16,257	{3} 23,257	{4} 20,150
1	Sacc	Contro		0,375494	0,039580	0,118927
2	Sacc	MS	0,375494		0,186641	0,432562
3	EtOH	Contro	0,039580	0,186641		0,530245
4	EtOH	MS	0,118927	0,432562	0,530245	

Table A5.85: Friedman ANOVA result for the time spent per minute in the inner zone of the Open Field

All Groups
Friedman ANOVA and Kendall Coeff. of Concordance (Spreadsheet8)
ANOVA Chi Sqr. (N = 33, df = 4) = 7,412141 p = ,11565
Coeff. of Concordance = ,05615 Aver. rank r = ,02666

Variable	Average Rank	Sum of Ranks	Mean	Std.Dev.
0-1 min	2,515152	83,0000	1,975758	1,835591
1-2 min	3,090909	102,0000	3,054545	2,314775
2-3 min	3,030303	100,0000	3,521212	3,682709
3-4 min	3,515152	116,0000	4,703030	4,593234
4-5 min	2,848485	94,0000	3,963636	5,219544

Table A5.86: Two-way ANOVA and Duncan's post-hoc test results for the number of entries into the inner zone during the Open Field Test

Univariate Tests of Significance for Inner Zone Frequency (Spreadsheet1)
Sigma-restricted parameterization
Effective hypothesis decomposition

Effect	SS	Degr. of Freedom	MS	F	p
Intercept	3238,764	1	3238,764	161,9550	0,000000
Treatment	164,578	1	164,578	8,2297	0,007609
Stress	15,633	1	15,633	0,7817	0,383886
Treatment*Stress	27,191	1	27,191	1,3597	0,253093
Error	579,940	29	19,998		

Duncan test; variable Inner Zone Frequency (Spreadsheet1)
Approximate Probabilities for Post Hoc Tests
Error: Between MS = 19,998, df = 29,000

Cell No.	Treatment	{1} 7,4444	{2} 12,333
1	Sacc		0,004155
2	EtOH	0,004155	

Duncan test; variable Inner Zone Frequency (Spreadsheet1)
Approximate Probabilities for Post Hoc Tests
Error: Between MS = 19,998, df = 29,000

Cell No.	Treatment	Stress	{1} 6,1818	{2} 9,4286	{3} 12,571	{4} 12,125
1	Sacc	Contro		0,158010	0,012674	0,016803
2	Sacc	MS	0,158010		0,195343	0,238447
3	EtOH	Contro	0,012674	0,195343		0,843512
4	EtOH	MS	0,016803	0,238447	0,843512	

Table A5.87: Friedman ANOVA result for the number of entries into the inner zone of the Open Field

All Groups
Friedman ANOVA and Kendall Coeff. of Concordance (Spreadsheet27)
ANOVA Chi Sqr. (N = 33, df = 4) = 8,888889 p = ,06394
Coeff. of Concordance = ,06734 Aver. rank r = ,03819

Variable	Average Rank	Sum of Ranks	Mean	Std.Dev.
0-1 min	2,454545	81,000(	1,333333	1,080123
1-2 min	3,333333	110,000(	2,181818	1,309927
2-3 min	3,090909	102,000(	2,060606	1,818987
3-4 min	3,303030	109,000(	2,212121	1,691109
4-5 min	2,818182	93,000(	2,090909	2,097076

Table A5.88: Kruskal-Wallis analysis of latency to the inner zone of the Open Field Test

Multiple Comparisons p values (2-tailed); Latency to InnerZone (s) (Spreadsheet22)
Independent (grouping) variable: Group
Kruskal-Wallis test: H (3, N= 33) =4,975641 p =,1736

Depend.: Latency to InnerZone (s)	Control R:20,000	MS R:17,000	EtOH R:10,071	EtOH+MS R:18,938
Control		1,000000(	0,202179	1,000000(
MS	1,000000(		1,000000(	1,000000(
EtOH	0,202179	1,000000(		0,458733
EtOH+MS	1,000000(	1,000000(	0,458733	

FORCED SWIM TEST

Table A5.89: Raw Data - Forced swim test

Rat Number	Group	Treatment	Stress	Time Immobile (s)	Time Climbing (s)	Time Swimming (s)	Latency to Immobility (s)
80	Control	Sacc	nMS	112	49	139	21
81	Control	Sacc	nMS	128	34	138	18
180	Control	Sacc	nMS	127	47	126	22
181	Control	Sacc	nMS	79	40	181	18
182	Control	Sacc	nMS	150	38	112	13
200	Control	Sacc	nMS	196	69	35	60
201	Control	Sacc	nMS	225	24	51	15
202	Control	Sacc	nMS	198	11	91	11
210	Control	Sacc	nMS	197	67	36	64
211	Control	Sacc	nMS	193	30	77	5
212	Control	Sacc	nMS	118	54	128	7
50	MS	Sacc	MS	189	17	94	19
51	MS	Sacc	MS	210	9	81	14
150	MS	Sacc	MS	69	39	192	51
151	MS	Sacc	MS	70	24	206	22
170	MS	Sacc	MS	128	99	73	61
171	MS	Sacc	MS	144	41	115	20
172	MS	Sacc	MS	108	53	139	45
60	EtOH	EtOH	nMS	114	40	146	21
61	EtOH	EtOH	nMS	231	6	63	12
130	EtOH	EtOH	nMS	123	37	140	67
131	EtOH	EtOH	nMS	63	65	172	51
190	EtOH	EtOH	nMS	193	53	54	44
191	EtOH	EtOH	nMS	184	48	68	21
192	EtOH	EtOH	nMS	212	33	55	9
40	EtOH+MS	EtOH	MS	103	58	139	43
41	EtOH+MS	EtOH	MS	87	66	147	68
70	EtOH+MS	EtOH	MS	141	29	130	34
71	EtOH+MS	EtOH	MS	143	21	136	19
140	EtOH+MS	EtOH	MS	157	44	99	17
141	EtOH+MS	EtOH	MS	91	31	178	21
160	EtOH+MS	EtOH	MS	62	60	178	21
161	EtOH+MS	EtOH	MS	71	43	186	26

Table A5.90: Shapiro-Wilk test results for variables measured in the FST

Variable	Shapiro-Wilk,W	P value
Time Immobile	0,94	0,068
Time Climbing	0,974	0,602
Time Swimming	0,959	0,241
Latency to immobility	0,0854	0,00043

Table A5.91: Two-way ANOVA and Duncan's post-hoc test for the time spent immobile in FST.

Univariate Tests of Significance for Time Immobile (s) (Spreadsheet6)
Sigma-restricted parameterization
Effective hypothesis decomposition

Effect	SS	Degr. of Freedom	MS	F	p
Intercept	613291,4	1	613291,4	249,5633	0,00000(
Treatment	871,1	1	871,1	0,3545	0,556201
Stress	12321,7	1	12321,7	5,0140	0,032979
Treatment*Stress	1522,1	1	1522,1	0,6194	0,437669
Error	71266,3	29	2457,5		

Duncan test; variable Time Immobile (s) (Spreadsheet6)
Approximate Probabilities for Post Hoc Tests
Error: Between MS = 2457,5, df = 29,000

Cell No.	Stress	{1} 157,94	{2} 118,20
1	nMS		0,029395
2	MS	0,029395	

Table A5.92: Two-way ANOVA and Duncan's post-hoc test for the time spent swimming in FST.

Univariate Tests of Significance for Time Swimming (s) (Spreadsheet6)
Sigma-restricted parameterization
Effective hypothesis decomposition

Effect	SS	Degr. of Freedom	MS	F	p
Intercept	456792,6	1	456792,6	217,4482	0,00000(
Treatment	719,3	1	719,3	0,3424	0,562969
Stress	11730,6	1	11730,6	5,5841	0,025043
Treatment*Stress	974,7	1	974,7	0,4640	0,501165
Error	60920,2	29	2100,7		

Duncan test; variable Time Swimming (s) (Spreadsheet6)
Approximate Probabilities for Post Hoc Tests
Error: Between MS = 2100,7, df = 29,000

Cell No.	Stress	{1} 100,67	{2} 139,53
1	nMS		0,021866
2	MS	0,021866	

Table A5.93: Two-way ANOVA of the time spent climbing in FST.

Univariate Tests of Significance for Time Climbing (s) (Spreadsheet6)
Sigma-restricted parameterization
Effective hypothesis decomposition

Effect	SS	Degr. of Freedom	MS	F	p
Intercept	55372,89	1	55372,89	129,3575	0,00000(
Treatment	7,27	1	7,27	0,0170	0,897243
Stress	7,27	1	7,27	0,0170	0,897243
Treatment*Stress	60,73	1	60,73	0,1419	0,709164
Error	12413,77	29	428,06		

Table A5.94: Kruskal-Wallis analysis of the latency to immobility in the FST.

	Multiple Comparisons p values (2-tailed); Latency to Immobility (sec) (Spreadsheet1 Independent (grouping) variable: Group Kruskal-Wallis test: H (3, N= 33) =3,434346 p =,3294			
Depend.: Latency to Immobility (sec)	Control R:12,682	MS R:19,643	EtOH R:18,071	EtOH+MS R:19,688
Control		0,819018	1,000000	0,713657
MS	0,819018		1,000000	1,000000
EtOH	1,000000	1,000000		1,000000
EtOH+MS	0,713657	1,000000	1,000000	

Table A5.95: Western blot analysis in the PREFRONTAL CORTEX of MALE RATS - UN-SCAN-IT pixel density percentage - RAW DATA

Male Rats				Prefrontal Cortex										
Rat Number	Group	Treatment	Stress	P-ERK1/2 / Alpha Tubulin	ERK1/2 / Alpha Tubulin	P-ERK1/2 / ERK1/2	P-GSK3β / Alpha Tubulin	GSK3β / Alpha Tubulin	P-GSK3β / GSK3β	P-CREB / Alpha Tubulin	CREB / Alpha Tubulin	P-CREB / CREB	Synaptophysin / Alpha Tubulin	ATP5A / Alpha Tubulin
82	Control	Sacc	nMS	112,36	122,01	92,09	78,66	106,65	73,75	153,30	92,97	164,89	108,36	90,20
112	Control	Sacc	nMS	95,57	87,84	108,79	123,75	99,29	124,64	37,46	57,87	138,74	68,27	115,31
183	Control	Sacc	nMS	61,94	72,49	85,44	76,39	95,79	79,75	80,29	131,16	75,07	94,26	100,24
203	Control	Sacc	nMS	115,27	111,65	103,24	120,33	82,54	145,80	98,46	121,01	60,53	106,59	77,37
85	Control	Sacc	nMS	79,33	103,77	76,45	79,52	96,01	82,82	73,25	82,45	65,71	96,45	78,20
114	Control	Sacc	nMS	97,24	102,25	95,10	72,76	79,29	91,76	54,18	90,56	106,56	94,88	95,97
184	Control	Sacc	nMS	76,21	88,79	85,83	77,42	104,12	74,36	96,51	65,73	84,97	86,69	98,29
215	Control	Sacc	nMS	109,38	123,64	88,47	77,58	107,21	72,37	55,85			86,95	74,43
120	MS	Sacc	MS	120,82	98,49	122,67	77,78	99,03	78,54	106,90	128,98	82,88	95,57	97,79
152	MS	Sacc	MS	112,41	93,52	120,20	81,82	88,55	92,40	95,84	84,29	130,54	103,49	103,45
173	MS	Sacc	MS	76,33	77,81	98,09	55,64	99,59	55,86	110,03	153,55	76,85	108,49	79,88
54	MS	Sacc	MS	145,49	132,26	110,00	103,88	103,79	100,08	118,01	108,21	94,77	99,20	117,06
125	MS	Sacc	MS	71,55	71,48	100,10	106,42	106,15	100,26	102,56	108,09	105,32	121,73	87,62
155	MS	Sacc	MS	132,02	118,18	111,71	104,62	107,59	97,24	113,84	94,42	96,06	94,44	102,59
174	MS	Sacc	MS	76,27	86,12	88,57	107,83	90,01	119,79	90,71	91,99	125,19	58,02	95,06
53	MS	Sacc	MS	115,03	128,12	89,78	116,07	95,35	121,73	115,16			118,59	102,78
62	EtOH	EtOH	nMS	84,57	102,34	82,64	125,97	94,16	133,79	87,53	107,95	81,08	108,02	96,90
90	EtOH	EtOH	nMS	110,81	89,76	123,45	131,16	114,41	114,64	117,19	76,71	152,76	109,43	102,52
93	EtOH	EtOH	nMS	93,81	85,11	110,22	109,28	100,28	108,97	143,29	74,58	192,13	116,57	96,56
132	EtOH	EtOH	nMS	141,21	140,99	100,16	101,94	111,82	91,16	90,90	133,31	68,19	83,91	141,33
65	EtOH	EtOH	nMS	101,41	94,29	107,55	60,83	94,51	64,36	100,55	108,41	92,75	98,47	88,19
135	EtOH	EtOH	nMS	111,45	97,18	114,69	127,37	112,40	113,32	101,81	112,90	90,17	84,72	137,15
194	EtOH	EtOH	nMS	98,62	97,10	101,57	115,46	91,49	126,19	74,86	85,07	88,00	95,74	137,90
195	EtOH	EtOH	nMS	112,18	96,40	116,37	115,53	105,79	109,21	157,32	179,21	87,78	93,07	119,10
72	EtOH+MS	EtOH	MS	94,31	95,90	98,34	107,61	93,86	114,65	52,58			63,14	91,38
73	EtOH+MS	EtOH	MS	81,05	89,69	90,36	83,15	105,07	79,14	137,01	80,99	169,18	164,33	105,88
100	EtOH+MS	EtOH	MS	92,93	98,96	93,91	127,01	90,40	140,49	84,62	58,89	143,69	106,34	91,72
142	EtOH+MS	EtOH	MS	124,09	138,22	89,78	117,74	125,38	93,90	78,87	99,05	79,63	86,54	108,02
143	EtOH+MS	EtOH	MS	116,49	92,71	125,65	99,24	102,77	96,57	62,45	77,58	80,49	104,37	82,39
44	EtOH+MS	EtOH	MS	95,89	120,46	79,60	159,49	99,64	160,07	191,49	79,05	242,24	103,09	167,16
45	EtOH+MS	EtOH	MS	110,13	112,71	97,71	70,76	94,27	75,06	128,89	93,85	137,33	132,59	103,17
101	EtOH+MS	EtOH	MS	117,11	102,53	114,23	133,09	119,57	111,30	94,09	119,93	78,45	124,84	70,06

Table A5.96: Western blot analysis in the DORSAL HIPPOCAMPUS of MALE RATS - UN-SCAN-IT pixel density percentage - RAW DATA

Male Rats				Dorsal Hippocampus										
Rat Number	Group	Treatment	Stress	P-ERK1/2 / Alpha Tubulin	ERK1/2 / Alpha Tubulin	P-ERK1/2 / ERK1/2	P-GSK3β / Alpha Tubulin	GSK3β / Alpha Tubulin	P-GSK3β / GSK3β	P-CREB / Alpha Tubulin	CREB / Alpha Tubulin	P-CREB / CREB	Synaptophysin / Alpha Tubulin	ATP5A / Alpha Tubulin
82	Control	Sacc	nMS	66,01	91,55	72,10	85,12	75,99	112,01	90,31	53,30	169,44	128,12	147,74
112	Control	Sacc	nMS	119,62	101,29	118,10	125,37	103,28	121,39	100,22	105,20	95,26	88,99	110,63
183	Control	Sacc	nMS	74,47	93,48	79,66	108,63	105,61	102,86	101,70	104,56	97,27	105,66	83,26
203	Control	Sacc	nMS	107,67	110,49	97,45	105,75	74,85	141,29	100,31	100,39	99,92	97,43	110,73
85	Control	Sacc	nMS	77,79	98,78	78,75	105,64	103,41	102,15	107,38	97,59	110,03	113,23	72,81
114	Control	Sacc	nMS	108,36	103,51	104,69	83,63	96,22	86,91	90,67	90,82	99,84	73,38	116,91
184	Control	Sacc	nMS	80,99	91,93	88,09	109,91	103,50	106,19	100,36	112,05	89,57	98,63	84,70
215	Control	Sacc	nMS	113,50	109,51	103,64	85,04	102,10	83,29	103,52	85,30	121,36	80,08	103,22
120	MS	Sacc	MS	62,76	90,29	69,51	66,94	80,89	82,75	74,67	46,42	160,88	102,12	65,24
152	MS	Sacc	MS	136,06	126,90	107,22	127,22	120,60	105,49	112,66	130,44	86,37	66,61	121,64
173	MS	Sacc	MS	80,75	91,51	88,24	83,49	87,19	95,76	92,46	113,12	81,74	107,91	89,47
54	MS	Sacc	MS	124,78	106,28	117,40	88,25	105,96	83,29	106,14	119,15	89,08	87,99	108,88
125	MS	Sacc	MS	104,32	97,51	106,98	111,43	92,47	120,51	122,76	112,89	108,74	121,63	92,30
155	MS	Sacc	MS	107,87	92,13	117,09	104,31	115,50	90,31	78,24	91,69	85,33	94,21	133,02
174	MS	Sacc	MS	86,52	109,88	78,75	40,62	81,92	49,59	89,31	95,93	93,09	79,25	63,32
53	MS	Sacc	MS	128,10	103,28	124,04	124,24	104,72	118,64	115,30	148,21	77,79	99,46	99,35
62	EtOH	EtOH	nMS	104,81	91,03	115,13	87,63	87,96	99,62	96,26	81,23	118,50	110,69	87,35
90	EtOH	EtOH	nMS	130,35	109,73	118,79	138,56	143,25	96,73	107,44	144,86	74,16	82,12	97,66
93	EtOH	EtOH	nMS	93,97	100,79	93,23	101,36	96,00	105,58	114,81	112,85	101,74	111,17	85,87
132	EtOH	EtOH	nMS	125,70	102,14	123,06	99,54	129,29	76,99	100,31	84,06	119,33	91,03	117,22
65	EtOH	EtOH	nMS	89,43	84,85	105,40	89,86	77,23	116,35	122,82	109,69	111,96	125,00	98,67
135	EtOH	EtOH	nMS	86,07	93,04	92,51	104,73	116,50	89,90	78,80	89,90	87,65	85,94	128,94
194	EtOH	EtOH	nMS	113,82	104,17	109,26	101,27	87,08	116,30	77,74	120,42	64,56	93,74	92,06
195	EtOH	EtOH	nMS	106,85	102,85	103,89	111,75	119,25	93,71	102,43	86,16	118,89	94,13	119,13
72	EtOH+MS	EtOH	MS	105,64	78,36	134,80	120,79	103,59	116,60	105,49	90,31	116,80	121,04	100,51
73	EtOH+MS	EtOH	MS	117,18	98,43	119,04	47,80	102,08	46,83	112,63	148,54	75,82	91,90	73,00
100	EtOH+MS	EtOH	MS	88,39	103,38	85,50	102,39	76,22	134,35	122,37	119,37	102,52	118,70	95,07
142	EtOH+MS	EtOH	MS	119,49	116,08	102,93	109,42	130,87	83,61	55,75	38,64	144,26	97,89	121,44
143	EtOH+MS	EtOH	MS	104,34	102,25	102,05	102,68	96,12	106,83	98,43	96,00	102,53	109,72	93,14
44	EtOH+MS	EtOH	MS	106,49	115,14	92,49	96,36	115,53	83,40	99,23	115,15	86,18	61,24	91,00
45	EtOH+MS	EtOH	MS	94,59	116,06	81,50	109,14	95,67	114,08	90,78	73,67	123,22	104,65	120,46
101	EtOH+MS	EtOH	MS	96,02	88,76	108,18	139,80	119,69	116,79	121,57	74,36	163,50	104,65	118,96

Table A5.97: Shapiro-Wilk Test results for Western Blot analysis in the prefrontal cortex (PFC) and dorsal hippocampus (DH) of male rats.

Sex	Brain Area	Variable	Shapiro-Wilk, W	*P* Value
Male	PFC	P-ERK1/2	0,975	0,632
Male	PFC	ERK1/2	0,878	0,002
Male	PFC	P-ERK1/2 / ERK1/2	0,969	0,475
Male	PFC	P-GSK3β	0,959	0,260
Male	PFC	GSK3β	0,986	0,944
Male	PFC	P-GSK3β / GSK3β	0,979	0,795
Male	PFC	P-CREB	0,973	0,596
Male	PFC	CREB	0,946	0,143
Male	PFC	P-CREB/CREB	0,862	0,001
Male	PFC	Synaptophysin	0,943	0,089
Male	PFC	ATP5A	0,906	0,009
Male	DH	P-ERK1/2	0,976	0,686
Male	DH	ERK1/2	0,980	0,810
Male	DH	P-ERK1/2 / ERK1/2	0,973	0,584
Male	DH	P-GSK3β	0,936	0,060
Male	DH	GSK3β	0,966	0,386
Male	DH	P-GSK3β / GSK3β	0,954	0,189
Male	DH	P-CREB	0,951	0,149
Male	DH	CREB	0,968	0,437
Male	DH	P-CREB/CREB	0,917	0,017
Male	DH	Synaptophysin	0,986	0,938
Male	DH	ATP5A	0,982	0,860

Table A5.98: Two-way ANOVA result of P-ERK1/2 pixel percentage in the prefrontal cortex of male rats

	Univariate Tests of Significance for Pixel Total % (Spreadsheet1) Sigma-restricted parameterization Effective hypothesis decomposition				
Effect	SS	Degr. of Freedom	MS	F	p
Intercept	336872,5	1	336872,5	805,3164	0,000000
Treatment	246,8	1	246,8	0,5901	0,448818
Stress	202,9	1	202,9	0,4850	0,491894
Treatment*Stress	485,9	1	485,9	1,1616	0,290324
Error	11712,7	28	418,3		

Table A5.99: Kruskal-Wallis test result of ERK1/2 pixel percentage in the prefrontal cortex of male rats

	Multiple Comparisons p values (2-tailed); Pixel Total % (Spreadsheet10) Independent (grouping) variable: Group Kruskal-Wallis test: H (3, N= 32) =,8323864 p =,8417			
Depend.: Pixel Total %	Control R:16,750	MS R:15,125	EtOH R:15,250	EtOH+MS R:18,875
Control		1,000000	1,000000	1,000000
MS	1,000000		1,000000	1,000000
EtOH	1,000000	1,000000		1,000000
EtOH+MS	1,000000	1,000000	1,000000	

Table A5.100: Two-way ANOVA and Duncan's post-hoc test results for P-ERK1/2 / ERK1/2 pixel percentage in the prefrontal cortex male rats

Univariate Tests of Significance for Pixel Total % (Spreadsheet24)
Sigma-restricted parameterization
Effective hypothesis decomposition

Effect	SS	Degr. of Freedom	MS	F	p
Intercept	324565,9	1	324565,9	2000,551	0,000000
Treatment	151,9	1	151,9	0,936	0,341527
Stress	46,7	1	46,7	0,288	0,596016
Treatment*Stress	932,9	1	932,9	5,750	0,023398
Error	4542,7	28	162,2		

Duncan test; variable Pixel Total % (Spreadsheet18)
Approximate Probabilities for Post Hoc Tests
Error: Between MS = 162,24, df = 28,000

Cell No.	Treatment	Stress	{1} 91,925	{2} 105,14	{3} 107,08	{4} 98,698
1	Sacc	Contro		0,058481	0,036140	0,296823
2	Sacc	MS	0,058481		0,762741	0,320611
3	EtOH	Contro	0,036140	0,762741		0,224249
4	EtOH	MS	0,296823	0,320611	0,224249	

Table A5.101: Two-way ANOVA result of P-ERK1/2 pixel percentage in the dorsal hippocampus of male rats

Univariate Tests of Significance for Pixel Total % (Spreadsheet31)
Sigma-restricted parameterization
Effective hypothesis decomposition

Effect	SS	Degr. of Freedom	MS	F	p
Intercept	329540,3	1	329540,3	895,6266	0,000000
Treatment	316,6	1	316,6	0,8604	0,361544
Stress	121,9	1	121,9	0,3312	0,569560
Treatment*Stress	327,7	1	327,7	0,8907	0,353365
Error	10302,4	28	367,9		

Table A5.102: Two-way ANOVA result of ERK1/2 pixel percentage in the dorsal hippocampus of male rats

Univariate Tests of Significance for Pixel Total % (Spreadsheet1)
Sigma-restricted parameterization
Effective hypothesis decomposition

Effect	SS	Degr. of Freedom	MS	F	p
Intercept	324420,3	1	324420,3	3075,904	0,000000
Treatment	0,1	1	0,1	0,001	0,974933
Stress	264,8	1	264,8	2,511	0,124295
Treatment*Stress	104,2	1	104,2	0,988	0,328694
Error	2953,2	28	105,5		

Table A5.103: Two-way ANOVA result of P-ERK1/2 / ERK1/2 pixel percentage in the dorsal hippocampus of male rats

Univariate Tests of Significance for Pixel Total % (Spreadsheet10)
Sigma-restricted parameterization
Effective hypothesis decomposition

Effect	SS	Degr. of Freedom	MS	F	p
Intercept	322989,4	1	322989,4	1274,444	0,000000
Treatment	478,3	1	478,3	1,887	0,180416
Stress	24,6	1	24,6	0,097	0,757735
Treatment*Stress	810,2	1	810,2	3,197	0,084606
Error	7096,2	28	253,4		

Table A5.104: Two-way ANOVA and Duncan's post-hoc test results of P-GSK3β in the prefrontal cortex of male rats

Effect	SS	Degr. of Freedom	MS	F	p
Intercept	329287,7	1	329287,7	606,2270	0,00000(
Treatment	3304,2	1	3304,2	6,0830	0,02003[illegible]
Stress	105,8	1	105,8	0,1948	0,66236[illegible]
Treatment*Stress	43,0	1	43,0	0,0791	0,78058[illegible]
Error	15208,[illegible]	28	543,2		

Univariate Tests of Significance for Pixel Total % (Spreadsheet42)
Sigma-restricted parameterization
Effective hypothesis decomposition

Duncan test; variable Pixel Total % (Spreadsheet1)
Approximate Probabilities for Post Hoc Tests
Error: Between MS = 543,18, df = 28,000

Cell No.	Treatment	{1} 91,279	{2} 111,60
1	Sacc		0,02016[illegible]
2	EtOH	0,02016[illegible]	

Table A5.105: Two-way ANOVA result of GSK3β in the prefrontal cortex of male rats

Effect	SS	Degr. of Freedom	MS	F	p
Intercept	323369,[illegible]	1	323369,[illegible]	3205,79(	0,00000(
Treatment	281,4	1	281,4	2,789	0,10603[illegible]
Stress	19,9	1	19,9	0,198	0,65994[illegible]
Treatment*Stress	5,3	1	5,3	0,053	0,81988[illegible]
Error	2824,4	28	100,9		

Univariate Tests of Significance for Pixel Total % (Spreadsheet63)
Sigma-restricted parameterization
Effective hypothesis decomposition

Table A5.106: Two-way ANOVA result of P-GSK3β/GSK3β in the prefrontal cortex of male rats

Effect	SS	Degr. of Freedom	MS	F	p
Intercept	328857,3	1	328857,3	519,4261	0,00000(
Treatment	1535,5	1	1535,5	2,4253	0,13062(
Stress	28,5	1	28,5	0,0450	0,83348[illegible]
Treatment*Stress	3,9	1	3,9	0,0061	0,93825[illegible]
Error	17727,3	28	633,1		

Univariate Tests of Significance for Pixel Total % (Spreadsheet72)
Sigma-restricted parameterization
Effective hypothesis decomposition

Table A5.107: Two-way ANOVA result of P-GSK3β in the Dorsal Hippocampus of male rats

Effect	SS	Degr. of Freedom	MS	F	p
Intercept	323748,(	1	323748,(	632,625(	0,00000(
Treatment	361,(	1	361,(	0,7054	0,40809[illegible]
Stress	148,3	1	148,3	0,2898	0,59460[illegible]
Treatment*Stress	98,9	1	98,9	0,1932	0,66360[illegible]
Error	14329,1	28	511,8		

Univariate Tests of Significance for Pixel Total % (Spreadsheet109)
Sigma-restricted parameterization
Effective hypothesis decomposition

Table A5.108: Two-way ANOVA result of GSK3β in the dorsal hippocampus of male rats

Effect	Univariate Tests of Significance for Pixel Total % (Spreadsheet118) Sigma-restricted parameterization Effective hypothesis decomposition SS	Degr. of Freedom	MS	F	p
Intercept	330189,9	1	330189,9	1077,472	0,000000
Treatment	631,2	1	631,2	2,060	0,162315
Stress	1,8	1	1,8	0,006	0,940089
Treatment*Stress	52,7	1	52,7	0,172	0,681550
Error	8580,6	28	306,4		

Table A5.109: Two-way ANOVA result of P-GSK3β/GSK3β in the dorsal hippocampus male rats

Effect	Univariate Tests of Significance for Pixel Total % (Spreadsheet127) Sigma-restricted parameterization Effective hypothesis decomposition SS	Degr. of Freedom	MS	F	p
Intercept	320021,4	1	320021,4	706,7394	0,000000
Treatment	0,7	1	0,7	0,0016	0,968672
Stress	328,0	1	328,0	0,7244	0,401922
Treatment*Stress	428,2	1	428,2	0,9456	0,339156
Error	12678,8	28	452,8		

Table A5.110: Two-way ANOVA of P-CREB pixel percentage in the prefrontal cortex of male rats

Effect	Univariate Tests of Significance for Pixel Total % (Spreadsheet29) Sigma-restricted parameterization Effective hypothesis decomposition SS	Degr. of Freedom	MS	F	p
Intercept	321158,6	1	321158,6	297,5027	0,000000
Treatment	1263,6	1	1263,6	1,1705	0,288525
Stress	803,1	1	803,1	0,7440	0,395716
Treatment*Stress	1909,8	1	1909,8	1,7691	0,194222
Error	30226,4	28	1079,5		

Table A5.111: Two-way ANOVA result of CREB pixel percentage in the prefrontal cortex of male rats

Effect	Univariate Tests of Significance for Pixel Total % (Spreadsheet38) Sigma-restricted parameterization Effective hypothesis decomposition SS	Degr. of Freedom	MS	F	p
Intercept	286768,0	1	286768,0	389,5761	0,000000
Treatment	41,6	1	41,6	0,0565	0,814112
Stress	36,0	1	36,0	0,0489	0,826750
Treatment*Stress	3032,9	1	3032,9	4,1203	0,053143
Error	18402,6	25	736,1		

Table A5.112: Kruskal-Wallis analysis result of P-CREB/CREB pixel percentage in the Prefrontal Cortex of male rats

Depend.: Pixel Total %	Multiple Comparisons p values (2-tailed); Pixel Total % (Spreadsheet47) Independent (grouping) variable: Group Kruskal-Wallis test: H (3, N= 29) =1,359360 p =,7151 Control R:12,286	MS R:15,286	EtOH R:14,875	EtOH+MS R:17,571
Control		1,000000	1,000000	1,000000
MS	1,000000		1,000000	1,000000
EtOH	1,000000	1,000000		1,000000
EtOH+MS	1,000000	1,000000	1,000000	

Table A5.113: Two-way ANOVA result of P-CREB pixel percentage in the dorsal hippocampus of male rats

Univariate Tests of Significance for Pixel Total % (Spreadsheet81) Sigma-restricted parameterization Effective hypothesis decomposition					
Effect	SS	Degr. of Freedom	MS	F	p
Intercept	318577,8	1	318577,8	1200,341	0,00000(
Treatment	13,6	1	13,6	0,051	0,82273
Stress	0,2	1	0,2	0,001	0,97668
Treatment*Stress	2,3	1	2,3	0,009	0,92654
Error	7431,4	28	265,4		

Table A5.114: Two-way ANOVA result of CREB pixel total percentage in the dorsal hippocampus of male rats

Univariate Tests of Significance for Pixel Total % (Spreadsheet90) Sigma-restricted parameterization Effective hypothesis decomposition					
Effect	SS	Degr. of Freedom	MS	F	p
Intercept	318458,2	1	318458,2	439,715	0,00000(
Treatment	14,9	1	14,9	0,0206	0,88682
Stress	39,4	1	39,4	0,0545	0,81719(
Treatment*Stress	1032,5	1	1032,5	1,4257	0,24249
Error	20278,6	28	724,2		

Table A5.115: Kruskal-Wallis analysis of P-CREB/CREB pixel percentage in the dorsal hippocampus of male rats

Multiple Comparisons p values (2-tailed); Pixel Total % (Spreadsheet99) Independent (grouping) variable: Group Kruskal-Wallis test: H (3, N= 32) =3,366477 p =,3385				
Depend.: Pixel Total %	Control R:18,625	MS R:11,875	EtOH R:15,750	EtOH+MS R:19,750
Control		0,90072	1,00000(	1,00000(
MS	0,90072		1,00000(	0,55896
EtOH	1,00000(	1,00000(		1,00000(
EtOH+MS	1,00000(	0,55896	1,00000(	

Table A5.116: Two-way ANOVA of Synaptophysin pixel percentage in the prefrontal cortex of male rats

Univariate Tests of Significance for Pixel Total % (Spreadsheet52) Sigma-restricted parameterization Effective hypothesis decomposition					
Effect	SS	Degr. of Freedom	MS	F	p
Intercept	323437,9	1	323437,9	798,961	0,00000(
Treatment	554,2	1	554,2	1,3691	0,25183
Stress	725,7	1	725,7	1,7926	0,19138
Treatment*Stress	45,6	1	45,6	0,1127	0,73956
Error	11335,(	28	404,8		

Table A5.117: Two-way ANOVA of Synaptophysin pixel percentage in the dorsal hippocampus of male rats

Univariate Tests of Significance for Pixel Total % (Spreadsheet61) Sigma-restricted parameterization Effective hypothesis decomposition					
Effect	SS	Degr. of Freedom	MS	F	p
Intercept	309747,6	1	309747,6	1047,72	0,00000(
Treatment	108,5	1	108,5	0,367	0,54946
Stress	3,4	1	3,4	0,011	0,91594(
Treatment*Stress	56,0	1	56,0	0,189	0,66672
Error	8277,9	28	295,6		

Table A5.118: Kruskal-Wallis analysis of ATP5A pixel percentage in the Prefrontal Cortex of male rats

	Multiple Comparisons p values (2-tailed); Pixel Total % (Spreadsheet1) Independent (grouping) variable: Group Kruskal-Wallis test: H (3, N= 32) =4,781250 p =,1885			
Depend.: Pixel Total %	Control R:11,500	MS R:16,375	EtOH R:21,750	EtOH+MS R:16,375
Control		1,00000(	0,17319{	1,00000(
MS	1,00000(		1,00000(	1,00000(
EtOH	0,17319{	1,00000(		1,00000(
EtOH+MS	1,00000(	1,00000(	1,00000(	

Table A5.119: Kruskal-Wallis analysis of ATP5A pixel percentage in the Dorsal Hippocampus of male rats

	Univariate Tests of Significance for Pixel Total % (Spreadsheet30) Sigma-restricted parameterization Effective hypothesis decomposition				
Effect	SS	Degr. of Freedom	MS	F	p
Intercept	328798,7	1	328798,7	757,5481	0,00000(
Treatment	43,3	1	43,3	0,0998	0,754447
Stress	153,5	1	153,5	0,3537	0,556815
Treatment*Stress	58,9	1	58,9	0,1358	0,715266
Error	12152,8	28	434,0		

Table A5.120: Western Blot Analysis in the PREFRONTAL CORTEX of FEMALE RATS - UN-SCAN-IT pixel density percentage - RAW DATA

Female Rats				Prefrontal Cortex										
Rat Number	Group	Treatment	Stress	P-ERK1/2 / Alpha Tubulin	ERK1/2 / Alpha Tubulin	P-ERK1/2 / ERK1/2	P-GSK3β / Alpha Tubulin	GSK3β / Alpha Tubulin	P-GSK3β / GSK3β	P-CREB / Alpha Tubulin	CREB / Alpha Tubulin	P-CREB / CREB	Synaptophysin / Alpha Tubulin	ATP5A / Alpha Tubulin
86	Control	Sacc	nMS	155,55	134,58	115,58	87,76	101,19	86,73	118,76	129,26	91,88	106,84	39,58
116	Control	Sacc	nMS	85,04	92,51	91,92	92,74	93,14	99,57	88,01	69,72	126,24	132,58	127,99
117	Control	Sacc	nMS	76,32	92,61	82,41	93,36	107,46	86,88	55,88	52,36	106,73	135,31	98,69
186	Control	Sacc	nMS	99,33	100,25	99,08	100,08	105,43	94,92	134,76	205,76	65,49	54,40	93,30
187	Control	Sacc	nMS	86,22	97,89	88,08	44,09	104,29	42,28	60,98	57,83	105,44	147,39	102,65
206	Control	Sacc	nMS	85,09	85,48	99,54	111,92	129,79	86,23	105,46	102,89	102,51	106,14	128,86
207	Control	Sacc	nMS	84,21	106,39	79,15	69,79	63,50	109,90	116,49	73,83	157,80	100,70	81,91
216	Control	Sacc	nMS	90,53	99,61	90,89	157,79	161,60	97,65	87,95	64,55	136,24	98,79	105,84
56	MS	Sacc	MS	99,46	98,61	100,86	102,40	108,56	94,33	92,56	90,60	102,16	44,90	112,86
57	MS	Sacc	MS	89,51	99,94	89,57	92,87	114,01	81,45	103,39	99,91	103,49	68,44	96,63
126	MS	Sacc	MS	74,61	89,59	83,28	96,65	128,63	75,14	56,86	68,39	83,15	85,18	89,76
127	MS	Sacc	MS	121,15	109,83	110,31	73,24	97,84	74,85	140,03	74,81	187,19	87,70	103,39
156	MS	Sacc	MS	93,87	98,28	95,51	114,17	96,62	118,16	94,03	120,36	78,13	123,49	101,68
157	MS	Sacc	MS	120,40	88,70	135,74	137,99	114,13	120,90	125,00	146,65	85,23	38,76	103,53
176	MS	Sacc	MS	93,49	106,35	87,91	94,30	69,27	136,14	119,04	112,13	106,16	127,10	93,07
177	MS	Sacc	MS	115,52	100,22	115,27	99,10	121,36	81,66	76,85			83,46	98,55
66	EtOH	EtOH	nMS	99,06	97,16	101,95	133,61	106,31	125,68	90,01	114,08	78,90	49,60	97,37
67	EtOH	EtOH	nMS	98,64	97,71	100,95	92,30	111,32	82,92	124,81	152,75	81,71	125,94	81,92
96	EtOH	EtOH	nMS	98,57	95,42	103,30	114,31	86,03	132,86	75,93	48,05	158,04	90,30	105,96
97	EtOH	EtOH	nMS	143,52	120,28	119,33	130,10	111,17	117,03	123,73	85,75	144,30	103,17	111,55
136	EtOH	EtOH	nMS	97,40	101,45	96,01	136,78	94,73	144,40	113,40	138,53	81,86	72,85	106,18
137	EtOH	EtOH	nMS	135,12	104,46	129,35	113,95	105,23	108,29	120,72	93,48	129,14	85,58	95,24
196	EtOH	EtOH	nMS	107,05	109,63	97,64	91,34	70,97	128,69	121,81	105,77	115,17	115,21	102,51
197	EtOH	EtOH	nMS	118,74	98,75	120,24	90,83	159,80	56,84	80,78			93,86	119,60
46	EtOH+MS	EtOH	MS	88,46	89,49	98,85	109,96	99,23	110,81	79,06	70,20	112,62	81,36	129,06
75	EtOH+MS	EtOH	MS				84,61	64,92	130,33	118,44	88,10	134,44	202,68	107,31
77	EtOH+MS	EtOH	MS	116,63	102,93	113,31	95,27	91,94	103,61	104,13	263,17	39,57	97,64	103,83
106	EtOH+MS	EtOH	MS	97,80	101,60	96,26	94,32	68,59	137,50	114,18	28,36	402,60	152,38	96,33
144	EtOH+MS	EtOH	MS	86,40	102,09	84,63	97,11	108,76	89,29	111,38	97,76	113,93	137,52	101,29
146	EtOH+MS	EtOH	MS	103,78	124,21	83,55	55,76	58,61	95,13	94,33	45,46	207,48	96,72	66,44
164	EtOH+MS	EtOH	MS	111,85	99,44	112,48	136,24	111,53	122,15	115,95	104,16	111,32	100,99	91,67
107	EtOH+MS	EtOH	MS	75,12	81,03	92,71	99,91	96,73	103,29	64,12			86,16	117,93

Table A5.121: Western Blot Analysis in the DORSAL HIPPOCAMPUS of FEMALE RATS - UN-SCAN-IT pixel density percentage - RAW DATA

Female Rats				Dorsal Hippocampus										
Rat Number	Group	Treatment	Stress	P-ERK1/2 / Alpha Tubulin	ERK1/2 / Alpha Tubulin	P-ERK1/2 / ERK1/2	P-GSK3β / Alpha Tubulin	GSK3β / Alpha Tubulin	P-GSK3β / GSK3β	P-CREB / Alpha Tubulin	CREB / Alpha Tubulin	P-CREB / CREB	Synaptophysin / Alpha Tubulin	ATP5A / Alpha Tubulin
86	Control	Sacc	nMS	71,58	104,31	68,62	102,19	77,09	132,55	98,11	90,95	107,87	92,96	112,28
116	Control	Sacc	nMS	105,11	111,18	94,54	105,07	127,58	82,36	107,07	125,78	85,12	90,07	98,79
117	Control	Sacc	nMS	88,74	97,82	90,71	92,28	84,17	109,64	84,61	59,25	142,81	95,43	110,94
186	Control	Sacc	nMS	105,88	113,27	93,47	77,32	84,06	91,98	94,02	121,56	77,34	87,94	112,79
187	Control	Sacc	nMS	114,79	88,87	129,16	126,46	76,29	165,77	77,12	71,10	108,48	171,86	91,17
206	Control	Sacc	nMS	79,08	122,23	64,70	92,66	80,19	115,56	99,92	77,25	129,34	72,56	112,86
207	Control	Sacc	nMS	64,36	82,05	78,45	106,71	101,58	105,05	97,45	77,23	126,18	105,54	118,07
216	Control	Sacc	nMS	132,84	119,55	111,12	96,27	119,05	80,86	92,03	143,02	64,34	99,76	84,01
56	MS	Sacc	MS	93,51	102,16	91,54	128,95	120,62	106,91	116,92	110,35	105,95	73,11	104,83
57	MS	Sacc	MS	106,03	95,56	110,96	49,93	52,47	95,15	108,95	120,88	90,13	81,91	86,03
126	MS	Sacc	MS	117,36	104,32	112,50	107,70	115,32	93,39	105,63	102,16	103,40	100,95	111,84
127	MS	Sacc	MS	111,08	103,05	107,79	80,25	96,76	82,94	117,95	166,79	70,72	110,14	95,85
156	MS	Sacc	MS	125,30	91,64	136,74	95,17	100,43	94,76	93,51	93,16	100,37	80,09	97,95
157	MS	Sacc	MS	106,51	119,63	89,03	103,29	102,93	100,36	107,57	93,27	115,33	56,89	88,01
176	MS	Sacc	MS	80,76	85,02	94,98	100,22	99,55	100,67	80,65	54,83	147,10	80,68	109,73
177	MS	Sacc	MS	113,32	106,57	106,34	97,41	106,13	91,79	108,90	166,99	65,21	129,54	77,64
66	EtOH	EtOH	nMS	103,03	96,97	106,25	145,62	92,12	158,08	102,88	106,74	96,38	76,89	118,53
67	EtOH	EtOH	nMS	121,53	85,89	141,50	76,37	153,67	49,69	100,53	100,68	99,85	122,21	83,36
96	EtOH	EtOH	nMS	93,36	98,09	95,18	119,44	95,16	125,52	105,72	77,43	136,53	114,14	102,09
97	EtOH	EtOH	nMS	94,60	90,45	104,59	118,98	109,00	109,16	117,75	169,87	69,32	96,23	92,72
136	EtOH	EtOH	nMS	100,83	90,23	111,74	99,88	98,69	101,20	88,19	90,28	97,69	79,36	98,93
137	EtOH	EtOH	nMS	90,00	105,51	85,30	117,17	100,62	116,44	141,78	187,13	75,77		100,08
196	EtOH	EtOH	nMS	94,16	91,85	102,51	130,64	88,98	146,82	96,91	54,13	179,04	58,62	107,83
197	EtOH	EtOH	nMS	118,56	107,22	110,58	92,54	118,12	78,35	127,81			120,16	87,87
46	EtOH+MS	EtOH	MS	105,69	115,65	91,39	118,86	104,08	114,21	94,29	120,33	78,36	108,40	95,46
75	EtOH+MS	EtOH	MS	95,85	87,54	109,49	81,80	94,95	86,15	75,35	30,83	244,39	160,63	104,83
77	EtOH+MS	EtOH	MS	104,57	103,55	100,99	90,52	78,93	114,70	76,82	59,74	128,59	105,81	93,15
106	EtOH+MS	EtOH	MS	85,95	90,63	94,83	105,61	108,64	97,21	107,47	76,33	140,79	89,67	86,94
144	EtOH+MS	EtOH	MS	112,24	103,68	108,26	81,17	117,41	69,13	86,09	115,06	74,82	88,35	108,72
146	EtOH+MS	EtOH	MS	64,82	90,05	71,98	103,14	128,22	80,44	126,42	93,12	135,76	155,09	103,59
164	EtOH+MS	EtOH	MS	118,86	115,18	103,20	101,83	110,92	91,80	82,14			69,04	118,30
107	EtOH+MS	EtOH	MS	94,11	103,42	91,00	76,95	98,73	77,94	130,97			136,86	93,61

Table A5.122: Shapiro-Wilk Test results for Western Blot analysis in the prefrontal cortex (PFC) and dorsal hippocampus (DH) of female rats.

Sex	Brain Area	Variable	Shapiro-Wilk, W	*P* Value
Female	PFC	P-ERK1/2	0,922	0,027
Female	PFC	ERK1/2	0,906	0,100
Female	PFC	P-ERK1/2 / ERK1/2	0,950	0,153
Female	PFC	P-GSK3β	0,953	0,183
Female	PFC	GSK3β	0,935	0,053
Female	PFC	P-GSK3β / GSK3β	0,976	0,691
Female	PFC	P-CREB	0,947	0,115
Female	PFC	CREB	0,883	0,004
Female	PFC	P-CREB/CREB	0,699	0,000
Female	PFC	Synaptophysin	0,962	0,321
Female	PFC	ATP5A	0,891	0,004
Female	DH	P-ERK1/2	0,974	0,617
Female	DH	ERK1/2	0,959	0,260
Female	DH	P-ERK1/2 / ERK1/2	0,958	0,244
Female	DH	P-GSK3β	0,978	0,736
Female	DH	GSK3β	0,976	0,675
Female	DH	P-GSK3β / GSK3β	0,949	0,133
Female	DH	P-CREB	0,971	0,518
Female	DH	CREB	0,961	0,339
Female	DH	P-CREB/CREB	0,874	0,002
Female	DH	Synaptophysin	0,939	0,077
Female	DH	ATP5A	0,965	0,395

Table A5.123: Kruskal-Wallis analysis of P-ERK1/2 in the prefrontal cortex of female rats

	Multiple Comparisons p values (2-tailed); P-ERK/Tubulin Pixel Total % (Spreadsheet1) Independent (grouping) variable: Group Kruskal-Wallis test: H (3, N= 31) =5,808828 p =,1213			
Depend.: P-ERK/Tubulin Pixel Total %	Control R:10,750	MS R:16,875	EtOH R:21,500	EtOH+MS R:14,714
Control		1,000000	0,108273	1,000000
MS	1,000000		1,000000	1,000000
EtOH	0,108273	1,000000		0,895738
EtOH+MS	1,000000	1,000000	0,895738	

Table A5.124: Kruskal-Wallis analysis of ERK1/2 in the prefrontal cortex of female rats

	Multiple Comparisons p values (2-tailed); ERK/Alpha Tubulin Pixel Total % (Spreadsheet7) Independent (grouping) variable: Group Kruskal-Wallis test: H (3, N= 31) =,5084965 p =,9170			
Depend.: ERK/Alpha Tubulin Pixel Total %	Control R:14,750	MS R:15,125	EtOH R:17,625	EtOH+MS R:16,571
Control		1,000000	1,000000	1,000000
MS	1,000000		1,000000	1,000000
EtOH	1,000000	1,000000		1,000000
EtOH+MS	1,000000	1,000000	1,000000	

Table A5.125: Two-way ANOVA and Duncan's post-hoc test results for P-ERK1/2 / ERK1/2 in the prefrontal cortex female rats

Univariate Tests of Significance for P-ERK/ERK Pixel Total % (Spreadsheet13)
Sigma-restricted parameterization
Effective hypothesis decomposition

Effect	SS	Degr. of Freedom	MS	F	p
Intercept	311492,7	1	311492,7	1681,08(	0,00000(
Treatment	207,3	1	207,3	1,119	0,299560
Stress	9,6	1	9,6	0,052	0,822015
Treatment*Stress	785,8	1	785,8	4,241	0,04922(
Error	5002,9	27	185,3		

Duncan test; variable P-ERK/ERK Pixel Total % (Spreadsheet13)
Approximate Probabilities for Post Hoc Tests
Error: Between MS = 185,29, df = 27,000

Cell No.	Treatment	Stress	{1} 93,331	{2} 102,30	{3} 108,60	{4} 97,399
1	Sacc	nMS		0,231821	0,051910	0,562017
2	Sacc	MS	0,231821		0,371811	0,484983
3	EtOH	nMS	0,051910	0,371811		0,137492
4	EtOH	MS	0,562017	0,484983	0,137492	

Table A5.126: Two-way ANOVA of P-ERK1/2 in the dorsal hippocampus of female rats

Univariate Tests of Significance for P-ERK/ Alpha Tubulin Pixel Total % (Spreadsheet25)
Sigma-restricted parameterization
Effective hypothesis decomposition

Effect	SS	Degr. of Freedom	MS	F	p
Intercept	322886,2	1	322886,2	1103,599	0,00000(
Treatment	10,2	1	10,2	0,035	0,852959
Stress	103,3	1	103,3	0,353	0,557103
Treatment*Stress	492,0	1	492,0	1,682	0,205280
Error	8192,1	28	292,6		

Table A5.127: Two-way ANOVA of total ERK1/2 in the dorsal hippocampus of female rats

Univariate Tests of Significance for ERK / Alpha Tubulin Pixel Total % (Spreadsheet30)
Sigma-restricted parameterization
Effective hypothesis decomposition

Effect	SS	Degr. of Freedom	MS	F	p
Intercept	324639,6	1	324639,6	2619,863	0,000000
Treatment	159,0	1	159,0	1,283	0,266884
Stress	4,6	1	4,6	0,037	0,848448
Treatment*Stress	174,8	1	174,8	1,411	0,244890
Error	3469,6	28	123,9		

Table A5.128: Two-way ANOVA and Duncan's post-hoc test results for P-ERK1/2 / ERK1/2 in the dorsal hippocampus female rats

Univariate Tests of Significance for P-ERK/ERK Pixel Total % (Spreadsheet35)
Sigma-restricted parameterization
Effective hypothesis decomposition

Effect	SS	Degr. of Freedom	MS	F	p
Intercept	321891,2	1	321891,2	1161,934	0,000000
Treatment	72,4	1	72,4	0,261	0,613139
Stress	33,2	1	33,2	0,120	0,731907
Treatment*Stress	1321,0	1	1321,0	4,768	0,037524
Error	7756,9	28	277,0		

Duncan test; variable P-ERK/ERK Pixel Total % (Spreadsheet35)
Approximate Probabilities for Post Hoc Tests
Error: Between MS = 277,03, df = 28,000

Cell No.	Treatment	Stress	{1} 91,347	{2} 106,23	{3} 107,21	{4} 96,393
1	Sacc	nMS		0,101000	0,090929	0,549374
2	Sacc	MS	0,101000		0,907901	0,247051
3	EtOH	nMS	0,090929	0,907901		0,230187
4	EtOH	MS	0,549374	0,247051	0,230187	

Table A5.129: Two-way ANOVA of P-GSK3β pixel total percentage in the prefrontal cortex of female rats

Univariate Tests of Significance for P-GSK/AT - Pixel Total % (Spreadsheet1)
Sigma-restricted parameterization
Effective hypothesis decomposition

Effect	SS	Degr. of Freedom	MS	F	p
Intercept	328993,2	1	328993,2	567,1178	0,000000
Treatment	365,5	1	365,5	0,6300	0,434014
Stress	184,6	1	184,6	0,3183	0,577146
Treatment*Stress	1049,2	1	1049,2	1,8086	0,189465
Error	16243,2	28	580,1		

Table A5.130: Two-way ANOVA of GSK3β pixel total percentage in the prefrontal cortex of female rats

Univariate Tests of Significance for GSK /AT - Pixel Total % (Spreadsheet10)
Sigma-restricted parameterization
Effective hypothesis decomposition

Effect	SS	Degr. of Freedom	MS	F	p
Intercept	332669,5	1	332669,5	594,1103	0,000000
Treatment	913,1	1	913,1	1,6308	0,212088
Stress	812,1	1	812,1	1,4503	0,238559
Treatment*Stress	522,2	1	522,2	0,9326	0,342463
Error	15678,5	28	559,9		

Table A5.131: Two-way ANOVA and Duncan's post-hoc analysis of P-GSK3β/GSK3β pixel total percentage in the prefrontal cortex of female rats

Univariate Tests of Significance for P-GSK/GSK - Pixel Total % (Spreadsheet1)
Sigma-restricted parameterization
Effective hypothesis decomposition

Effect	SS	Degr. of Freedom	MS	F	p
Intercept	335298,4	1	335298,4	635,9621	0,000000
Treatment	2850,7	1	2850,7	5,4069	0,027527
Stress	170,6	1	170,6	0,3235	0,574021
Treatment*Stress	215,6	1	215,6	0,4089	0,527706
Error	14762,4	28	527,2		

Duncan test; variable P-GSK/GSK - Pixel Total % (Spreadsheet1)
Approximate Probabilities for Post Hoc Tests
Error: Between MS = 527,23, df = 28,000

Cell No.	Treatment	{1} 92,924	{2} 111,80
1	Sacc		0,027650
2	EtOH	0,027650	

Table A5.132: Two-way ANOVA of P-GSK3β pixel total percentage in the dorsal hippocampus of female rats

Univariate Tests of Significance for P-GSK/AT Pixel Total % (Spreadsheet38)
Sigma-restricted parameterization
Effective hypothesis decomposition

Effect	SS	Degr. of Freedom	MS	F	p
Intercept	324495,7	1	324495,7	909,5685	0,000000
Treatment	304,1	1	304,1	0,8523	0,363799
Stress	976,6	1	976,6	2,7373	0,109196
Treatment*Stress	342,8	1	342,8	0,9609	0,335365
Error	9989,2	28	356,8		

Table A5.133: Two-way ANOVA of GSK3β pixel total percentage in the dorsal hippocampus of female rats

	Univariate Tests of Significance for GSK/Tubulin - Pixel Total % (Spreadsheet47) Sigma-restricted parameterization Effective hypothesis decomposition				
Effect	SS	Degr. of Freedom	MS	F	p
Intercept	328548,4	1	328548,4	881,7017	0,000000
Treatment	741,4	1	741,4	1,9896	0,169399
Stress	27,6	1	27,6	0,0741	0,787492
Treatment*Stress	107,7	1	107,7	0,2890	0,595112
Error	10433,6	28	372,6		

Table A5.134: Two-way ANOVA of P-GSK3β/GSK3β pixel total percentage in the dorsal hippocampus female rats

	Univariate Tests of Significance for P-GSK/GSK - Pixel Total % (Spreadsheet29) Sigma-restricted parameterization Effective hypothesis decomposition				
Effect	SS	Degr. of Freedom	MS	F	p
Intercept	333450,4	1	333450,4	564,0799	0,000000
Treatment	33,8	1	33,8	0,0572	0,812687
Stress	2303,1	1	2303,1	3,8960	0,058342
Treatment*Stress	40,2	1	40,2	0,0681	0,796086
Error	16551,9	28	591,1		

Table A5.135: Two-way ANOVA of P-CREB/α-tubulin in the prefrontal cortex of female rats

	Univariate Tests of Significance for P-CREB / Alpha Tubulin Pixel Total % (Spreadsheet1) Sigma-restricted parameterization Effective hypothesis decomposition				
Effect	SS	Degr. of Freedom	MS	F	p
Intercept	325800,7	1	325800,7	561,0451	0,000000
Treatment	184,1	1	184,1	0,3170	0,577901
Stress	3,2	1	3,2	0,0055	0,941271
Treatment*Stress	248,0	1	248,0	0,4270	0,518771
Error	16259,7	28	580,7		

Table A5.136: Kruskal-Wallis analysis of CREB/α-tubulin pixel total percentage in the prefrontal cortex of female rats

	Multiple Comparisons p values (2-tailed); Creb / Alpha Tubulin Pixel Total % (Spreadsheet10) Independent (grouping) variable: Group Kruskal-Wallis test: H (3, N= 29) =2,100246 p =,5519			
Depend.: Creb / Alpha Tubulin Pixel Total %	Control R:12,875	MS R:17,000	EtOH R:17,714	EtOH+MS R:12,714
Control		1,000000	1,000000	1,000000
MS	1,000000		1,000000	1,000000
EtOH	1,000000	1,000000		1,000000
EtOH+MS	1,000000	1,000000	1,000000	

Table A5.137: Two-way ANOVA of P-CREB/CREB pixel total percentage in the prefrontal cortex of female rats

Multiple Comparisons p values (2-tailed); P-CREB/CREB - Pixel Total % (Sprea
Independent (grouping) variable: Group
Kruskal-Wallis test: H (3, N= 29) =2,473892 p =,4800

Depend.: P-CREB/CREB - Pixel Total %	Control R:14,750	MS R:11,571	EtOH R:15,000	EtOH+MS R:18,714
Control		1,000000(	1,000000(	1,000000(
MS	1,000000(		1,000000(	0,699312
EtOH	1,000000(	1,000000(		1,000000(
EtOH+MS	1,000000(	0,699312	1,000000(	

Table A5.138: Two-way ANOVA and Duncan's post-hoc test results for P-CREB pixel total percentage in the dorsal hippocampus of female rats

Univariate Tests of Significance for P-CREB/Alpha Tubulin - Pixel Total % (Spreadsheet30)
Sigma-restricted parameterization
Effective hypothesis decomposition

Effect	SS	Degr. of Freedom	MS	F	p
Intercept	330387,1	1	330387,1	1279,995	0,000000
Treatment	156,4	1	156,4	0,606	0,442891
Stress	4,7	1	4,7	0,018	0,893601
Treatment*Stress	1149,2	1	1149,2	4,452	0,043921
Error	7227,2	28	258,1		

Duncan test; variable P-CREB/Alpha Tubulin - Pixel Total % (Spreadsheet1)
Approximate Probabilities for Post Hoc Tests
Error: Between MS = 258,12, df = 28,000

Cell No.	Treatment	Stress	{1} 93,790	{2} 105,01	{3} 110,20	{4} 97,445
1	Sacc	Contro		0,19774	0,07056	0,65279
2	Sacc	MS	0,19774		0,52379	0,35457
3	EtOH	Contro	0,07056	0,52379		0,14424
4	EtOH	MS	0,65279	0,35457	0,14424	

Table A5.139: Two-way ANOVA of CREB pixel total percentage in the dorsal hippocampus of female rats

Univariate Tests of Significance for CREB/Alpha Tubulin - Pixel Total % (Spreadsheet11)
Sigma-restricted parameterization
Effective hypothesis decomposition

Effect	SS	Degr. of Freedom	MS	F	p
Intercept	292011,7	1	292011,7	199,4434	0,000000
Treatment	372,1	1	372,1	0,2542	0,618565
Stress	255,9	1	255,9	0,1748	0,679455
Treatment*Stress	4038,9	1	4038,9	2,7586	0,109226
Error	36603,3	25	1464,1		

Table A5.140: Kruskal-Wallis analysis of P-CREB/CREB pixel total percentage in the dorsal hippocampus female rats

Multiple Comparisons p values (2-tailed); P-CREB/CREB - Pixel Total % (Spreadsheet2
Independent (grouping) variable: Group
Kruskal-Wallis test: H (3, N= 29) =1,431281 p =,6982

Depend.: P-CREB/CREB - Pixel Total %	Control R:15,000	MS R:13,375	EtOH R:13,857	EtOH+MS R:18,500
Control		1,000000(	1,000000(	1,000000(
MS	1,000000(		1,000000(	1,000000(
EtOH	1,000000(	1,000000(		1,000000(
EtOH+MS	1,000000(	1,000000(	1,000000(	

Table A5.141: Two-way ANOVA and Duncan's post-hoc test results for Synaptophysin pixel total percentage in the prefrontal cortex of female rats

Univariate Tests of Significance for Synap/ Alpha Tubulin - Pixel Total % (Spreadsheet120)
Sigma-restricted parameterization
Effective hypothesis decomposition

Effect	SS	Degr. of Freedom	MS	F	p
Intercept	326663,1	1	326663,1	311,5109	0,000000
Treatment	710,6	1	710,6	0,6776	0,417371
Stress	0,5	1	0,5	0,0005	0,982022
Treatment*Stress	6107,5	1	6107,5	5,8243	0,022598
Error	29361,9	28	1048,6		

Duncan test; variable Synap/ Alpha Tubulin - Pixel Total % (Spreadsheet120)
Approximate Probabilities for Post Hoc Tests
Error: Between MS = 1048,6, df = 28,000

Cell No.	Treatment	Stress	{1} 110,27	{2} 82,378	{3} 92,063	{4} 119,43
1	Sacc	Contro		0,113856	0,270501	0,576041
2	Sacc	Stress	0,113856		0,554684	0,043561
3	EtOH	Contro	0,270501	0,554684		0,120573
4	EtOH	Stress	0,576041	0,043561	0,120573	

Table A5.142: Two-way ANOVA of Synaptophysin pixel total percentage in the dorsal hippocampus of female rats

Univariate Tests of Significance for Synaptophysin/Alpha tubulin - Pixel Total % (Spreadsheet144)
Sigma-restricted parameterization
Effective hypothesis decomposition

Effect	SS	Degr. of Freedom	MS	F	p
Intercept	310181,1	1	310181,1	392,5017	0,000000
Treatment	655,5	1	655,5	0,8295	0,370469
Stress	69,7	1	69,7	0,0882	0,768705
Treatment*Stress	1941,5	1	1941,5	2,4567	0,128668
Error	21337,2	27	790,3		

Table A5.143: Kruskal-Wallis analysis of ATP5A pixel total percentage in the prefrontal cortex of female rats

Multiple Comparisons p values (2-tailed); Pixel Total % (Spreadsheet1)
Independent (grouping) variable: Group
Kruskal-Wallis test: H (3, N= 32) =,5880682 p =,8992

Depend.: Pixel Total %	Control R:15,875	MS R:14,750	EtOH R:18,000	EtOH+MS R:17,375
Control		1,000000	1,000000	1,000000
MS	1,000000		1,000000	1,000000
EtOH	1,000000	1,000000		1,000000
EtOH+MS	1,000000	1,000000	1,000000	

Table A5.144: Two-way ANOVA of ATP5A pixel total percentage in the dorsal hippocampus of female rats

Univariate Tests of Significance for A/T Pixel Total % (Spreadsheet11)
Sigma-restricted parameterization
Effective hypothesis decomposition

Effect	SS	Degr. of Freedom	MS	F	p
Intercept	321759,4	1	321759,4	2452,531	0,000000
Treatment	8,8	1	8,8	0,067	0,797133
Stress	97,4	1	97,4	0,742	0,396240
Treatment*Stress	211,1	1	211,1	1,609	0,215030
Error	3673,5	28	131,2		

EXPLORATORY PAIRWISE CORRELATIONS

Table A5.145: Exploratory pairwise correlations within behavioural measures.

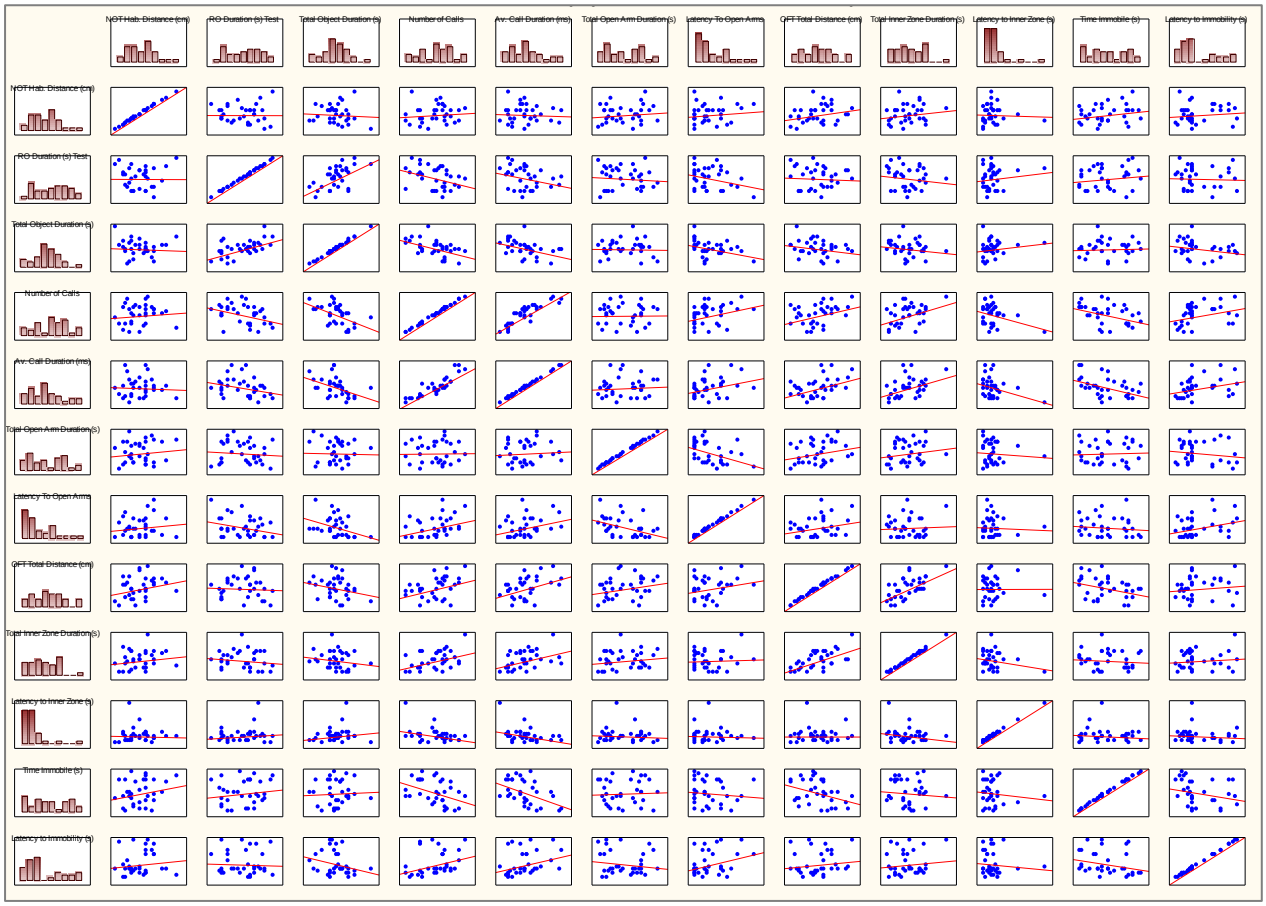

Table A5.146: Exploratory pairwise correlations within neurochemical measures of male rats.

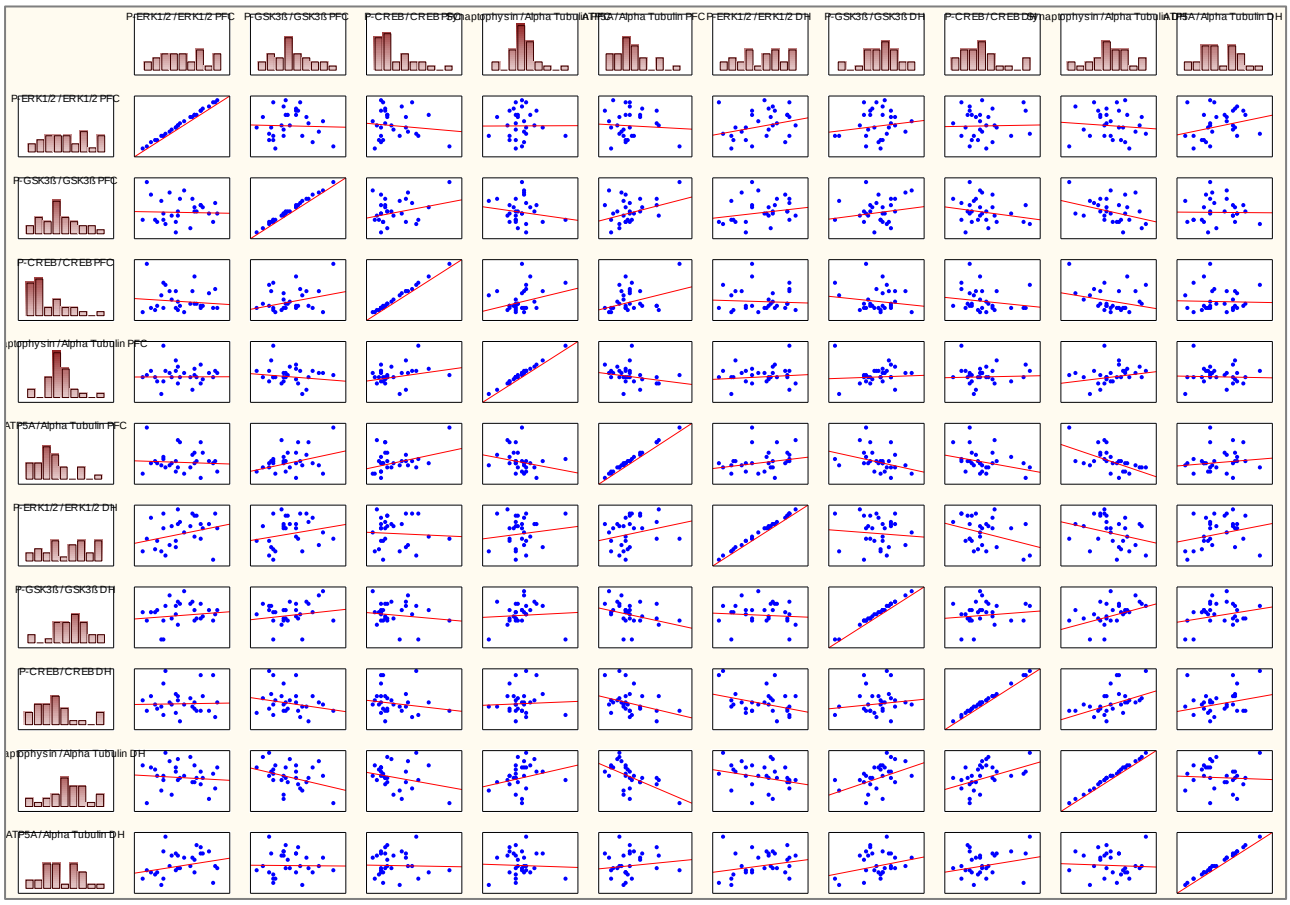

Table A5.147: Exploratory pairwise correlations within neurochemical measures of female rats.

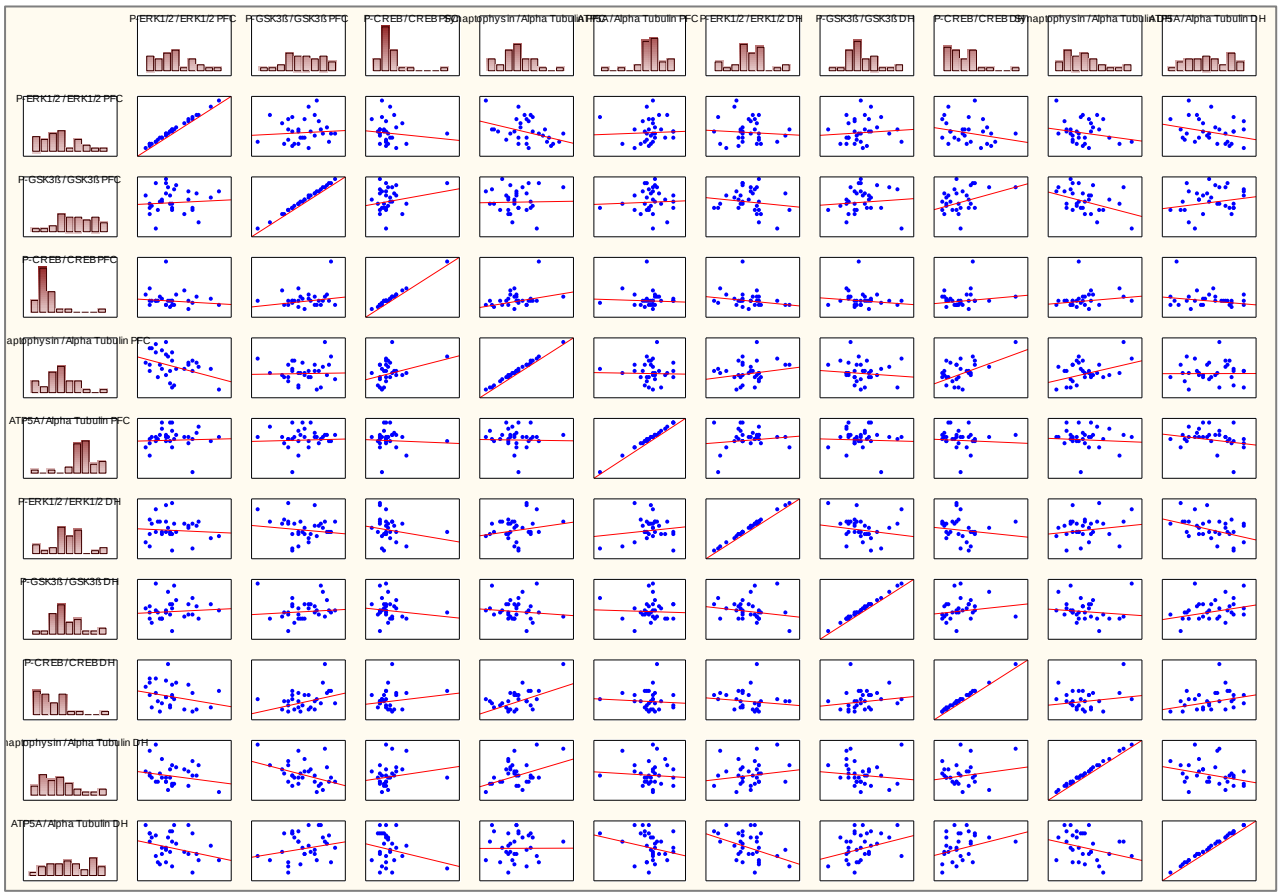

A6: CHAPTER 6

NETWORK ANALYSIS OF SIGNIFCANTLY CHANGED PROTEINS (> 2-FOLD)

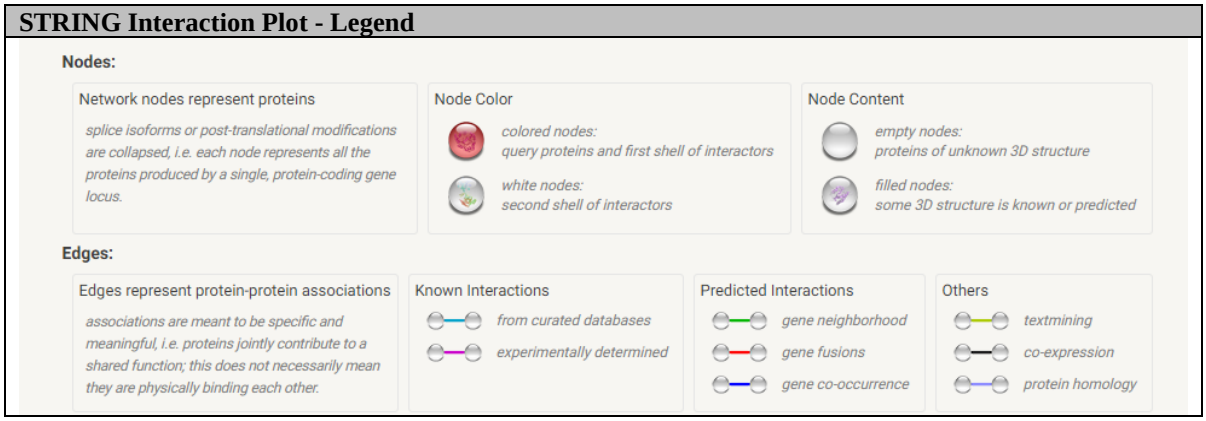

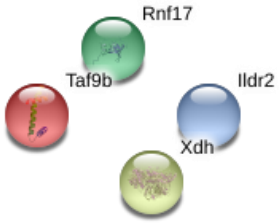

Figure A6.1: Protein-protein interaction plot of the significantly changed proteins (> 2-fold) in the PFC of EtOH-rats versus controls. No significant interactions were observed.

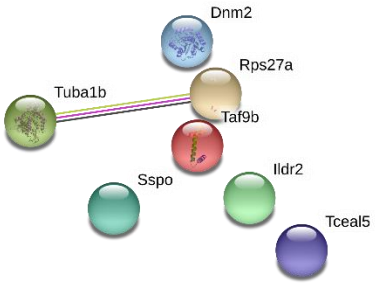

Figure A6.2: Protein-protein interaction plot of the significantly changed proteins (> 2-fold) in the PFC of EtOH+MS-rats versus controls. No significant interactions were observed.

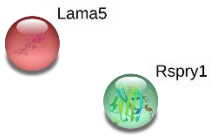

Figure A6.3 Protein-protein interaction plot of the significantly changed proteins (> 2-fold) in the DH of MS-rats versus controls. No significant interactions were observed.

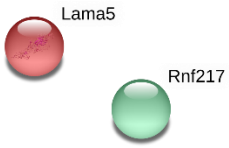

Figure A6.4 Protein-protein interaction plot of the significantly changed proteins (> 2-fold) in the DH of EtOH+MS-rats versus controls. No significant interactions were observed.

Table A6.5: Full list of proteins altered by prenatal-ethanol exposure (fold change > 1.2) in the *dorsal hippocampus* of EtOH-rats

DH	Category	Protein	Accession no.	Cov (%)	Pep	Control : Control	EtOH : Control	Fold △	
	Energy metabolism	**ATP synthase subunit delta, mitochondrial**	**G3V7Y3_RAT**	**48,81**	**11**	**1,000**	**2,769**	**2,769**	↑
		Acyl carrier protein	**D3ZF13_RAT**	**13,46**	**3**	**1,000**	**2,661**	**2,661**	↑
		Cytochrome c, somatic	**CYC_RAT**	**69,52**	**32**	**1,000**	**2,211**	**2,211**	↑
		Acyl-CoA-binding protein	**Q6TXF3_RAT**	**6,00**	**11**	**1,000**	**2,027**	**2,027**	↑
		Gene - DLST - dihydrolipoamide S-succinyltransferase	Q8CJG5_RAT	23,13	16	1,000	1,886	1,886	↑
		Gamma-enolase	ENOG_RAT	63,36	66	1,000	1,770	1,770	↑
		Transketolase	TKT_RAT	49,12	40	1,000	1,674	1,674	↑
		Glycogenin-1 (Fragment)	F8WFR6_RAT	7,25	2	1,000	1,458	1,458	↑
		Cytochrome c oxidase subunit 5A, mitochondrial	COX5A_RAT	41,78	7	1,000	1,383	1,383	↑
		Fatty acid-binding protein, heart	FABPH_RAT	61,65	10	1,000	1,338	1,338	↑
		Long-chain-fatty-acid--CoA ligase ACSBG1	ACBG1_RAT	4,44	3	1,000	1,335	1,335	↑
		6-phosphofructokinase	C7C5T2_RAT	33,38	51	1,000	1,315	1,315	↑
		Cytochrome b-c1 complex subunit 1, mitochondrial	QCR1_RAT	7,08	3	1,000	1,296	1,296	↑
		3-ketoacyl-CoA thiolase, mitochondrial	G3V9U2_RAT	9,60	2	1,000	1,279	1,279	↑
		ATP synthase-coupling factor 6, mitochondrial	ATP5J_RAT	35,19	4	1,000	1,236	1,236	↑
		Acyl-CoA thioesterase 7, isoform CRA_a	F8WG67_RAT	35,48	18	1,000	1,220	1,220	↑
		6-phosphofructokinase	Q6P783_RAT	25,51	13	1,000	1,217	1,217	↑
		L-lactate dehydrogenase	B5DEN4_RAT	48,49	35	1,000	0,506	1,977	↓
		Glucose-6-phosphate isomerase	G6PI_RAT	18,10	3	1,000	0,537	1,862	↓
		Creatine kinase B-type	KCRB_RAT	64,04	79	1,000	0,621	1,609	↓
		Glyceraldehyde-3-phosphate dehydrogenase	G3P_RAT	58,26	54	1,000	0,625	1,599	↓
		Phosphoglycerate kinase 1	PGK1_RAT	57,79	72	1,000	0,640	1,563	↓
		Pyruvate kinase PKM	KPYM_RAT	59,51	85	1,000	0,645	1,551	↓
		Glycerol-3-phosphate dehydrogenase [NAD(+)], cytoplasmic	GPDA_RAT	11,46	4	1,000	0,649	1,541	↓
		Hexokinase-1	HXK1_RAT	22,88	30	1,000	0,687	1,456	↓

DH	Category	Protein	Accession no.	Cov (%)	Pep	Control : Control	EtOH : Control	Fold △	
	Energy metabolism (cont.)	Citrate synthase	G3V936_RAT	41,20	32	1,000	0,706	1,416	↓
		Isoform M2 of Pyruvate kinase PKM	KPYM_RAT	59,32	4	1,000	0,715	1,398	↓
		Alpha-1,4 glucan phosphorylase	B1WBU9_RAT	27,91	17	1,000	0,730	1,369	↓
		Acad9 protein -Acyl-CoA dehydrogenase family member 9	B1WC61_RAT	6,08	4	1,000	0,732	1,365	↓
		ATP synthase subunit alpha	F1LP05_RAT	48,82	45	1,000	0,733	1,365	↓
		Pdhx protein (Fragment) - Pyruvate dehydrogenase complex component X	Q5BJX2_RAT	5,26	2	1,000	0,744	1,345	↓
		Ab2-076 - Acetyl-CoA Acetyltransferase 2	Q7TP61_RAT	7,58	5	1,000	0,748	1,337	↓
		Phosphoglucomutase 1	Q499Q4_RAT	38,08	23	1,000	0,751	1,331	↓
		Fumarate hydratase 1	Q5M964_RAT	41,42	24	1,000	0,755	1,325	↓
		Acyl-CoA thioesterase 9	Q5U2X8_RAT	19,82	6	1,000	0,757	1,320	↓
		Malate dehydrogenase, cytoplasmic	MDHC_RAT	34,13	2	1,000	0,760	1,316	↓
		Fructose-bisphosphate aldolase C	ALDOC_RAT	75,48	42	1,000	0,761	1,314	↓
		Mitochondrial 2-oxoglutarate/malate carrier protein	G3V6H5_RAT	22,61	5	1,000	0,764	1,308	↓
		Pyruvate dehydrogenase E1 component subunit beta, mitochondrial	ODPB_RAT	35,93	25	1,000	0,781	1,281	↓
		NADP-dependent malic enzyme	MAOX_RAT	19,23	8	1,000	0,783	1,278	↓
		Cytochrome c oxidase subunit 2	B0FTB8_RATLE	17,62	4	1,000	0,798	1,253	↓
	Redox regulation	**Lactoylglutathione lyase**	**LGUL_RAT**	**52,72**	**11**	**1,000**	**2,703**	**2,703**	↑
		Superoxide dismutase [Mn], mitochondrial	**SODM_RAT**	**52,25**	**21**	**1,000**	**2,147**	**2,147**	↑
		Superoxide dismutase [Cu-Zn]	**Q6LDS4_RAT**	**32,89**	**7**	**1,000**	**2,137**	**2,137**	↑
		Thioredoxin (Fragment)	**R4GNK3_RAT**	**31,73**	**12**	**1,000**	**2,024**	**2,024**	↑
		Ac1002	Q7TQ90_RAT	8,03	8	1,000	1,730	1,730	↑
		Peroxiredoxin-2	PRDX2_RAT	18,69	8	1,000	1,668	1,668	↑
		Copper transport protein ATOX1	ATOX1_RAT	32,35	4	1,000	1,657	1,657	↑
		Glutathione S-transferase omega 1	B6DYQ5_RAT	26,97	10	1,000	1,559	1,559	↑
		Peroxiredoxin-1	PRDX1_RAT	49,75	22	1,000	1,475	1,475	↑
		Isoform 2 of Hydroxyacylglutathione hydrolase, mitochondrial	GLO2_RAT	8,85	3	1,000	1,374	1,374	↑
		Peroxiredoxin 3	G3V7I0_RAT	33,07	21	1,000	1,255	1,255	↑
		Protein Mgst3 - Microsomal glutathione S-transferase 3	D4ADS4_RAT	17,76	2	1,000	0,670	1,493	↓
		Glutathione S-transferase Yb-3	GSTM4_RAT	47,25	16	1,000	0,731	1,369	↓

DH	Category	Protein	Accession no.	Cov (%)	Pep	Control : Control	EtOH : Control	Fold △	
	Redox regulation (cont.)	Glutathione S-transferase pi	B6DYQ7_RAT	47,14	11	1,000	0,767	1,304	↓
		Peroxiredoxin-5, mitochondrial (Fragment)	D3ZEN5_RAT	47,83	15	1,000	0,792	1,263	↓
	Neurotransmission / signalling	**Aspartate aminotransferase, cytoplasmic**	**AATC_RAT**	**64,65**	**57**	**1,000**	**2,045**	**2,045**	↑
		Complexin-1	CPLX1_RAT	39,55	12	1,000	1,978	1,978	↑
		ATP-dependent (S)-NAD(P)H-hydrate dehydratase	D3ZLK9_RAT	12,84	3	1,000	1,970	1,970	↑
		Protein S100-B	S100B_RAT	40,22	22	1,000	1,961	1,961	↑
		Na(+)/H(+) exchange regulatory cofactor NHE-RF1	NHRF1_RAT	10,39	4	1,000	1,946	1,946	↑
		Protein Pkn3 - Protein kinase N3	D3ZC07_RAT	6,89	5	1,000	1,849	1,849	↑
		Receptor-type tyrosine-protein phosphatase zeta	PTPRZ_RAT	9,28	27	1,000	1,767	1,767	↑
		Neurogranin	NEUG_RAT	55,13	8	1,000	1,730	1,730	↑
		Voltage-gated potassium channel subunit beta-2	KCAB2_RAT	20,16	6	1,000	1,730	1,730	↑
		Protein Pgp - Glycerol-3-phosphate phosphatase	D3ZDK7_RAT	8,72	2	1,000	1,700	1,700	↑
		Adenine phosphoribosyltransferase	APT_RAT	30,00	6	1,000	1,668	1,668	↑
		Calretinin	CALB2_RAT	15,50	2	1,000	1,659	1,659	↑
		Astrocytic phosphoprotein PEA-15	PEA15_RAT	44,62	11	1,000	1,644	1,644	↑
		EF-hand domain-containing protein D2	EFHD2_RAT	41,00	12	1,000	1,604	1,604	↑
		Calbindin	CALB1_RAT	49,04	15	1,000	1,571	1,571	↑
		Isoform 2 of Alpha-endosulfine	ENSA_RAT	53,85	5	1,000	1,571	1,571	↑
		Calmodulin	CALM_RAT	69,13	35	1,000	1,538	1,538	↑
		Neuromodulin (signalling)	NEUM_RAT	71,68	22	1,000	1,531	1,531	↑
		Myristoylated alanine-rich C-kinase substrate	MARCS_RAT	44,98	12	1,000	1,515	1,515	↑
		Protein Prkcsh - Protein kinase C substrate 80K-H	B1WC34_RAT	8,57	6	1,000	1,495	1,495	↑
		Sn1-specific diacylglycerol lipase beta	DGLB_RAT	2,10	2	1,000	1,472	1,472	↑
		Amyloid beta A4 protein	A4_RAT	6,10	5	1,000	1,447	1,447	↑
		Purkinje cell protein 4	PCP4_RAT	27,42	13	1,000	1,443	1,443	↑
		Serine/threonine-protein phosphatase 2B catalytic subunit alpha isoform	PP2BA_RAT	38,00	43	1,000	1,430	1,430	↑
		Protein Aimp1 - Aminoacyl tRNA synthetase complex-interacting multifunctional protein 1	Q4G079_RAT	10,79	2	1,000	1,424	1,424	↑
		Calcineurin subunit B type 1	CANB1_RAT	51,18	24	1,000	1,413	1,413	↑

DH	Category	Protein	Accession no.	Cov (%)	Pep	Control : Control	EtOH : Control	Fold △	
	Neurotransmission / signalling(cont.)	Serine/threonine-protein phosphatase PP1-gamma catalytic subunit	PP1G_RAT	23,84	6	1,000	1,410	1,410	↑
		Ras-related protein Ral-A	RALA_RAT	31,55	7	1,000	1,396	1,396	↑
		Synaptopodin	SYNPO_RAT	10,10	8	1,000	1,373	1,373	↑
		ProSAAS	PCSK1_RAT	30,38	7	1,000	1,369	1,369	↑
		Protein Psd3 - Pleckstrin and Sec7 domain-containing 3	D3ZFY7_RAT	8,74	7	1,000	1,360	1,360	↑
		Guanine deaminase	Q9JKB7_RAT	42,51	43	1,000	1,352	1,352	↑
		Protein Srgap3 - slit-robo rho GTPase activating protein	F1M5M9_RAT	2,46	2	1,000	1,344	1,344	↑
		Inosine triphosphate pyrophosphatase	ITPA_RAT	34,85	12	1,000	1,305	1,305	↑
		B-cell CLL/lymphoma 6	B2GUV8_RAT	2,26	2	1,000	1,299	1,299	↑
		Serine/threonine-protein phosphatase 2B catalytic subunit beta isoform	PP2BB_RAT	29,90	9	1,000	1,293	1,293	↑
		Synaptogyrin-1	SNG1_RAT	10,26	4	1,000	1,279	1,279	↑
		Protein kinase C and casein kinase substrate in neurons protein 1	PACN1_RAT	37,19	29	1,000	1,276	1,276	↑
		Protein Eea1 (Fragment) - Early endosome antigen 1	F1LUA1_RAT	3,40	5	1,000	1,263	1,263	↑
		Protein Ranbp1 - RAN-binding protein 1	D4A2G9_RAT	10,84	2	1,000	1,257	1,257	↑
		14-3-3 protein gamma	1433G_RAT	63,56	22	1,000	1,248	1,248	↑
		COP9 signalosome complex subunit 8	CSN8_RAT	23,44	3	1,000	1,247	1,247	↑
		Sirpa protein - signal-regulatory protein alpha	Q499T3_RAT	10,72	4	1,000	1,242	1,242	↑
		Rabphilin-3A	F1LPB9_RAT	14,91	10	1,000	1,233	1,233	↑
		Sodium/calcium exchanger 2	F1M9A2_RAT	10,11	9	1,000	1,223	1,223	↑
		Protein Rab6b - RAB6B, member RAS oncogene family	F1LVC3_RAT	33,71	3	1,000	1,217	1,217	↑
		Syntaxin 1A	Q9QXG3_RAT	31,25	11	1,000	1,215	1,215	↑
		Importin 7 (Predicted), isoform CRA_c	D4AE96_RAT	2,60	2	1,000	1,206	1,206	↑
		Neurocalcin-delta	NCALD_RAT	33,16	7	1,000	1,204	1,204	↑
		Protein Rab5b	A1L1J8_RAT	25,58	4	1,000	1,200	1,200	↑
		Protein Nbea - neurobeachin (Fragment)	F1LXU4_RAT	1,59	2	1,000	0,611	1,638	↓
		Protein Atp6v1h - ATPase H+-transporting V1 subunit H	E9PTI1_RAT	24,04	12	1,000	0,614	1,629	↓
		Serine/threonine-protein phosphatase 2A activator	B2RYQ2_RAT	23,53	7	1,000	0,632	1,582	↓
		14-3-3 protein theta	1433T_RAT	48,98	21	1,000	0,644	1,554	↓

DH	Category	Protein	Accession no.	Cov (%)	Pep	Control : Control	EtOH : Control	Fold △	
	Neurotransmission / signalling(cont.)	Calcium/calmodulin-dependent protein kinase type II subunit beta	F1LNI8_RAT	26,83	14	1,000	0,649	1,542	↓
		UDP-N-acetylglucosamine--peptide N-acetylglucosaminyltransferase 110 kDa subunit	OGT1_RAT	4,05	3	1,000	0,653	1,531	↓
		Vacuolar protein sorting-associated protein 35	G3V8A5_RAT	17,96	11	1,000	0,662	1,511	↓
		Beta-arrestin-1	ARRB1_RAT	10,53	5	1,000	0,663	1,508	↓
		14-3-3 protein beta/alpha	1433B_RAT	67,89	25	1,000	0,665	1,504	↓
		V-type proton ATPase subunit C 1	VATC1_RAT	40,05	19	1,000	0,684	1,462	↓
		14-3-3 protein eta	1433F_RAT	57,72	28	1,000	0,692	1,445	↓
		Synapsin-2 OS=Rattus norvegicus GN=Syn2 PE=1 SV=1	SYN2_RAT	52,22	45	1,000	0,709	1,410	↓
		Calcium binding protein 39 (Predicted), isoform CRA_a	D3ZJ77_RAT	13,78	2	1,000	0,711	1,407	↓
		Galectin	B4F7A3_RAT	30,81	4	1,000	0,715	1,399	↓
		Rab GDP dissociation inhibitor beta	GDIB_RAT	55,28	26	1,000	0,721	1,388	↓
		Hsc70-interacting protein	F10A1_RAT	10,87	6	1,000	0,742	1,348	↓
		14-3-3 protein zeta/delta	1433Z_RAT	73,88	59	1,000	0,752	1,331	↓
		Serine/threonine-protein kinase PAK 3	PAK3_RAT	17,83	4	1,000	0,752	1,330	↓
		Protein Ank2 (Fragment)	F1M9N9_RAT	10,97	3	1,000	0,759	1,318	↓
		ADP-ribosylation factor 1	ARF1_RAT	54,70	31	1,000	0,767	1,304	↓
		MAP2K4delta	S4VP54_RAT	5,39	2	1,000	0,769	1,301	↓
		Isoform 2 of Mitogen-activated protein kinase 3	MK03_RAT	17,24	2	1,000	0,772	1,296	↓
		Phospholipase D3	PLD3_RAT	6,76	2	1,000	0,780	1,283	↓
		Protein Asmtl - Acetylserotonin O-methyltransferase-like	D4AA35_RAT	13,72	2	1,000	0,792	1,263	↓
	Protein synthesis	**Histone H4**	**H4_RAT**	**63,11**	**30**	**1,000**	**2,473**	**2,473**	↑
		Protein Hnrnpab - Heterogeneous nuclear ribonucleoprotein A/B	Q9QX81_RAT	18,37	8	1,000	1,940	1,940	↑
		Protein Tceal5 - transcription elongation factor A-like 5, isoform CRA_a	M0RDJ7_RAT	20,00	4	1,000	1,868	1,868	↑
		Ubiquitin-40S ribosomal protein S27a	RS27A_RAT	19,23	4	1,000	1,864	1,864	↑
		Histone H3	D3ZJ08_RAT	23,53	4	1,000	1,820	1,820	↑
		Far upstream element-binding protein 2	M0R961_RAT	8,60	4	1,000	1,783	1,783	↑
		Protein LOC684828	M0R7B4_RAT	17,39	8	1,000	1,766	1,766	↑
		Brain acid soluble protein 1	BASP1_RAT	68,64	37	1,000	1,762	1,762	↑

DH	Category	Protein	Accession no.	Cov (%)	Pep	Control : Control	EtOH : Control	Fold △	
	Protein synthesis (cont.)	Caprin-1	CAPR1_RAT	2,69	3	1,000	1,708	1,708	↑
		Hepatoma-derived growth factor	F1LPC7_RAT	20,86	2	1,000	1,702	1,702	↑
		RNA-binding motif protein, X chromosome retrogene-like	RMXRL_RAT	14,43	7	1,000	1,701	1,701	↑
		Nucleobindin-1	NUCB1_RAT	12,42	4	1,000	1,664	1,664	↑
		Single-stranded DNA-binding protein	G3V7K6_RAT	22,30	2	1,000	1,632	1,632	↑
		Psip1 protein - PC4 and SFRS1-interacting protein	Q566D6_RAT	12,08	2	1,000	1,583	1,583	↑
		Histone H1.5	H15_RAT	18,47	4	1,000	1,529	1,529	↑
		Histone H1.0	H10_RAT	11,86	2	1,000	1,521	1,521	↑
		Protein LOC689899 - Uncharacterized protein	D3ZTH8_RAT	34,62	5	1,000	1,489	1,489	↑
		Heterogeneous nuclear ribonucleoprotein D, isoform CRA_b	G3V6A4_RAT	17,43	8	1,000	1,472	1,472	↑
		Calumenin	G3V6S3_RAT	11,11	2	1,000	1,466	1,466	↑
		LOC687565 protein - Density-regulated protein	B0BNB2_RAT	13,40	2	1,000	1,452	1,452	↑
		Protein Srsf1 - serine/arginine-rich splicing factor	D4A9L2_RAT	14,11	4	1,000	1,447	1,447	↑
		Eukaryotic translation initiation factor 3 subunit B	EIF3B_RAT	3,26	2	1,000	1,371	1,371	↑
		Protein LZIC - Leucine zipper and CTNNBIP1 domain containing	LZIC_RAT	17,37	2	1,000	1,326	1,326	↑
		40S ribosomal protein S9	RS9_RAT	8,25	2	1,000	1,291	1,291	↑
		60S ribosomal protein L17	RL17_RAT	21,74	3	1,000	1,266	1,266	↑
		Transcriptional activator protein Pur-beta	PURB_RAT	48,57	9	1,000	1,226	1,226	↑
		AXIN1 up-regulated 1 (Predicted)	D4AAK3_RAT	0,00	3	1,000	1,225	1,225	↑
		Protein Chmp4bl1 - Chromatin-modifying protein 4B-like 1	D4A9Z8_RAT	13,39	2	1,000	1,220	1,220	↑
		Protein Chmp4bl1 - Chromatin-modifying protein 4B-like 1	D4A9Z8_RAT	13,39	2	1,000	1,220	1,220	↑
		60S ribosomal protein L18	**RL18_RAT**	**13,83**	**3**	**1,000**	**0,038**	**26,178**	↓
		Protein RGD1563570 - ribosomal protein S23-like	**D3Z9X6_RAT**	**14,15**	**3**	**1,000**	**0,316**	**3,168**	↓
		Transcription initiation factor TFIID subunit 9B	**TAF9B_RAT**	**6,20**	**2**	**1,000**	**0,452**	**2,214**	↓
		Peptidyl-prolyl cis-trans isomerase B	PPIB_RAT	12,96	3	1,000	0,567	1,765	↓
		Profilin	D3ZDU5_RAT	48,65	17	1,000	0,613	1,630	↓
		Profilin-1	PROF1_RAT	65,00	26	1,000	0,651	1,536	↓
		Protein Cct7 - Chaperonin-containing TCP1 subunit 7	D4AC23_RAT	14,71	7	1,000	0,664	1,507	↓

DH	Category	Protein	Accession no.	Cov (%)	Pep	Control : Control	EtOH : Control	Fold △	
	Protein synthesis (cont.)	Peptidyl-prolyl cis-trans isomerase A	PPIA_RAT	42,07	24	1,000	0,680	1,470	↓
		Elongation factor 1-gamma	EF1G_RAT	20,37	12	1,000	0,723	1,384	↓
		40S ribosomal protein S10	RS10_RAT	23,64	3	1,000	0,725	1,380	↓
		Rps16 protein - ribosomal protein S16 (Fragment)	B0K038_RAT	13,13	2	1,000	0,729	1,372	↓
		Protein Nt5dc3 - 5'-nucleotidase domain-containing 3	D3ZAI6_RAT	14,84	7	1,000	0,735	1,361	↓
		Lupus La protein homolog	Q66HM7_RAT	5,78	2	1,000	0,737	1,357	↓
		Protein Wfs1 - Wolframin ER transmembrane glyoprotein	E9PT53_RAT	8,43	5	1,000	0,739	1,353	↓
		Cytoplasmic FMR1 interacting protein 1 (Predicted)	D4A8H8_RAT	7,18	11	1,000	0,750	1,334	↓
		Protein Tardbp	I6L9G6_RAT	8,07	3	1,000	0,755	1,324	↓
		Elongation factor 1-alpha 2	EF1A2_RAT	43,41	40	1,000	0,760	1,316	↓
		Protein Scai	F1M3P6_RAT	12,71	8	1,000	0,768	1,303	↓
		Bifunctional purine biosynthesis protein PURH	PUR9_RAT	27,36	14	1,000	0,780	1,282	↓
		Histidine triad nucleotide-binding protein 1	HINT1_RAT	35,71	8	1,000	0,785	1,274	↓
		40S ribosomal protein S12	RS12_RAT	6,06	2	1,000	0,787	1,271	↓
		Protein Nars - Asparaginyl-tRNA synthetase	F1LPV0_RAT	7,35	3	1,000	0,791	1,264	↓
		Protein LOC681195 - similar to ribosomal protein L21	D3ZZH9_RAT	20,63	3	1,000	0,793	1,261	↓
		60S ribosomal protein L12	RL12_RAT	15,15	2	1,000	0,797	1,254	↓
	Protein degradation	**Aspartyl aminopeptidase**	**Q4V8H5_RAT**	**7,58**	**4**	**1,000**	**2,161**	**2,161**	↑
		Calpastatin	D3ZL24_RAT	11,03	4	1,000	1,592	1,592	↑
		Cytosolic non-specific dipeptidase	CNDP2_RAT	26,74	15	1,000	1,565	1,565	↑
		Aminoacylase-1A	ACY1A_RAT	16,18	5	1,000	1,539	1,539	↑
		Alpha-1-inhibitor 3	A1I3_RAT	12,32	16	1,000	1,481	1,481	↑
		26S protease regulatory subunit 7	G3V7L6_RAT	9,70	3	1,000	1,460	1,460	↑
		Alpha-1-macroglobulin	A1M_RAT	3,80	6	1,000	1,379	1,379	↑
		Clusterin	CLUS_RAT	9,62	3	1,000	1,353	1,353	↑
		Ubiquitin carboxyl-terminal hydrolase isozyme L1	UCHL1_RAT	47,53	30	1,000	1,258	1,258	↑
		Isoform 2 of Basigin	BASI_RAT	10,66	2	1,000	1,222	1,222	↑
		Antisecretory factor	O88321_RAT	9,74	2	1,000	1,218	1,218	↑

DH	Category	Protein	Accession no.	Cov (%)	Pep	Control : Control	EtOH : Control	Fold △	
	Protein degradation (cont.)	Ubiquitin carboxyl-terminal hydrolase	D4ABI6_RAT	21,74	3	1,000	1,218	1,218	↑
		Protein Serpinb9	Q6AYF8_RAT	6,15	3	1,000	0,588	1,701	↓
		Protein Npepps - puromycin-sensitive aminopeptidase	F1M9V7_RAT	29,67	33	1,000	0,698	1,432	↓
		Calcyclin-binding protein	CYBP_RAT	23,14	4	1,000	0,738	1,355	↓
		Prolyl endopeptidase-like	PPCEL_RAT	9,50	4	1,000	0,751	1,331	↓
		Cystatin-B	CYTB_RAT	18,37	3	1,000	0,763	1,311	↓
		Dipeptidyl peptidase 3	DPP3_RAT	17,48	10	1,000	0,768	1,302	↓
		Proteasome (Prosome, macropain) 26S subunit, non-ATPase, 3	Q5U2S7_RAT	4,53	3	1,000	0,777	1,286	↓
		Cathepsin D	Q6P6T6_RAT	8,85	4	1,000	0,783	1,277	↓
		Xaa-Pro aminopeptidase 1	XPP1_RAT	13,64	8	1,000	0,795	1,258	↓
	Cytoskeletal / structural	**Isoform 2 of Tropomyosin beta chain**	**TPM2_RAT**	**17,61**	**3**	**1,000**	**2,406**	**2,406**	↑
		HMW-MAP2 (Fragment) - High molecular weight - microtubule-associated protein	**P70652_9MURI**	**57,30**	**8**	**1,000**	**2,342**	**2,342**	↑
		Tropomyosin 5	**P97726_9MURI**	**38,31**	**22**	**1,000**	**2,284**	**2,284**	↑
		Microtubule-associated protein 4	**MAP4_RAT**	**4,26**	**3**	**1,000**	**2,169**	**2,169**	↑
		Clathrin light chain A	**CLCA_RAT**	**22,18**	**9**	**1,000**	**2,066**	**2,066**	↑
		Microtubule-associated protein	Q63724_RATRT	57,11	180	1,000	1,983	1,983	↑
		Isoform 5 of Tropomyosin alpha-1 chain	TPM1_RAT	38,78	10	1,000	1,942	1,942	↑
		Nucleolin	NUCL_RAT	19,64	18	1,000	1,932	1,932	↑
		Protein Krtap9-1 - Keratin-associated protein 9-1	F1M294_RAT	33,33	2	1,000	1,887	1,887	↑
		Neuronal membrane glycoprotein M6-a	GPM6A_RAT	8,99	2	1,000	1,735	1,735	↑
		Beta-synuclein	SYUB_RAT	53,28	43	1,000	1,723	1,723	↑
		Spna2 protein - Spectrin alpha chain, non-erythrocytic 1	Q6IRK8_RAT	60,07	256	1,000	1,689	1,689	↑
		Stathmin	STMN1_RAT	52,35	21	1,000	1,684	1,684	↑
		Myelin proteolipid protein	MYPR_RAT	14,08	10	1,000	1,675	1,675	↑
		Mammalian ependymin-related protein 1	EPDR1_RAT	8,93	2	1,000	1,657	1,657	↑
		Clathrin light chain B	CLCB_RAT	23,14	10	1,000	1,644	1,644	↑
		Laminin, alpha 5, isoform CRA_a	F1MAN8_RAT	0,51	3	1,000	1,617	1,617	↑
		Protein piccolo	PCLO_RAT	4,09	13	1,000	1,577	1,577	↑

DH	Category	Protein	Accession no.	Cov (%)	Pep	Control : Control	EtOH : Control	Fold △	
	Cytoskeletal / structural (cont.)	Microtubule-associated protein	D3ZNA6_RAT	25,68	25	1,000	1,572	1,572	↑
		Neurofilament medium polypeptide	NFM_RAT	27,19	33	1,000	1,563	1,563	↑
		Drebrin	DREB_RAT	31,68	29	1,000	1,563	1,563	↑
		Protein Clip1 - CAP-Gly domain-containing linker protein 1	F1MAH8_RAT	2,20	2	1,000	1,559	1,559	↑
		ERC protein 2	ERC2_RAT	9,51	10	1,000	1,525	1,525	↑
		Microtubule-associated protein 6	MAP6_RAT	32,56	35	1,000	1,509	1,509	↑
		Protein bassoon	G3V984_RAT	9,84	28	1,000	1,482	1,482	↑
		Neurabin-1	NEB1_RAT	7,31	6	1,000	1,456	1,456	↑
		Isoform 2 of Myelin basic protein	MBP_RAT	40,24	19	1,000	1,444	1,444	↑
		Glia maturation factor beta	GMFB_RAT	37,32	8	1,000	1,434	1,434	↑
		Neurofilament heavy polypeptide	NFH_RAT	12,59	12	1,000	1,417	1,417	↑
		Translationally-controlled tumor protein	TCTP_RAT	36,63	8	1,000	1,397	1,397	↑
		Neural cell adhesion molecule 1 (Fragment)	F1LNY3_RAT	36,60	35	1,000	1,391	1,391	↑
		Paralemmin-1	PALM_RAT	18,54	5	1,000	1,379	1,379	↑
		Neurabin-2	NEB2_RAT	8,32	4	1,000	1,370	1,370	↑
		Alpha-synuclein	SYUA_RAT	60,00	22	1,000	1,370	1,370	↑
		Tropomyosin alpha-1 chain	TPM1_RAT	32,04	3	1,000	1,368	1,368	↑
		Dync1li2 protein	Q5D023_RAT	6,71	4	1,000	1,363	1,363	↑
		Cell adhesion molecule 2	CADM2_RAT	14,25	8	1,000	1,335	1,335	↑
		Alpha II spectrin	C9EH87_RAT	59,85	3	1,000	1,318	1,318	↑
		GRIP1-associated protein 1	GRAP1_RAT	6,93	6	1,000	1,308	1,308	↑
		C38 protein	B7X6I3_RAT	14,77	4	1,000	1,292	1,292	↑
		Neural cell adhesion molecule L1	D3ZPC4_RAT	5,18	5	1,000	1,292	1,292	↑
		Isoform 4 of Drebrin-like protein	DBNL_RAT	18,10	9	1,000	1,290	1,290	↑
		Myosin regulatory light chain	Q63781_RAT	33,72	6	1,000	1,280	1,280	↑
		Myotrophin	MTPN_RAT	38,14	10	1,000	1,272	1,272	↑
		Reticulon	F1LQN3_RAT	27,43	26	1,000	1,268	1,268	↑
		Neuroplastin	NPTN_RAT	11,96	7	1,000	1,254	1,254	↑

DH	Category	Protein	Accession no.	Cov (%)	Pep	Control : Control	EtOH : Control	Fold △	
	Cytoskeletal / structural (cont.)	Nucleophosmin	NPM_RAT	28,42	8	1,000	1,242	1,242	↑
		Band 4.1-like protein 1	D3ZMI4_RAT	5,29	8	1,000	1,232	1,232	↑
		C-fos induced growth factor, isoform CRA_b	G3V9S8_RAT	5,83	2	1,000	1,225	1,225	↑
		Uncharacterized protein - Tenascin-R	TENR_RAT	22,35	4	1,000	1,218	1,218	↑
		Neurotrimin	G3V964_RAT	18,02	9	1,000	1,208	1,208	↑
		Kinesin heavy chain isoform 5A	F1M8F2_RAT	3,99	2	1,000	1,205	1,205	↑
		Gamma-synuclein	F1LQ96_RAT	36,89	3	1,000	1,204	1,204	↑
		Tubulin alpha-1A chain	**TBA1A_RAT**	**75,17**	**11**	**1,000**	**0,371**	**2,697**	↓
		Actin, aortic smooth muscle	ACTA_RAT	43,50	6	1,000	0,529	1,891	↓
		Actin, cytoplasmic 2	ACTG_RAT	70,40	95	1,000	0,613	1,632	↓
		Septin 8 (Predicted)	G3V9Z6_RAT	15,38	5	1,000	0,631	1,585	↓
		Prelamin-A/C	LMNA_RAT	3,46	2	1,000	0,658	1,520	↓
		Vesicle-fusing ATPase	NSF_RAT	43,41	54	1,000	0,678	1,474	↓
		WD repeat-containing protein 1	WDR1_RAT	37,79	29	1,000	0,680	1,472	↓
		Tubulin beta-2A chain	TBB2A_RAT	69,44	152	1,000	0,687	1,456	↓
		Tubulin alpha-4A chain	TBA4A_RAT	66,29	12	1,000	0,694	1,441	↓
		Septin-11	SEP11_RAT	32,71	23	1,000	0,697	1,434	↓
		Protein Krtap9-1 - Keratin-associated protein 9-1	D3ZD90_RAT	20,75	4	1,000	0,699	1,431	↓
		Tubulin beta-5 chain	TBB5_RAT	69,59	20	1,000	0,700	1,429	↓
		Protein Tubb6	Q4QQV0_RAT	48,77	11	1,000	0,715	1,399	↓
		F-actin-capping protein subunit alpha-2	CAZA2_RAT	49,30	21	1,000	0,736	1,359	↓
		Neurochondrin	NCDN_RAT	15,50	17	1,000	0,740	1,351	↓
		Tubulin beta-3 chain	TBB3_RAT	66,44	41	1,000	0,742	1,348	↓
		Tubulin beta-4B chain	TBB4B_RAT	68,31	31	1,000	0,757	1,321	↓
		Coactosin-like protein	COTL1_RAT	45,07	7	1,000	0,762	1,312	↓
		Destrin	DEST_RAT	40,00	9	1,000	0,765	1,307	↓
		Endophilin-A1 (Fragment)	F1LQ05_RAT	38,46	26	1,000	0,770	1,299	↓
		Actin-related protein 2	ARP2_RAT	29,70	22	1,000	0,771	1,297	↓

DH	Category	Protein	Accession no.	Cov (%)	Pep	Control : Control	EtOH : Control	Fold △	
	Cytoskeletal / structural (cont.)	Isoform 4 of Dynamin-1	DYN1_RAT	51,87	75	1,000	0,778	1,286	↓
		Adaptor-related protein complex 2, beta 1 subunit, isoform CRA_b	Q3ZB97_RAT	29,97	47	1,000	0,785	1,275	↓
		Fascin	FSCN1_RAT	35,29	25	1,000	0,787	1,270	↓
		Coronin-1A	COR1A_RAT	17,35	7	1,000	0,788	1,269	↓
		Septin 7	A2VCW8_RAT	34,10	22	1,000	0,793	1,261	↓
		Isoform 8 of Dynamin-1	DYN1_RAT	51,05	2	1,000	0,798	1,254	↓
	Other	**Hemoglobin subunit alpha-1/2**	**HBA_RAT**	**72,54**	**50**	**1,000**	**2,787**	**2,787**	↑
		Hemoglobin subunit beta-1	**HBB1_RAT**	**89,12**	**72**	**1,000**	**2,706**	**2,706**	↑
		Hemoglobin subunit beta-2	**HBB2_RAT**	**78,91**	**12**	**1,000**	**2,653**	**2,653**	↑
		Prothymosin alpha	**PTMA_RAT**	**34,82**	**6**	**1,000**	**2,471**	**2,471**	↑
		Parathymosin	**PTMS_RAT**	**22,55**	**5**	**1,000**	**2,414**	**2,414**	↑
		Ab2-417	**Q7TMC7_RAT**	**11,75**	**10**	**1,000**	**2,360**	**2,360**	↑
		Protein Vat1l - Vesicle Amine Transport 1 Like	**D3ZE32_RAT**	**8,41**	**3**	**1,000**	**2,111**	**2,111**	↑
		Pyridoxal kinase	G3V647_RAT	41,03	12	1,000	1,968	1,968	↑
		Pdxp protein - pyridoxal phosphatase	B2GV79_RAT	24,66	6	1,000	1,948	1,948	↑
		SCO-spondin	SSPO_RAT	0,37	2	1,000	1,934	1,934	↑
		D-dopachrome decarboxylase	DOPD_RAT	50,85	9	1,000	1,889	1,889	↑
		Sulfated glycoprotein 1	SAP_RAT	8,48	10	1,000	1,799	1,799	↑
		Protein LOC100912106 - Programmed cell death 5	D4ADF5_RAT	28,80	7	1,000	1,781	1,781	↑
		Protein LOC100909983	M0R9D0_RAT	17,96	6	1,000	1,763	1,763	↑
		Uncharacterized protein	D3ZWT8_RAT	29,92	3	1,000	1,735	1,735	↑
		Zero beta-globin (Fragment)	Q63011_RAT	81,51	22	1,000	1,727	1,727	↑
		Hemopexin	HEMO_RAT	5,00	2	1,000	1,724	1,724	↑
		Reticulocalbin-2	RCN2_RAT	29,38	11	1,000	1,687	1,687	↑
		Protein RGD1310819 - Similar to putative protein (5S487)	D3ZEA1_RAT	14,95	3	1,000	1,640	1,640	↑
		Ribonuclease UK114	UK114_RAT	67,15	13	1,000	1,625	1,625	↑
		Protein Naca - Nascent polypeptide-associated complex alpha subunit	M0R9L0_RAT	1,94	6	1,000	1,605	1,605	↑
		Cortactin	Q66HL2_RAT	19,25	17	1,000	1,510	1,510	↑
	Other (cont.)	Stress-induced-phosphoprotein 1	STIP1_RAT	26,70	17	1,000	1,428	1,428	↑

DH	Category	Protein	Accession no.	Cov (%)	Pep	Control : Control	EtOH : Control	Fold △	
		Alpha globin	Q63910_RAT	19,72	3	1,000	1,426	1,426	↑
		Tumor protein D54	TPD54_RAT	11,82	2	1,000	1,410	1,410	↑
		Uncharacterized protein	M0R9D5_RAT	0,47	2	1,000	1,402	1,402	↑
		Complement C3	M0RBJ7_RAT	5,84	7	1,000	1,399	1,399	↑
		Protein Timm8a1 - Uncharacterized protein	F1LP21_RAT	22,68	2	1,000	1,382	1,382	↑
		Ferritin (Fragment)	A0JPM7_RAT	10,13	2	1,000	1,369	1,369	↑
		Protein FAM136A - Family With Sequence Similarity 136 Member A	F136A_RAT	18,12	2	1,000	1,318	1,318	↑
		Pcbp2 protein -poly(rc)-binding protein 2	Q4V8F6_RAT	8,66	2	1,000	1,256	1,256	↑
		Protein Ubap2l - Ubiquitin associated protein like 2	E9PTR4_RAT	5,25	4	1,000	1,255	1,255	↑
		Uncharacterized protein	Q6P769_RAT	19,44	5	1,000	1,254	1,254	↑
		Protein Tfg - TRK fused gene	Q6AYR1_RAT	9,05	2	1,000	1,250	1,250	↑
		Protein LOC100363408	D3ZVA6_RAT	27,91	2	1,000	1,240	1,240	↑
		Acylphosphatase-2	ACYP2_RAT	20,62	5	1,000	1,233	1,233	↑
		Annexin A3	**ANXA3_RAT**	**17,28**	**5**	**1,000**	**0,233**	**4,286**	↓
		Protein LOC685544 - Hypothetical protein LOC685544	**D3ZQT2_RAT**	**0,00**	**2**	**1,000**	**0,460**	**2,175**	↓
		Protein LOC679816 - RCG31390 (submitted name, UniProt)	**G3V9A3_RAT**	**23,79**	**3**	**1,000**	**0,479**	**2,089**	↓
		LOC681996 protein - Activator of Hsp90 ATPase activity 1	B0BN63_RAT	9,76	3	1,000	0,502	1,992	↓
		Uncharacterized protein	M0RCB1_RAT	8,33	2	1,000	0,565	1,769	↓
		Protein Ppidl1 - Uncharacterized protein	M0RB67_RAT	21,35	10	1,000	0,686	1,459	↓
		Protein LOC100911918 (Fragment) - Microtubule-associated protein RP/EB family member 2	M0R7M8_RAT	15,85	2	1,000	0,698	1,433	↓
		Heat shock cognate 71 kDa protein	F1LZI1_RAT	65,02	8	1,000	0,743	1,346	↓
		Uncharacterized protein	F1M2D3_RAT	38,30	2	1,000	0,749	1,335	↓
		Endophilin-B2	D4A7V1_RAT	23,02	8	1,000	0,776	1,288	↓
		60 kDa heat shock protein, mitochondrial	CH60_RAT	50,96	42	1,000	0,786	1,273	↓
		NAD(P)H-hydrate epimerase	NNRE_RAT	9,22	3	1,000	0,788	1,270	↓
		Fam49b protein	B2GUZ9_RAT	31,48	13	1,000	0,794	1,259	↓